A CORE-BASED ASSESSMENT OF THE SPATIAL RELATIONSHIP OF SMALL FAULTS ASSOCIATED WITH A BASEMENT-CONTROLLED, LARGE NORMAL FAULT IN THE HICKORY SANDSTONE

A Thesis

by

MITCHELL C. GRAFF

Submitted to the Office of Graduate Studies of
Texas A&M University
in partial fulfillment of the requirements for the degree of

MASTER OF SCIENCE

August 2006

Major Subject: Geology

A CORE-BASED ASSESSMENT OF THE SPATIAL RELATIONSHIP OF SMALL FAULTS ASSOCIATED WITH A BASEMENT-CONTROLLED, LARGE NORMAL FAULT IN THE HICKORY SANDSTONE

A Thesis

by

MITCHELL C. GRAFF

Submitted to the Office of Graduate Studies of
Texas A&M University
in partial fulfillment of the requirements for the degree of

MASTER OF SCIENCE

Approved by:

Chair of Committee,	Brann Johnson
Committee Members,	Frederick Chester
	Akhil Datta-Gupta
Head of Department,	Richard Carlson

August 2006

Major Subject: Geology

ABSTRACT

A Core-Based Assessment of the Spatial Relationship of Small Faults Associated with a Basement-Controlled, Large Normal Fault in the Hickory Sandstone. (August 2006)
Mitchell C. Graff, B.S., The University of Texas of the Permian Basin
Chair of Advisory Committee: Dr. Brann Johnson

This research characterized a system of small faults (displacement < 0.3 m) in seven closely-spaced continuous 2.4 inch (6.1 cm) diameter cores. Cores were obtained from central Texas, on the western edge of the Llano Uplift. Cores penetrate a dip-slip dominant, normal fault (Nobles Fault) with 18.3 m (60 ft) of stratigraphic throw. The spatial, geometric and kinematic attributes of small faults within the Nobles Fault system were characterized to explore potential cause-and-effect relationships.

To quantify spatial distributions, a "density" measure based on individual small fault magnitude was utilized. Approximately half of the small faults in the core possessed no discernible offset markers; thus displacement amount for these faults could not be measured directly. Using a nonparametric method in which an alternating conditional expectation determined optimal transformations for the data, a statistically significant empirical correlation was established for faults with measurable gouge thickness, displacement, protolith mean grain size and sorting. Gouge thickness of small faults was found to be dependant upon the displacement amount of the small fault and the textural characteristics of the host protolith.

The role of protolith lithology, proximity to crystalline basement, and structural position relative to the Nobles Fault system were examined to explain observed ubiquitous spatial distribution of small faults. Small faults were found to occur in clusters and the number of faults per foot only weakly correlates to the cumulative displacement of the corresponding faults. The amount of mudstone present is the dominant factor controlling small fault formation. Intervals with only minor quantities

of mudstone have the largest number of faults per foot as well as largest associated cumulative displacement per foot. Frequency of occurrence of small faults near the basement is greater when compared to similar lithologies higher in the core. Intensity of small faults do not universally increase with proximity to large faults. To observe an increase in small faults, it is necessary to use a mean global cumulative displacement approach. Zones of greater than average cumulative displacement of small faults in close proximity to large faults were observed in zones that are compatible with fault-fault interaction.

ACKNOWLEDGEMENTS

I would like to thank Brann Johnson for giving me the opportunity to work on this project. Your mentoring and friendship has helped me mentally grow and for that, I thank you. Although, I might never want to study such an immense amount of core in such a detailed manner, I hope that my work offers some hints as to how fault systems evolve. Without substantial help from Stephen Schneider and Brian Bagley, I would have never finished digitizing all 222 pages of strip maps. To the ever patient Jessica Fallon, without your encouragement, editing abilities and digitizing skills, I might still be working on this thesis.

TABLE OF CONTENTS

Page

LIST OF FIGURES

FIGURE Page

FIGURE Page

FIGURE Page

FIGURE Page

FIGURE Page

LIST OF TABLES

1. INTRODUCTION

Field studies show that brittle failure of a large volume of rock results in the development of a system of faults that accommodates the inelastic strain field. Typically, members of the fault system exhibit a broad range of dimensions and displacements. Most small-scale field studies focus on the larger fault members, which normally have the larger displacements (e.g. Dawer and Anders, 1995; Ackermann and Schlische, 1997; Fossen and Hesthammer, 1997*)*. With an increase of mapping scale, one can document the spatial attributes of a large number of shorter faults with smaller displacements.

The mechanical significance of these smaller faults has received only limited study and remains open to debate. Some workers suggest that small faults represent early-formed features that did not evolve into a larger fault due to mechanical effects associated with preferential strain accommodation and growth of other faults in a neighboring region (Antonellini and Aydin, 1995; Cruikshank et al., 1991; Cowie and Scholz, 1992; Davis et al., 1999; Fossen and Hesthammer, 1997). In contrast, some workers suggest that small faults need not be solely, early-formed elements with arrested growth, but that some faults are nucleating through out the deformation interval and reflect spatial and temporal variations of the inelastic strain field associated with larger structures (Childs et al., 1996; Davison, 1994; Hedgcoxe, 1987; Johnson, 1993; Schafer, 2002; Walsh et al., 1999; Peacock and Sanderson, 1991).

The latter model for formation of small faults may be particularly appropriate when studying large faults that evolve by interaction between and linkage of early-formed, smaller faults. The fault-linkage model has been proposed to explain the highly segmented character and the multiple, fault-element architecture of large faults (Hedgcoxe, 1987; Cruikshank et al., 1991; Zhao and Johnson, 1991; Johnson, 1993; Fossen and Hesthammer, 1997; Schafer, 2002; Bernard and Labaume, 2002). This model of fault growth predicts the occurrence of spatial and temporal variations of the

---

This thesis follows the style of Journal of Structural Geology.

strain field in the vicinity of the large fault with larger inelastic strains in regions between interacting neighboring faults. In this model, later-forming small faults are interpreted to be subsidiary faults forming in close association with the larger fault and are a direct consequence of the evolution of the larger fault. This model of small-fault formation would predict differing relative times of formation of the small faults. This model also explains the common observation that the number of small faults increases with increasing proximity to a large fault, although spatial variation along the fault also can occur.

This thesis research has studied a system of small faults (displacements less than 0.3 m) in a volume of faulted siliciclastic rock in central Texas. This study builds upon and extends the earlier study of Wilson (2001), which documented several closely associated, moderate displacement, segmented faults. Wilson (2001) used 1050 m (3445 ft) of continuous core from eleven, closely spaced boreholes to construct a high-resolution stratigraphic model and structural architecture of the segmented faults. Wilson used the fault-linkage model to interpret the structural evolution of the faults. The primary segmented fault has a net displacement of 18.3 m (60 ft) distributed on the multiple fault elements.

This thesis has characterized the spatial, geometric and kinematic attributes of small faults within core for the purpose of exploring several potential cause and effect relationships that account for the observed spatial variations of small faults. The cause and effect relationships that were investigated are: 1) lithologic control, 2) bedding rotation 3) reactivation of basement fractures, 4) lateral proximity to large faults, and 5) fault-fault interaction.

2. PREVIOUS WORK

The study area is located in central Texas, in northern Mason County, northeast of the town of Katemcy, on the western edge of the structural province know as the Llano Uplift (Fig. 1). The Llano Uplift is a broad domal structural high that trends NW-SE. Within the Llano uplift, 1000 m (3281 ft) of Paleozoic clastics and carbonates strata have been tilted and faulted and are primarily exposed along the flanks of the uplift. The central region of the uplift is primarily composed of exposed Precambrian igneous and metamorphic rocks.

2.1 Stratigraphy

The Hickory Sandstone is the only Paleozoic unit present within the study area and consists of 137 m (450 ft) of quartzose and sub-arkosic sandstone with interbeds of mudstone and siltstone (Randolph, 1991; Wilson, 2001). The Hickory Sandstone is the basal member of the Riley Formation and is Upper Middle to Late Cambrian in age (Cloud, et al. 1945) and unconformabliy overlies the Precambrian Town Mountain Granite.

The Hickory Sandstone is subdivided into three units for field mapping purposes: Lower, Middle and Upper Hickory as defined by Barnes and Bell (1977). Only the Lower and Middle subunits are of importance for this study. Based on core and geophysical logs, the Middle Hickory has been further subdivided into Lower Middle and Upper Middle subunits.

At the study site, the Lower Hickory is 57 m (187 ft) in thickness and consists of two subfacies XB1 and XB2 as defined by Wilson (2001). The lithology of the Lower Hickory consist of a friable to weakly cemented, high porosity, coarse to medium, angular to subangular, poorly sorted, quartzose to subarkosic sandstone (Bridge et al., 1947; Barnes and Bell, 1977; Randolph, 1991; Wilson, 2001). Large festoon cross bedding is prominent along with a few interbedded, laterally discontinuous mudstone and siltstone beds that increase in frequency upsection (Wilson, 2001).

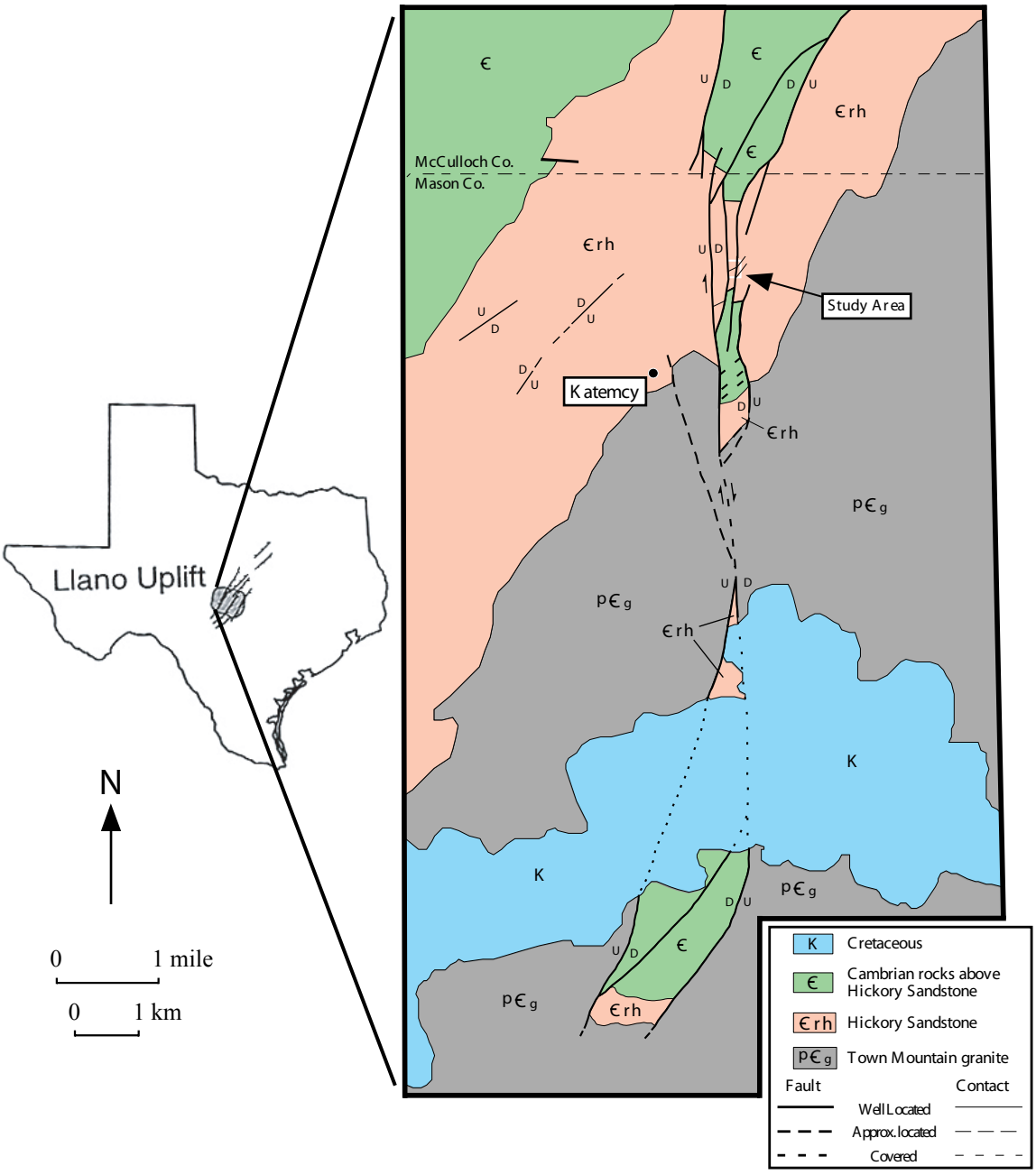

Fig. 1. Map of regional geology and location of study area. Modified from Randolph, (1991).

The Lower Middle Hickory is 35 m (115 ft) in thickness and consists of two subfacies MS1 and MS2. Lithology of the Lower Middle Hickory consists of fine grained to medium grain, poor to moderately sorted, quartzose sandstone, siltstone and mudstone, which are commonly bioturbated (Wilson, 2001). Laterally extensive siltstone and mudstone beds are prominent and range from 0.02 - 1 m (0.07 – 3.3 ft) in thickness.

2.2 Structure

Faults within Paleozoic strata formed during the Quachita orogeny of Middle Pennsylvanian time (Cheny and Goss, 1952). According to Becker (1985), Johnson and Becker (1986) and Johnson (1990), faulting can be reconciled with a NNW-SSE regional extension, which was due to plate flexure induced by vertical loads associated with crustal thickening on the convergent plate margin to the E and SE. Stratigraphic constraints (Becker, 1985) and diagenesis studies of the Hickory Sandstone (El-Jard, 1982; McBride et al., 2002) indicate that at the time of faulting approximately, 1km (0.62 mi) of sedimentary overburden was over the crystalline basement. Due to the shallow depth of burial, re-activation of pre-existing weaknesses in the basement is inferred to strongly control faulting during the Pennsylvanian deformation interval (Becker, 1985; Johnson and Becker, 1986; Schmittle, 1987; Hedgcoxe, 1987; Johnson, 1990).

In the vicinity of the study area, Randolph (1991) mapped a 600 m (2000 ft) wide, N-trending structural graben within the Precambrian Granite and overlying Lower Paleozoic strata (Fig. 2). Within the graben, two N-trending, large displacement, normal dip-slip dominant faults with some right-lateral slip structurally partition the graben. Smaller NE-trending normal and oblique faults further partition the graben into a number of partially to completely fault-bounded blocks. The focus of this study is on one of these normal faults, which trends approximately N60E and dips to the SE. For ease of presentation, the study fault is denoted as the Nobles Fault. The Nobles Fault is

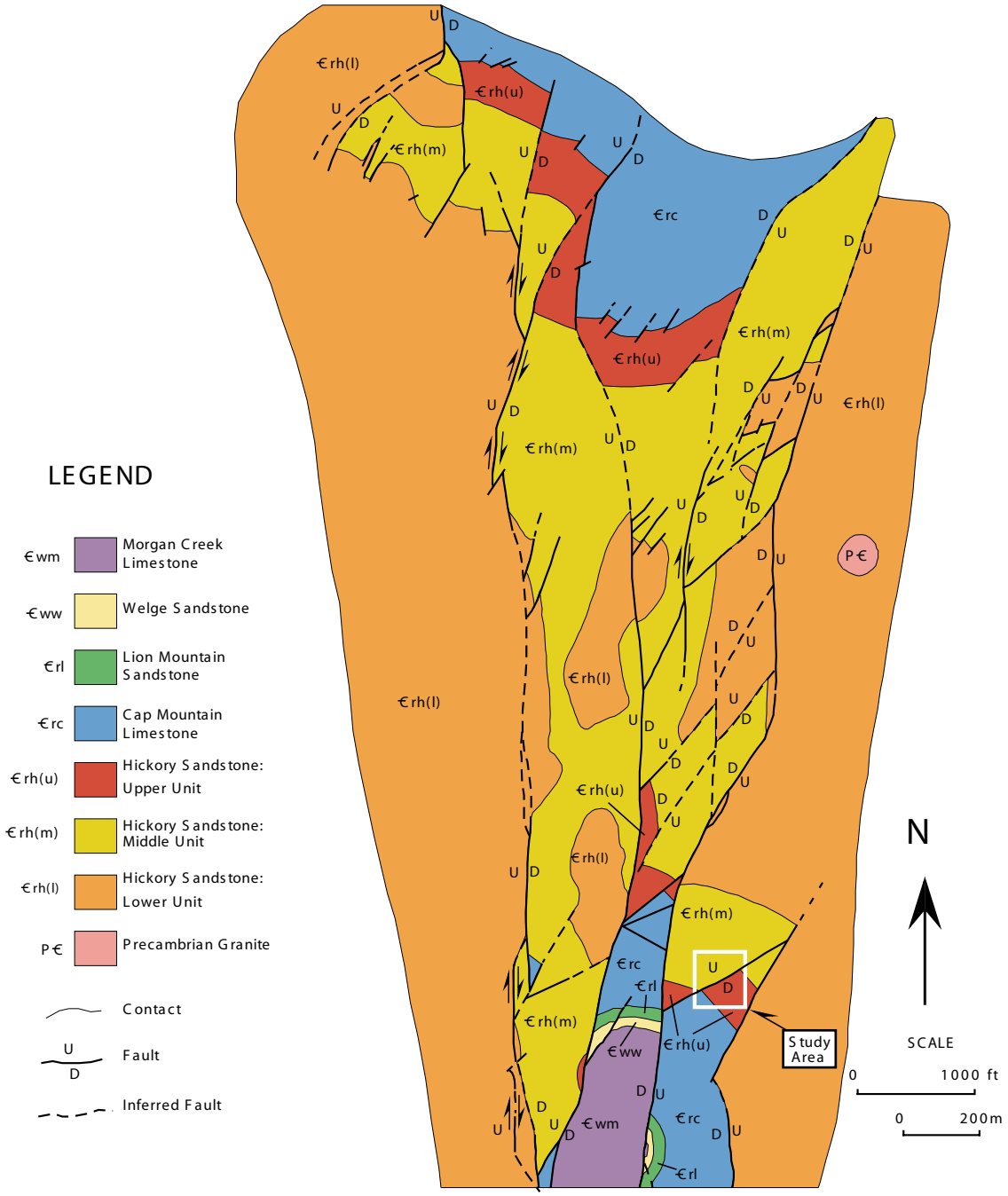

Fig. 2. Geologic map showing structural graben in which the study area lies. Modified from Randolph, (1991

bounded to the east by a dip-slip dominant fault that trends approximately N30E and to the west by one of the two N-trending, dip-slip dominant, large displacement faults.

2.2a Architecture of Nobles Fault System

Wilson (2001) constructed a structural model for the Nobles Fault using continuous core and geophysical logs from boreholes drilled through the fault system. The Nobles Fault is a linked-fault system consisting of several hard-linked, large fault segments (Fig. 3), with a maximum net stratigraphic throw of 18.3 m (60 ft). The dominate slip surface of the Nobles Fault system is comprised of three main segments. Due to limited data, only the lower two segments (1 and 2) were used in this study. The lower half of Segment 1 is subdivided into two Sub-Segments: 1a and 1b. In the hanging wall in close proximity to Segment 1 is a prominent fault with 2 m (7 ft) of displacement, which is denoted as the Upper Fault.

Wilson (2001) interpreted that the Nobles Fault evolved from upward and lateral growth and eventual hard linkage of two closely spaced, ENE-trending, left-stepping en echelon faults contained within the granite basement. Segment 2 is inferred to hard link with Segment 1 near the Precambrian contact and along strike to the east and up dip. The inferred linkage along strike is based on observed strike change of Segment 1 to the east. The up-dip linkage is supported by the shallowing of dip of Segment 1 as it approaches Segment 2. Transfer of displacement between the Segments 1 and 2 is inferred from along fault variation of fault throw. Displacement transfer between the two segments is supported by Segment 1 having the largest throw along strike to the east, while to the west Segment 2 has the largest throw. Also, where the segments overlap, displacement variations both laterally and vertically show complimentary variations; increase of displacement on one segment is matched by a similar decrease on the neighboring segment.

Wilson (2001) proposed two models for the development of the Upper Fault. The preferred model relates the genesis of the Upper Fault with the hard linkage of the main segments. Hard linkage of the main segments resulted in the formation of a large

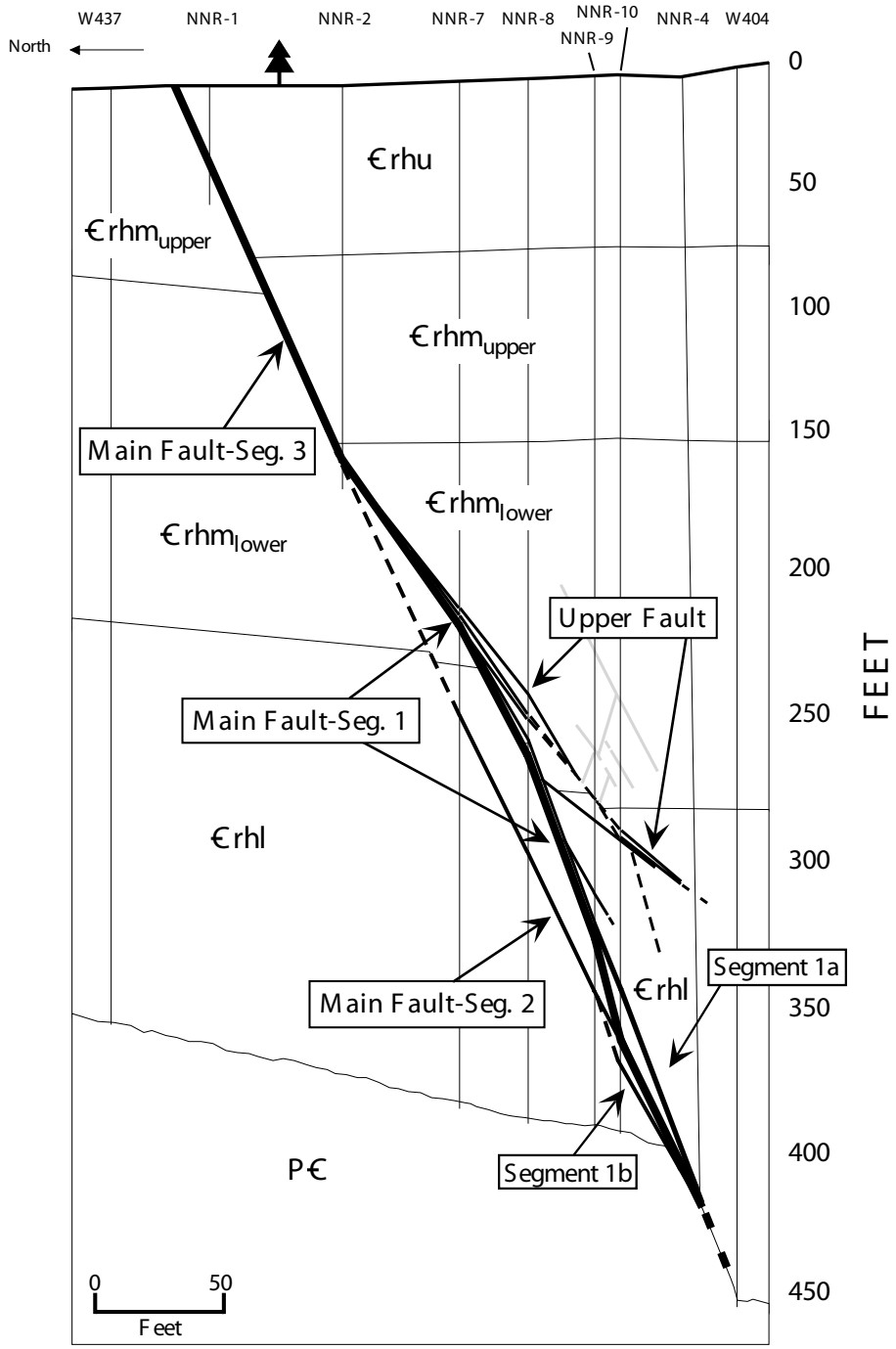

Fig. 3. Eastern cross section of the study area showing major segments of the Nobles Fault. Modified from Wilson, (2001).

geometric perturbation. With increasing displacement on the main segments this perturbation concentrated deformation in the adjacent hanging wall, which resulted in formation of the Upper Fault. The alternative model proposes an early formation of the Upper Fault independent of the effect of the hard linkage-induced perturbation. This model associates the low dip to mechanical behavior of interbedded sandstone and mudstone.

3. METHODOLOGY

3.1 Nature of Data

The data set consists of measurements acquired from core and geophysical logs in seven closely spaced boreholes. The boreholes were continuously cored using a HX-size, 10 ft (3.05 m) long, core barrel, which produced 2.4 inch (6.1 cm) diameter core. Core recovery averaged 99 % for boreholes ranging in depth from 320 - 405 ft (97.54 - 123.44 m). The core used is part of a larger data set from eleven boreholes (NNR-1 through 10 and GKR-5) drilled through or in immediate proximity to the Nobles Fault (Fig. 4). NNR-1 and 2 were early exploratory boreholes drilled through the shallow portion of the Nobles Fault and terminate a short distance after penetrating the Nobles Fault in the unsaturated interval above the aquifer. NNR-3 through 10 penetrate the Nobles Fault in the saturated interval within the aquifer, and all but NNR-3 terminate in the Precambrian granite. GKR-5 is in the footwall and also terminates in the granite. Gamma ray logs were taken in all of the boreholes and used to quantify lithology. Acoustic borehole televiewer logs (BHTV) were taken in the saturated interval of boreholes NNR-3, 4, 7, 8, 9 and 10 and used to orient the core with respect to a true west datum. Once the core was oriented, it was mapped onto strip maps. Data contained within strip maps was then tabulated into a Microsoft Excel spreadsheet which facilitated quantitative analysis of spatial relationships.

3.2 Gamma Ray Logs

The mudstone content of the Hickory Sandstone varies with stratigraphic position. Normalized gamma ray values from the gamma ray logs taken in each borehole were used to quantify the fraction of mudstone within any given depth interval. This gamma ray derived mudstone fraction was used to investigate the effect of lithology on fault distribution in the boreholes.

Gamma ray logs detect the natural gamma radiation emitted by decay of potassium-40 and trace amounts of uranium and thorium. Shales and mudstones typically have greater concentrations of these natural radioactive elements as compared

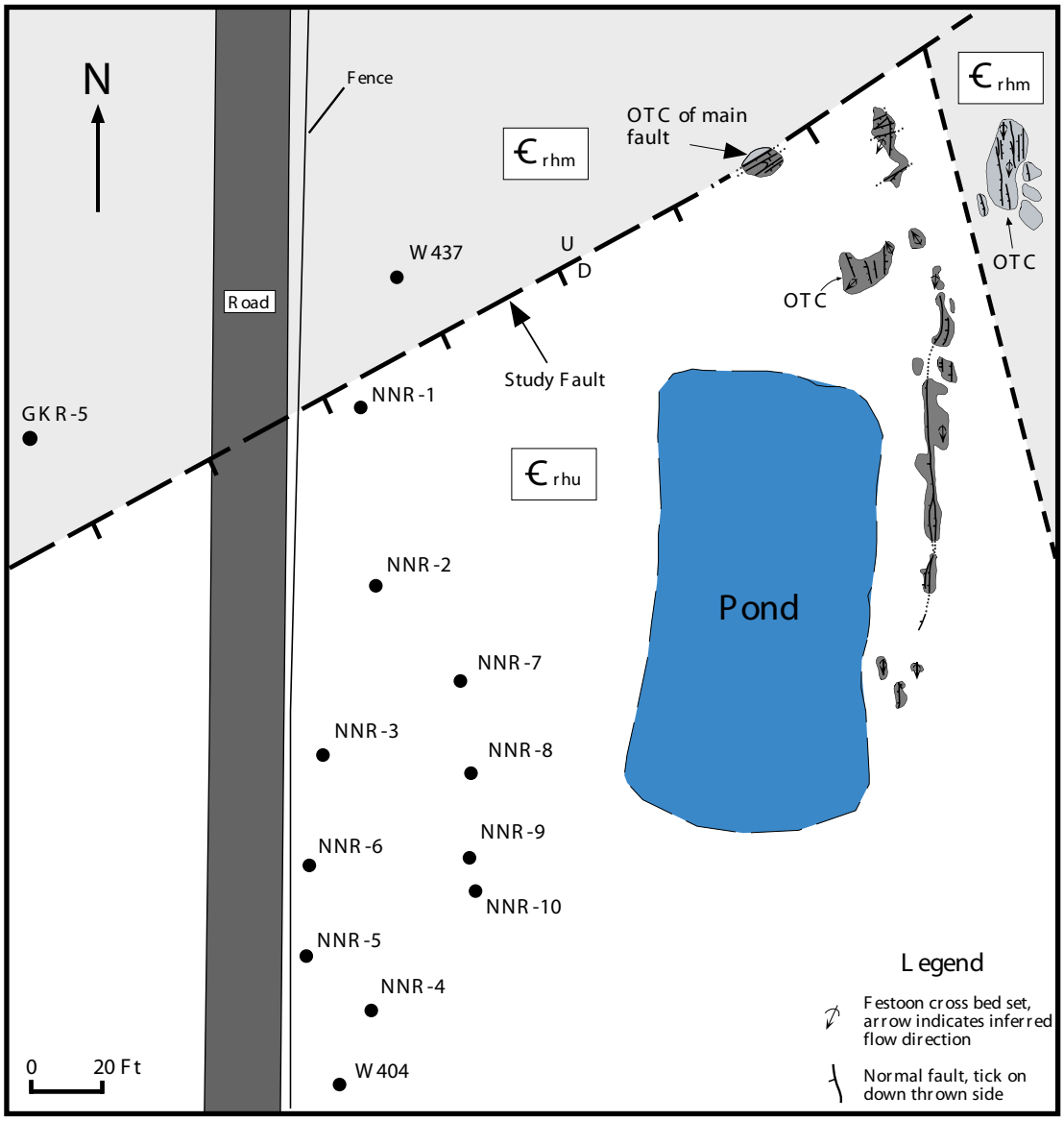

Fig. 4. Map showing surface trace of the Nobles Fault, surface geology and location of cored boreholes. Modified from Wilson, (2001).

to siliciclastic-rich sandstone. Some discrepancy in gamma ray counts can occur because they are slightly dependent on how fast the geophysical tool is pulled up the borehole.

Normalization of the gamma ray logs is necessary to insure a consistent magnitude in gamma ray counts in correlated units. A commercial gamma ray log obtained for NNR-3 is used to shift gamma ray curves of the other boreholes. Two stratigraphic intervals that are distinct and readily correlated across all boreholes and are located at approximately 18 m (59.05 ft) and 21 m (68.9 ft) in NNR-3 were chosen to normalize the gamma ray logs.

The normalized gamma ray logs were used to distinguish between sandstone-dominant and mudstone-dominant intervals. Based on gamma ray response and the equivalent lithology observed in the core, a value of 60 API was deemed reasonable to separate clean sandstone from interbedded sandstone and mudstone. The total cumulative footage greater than 60 API for any chosen interval length is divided by the interval length in order to determine the mudstone fraction within that interval.

3.3 Orientation of Core Using Acoustic Borehole Televiewer Logs

Orientation of the core relative to a geographic directional datum was achieved using acoustic borehole televiewer logs. An acoustic borehole televiewer (BHTV) is an ultrasonic imaging tool that produces a continuous three-dimensional image of the borehole wall. The differences in acoustic reflectivity allow joints, faults and bedding features, hereafter referred to as structural elements, to be distinguished from one another. Absolute orientations for these elements can be determined, because the BHTV logs were magnetically oriented and have a resolution within the millimeters range. Absolute orientation for structural elements in the BHTV log is measured at the dip line point. Since strike is perpendicular to the dip line point, one only needs to subtract or add 90 ˚ to obtain strike (Fig. 5). In order to determine the dip amount (θ), the vertical distance between the two dip line points (h) and the diameter of the borehole (d) are needed to calculate the dip from:

$$\text{TAN } \theta = h/d \qquad (1)$$

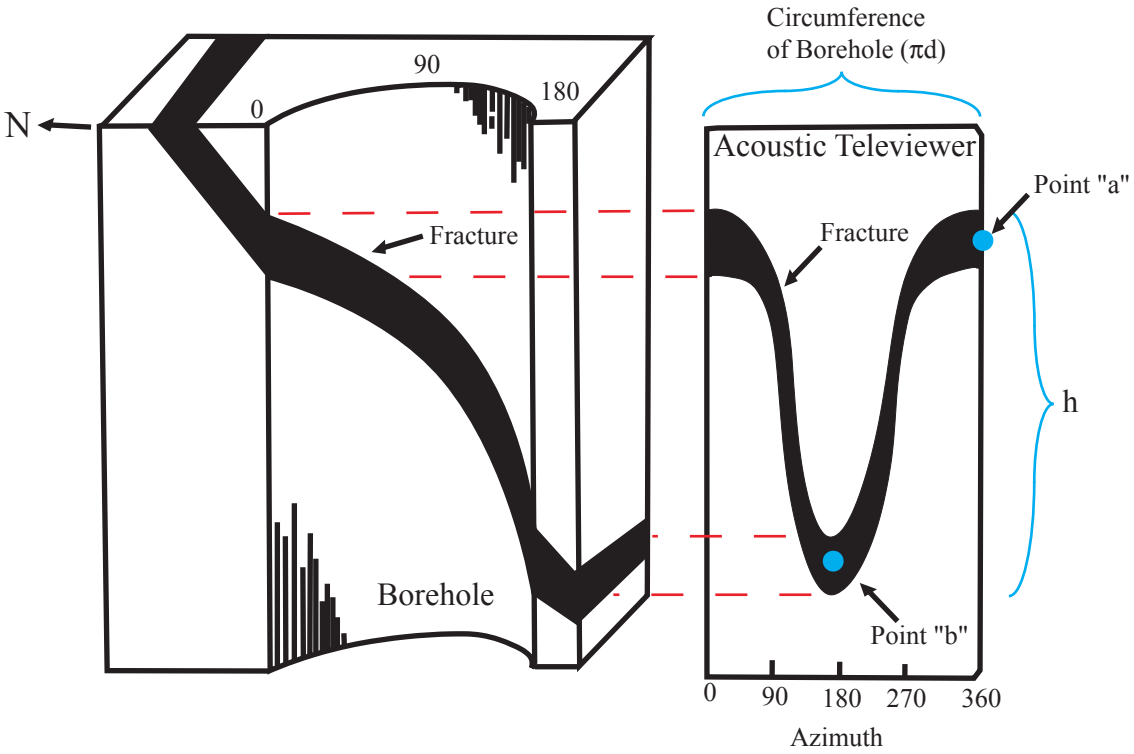

Strike of Fracture (α)

α = [Point "a" or "b" of Dip Line] + 90

Dip of Fracture (θ)

$\tan\theta = h / d$

Fig. 5. Illustration of acoustic borehole televiewer log and method for obtaining the attitude of fractures within boreholes. Example fracture strikes E-W and dips to the south. Modified form Davison et al., (1982).

BHTV logs were obtained in the saturated interval of boreholes NNR-3, 4, 7, 8, 9 and 10 and are used to determine absolute orientation of select structural elements. Structural elements with attitudes determined using the BHTV log were first located in core, then the core was rotated to match the directional datum of the BHTV (in this case, west) (Fig. 6). These correlated elements were then used to orient the rest of the core by carefully piecing together the intermediary core pieces. Quality of core orientation was checked by comparing the inferred west datum direction as carried from one correlation element to that of the next correlation element. If the two directions differed by less than 10˚, the core interval between the correlation elements was considered properly oriented. This method was highly successful because broken pieces of core were easily put back together. In cases where the core was missing or damaged, and pieces could not be placed together easily, the dip line of local mudstone beds was assumed to trend west, because the average strike of mudstone beds calculated within BHTV logs strike approximately to the north and dip to the west.

Once the core was oriented the absolute orientation for faults, joints and bedding elements that are not visible in BHTV logs were determined. Bedding attitudes measured in core were determined primarily on clay surfaces and interfaces between sandstones layers of significantly different grain sizes. Care was taken to not measure attitudes of large scale cross bedding in sandstone. In a sand quarry near the study area, clay drapes in the Lower Hickory occur on dune and bar surfaces (Johnson personal communication), thus measured bedding attitudes reflect both stratigraphic and structural controls.

Bedding attitudes also were obtained independently from the BHTV logs. Attitudes of low dipping beds were not attempted because of the inherent error associated with the measurement. When BHTV bedding attitudes were compared with bedding attitudes obtained from core, the two measurements were usually similar.

3.4 Core Description

This study describes 1,652 ft (503.53 m) of core in detail. The types of data recorded are: 1) type of structural element (fault, joint and bedding), 2) depth of

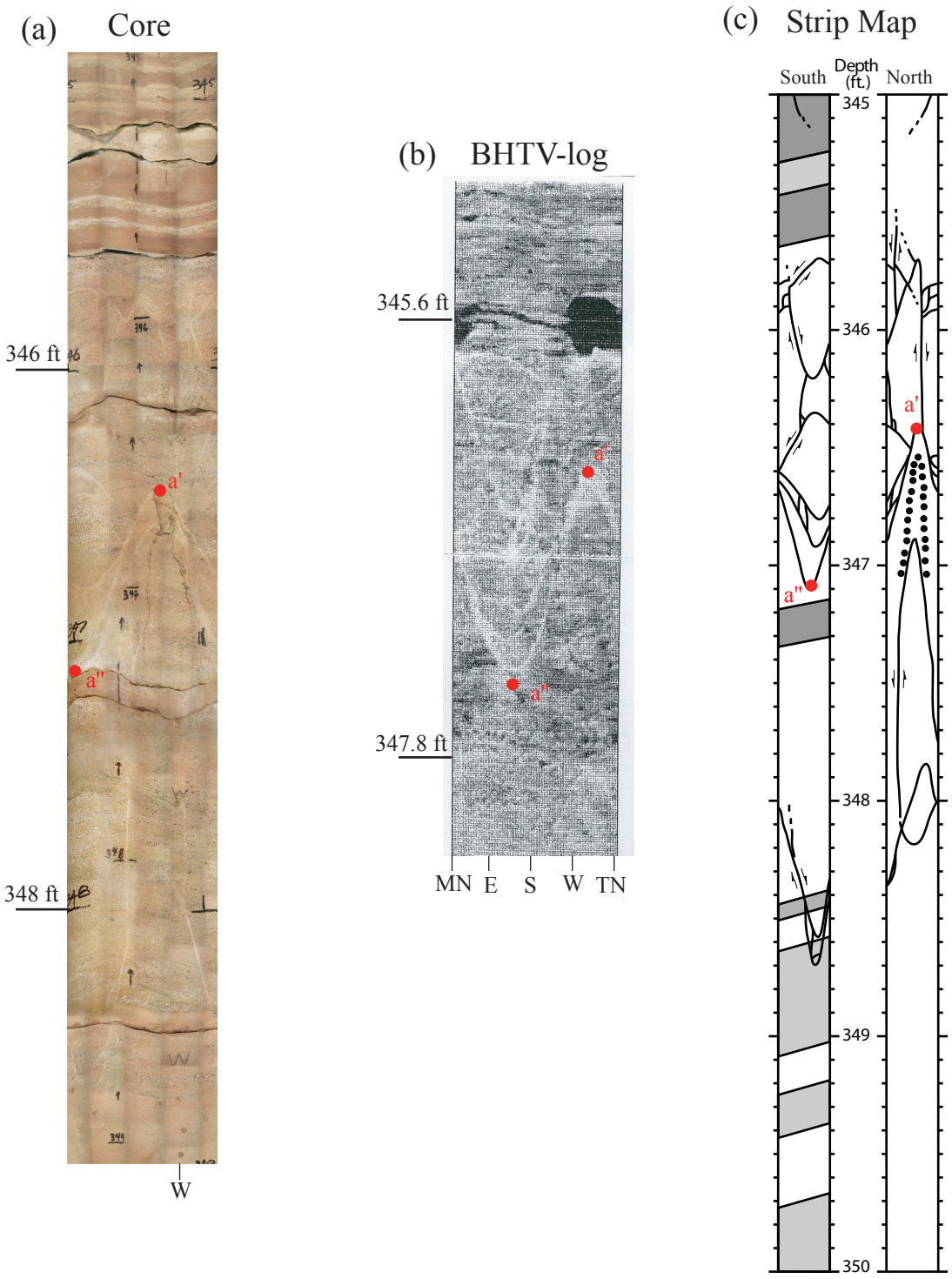

Fig. 6. Example of method for orienting core by use of acoustic borehole televiewer logs (BHTV). (a) Structural element within core (360˚ view) with corresponding correlation points found in (b) acoustic borehole televiewer log. (c) Strip map created for this depth interval showing bedding, faults and open crack (dots).

structural element, 3) orientation of structural element, 4) gouge thickness of small fault, 5) sense of slip and magnitude of small fault, 6) pitch of displacement vector when striae visible, 7) cross-cutting relationship with other structural elements and 8) lithology.

Faults, joints and bedding are the three types of structural elements that are distinguishable in core. Joints within the core are purely mode I and commonly have Fe or Mn oxide surface coatings. Of the 2523 structural elements recorded only 81 are joints and they are younger in age than faults. The joints were documented for completeness, but were not analyzed in this study. Faults are discernable by the presence of a well-defined, quasi-planar, continuous zone of cataclasis. Faults were subdivided into three subcategories based on magnitude of displacement. Large faults have a displacement greater than 3 ft (0.91 m), intermediate faults have a displacement ranging from 1 - 3 ft (0.3 - 0.91 m) and small faults have a displacement of less than 1 ft (0.3 m).

A midpoint depth (i.e. depth in core below the earth's surface) is used as the spatial location for each structural element in core. In many cases, structural elements cut entirely across the core (Fig. 7a). In some cases the elements cut only partway across the core and either die out or terminate against another structural element (Figs. 7b and 7c). The midpoint depth is the maximum depth minus the minimum depth divided by two. All depth measures were measured to the nearest 0.05 ft (1.52 cm).

The absolute attitude of each structural element was possible because the core was oriented using BHTV logs, as described above. Strike was recorded to the nearest 5° increment, while dip amount was measured with a contact goniometer and recorded to the nearest 1° increment.

Displacement amount and thickness of gouge for each small fault was measured from core and used as a substitute measure of strain. Values of shear displacements were determined from offset of sedimentary structures and measured to the nearest 0.5 mm (0.02 in). Gouge thickness was measured to the nearest 0.25 mm (0.01 in) in close proximity to the location where displacement is measured. If a small fault exhibited

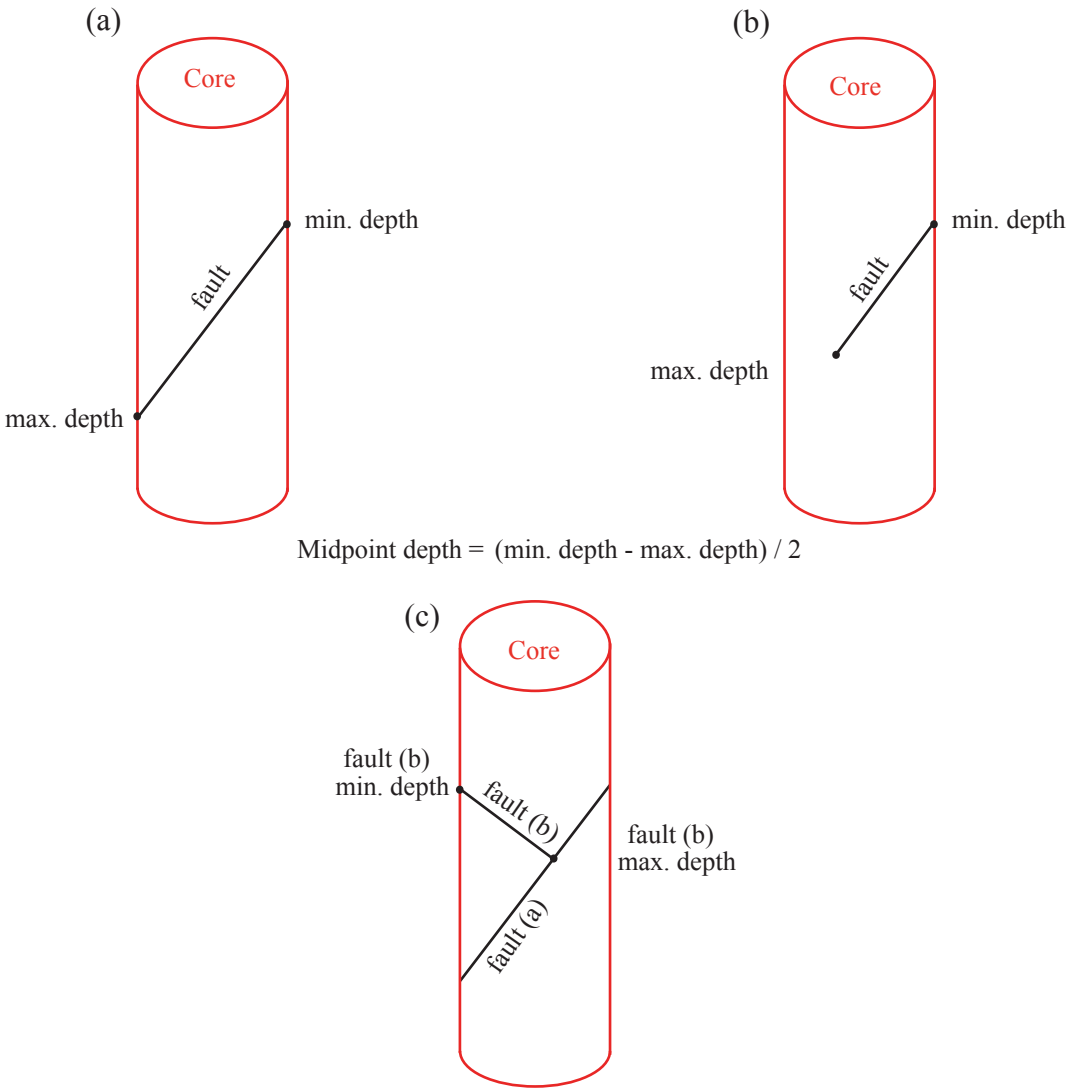

Fig. 7. Illustration of method for determining midpoint depth of structural elements within core from maximum and minimum depths. Structural element cut entirely across the core (a) or terminates within core by either dying out (b) or terminating against another structural element (c).

variable gouge thickness along its length in core, an average gouge thickness was recorded. Displacement and gouge thickness are addressed in further detail in section 4.

Core breakage occasionally occurs along faults, especially for large and intermediate faults. Fault slip striae are often visible on these exposed fault surfaces. The rake of the striae was measured and considered to be parallel to the slip vector.

The small diameter of the core constrains the lateral dimensions of faults sampled by the core and provides a limited sampling of cross-cutting relationships. If a fault appeared to cut another fault, a cross-cutting relationship was recorded if the following criteria were met: 1) the displacement magnitude and direction of the younger fault could be determined independently using sedimentary markers, 2) the apparent magnitude and direction of displacement of the younger fault as determined by offset of the older (cross-cut) fault was similar to the independently determined measurement obtained using sedimentary markers, and 3) the strike and dip of the offset fault segments were similar.

Six lithologies were distinguished based on grain size and sorting: 1) coarse to very coarse grained sand, 2) fine to medium grained sand, 3) coarse grained sand with only a few clay interbeds, 4) interbedded medium grained sand and clay, 5) mudstone with a few sand interbeds, and 6) mudstone. These six lithofacies are equivalent to the lithofacies described by Wilson (2001).

3.5 Core Data Illustration

An illustrated three-dimensional representation of structural features in the core was documented using strip maps (Fig. 8). The strip maps were drawn such that one view is seen looking to the north (front) and the reverse side is seen looking to the south (back). Lithologic changes within core and bedding dip amounts were illustrated only on the view looking to the north. Documented within the stripmap are: 1) sense of slip, displacement magnitude of small faults, 2) pitch of displacement vector if visible, 3) gouge thickness of small faults, and 4) mean grain size of the protolith adjacent to the measured gouge zone. Orientations of bedding features measured within BHTV logs are noted. Faults and joints used as correlations points to orient the core, ancillary notes and

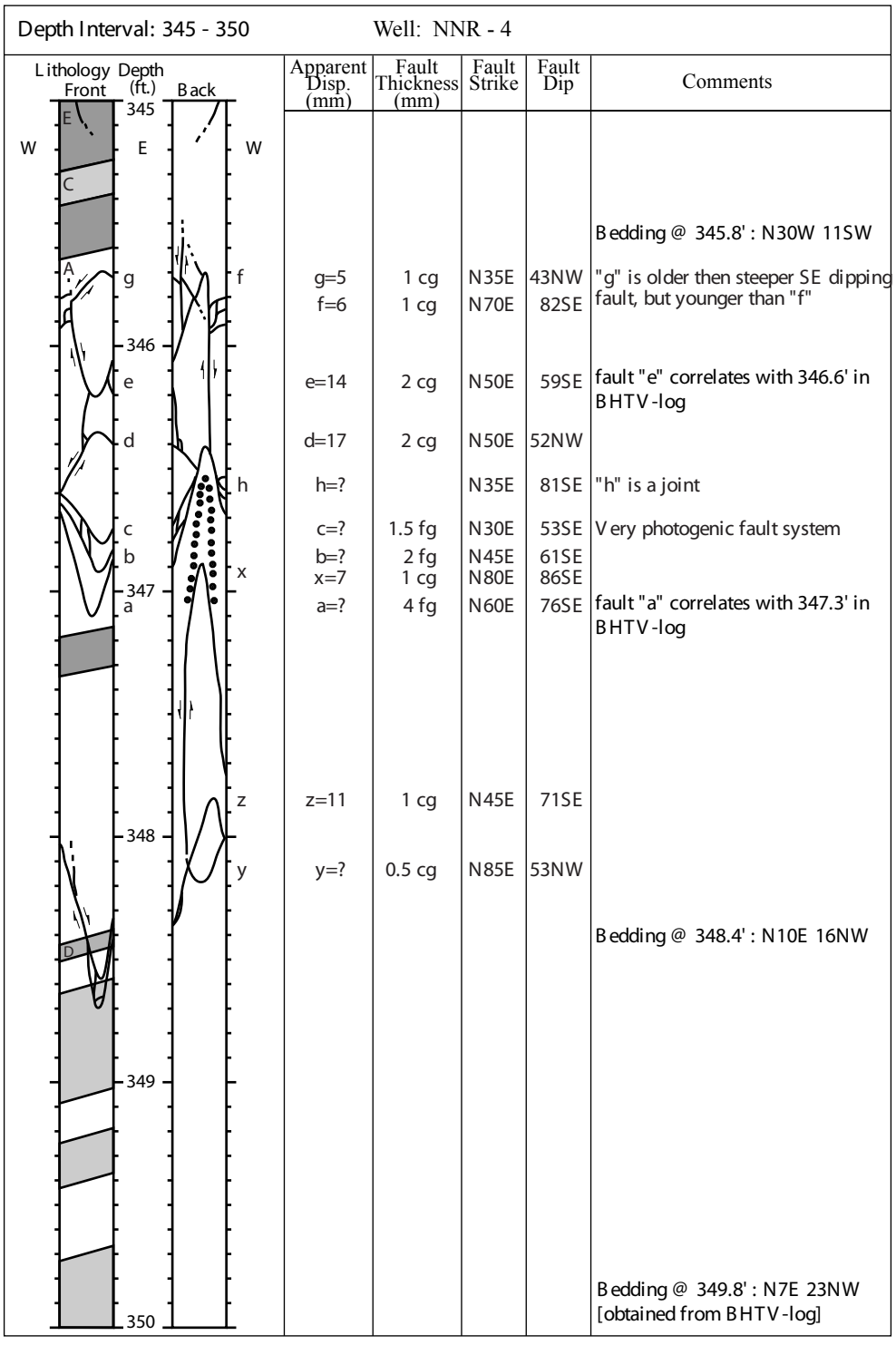

Fig. 8. Strip map example of core within NNR-4 from depth interval of 345 – 350 ft.

drawings are also included within the margins of the strip maps. Individual small faults were illustrated as observed. Near or within faults of intermediate to large displacements the complexity occasionally became too great to accurately capture at this scale of observation. Since large and intermediate faults were not the focus of this study, only the dominant characteristics of small faults were captured in these complex areas.

3.6 Defining Clusters of Fault Elements

Preliminary observations of small faults show they tend to form clusters. A cluster is comprised of two or more fault elements that occur close together relative to the proximity of the next cluster of faults. To facilitate data analysis, the faults were grouped into clusters using the criteria outlined below.

The first step in identifying a cluster of faults was to determine the average distance between adjacent faults using a nearest-neighbor-distance method. The distance between neighboring faults was measured perpendicular to the faults, which for neighboring faults that have the same orientation is the shortest distance between the faults (Fig. 9a). Since most faults are not parallel four different distances were calculated for each neighboring pair and the average distance was used (Fig. 9a - e):

$$d_1 = (Y_1 - X_1) \cos \theta_Y \quad (2)$$

$$d_2 = (Y_2 - X_2) \cos \theta_Y \quad (3)$$

$$d_3 = (Y_1 - X_1) \cos \theta_X \quad (4)$$

$$d_4 = (Y_2 - X_2) \cos \theta_X \quad (5)$$

$$d_{ave} = (d_1 + d_2 + d_3 + d_4) / 4 \quad (6)$$

The frequency distribution of the average distance between nearest-neighbor faults was examined (Fig. 10) and used to establish the criterion to define a fault-cluster distance threshold. The histogram of average distance between nearest-neighbor faults is highly skewed with a maximum average distance of 7.4 ft (2.26 m), while the arithmetic mean is 0.41 ft (0.12 m). Based on the distributional characteristic of fault spacing, a threshold distance of 1 ft (0.3 m) was selected to discriminate two

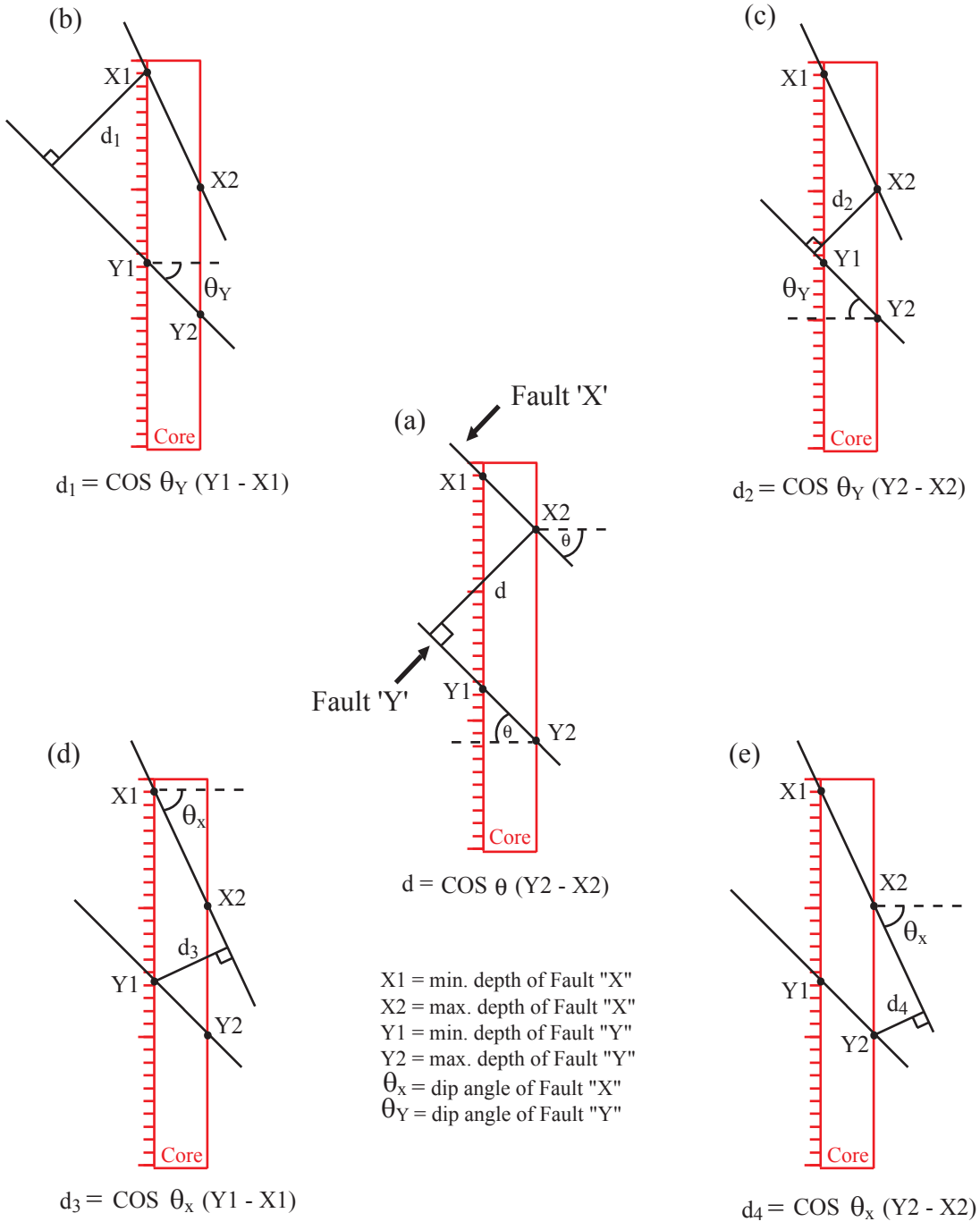

Fig. 9. Illustration for calculating the average distance between neighboring faults in core. (a) Ideal case in which faults are parallel and (b through e) four different algorithms used to calculate average distance

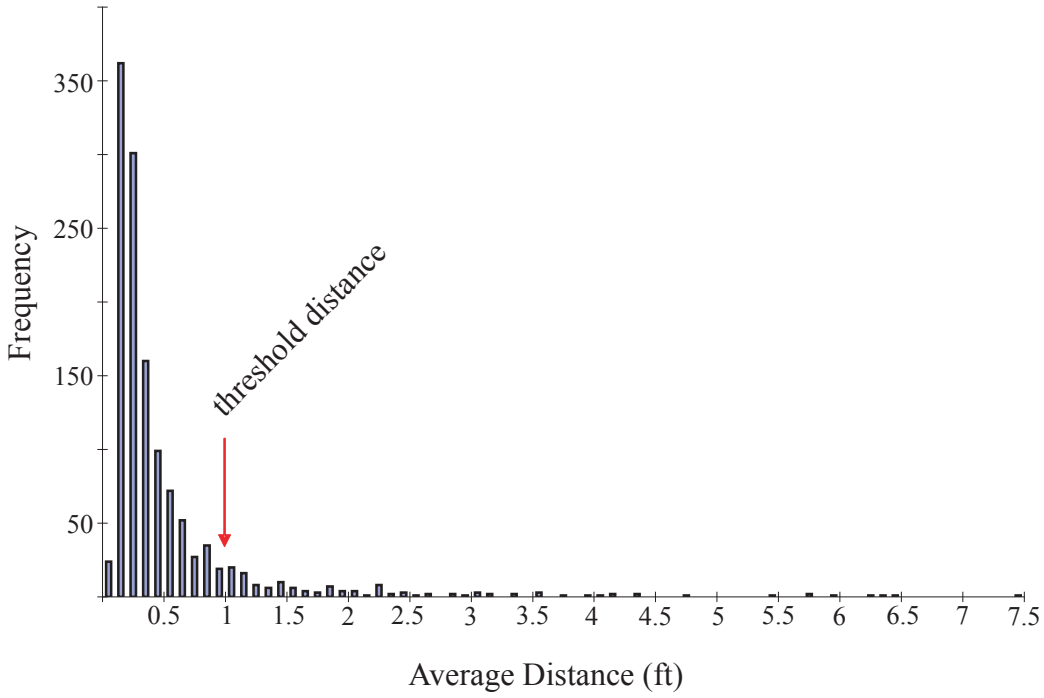

Fig. 10. Histogram of average distance between nearest-neighbor faults in core. Data for faults within core from GKR-5, NNR-3, 4, 7, 8, 9 and 10.

neighboring clusters. This threshold distance is approximately one standard deviation larger than the mean spacing.

A cluster is typically composed of multiple faults, although a single fault element can represent a cluster in some cases. Some clusters consist of faults with similar attitudes and shear sense (Fig. 11). Whereas, clusters with a more complex architecture have fault elements with different attitudes and shear sense, which can be grouped into several sets (Fig. 12). A fault set consists of fault elements with a similar strike, dip direction and shear sense.

Fault elements were grouped into sets using stereonet plots and the following criteria: 1) Fault elements of a set have a similar dip direction and dip magnitude. Fault elements with similar dip directions were placed into different sets only if their dip magnitude differed by more than 60˚. 2) The strike of fault elements in a set must differ by no more than 30˚, unless hard linkage occurs, if the latter occurs, the range in strike is increased up to 60˚. 3) Fault elements in a set must also have the same apparent sense of displacement. If the sense of slip of a fault could not be determined, then it was assumed to have the same slip sense as the nearest-fault element with similar strike and dip direction. Once the fault sets in a cluster were identified, the average strike and dip of set members was determined. This average orientation was then assigned to each member of the set.

Determination of fault sets comprising a cluster of fault elements served two purposes. Firstly, it permitted representation of each cluster by a simplified idealization that contained the architectural essence of the dominant fault set or sets within the cluster. The idealized clusters show orientation of fault sets as well as observed or inferred abutting and cross-cutting relationships between sets, shear sense on each set and cumulative shear displacement for each set in the cluster. It was anticipated that representation of complex clusters of faults by the idealized versions would facilitate correlation of faults between neighboring boreholes and thus aid in construction of a cross section containing boreholes NNR-7, 8, 9, 10 and 4 (sequenced N to S). Secondly,

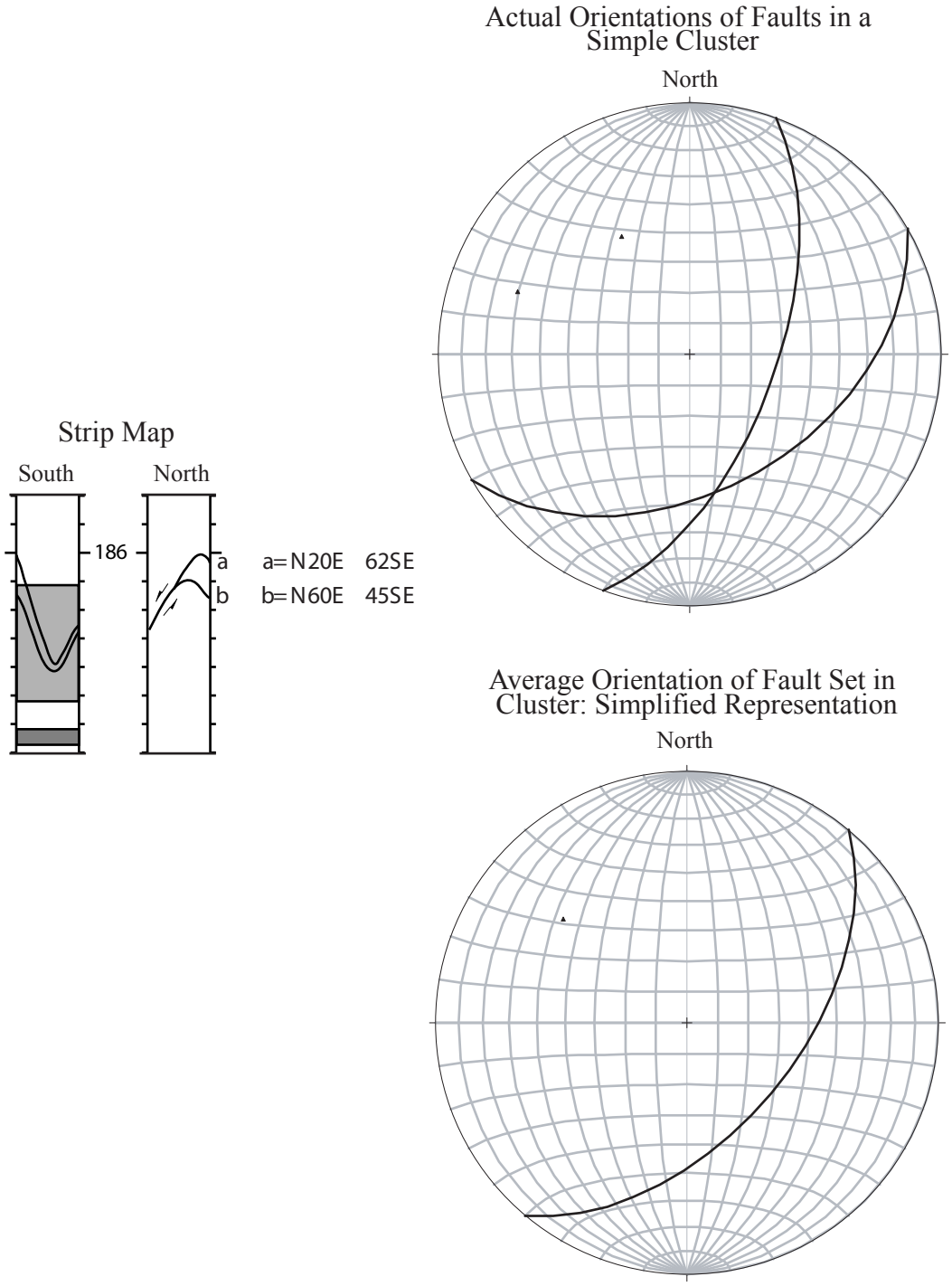

Fig. 11. Example of a simple fault cluster showing the actual architecture and its simplified representation. Example is from NNR-9. Stereonets are equal area, lower hemisphere projections, showing planes and associated poles.

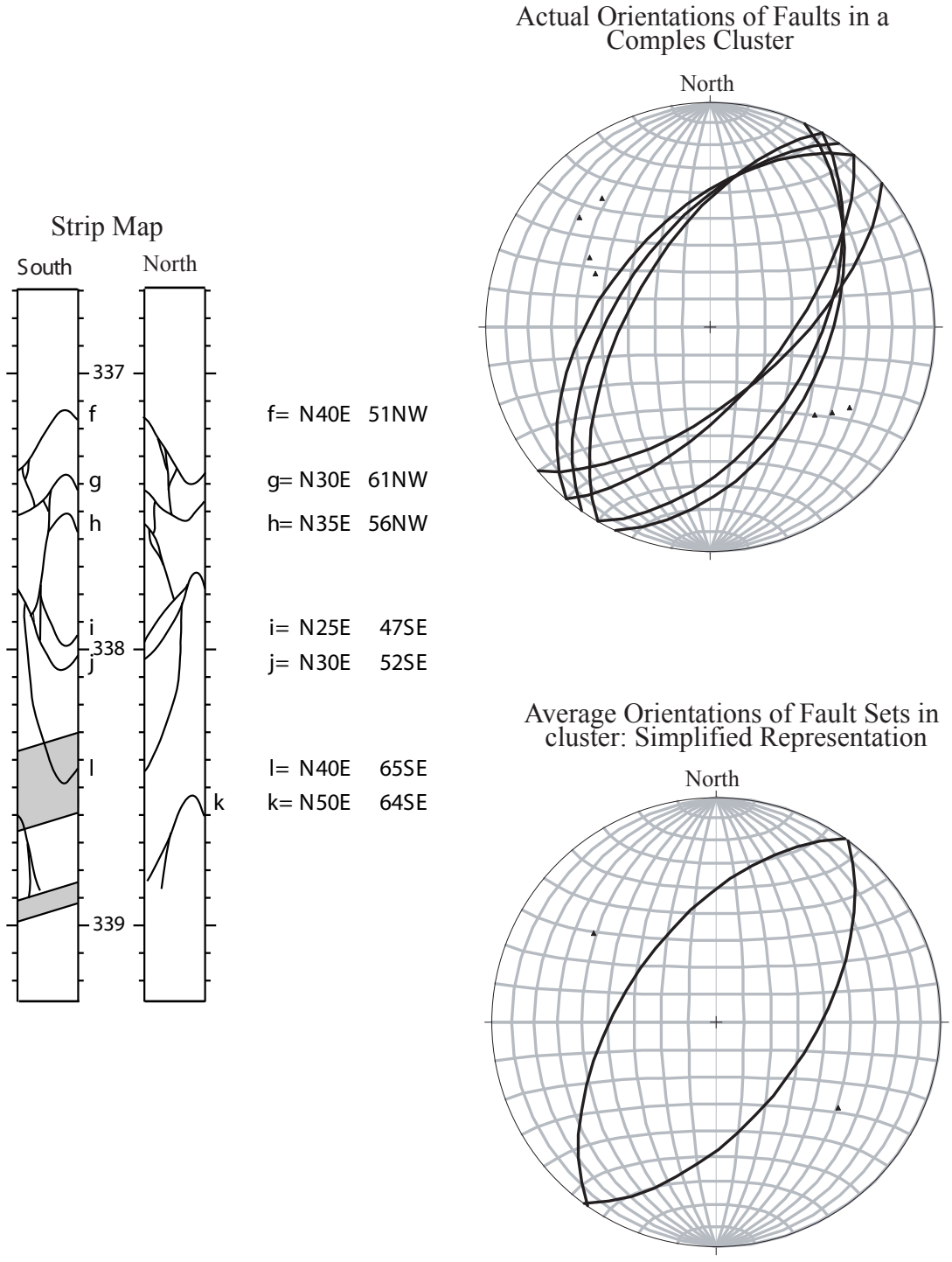

Fig. 12. Example of a complex fault cluster showing the actual architecture and its simplified representation. Example is from NNR-7. Stereonets are equal area, lower hemisphere projections, showing planes and associated poles.

differentiation of fault sets in fault clusters aided in establishing strike and dip cutoff limits used to define fault sets in the global data set as discussed below.

3.7 Orientation of Small Faults Analysis Method

Stereonet and rose diagrams plots show existence of multiple fault sets (Fig. 13). In order to allow easier visualization of spatial patterns of faults as a function of fault orientation, faults were assigned to one of four strike bins. Faults within a strike bin were further differentiated according to dip polarity.

Initial efforts to define the range of strike associated with each bin utilized the actual orientation data to construct global stereonet and rose diagrams plots (Fig. 13). These plots provided insight into possible strike intervals for each bin, but cutoffs limits were uncertain due to significance dispersion about the mean.

An alternative approach was to utilized "smoothed" fault attitudes. Each actual fault attitude was replaced by the average attitude of the set to which it was assigned in the cluster idealization (Section 3.6). This process reduced the inherent variability of fault attitudes (Fig. 13), yet insured that small faults that are in close proximity to one another but with minor variability in strike were placed in the same strike bin. For example, a bin could be defined from faults that dip to the SE and range in strike from N30E to N70E. If the actual orientation of faults is used, this cutoff (N30E to N80E) would place small faults with similar attitudes that are in close proximity to one another into separate bins, see Figures 11 and 12 as examples.

Global stereonet and rose diagram plots using the smoothed data allowed easier discrimination of fault bins and strike cutoffs to separate global fault sets. Four strike bins were discriminated: 1) NE strike (N30-70E), 2) N strike (N29W-N29E), 3) E strike (N71E–S71E) and 4) NW strike (N30-70W). Each strike bin was then subdivided based on dip direction. All orientation data were plotted using Allmendingers's StereoWin 1.2 software (2002).

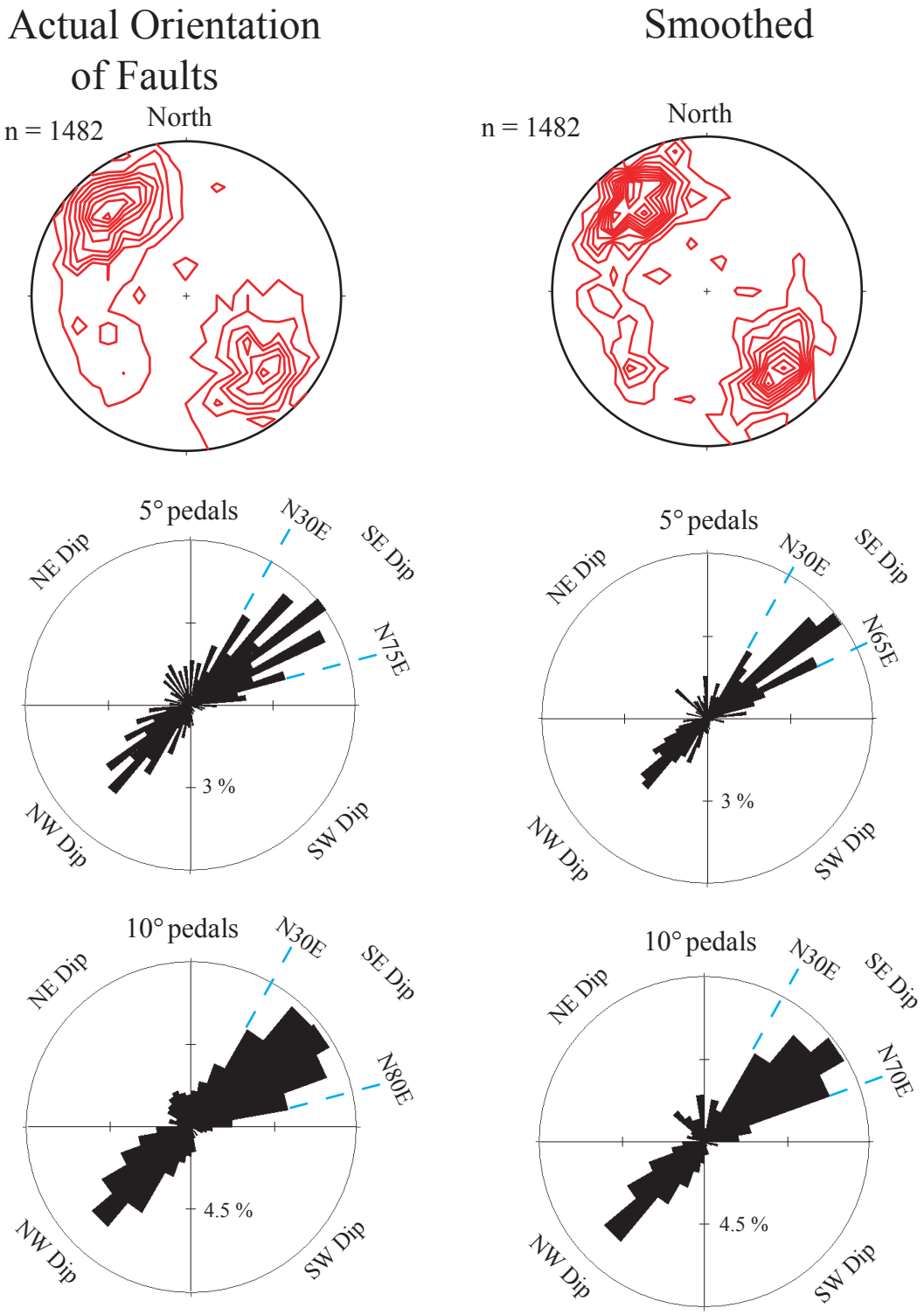

Fig. 13. Rose diagrams and stereonets of actual and smoothed small fault orientations. Equal area, lower hemisphere projection, stereonet plots with Kamb contouring of poles with a contour interval of 2σ.

3.8 Density Measures of Small Faults

Three measures of small fault occurrence are used to represent "density" measures within the core as function of depth. These measures are: 1) frequency of small faults per foot, 2) cumulative displacement of all small faults per foot, and 3) average displacement of all faults per foot (i.e. cumulative displacement per foot \ frequency per foot). Though large and intermediate displacement faults were mapped in core, they were purged from the data set before the three measures of "density" were quantified (Table 1).

Density measures of cumulative displacement and average displacement require all faults to have measures of displacement. For approximately half of the small faults in core, no displacement was able to be determined directly. The following section outlines the method used to obtain estimated measures of displacement for these faults from measures of fault gouge thickness and textural characteristics of the host protolith. On occasion neither displacement nor gouge thickness could be determined for a small fault. Typically when this occurred a discernible lithologic marker could be seen, either on the footwall or hanging wall portion of the fault. The distance from the lithologic marker to the dip line of the fault represents a minimum displacement. This minimum displacement was assigned as the displacement value. On rare occasion no minimum displacement could be determined for a small fault because of lack of discernible lithologic markers. When this occurred these faults were purged from the data set (Table 2).

Table 1. Large and intermediate displacement faults that correlate with Wilson (2001) and were purged from "density" measures.

Borehole	Midpoint (ft)	Borehole	Midpoint (ft)	Borehole	Midpoint (ft)
NNR-10	232.30	NNR-4	228.05	NNR-9	250.50
NNR-10	232.48	NNR-4	255.65	NNR-9	250.55
NNR-10	255.55	NNR-4	298.83	NNR-9	252.10
NNR-10	280.05	NNR-4	299.15	NNR-9	252.20
NNR-10	282.33	NNR-4	299.68	NNR-9	253.23
NNR-10	282.60	NNR-4	300.33	NNR-9	268.53
NNR-10	283.15	NNR-4	396.40	NNR-9	276.50
NNR-10	286.03	NNR-4	403.35	NNR-9	276.95
NNR-10	286.20	NNR-4	404.53	NNR-9	303.68
NNR-10	286.53	NNR-7	196.10	NNR-9	315.00
NNR-10	286.70	NNR-7	196.50	NNR-9	315.08
NNR-10	338.35	NNR-7	198.65	NNR-9	315.20
NNR-10	338.95	NNR-7	202.13	NNR-9	320.23
NNR-10	339.35	NNR-7	203.00	NNR-9	321.70
NNR-10	340.13	NNR-7	205.13	NNR-9	340.95
NNR-10	340.38	NNR-7	205.20	NNR-9	342.00
NNR-10	341.30	NNR-7	236.35	GKR-5	368.50
NNR-10	357.03	NNR-7	236.95	GKR-5	136.63
NNR-10	357.28	NNR-7	304.20	GKR-5	296.90
NNR-10	359.28	NNR-7	304.50	GKR-5	364.60
NNR-10	360.10	NNR-7	304.55	GKR-5	376.80
NNR-10	362.75	NNR-7	327.35	GKR-5	298.15
NNR-10	363.33	NNR-8	228.05		
NNR-10	367.70	NNR-8	228.10		
NNR-3	192.45	NNR-8	236.23		
NNR-3	192.63	NNR-8	238.10		
NNR-3	202.93	NNR-8	238.13		
NNR-3	230.30	NNR-8	245.95		
NNR-3	230.83	NNR-8	251.05		
NNR-3	269.15	NNR-8	252.20		
NNR-4	200.85	NNR-8	287.23		
NNR-4	201.00	NNR-9	215.80		

Table 2. Small faults in which estimated or minimum displacement could not be determined, thusly they were purged from the "density" measures.

Borehole	Midpoint (ft)	Borehole	Midpoint (ft)
NNR-4	266.8	GKR-5	90.33
NNR-4	274.13	GKR-5	90.83
NNR-4	274.5	GKR-5	91.68
NNR-7	178.4	GKR-5	101.68
NNR-7	235.8	GKR-5	127.20
NNR-7	235.9	GKR-5	143.10
NNR-7	238.6	GKR-5	164.20
NNR-7	239.3	GKR-5	164.45
NNR-7	287.425	GKR-5	181.70
NNR-7	296.7	GKR-5	185.25
NNR-7	309.9	GKR-5	219.95
NNR-7	317.275	GKR-5	228.75
NNR-7	321	GKR-5	238.60
NNR-7	323.6	GKR-5	258.45
NNR-7	326.425	GKR-5	299.15
NNR-7	380.1	GKR-5	299.65
NNR-8	198.825	GKR-5	300.40
NNR-8	227.175	GKR-5	300.60
NNR-8	236.125	GKR-5	349.65
NNR-8	237.4	GKR-5	351.65
NNR-8	245.625	GKR-5	351.75
NNR-8	247.7	GKR-5	352.31
NNR-9	188.3	GKR-5	352.70
NNR-9	202.05	GKR-5	371.40
NNR-9	216.675		
NNR-9	275.475		
NNR-9	317.1		
NNR-9	384.125		
NNR-10	388.8		

4. ESTIMATING SMALL FAULT DISPLACEMENT USING FAULT GOUGE THICKNESS AND PROTOLITH TEXTURE

The focus of this section is two fold. First, using data for small faults with measurable displacement, a statistically significant empirical correlation was established between the dependent variable, gouge thickness and the independent variables of fault displacement, protolith mean grain size and protolith sorting.

Second, in subsequent analysis displacement amount was used to weight each fault. Approximately half of the small faults in core possessed no discernible offset markers, and thus displacement amount for these faults could not be measured directly. In instances where displacement amount could not be directly measured for a fault, the empirical correlation established for faults with measurable gouge thickness, displacement, protolith mean grain size and sorting of the protolith were used to generate an estimate of displacement.

4.1 Previous Work

Experimental deformation studies have observed that both the mean gouge thickness (Engelder, 1974) and the frequency of associated deformation bands comprising a fault (Mair et al., 2000) increase approximately linearly with displacement. Field observations have established that the fault zone thickness increases with net displacement at a constant proportion over several orders of magnitude (Otsuki, 1978; Robertson, 1983; Wallace and Morris, 1986; Hull, 1988). Subsequent work has focused on defining measures of fault zone thickness in order to better understand the interdependence of fault thickness and displacement. Two approaches have been taken; one is to measure attributes of individual faults, while the other is to measure attributes of the zone associated with deformation. Field work by Knott (1994) observed that thickness of deformation bands or zones of deformation bands increases with displacement of individual deformation bands, or zones of deformation bands. Net thickness of individual faults has been observed to scale with net displacement (Child et al., 1996). The thickness of damage zones also have been observed to increases with net

displacement of the zone (Beach et al., 1999; Fossen and Hesthammer, 2000; Shipton and Cowie, 2001; Bernard and Labaume, 2002). Even though a crude linear relationship exists for displacement and gouge thickness, the wide statistical variability implies that a simple relationship does not exist for the two variables. Lithology, cementation, porosity and burial depth are all secondary variables that could account for the variability of gouge thickness for a given displacement.

Textural attributes of siliciclastic granular protoliths in which the fault forms appears to explain some of the variability of shear zone thickness associated with a given displacement. Fault thickness has been observed to be narrower in clay-rich horizons as compared to coarser siliciclastic layers (Antonellin et al., 1994; Knott et al., 1996; Heynekamp et al., 1999). For high porosity sandstone, the finer-grained sandstone tends to have less gouge development than coarse-grained sandstone (Schmittle, 1987; Beach et al., 1999; Fossen and Hesthammer, 2000). The effective pressure in which cataclastic flow occurs in high porosity sandstone is dependent upon grain size and porosity (Zhang et al., 1990; Wong et al., 1997). Karner et al., (2005) deformed samples of unconsolidated sand and found that the critical pressure for grain crushing has an inverse power-law relationship with grain size.

Cementation of grains potentially can decrease the amount of gouge formed during shear deformation. Experimental work has shown that intragranular failure is inhibited by cemented regions around the grains (Bernabe et al., 1992; Menendez et al., 1996) which is inferred to result from contact tractions on grains becoming more uniformly distributed (Yin and Dvorkin, 1994). Field observations of deformation bands with thin zones of gouge development as compared to deformation bands with thicker zones of gouge thickness suggests that secondary cementation in the porous sandstone affects the thickness of deformation bands (Johansen et al., 2005).

Experimental studies show fracture strength of quartz sandstone increases with a decrease of porosity (Dunn et al., 1973; Wong et al., 1997). Porosity also affects the brittle-ductile transition, such that at the same confining pressure a high porosity material will respond in a brittle manner as compared to a low porosity material (Scott

and Nielsen, 1991). Field work by Young (1982) observed that porosity affects the relationship between gouge thickness and displacement of a single fault, such that for a fixed displacement, the gouge thickness is smaller with a decrease in porosity of the protolith. A weak correlation between porosity of the host protolith and the thickness of deformation bands within the same mean pressure regime has also been observed (Antonellini et al., 1994).

Experimental studies on precut high porosity sandstone have shown that normal stress influences the thickness of gouge, such that an increase in normal stress is accompanied by an increase in gouge development (Teufel, 1981). Conversely, experimentally deformed samples of intact porous sandstone have shown that with an increase in normal stress, the thickness of gouge decreases although the relationship appears not to be monotonic at high normal stress (El Bied et al., 2002).

Although these studies have investigated several variables that can affect the relationship between gouge thickness and displacement, none limited the range of analysis for displacement and gouge thickness to less than three orders of magnitude, analyzed samples within the same lithology, mean pressure regime or established any statistically significant linear correlation.

4.2 Controls on Gouge Thickness Development

Small faults, which are also called deformation bands (Aydin and Johnson, 1978), within the sandstones of the Hickory Sandstone are seen as narrow, quasi-planar cataclastic zones in which the grains of the protolith have undergone comminution. These well-defined zones are lighter in color than the buff to tan protolith. The thickness of the cataclastic material comprising the narrow zone of shear deformation is denoted as gouge thickness in this thesis.

Statistical analysis was performed on 692 small faults with measurable displacement in order to explore empirical relationship between the dependent variable, gouge thickness and the independent variables; displacement, protolith mean grain size and sorting of the protolith. In agreement with prior workers and shown subsequently, a weak statistical correlation was found between displacement and gouge thickness. The

incorporation of protolith mean grain size and sorting in addition to displacement improved the correlation and demonstrates the importance of protolith texture on gouge development.

The role of effective mean pressure and protolith cementation were not assessed. It was assumed all faults studied formed under a similar effective mean pressure, because the faults occur within a small vertical sample window of 245 ft (74.68 m) and a horizontal window of approximately 110 ft (33.53 m). Cementation also was expected to marginally contribute to the variability, because diagenesis of the Hickory Sandstone resulted in only minor cementation (El-Jard 1982; McBride et al., 2002).

4.2a Variables and Data Collection Techniques

Gouge thickness is a quantitative continuous variable and was defined as the dependent variable. Thickness of gouge for most faults was readily measurable with the unaided eye via a ruler marked in 1 mm (0.04 in) increments. For thickness less than or equal to 1 mm (0.04 in), the thickness recorded was reported to the nearest 0.25 mm (0.01 in); for thickness greater than 1 mm (0.04 in), the thickness recorded was reported to the nearest 0.5 mm (0.02 in). Measures of thickness were obtained in close proximity to locations where displacement was measured. If a small fault exhibited variable gouge thickness along its length in core, an average gouge thickness was recorded. Thickness measurements were not taken in the vicinity of dip lines, because gouge thickness has a grossly enlarged apparent thickness at these locations in core.

Displacement was determined by offset of sedimentary structures and was considered a quantitative, independent variable. Slip striae on fault surfaces demonstrate that faults are nearly dip-slip (Fig. 14), so for displacement measurements the slip vector was assumed to be parallel to fault dip. A ruler marked in 1 mm (0.04 in) increments was used to measure displacement, which was reported to the nearest 0.5 mm (0.02 in).

Grain size also was defined as an independent variable and was the main textural variable quantified. In order to address the effect of grain size on gouge thickness, mean grain size of the protolith adjacent to a fault was determined and assigned to one of four grain size categories. Juxtaposition of lithologies with a different mean grain size across

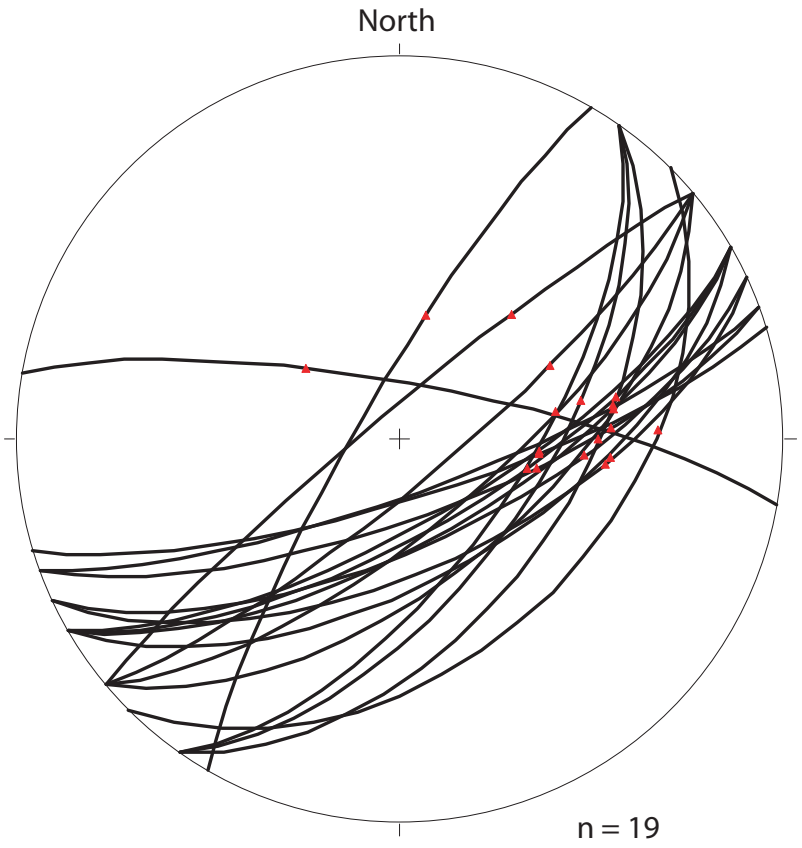

Fig. 14. Equal area, lower hemisphere stereonet projection of faults with observable fault striae. Red symbols represent fault striae orientation.

a small fault was of limited occurrence, since 99.8 % of the small faults analyzed have a displacement less than 8 cm (3.15 in) and 97.8 % of the faults have a thickness less than 4 mm (0.16 in), thus grain size measurement was limited to a single lithology. The mean grain size was determined using a 10x hand-lenses and a grain size comparative card. The four mean grain size categories correspond to the Wentworth's categories and are: 1) very coarse to coarse sand (2 - 0.5 mm), 2) medium sand (0.5 - 0.25 mm), 3) fine sand (0.25 - 0.0625 mm) and 4) mud (< 0.0625 mm).

Sorting is a qualitative independent variable that was explored in a preliminary fashion. A measure of sorting was not acquired for the protolith adjacent to a fault but was inferred by the stratigraphic position of the fault. Wilson (2001) observed that the sandstone in the Lower Hickory is more poorly sorted than that of the Middle Hickory, which reflects a difference in the depositional environment. Faults in the Lower Hickory were distinguished from faults in the Middle Hickory and assigned to a different sorting category.

4.2b Linear Regressions for Gouge Thickness Versus Displacement

A linear-linear scatterplot of gouge thickness versus displacement was used initially to assess the relationship between the two variables (Fig. 15). As seen with prior studies, small faults with a specific displacement exhibit a wide range of gouge thickness. A linear, least-square-fit regression was preformed and results in a correlation $R^2 = 0.431$, which indicates a weak relationship between the two variables. However, if mean gouge thicknesses for a given displacement only were considered, better correlations can be found because averaging inherently smooth statistical variability (Fig. 16).

Several approaches were available to seek better empirical correlations between displacement and thickness of gouge that did not require averaging of the data. One approach utilized a transformation of the data. The other incorporated additional independent variables together with transformations of the variable.

Frequency histograms of displacement and gouge thickness are not Gaussian but are markedly skewed to the right (Figs. 17a, 17c, 18a and 18c). The skewed distribution

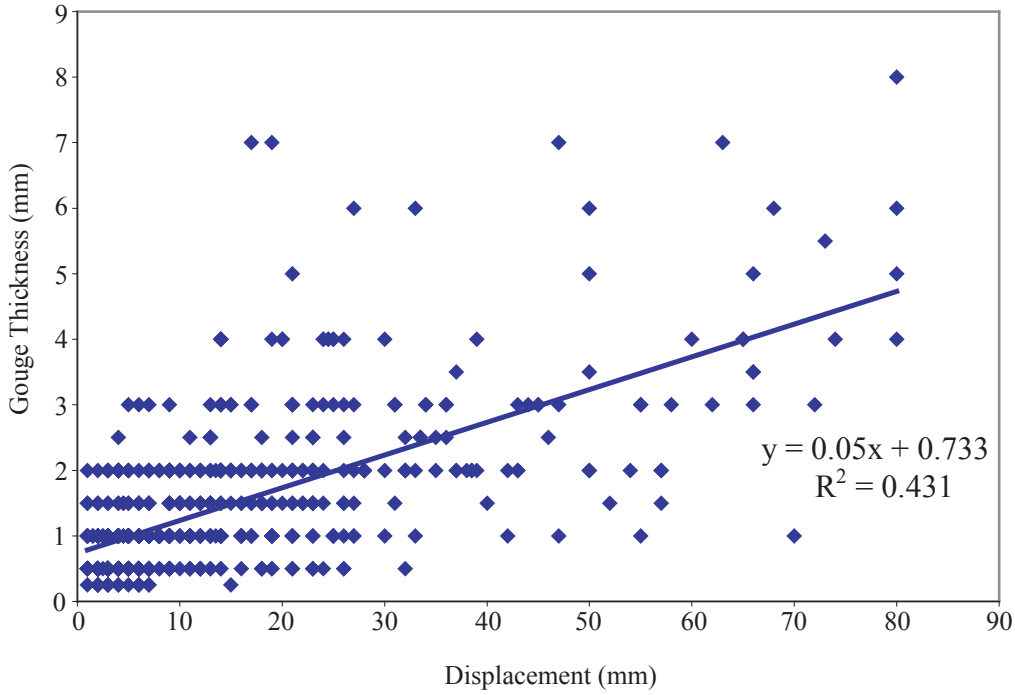

Fig.15. Scatterplot of gouge thickness versus displacement with linear least-square-fit regression line.

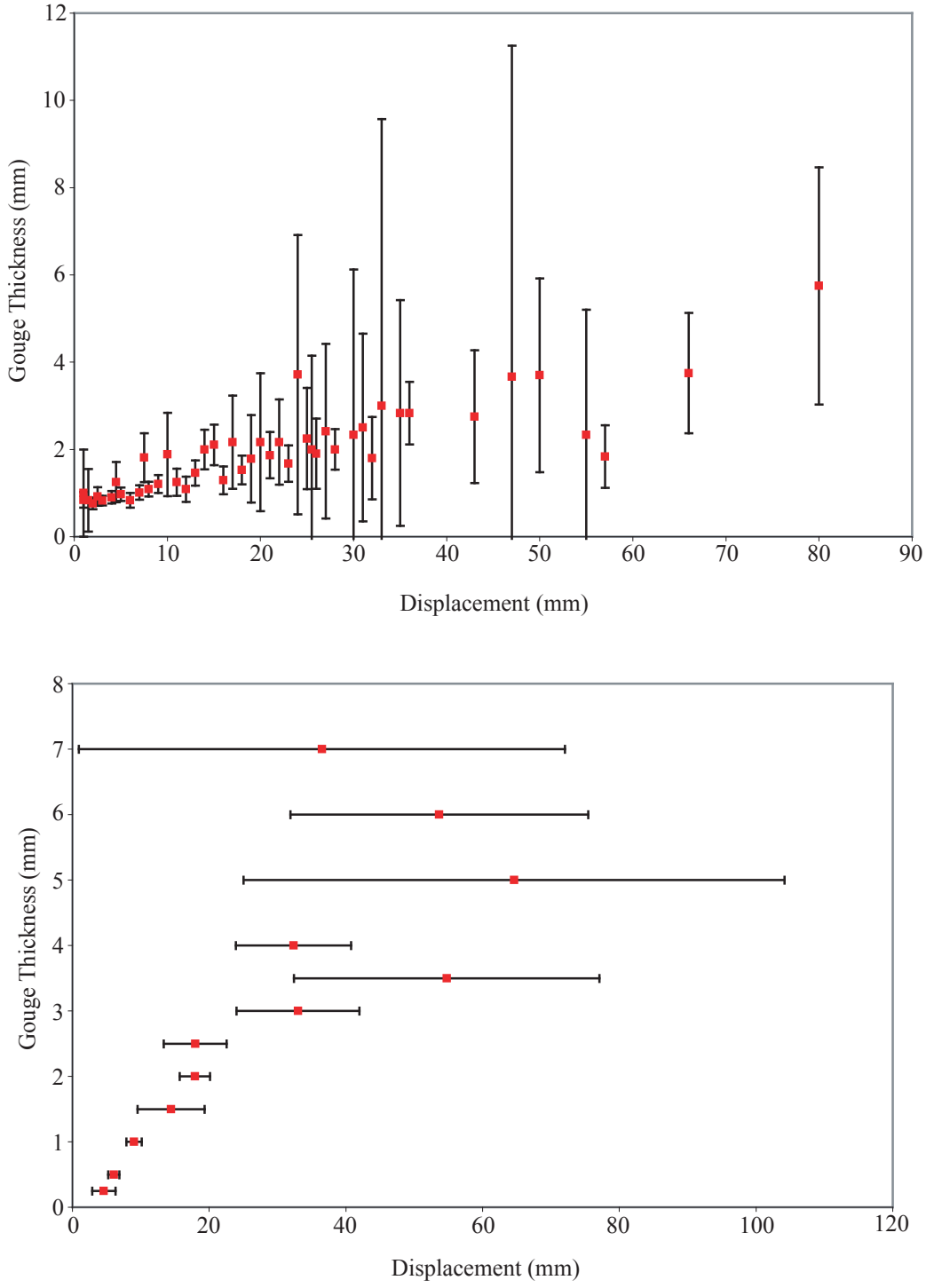

Fig. 16. Distributions of the mean gouge thickness for a given displacement amount and mean displacement for a given gouge thickness. Error bars represent 95% confidence intervals of mean.

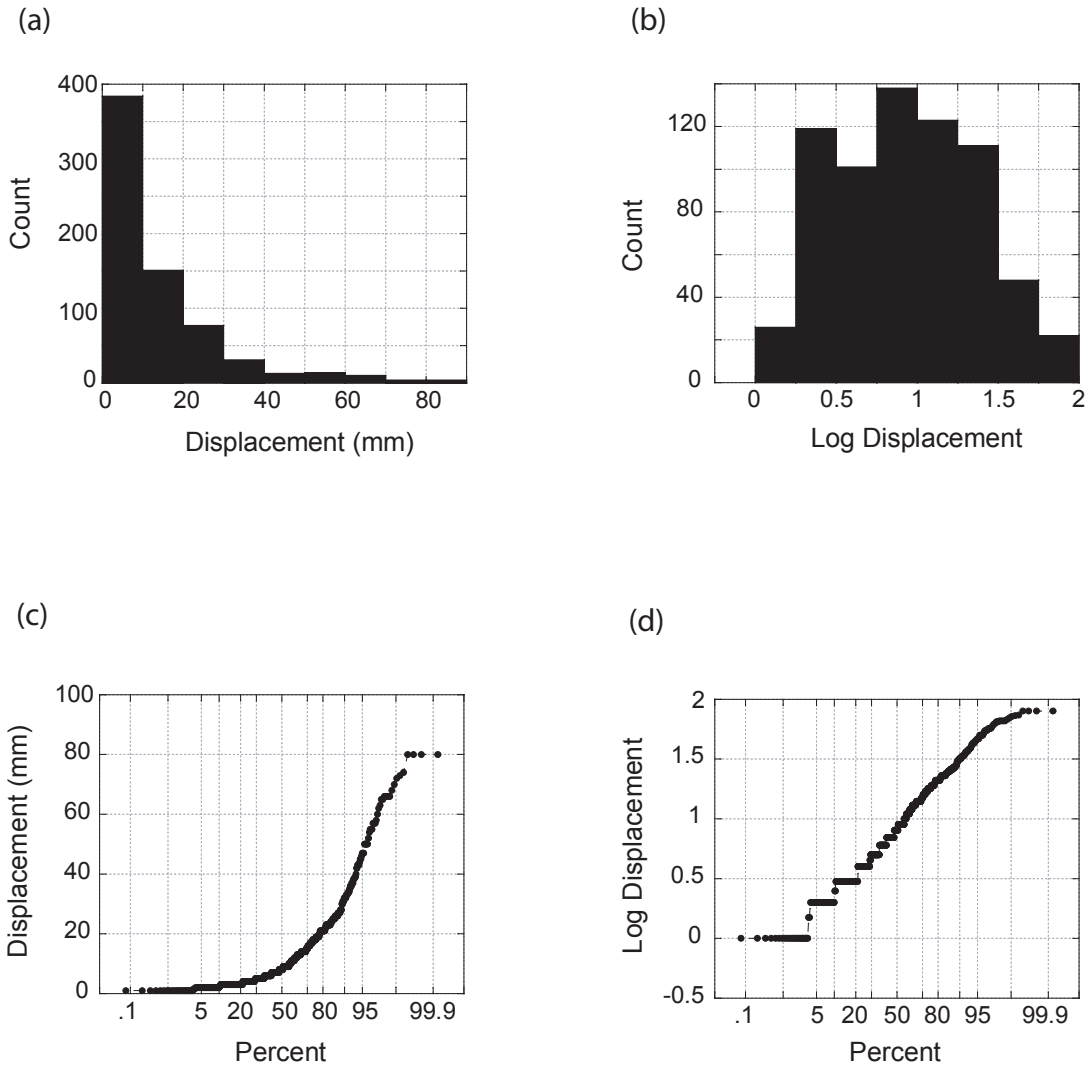

Fig. 17. Frequency and cumulative frequency plots of untransformed and logarithmically transformed displacement. (a) Frequency distribution of displacement; (b) frequency distribution of log displacement; (c) probability distribution function for displacement; and (d) probability distribution function for log displacement.

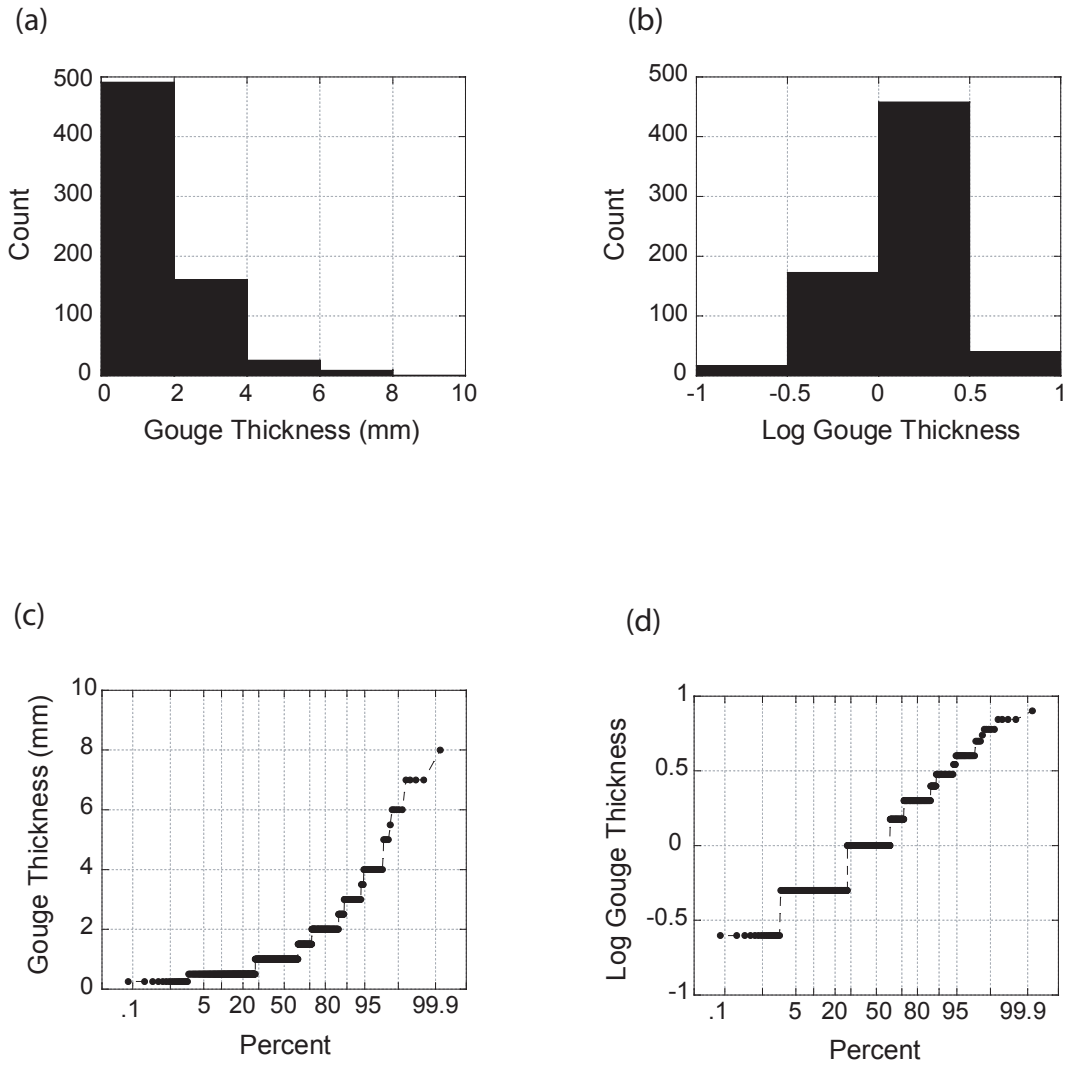

Fig. 18. Frequency and cumulative frequency plots of untransformed and logarithmically transformed gouge thickness. (a) Frequency distribution of gouge thickness; (b) frequency distribution of log gouge thickness; (c) probability distribution function for gouge thickness; and (d) probability distribution function for log gouge thickness.

toward small values is suggestive of a log-normal distribution. For such skewed distributions, conventional practice is to transform the variables via a log or ln function. A base 10, logarithmic transformation resulted in a more symmetric distribution (Figs. 17b, 17d, 18c and 18d), suggesting the data are approximately log-normal. Kurtosis values (Table 3) indicate that both transformed variables are not Gaussian and are sparser in the tails than a normal distribution. A linear least-square-fit regression on the two logarithmic transformed variable results in a correlation $R^2 = 0.376$, which is a weaker correlation than for linear regression on the untransformed data (Fig. 19a).

In lieu of a trial and error approach to correctly transform data to a Gaussian distribution, normal score transformations are commonly used in regression analysis. A normal score distribution is said to be achieved when the transformed data approximates the standard normal distribution (i.e. mean = 0 and variance = 1). A linear least-square-fits regression for the normal score of gouge thickness and displacement results in a correlation $R^2 = 0.492$ (Fig. 19b), which represents a stronger correlation than for the untransformed data. The premise behind normal score transformations is that if two variable have an interdependence and a normal distribution, then the relationship between the two variables is linear. Since normal transformations of gouge thickness and displacement still exhibit a weak relationship, one might infer that additional independent variables have yet to be identified.

4.2c Optimal Transformations

The conventional regression methods described above assume that the independent variable is error free and that the proper transformation function of the variables is identified. The following nonparametric method requires no prior knowledge of the functional form of the probability distribution function in order to obtain optimal transformations for correlations in the transformed space. The basis of this method involves an alternating conditional expectation (ACE) to derive the optimal transformations for the data (Breiman and Friedman, 1985) and is described briefly below following the presentation given by Breiman and Friedman (1985).

Table 3. Descriptive statistics for sample data (n = 692) of displacement, gouge thickness and corresponding log transforms.

	Mean	Standard Error	Median	Mode	Standard Deviation	Variance	Kurtosis	Skewness
Thickness	1.42	0.04	1	1	1.12	1.25	6.72	2.23
Log Thickness	0.05	0.01	0	0	0.3	0.09	-0.33	0.22
Displacement	13.77	0.57	8	3	15.03	225.94	6.22	2.29
Log Displacement	0.93	0.02	0.9	0.48	0.44	0.19	-0.56	0.04

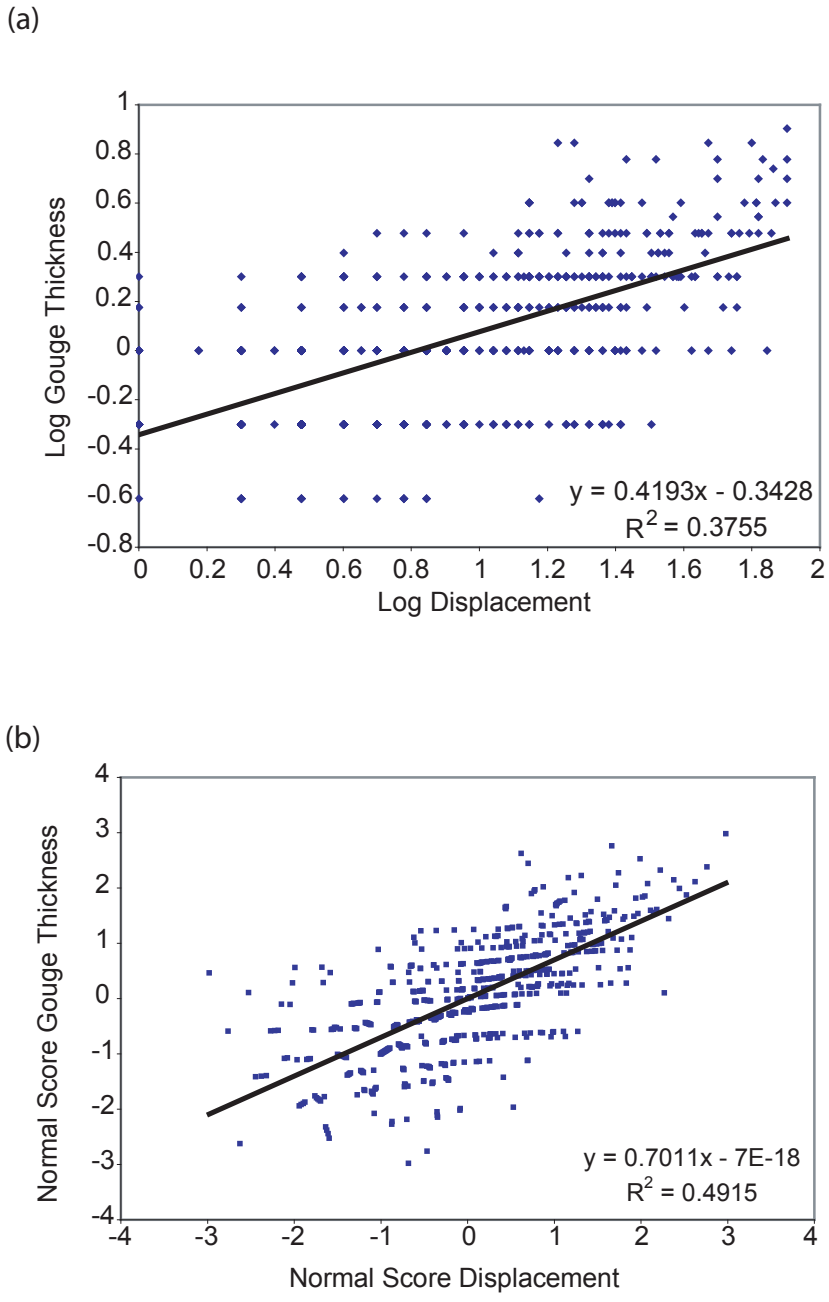

Fig. 19. Scatterplot of transformed gouge thickness versus transformed displacement with linear least-square-fit regressions. (a) Logarithmic transform; (b) normal score transform.

Let Y be the dependent random variable and $X_1,...,X_p$ be independent random variables. Also let $\theta(Y),\phi_1(X_1),....,\phi_p(X_p)$ be arbitrary mean-zero transforms. The error (e^2) that is not explained by a linear regression between the transformed dependent and sum of independent variables is:

$$e^2(\theta,\phi_1,....,\phi_p) = \frac{E\{[\theta(Y) - \sum_{i=1}^{p}\phi_i(X_i)]^2\}}{E\theta^2(Y)} \tag{7}$$

Transformations of $\theta^*(Y),\phi_1^*(X_1),....,\phi_p^*(X_p)$ are optimal if they satisfy the following:

$$e^{*2}(\theta^*,\phi_1^*,....,\phi_p^*) = \min_{\theta,\phi_1,....\phi_p} e^2(\theta,\phi_1,....,\phi_p) \tag{8}$$

Consider the bivariate case (p = 1) in which $E[\theta^2(Y)] = 1$ and the expectation of all functions is zero. Thus,

$$e^2(\theta,\phi) = E\{[\theta(Y) - \phi(X)]^2\} \tag{9}$$

The minimization of e^2 for $\phi(X)$ given $\theta(Y)$ is:

$$\phi(X) = E[\theta(Y) \mid X] \tag{10}$$

Conversely, the minimization of e^2 for $\theta(Y)$ given $\phi(X)$ is:

$$\theta(Y) = E[\phi(X) \mid Y / \left\|E[\phi(X) \mid Y]\right\| \tag{11}$$

When the data set is finite, the conditional expectation is replaced by a suitable estimate derived from a data smoothing process. The estimates of the optimal transformations are derived by a moving average in which the window is determined by local cross-validation. See Breiman and Friedman (1985) for further details concerning the smoothing process.

An ACE algorithm program supplied by Xue et al. (1997) was used to obtain optimal transformations of gouge thickness and displacement (Fig. 20). It is clear from the linear shape of the transformations that the conventional logarithmic transformation is unnecessary for this data set. Rather, it appears that transformation of the data set is unwarranted. This explains why the logarithmic transformation has a lower correlation

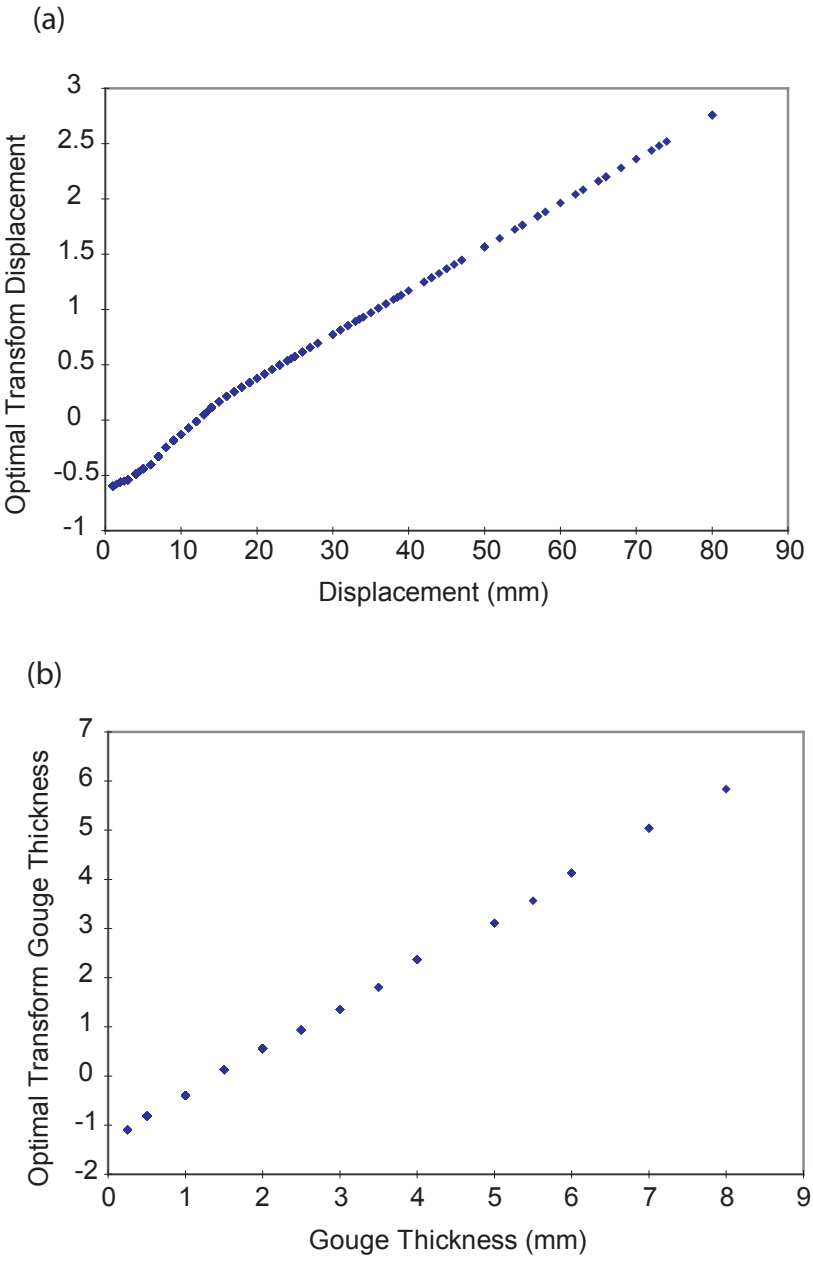

Fig. 20. Optimal transformations of gouge thickness and fault displacement using alternating conditional expectation. (a) Displacement versus optimally transformed displacement; and (b) gouge thickness versus optimally transformed gouge thickness.

than the untransformed data. A linear regression for optimal transformed gouge thickness and displacement results in a correlation $R^2 = 0.436$ (Fig. 21), which is similar to the correlation for untransformed data.

As shown above only a weak relationship exists between the sole independent variable, displacement and dependent variable, gouge thickness. The scatter in the data cannot reflect solely uncertainty in displacement. Instead, the weak correlation suggests that one or more independent variables influence the thickness of gouge developed for a given displacement. As noted earlier, grain size, grain sorting, porosity and effective mean pressure are additional factors that appear to qualitatively influence gouge thickness.

A multiple parameter regression method was used to seek an improved relationship that incorporates the influence of mean grain size and sorting. Since sorting and grain size are categorical predictor variables and assumptions of linearly responsiveness with gouge thickness is unwarranted, they were treated as indicator variables taking on a numerical value of 1 or 0. A conventional multiple parameter linear regression method results in a correlation $R^2 = 0.538$, for the dependent variable gouge thickness and independent variables displacement, grain size and sorting. Using ACE to generate optimal transformations for the same variables results in an improved correlation $R^2 = 0.592$ (Figs. 22 and 23).

Incorporation of grain size and sorting of the protolith strengths the predictability of gouge thickness amount as compared to using only displacement as the sole independent variable. Comparisons between the correlation coefficient for a single predictor variable (displacement) and multiple predictor variables (displacement, grain size and sorting) indicate that displacement is the dominant predictor variable. In order to assess the individual contribution that grain size and sorting have on the predicted gouge thickness amount, the ACE method was performed using one dependent variable at a time. The regression between gouge thickness and grain size results in $R^2 = 0.230$, while the regression between gouge thickness and sorting have a correlation $R^2 = 0.096$.

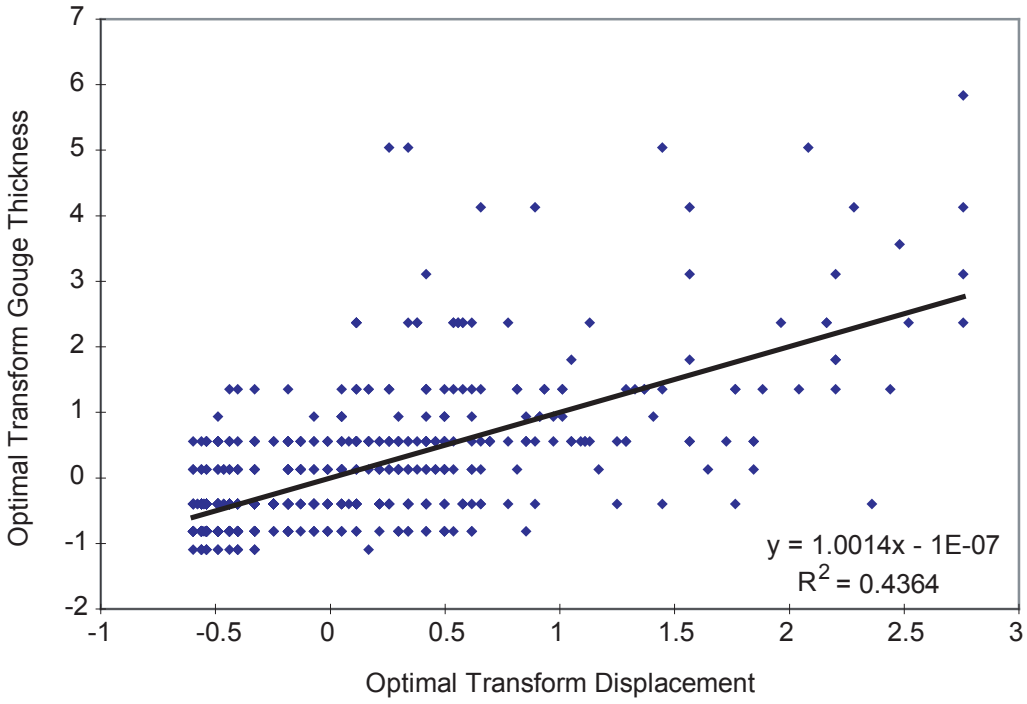

Fig. 21. Scatterplot of optimally transformed gouge thickness versus optimally transformed displacement with linear least-square-fit regression.

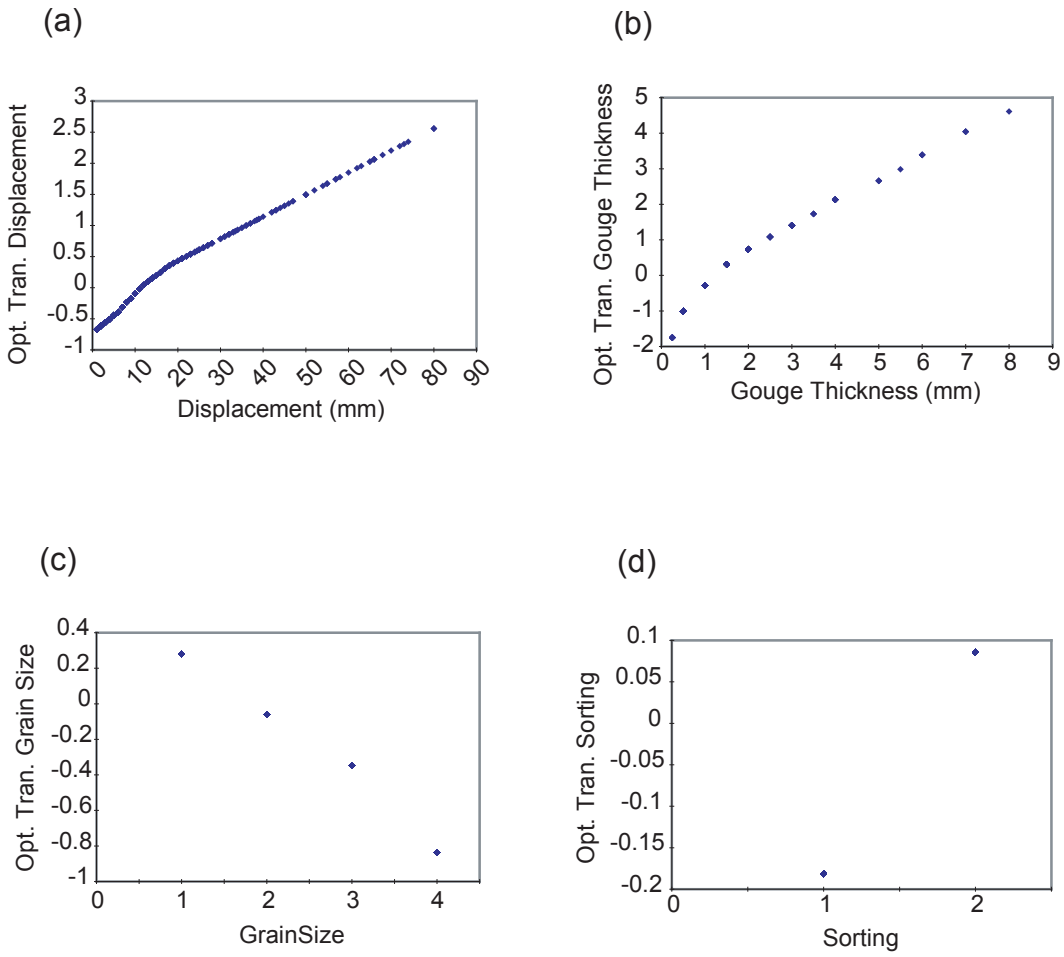

Fig. 22. Optimal transformations for multivariant case (gouge thickness, displacement, grain size & sorting) using alternating conditional expectation method. (a) Displacement versus optimally transformed displacement; (b) gouge thickness versus optimally transformed gouge thickness; (c) grain size (1 = coarse, 2 = medium, 3 = fine and 4 = mud) versus optimally transformed grain size; and (d) sorting (1 = Lower Middle Hickory and 2 = Lower Hickory) versus optimally transformed sorting.

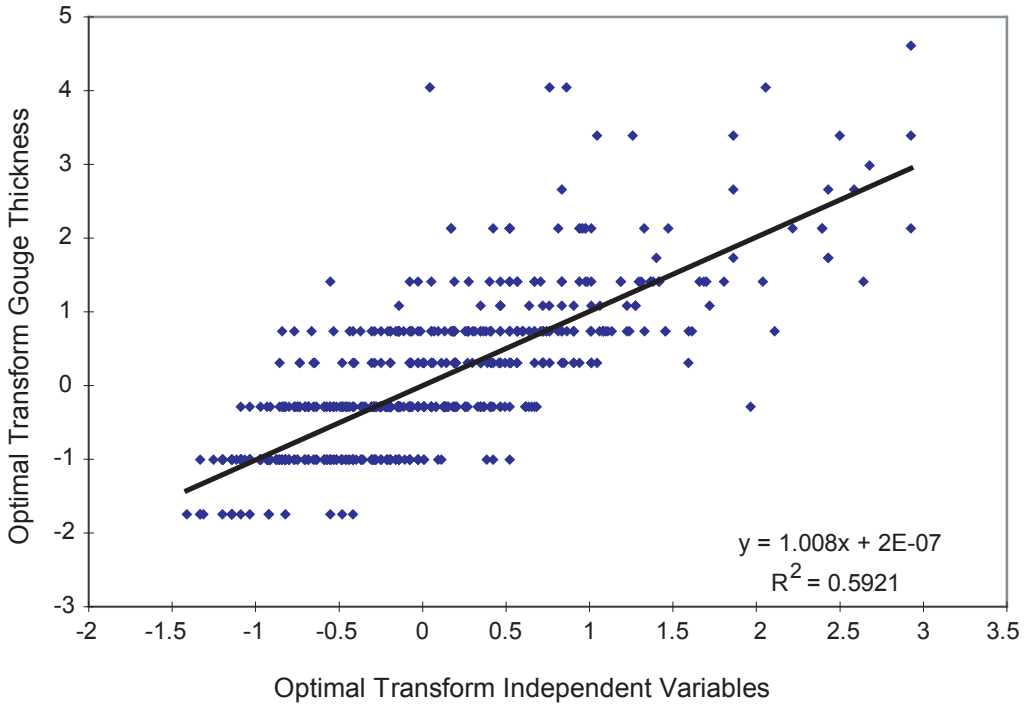

Fig. 23. Scatterplot of optimally transformed gouge thickness versus sum of optimally transformed independent variables (displacement, grain size & sorting) with linear least-square-fit regression.

Theses results indicate that grain size has the second largest contribution in determining gouge thickness, while sorting contributes very little to explaining the variability.

Some words of caution are warranted about interpretations of the population based on the optimal transformation of the sample data. It is unclear if the optimally transformed functional forms of the samples truly represent the functional forms of the populations or are a consequence of the variability within the samples, because not all relevant variables have been identified. Many field studies, including Shipton and Cowie (2001) have shown that inherent variability of the shear zone exists along the fault trace. Child et al. (1996) and Shafer (2002) have shown that this variability is associated with fault segmentation. This fault architecture could contribute to the limited linear correlation established for displacement, mean grain size and sorting to the dependent gouge thickness. Such an effect has not been incorporated into the current study.

4.2d Mean Displacement Analysis

In order to validate the results from ACE, probabilities of mean displacements were calculated. Data were sorted into the four grain size categories and the distributions of displacement at 1 mm gouge thickness were computed. The 1 mm (0.04 in) gouge thickness was chosen because the number (power) of displacement values for all four grain sizes (Table 4) were sufficient to discriminate between differences in the mean displacement of each sample, thusly eliminating the potentially of a type II error (rejection of the null hypothesis when false) at the 95 % confidence level.

Gouge thickness and displacement were transformed logarithmically to approximate a normal distribution in order to use parametric analysis techniques. In order to formally test for a difference between the mean displacement of each grain size, independent t-tests were used. Even thought most samples have similar variance, the sample sizes are unequal. Consequently, the pooled variance method was not used. Instead, the more robust Welch-Satterthwaite (Tamhane and Dunlop, 2000) method of separate variance was used. A significance level of 0.05 was used for a cut-off point for the null hypothesis to be ruled out. For the 1 mm gouge thickness, the mean

Table 4. Summary statistics for ln displacement of all four grain sizes for a given gouge thickness.

Grain Size	Ln Gouge Thickness	Count	Mean Ln Displacement	95% Confidence Interval	Standard Error	Min	Median	Max	Variance	Standard Deviation	Kurtosis	Skewness
Coarse	-0.693	36	1.154	0.954 to 1.354	0.099	0.000	1.099	2.639	0.349	0.591	0.415	-0.240
Coarse	0.000	126	1.614	1.497 to 1.732	0.059	0.000	1.701	3.332	0.441	0.664	-0.408	-0.355
Coarse	0.405	47	2.354	2.151 to 2.558	0.101	0.000	2.485	3.296	0.481	0.694	2.053	-1.264
Coarse	0.693	68	2.547	2.350 to 2.744	0.099	0.000	2.674	4.043	0.660	0.813	0.511	-0.733
Coarse	0.916	15	2.988	2.644 to 3.331	0.160	1.386	3.135	3.829	0.385	0.620	1.881	-1.154
Coarse	1.099	27	3.135	2.823 to 3.447	0.152	1.609	3.178	5.193	0.623	0.789	0.705	0.246
Coarse	1.253	4	3.976	3.536 to 4.415	0.138	3.611	4.051	4.190	0.076	0.276	-0.937	-0.922
Coarse	1.386	16	3.343	3.028 to 3.659	0.148	2.639	3.209	4.382	0.350	0.591	-0.912	0.482
Coarse	1.609	3	3.715	2.231 to 5.199	0.345	3.045	3.912	4.190	0.357	0.597		-1.321
Coarse	1.792	5	3.861	3.287 to 4.435	0.207	3.296	3.912	4.382	0.214	0.462	-2.255	-0.176
Coarse	1.946	2	3.544		0.599	2.944	3.544	4.143	0.718	0.848		
Mud	-1.386	5	1.898	1.187 to 2.609	0.256	1.099	1.946	2.708	0.328	0.573	1.763	0.043
Mud	-0.693	21	2.621	2.388 to 2.854	0.112	1.609	2.565	3.466	0.262	0.512	-0.939	-0.199
Mud	0.000	8	3.304	2.960 to 3.648	0.145	2.833	3.177	4.007	0.169	0.411	-0.197	1.004
Mud	0.405	2	3.866		0.177	3.689	3.866	4.043	0.063	0.250		
Mud	0.693	4	3.578	2.749 to 4.406	0.260	2.890	3.689	4.043	0.271	0.521	-0.673	-0.889
Mud	1.099	2	3.617		0.573	3.045	3.617	4.190	0.656	0.810		

Table 4 Continued

Fine	-1.386	10	0.994	0.595 to 1.393	0.176	0.000	0.896	1.792	0.311	0.558	-0.180	-0.010
Fine	-0.693	80	1.415	1.245 to 1.585	0.085	0.000	1.386	4.143	0.584	0.764	1.580	0.678
Fine	0.000	40	2.237	1.972 to 2.502	0.131	0.000	2.197	3.738	0.687	0.829	-0.203	-0.272
Fine	0.405	3	1.600	1.187 to 2.013	0.096	1.504	1.504	1.792	0.028	0.166		1.732
Fine	0.693	12	2.833	2.376 to 3.291	0.208	1.386	2.943	3.989	0.518	0.720	0.271	-0.542
Fine	1.099	4	3.638	2.975 to 4.300	0.208	3.135	3.644	4.127	0.173	0.416	-0.003	-0.080
Fine	1.386	2	2.996		0.000	2.996	2.996	2.996	0.000	0.000	0.000	0.000
Fine	1.946	2	3.342		0.508	2.833	3.342	3.850	0.517	0.719		
Medium	-1.386	2	1.498		0.112	1.386	1.498	1.609	0.025	0.158		
Medium	-0.693	38	1.441	1.211 to 1.671	0.114	0.000	1.609	2.944	0.490	0.700	0.192	-0.187
Medium	0.000	59	1.923	1.708 to 2.139	0.108	0.000	1.946	4.248	0.685	0.827	0.259	-0.060
Medium	0.405	19	2.534	2.069 to 2.999	0.221	0.000	2.890	3.951	0.932	0.965	1.782	-1.349
Medium	0.693	21	2.778	2.438 to 3.119	0.163	1.099	2.639	3.761	0.559	0.748	-0.387	-0.436
Medium	1.099	4	3.803	3.247 to 4.360	0.175	3.296	3.929	4.060	0.122	0.350	2.604	-1.637
Medium	1.386	2	3.173		0.228	2.944	3.173	3.401	0.104	0.323		

displacement associated with all four grain sizes was statistically significant which allows one to conclude that the samples come from different populations (Table 5). The test was repeated using the non-parametric Mann-Whitney U-test (Tamhane and Dunlop, 2000) in order to insure that the probabilities generated via the independent t-test are not underestimated due to departures from normality, especially at the tails. A significance level of 0.05 was used and all tests were determined also to be statistically significant (Table 6).

4.3 Estimating Fault Displacement Using Gouge Thickness and Protolith Textural Data

Only approximately half of the small faults observed in the core cut passive markers that allowed direct measurement of fault displacement. In subsequent analysis of fault in core, it was desired to weight faults by their displacement. Faults without a direct measure of displacement were assigned an estimate of displacement based on the observed relationship between gouge thickness, displacement, mean grain size and sorting as explored in the prior section. The assigned estimate also contained statistical variability approximately similar to that of faults with known displacement.

The first step was to find the best correlation between fault displacement, now treated as a dependent variable and the independent variables of gouge thickness, mean grain size and sorting using the ACE algorithm. The multivariante regression using ACE resulted in a correlation $R^2 = 0.536$ (Fig. 24).

Since significant unaccounted variability is inherent within the data set, a random number generator was used to simulate this variability when calculating the estimated displacement. The difference between the data values and the corresponding fitted values from the best-fit regression line, referred to as residuals, was calculated to check the model assumption of constant variance. Examination of the optimal transformed displacement residuals versus sum of optimal transformed independent variables (Fig. 25) shows that constant variance does not exist for the entire range of independent variables. Instead, it appears that the variance is proportional to the mean. The distribution for a given sum of optimally transformed independent variables is skewed, especially for low values. Thus, a log-normal random number generator was used for

Table 5. Results of parametric independent Welch-Satterthwaite T-test for distribution of Ln displacement with 1 mm gouge thickness.

Alternative hypothesis	Difference between means	95% CI	T statistic	1-tailed p	Statistical Power	Degrees of Freedom	Effect Size	Cohen's d
coarse ≤ Medium	-0.309	−∞ to -0.105	-2.51	0.0068	80.70%	94.31	0.2502	-0.5169
coarse ≤ Fine	-0.623	−∞ to -0.382	-4.33	<0.0001	99.60%	55.81	0.5014	-1.1592
coarse ≤ Clay	-1.689	−∞ to -1.403	-10.76	<0.0001	100%	9.49	0.9613	-6.9856
Medium ≤ Fine	-0.314	−∞ to -0.032	-1.85	0.0338	58.20%	83.8	0.19808	-0.4041
Medium ≤ Clay	-1.380	−∞ to -1.065	-7.63	<0.0001	100%	16.19	0.8845	-3.7925
Fine ≤ Clay	-1.066	−∞ to -0.729	-5.45	<0.0001	100%	20.54	0.76888	-2.405

Table 6. Results of nonparametric Mann-Whitney U-test for distribution of Ln displacement with 1 mm gouge thickness.

Alternative hypothesis	GrainSize	n	Rank sum	Mean rank	U	Difference between medians	95% CI	Mann-Whitney U statistic	1-tailed p
coarse ≤ Medium	**Coarse**	-8	1840.5	129.04	1132.5	-0.288	−∞ to -0.118	4578.5	0.0054
	Medium	-75	-2667.5	150.48	-590.5				
coarse ≤ Fine	**Coarse**	-46	-596.5	146.16	-724.5	-0.606	−∞ to -0.405	3601.5	<0.0001
	Fine	-132	-5614.5	181.78	-2887.5				
coarse ≤ Clay	**Coarse**	-110	-5914.5	197.37	-1006.5	-1.658	−∞ to -1.253	1007.5	<0.0001
	Clay	-228	-12872.5	264.30	-2013.5				
Medium ≤ Fine	**Medium**	21	1804.5	66.84	425.5	-0.336	−∞ to 0	1431.5	0.0362
	Fine	2	1357.5	77.39	-77.5				
Medium ≤ Clay	**Medium**	-43	-820.0	91.13	-406.0	-1.344	−∞ to -0.916	450	<0.0001
	Clay	-94	-2126.0	121.50	-834.0				
Fine ≤ Clay	**Fine**	-24	-241.5	56.26	-186.5	-1.063	−∞ to -0.631	275.5	0.0007
	Clay	-56	-794.5	73.59	-417.5				

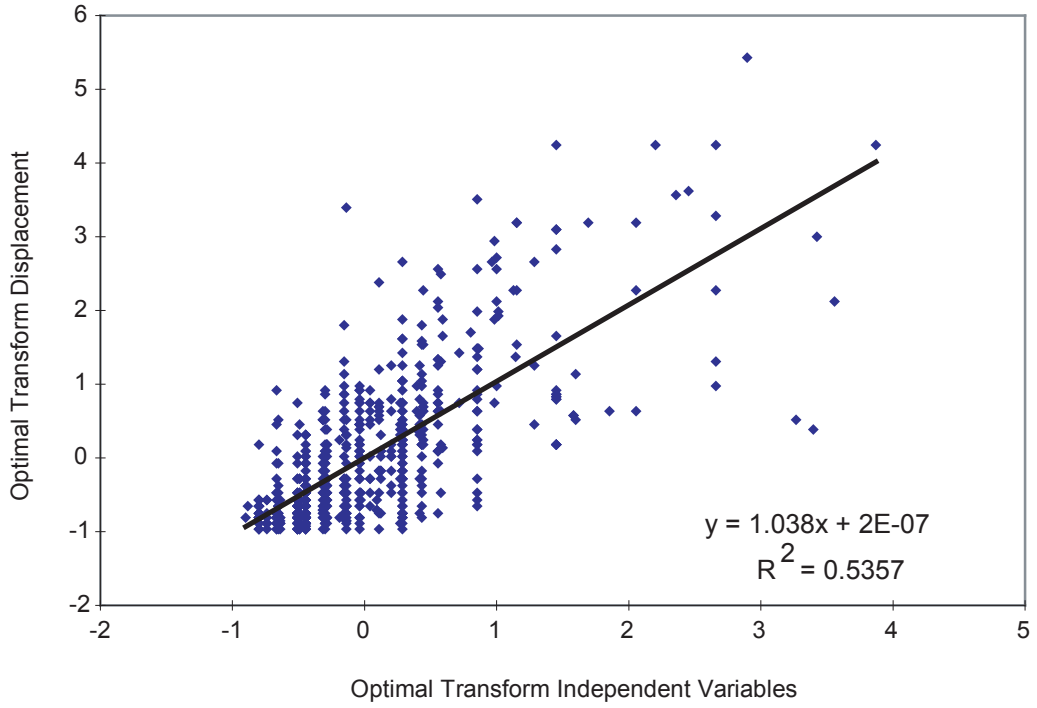

Fig. 24. Scatterplot of optimally transformed displacement versus sum of optimally transformed independent variables (gouge thickness, grain size & sorting) with linear least-square-fit regression.

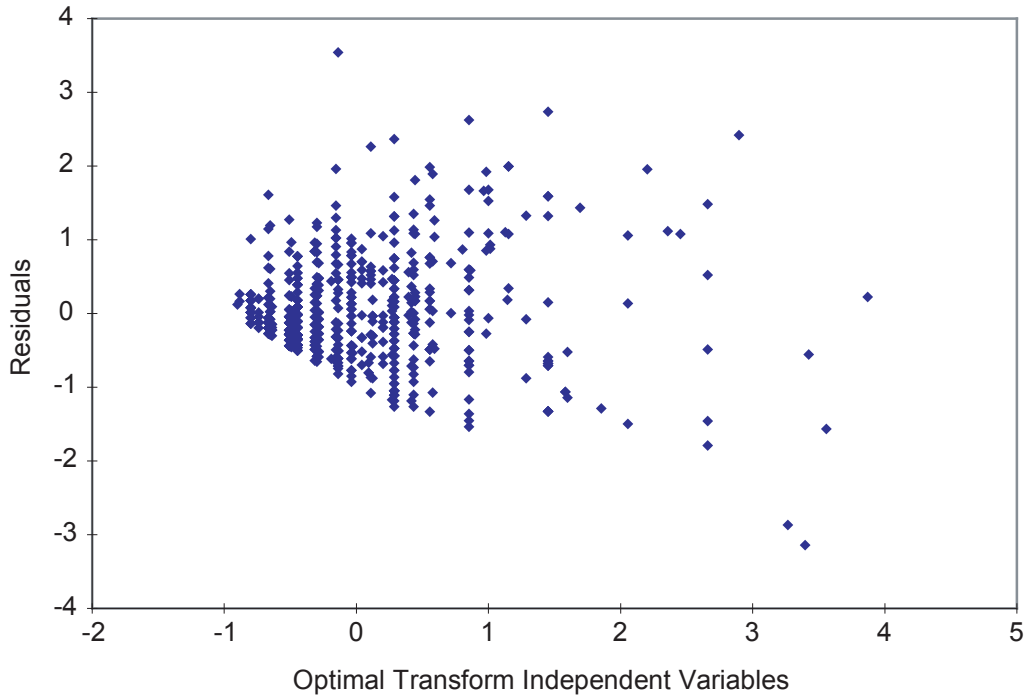

Fig. 25. Scatterplot of residuals (difference between best fit value and data value) versus sum of optimally transformed independent variables (gouge thickness, grain size and sorting) in which variance is proportional to mean.

faults that have up to 1 mm (0.04 in) of gouge thickness, whereas a Gaussian random number generator was used for faults that have gouge thickness greater than 1mm.

Figure 26 and Table 7 provide a comparison of measured fault displacement and estimated displacement as a function of gouge thickness. The estimated displacement values at large gouge thickness values tend to be underestimated and the variance of the estimated population is less than that of the known population. Though the two data sets are not truly identical, they are similar enough that the procedure used to produce an estimated displacement using measured gouge thickness produced an acceptable estimated population that is similar in most respects to that of measured displacement population.

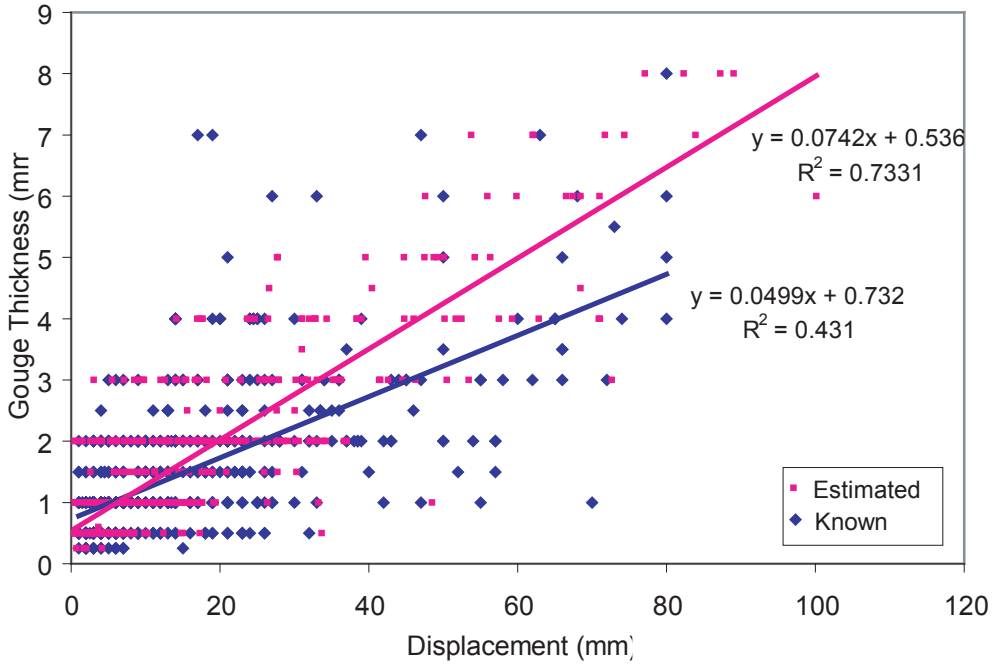

Fig. 26. Combined scatterplot of faults with known gouge thickness versus known displacement and faults with known gouge thickness versus estimated displacement.

Table 7. Descriptive statistics for estimated and know displacements for a given gouge thickness.

		Displacement (mm)			
		Mean	Confidence Level (95.0%)	Standard Deviation	Sample Variance
0.5 mm Gouge Thickness	Known	6.14	0.86	5.72	32.69
	Estimated	4.83	0.80	4.15	17.21
1 mm Gouge Thickness	Known	9.00	1.13	8.71	75.82
	Estimated	9.10	0.65	4.93	24.29
1.5 mm Gouge Thickness	Known	14.67	2.49	10.44	108.94
	Estimated	13.73	2.50	6.58	43.26
2 mm Gouge Thickness	Known	18.81	2.53	13.06	170.48
	Estimated	17.01	1.78	9.31	86.70
3 mm Gouge Thickness	Known	30.94	6.12	18.07	326.68
	Estimated	26.74	4.26	14.34	205.66
4 mm Gouge Thickness	Known	33.38	9.75	21.41	458.52
	Estimated	38.37	6.27	16.18	261.83
> 4mm Gouge Thickness	Known	51.60	12.95	23.39	546.97
	Estimated	60.06	6.78	18.49	341.88

5. RESULTS

The data recorded from core are presented in strip maps with complementary measurements (Appendix A) and the spreadsheet data table (Appendix B). A total of 1873 fault elements with subsidiary information and measurements as well as 569 bedding features were recorded from the boreholes GKR-5, NNR-3, 4, 7, 8, 9 and 10. The data are presented in several graphical formats that facilitate their visualization. Displacement amounts are reported in metric units, whereas the depths within the boreholes are reported in English units. The use of English units for length and depth are for pragmatic purposes. Coring was done with a 10 ft (3.05 m) core barrel and core was initially marked in 1 ft (0.3 m) increments.

5.1 Spatial Distribution of Small Faults

Each borehole is a vertical transect that provides a random sample of the fault population intersected. Three quantitative measures are used to capture the spatial attributes of small faults: 1) frequency of small faults per 1 ft, 2) cumulative displacement of small faults per 1 ft, and 3) average displacement of small faults per 1 ft. Figures 27 - 33 show the spatial distribution of these measures in all boreholes used in this study. Faults with intermediate and large displacement also are shown and highlighted in order to facilitate preliminary assessment of spatial associations with small faults.

Three measures of fault occurrence are used and represent 1-D “density” measures. A frequency measure (fault number density) is defined as number of faults per foot of core. For this measure, all faults, irrespective of their displacement are weighted equal. This is a common measure used in prior studies. In the case of Mode I cracks, it seems to be the logical measure that most closely reflects the local intensity of deformation. In the case of faults, however it is not necessarily an obvious measure of the inelastic deformation associated with the faults since no accounting of shear displacement is directly incorporated in the measure. In fact, solely using a frequency measure is at best a crude method for addressing the mechanical significance of smaller

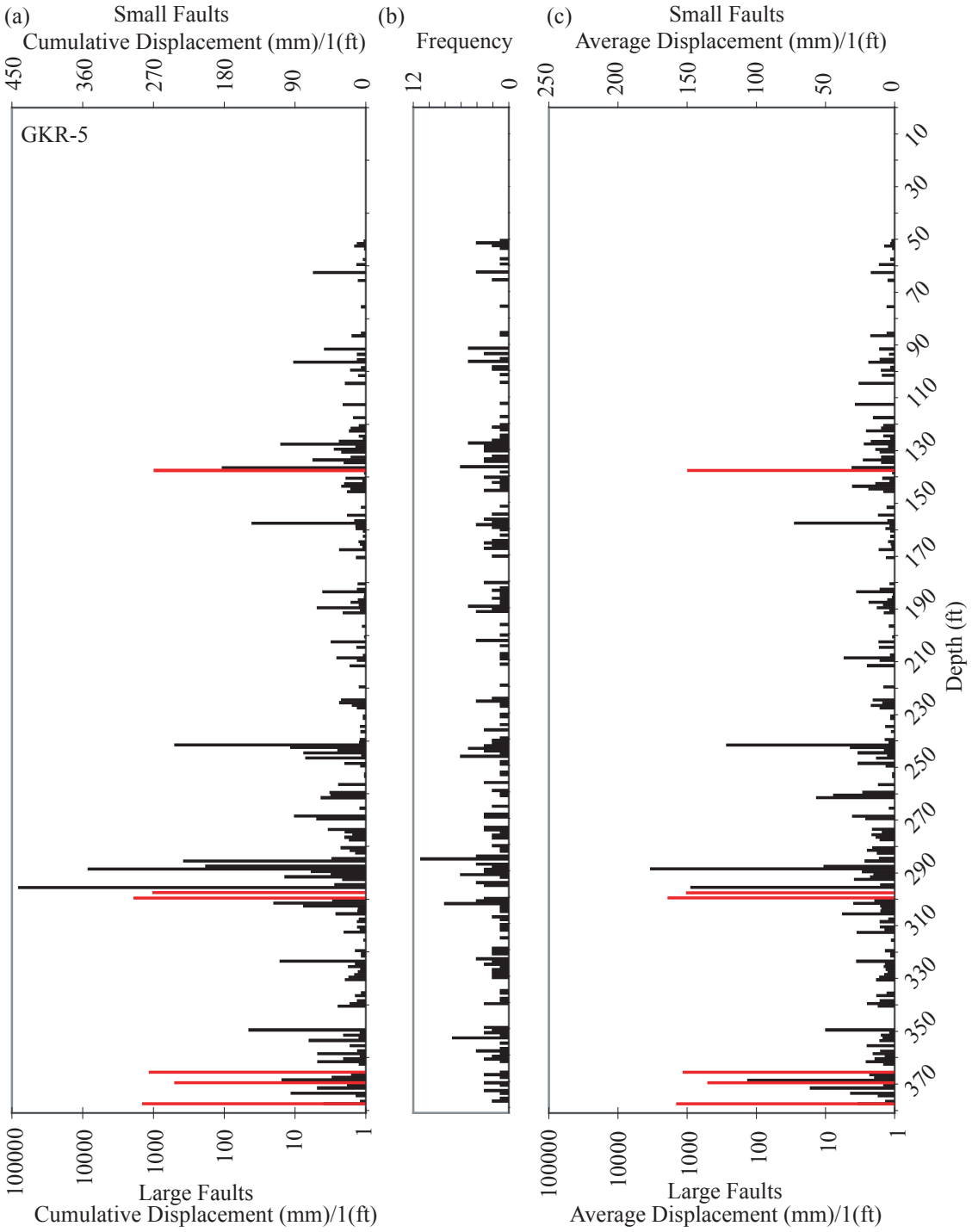

Fig. 27. Borehole GKR-5: vertical distribution of small faults shown using three 1-D "density" measures. (a) Cumulative displacement (mm) of all faults per foot; (b) number of small faults per foot; (c) average displacement (mm) of all faults per foot. Small fault measures (black) have a linear scale (top), whereas large faults (red) have a log scale (bottom).

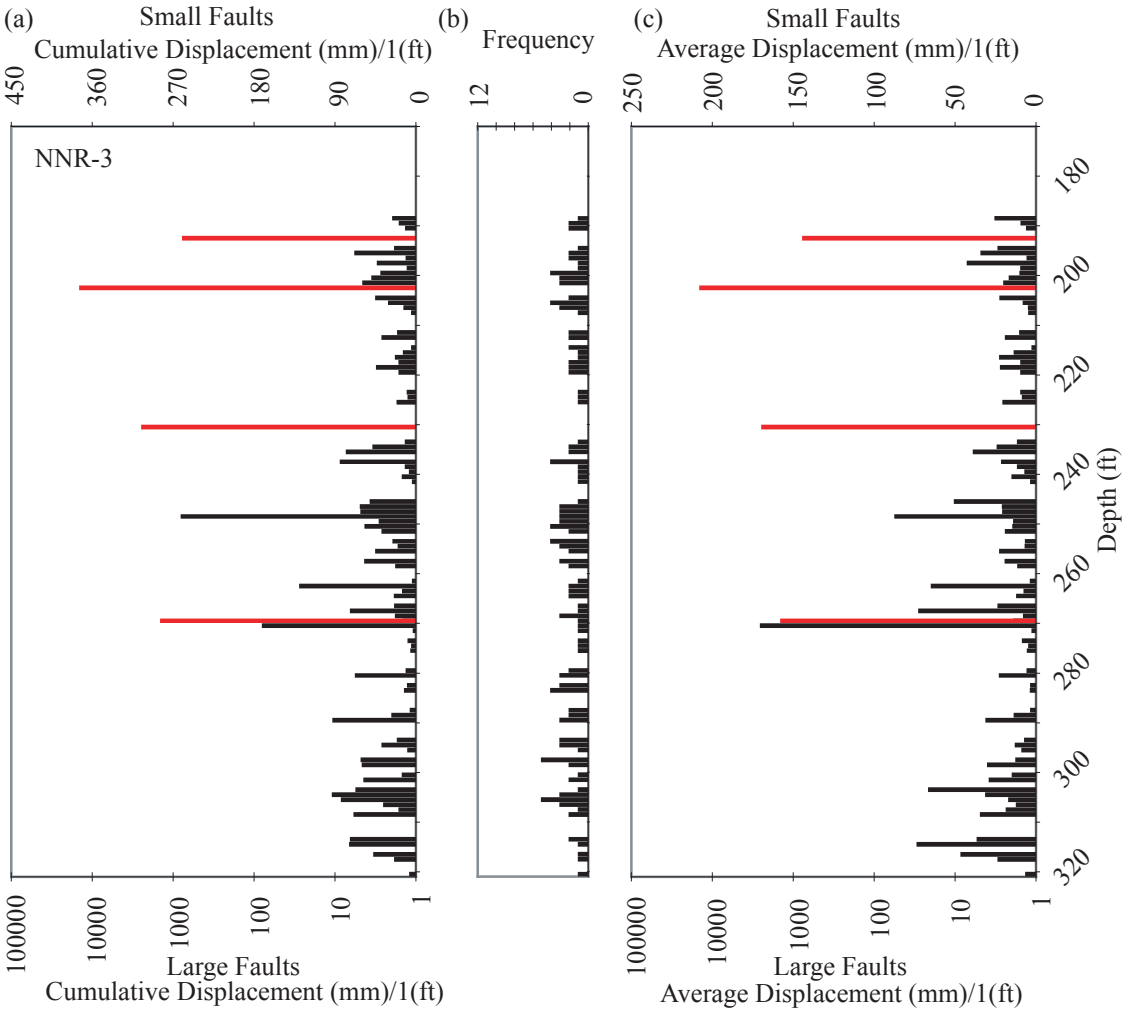

Fig. 28. Borehole NNR-3: vertical distribution of small faults shown using three 1-D "density" measures. (a) Cumulative displacement (mm) of all faults per foot; (b) number of small faults per foot; (c) average displacement (mm) of all faults per foot. Small fault measures (black) have a linear scale (top), whereas large faults (red) have a log scale (bottom).

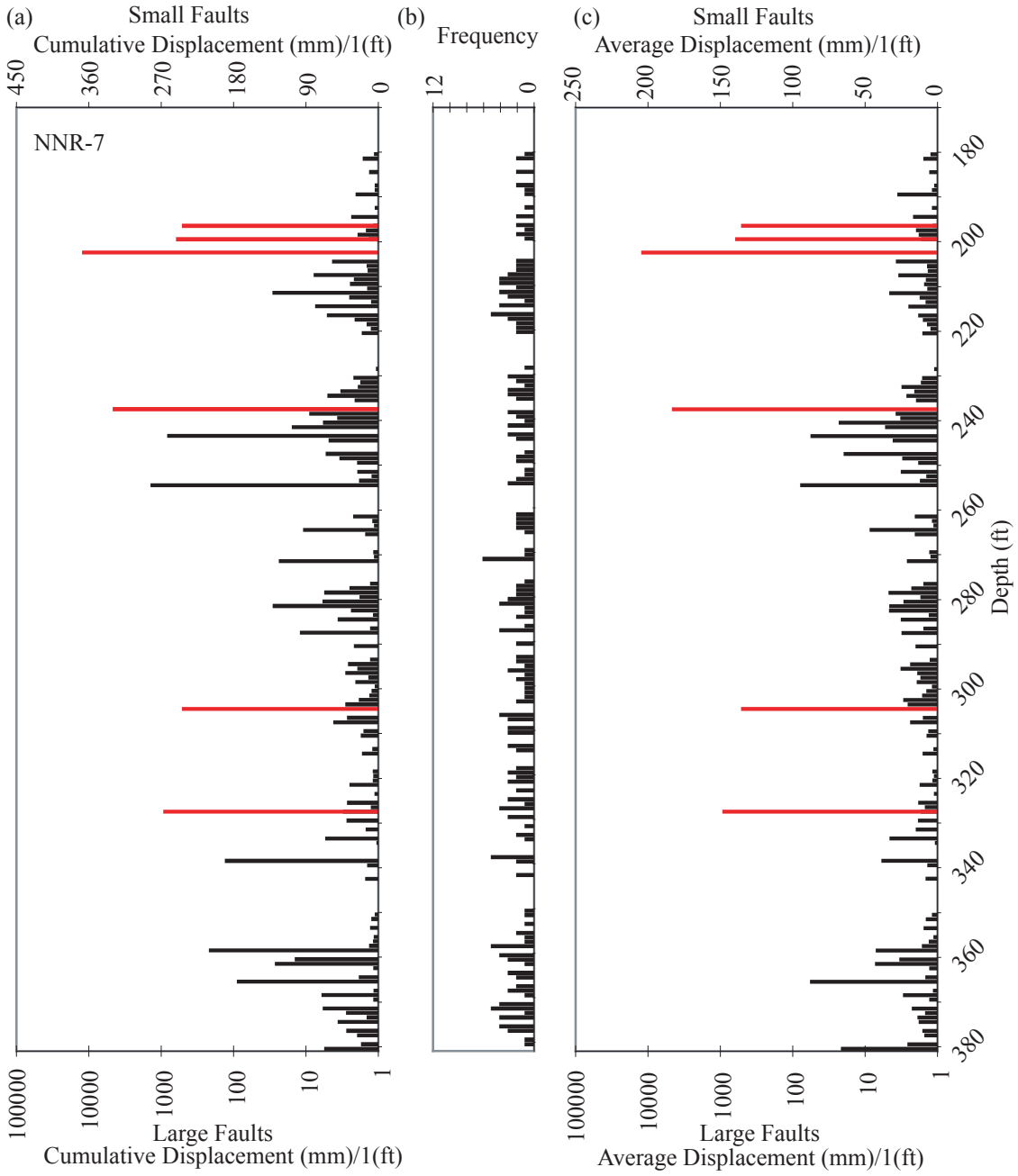

Fig. 29. Borehole NNR-7: vertical distribution of small faults shown using three 1-D "density" measures. (a) Cumulative displacement (mm) of all faults per foot; (b) number of small faults per foot; (c) average displacement (mm) of all faults per foot. Small fault measures (black) have a linear scale (top), whereas large faults (red) have a log scale (bottom).

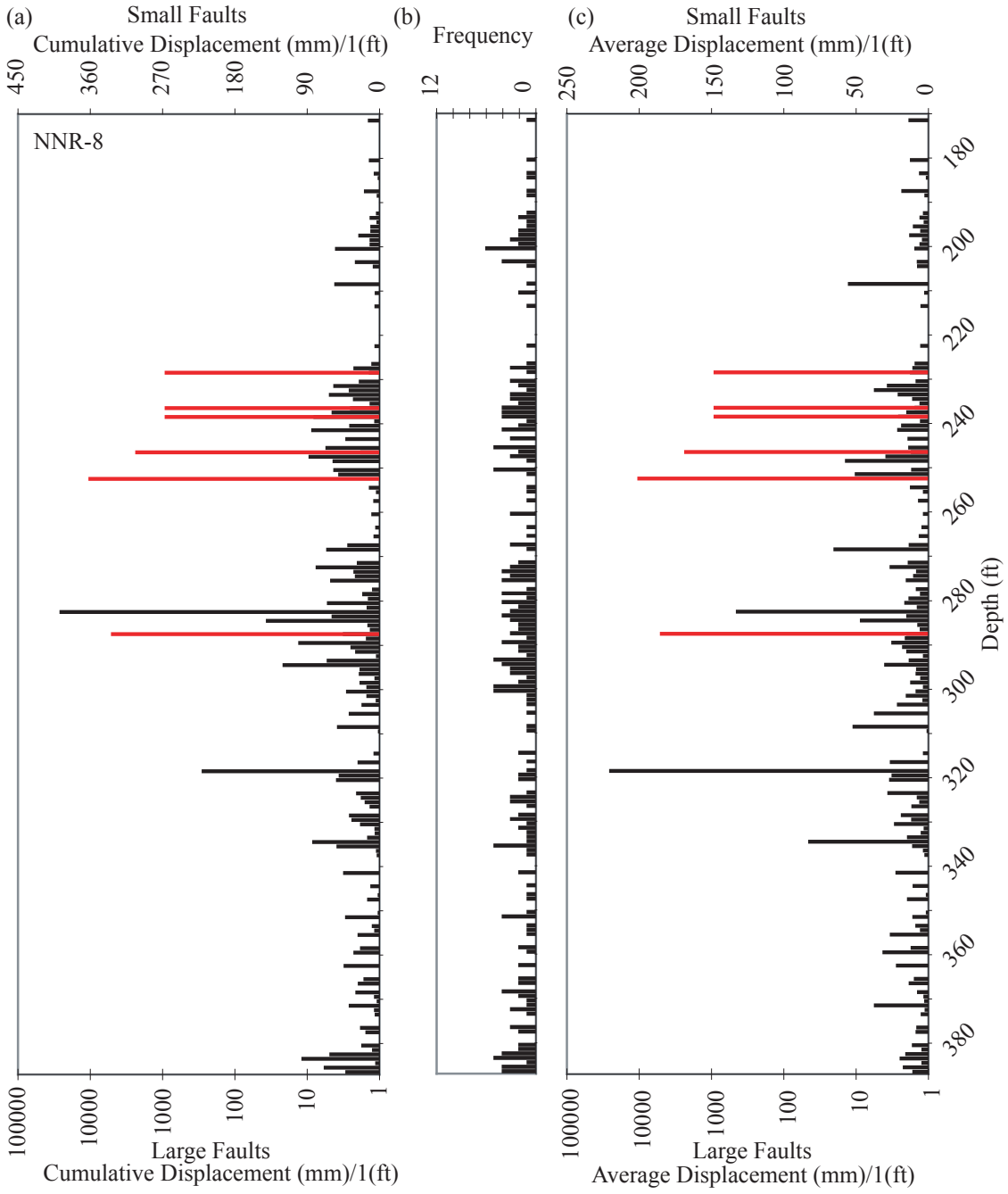

Fig. 30. Borehole NNR-8: vertical distribution of small faults shown using three 1-D "density" measures. (a) Cumulative displacement (mm) of all faults per foot; (b) number of small faults per foot; (c) average displacement (mm) of all faults per foot. Small fault measures (black) have a linear scale (top), whereas large faults (red) have a log scale (bottom).

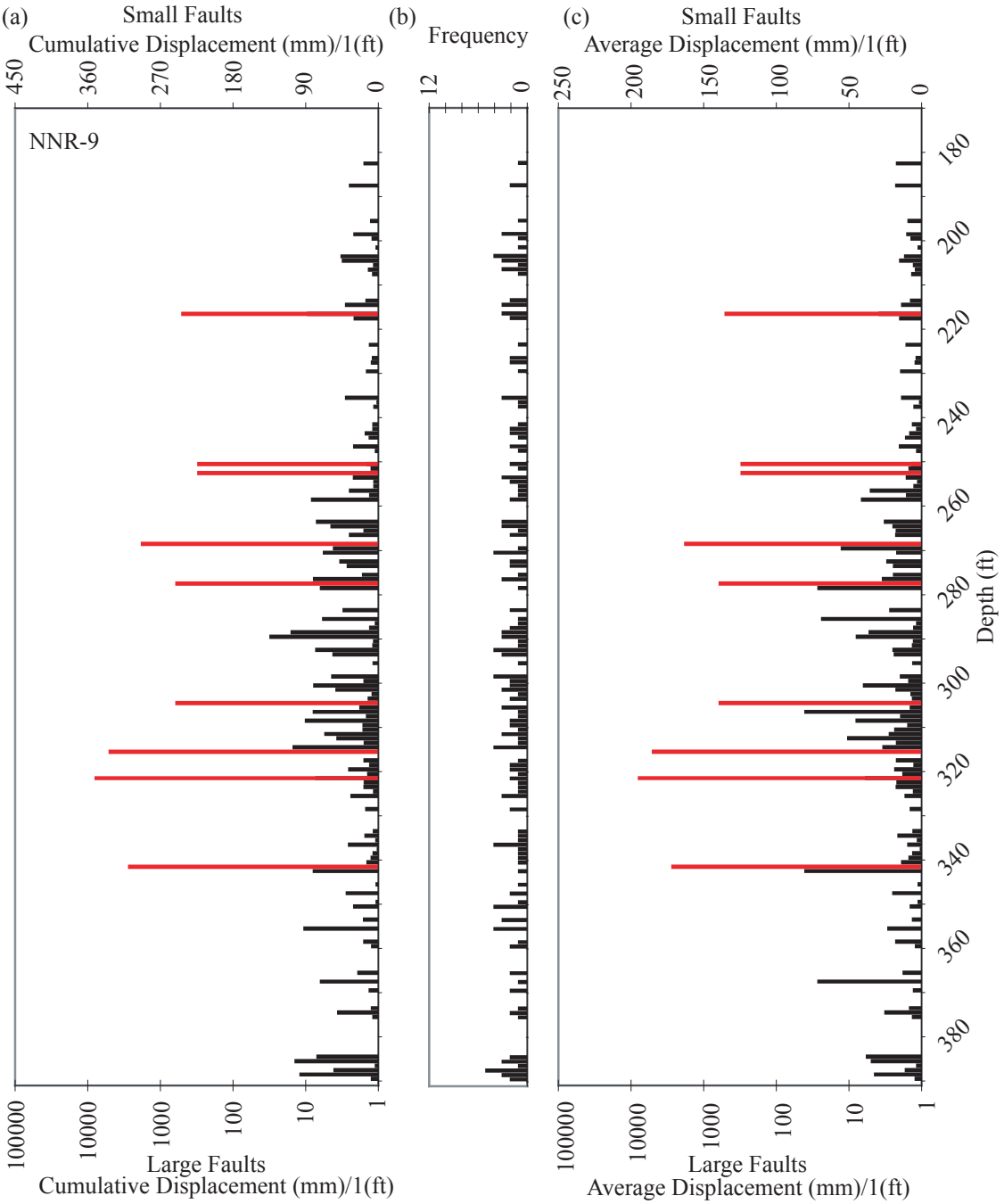

Fig. 31. Borehole NNR-9: vertical distribution of small faults shown using three 1-D "density" measures. (a) Cumulative displacement (mm) of all faults per foot; (b) number of small faults per foot; (c) average displacement (mm) of all faults per foot. Small fault measures (black) have a linear scale (top), whereas large faults (red) have a log scale (bottom).

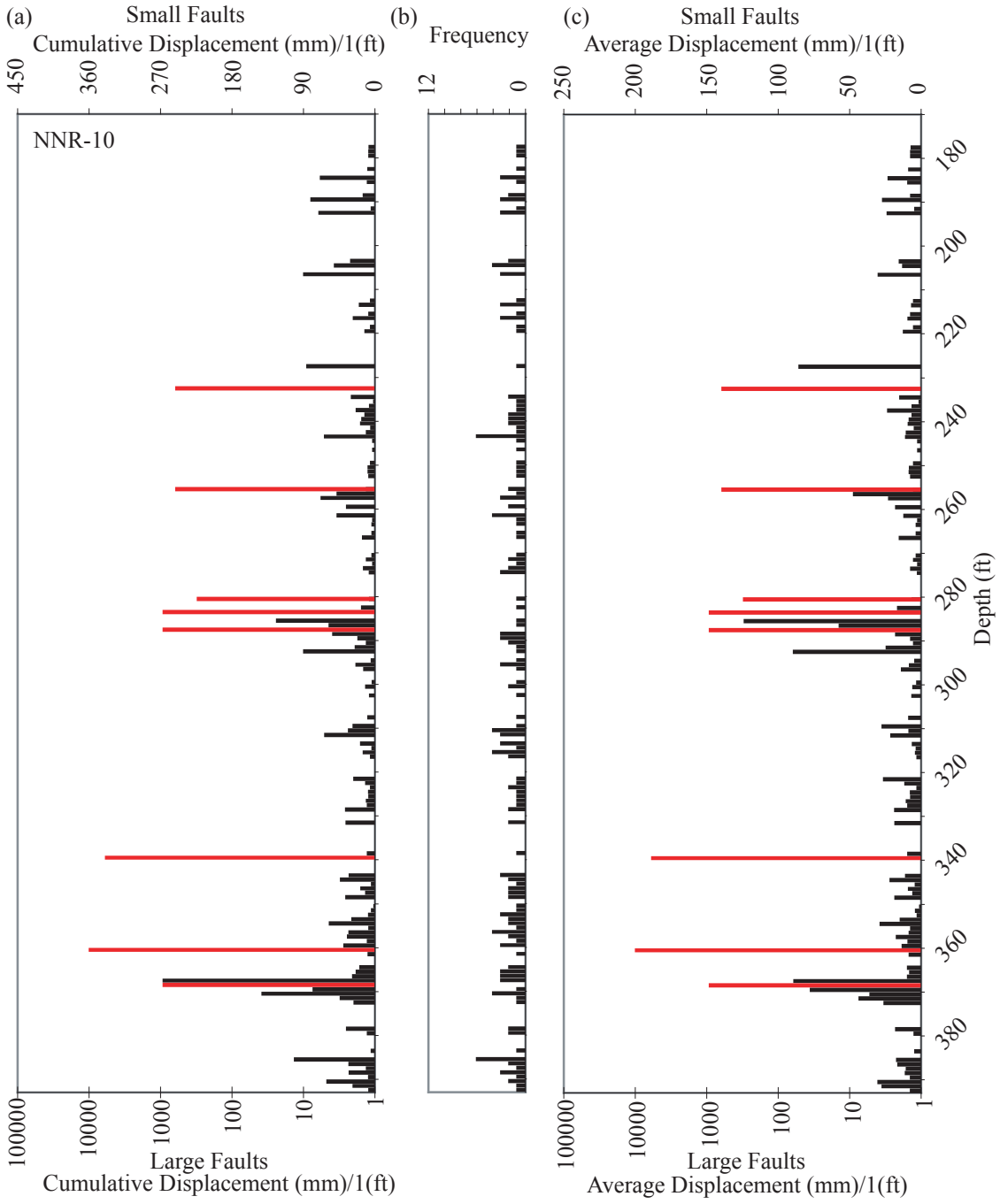

Fig. 32. Borehole NNR-10: vertical distribution of small faults shown using three 1-D "density" measures. (a) Cumulative displacement (mm) of all faults per foot; (b) number of small faults per foot; (c) average displacement (mm) of all faults per foot. Small fault measures (black) have a linear scale (top), whereas large faults (red) have a log scale (bottom).

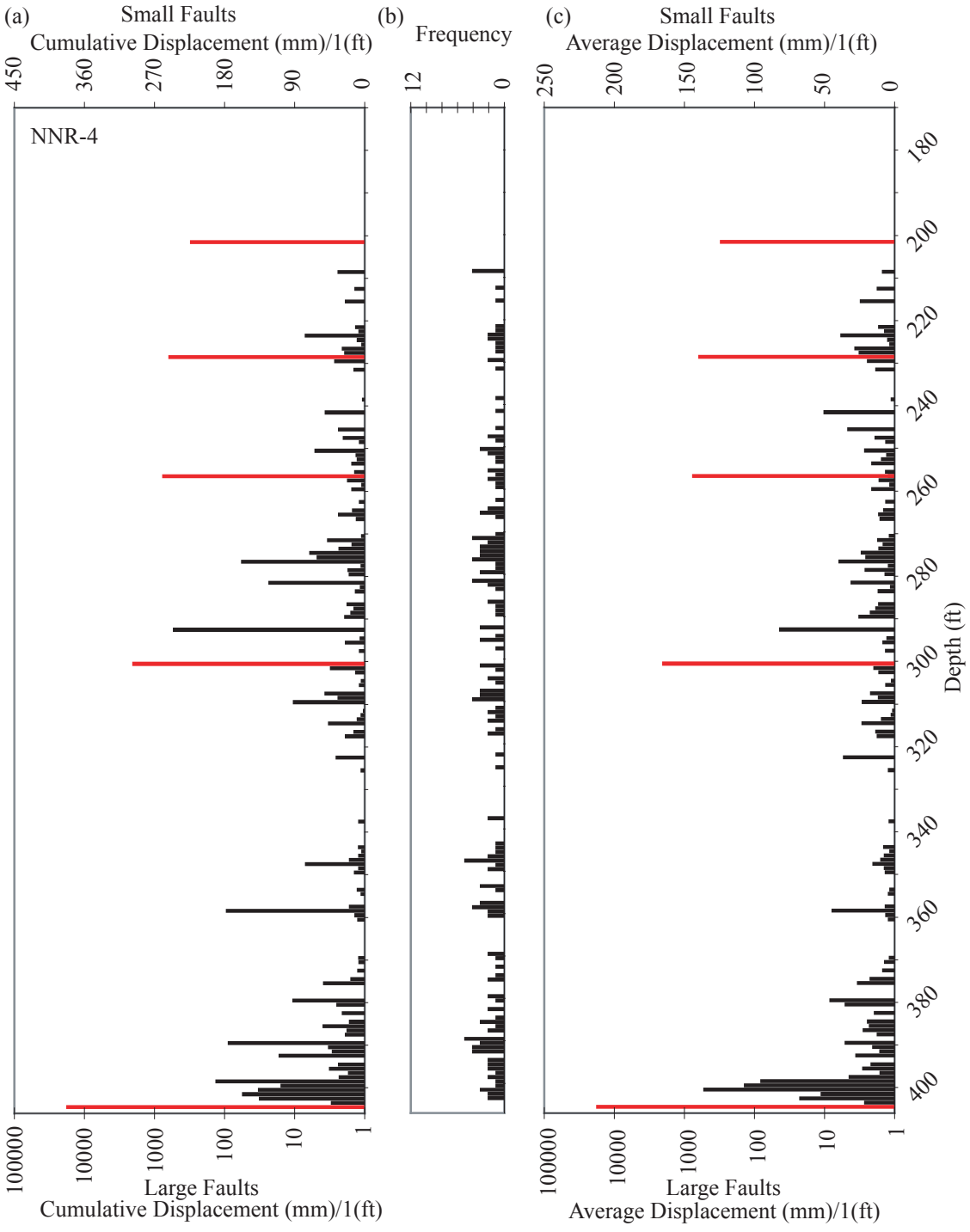

Fig. 33. Borehole NNR-4: vertical distribution of small faults shown using three 1-D "density" measures. (a) Cumulative displacement (mm) of all faults per foot; (b) number of small faults per foot; (c) average displacement (mm) of all faults per foot. Small fault measures (black) have a linear scale (top), whereas large faults (red) have a log scale (bottom).

faults (Fig. 34). Since inelastic strain and shear displacement on faults are related (e.g. Jamison, 1979), alternative measures incorporating fault displacement are anticipated to provide a more direct measure of local inelastic strain. This requires all faults to have a measured or estimated displacement if a measure is to be defined and useful. This was one of the primary reasons for exploring the relationship of gouge thickness to fault displacement and protolith textural parameters as presented in the prior section (4). Two measures incorporating fault displacement are used. Cumulative displacement of all faults per foot and average displacement of faults in a foot of core; the later represents a combination of number density and cumulative displacement density.

The spatial patterns of the small fault "density" measures clearly show the tendency of faults to occur in clusters. Using the 1 ft (0.3 m) threshold distance for discrimination of separate cluster, approximately 220 clusters were identified in the core from NNR-3, 4, 7, 8, 9 and 10. Cluster width (vertical dimension in core) is quite variable (Fig. 35), but 60 % of the clusters have a width less than 2 ft (0.61 m). There are some (~ 10 %) large clusters with a width greater or equal to 7 ft (2.13 m); however, nearly 80 % of the clusters are within 2 ft (0.61 m) of a neighboring cluster.

Spatial patterns of the frequency and displacement attributes of the small faults look similar on average in all boreholes. Faults are nearly ubiquitous throughout the core. There are, however, localized intervals where both the abundance of faults and associated cumulative displacement appear to be either anomalously high or low.

Some anomalous intervals appear to be associated with large displacement faults. There are examples where enhanced numbers of faults and cumulative displacement occur adjacent to or in close proximity to a large displacement fault. There also are examples of zones adjacent to a large fault with few faults and only small cumulative displacement. Consider for example, the large fault at 252 ft in NNR-8 (Fig. 30). Intensification of faults appears to exist in the zone above the large faults (hanging wall). But one also can see that the zone immediately below the large fault (footwall) has few faults and only small cumulative displacement. A quantitative assessment of the spatial correlation of small faults to large faults is explored in the following section (6.4 - 5).

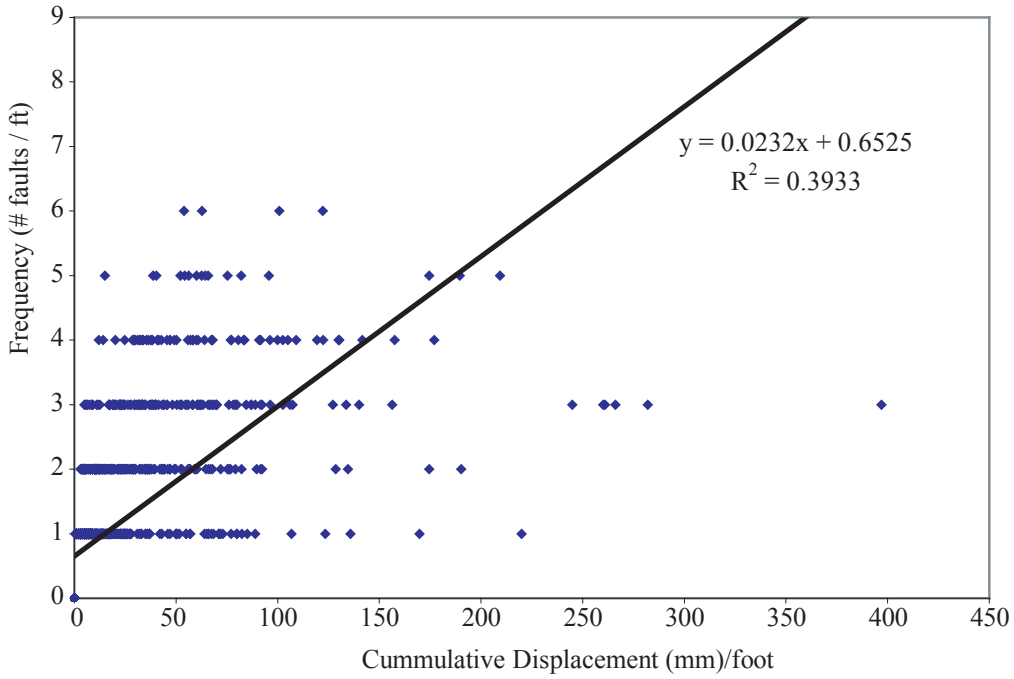

Fig. 34. Scatterplot of cumulative displacement versus frequency for small faults in a 1 ft interval.

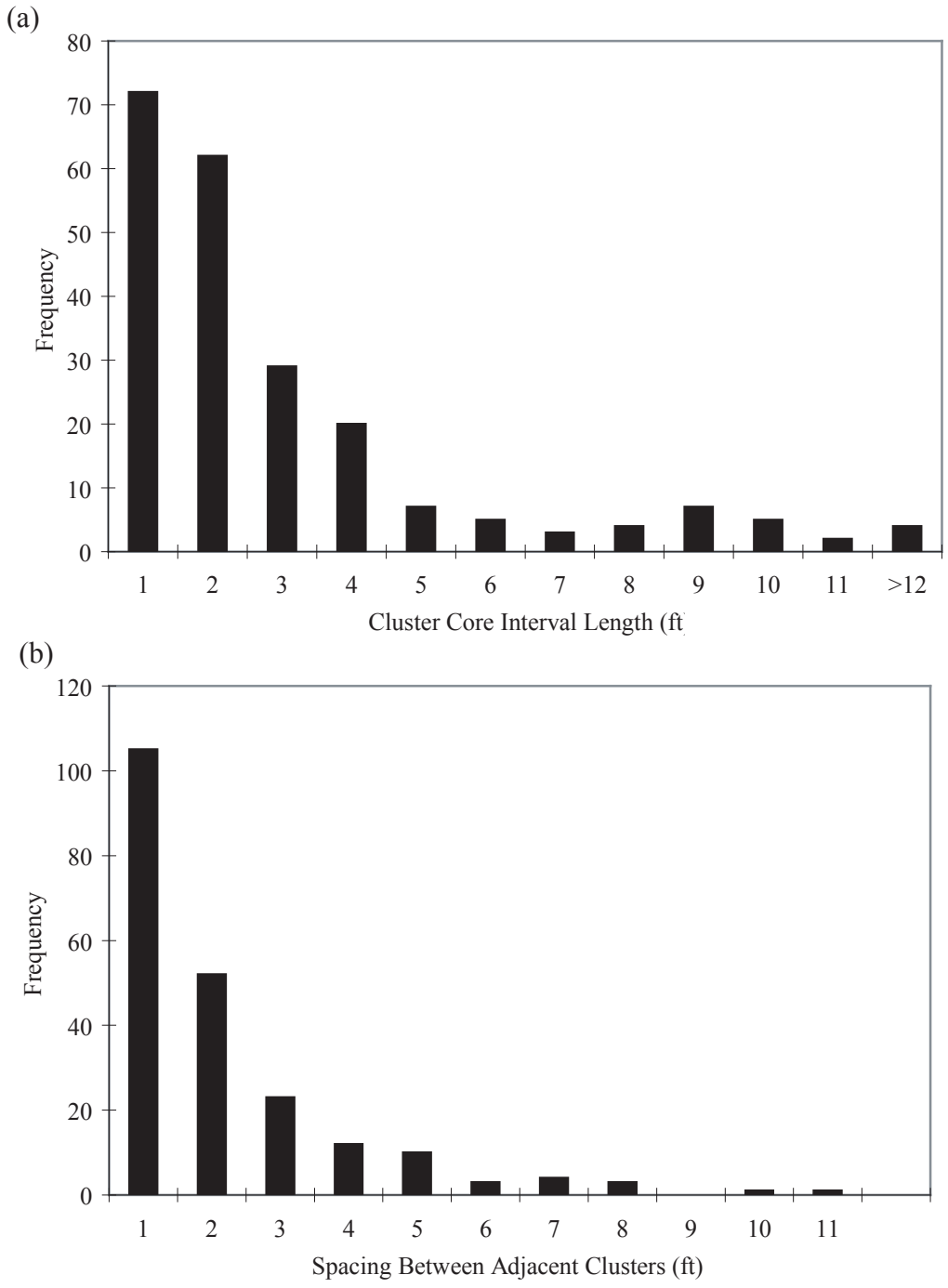

Fig. 35. Frequency histograms of distance between adjacent clusters and length (vertical width) of clusters based on a 1 ft interval in core.

Intervals with small, relatively widely spaced, fault clusters with small cumulative displacement are observed to be common in the upper portion of the boreholes within the more mudstone-rich Middle Hickory. In NNR-8 (Fig. 30) very little cumulative displacement is associated with the upper portions of the borehole (i.e. 170 - 220 ft), and the clusters in this portion of the borehole are separated by substantial distances. This same association is also observed in NNR-9 (Fig. 31), from 170 - 240 ft, and in NNR-10 (Fig. 32) from 170 - 270 ft. The role of mechanical stratigraphy is explored quantitatively in the following section (6.2).

5.2 Orientation of Small Faults

A global stereonet plot of attitudes of small faults shows that the dominant set of faults strike northeasterly with a SE dip (Fig. 36a). The attitudes of most large and intermediate displacement faults (Wilson 2001) are similar to this dominant set of small faults, although the larger faults tend to have a more easterly strike. A second prominent but less numerous set of small faults strike northeasterly, but dips to the NW. In addition to these prominent sets, there are a smaller number of small faults that strike northerly and northwesterly with easterly and northeasterly dips.

Slip vectors recorded from slip surfaces of large displacement faults reveal that overall, the larger faults are normal, dip-slip dominant with a small left-lateral component (Fig. 36b). The subgroup of small faults with known normal dip-slip displacements exhibits the same general fabric as the global distribution (Fig. 36c). Of the 776 faults with known sense of slip, 134 (17 %) have a reverse sense of dip-slip. The orientations of reverse-slip faults differ somewhat from that of the normal-slip faults (Fig. 36d). The most numerous reverse-slip faults strike northeasterly but dip to the NW. Some reverse-slip faults strike northerly and northwesterly, and like the normal-slip faults they dip to the E and NE. Although there are a few low angle, NE-striking reverse faults, most reverse faults are high angle (Fig. 37). Exposure of a normal fault in a near by quarry near Voca, Tx reveals that reverse-slip faults are the consequence of an upward propagating normal fault (personal communication Brann Johnson). These high

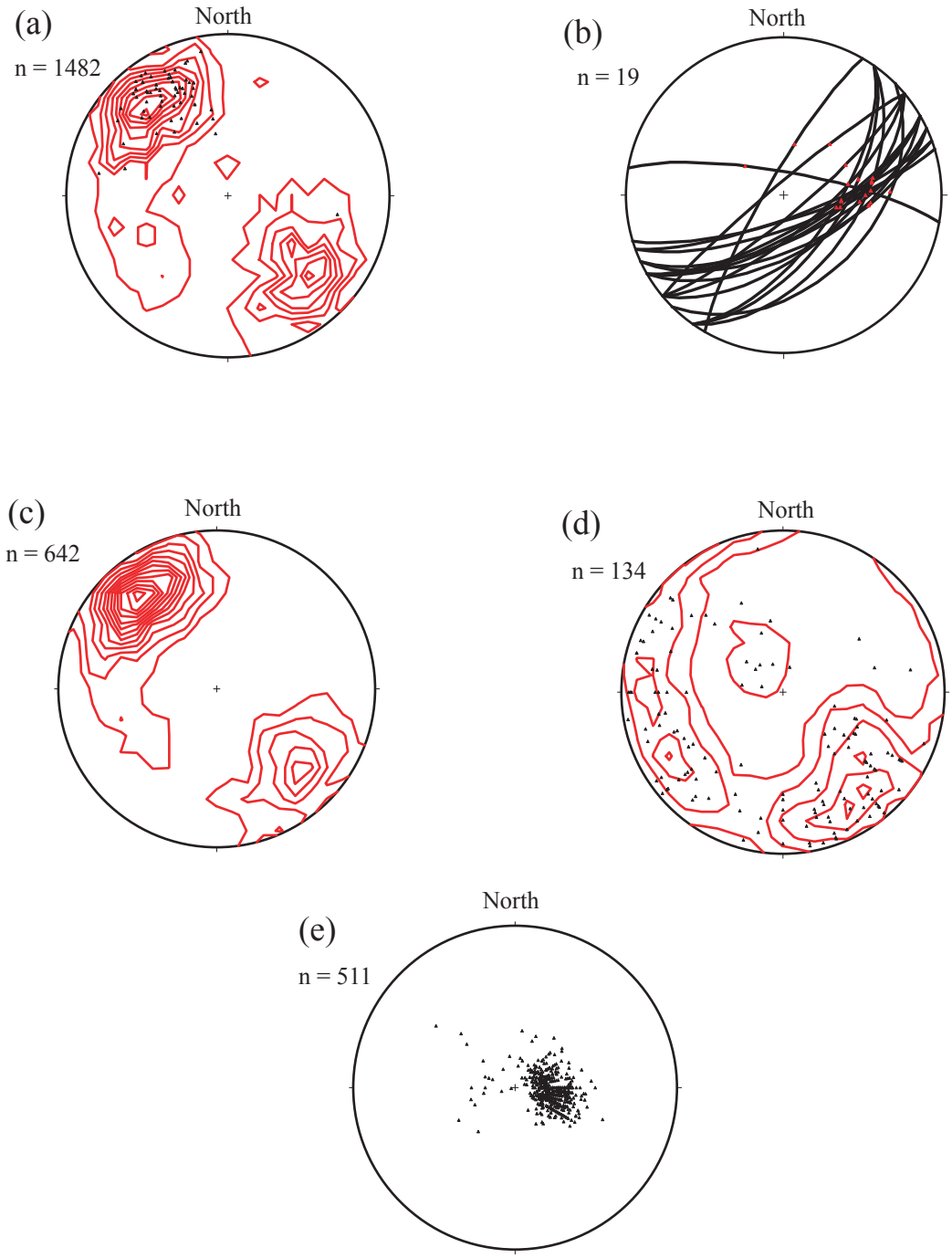

Fig. 36. Global stereonet of fault and bedding attitudes from boreholes NNR-3, 4, 7, 8, 9 and 10. (a) Kamb contour is for small displacement faults, while poles are for large displacement faults; (b) faults with fault striae, red symbols represents fault striae orientation; (c) Kamb contour of faults with normal displacement; (d) Kamb contour with poles of faults with reverse displacement; and (e) poles of bedding within core. Equal area, lower hemisphere projections, stereonet plots with best fit poles for Kamb contouring with contour interval of 2σ.

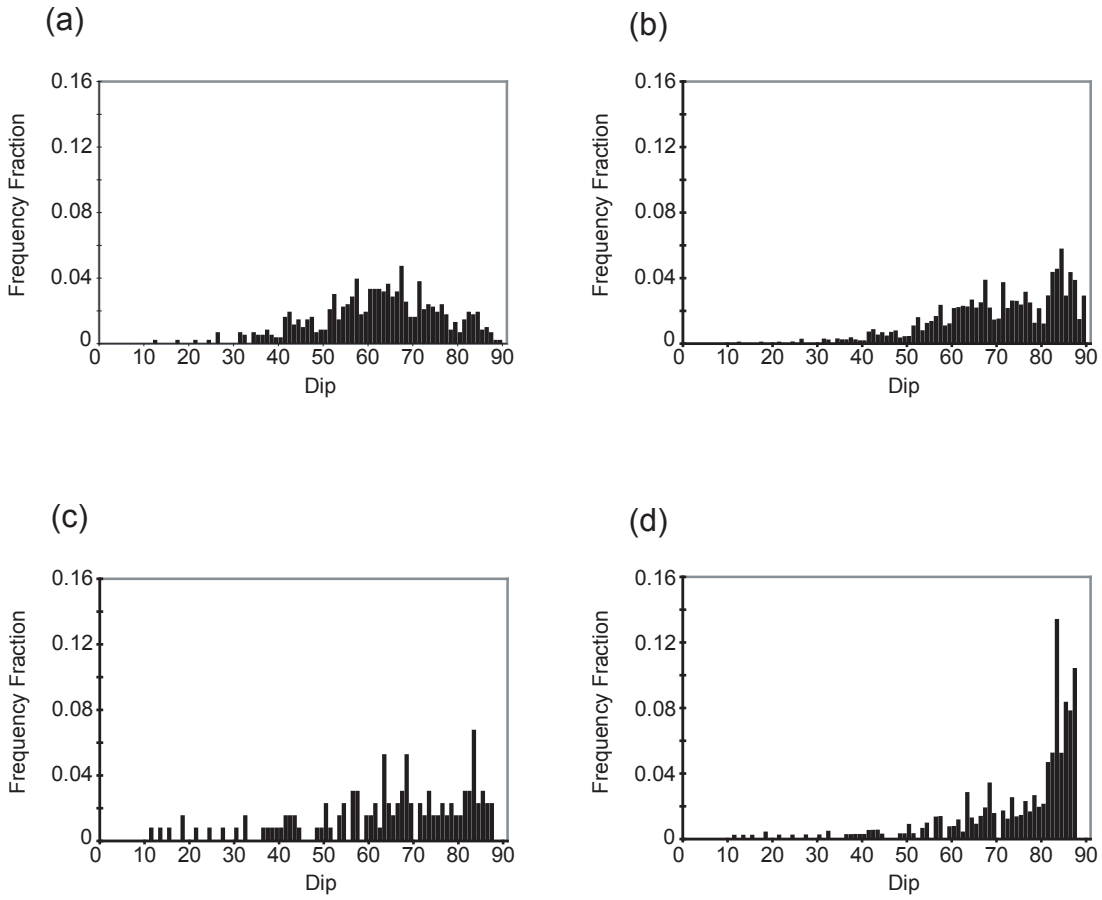

Fig. 37. Histograms of fault dips for small faults with known sense of displacement. (a) Frequency histogram for normal-slip faults, (b) corrected frequency of normal-slip faults, (b) frequency histogram for reverse-slip faults, (c) corrected frequency of reverse-slip faults. Corrected histogram used Terzaghi (1965) method for sample bias.

angle, reverse faults are also consistent with experimental work of an upper propagating normal fault (Patton, 1984).

In order to visualize spatial patterns of small faults, "smoothed" small fault orientations are used (see sections 3.6 and 3.7) to assign faults to one of four strike sets. Figures 38 - 49 show the spatial distribution of the faults separated into the four strike bins for all boreholes, while Figures 50 - 55 show only the locations of faults with reverse-slip. Within a given strike bin, different spatial pattern associated to dip polarity occur. In some intervals, faults of opposite polarity are of nearly equal occurrence; for example NNR-3 from 290 - 320 ft (Figs. 38 and 44). In other intervals, faults of one sense of polarity dominate; for example NNR-7 from 200 - 220 ft (Figs. 39 and 45). Faults striking NE are most common, but there are core intervals in which no NE-striking faults. In these intervals, faults of other orientations often occur; for example NNR-8 from 200 - 220 ft (Figs. 40 and 46). In some intervals, multiple fault sets occur together; for example NNR-10 from 260 - 280 ft (Figs. 42 and 48).

Cross-cutting relationships show no simple systematic differences in relative age between sets. If the age relationship data are separated based upon footwall and hanging wall domain of the Nobles Fault, some general patterns are evident. Within the hanging wall portion of the Nobles Fault, SE-dipping faults tend to be younger in age (Fig. 56b); while within the footwall, the NW-dipping faults dominantly are younger in age (Fig. 56d).

5.3 Bedding Attitudes

Bedding attitudes from BHTV logs and oriented core are restricted to depths greater than 170 ft in the saturated intervals. Bedding as determined in oriented core, strikes approximately NS with a shallow dip to the West (Fig. 36e). Strikes determined from BHTV logs are on average equivalent to strikes determined from oriented core, which gives confidence in the quality of the core orientation process (Figs. 57 – 62). These figures also show locations of faults and joints used to orient core in order to provide a sense of orientation control available at different depth intervals.

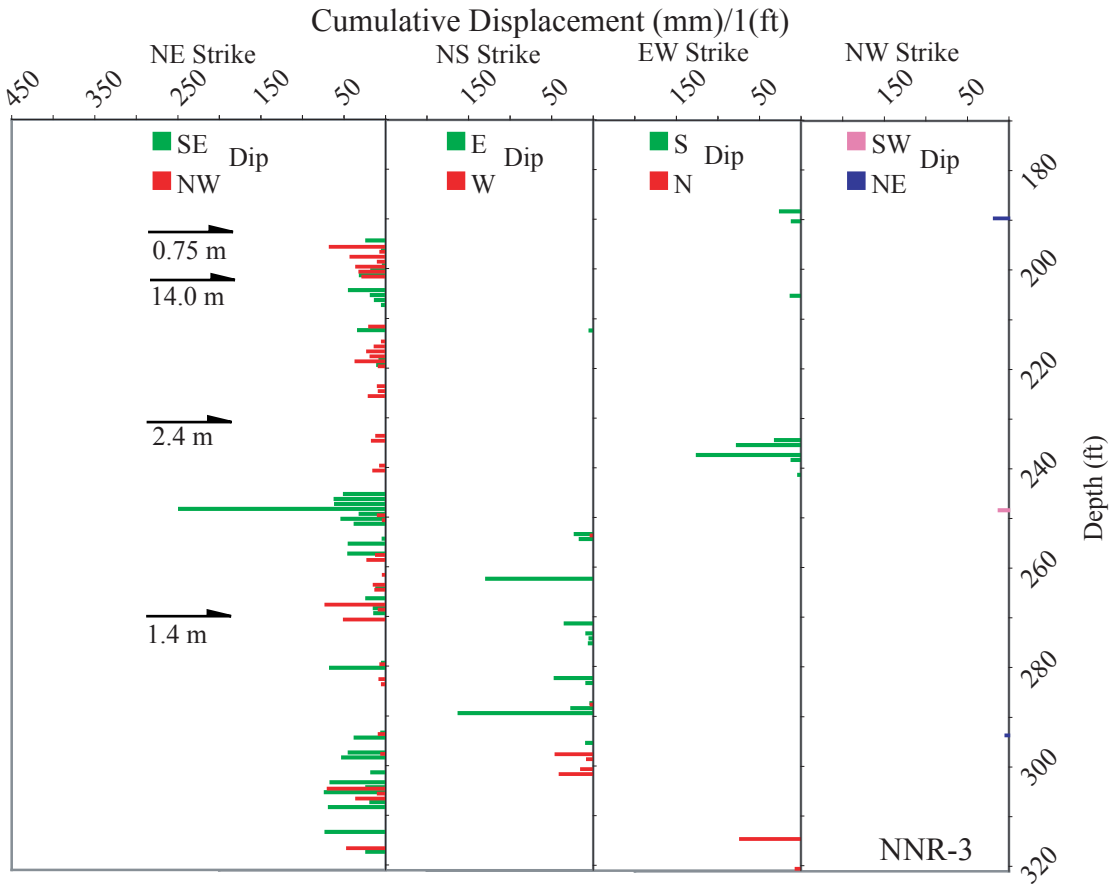

Fig. 38. Borehole NNR-3: Distribution of small faults showing associated strike, dip polarity and cumulative displacement per foot. Ranges in strike attitudes for bins are as follows: (NE strike) N30-70E, (NS strike) N29W to N29E, (EW strike) N71E to S71E and (NW strike) N30-70W. Small fault that dip synthetic to the Nobles fault are green; while antithetic dipping small faults are red. Small faults that are in the NW strike bin that dip to the SW are colored pink; while NE dipping faults are dark blue. Large fault locations (black arrow) are placed in strike bin of similar orientation, along with stratigraphic throw (m) determined by Wilson (2001).

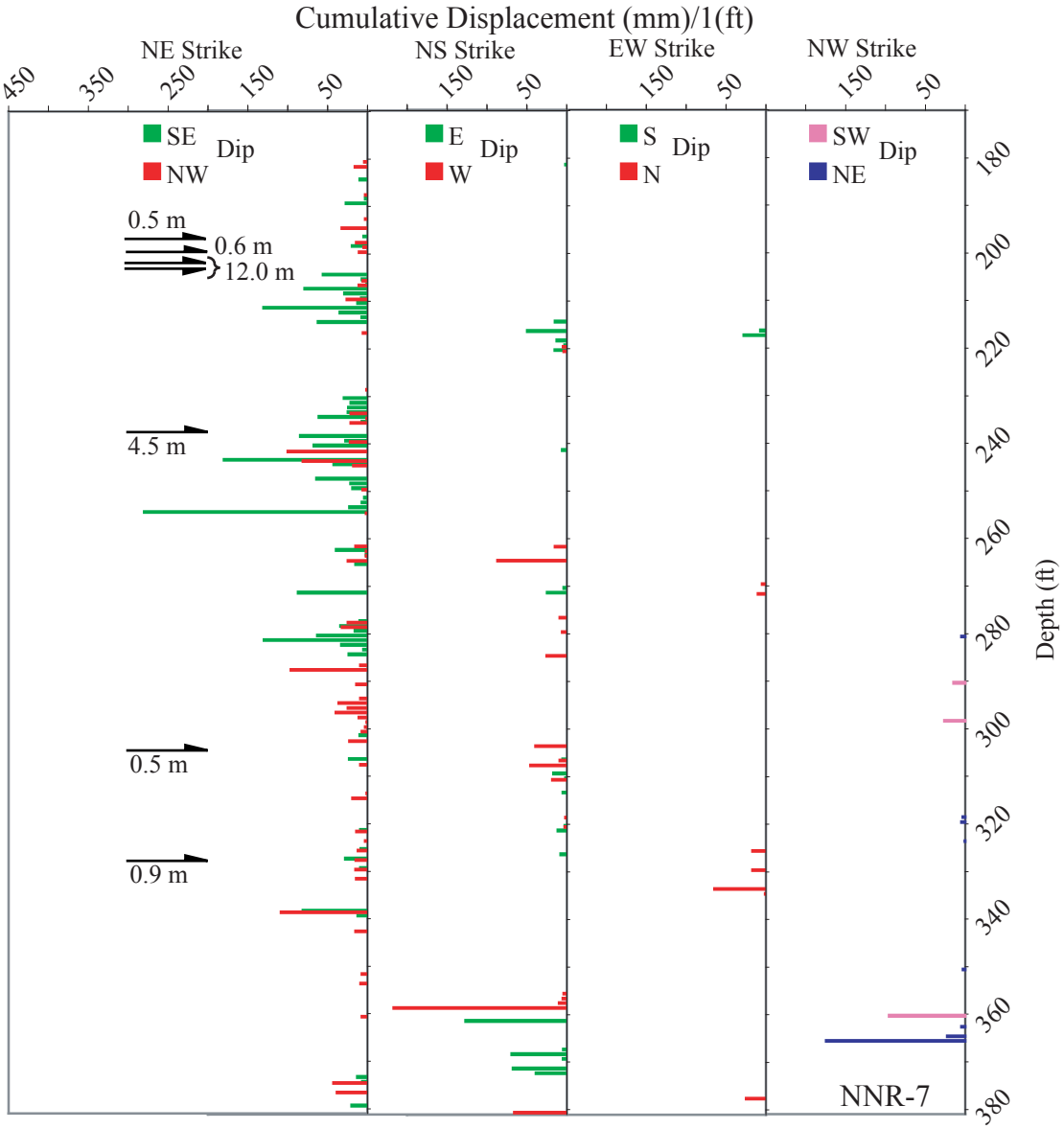

Fig. 39. Borehole NNR-7: Distribution of small faults showing associated strike, dip polarity and cumulative displacement per foot. Ranges in strike attitudes for bins are as follows: (NE strike) N30-70E, (NS strike) N29W to N29E, (EW strike) N71E to S71E and (NW strike) N30-70W. Small fault that dip synthetic to the Nobles fault are green; while antithetic dipping small faults are red. Small faults that are in the NW strike bin that dip to the SW are colored pink; while NE dipping faults are dark blue. Large fault locations (black arrow) are placed in strike bin of similar orientation, along with stratigraphic throw (m) determined by Wilson (2001).

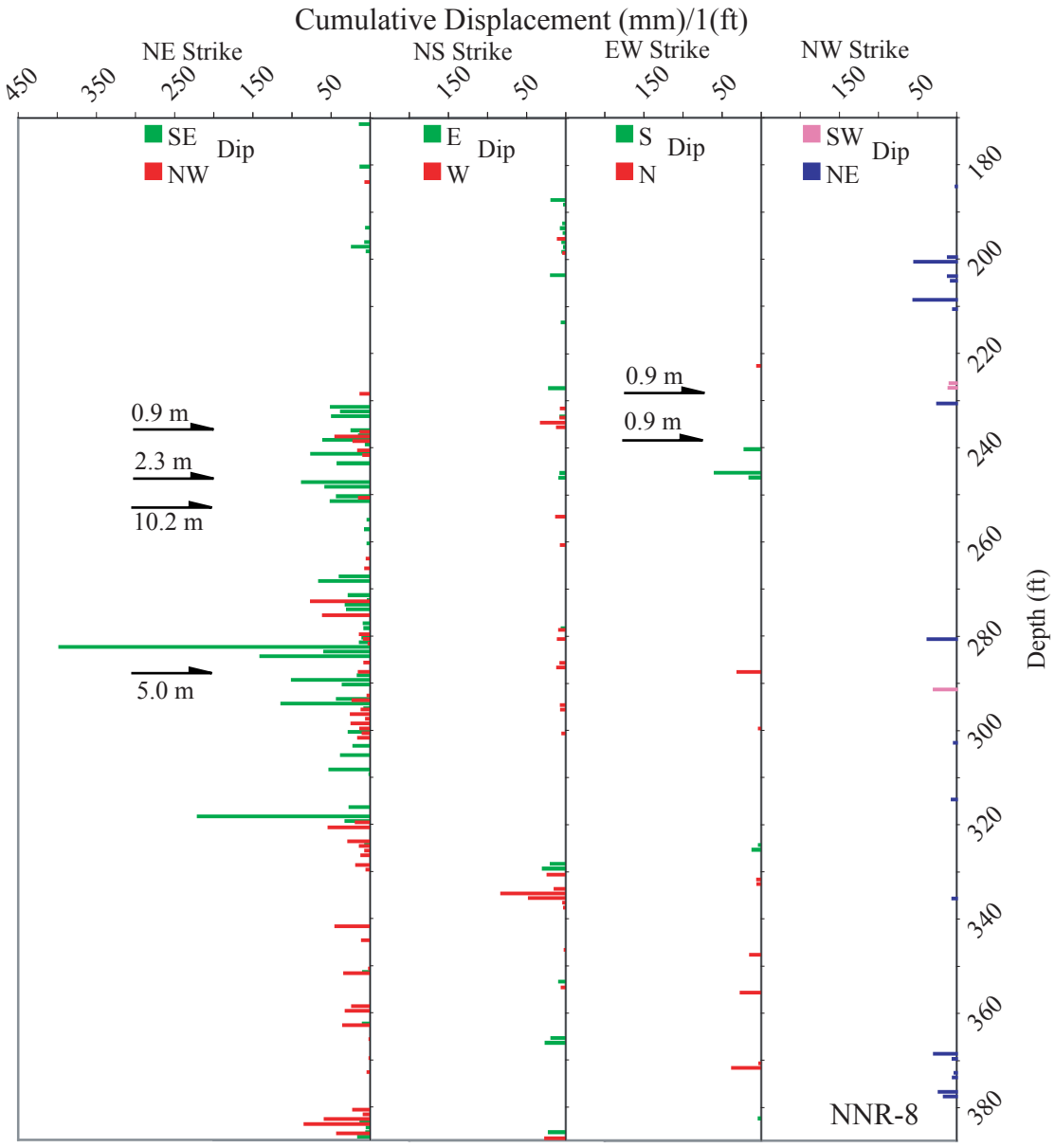

Fig. 40. Borehole NNR-8: Distribution of small faults showing associated strike, dip polarity and cumulative displacement per foot. Ranges in strike attitudes for bins are as follows: (NE strike) N30-70E, (NS strike) N29W to N29E, (EW strike) N71E to S71E and (NW strike) N30-70W. Small fault that dip synthetic to the Nobles fault are green; while antithetic dipping small faults are red. Small faults that are in the NW strike bin that dip to the SW are colored pink; while NE dipping faults are dark blue. Large fault locations (black arrow) are placed in strike bin of similar orientation, along with stratigraphic throw (m) determined by Wilson (2001).

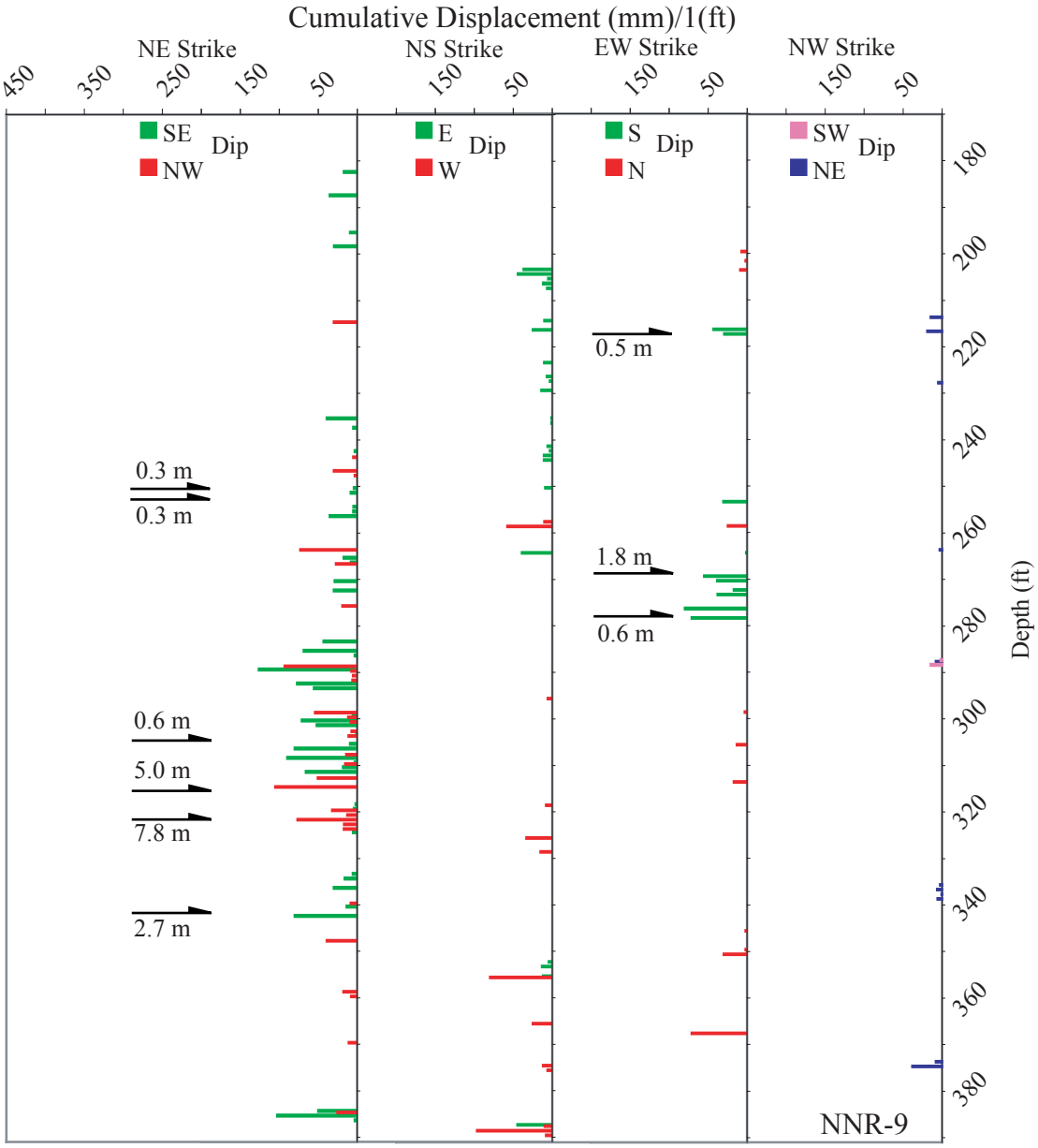

Fig. 41. Borehole NNR-9: Distribution of small faults showing associated strike, dip polarity and cumulative displacement per foot. Ranges in strike attitudes for bins are as follows: (NE strike) N30-70E, (NS strike) N29W to N29E, (EW strike) N71E to S71E and (NW strike) N30-70W. Small fault that dip synthetic to the Nobles fault are green; while antithetic dipping small faults are red. Small faults that are in the NW strike bin that dip to the SW are colored pink; while NE dipping faults are dark blue. Large fault locations (black arrow) are placed in strike bin of similar orientation, along with stratigraphic throw (m) determined by Wilson (2001).

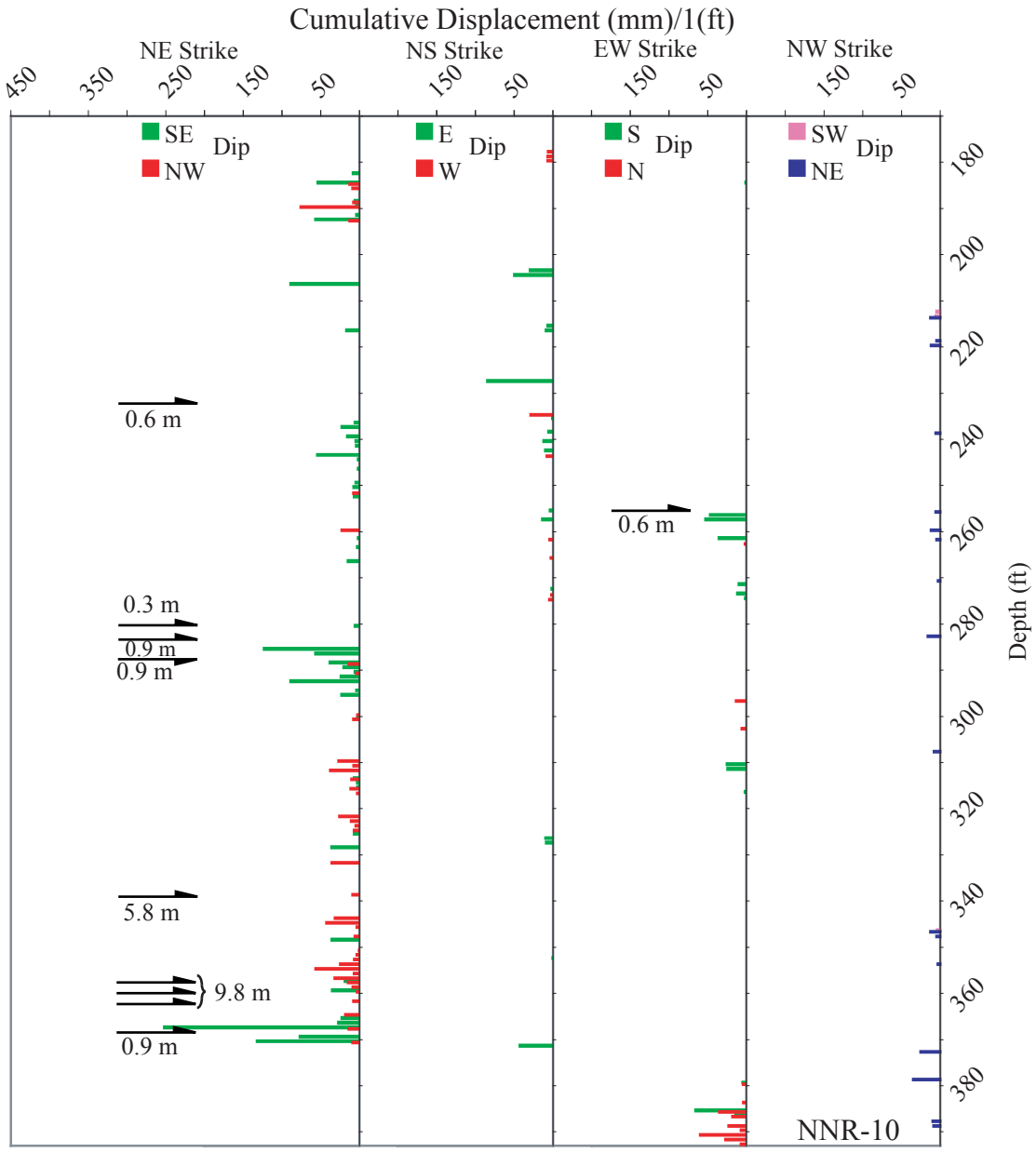

Fig. 42. Borehole NNR-10: Distribution of small faults showing associated strike, dip polarity and cumulative displacement per foot. Ranges in strike attitudes for bins are as follows: (NE strike) N30-70E, (NS strike) N29W to N29E, (EW strike) N71E to S71E and (NW strike) N30-70W. Small fault that dip synthetic to the Nobles fault are green; while antithetic dipping small faults are red. Small faults that are in the NW strike bin that dip to the SW are colored pink; while NE dipping faults are dark blue. Large fault locations (black arrow) are placed in strike bin of similar orientation, along with stratigraphic throw (m) determined by Wilson (2001).

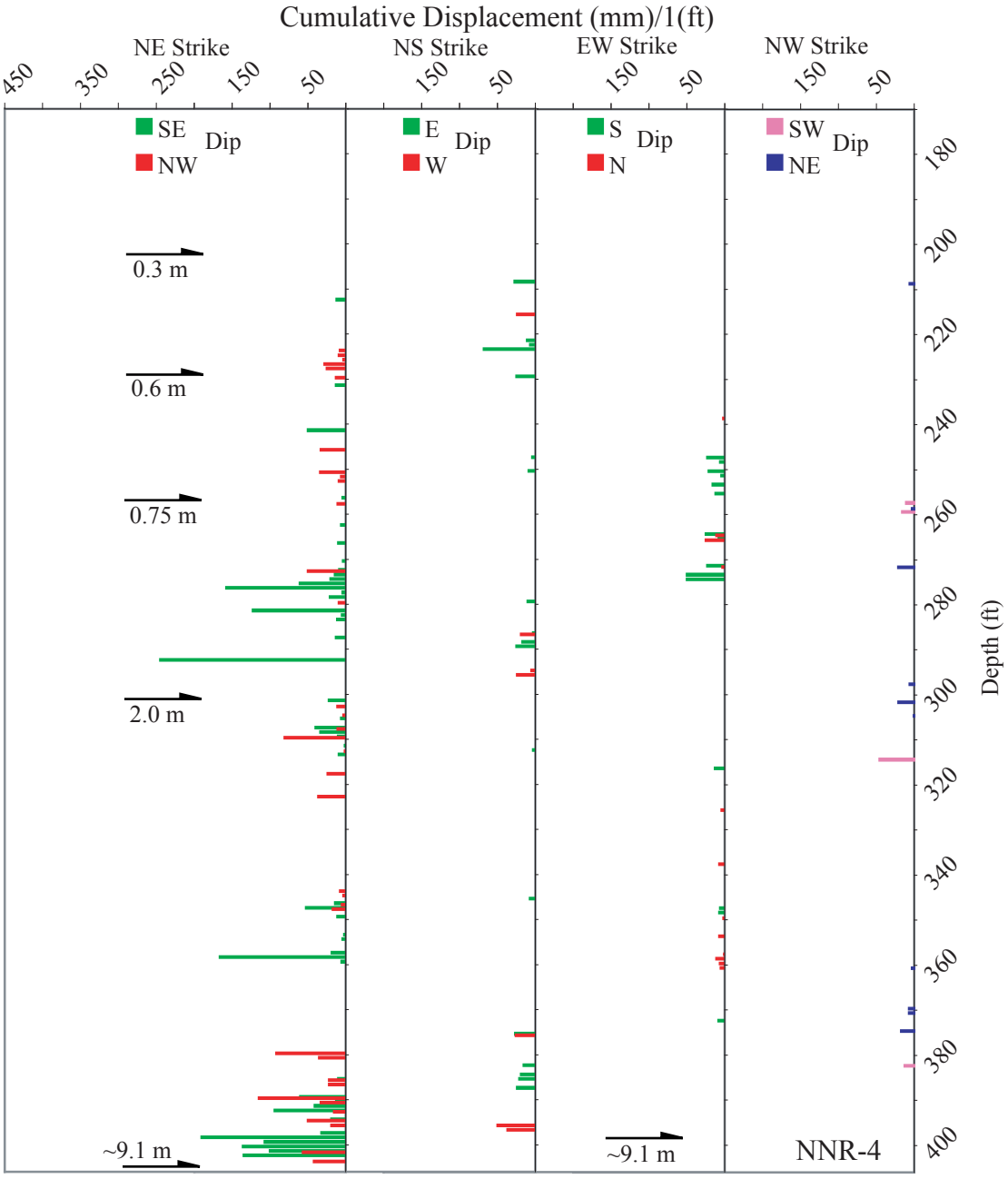

Fig. 43. Borehole NNR-4: Distribution of small faults showing associated strike, dip polarity and cumulative displacement per foot. Ranges in strike attitudes for bins are as follows: (NE strike) N30-70E, (NS strike) N29W to N29E, (EW strike) N71E to S71E and (NW strike) N30-70W. Small fault that dip synthetic to the Nobles fault are green; while antithetic dipping small faults are red. Small faults that are in the NW strike range and dip to the SW are colored pink, while NE dipping faults are dark blue. Large faults locations (black arrow) are placed in strike bin of similar orientation, along with stratigraphic throw (m) determined by Wilson (2001).

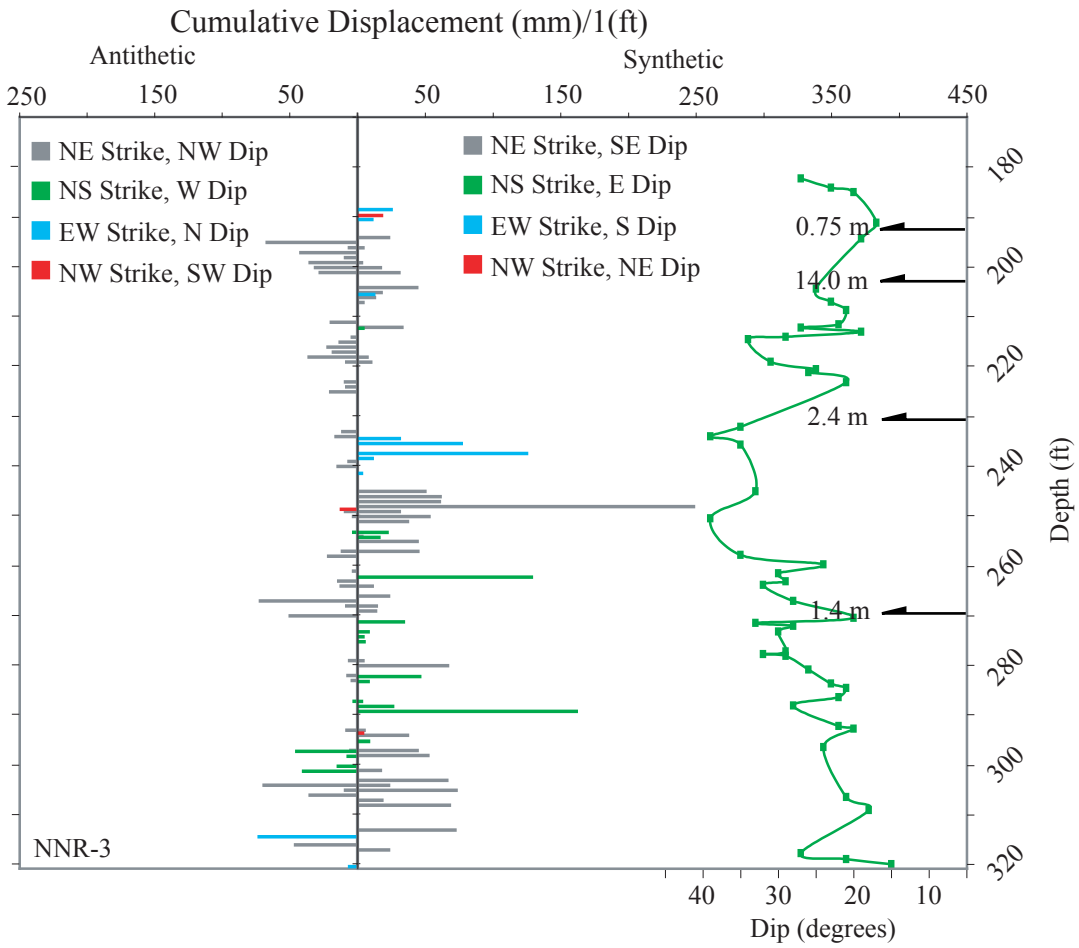

Fig. 44. Borehole NNR-3: Distribution of small faults showing associated fault strike, dip polarity and cumulative displacement per foot along with dip amount of bedding. Strike bins are as follows: (NE strike) N30-70E, (NS strike) N29W to N29E, (EW strike) N71E to S71E and (NW strike) N30-70W. Small faults that dip synthetic to the Nobles fault are the histograms on the right; while antithetic dipping small faults are the histogram on the left. Bedding dip is located on right (green) with associated scale below. Location of large faults (black arrows) and stratigraphic throw (m) determined by Wilson (2001) are noted on the far right.

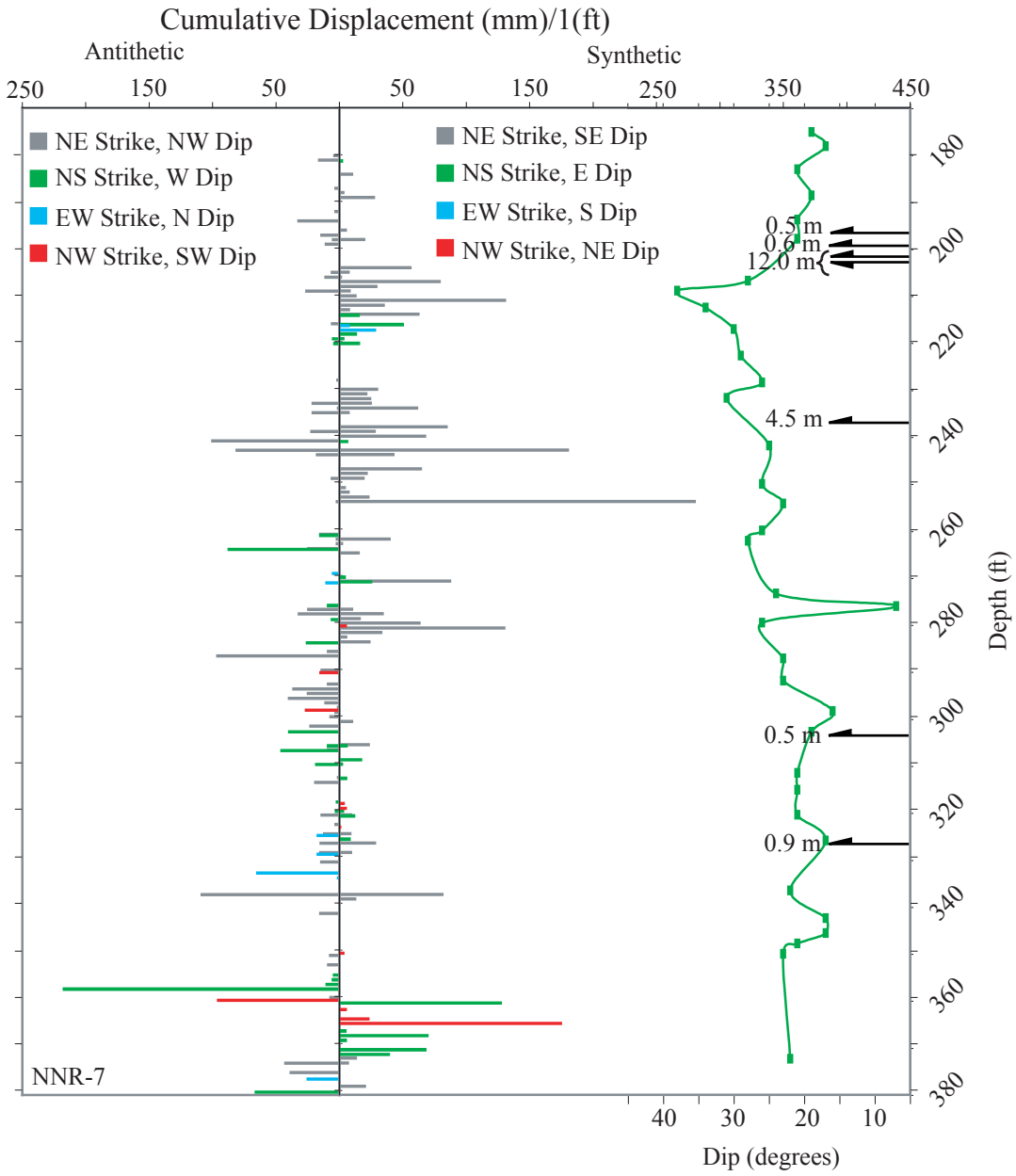

Fig. 45. Borehole NNR-7: Distribution of small faults showing associated fault strike, dip polarity and cumulative displacement per foot along with dip amount of bedding. Strike bins are as follows: (NE strike) N30-70E, (NS strike) N29W to N29E, (EW strike) N71E to S71E and (NW strike) N30-70W. Small faults that dip synthetic to the Nobles fault are the histograms on the right; while antithetic dipping small faults are the histogram on the left. Bedding dip is located on right (green) with associated scale below. Location of large faults (black arrows) and stratigraphic throw (m) determined by Wilson (2001) are noted on the far right.

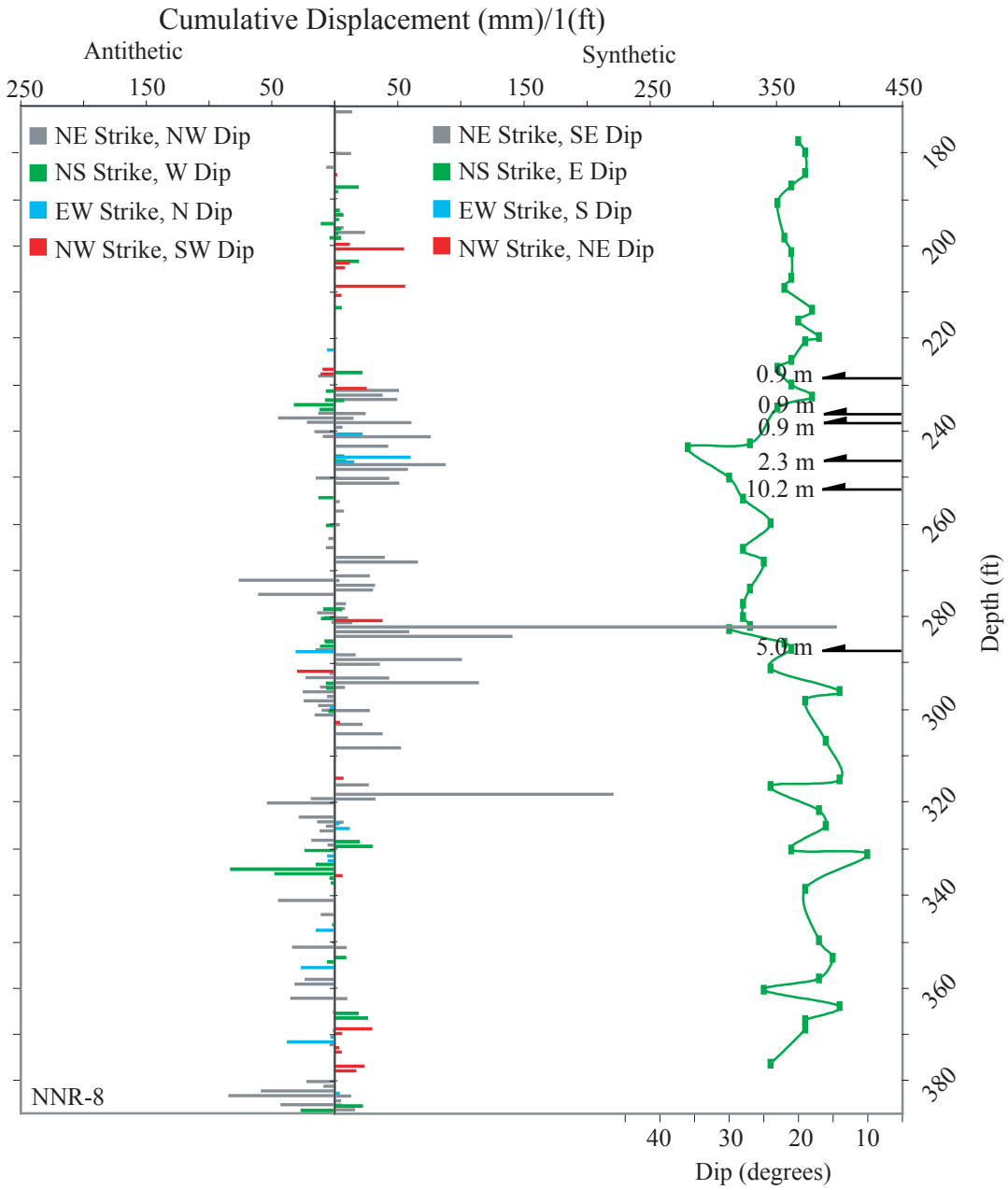

Fig. 46. Borehole NNR-8: Distribution of small faults showing associated fault strike, dip polarity and cumulative displacement per foot along with dip amount of bedding. Strike bins are as follows: (NE strike) N30-70E, (NS strike) N29W to N29E, (EW strike) N71E to S71E and (NW strike) N30-70W. Small faults that dip synthetic to the Nobles fault are the histograms on the right; while antithetic dipping small faults are the histogram on the left. Bedding dip is located on right (green) with associated scale below. Location of large faults (black arrows) and stratigraphic throw (m) determined by Wilson (2001) are noted on the far right.

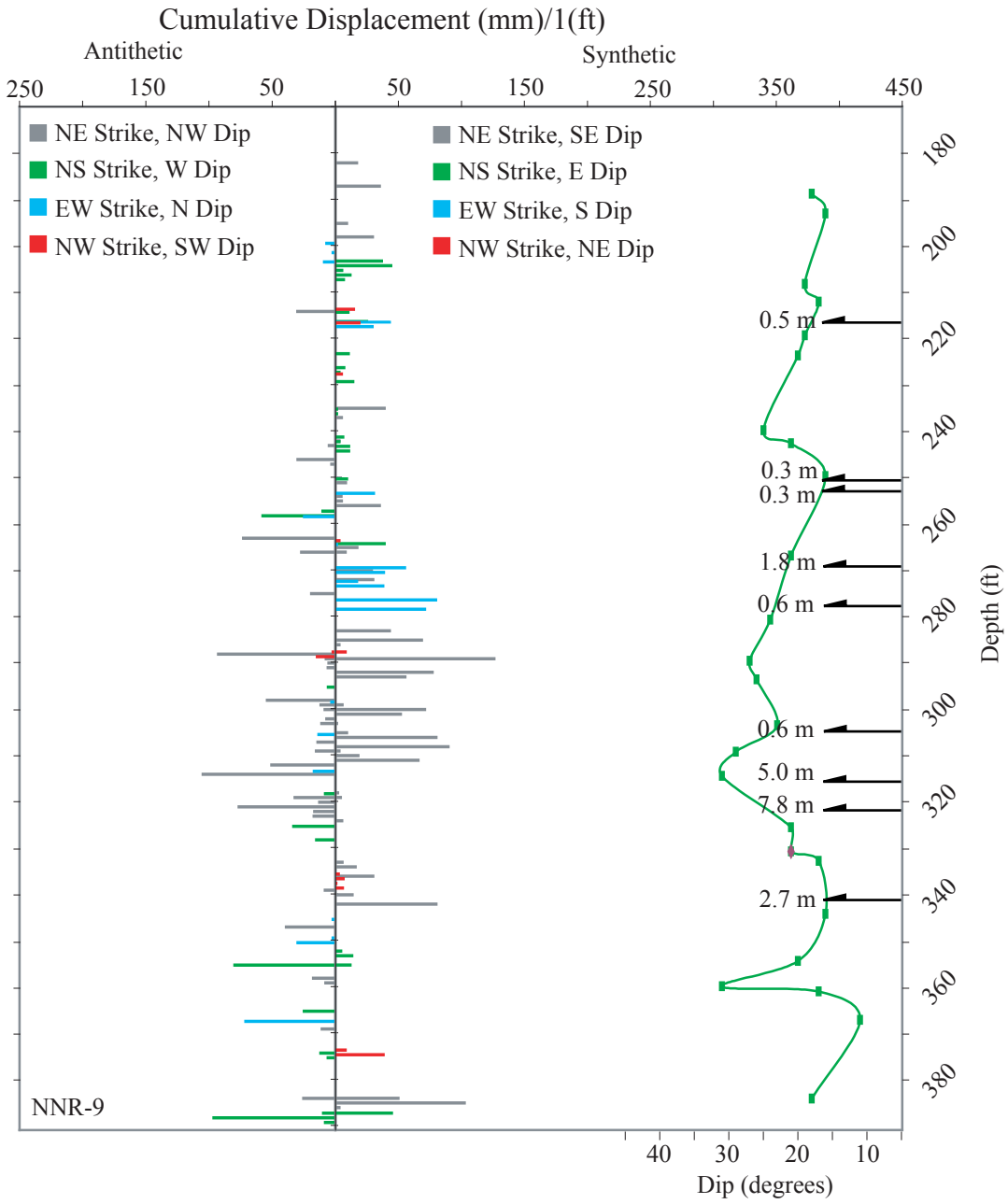

Fig. 47. Borehole NNR-9: Distribution of small faults showing associated fault strike, dip polarity and cumulative displacement per foot along with dip amount of bedding. Strike bins are as follows: (NE strike) N30-70E, (NS strike) N29W to N29E, (EW strike) N71E to S71E and (NW strike) N30-70W. Small faults that dip synthetic to the Nobles fault are the histograms on the right; while antithetic dipping small faults are the histogram on the left. Bedding dip is located on right (green) with associated scale below. Location of large faults (black arrows) and stratigraphic throw (m) determined by Wilson (2001) are noted on the far right.

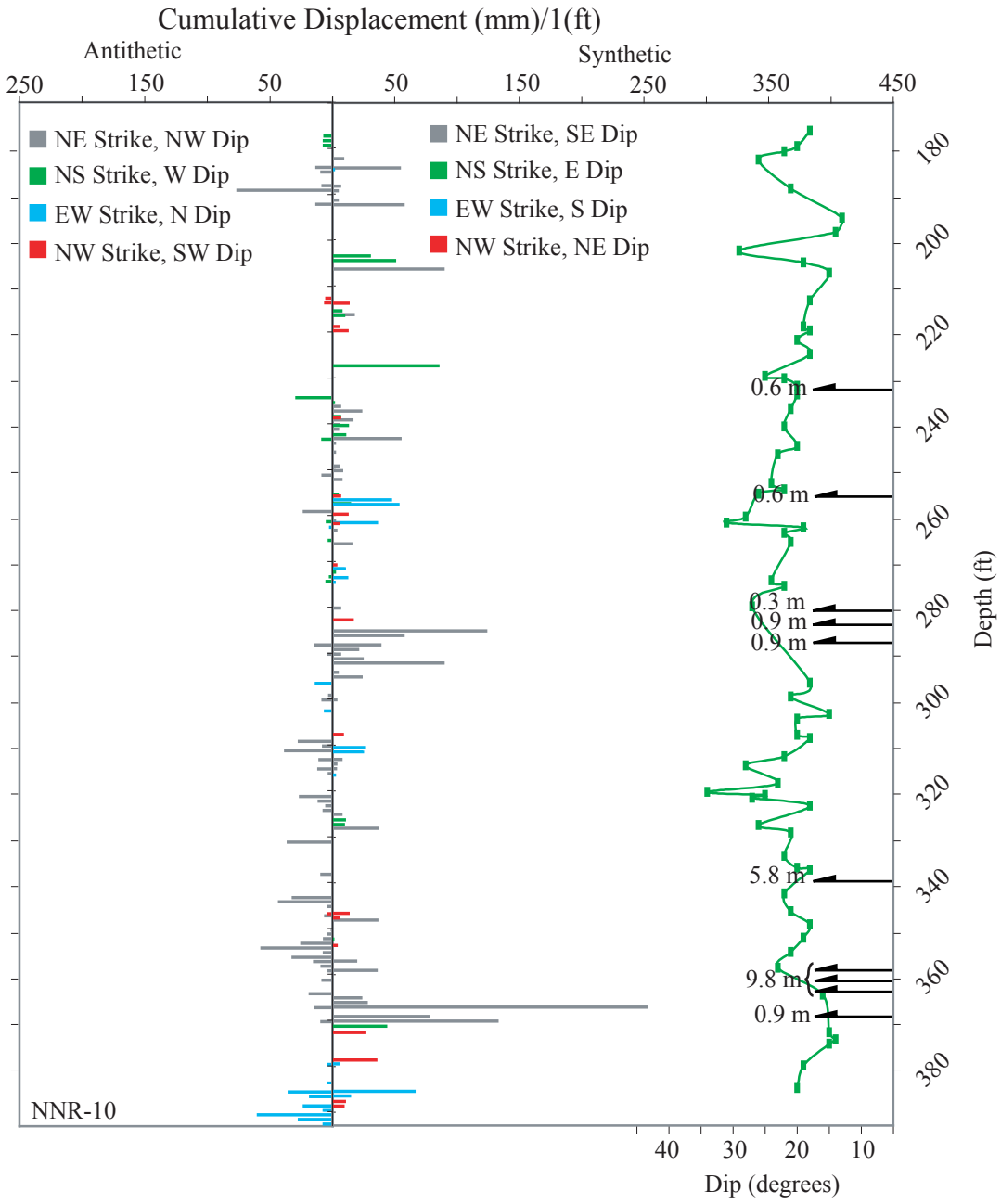

Fig. 48. Borehole NNR-10: Distribution of small faults showing associated fault strike, dip polarity and cumulative displacement per foot along with dip amount of bedding. Strike bins are as follows: (NE strike) N30-70E, (NS strike) N29W to N29E, (EW strike) N71E to S71E and (NW strike) N30-70W. Small faults that dip synthetic to the Nobles fault are the histograms on the right; while antithetic dipping small faults are the histogram on the left. Bedding dip is located on right (green) with associated scale below. Location of large faults (black arrows) and stratigraphic throw (m) determined by Wilson (2001) are noted on the far right.

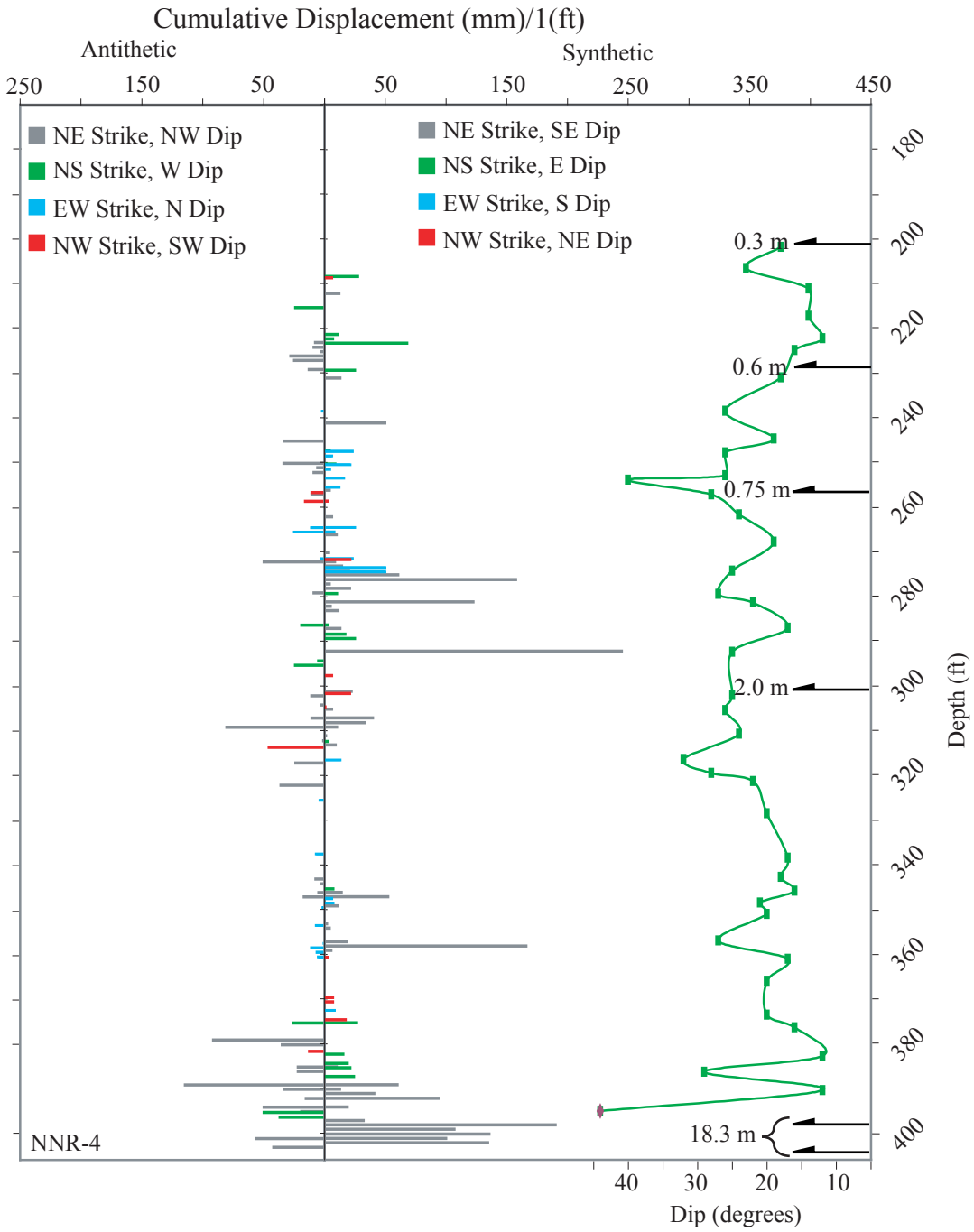

Fig. 49. Borehole NNR-4: Distribution of small faults showing associated fault strike, dip polarity and cumulative displacement per foot along with dip amount of bedding. Strike bins are as follows: (NE strike) N30-70E, (NS strike) N29W to N29E, (EW strike) N71E to S71E and (NW strike) N30-70W. Small faults that dip synthetic to the Nobles fault are the histograms on the right; while antithetic dipping small faults are the histogram on the left. Bedding dip is located on right (green) with associated scale below. Location of large faults (black arrows) and stratigraphic throw (m) determined by Wilson (2001) are noted on the far right.

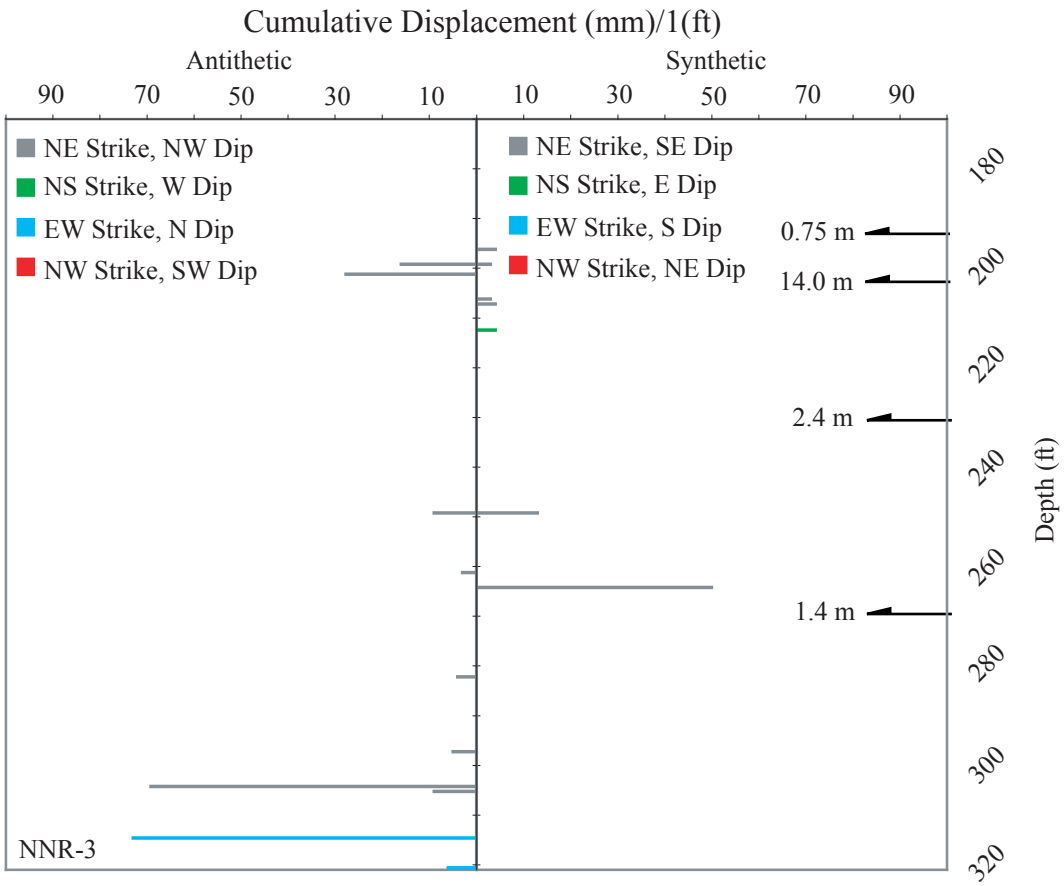

Fig. 50. Borehole NNR-3: Distribution of small faults with reverse-slip, showing associated fault strike, dip polarity and cumulative displacement per foot. Strike bins are as follows: (NE strike) N30-70E, (NS strike) N29W to N29E, (EW strike) N71E to S71E and (NW strike) N30-70W. Small faults that dip synthetic to the Nobles fault are the histograms on the right; while antithetic dipping small faults are the histogram on the left. Location of large faults (black arrows) and stratigraphic throw (m) determined by Wilson (2001) are noted on the far right.

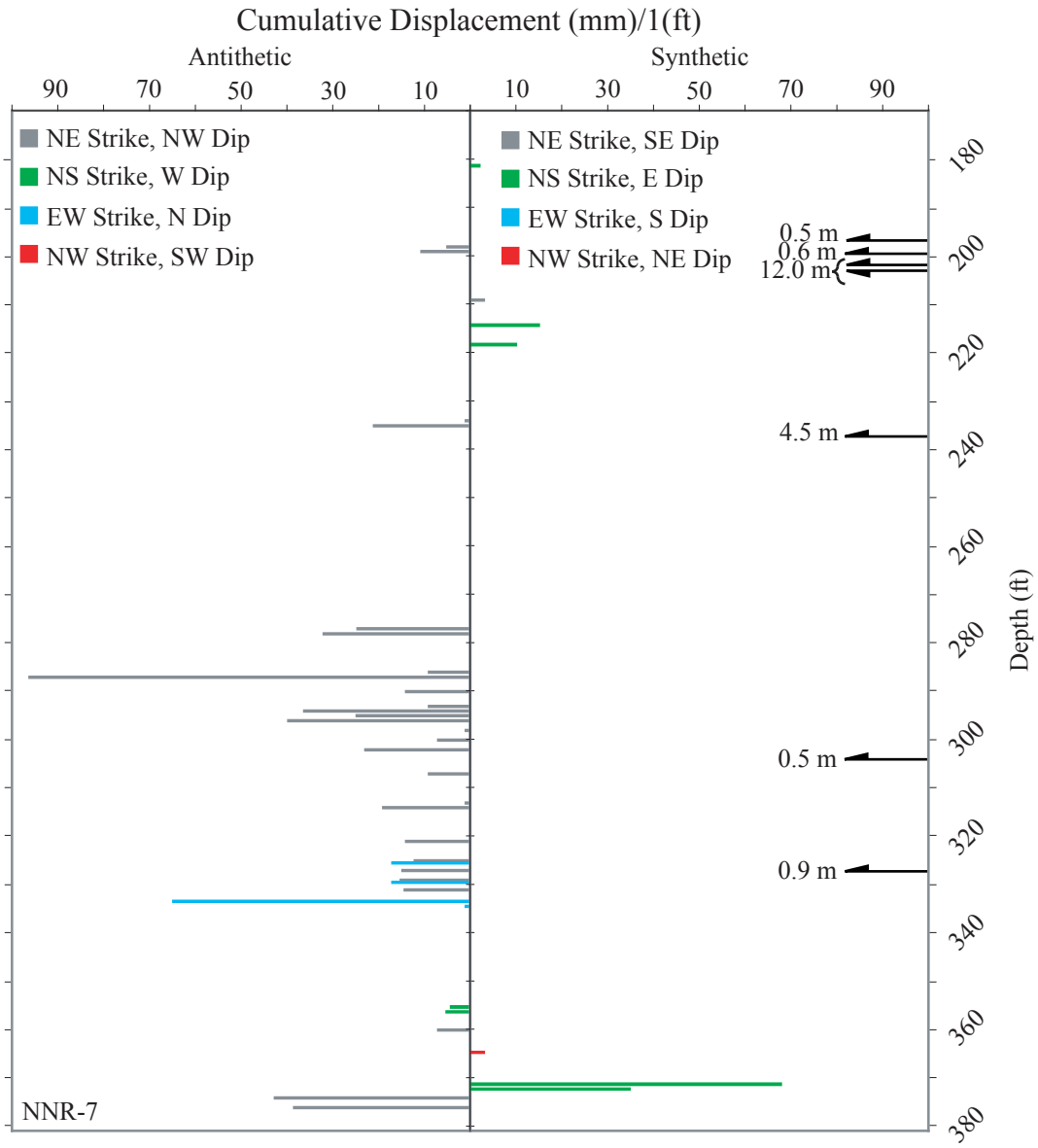

Fig. 51. Borehole NNR-7: Distribution of small faults with reverse-slip, showing associated fault strike, dip polarity and cumulative displacement per foot. Strike bins are as follows: (NE strike) N30-70E, (NS strike) N29W to N29E, (EW strike) N71E to S71E and (NW strike) N30-70W. Small faults that dip synthetic to the Nobles fault are the histograms on the right; while antithetic dipping small faults are the histogram on the left. Location of large faults (black arrows) and stratigraphic throw (m) determined by Wilson (2001) are noted on the far right.

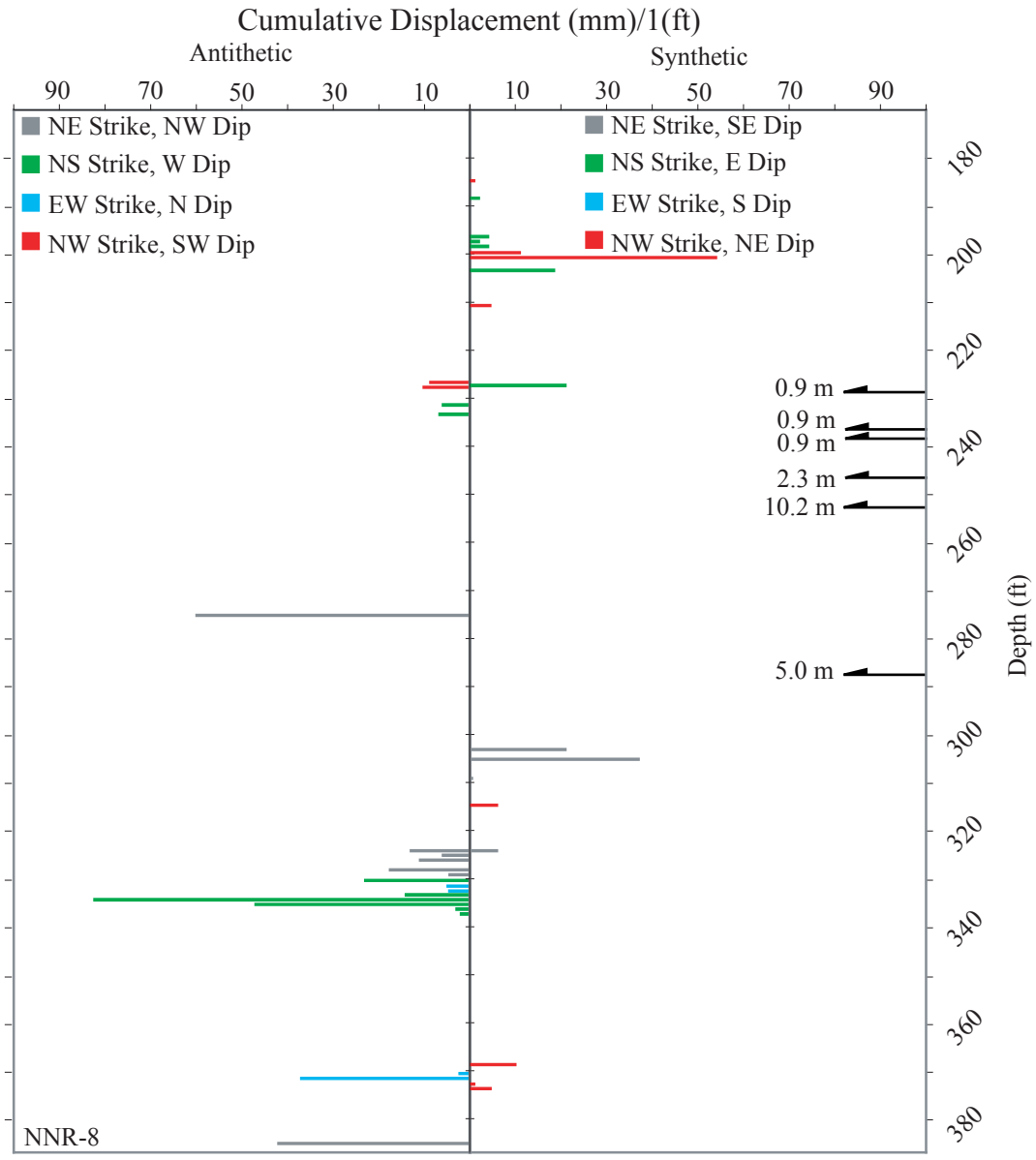

Fig. 52. Borehole NNR-8: Distribution of small faults with reverse-slip, showing associated fault strike, dip polarity and cumulative displacement per foot. Strike bins are as follows: (NE strike) N30-70E, (NS strike) N29W to N29E, (EW strike) N71E to S71E and (NW strike) N30-70W. Small faults that dip synthetic to the Nobles fault are the histograms on the right; while antithetic dipping small faults are the histogram on the left. Location of large faults (black arrows) and stratigraphic throw (m) determined by Wilson (2001) are noted on the far right.

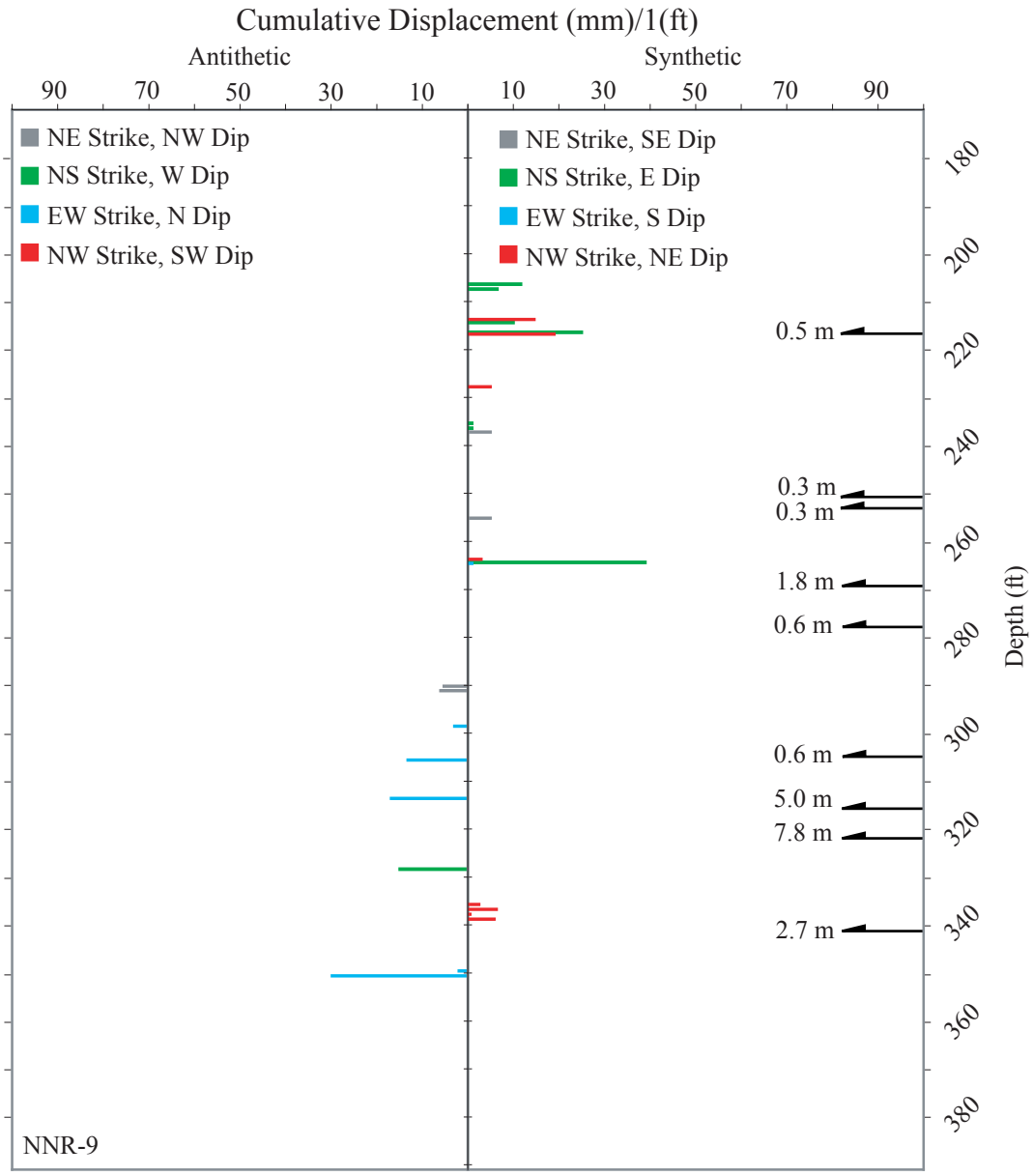

Fig. 53. Borehole NNR-9: Distribution of small faults with reverse-slip, showing associated fault strike, dip polarity and cumulative displacement per foot. Strike bins are as follows: (NE strike) N30-70E, (NS strike) N29W to N29E, (EW strike) N71E to S71E and (NW strike) N30-70W. Small faults that dip synthetic to the Nobles fault are the histograms on the right; while antithetic dipping small faults are the histogram on the left. Location of large faults (black arrows) and stratigraphic throw (m) determined by Wilson (2001) are noted on the far right.

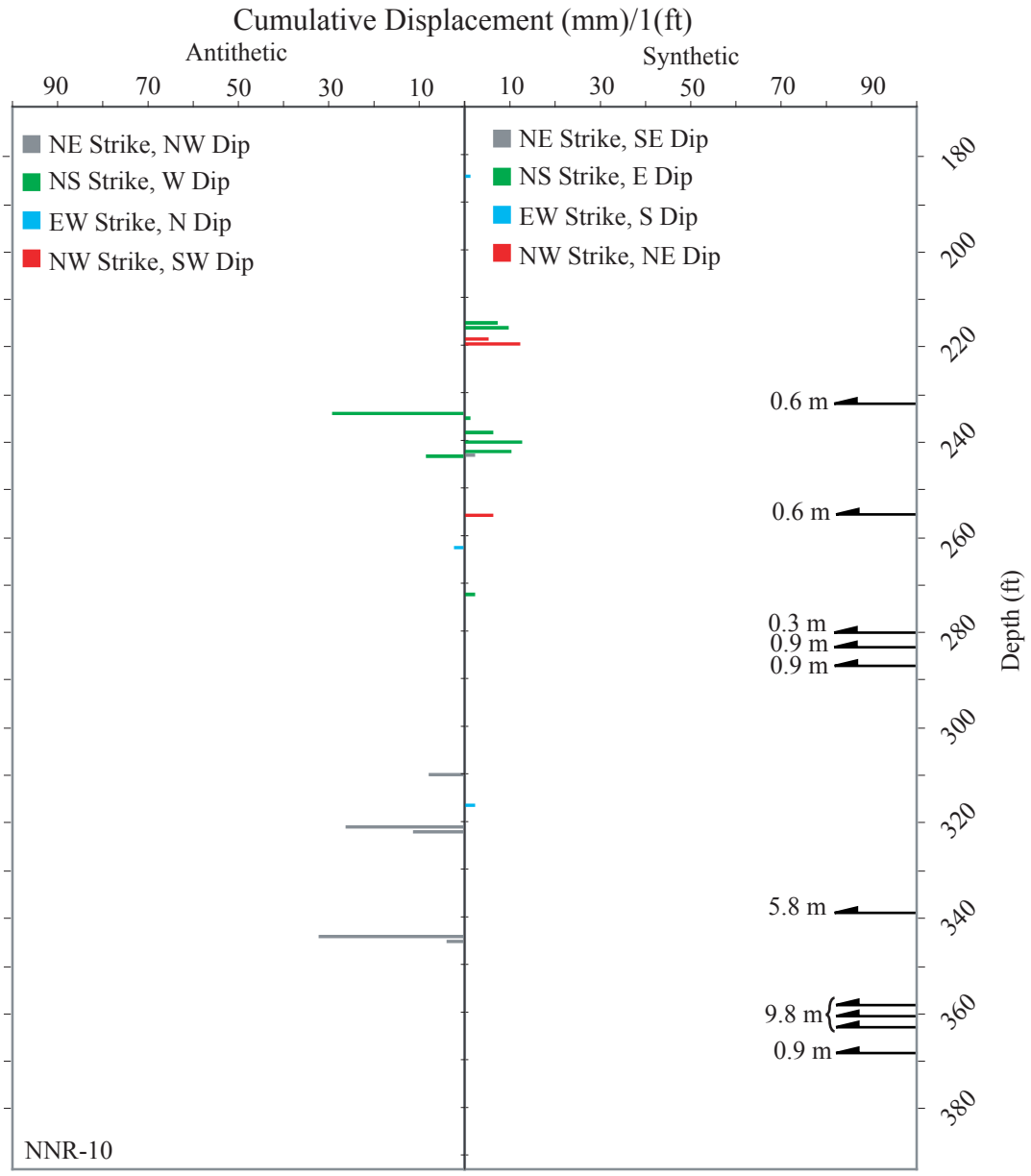

Fig. 54. Borehole NNR-10: Distribution of small faults with reverse-slip, showing associated fault strike, dip polarity and cumulative displacement per foot. Strike bins are as follows: (NE strike) N30-70E, (NS strike) N29W to N29E, (EW strike) N71E to S71E and (NW strike) N30-70W. Small faults that dip synthetic to the Nobles fault are the histograms on the right; while antithetic dipping small faults are the histogram on the left. Location of large faults (black arrows) and stratigraphic throw (m) determined by Wilson (2001) are noted on the far right.

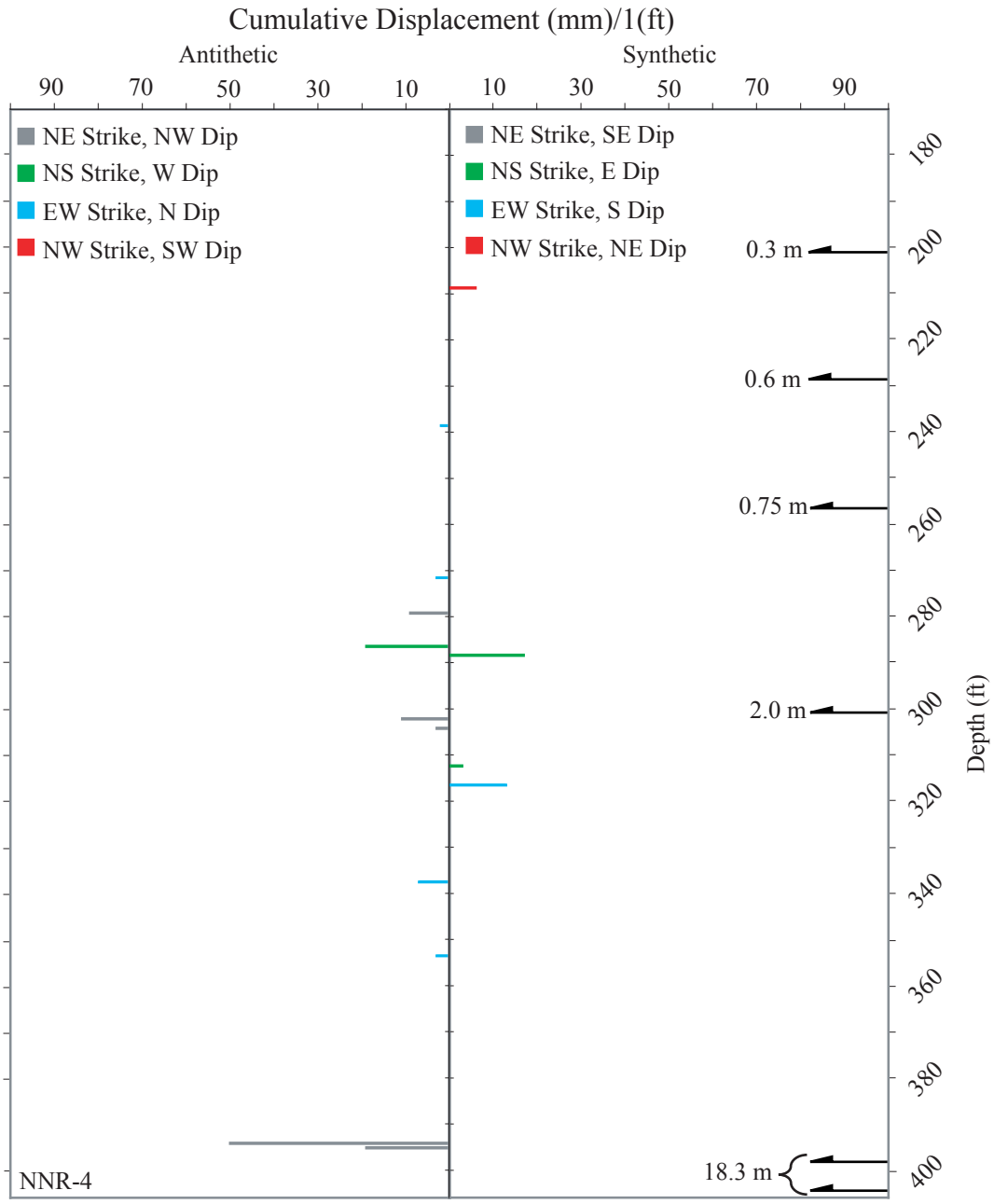

Fig. 55. Borehole NNR-4: Distribution of small faults with reverse-slip, showing associated fault strike, dip polarity and cumulative displacement per foot. Strike bins are as follows: (NE strike) N30-70E, (NS strike) N29W to N29E, (EW strike) N71E to S71E and (NW strike) N30-70W. Small faults that dip synthetic to the Nobles fault are the histograms on the right; while antithetic dipping small faults are the histogram on the left. Location of large faults (black arrows) and stratigraphic throw (m) determined by Wilson (2001) are noted on the far right.

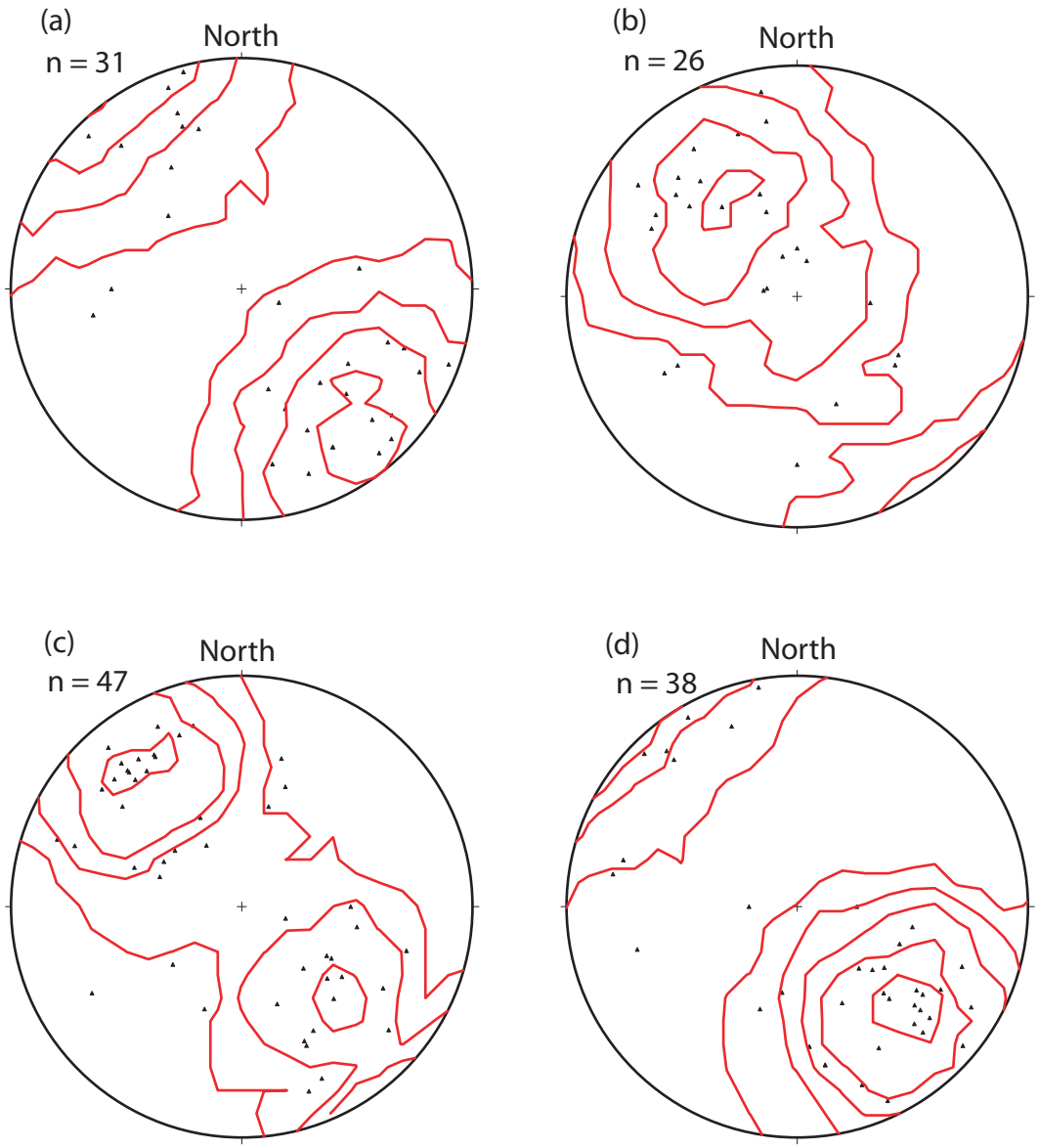

Fig. 56. Stereonet plots of faults with known cross-cutting relative ages. (a) Small faults within the hanging wall portion of the Nobles Fault that are older in age, (b) hanging wall younger faults, (c) footwall older faults, and (d) footwall younger faults. All plots are equal area, lower hemisphere projection, stereonet plots with best fit poles using Kamb contouring with contour interval of 2σ.

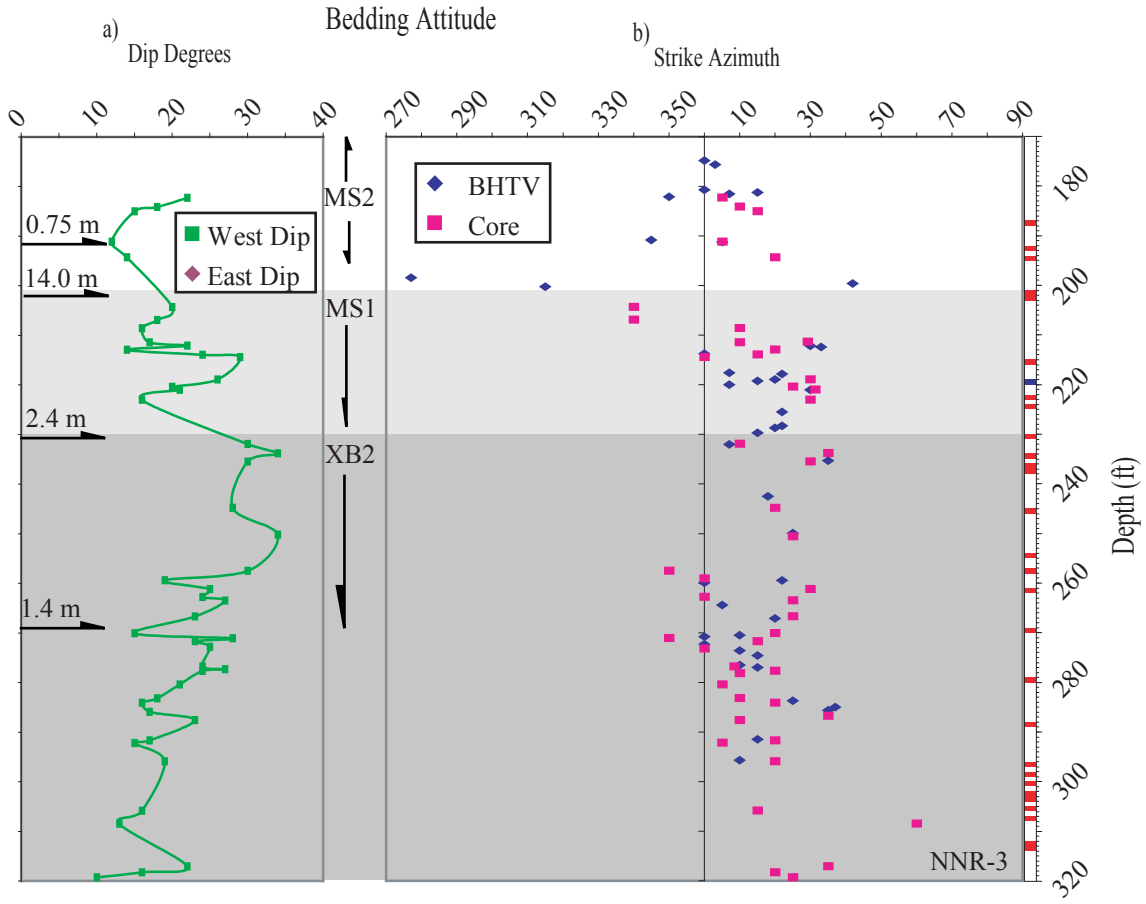

Fig. 57. Borehole NNR-3 bedding attitudes and BHTV-log correlations. (a) Bedding dip amount and dip direction East or West. Locations of large faults are marked with blacks arrows along with associated stratigraphic throw (m). (b) Bedding strike azimuth from core and BHTV. Right column show location where core and BHTV logs were correlated (red) as well as missing core intervals (blue). Lithofacies shown as shaded tones.

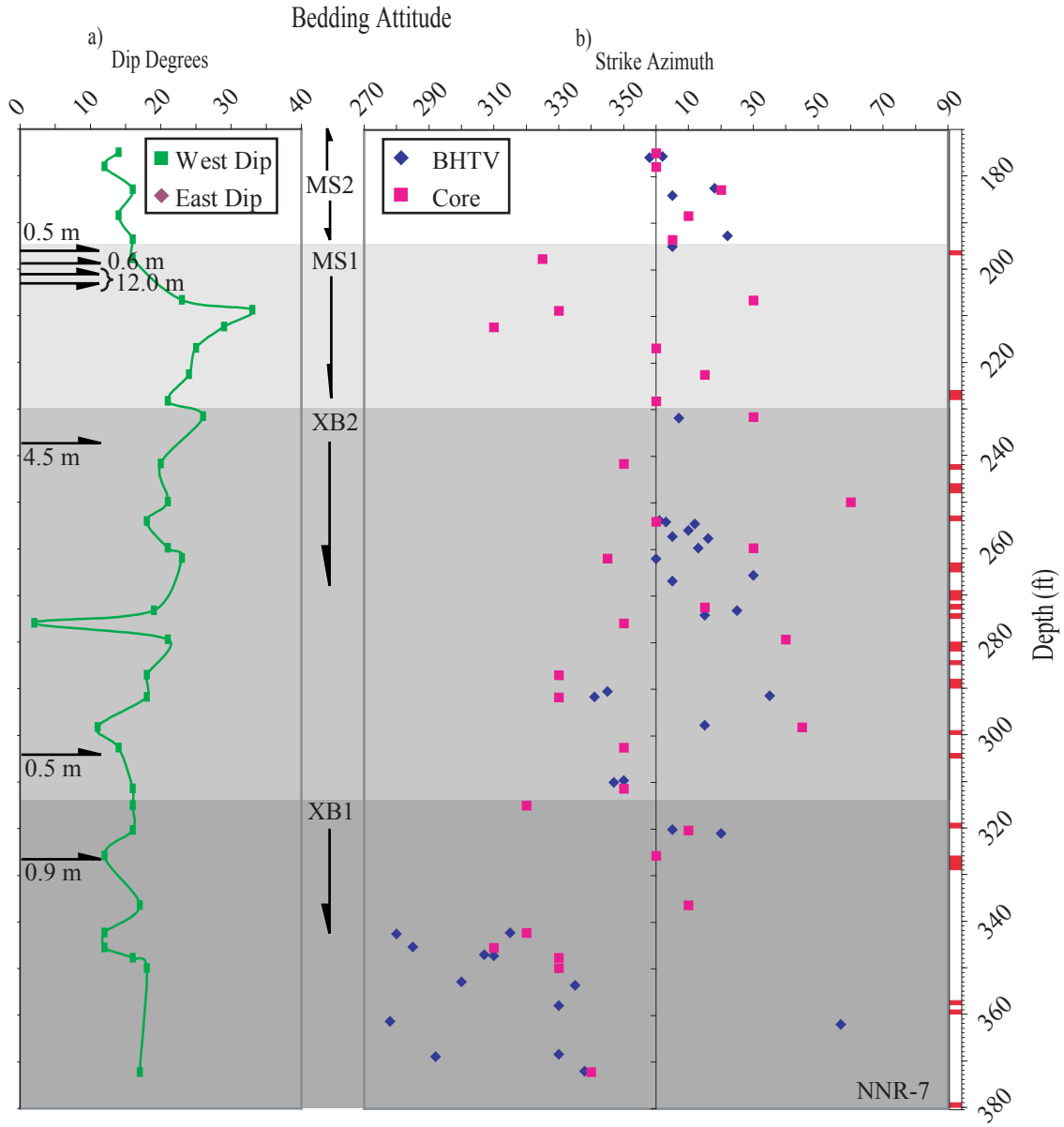

Fig. 58. Borehole NNR-7 bedding attitudes and BHTV-log correlations. (a) Bedding dip amount and dip direction East or West. Locations of large faults are marked with blacks arrows along with associated stratigraphic throw (m). (b) Bedding strike azimuth from core and BHTV. Right column show location where core and BHTV logs were correlated (red) as well as missing core intervals (blue). Lithofacies shown as shaded tones.

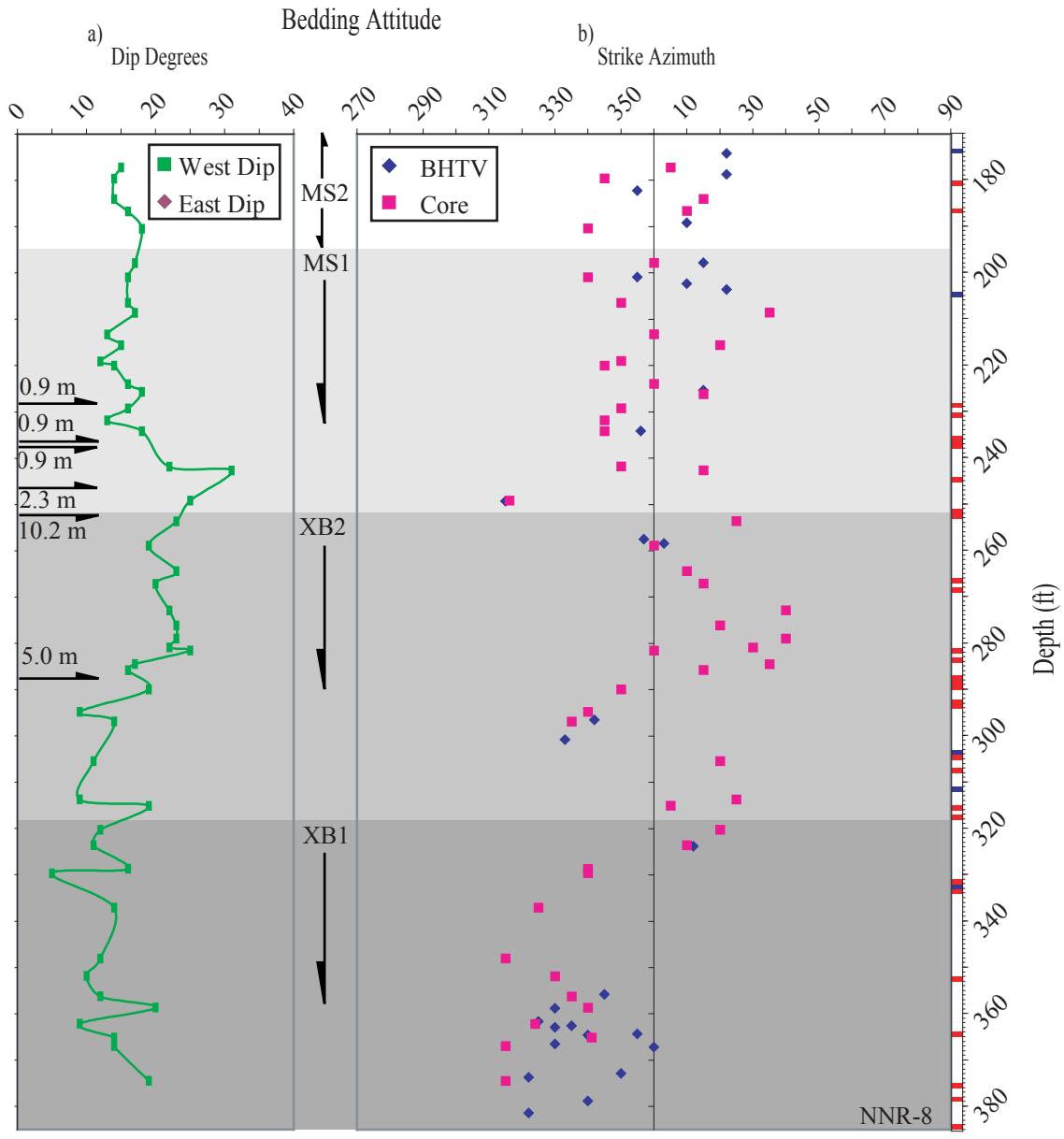

Fig. 59. Borehole NNR-8 bedding attitudes and BHTV-log correlations. (a) Bedding dip amount and dip direction East or West. Locations of large faults are marked with blacks arrows along with associated stratigraphic throw (m). (b) Bedding strike azimuth from core and BHTV. Right column show location where core and BHTV logs were correlated (red) as well as missing core intervals (blue). Lithofacies shown as shaded tones.

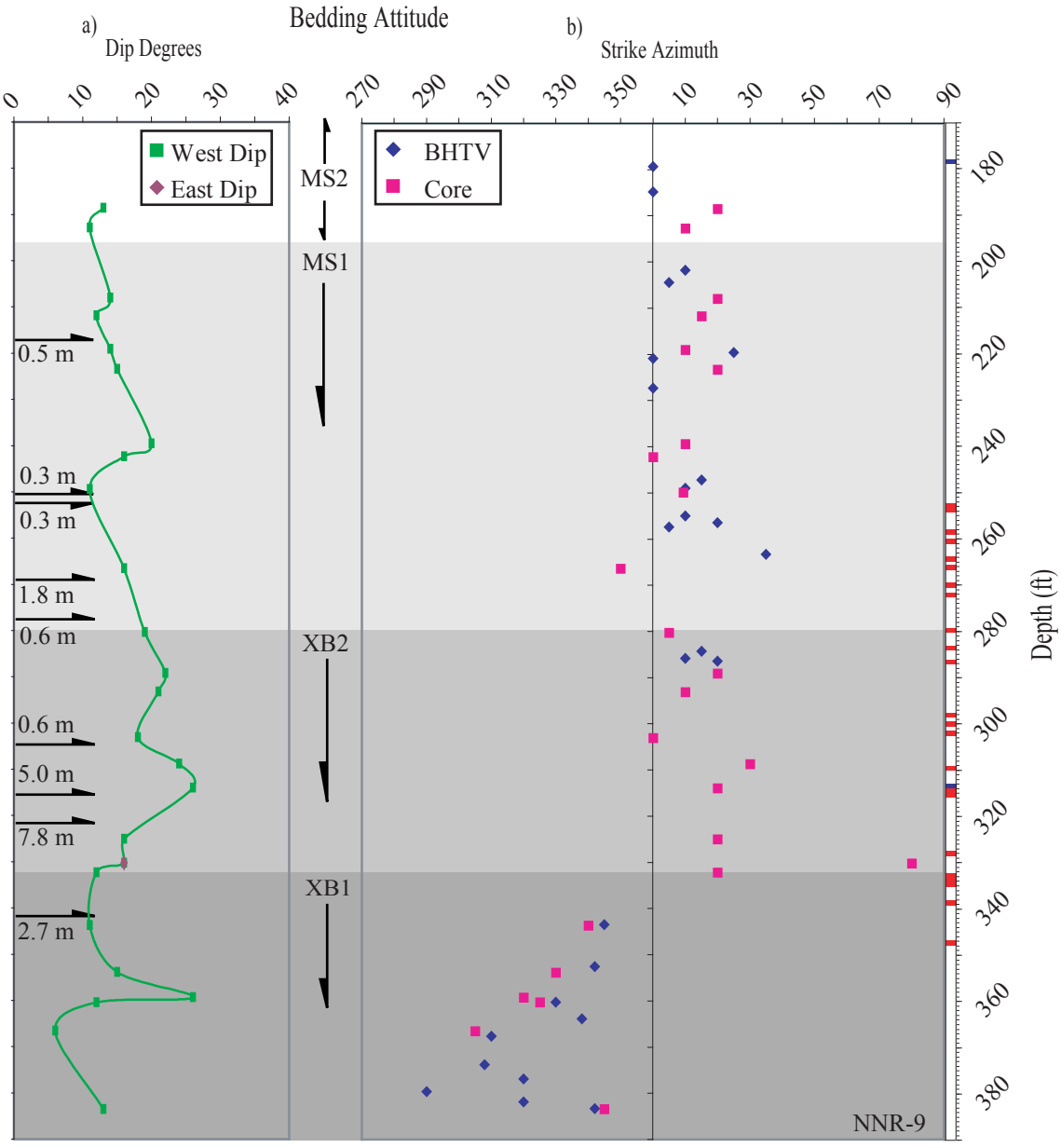

Fig. 60. Borehole NNR-9 bedding attitudes and BHTV-log correlations. (a) Bedding dip amount and dip direction East or West. Locations of large faults are marked with blacks arrows along with associated stratigraphic throw (m). (b) Bedding strike azimuth from core and BHTV. Right column show location where core and BHTV logs were correlated (red) as well as missing core intervals (blue). Lithofacies shown as shaded tones.

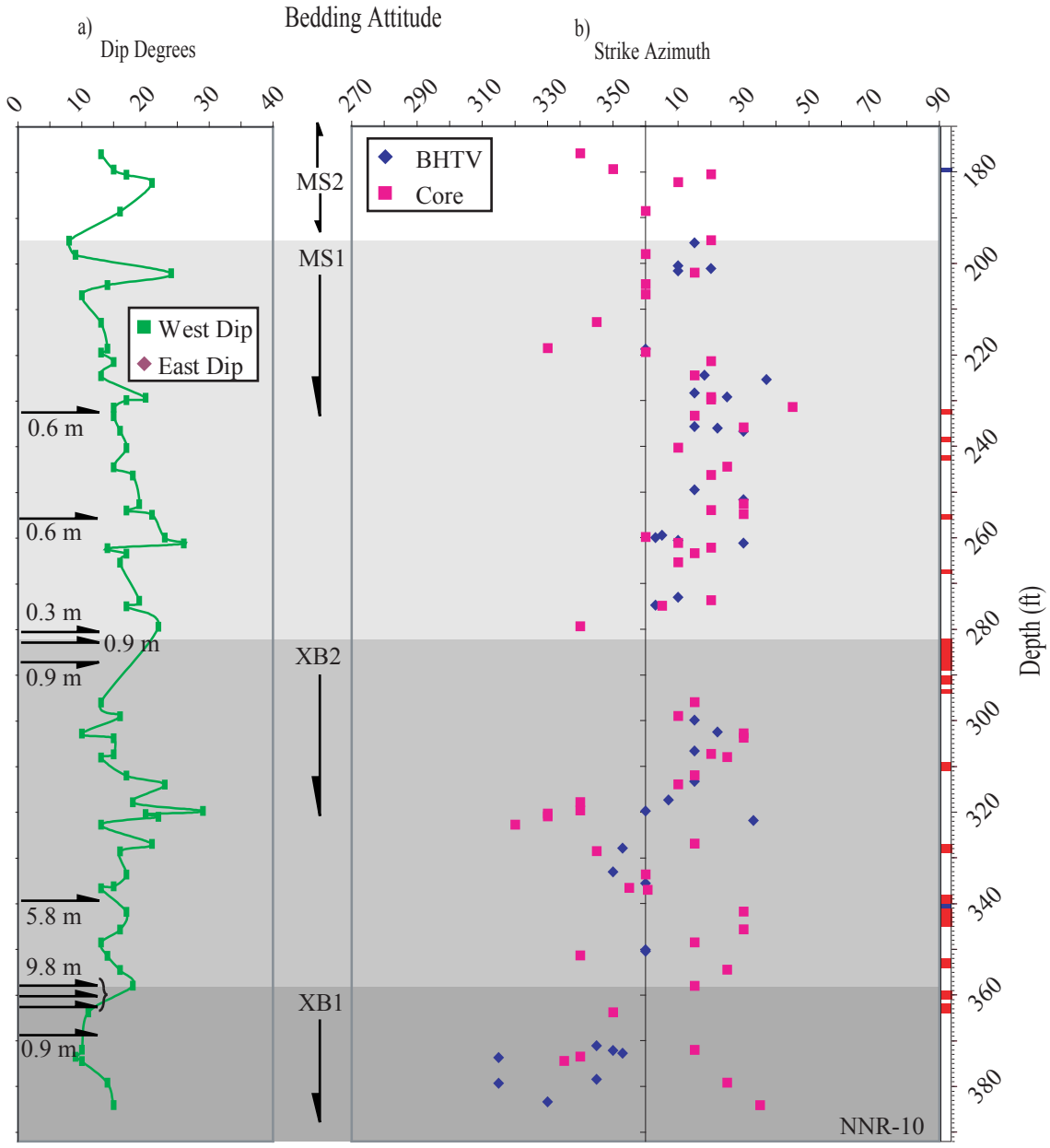

Fig. 61. Borehole NNR-10 bedding attitudes and BHTV-log correlations. (a) Bedding dip amount and dip direction East or West. Locations of large faults are marked with blacks arrows along with associated stratigraphic throw (m). (b) Bedding strike azimuth from core and BHTV. Right column show location where core and BHTV logs were correlated (red) as well as missing core intervals (blue). Lithofacies shown as shaded tones.

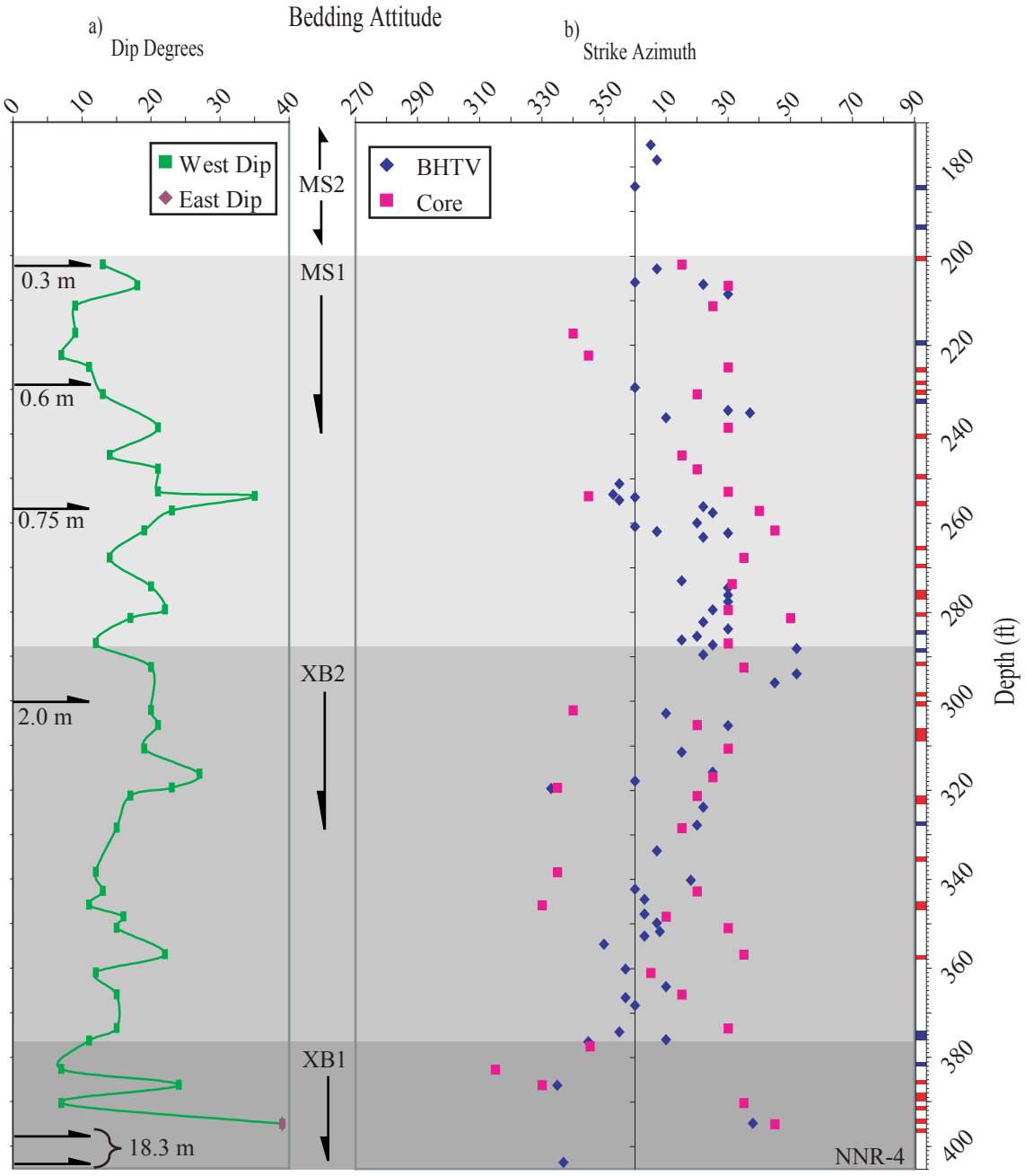

Fig. 62. Borehole NNR-4 bedding attitudes and BHTV-log correlations. (a) Bedding dip amount and dip direction East or West. Locations of large faults are marked with blacks arrows along with associated stratigraphic throw (m). (b) Bedding strike azimuth from core and BHTV. Right column show location where core and BHTV logs were correlated (red) as well as missing core intervals (blue). Lithofacies shown as shaded tones.

Bedding strike measurements exhibit significant variability. The approximate average strike is N to N15E, except for beds in the Lower Hickory XB1 subfacies. The variability probably is a result of bedding surfaces being non horizontal depositional surfaces. Dip amounts of bedding determined in oriented core, average 15° but range from a maximum of 40° to a minimum of 3°. All but two of the dips recorded are westerly. Dip angle reflects a combination of structural rotation of bedding and an initial, inclined depositional surface. The average dip of 15° to the west is interpreted to be a consequence of structural dip.

No systematic overall change in bedding dip angle occurs with depth, but local zones of steeper than average dip occur. For example, a zone of consistently large dip occurs within NNR-3 from 230 - 250 ft (Fig. 57). Within NNR-8 from 240 - 280 ft this same pattern of dip change also occurs (Fig. 59). The upper portion of NNR-7 has an average dip of 15°, then abruptly increases near a depth of 208 ft (Fig. 58), after which the dip amount generally decreases with depth.

6. INTERPRETATION OF RESULTS

This research examines small faults in detail and characterizes their spatial, geometric and kinematic attributes. Variability in observed spatial locations and magnitude of small faults can be accounted for by different cause and effect relationships. Cause and effect relationships for small faults are found to be either due to lithologic controls or structural position. Variability of structural elements within the core due to structural position is found to be a consequence of: 1) bedding rotation, 2) lithologic control, 3) reactivation of basement fractures, 4) lateral proximity to large faults and 5) fault-fault interaction. The following discussion seeks to explain the observed variability of structural elements found within core.

6.1 Bedding Rotation

Wilson (2001) noted a significant change of bedding strike and dip across the Nobles Fault, which implies that rotation of bedding occurred during deformation. To evaluate the possibility that bedding rotation occurred; bedding attitudes were determined in the oriented core with respect to depth and proximity to the Nobles Fault. Structural rotation of bedding during formation of the large fault system could have generated associated shear strain which might be manifested in small fault development.

Wilson (2001) reports bedding attitudes from surface exposures in the hanging wall and from three-point calculations for laterally continuous beds in the subsurface. At the surface, a single bedding attitude of N9W 13SW is measured. Three-point calculations for beds located 10 - 50 ft (3.05 - 15.24 m) below the surface, have an average attitude of N19W 5SW. Laterally continuous beds in the Lower Middle Hickory (MS1 and MS2 subfacies) are located in the hanging wall and in close proximity to the Nobles Faults have an average attitude of N5E 14NW. I independently determined bedding attitudes using BHTV and oriented core in the same region and observed that within MS1 and MS2 subfacies that bedding on average is oriented N10E 15NW, which agrees with the previous work of Wilson (2001) (Figs. 59 - 62). The observation that bedding attitudes change from a NW trend in the hanging wall near the

surface to a NNE strike in the hanging wall near the Nobles Fault suggests that during large fault development bedding rotated.

Assessing the structural influence of bedding attitudes in the footwall region of the Nobles Fault was difficult and open to debate because of a significant influence of primary depositional control on bedding attitudes. The dominant stratigraphic units in the footwall are the XB1 and XB2 facies of the Lower Hickory. As seen in Figures 58 - 60 bedding strike in XB2 is highly variable and differs significantly from that of XB1, which also exhibits significant variability. The strike of beds in the XB2 subfacies obtained from core dominantly strike to the NE, but alternates erratically between NW and NE directions. The strike then becomes dominantly NW within and near the XB1 subfacies. Three-point calculations of inferred laterally continuous beds in the lower portion of the XB2 subfacies near the transition to XB1 average N38W 12SW (Wilson 2001). Structural contours for the top of the Precambrian granite also have a NW strike with an average attitude of N56W 10SW (Wilson 2001). There is a readily discernable localized change in strike near the Nobles fault (e.g. NNR-3 at 200 ft; NNR-7 at 210 ft; NNR-8 at 250 ft; NNR-9 at 330 ft; and NNR-4 at 390 ft), but systematic change is unclear. The observation that bedding attitudes in the XB1 and XB2 subfacies change from NNE to NW near the XB1 depositional contact suggests that average bedding strike measured within core reflect primary depositional features that mask any systematic structural control, should it exist.

Although strike data provides little support for bedding rotation in the footwall, bedding dip does show spatial variation supportive of some enhanced rotation near the large faults. Bedding dips in excess of 30˚ are located within close proximity to larger faults (e.g. NNR-3 from 230 – 235 ft; NNR-4 at 255 ft, 395 ft; NNR-7 at 210 ft; and NNR-8 at 245 ft). The increase in dip amount on both sides of Nobles Fault suggests that bedding has undergone some rotation. There are several locations away from large faults with anomalously steep dips (e.g. NNR-3 from 215 – 220 ft, 245 – 260 ft; and NNR-4 at 315 ft). Whether these reflect local structural control or effects of primary depositional features can be argued. There are places where anomalously steep dips

correlate with significant small fault clusters (e.g. NNR-3 at 245 ft; and NNR-4 at 290 ft). It is fairly clear that bedding as a whole has been rotated 15˚ to the west and southwest. Dips that are greater than about 10˚ - 15˚ appear difficult to solely attribute to primary depositional features. Clay drapes on large bar surfaces within the XB2 subfacies seen in a quarry near Voca, Tx rarely dip more than 10˚ (personal communication Brann Johnson).

6.2 Lithologic Controls

Different lithologies exhibit different mechanical properties. Hence, they may exhibit different faulting characteristics under similar deformation conditions. In order to determine the effect of lithology on small fault occurrence, a comparison between small faults in the Lower Hickory (sandstone-dominant) and small faults in the Lower Middle Hickory (mudstone-rich) was investigated. This analysis utilized data in core from boreholes located most laterally distant from the Nobles Fault, in an effort to minimize possible effects associated directly with the larger fault system.

For sandstone-dominant lithologies, data on faults in core from the Lower Hickory in GKR-5, NNR-3 and NNR-7 were used. Small faults within these intervals have an average cumulative displacement of 24.0 mm/ft and an average occurrence frequency of 1.4 faults per foot (Table 8).

The Lower Middle Hickory consists of sandstone interbedded with mudstone and is discernibly different from the Lower Hickory. Boreholes GKR-5 and NNR-4 were used to assess small fault attributes in this lithology. The upper portion of the Lower Middle Hickory is primarily mudstone-dominant and the small faults within this interval have an average cumulative displacement of 9.8 mm/ft (Table 8). The lower portion of the Lower Middle Hickory contains interbedded sandstone intervals. The average cumulative displacement of small faults within this interval is 8.4 mm/ft (Table 8). Small faults in both the mudstone-dominant and interbedded sandstone intervals have an average frequency of occurrence of 0.8 faults per foot. The similarity of the average small fault attributes suggests that these lithologies have a similar effect on small fault formation.

Table 8. Locations and values of data used in Figures 63 – 65.

Test	Borehole	Top	Bottom	Length	GR Fraction	Displacement(mm)/Length(ft)	# Faults/ Length(ft)	Distance to Nobles Fault (m)
Mud Rich	GKR-5	140	155	15	0.96	10.13	0.93	
Mud Rich	NNR-4	201	229	28	0.81	9.50	0.61	22.39
Interbedded	GKR-5	165	220	55	0.62	7.11	0.82	
Interbedded	NNR-4	235	270	35	0.61	9.73	0.80	14.42
Sandstone Dominate	GKR-5	238	286	48	0.15	28.86	1.50	
Sandstone Dominate	GKR-5	310	345	35	0.51	10.43	1.00	
Sandstone Dominate	NNR-3	245	275	30	0.03	40.59	1.70	10.00
Sandstone Dominate	NNR-3	276	320	44	0.09	24.03	1.30	14.40
Sandstone Dominate	NNR-7	270	314	44	0.07	24.13	1.52	11.16
Sandstone Dominate	NNR-7	301	345	44	0.34	16.00	1.32	13.71
Mud Rich lateral proximity	NNR-10	196	226	30	0.80	8.12	0.63	15.26
Mud Rich lateral proximity	NNR-8	196	227	31	0.97	8.28	0.94	5.66
Clay Rich lateral proximity	NNR-9	197	226	29	0.76	12.00	1.10	12.58
Interbedded Lateral Proximity	NNR-10	235	270	35	0.75	11.90	1.14	9.82
Interbedded Lateral Proximity	NNR-9	230	260	30	0.80	10.66	0.93	7.95
Sandstone Dominate Lateral Proximity	NNR-8	310	355	45	0.48	18.64	1.04	7.37
Sandstone Dominate Lateral Proximity	NNR-9	350	380	30	0.25	11.15	0.77	3.24
Basement	NNR-10	386	392	6	0.00	29.15	1.83	
Basement	NNR-7	374	380	6	0.00	33.09	2.17	
Basement	NNR-8	380	386	6	0.00	49.85	3.67	
Basement	NNR9	383	389	6	0.00	56.57	2.67	

Since differences and similarities in lithology between the mudstone-dominant and interbedded sandstone intervals of Lower Middle Hickory and sandstone-dominant Lower Hickory was observed in core, a quantifiable variable was desirable to distinguish between these lithologies. Gamma ray logs values are susceptible to clay content and are used routinely within the petroleum industry to distinguish between clean sand intervals and clay-rich intervals. The fraction of mudstone calculated from Gamma Ray logs within any interval in core was used to objectively quantify differences in lithology. The procedure used to determine mudstone fraction was outlined in Section (3.2).

The average cumulative displacement and average frequency of faults within the mudstone-dominant, interbedded sandstone and sandstone-dominant intervals were plotted against the calculated mudstone ratio for these intervals (Fig. 63). In comparison to sandstone-rich intervals, small faults occur less frequently in mudstone-rich intervals and the average amount of displacement that they accrue also is less as compared to the sandstone-rich intervals. It appears that the fraction of mudstone within an interval, irrespective of interbedding aspects, controls the average amount of deformation manifested by faults within that interval.

6.3 Reactivation of Basement Weaknesses

Becker (1985) and Hegdcoxe (1987) concluded from outcrop studies that deformation within the Hickory Sandstone is strongly controlled by re-activation of pre-existing weaknesses within the Precambrian basement. They observed an increase in fault density and a greater variety of fault attitudes near the basement as compared to higher stratigraphic positions. Low angle, reverse faults also have been observed to be more common in exposures of Hickory Sandstone only a small distance above the crystalline basement (personal communication Brann Johnson). Small faults within the core near the basement exhibit a significant range of attitudes; in addition to differences between adjacent boreholes.

Direct determination of fault attitudes in the Precambrian granite at the study site was not possible, except for one fault in NNR-7. This fault is oriented N10W 32SW. The dominant strike of small faults within NNR-7 near the basement (i.e. 360 ft –

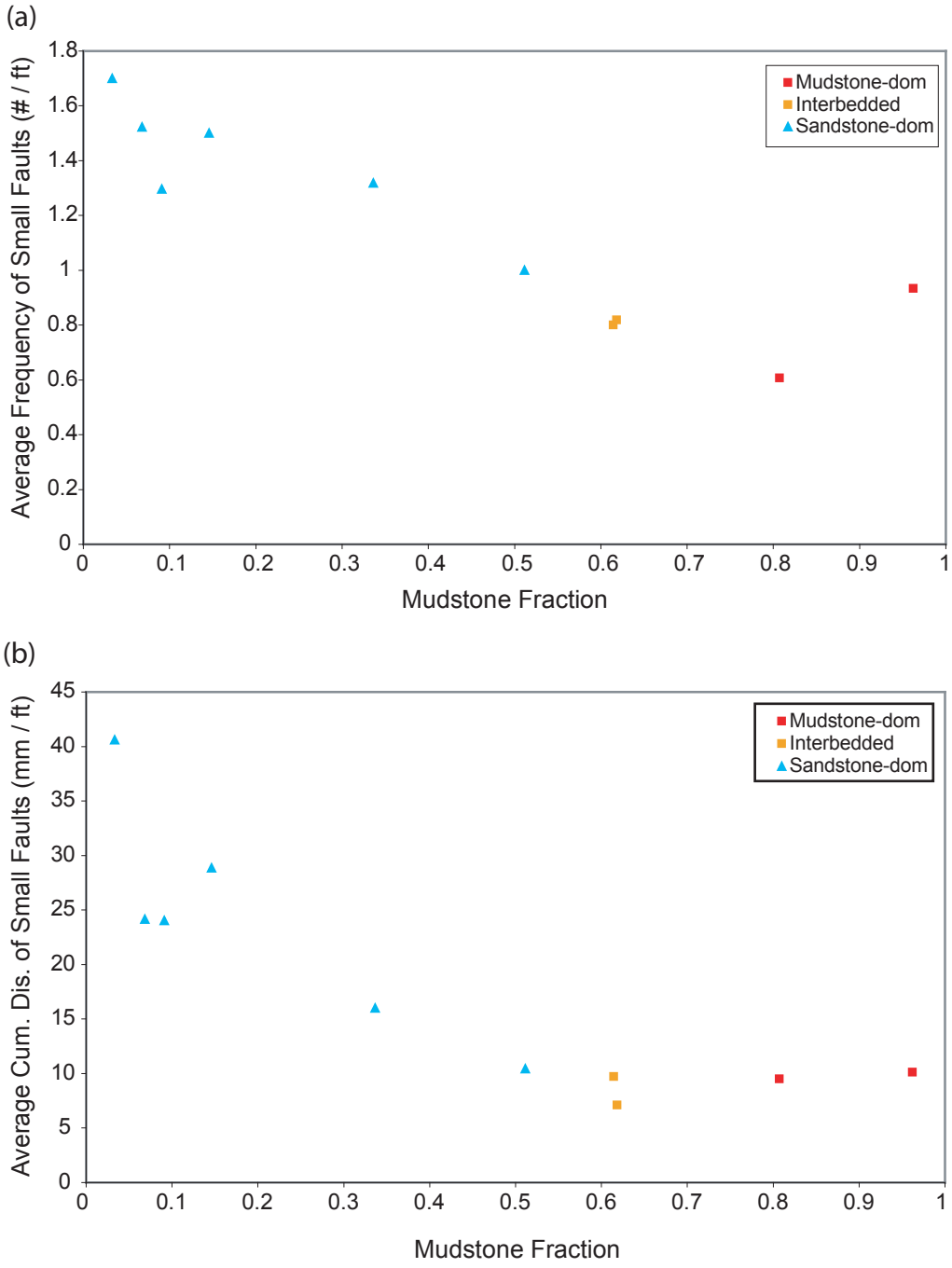

Fig. 63. Comparison of small fault "densities" for far-field test of small faults within mudstone-dominant, interbedded sandstone and sandstone-dominant intervals. (a) Frequency of small faults and (b) cumulative displacement of small faults.

basement) is N and NW (Figs. 39 and 45), which closely matches the orientation of the fault contained within the granite basement. Small faults in NNR-8, near the basement (i.e. 360 ft – basement) exhibit substantial variability in strike (NE and NW), as compared to NNR-7 (Figs. 40 and 46). This difference might be related to the influence of an intermediate fault in the interval, but it could also reflect a basement influence. Orientations of small faults within NNR-9 near the basement (i.e. 370 ft – basement) encompass both of the dominant characteristic of small faults in NNR-7 and 8 (N and NE trend in strike) (Figs. 41 and 47).

6.3a Fault Occurrence and Displacement Attributes

Variability in small faults attitudes near the basement strongly suggests that small faults in these locations are associated with some external influence. In order to address if this influence not only controls orientation, but also magnitude of small faults, average cumulative displacement and average frequency counts were generated for a 6 ft (1.83 m) interval immediately above the basement and was compared to similar lithologies stratigraphically higher in core (Table 8). The ability to objectively quantify mudstone fraction using Gamma Ray logs near the basement is hampered due to the presence of potassium feldspar minerals in the subarkosic basal Hickory. Visual inspection of core near the basement reveals that the lithology is essentially composed of 100 % mudstone-free sandstones. Thus, a value of zero was chosen to represent the fraction of mudstone within the interval above the basement. If the average frequency of small fault in the 6 ft (1.83 m) interval above the basement are compared to sandstone-dominate interval higher in the core, it is observed that small faults occur in higher concentrations near the basement (Fig. 64a). This observation is in agreement with the qualitative inferences of Becker (1985) and Hedgcoxe (1987). In addition to the increased fault density, the average cumulative displacement of small faults within the 6 ft (1.83 m) interval above the basement is greater than the average cumulative displacement for small faults in clean sandstone intervals higher stratigraphically in the core (Fig. 64b).

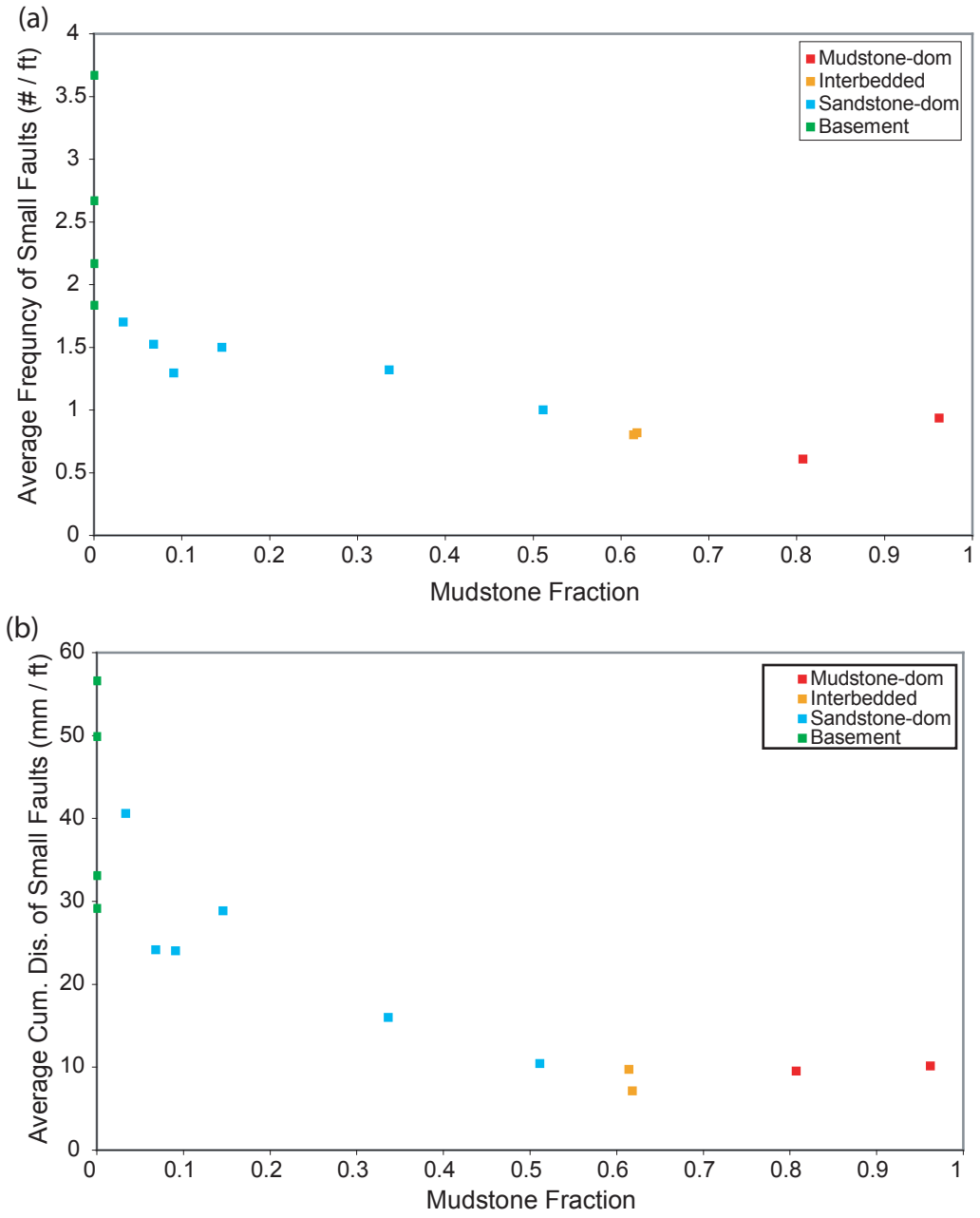

Fig. 64. Comparison of small fault "densities" immediately above the basement and data points of established lithologic control from far-field test. (a) Frequency of small faults and (b) cumulative displacement of small faults.

6.4 Lateral Proximity

A number of prior studies have noted that a higher density of small displacement faults occur with increasing proximity to larger faults (Jamison, 1979; Young, 1982; Hedgcoxe, 1987; Knott et al., 1996; Bernard and Labaume, 2002). In context to these observations, this study investigates whether higher frequencies of small faults are observed to occur in proximity to the large faults of the Nobles Fault system. As noted earlier (section 5.1), a qualitative examination of the spatial distribution of small faults shows that no simple systematic variability is universally observed with an increase in proximity to large faults for this data set. In fact, there are situations where small faults are only sparsely developed adjacent a large fault. The following text seeks to quantify and explain the variability of small faults in close proximity to large faults.

Since lithologic differences, especially mudstone content, affect the frequency and cumulative displacement of small faults in a given interval, any attempt to compare distributions of small faults as a function of lateral distance to larger faults must take lithologic controls into account. Consequently, average cumulative displacement and average frequency of small faults were determined for the same stratigraphic intervals but with different lateral positions relative to the Noble Fault. Some of the stratigraphic intervals are the same that were used to assess lithologic effects. To these have been added samples of the same stratigraphic interval but explicitly selected to be at different lateral distances relative to the Nobles Fault (Table 8). Note that these data come from samples intervals that are no closer than 3 m (9.84 ft) from the Noble Fault. Figure 65 clearly demonstrates that lateral proximity to the Noble Fault has no discernable effect on the development of small faults. The additional data points for stratigraphic intervals closer to the Nobles Fault only serve to re-enforce the importance of lithologic control.

On might postulate it is necessary to sample closer than 3 m (9.84 ft) to a large fault in order to discern an effect. Therefore, the distribution of small faults within a 10 ft (3.05 m) vertical window on both sides of all large faults (i.e. thus the window is 20 ft in length) was calculated and compared to measures farther away from the faults. A comparison of the frequency histogram for small faults density within the 20 ft (7.01 m)

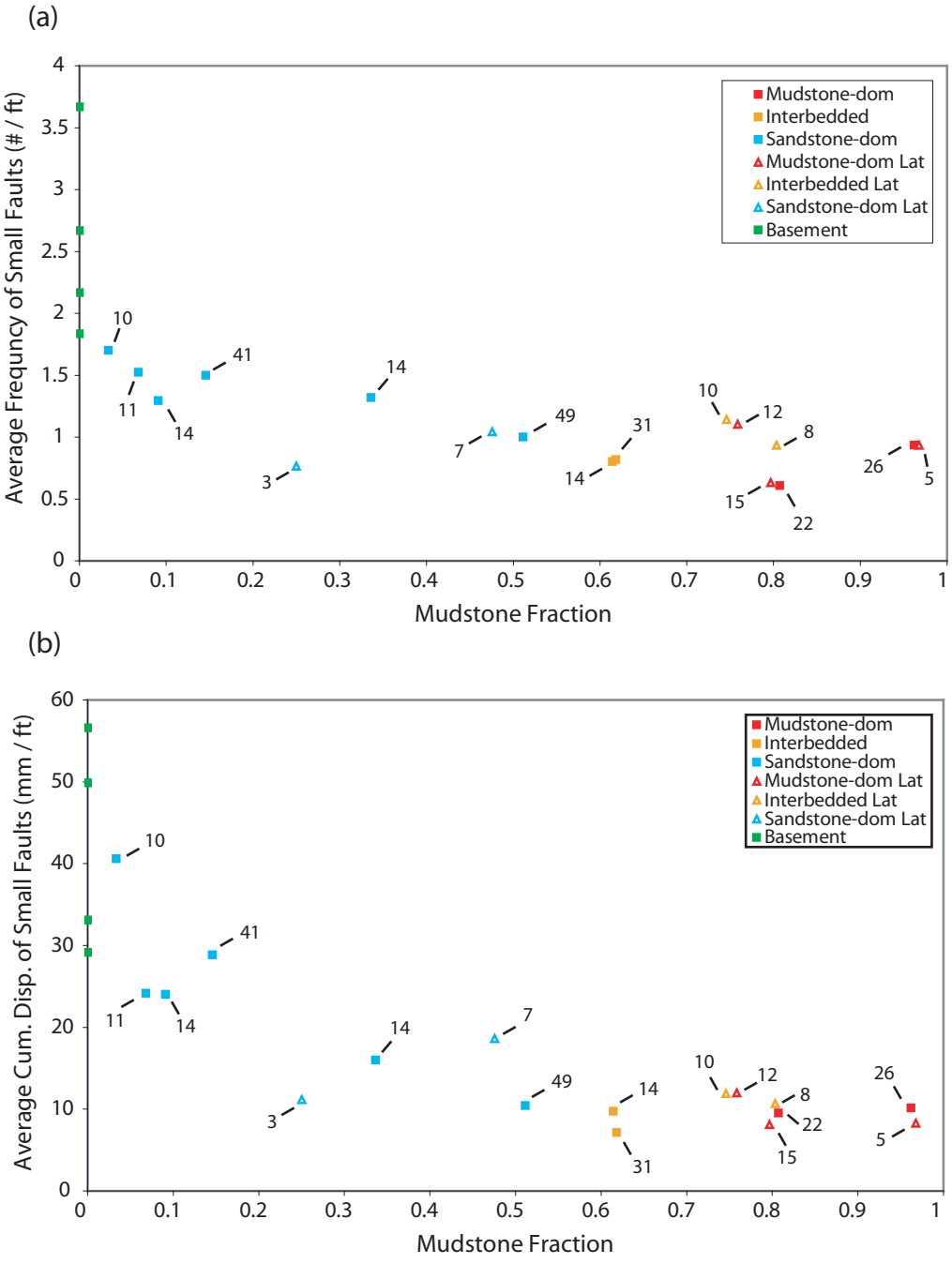

Fig. 65. Assessing the role of lateral proximity on small fault "density characteristics. (a) Frequency of small faults and (b) cumulative displacement of small faults. Lateral distance (m) to Nobles Fault is shown adjacent to data point.

windows adjacent to large faults and that of small fault density outside the 20 ft (7.01 m) windows, appear too have similar distributions (Fig. 66a and b). Although, the histogram for small faults within the 20 ft (7.01 m) windows has fewer intervals with no small fault occurrence. This is suggestive that, on average, there is a slight overall enhancement of small faults in the 20 ft (7.01 m) window.

One might expect that if small faults have a higher density near large faults, then cumulative displacement for these faults might be larger. Frequency distributions of cumulative displacement per foot for intervals within the 20 ft (7.01 m) window were compared with distributions outside the 20 ft (7.01 m) window (Fig 66c and d). Footage in which no cumulative displacement occurs was omitted and the data were logarithmically transformed in order to perform parametric tests. Histograms of log cumulative displacement for small faults within and outside the 20 ft (7.01 m) window appear bimodal with similar variances. An f-test with a 95% confidence interval confirms ($p = 0.8706$) that the distributions have similar variance (Table 9). In fact, the two sample distributions come from the same population ($p = 0.6052$), thusly an increase in cumulative displacement is not observed within 10ft (3.05 m) of large faults.

Since some of the large faults have a displacement as small as 1 ft (0.30 m), an increase in host rock damage might not be distinguishable within a sampling window as large as 10 ft (3.05 m) away from a large fault. Consequently, large faults with displacement greater than 1.5 m (4.92 ft) were separated from their smaller counter parts and reanalyzed. Histograms for the cumulative displacement per foot of small faults within the 20 ft (7.01 m) window and outside the window have similar variance ($p = 0.9289$), but the means appear to be substantially different (Fig. 66e). T-tests confirm with a 95% confidence level that the two samples have different means ($p = 0.0021$). This implies that the cumulative displacement for small faults is greater near large faults with a displacement greater than 1.5 m (4.92 ft).

Although an increase in average cumulative displacement for small faults within a vertical distance of 10 ft (3.05 m) from a large fault with a stratigraphic throw greater than 1.5 m (4.92 ft) is observed, this analysis does not incorporate lithologic controls.

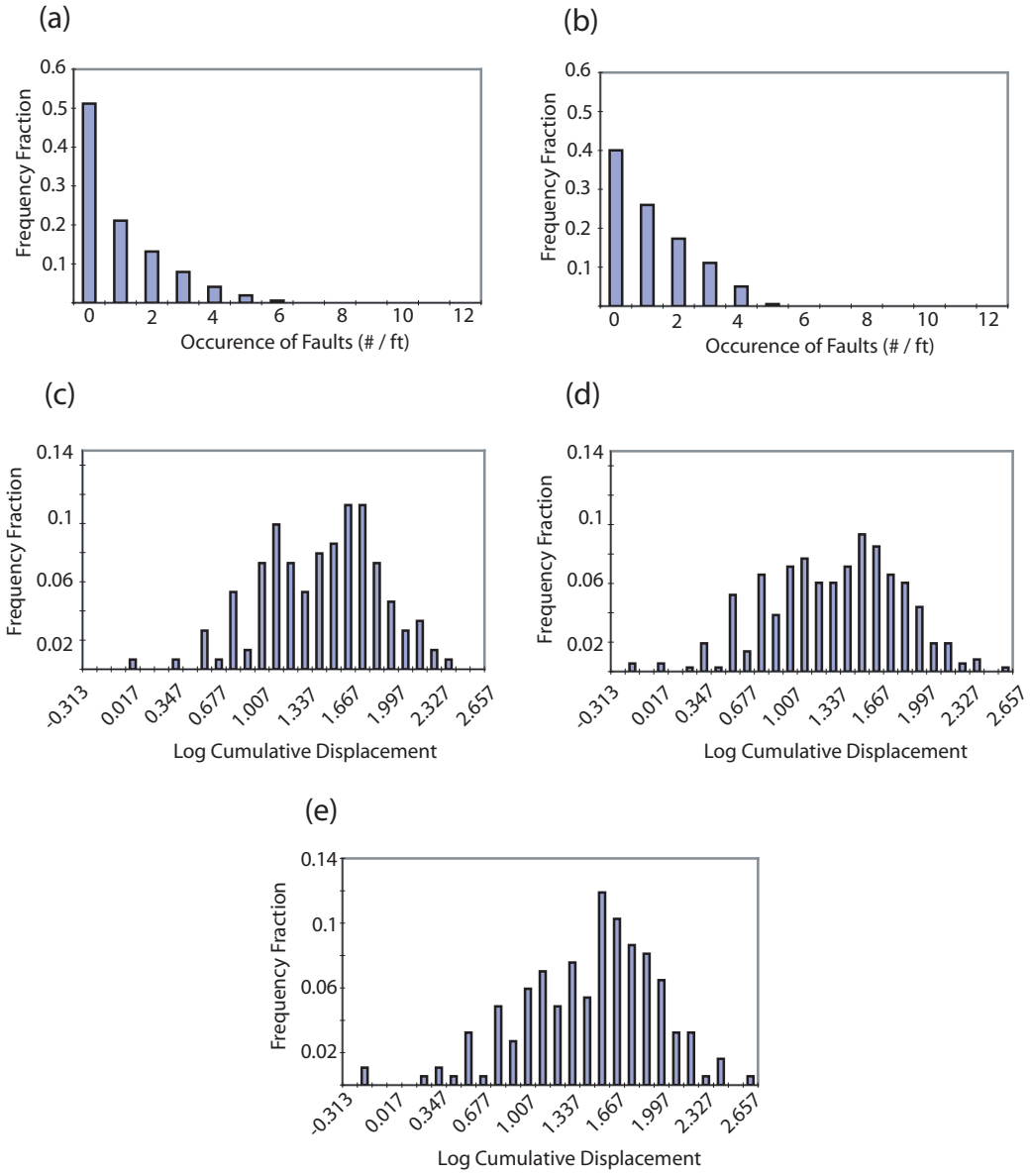

Fig. 66. Comparison of frequency characteristics of small fault measures inside and outside a 20 ft window adjacent large faults. (a) Frequency of small faults per foot outside the 20 ft windows, (b) frequency of small faults per foot inside the 20 ft windows. Logarithmically transformed cumulative displacement per foot of small faults (c) outside 20 ft windows, (d) inside 20 ft windows and (e) inside 20 ft windows only for larger faults with 1.5 m or greater displacement.

Table 9. Statistical tests of enhanced occurrence of small faults in close proximity to large faults. (a) Summary statistics (b) f-test and (c) t-test of small faults within 20 ft and 3 ft of large faults along with small faults outside the 20 ft and 3 ft window. Small faults within 20 ft and 3 ft of large faults with greater than 1.5 m of stratigraphic throw also are included.

(a)

	n	Mean	SD	SE
Outside 20ft	333	1.268	0.501	0.0275
Within 20ft	346	1.287	0.497	0.0267
Within 20ft > 1.5m	185	1.409	0.498	0.0366
Outside 3ft	528	1.242	0.507	0.0221
Within 3ft	151	1.403	0.445	0.0362
Within 3ft > 1.5m	64	1.484	0.417	0.0521

(b)

Alternative hypothesis	F statistic	95% CI	2-tailed p
Within 20ft ≠ Outside 20ft	0.98	0.79 to 1.22	0.8706
Within 20ft > 1.5m ≠ Outside 20ft	0.99	0.77 to 1.28	0.9289
Within 20ft ≠ Within 3ft	1.25	0.94 to 1.62	0.1214

(c)

Alternative hypothesis	Difference between means	95% CI	T statistic	2-tailed p
Outside 20ft ≠ Within 20ft	-0.020	-0.095 to 0.055	-0.52	0.6052
Outside 20ft ≠ Within 10ft > 1.5m	-0.141	-0.231 to -0.051	-3.09	0.0021
Outside 20ft ≠ Within 3ft	-0.116	-0.204 to -0.028	-2.58	0.0104

As shown earlier, mudstone content affects the average frequency and average cumulative displacement of small faults in a given interval. In order to asses the effect that lithology has on small faults within 10 ft (3.05 m) of all large faults, the average frequency and average cumulative displacement of these intervals is plotted against the mudstone fraction for these intervals (Fig. 67). Data from the basement and previous lateral proximity test are included for reference. From the scatterplots it is apparent that mudstone content still is a dominate control on small fault in close proximity to large faults, regardless of the magnitude of the large fault. All the extreme outliers associated with the "density" plots (Table 10) are found in borehole NNR-8 and are located between the Upper Fault and the main segment of the Nobles Fault (Segment 1). The extreme outliers associated with the cumulative displacement plot also come from the same locations in NNR-8; in addition, one data point is associated with the main portion of the Nobles Fault near the basement in NNR-4, approximately at a depth of 404 ft. All the extreme outliers are associated with zones of potential fault-fault interaction, thus the following section investigates this potential effect.

6.5 Fault-Fault Interaction

The Nobles Fault system is interpreted (Wilson 2001) to have evolved by interaction and linkage of two large faults. Field studies by Hedgcoxe (1987) and Schafer (2002) have observed that displacement transfer between interacting faults is accommodated by a number of small faults. Using the premise that an increase in cumulative displacement for small faults should reflect mechanical interactions of larger faults, cumulative displacement for small faults within a 3 ft (0.91 m) window around large faults was determined (Table 11). The sample window does not straddle large faults but was separated into a hanging wall and a footwall window. Although the sample windows are small, which will increase variability when comparing to large intervals, this window size was chosen because this is the maximum length in which two windows on adjacent large faults will not overlap one another. Thusly, a small fault will only be counted once.

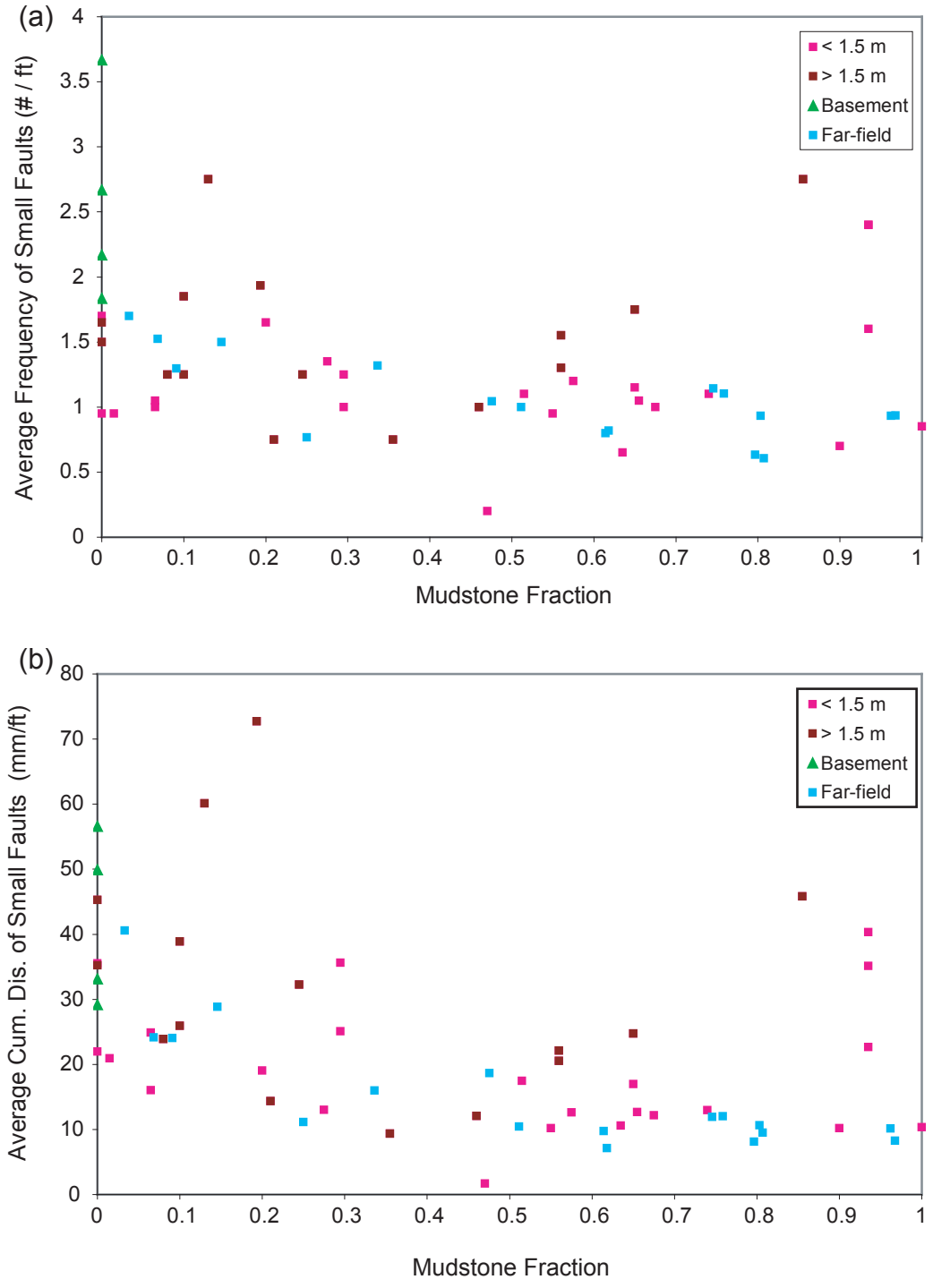

Fig. 67. Comparison of small fault "densities" within 10 ft of large fault that have greater than or less than 1.5 m of stratigraphic throw along with basement and data points of established lithologic control from far-field test. (a) Frequency of small faults and (b) cumulative displacement of small faults.

Table 10. Location and values of small fault "densities" within 10 ft of a large fault.

	Borehole	Top	Bottom	Length	GR Fraction	Displacement/Length	# Faults/ Length	Large fault Dis. (m)
Large Fault 232	NNR-10	222	242	20	0.90	10.19	0.70	0.6
Large Fault 255	NNR-10	245	265	20	0.68	12.19	1.00	0.6
Large Fault 280	NNR-10	270	290	20	0.07	16.05	1.05	0.6
Large Fault 283	NNR-10	273	293	20	0.02	20.95	0.95	0.9
Large Fault 287	NNR-10	277	297	20	0.00	21.96	0.95	0.9
Large Fault 339	NNR-10	329	349	20	0.36	9.35	0.75	5.8
Large Fault 358, 360, 363	NNR-10	350	370	20	0.10	38.91	1.85	9.8
Large Fault 368	NNR-10	358	378	20	0.30	35.61	1.25	0.9
Large Fault 192	NNR-3	182	202	20	0.52	17.46	1.10	0.75
Large Fault 202	NNR-3	192	212	20	0.56	22.11	1.55	14
Large Fault 231	NNR-3	221	241	20	0.21	14.34	0.75	2.4
Large Fault 269	NNR-3	259	279	20	0.07	24.91	1.00	1.4
Large Fault 201	NNR-4	191	211	20	0.47	1.67	0.20	0.3
Large Fault 228	NNR-4	218	238	20	0.64	10.58	0.65	0.6
Large Fault 256	NNR-4	246	266	20	0.58	12.60	1.20	0.75
Large Fault 300	NNR-4	290	310	20	0.10	25.93	1.25	2
Large Fault 396, 404	NNR-4	390	405	15	0.19	72.74	1.93	18.29
Large Fault 196	NNR-7	186	206	20	0.55	10.18	0.95	0.5
Large Fault 199	NNR-7	189	209	20	0.65	16.98	1.15	0.6
Large Fault 202, 205	NNR-7	193	213	20	0.65	24.74	1.75	12
Large Fault 237	NNR-7	227	247	20	0.00	45.26	1.50	4.5
Large Fault 304	NNR-7	294	314	20	0.20	19.06	1.65	0.5
Large Fault 327	NNR-7	317	337	20	0.28	13.01	1.35	0.9
Large Fault 228	NNR-8	218	238	20	0.94	22.65	1.60	0.9
Large Fault 236	NNR-8	226	246	20	0.94	35.14	2.40	0.9
Large Fault 238	NNR-8	228	248	20	0.94	40.34	2.40	0.9
Large Fault 246	NNR-8	236	256	20	0.86	45.81	2.75	2.3
Large Fault 252	NNR-8	242	262	20	0.56	20.53	1.30	10.2
Large Fault 287	NNR-8	277	297	20	0.13	60.11	2.75	5
Large Fault 216	NNR-9	206	226	20	1.00	10.32	0.85	0.5
Large Fault 250	NNR-9	240	260	20	0.74	12.98	1.10	0.3
Large Fault 252	NNR-9	242	262	20	0.66	12.68	1.05	0.3
Large Fault 268	NNR-9	258	278	20	0.25	32.26	1.25	1.8
Large Fault 277	NNR-9	267	287	20	0.30	25.07	1.00	0.6
Large Fault 304	NNR-9	294	314	20	0.00	35.52	1.70	0.6
Large Fault 315	NNR-9	305	325	20	0.00	35.24	1.65	5
Large Fault 321	NNR-9	311	331	20	0.08	23.88	1.25	7.8
Large Fault 341	NNR-9	331	351	20	0.46	12.07	1.00	2.7

Table 11. Location and values of small fault "densities" within 3 ft of a large fault.

	Borehole	Top	Bottom	Length	GR Fraction	Displacement/Length	# Faults/ Length	Large fault Dis. (m)
Large Fault 232	NNR-10	229	232	3	0.43	0.00	0.00	0.6
Large Fault 232	NNR-10	232	235	3	1.00	10.00	1.00	0.6
Large Fault 255	NNR-10	252	255	3	1.00	5.67	1.00	0.6
Large Fault 255	NNR-10	255	258	3	0.43	41.33	2.00	0.6
Large Fault 280	NNR-10	277	280	3	0.00	2.00	0.33	0.6
Large Fault 280	NNR-10	280	283	3	0.00	7.39	0.67	0.6
Large Fault 283	NNR-10	280	283	3	0.00	7.39	0.67	0.9
Large Fault 283	NNR-10	283	286	3	0.00	60.13	0.67	0.9
Large Fault 287	NNR-10	284	287	3	0.00	60.13	0.67	0.9
Large Fault 287	NNR-10	287	290	3	0.00	27.70	2.67	0.9
Large Fault 339	NNR-10	336	339	3	1.00	3.00	0.33	5.8
Large Fault 339	NNR-10	339	342	3	1.00	0.00	0.00	5.8
Large Fault 358, 360, 363	NNR-10	357	360	3	0.43	27.02	2.00	9.8
Large Fault 358, 360, 363	NNR-10	360	363	3	0.00	2.67	0.33	9.8
Large Fault 368	NNR-10	365	368	3	0.10	105.50	3.00	0.9
Large Fault 368	NNR-10	368	371	3	0.23	87.22	2.00	0.9
Large Fault 192	NNR-3	189	192	3	0.67	17.84	1.67	0.75
Large Fault 192	NNR-3	192	195	3	0.67	30.00	1.00	0.75
Large Fault 202	NNR-3	199	202	3	0.67	48.23	3.33	14
Large Fault 202	NNR-3	202	205	3	0.67	24.49	2.00	14
Large Fault 231	NNR-3	228	231	3	0.00	0.00	0.00	2.4
Large Fault 231	NNR-3	231	234	3	0.00	19.35	1.00	2.4
Large Fault 269	NNR-3	266	269	3	0.00	43.47	2.00	1.4
Large Fault 269	NNR-3	269	272	3	0.43	61.71	1.00	1.4
Large Fault 201	NNR-4	198	201	3	0.70	0.00	0.00	0.3
Large Fault 201	NNR-4	201	204	3	0.40	0.00	0.00	0.3
Large Fault 228	NNR-4	225	228	3	0.97	18.67	1.00	0.6
Large Fault 228	NNR-4	228	231	3	0.00	16.98	1.00	0.6
Large Fault 256	NNR-4	253	256	3	0.13	10.71	1.33	0.75
Large Fault 256	NNR-4	256	259	3	0.00	14.75	1.67	0.75
Large Fault 300	NNR-4	297	300	3	0.00	2.03	0.33	2
Large Fault 300	NNR-4	300	303	3	0.00	18.02	1.33	2
Large Fault 396, 404	NNR-4	397	400	3	0.00	154.93	1.67	18.29
Large Fault 396, 404	NNR-4	400	403	3	0.13	156.22	2.67	18.29
Large Fault 196	NNR-7	193	196	3	0.00	12.45	1.33	0.5
Large Fault 196	NNR-7	196	199	3	0.43	18.06	2.00	0.5
Large Fault 199	NNR-7	196	199	3	0.43	18.06	2.00	0.6
Large Fault 199	NNR-7	199	202	3	1.00	11.68	1.00	0.6
Large Fault 202, 205	NNR-7	200	203	3	1.00	0.00	0.00	12
Large Fault 202, 205	NNR-7	203	206	3	1.00	27.00	2.00	12

Table 11 Continued

Large Fault 237	NNR-7	234	237	3	0.00	30.04	1.67	4.5
Large Fault 237	NNR-7	237	240	3	0.00	67.24	2.00	4.5
Large Fault 304	NNR-7	301	304	3	0.23	24.07	1.33	0.5
Large Fault 304	NNR-7	304	307	3	0.00	30.70	2.33	0.5
Large Fault 327	NNR-7	324	327	3	0.33	29.45	2.67	0.9
Large Fault 327	NNR-7	327	330	3	0.67	26.93	2.33	0.9
Large Fault 228	NNR-8	225	228	3	1.00	17.32	1.67	0.9
Large Fault 228	NNR-8	228	231	3	0.67	30.84	2.00	0.9
Large Fault 236	NNR-8	233	236	3	1.00	46.55	4.00	0.9
Large Fault 238	NNR-8	235	238	3	1.00	61.75	4.67	0.9
Large Fault 236	NNR-8	236	239	3	1.00	59.82	4.33	0.9
Large Fault 238	NNR-8	238	241	3	1.00	68.54	3.67	0.9
Large Fault 246	NNR-8	243	246	3	1.00	43.29	3.33	2.3
Large Fault 246	NNR-8	246	249	3	1.00	55.57	2.00	2.3
Large Fault 252	NNR-8	249	252	3	0.87	35.46	2.00	10.2
Large Fault 252	NNR-8	252	255	3	0.67	5.00	0.67	10.2
Large Fault 287	NNR-8	284	287	3	0.00	69.58	3.33	5
Large Fault 287	NNR-8	287	290	3	0.53	64.81	3.33	5
Large Fault 216	NNR-9	213	216	3	1.00	47.23	2.67	0.5
Large Fault 216	NNR-9	216	219	3	1.00	38.80	1.67	0.5
Large Fault 250	NNR-9	247	250	3	1.00	5.33	1.00	0.3
Large Fault 252	NNR-9	249	252	3	0.90	7.08	1.00	0.3
Large Fault 250	NNR-9	250	253	3	0.87	17.19	2.00	0.3
Large Fault 252	NNR-9	252	255	3	0.77	13.38	2.00	0.3
Large Fault 268	NNR-9	265	268	3	0.77	17.39	1.00	1.8
Large Fault 268	NNR-9	268	271	3	0.87	40.79	1.67	1.8
Large Fault 277	NNR-9	274	277	3	0.00	32.89	1.33	0.6
Large Fault 277	NNR-9	277	280	3	0.10	23.67	0.33	0.6
Large Fault 304	NNR-9	301	304	3	0.00	23.59	2.00	0.6
Large Fault 304	NNR-9	304	307	3	0.00	38.73	1.67	0.6
Large Fault 315	NNR-9	312	315	3	0.00	57.45	2.00	5
Large Fault 315	NNR-9	315	318	3	0.00	9.00	1.00	5
Large Fault 321	NNR-9	318	321	3	0.00	45.08	2.33	7.8
Large Fault 321	NNR-9	321	324	3	0.00	0.00	1.67	7.8
Large Fault 341	NNR-9	338	341	3	0.10	9.19	1.00	2.7
Large Fault 341	NNR-9	341	344	3	0.90	26.67	0.33	2.7

For comparison purposes, the frequency histogram for small faults density within the 3 ft (0.91 m) windows adjacent to large faults and cumulative displacement for these faults are compared to distributions of small faults within a the 20 ft (7.01 m) windows adjacent to large faults (Fig. 68). Histograms of log cumulative displacement for small faults within 3 ft (0.91 m) and 20 ft (7.01 m) of large faults have the same variance (Table 9) but do not have the same mean ($p = 0.0104$). Rather, with an increase from 10 ft (3.05 m) to 3 ft (0.91 m) from a large fault, the mean cumulative displacement per foot also increases. This further re-enforces the quantitative conclusion that on average the mean cumulative displacement increases with proximity to large faults.

Average cumulative displacement of small fault within the 3 ft (0.91 m) window was plotted against mudstone fraction for comparison purposes; data points from laterally distant locations were added to assess major deviations from expected values (Fig. 69). Cumulative displacement measurements of small faults within the 3 ft (0.91 m) windows from large faults have a substantial amount of variability that does not appear to fit the expected values if mudstone fraction were the sole controlling factor on small fault cumulative displacement.

Examination of spatial locations of extreme outliers reveals that the majority are located in zones of inferred hard linkage (Fig. 70). Wilson (2001) interpreted that hard linkage between Segments 1 and 2 should occur near the basement in the vicinity of NNR-4. Extreme outliers with greater than 140 mm/ft of average cumulative displacement are located within NNR-4 near the basement. Extreme outliers with greater than 80 mm/ft but less than 120 mm/ft of average cumulative displacement are located in NNR-10 and comprise the footwall and hanging wall portion of the large fault found at 368 ft. This is very suggestive of interactions between Sub-segments 1a with 1b and Segments 1 with 2. Additionally, the extreme outliers with 100 % mudstone and greater than 38 mm/ft average cumulative displacement are located in NNR-8 between the Upper fault and Segment 1. Even though the average cumulative displacements for small faults near large faults are variable, most of the outliers are located in areas in which Wilson (2001) inferred hard linkage. Although most extreme outliers are located

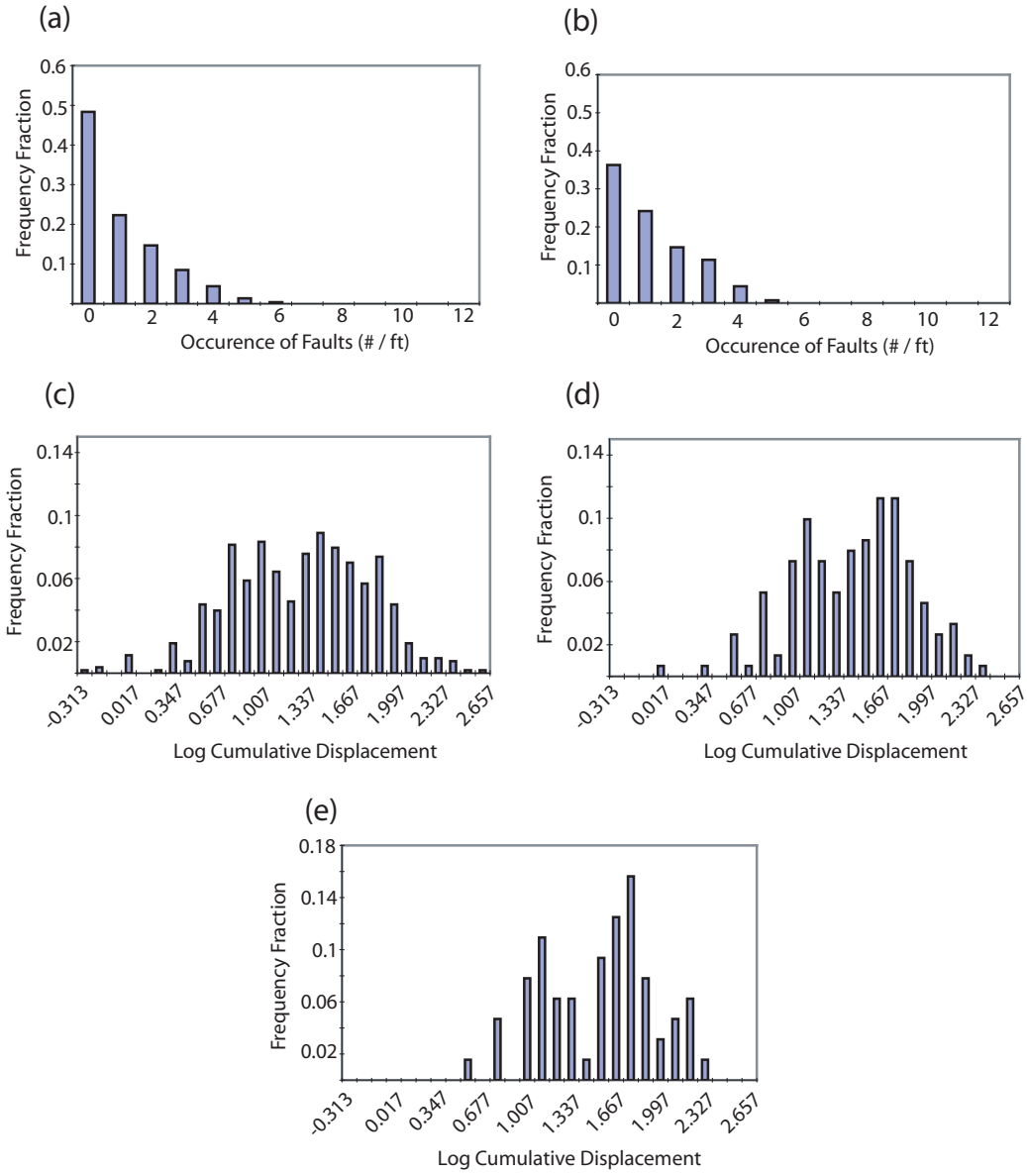

Fig. 68. Comparison of frequency characteristics of small fault measures inside and outside a 3 ft window adjacent large faults. (a) Frequency of small faults per foot outside the 3 ft windows, (b) frequency of small faults per foot inside the 3 ft windows. Logarithmically transformed cumulative displacement per foot of small faults (c) outside 3 ft windows, (d) inside 3 ft windows and (e) inside 3 ft windows only for larger faults with 1.5 m or greater displacement.

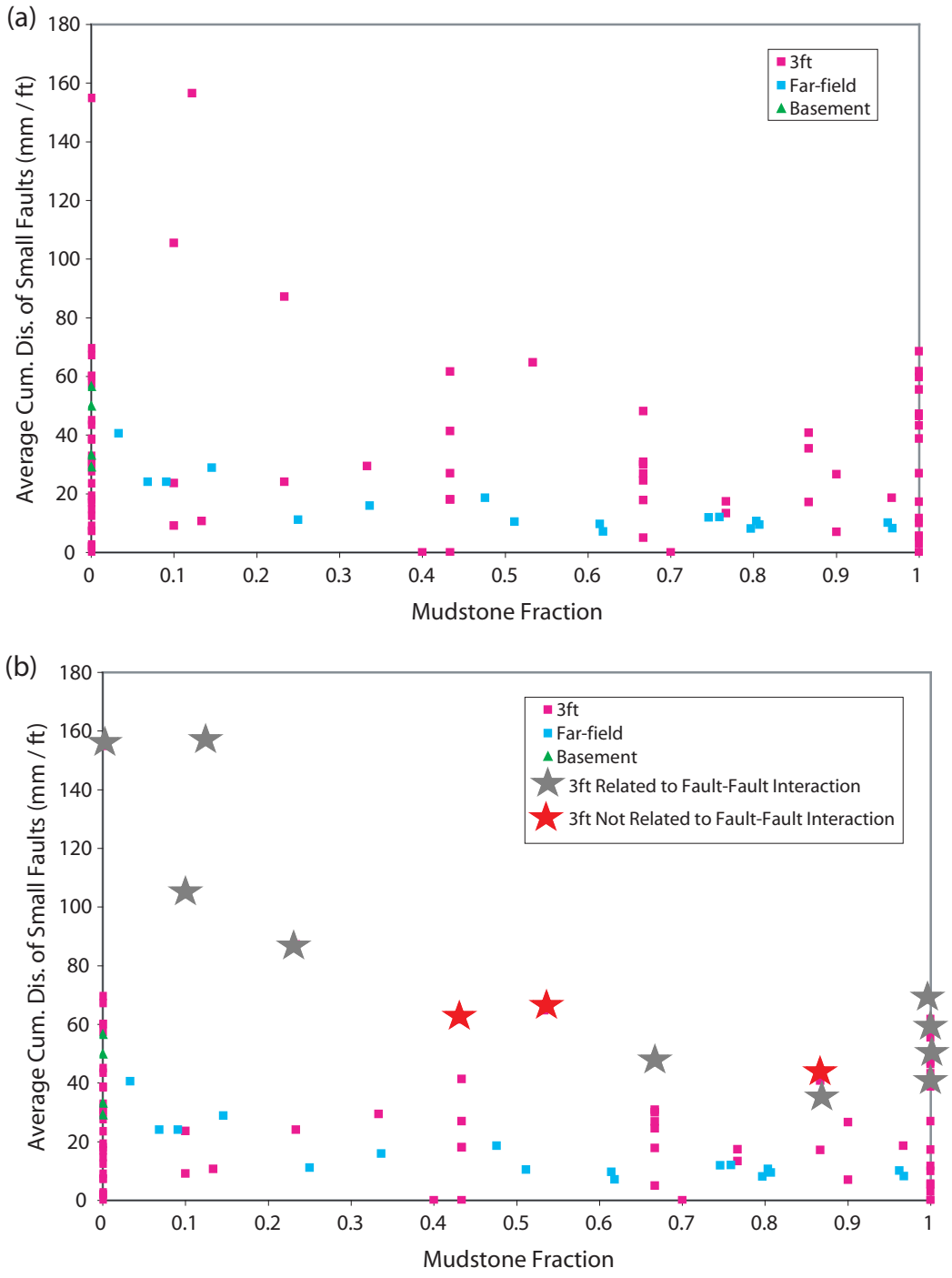

Fig. 69. Scatterplots of cumulative displacement of small fault versus mudstone percent for the small faults within 3 ft window adjacent to large faults, in addition to far-field and basement test data points. (a) Actual data points; (b) extreme outliers that are either spatially located in zones of large fault-fault interaction (grey stars) or not located in zones of large fault-fault interaction (red stars).

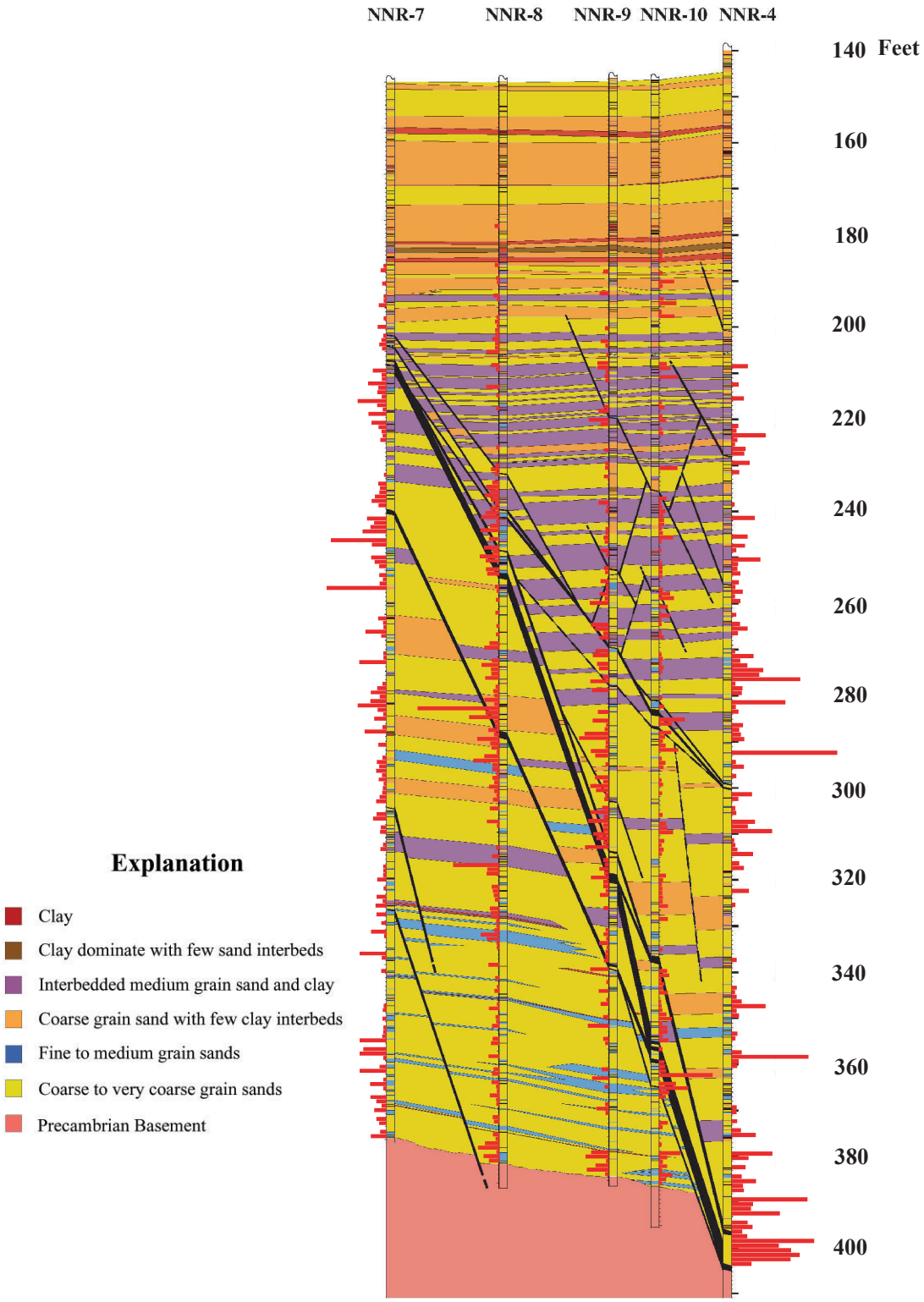

Fig. 70. Eastern cross section with cumulative displacement of small faults, finalized stratigraphic and structural model. Modified from Wilson (2001).

in areas of inferred hard linkage, it appears that mudstone fraction within the protolith still grossly controls the amount of displacement of a small fault.

7. SUMMARY AND CONCLUSIONS

On the basis of examining the spatial and kinematic attributes of small faults the following summary and conclusion can be drawn:

1) Nearly half of the 1873 small faults sampled in the core have measurable displacements and provided the basis for studying the correlation between fault displacement and associated gouge thickness. In sandstone, siltstone and mudstone protoliths in the Hickory Sandstone, faults with displacements less than 80 mm (6.1 in) exhibit only a weak linear correlation between displacement and thickness of the cataclastic gouge zone. As also seen in prior studies there is significant variability of gouge thickness for a specific displacement. Optimal transformation of the data using an alternating conditional expectation method did not improve the correlation and showed that the commonly used logarithmic transformation of data is not justified. Incorporation of categorical measures of mean grain size and sorting of the protolith in a multivariable, optimal transformation, linear regression improved the correlation between gouge thickness and displacement. For a specific displacement, a larger mean grain size of the protolith results, on average, in a thicker gouge zone. The empirical correlation developed was used to assign a statistical-based, displacement value to every small fault in core with unknown displacement by using measured gouge zone thickness and protolith texture.
2) Within the rock volume studied that envelopes the Nobles Fault system, small faults are numerous and nearly ubiquitous spatially. Three “1-D density” measures associated with small faults were used to quantify intensity of occurrence of small faults: 1) number of faults in a 1 ft (0.3 m) interval, 2) cumulative displacement of all faults in a 1 ft (0.3 m) interval, and 3) average displacement of all faults in a 1 ft (0.3 m) interval. The latter two measures, weight the faults by their displacement and provide a more direct relationship to inelastic strain associated with the fault. The number of faults per ft only weakly correlates to the cumulative displacement of the corresponding faults, which

indicates that a frequency measure of fault occurrence should be used with caution when inferring intensity of deformation and associated inelastic strain.

3) Small faults exhibit a range of attitudes but can be grouped into four sets based on strike. The dominant set strikes NE, approximately parallel to the large faults of the Noble Fault system. The NE-trending small faults dip SE (synthetic to large faults) and NW (antithetic), with the former being more frequent. A smaller number of small faults strike either NNW – NNE or NW – WNW and typically dip easterly. No systematic differences in relative age between sets could be documented. Most small faults are normal dip-slip faults, but there are a significant number of reverse dip-slip faults, which tend to dip steeply. The latter show no consistent spatial distribution; some may reflect effects of local fault-fault interaction, whereas others may be related to upward propagation of faults from the basement.
4) Small faults are not evenly distributed but tend to occur in clusters. Based upon the spacing attributes of neighboring faults, a limiting threshold of 1 ft (0.3 m) was defined. Faults closer than 1 ft (0.3 m) were considered to be in the same cluster, whereas faults farther apart than 1 ft (0.3 m) were considered to be in different clusters. The width, the number of faults and the associated cumulative displacement of faults of a cluster are highly variable, but small clusters dominate. Spacing between clusters ranges from 1 – 10 ft (0.3 – 3.05 m), with spacing less than 2 ft (0.61 m) most common.
5) Intensity of small faults and associated cumulative displacement vary spatially. There are intervals with high fault frequency and large cumulative displacement and there are intervals with sparse numbers of faults with only small cumulative displacement. These anomalous intervals do not exhibit a simple relationship to the large faults of the Nobles Fault system. There are examples where zones of intense faulting are closely associated with a large fault, but there also are examples where zones of sparse faulting occur adjacent to large faults. The role of protolith lithology, proximity to crystalline basement and structural position

relative to the Nobles Fault system were explored in an effort to explain the observed spatial distribution of small faults.

6) In order to asses the role of lithology on small faults occurrences, a far-field test was conducted. Sample intervals were located as far from the Noble Fault as feasible in order to minimize possible structural deformation influences. Sample intervals were selected to provide a range in relative amounts of sandstone and mudstone within the interval; Gamma Ray logs were used to provide a quantitative measure of mudstone in the stratigraphic interval. Mudstone content in an interval clearly affects the occurrence of small faults. Intervals with only minor mudstone interbeds have the largest number of faults per foot as well as the largest associated cumulative displacement per foot. With an increase of mudstone content, both these measures of fault intensity decrease until a content of 50 % mudstone is reached. A further increase of mudstone content does not appear to have an effect on the fault intensity measures.
7) In order to assess the effect that pre-existing weaknesses within the Precambrian Granite have on the "density" of small faults near the basement, a basement test was conducted. Samples were taken from intervals that were no greater than 6 ft above basement and no less than a lateral distance of 10 ft away from the Nobles Fault. No simple systematic pattern of fault strike was observed. Rather, the dips of small faults within these intervals tend to dip to the W, which is indicative of faults in the footwall portion of the Nobles Fault. The frequency of occurrence of small faults near the basement is greater as compared to similar lithologies higher in the core.
8) Intensity of small faults and associated cumulative displacement do not universally increase with proximity to large faults. Rather, in order to observe an increase in small faults, a mean global cumulative displacement approach is necessary. For large faults with greater than 1.5 m of stratigraphic throw, an increase in small fault mean cumulative displacement is observed within 10 ft of the large fault. If the sample window is reduced to 3 ft from a large fault. An

increase in small fault mean cumulative displacement is observed for all large faults.

9) In order to assess the role of fault-fault interaction on small fault development, a scatterplot of average cumulative displacement of small faults versus mudstone fraction was generated. The scatterplot reveals that mudstone fraction still grossly controls the amount of displacement of small faults within 3 ft of a large fault. Although the small sampling window increased variability, several internal adjacent large faults exhibit anomalously high values of cumulative displacement. Examination of the locations of these outliers reveals that they tend to be located in zones compatible with a fault-fault interaction.
10) Bedding attitudes determined from BHTV logs and three-point calculation are used to assess the occurrence of bedding rotation and potential effect on small fault formation. Within the hanging wall portion of the Noble Fault, bedding strike changes from a NW trend to a NNE strike near the Nobles Fault. Unfortunately primary depositional influences within the footwall region of the Nobles Fault mask recognition of systematic changes in bedding strike. The average structural dip is 15˚ with a westerly direction. Bedding dips near the Nobles Fault are routinely in excess of 30˚ on both sides of the fault. Places where anomalously steep dips occur typically are associated with clusters of significant small faults.

REFERENCES

Ackermann, R.V., Schlische, R.W., 1997. Anticlustering of small normal faults around larger faults. Geology 25 (12), 1127-1130.

Allmendinger, R. W., 2002. Allmendingers's Stereonet for Windows Version 1.16. Cornell University, Ithaca, NY.

Antonellini, M., Aydin, A., 1995. Effect of faulting on fluid flow in porous sandstones: geometry and spatial distribution. The American Association of Petroleum Geologist 79 (5), 642-671.

Antonellini, M.A., Aydin, A., Pollard, D.D. 1994. Microstructures of deformation bands in porous sandstones at Arches National Park, Utah. Journal of Structural Geology 16 (7), 941-959.

Barnes, V.E., Bell, W.C., 1977. The Moore Hollow group of central Texas. University of Texas at Austin, Bureau of Economic Geology, Report of Investigations 88, 1–169.

Beach, A., Welbon, A.L., Brockbank, P., McCallum, J.E., 1999. Reservoir damage around faults: outcrop examples from the Suez rift. Petroleum Geoscience 5, 109-116.

Becker, J.E., 1985. Structural analysis of the western Llano Uplift with emphasis on the Mason Fault. M.S. thesis, Texas A&M University, College Station, TX.

Bernabe, Y., Fryer, D.T., Hayes, J.A., 1992. The effect of cement on the strength of granular rocks. Geophysical Research Letters 19 (14), 1511-1514.

Bernard, X.D., Labaume, P., 2002. Cataclastic slip band distribution in normal fault damage zones, Nubian Sandstone, Suez rift. Journal of Geophysical Research 107 (B7), 2141, ETG 6, 1-12.

Breiman, L., Friedman, J.H., 1985. Estimating optimal transformations for multiple regression and correlation., Journal of the American Statistical Association, 80 (391), 580-598.

Bridge, J., Barnes, V.E., Cloud, Jr. P.E., 1947. Stratigraphy of the Upper Cambrian, Llano Uplift, Texas. Geologic Society of America Bulletin 58 (1), 109-123.

Cheny, M.G., Goss, L.F., 1952. Tectonics of central Texas. American Association of Petroleum Geologist Bulletin 36, 2237-2265.

Child, C., Nicol, A., Walsh, J.J., Watterson, J., 1996. Growth of vertically segmented normal faults. Journal of Structural Geology 18 (12), 1389-1397.

Childs, C.J., Watterson, Walsh, J.J., 1996. A model for the structure and development of fault zones. Journal of the Geological Society of London 153, 337-340.

Cloud, Jr. P.E., Barnes, V.E., Bridges, J., 1945. Stratigraphy of the Ellenburger group in central Texas: a progress report. University of Texas at Austin, Bureau of Economic Geology, University of Texas Publication 4301, 133-161.

Cowie, P.A., Scholz, C.H., 1992. Physical explanation for displacement-length relationship of faults using post-yield fracture mechanics model. Journal of Structural Geology 14 (10), 1133-1148.

Cruikshank, K.M., Zha, G., Johnson, A.M., 1991. Duplex structures connecting fault segments in Entrada Sandstone. Journal of Structural Geology 13 (10), 1185-1196.

Davis, G.H., Bump, A.P., Garcia, P.E., Ahlgren, S.G., 1999. Conjugate riedel Deformation band shear zones. Journal of Structural Geology 22, 121-142.

Davison, C.C., Keys, W.S., Paillet, F.L., 1982. Use of borehole-geophysical logs and hydrologic test to characterize crystalline rock for nuclear-waste storage, Whiteshell Nuclear Research Establishment, Manitoba, and Chalk River Nuclear Laboratory, Ontario, Canada: U.S. Department of Energy, issued by the U.S. Department of Commerce, National Technical Information Service, Report ONWI-418, p. 103

Davison, I., 1994. Linked fault systems; extensional, strike-slip and contractional. In: P.L. Hancock, (Ed.), Continental Deformation, Tarrytown, NY, Pergamon Press, pp. 121-142.

Dawer, N. H., Anders, M.H., 1995. Displacement-length scaling and fault linkage. Journal of Structural Geology 17 (5), 607-614.

Dunn, D.E., LaFountain, L.J., Jackson, R.E., 1973. Porosity dependence and mechanism of brittle fracture in sandstones. Journal of Geophysical Research 78 (14), 2403-2417.

El Bied, A., Sulem, J., Martineau, F., 2002. Microstructures of shear zones in Fontainebleau Sandstone. International Journal of Rock Mechanics and Mining Science 39, 917-932.

El-Jard, M.R., 1982. Diagenesis of the Hickory Sandstone (Cambrian), McCulloch and Mason Counties, central Texas. M.A. Thesis, University of Texas at Austin, Austin, TX.

Engelder, J.T., 1974. Cataclasis and the generation of fault gouge. Geological Society of America Bulletin 85, 1515-1522.

Fossen, H., Hesthammer, J., 1997. Geometric analysis and scaling relationships of deformation bands in porous sandstone. Journal of Structural Geology 19 (12), 1479-1493.

Fossen, H., Hesthammer, J., 2000. Possible absence of small faults in the Gullfaks Field, northern North Sea: implication for downscaling of faults in some porous sandstones. Journal of Structural Geology 22, 851-863.

Heynekamp, M.R., Goodwin, L.B., Mozley, P.S., Haneberg, W.C., 1999. Controls on fault zone architecture in poorly lithified sediments, Rio Grande Rift, New Mexico: implications for fault zone permeability and fluid-flow. In: Haneberg, W.C., Mozley, P.S., Moore, C.J., Goodwin, L.B. (Eds.), Faults and Subsurface Fluid Flow, American Geophysical Union Geophysical Monograph 113, pp. 27-49.

Hedgcoxe, H.R., 1987. Development of secondary faults between en echelon, oblique-slip faults: example from basement controlled, small-fault systems in the Llano Uplift of central Texas. M.S. thesis, Texas A&M University, College Station, TX.

Hull, J., 1988. Thickness-displacement relationships for deformation zones. Journal of Structural Geology 10, 431-435.

Jamison, W.R.,1979. Laramide deformation of the Windgate Sandstone, Colorado National Monument: a study of cataclastic flow. Ph.D. dissertation, Texas A&M University, College Station, TX.

Johansen, T.E.S., Fossen, H., Kluge, R., 2005. The impact of syn-faulting porosity reduction on damage zone architecture in porous sandstone: an outcrop example from Moab Fault, Utah. Journal of Structural Geology 27, 1469-1485.

Johnson, B., 1993. Detailed field characterization of normal and oblique-slip faults in siliciclastic sequences: fault structure, nature of fault interaction and linkage, and hanging wall-footwall deformation. In: Industrial Associates Program in migration and structural trapping of fluids: Center for Tectonophysics, Texas A&M University, College Station, TX.

Johnson, B., 1990. The Llano Uplift: a plate flexural model and its associate implications. Geological Society of America Abstracts with Programs 22, 21.

Johnson, B., Becker, J.E., 1986. Normal fault development in the western Llano Uplift of Cental Texas. Geological Society of America Abstracts with Programs 18, 646.

Karner, S.L., Chester, J.S., Chester, F.M., Kronenberg, A.K., Hajash, A., 2005 Laboratory deformation of granular quartz sand: implications for the burial of clastic rocks. American Association of Petroleum Geologist Bulletin 89 (5), 603-625.

Knott, S.D., 1994. Fault zone thickness versus displacement in the Permo-Triassic sandstone of NW England. Journal of the Geological Society of London 151, 17-25.

Knott, S.D., Beach, A., Brockbank, J., Lawson, B., McCallum, J.E., Welbon, A.I., 1996. Spatial and mechanical controls on normal fault populations. Journal of Structural Geology 18, 359-372.

Mair, K., Main, I., Elphick, S., 2000. Sequential growth of deformation bands in the laboratory. Journal of Structural Geology 22, 25-42.

McBride, E.F., Abdel-Wahab, A.A., Milliken, K.L., 2002. Petrography and diagenesis of a half-billion-year-old cratonic sandstone (Hickory), Llano region, Texas. University of Texas at Austin, Bureau of Economic Geology, Report of Investigations 264, 1-77.

Menendez, B., Zhu, W., Wong, T.F., 1996. Micromechanics of brittle faulting and cataclastic flow in Berea Sandstone. Journal of Structural Geology 18 (1), 1-16.

Otsuki, K. 1978. On the relationship between the width of shear zone and the displacement along fault. Journal of Geologic Society Japan 84, 661-669.

Patton, T.L, III., 1984. Normal-fault and fold development in sedimentary rock above a pre-existing basement normal fault. Ph.D. dissertation, Texas A&M University, College Station, TX.

Peacock, D.C.P., Sanderson, D.J., 1991. Displacement and segment linkage and relay ramps in normal fault zones. Journal of Structural Geology 13 (6), 721-733.

Randolph, L.C., 1991. The effects of faulting on the ground water system in the Hickory Sandstone aquifer. M.S. thesis, Texas A&M University, College Station, TX.

Robertson, E.C, 1983. Relationship of fault displacement to gouge and breccia thickness. Society of Mining engineers, American Institute of Minning Engineers Transactions 274, 1426-1432.

Schafer, K.W., 2002. The structure and evolution of small-displacement strike-slip faults in porous sandstone. M.S. thesis, Texas A&M University, College Station, TX.

Schmittle, J.M.,1987. Brittle deformation and cataclasis on the southwest flank of the Llano Uplift, Mason County, Texas. M.S. thesis, Texas A&M University, College Station, TX.

Scott, T.E., Nielsen, K.C., 1991. The effects of porosity on the brittle-ductile transition in sandstones. Journal of Geophysical Research 96 (B1), 405-414.

Shipton, Z.K., Cowie, P.A., 2001. Damage zone and slip-surface evolution over micrometers to kilometers scales in high-porosity Navajo Sandstone, Utah. Journal of Structural Geology 23, 1825-1844.

Tamhane, A.C., Dunlop, D.D., 2000. Statistics and Data Analysis from Elementary to Intermediate. Prentice-Hall, Upper Saddle River, NJ.

Terzahi, R.D., 1965. Source of error in joint surveys. Geotechnique 15, 287.

Teufel, L.W. 1981. Pore volume changes during frictional sliding of simulated faults. In Mechanical Behavior of Crustal Rocks (edited by Carter N.L., Friedman M., Logan J.M., and Stearns D.W.) American Geophysical Union Monograph 24, 135-145.

Wallace, R.E., Morris, H.T., 1986. Characteristics of faults and shear zones in deep mines. Pure and Applied Geophysics 124, 107-126.

Walsh, J.J., Watterson, J., Bailey, W.R., Childs, C., 1999. Faults relays, bends and branch lines. Journal of Structural Geology 21, 1019–1026.

Wilson, J.S., 2001. High–resolution stratigraphic and structural characterization of the fault-partitioned Hickory Sandstone aquifer system, Mason County, central Texas. M.S. thesis, Texas A&M University, College Station, TX.

Wong, T.F., Christian, D., Zhu, Wenlu., 1997. The transition from brittle faulting to cataclastic flow in porous sandstone: mechanical deformation. Journal of Geophysical Research 102 (B2), 3009-3025.

Yin, H., Dvorkin, J., 1994. Strength of cemented grains. Geophysical Research Letters 21 (10), 903-906.

Young, S.T., 1982. Characterization of and parameters controlling small faults in naturally deformed, porous sandstone. M.S. thesis, Texas A&M University, College Station, TX.

Zhang, J., Wong, T.F., Davis, D.M., 1990. Micromechanics of pressure-induced grain crushing in porous rocks. Journal of Geophysical Research 95 (B1), 341-352.

Zhao, G., Johnson, A., 1991. Sequential and incremental formation of conjugate sets of faults. Journal of Structural Geology 13, 887-895.

Xue, G., Datta-Gupta, A., Valko, P., Blasingame., 1997. Optimal transformation for multiple regression: application to permeability estimation from well logs. Society of Petroleum Engineers 12 (2), 85-93.

APPENDIX A

Structural Explanation

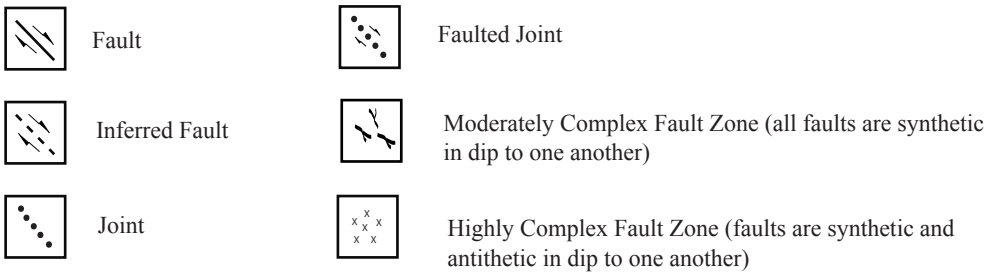

For each structural element a different alphabetical identification is assigned to it. The alphabetically identification is placed next to the top or bottom of the structural element on the outside margins of the illustrated core. Apparent displacement amount for each structural element also contains the alphabetically identification. Attitudes and gouge thickness are aligned laterally parallel to apparent displacement along with notes. Qualitative measures of mean grain size (cg = coarse grained, mg = medium grained, fg = fine grained, cl = clay) are included within the margin containing the gouge thickness.

Joints within the core are mapped as dotted traces in the strip maps, while faults are mapped as a solid trace. Instances were the fault trace was inferred a non-continuous trace was used. On occasion an older fault with discernable offset later under went an extensional phase (i.e. faulted joint) and is manifested as a mode I opening. When this occurs the trace is mapped as a joint but with apparent displacement direction and magnitude. Individual small faults were mapped until the complexity became too great to accurately capture at this scale of observation, this typically occurred near to or within large and intermediate faults.

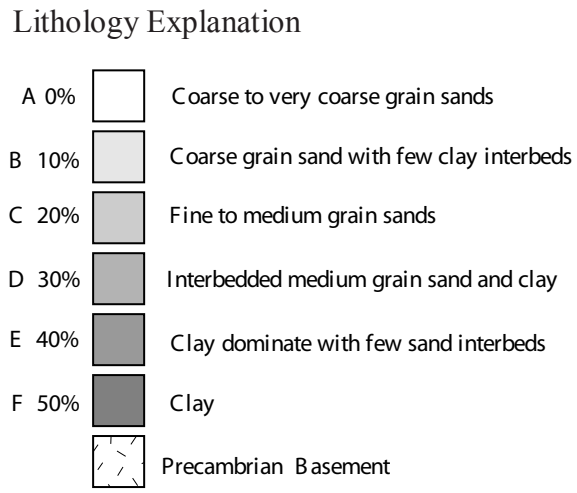

The first time a lithology appears within an individual (5 ft) strip map, the lithology is alphabetically identified and colored with the appropriate gray tone within the portion of the core illustration that is seen looking North (i.e. front). Subsequent appearances of the same lithology within the 5 ft strip map are not alphabetically identified. If a bedding dip amount was recorded from the core then the direction an amount were used in the lithologic illustration for all lithologies until the next bedding measurement further down in core was recorded.

Depth Interval: 170 - 175 Well: NNR - 7

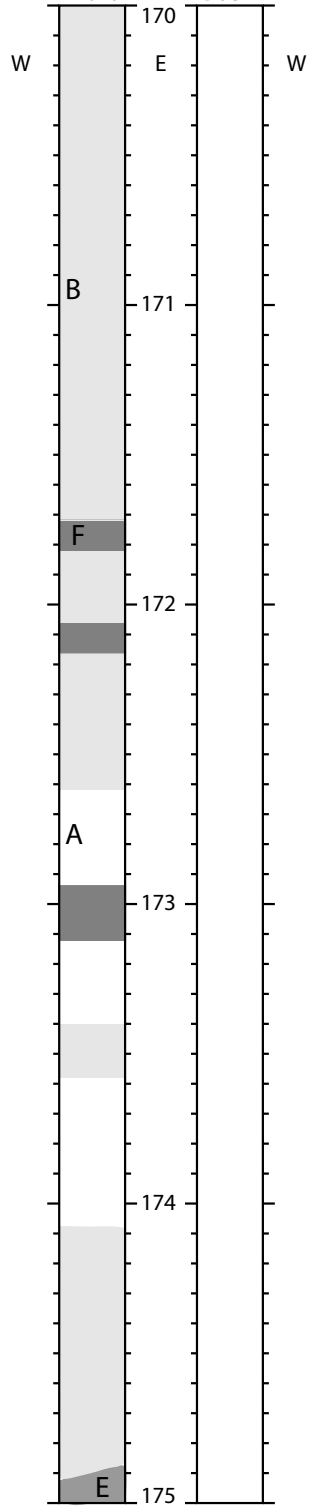

Apparent Disp. (mm)	Fault Thickness (mm)	Fault Strike	Fault Dip	Comments
				171.2 possible fault NS 57E within normal displacement. Difficult to see due to clay rich horizon Bedding @ 171.6': N7W 9SW [obtained from BHTV-log] Bedding @ 175' : NS 14W

Depth Interval: 175 - 180 Well: NNR - 7

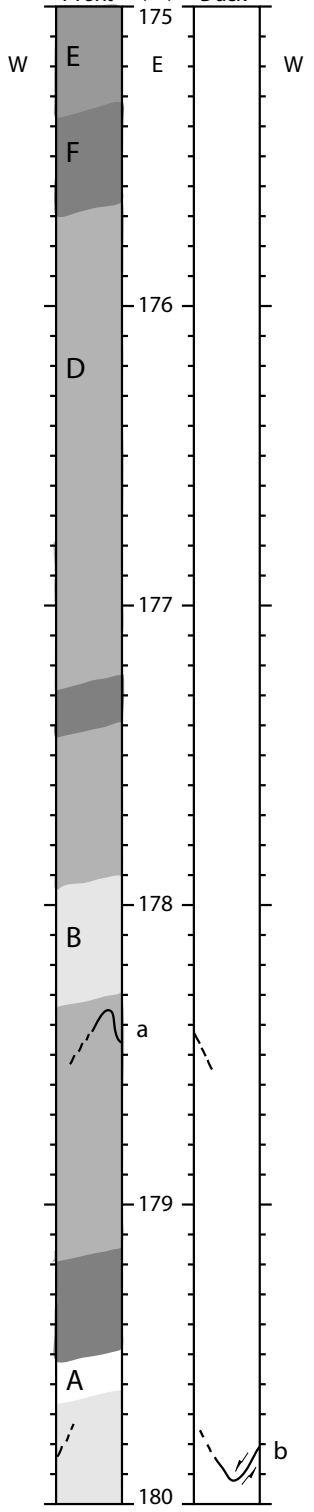

Apparent Disp. (mm)	Fault Thickness (mm)	Fault Strike	Fault Dip	Comments
				Bedding @ 175.7': N2E 18NW [obtained form BHTV-log]
				Bedding @ 175.9': N2W 14SW [obtained form BHTV-log]
				Bedding @ 178.0' : NS 12W
a=?		N40E	53NW	
b=4	1 fg	N70E	57NW	

Depth Interval: 180 - 185 Well: NNR - 7

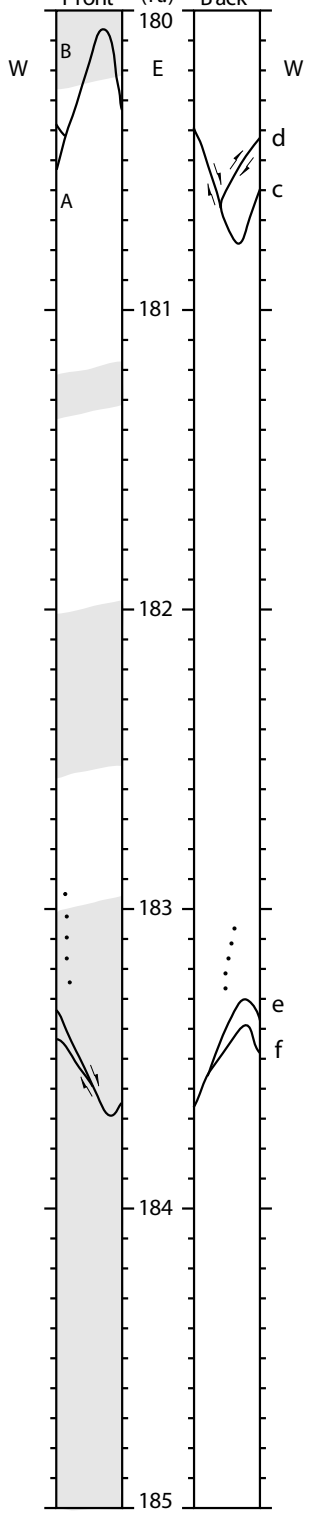

Apparent Disp. (mm)	Fault Thickness (mm)	Fault Strike	Fault Dip	Comments
d=2	1.5 mg	NS	50E	
c=6	1 mg	N45E	66NW	
				Run #17 Score card: 181.1' 181.1' - 191.3' Drilled: 10.0' Recovered: 10.2'
				Bedding @ 182.5': N18E 14NW [obtained from BHTV-log]
				Bedding @ 182.9' : N20E 16NW
e=3	1 fg	N30E	56SE	
f=7	2 fg	N35E	52SE	
				Bedding @ 184.1': N5E 12NW [obtained from BHTV-log]

Depth Interval: 185 - 190 Well: NNR - 7

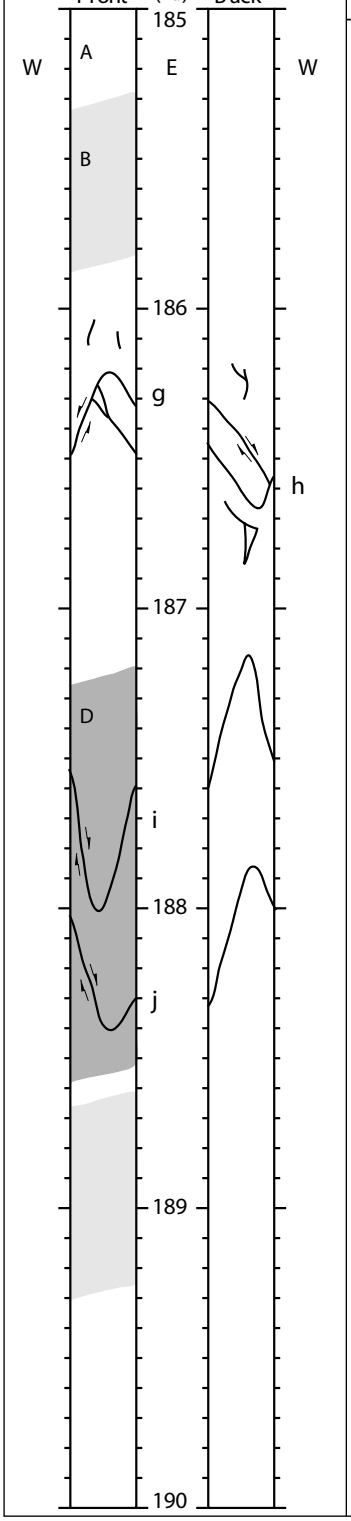

Apparent Disp. (mm)	Fault Thickness (mm)	Fault Strike	Fault Dip	Comments
				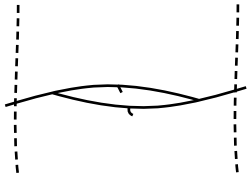
g=2	1 mg	N80E	60NW	Plan view of "g" & "h"
h=1	1 mg	N30E	61NW	
i=3	0.5 fg	N80E	69SE	
j=27	1 fg	N50E	65SE	
				Bedding @ 188.5' : N10E 14NW

Depth Interval: 190 - 195 Well: NNR - 7

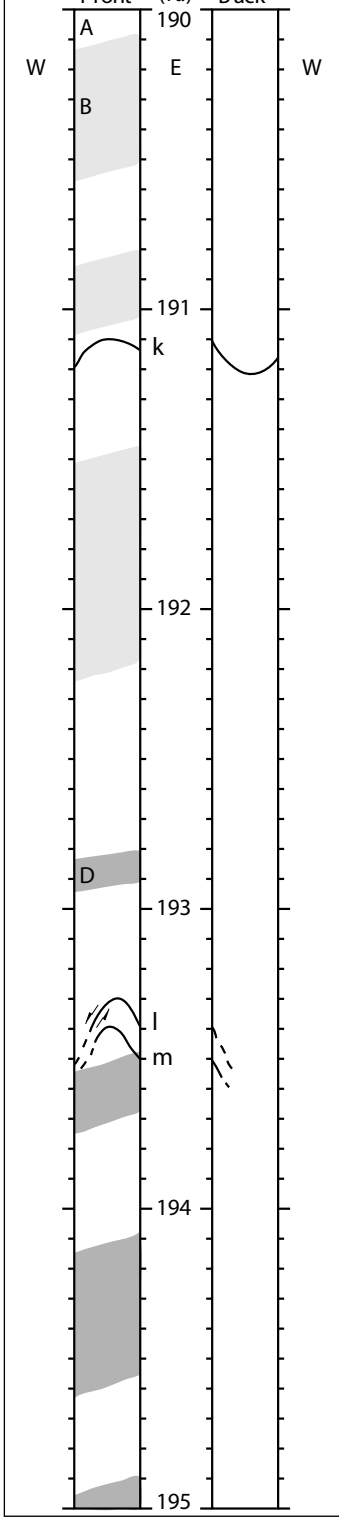

Apparent Disp. (mm)	Fault Thickness (mm)	Fault Strike	Fault Dip	Comments
k=?	0.5 fg	N70E	30NW	Run #18 Score card: 191.25' 191.1' - ? Drilled: ? Recovered: ?
				Bedding @ 192.7': N22W 14SW [obtained from BHTV-log]
				Bedding @ 192.9' : N20W 8SW
l=6	1 mg	N50E	49NW	
m=?	1 mg	N85E	61NW	Bedding @ 193.6' : N5W 16SW
				Bedding @ 195': N5E 19NW [obtained from BHTV-log]

Depth Interval: 195 - 200 Well: NNR - 7

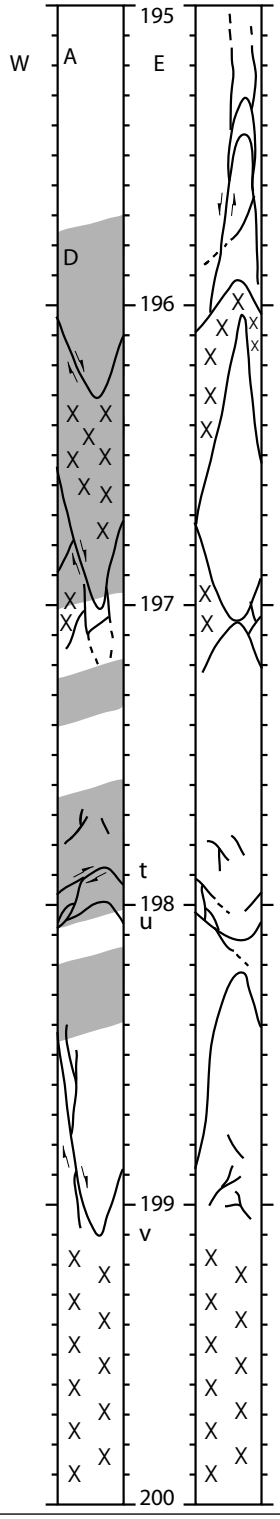

Apparent Disp. (mm)	Fault Thickness (mm)	Fault Strike	Fault Dip	Comments
n=2.5	0.5 mg	N55E	78SE	
o=2.5	0.5 mg	N55E	75SE	
p=?		N50E	58SE	
q=?		N50E	80SE	Rake on "q": 55NE
r=?	1 mg	N60E	61NW	
s=?	1 mg	N60E	64SE	
				Bedding @ 197.7' : N35W 16SW
t=5	1 mg	N35E	32NW	
u=?	1 mg	N30E	30NW	
v=?		N40E	72SE	Core is to fragile and broken to accurately map faults from 199'-200'

Depth Interval: 200 - 205 Well: NNR - 7

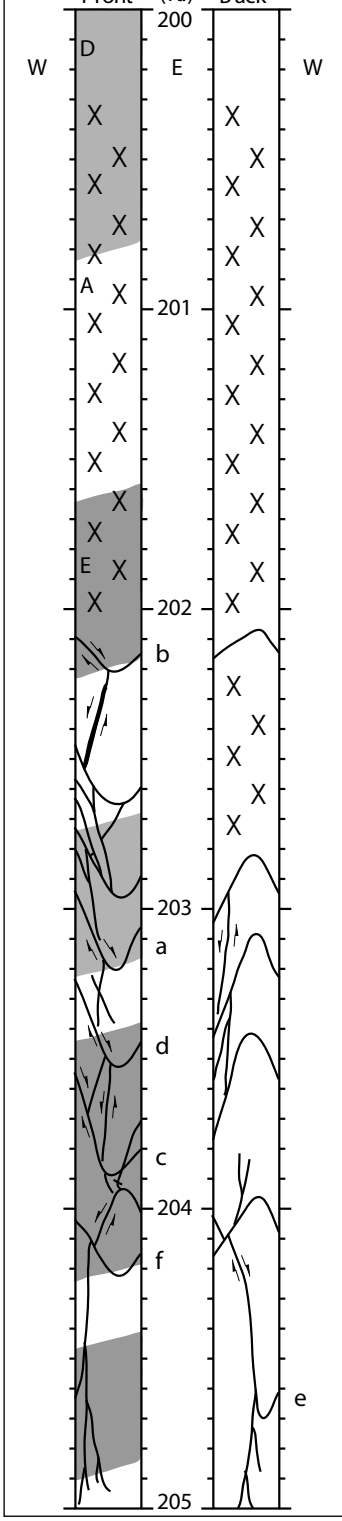

Apparent Disp. (mm)	Fault Thickness (mm)	Fault Strike	Fault Dip	Comments
				Multiple faults from 200' - 202' beyond resolution
				Run #19 Score card: 201.1' 201.1' - 211.1' Drilled: 10.0' Recovered: 9.9'
b=?		N60E	41SE	
a=?		N60E	60SE	Fault "a" correlates w/202.2' in BHTV Rake on "a": 57NE ○
d=9	1 fg	N50E	56SE	
c=47	7 fg	N70E	63SE	
f=7	0.5 clay	N40E	51SE	"f" is younger than "e"
e=6		N40E	74NW	

Depth Interval: 205 - 210 Well: NNR - 7

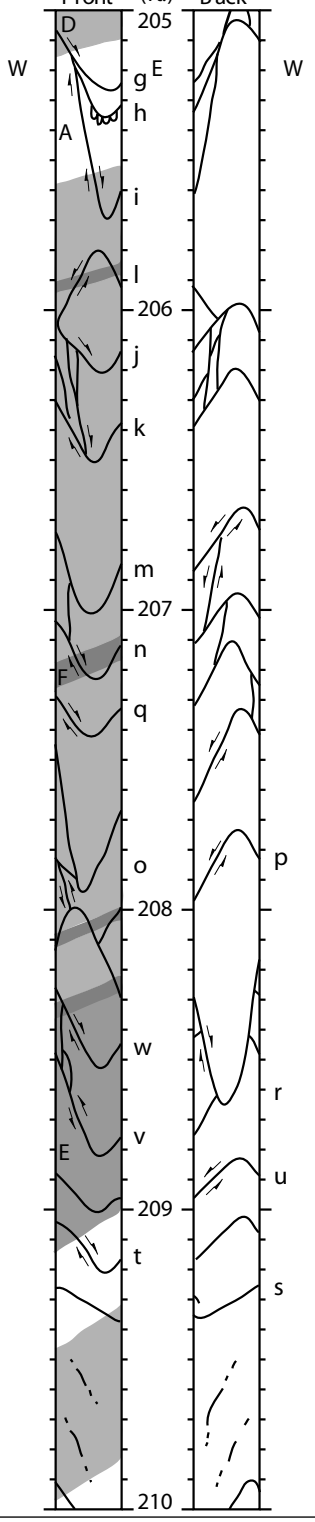

Apparent Disp. (mm)	Fault Thickness (mm)	Fault Strike	Fault Dip	Comments
g=?	1 cg	N50E	37SE	
h=?	21 cg	N50E	45SE	
i=1	0.5 fg	N50E	67SE	
l=11	0.5 fg	N60E	55NW	
j=32	2 fg	N60E	58SE	
k=28	2 cg	N70E	51SE	
				Bedding @ 206.6' : N30E 23NW
m=19	1 fg	N50E	41SE	
n=7	0.5 fg	N60E	56SE	
q=3	0.5 fg	N55E	54SE	
o=16	2 mm fg	N50E	70SE	
p=3	0.5 fg	N60E	53SE	
w=3	0.5 fg	N45E	65SE	
r=26	0.5 fg	N80W	62NE	
v=3	0.5 fg	N40E	63SE	Bedding @ 208.8' : N30W 33SW
u=2	0.5 fg	N50E	37SE	
t=3	2 mg	N40E	44SE	
s=?	1 mg	N20E	24SE	

Depth Interval: 210 - 215 Well: NNR - 7

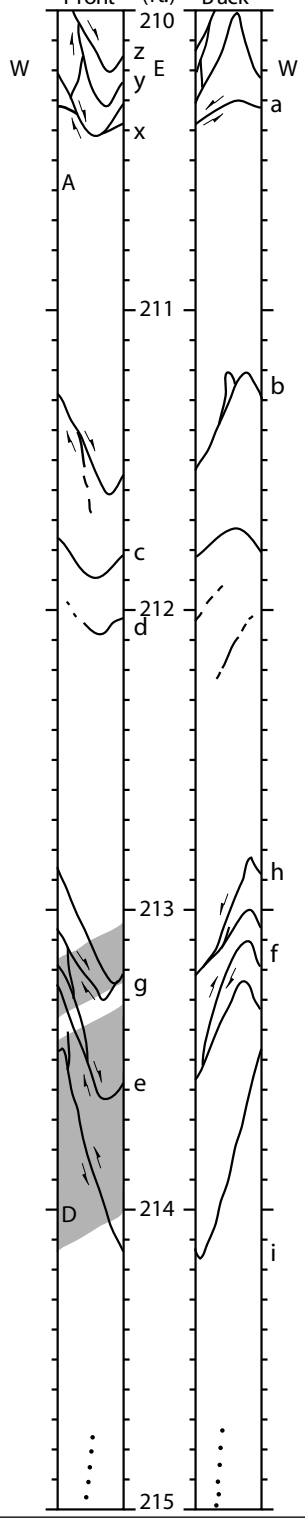

Apparent Disp. (mm)	Fault Thickness (mm)	Fault Strike	Fault Dip	Comments
		N25E	51SE	
z+y=67	z+y=5 cg	N40E	67SE	
a=?	3 cg	N55E	31SE	
x=?	7 cg	N70E	52SE	
				Run #20 Score card: 211.02' 211.1' - 221.1' Drilled: 10.0' Recovered: ?'
b=3	1 mg	N20E	54SE	
c=?	1 mg	N60E	43SE	
d=?	1 mg	N55E	41SE	
				Bedding @ 212.4' : N50W 29SW
h=?	1 fg	N20E	61SE	
f=7	1 fg	N30E	68SE	
g=3	1 fg	N30E	46SE	
e=?	4 fg	N50E	61SE	
i=8	2 mg	N10W	71NE	

Depth Interval: 215 - 220 Well: NNR - 7

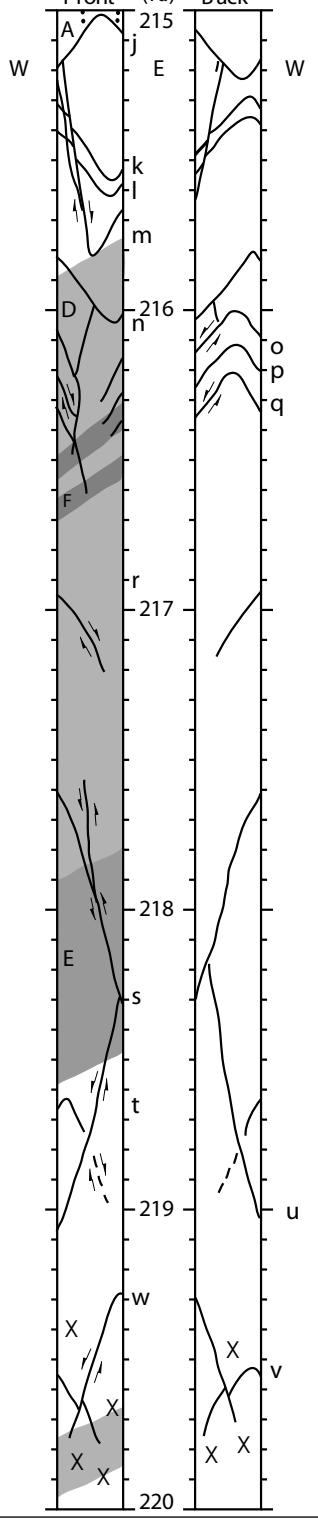

Apparent Disp. (mm)	Fault Thickness (mm)	Fault Strike	Fault Dip	Comments
j=?	1.5 mg	N50E	43NW	
k=?	2 mg	N30E	32SE	
l=?	2 mg	N20E	31SE	
m=7	1.5 mg	N70E	72SE	"m" is younger than "k" & "l"
n=?	1 mg	N10E	42SE	
o=12	1 fg	N70E	60SE	
p=4	0.5 fg	N70E	62SE	
q=12	0.5 clay	N75E	66SE	
r=3	0.25 clay	NS	42E	Bedding @ 216.9' : NS 25W
s=10	1 fg	NS	61E	
t=3	0.5 mg	N10E	41SE	
u=5	1 cg	N10E	80NW	
w=4	1 mg	N20E	65NW	
v=?		N20E	41SE	"v" is older than "w"

Depth Interval: 220 - 225 Well: NNR - 7

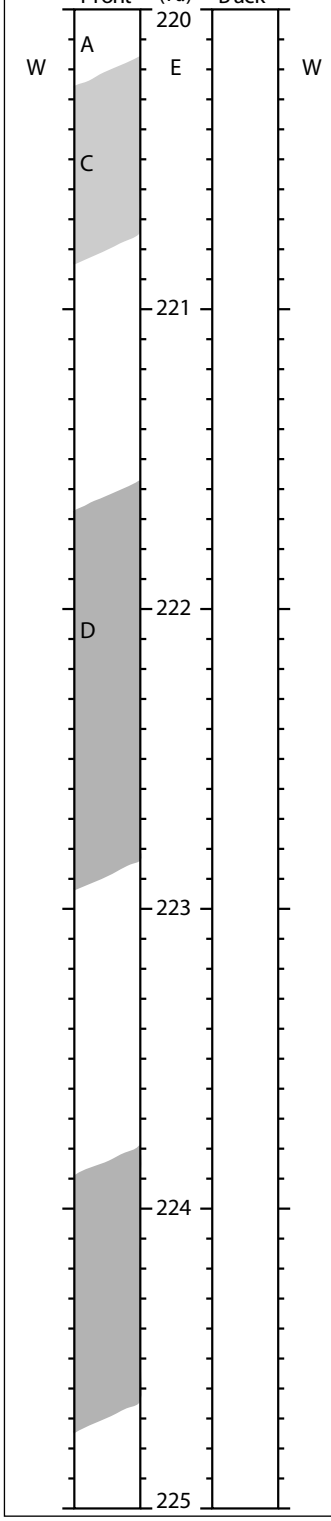

Apparent Disp. (mm)	Fault Thickness (mm)	Fault Strike	Fault Dip	Comments
				Run #21 Score card: 221.1' 221.1' - 231.1' Drilled: 10.0' Recovered: 10.0w'
				Bedding @ 222.6' : N15E 24NW

Depth Interval: 225 - 230 Well: NNR - 7

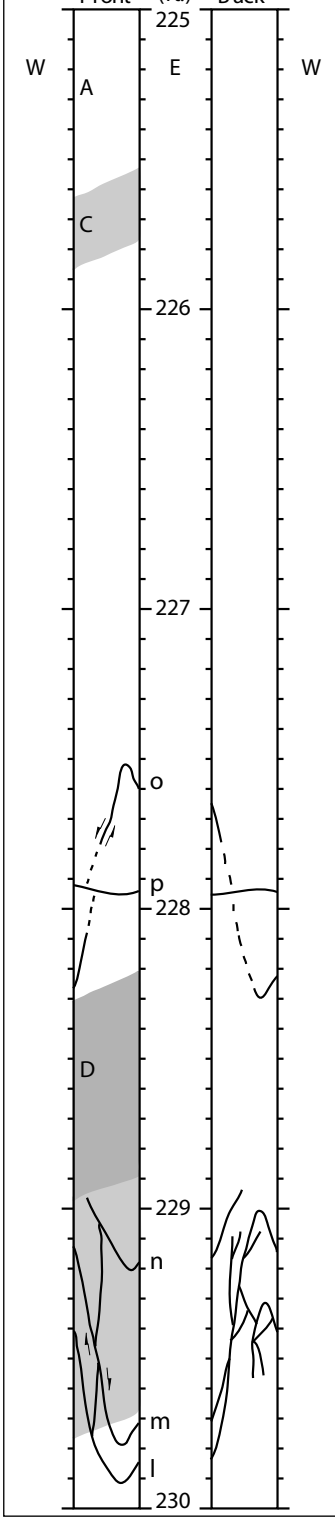

Apparent Disp. (mm)	Fault Thickness (mm)	Fault Strike	Fault Dip	Comments
o=1.5	1 cg	N30E	77NW	
p=?	1 cg		14S	Strike for fault "p'" is N20E or EW ?
				Bedding @ 228.3' : NS 21W
n=?	0.5 fg	N20E	51SE	
m=19	1 fg	N40E	73SE	
l=?	0.5 fg	N40E	69SE	

Depth Interval: 230 - 235 Well: NNR - 7

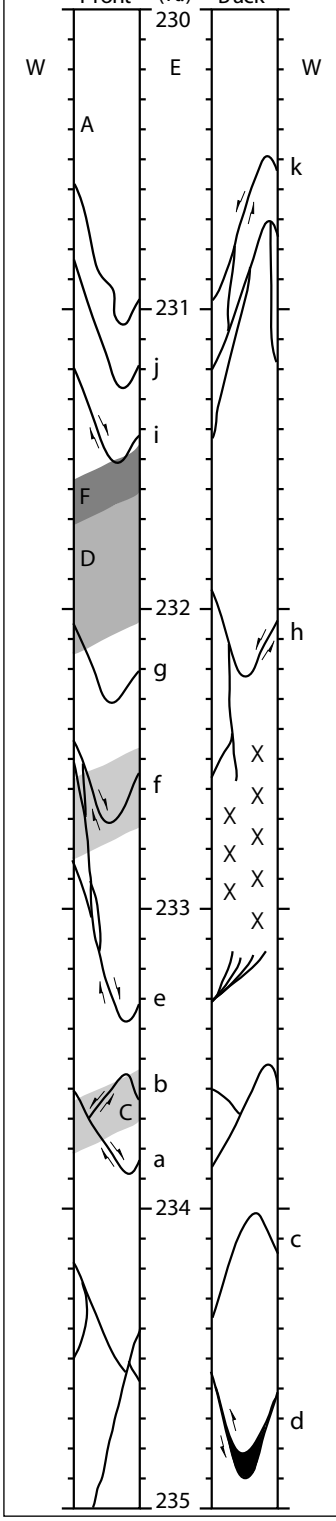

Apparent Disp. (mm)	Fault Thickness (mm)	Fault Strike	Fault Dip	Comments
k=9	3 cg	N40E	63SE	Strike changes to N20E at top of faults "k", "j", and "i"
j=?	2 cg	N45E	64SE	Run #22 Score card: 231.1' 231.1' - 241.0' Drilled: 10.0'
i=24	4 cg	N50E	76SE	Recovered: 9.9' Bedding @ 231.6' : N30E 26NW Bedding @ 231.8': N7E 22NW [obtained from BHTV-log]
h=21	1 clay	N70E	75NW	
g=?	1 cg	N60E	57SE	
f=14	4 cg	N70E	51SE	
e=39	4 cg	N30E	74SE	
b=1		N30E	43NW	
a=22	4	N20E	46SE	
c=?	3 cg	N50E	77SE	"c" is probably younger than "d"
d=21	5 cg	N70E	74NW	

Depth Interval: 235 - 240 Well: NNR - 7

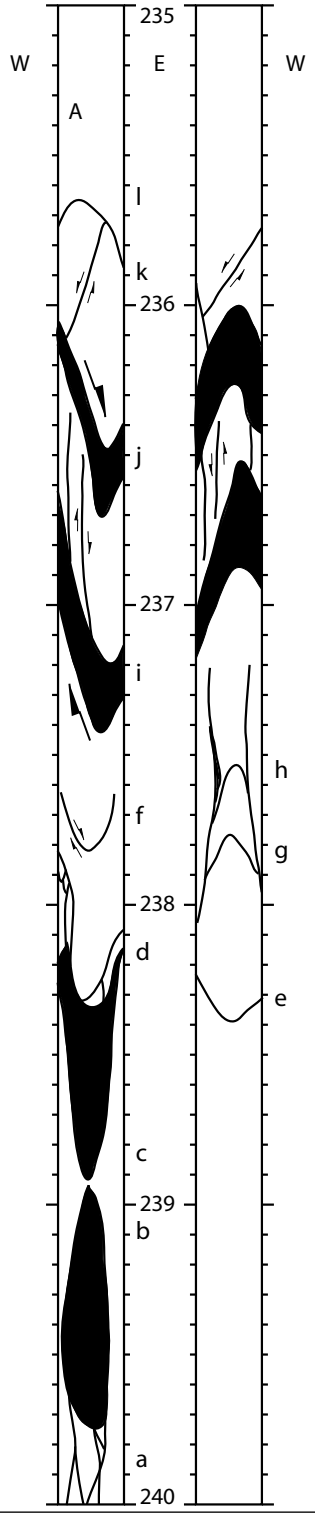

Apparent Disp. (mm)	Fault Thickness (mm)	Fault Strike	Fault Dip	Comments
l=?		N50W	43NE	
k=?		N50E	64NW	
j=?		N60E	70SE	Rake on "j": 46NE Fault "j" correlates w/235.8' in BHTV-log
i=?		N60E	72SE	Rake on "i": 66NE Fault "i" correlates w/237.7' in BHTV-log
h=?	3.5 cg	N40E	79SE	
f=9	2 cg	N40E	66SE	
g=?	3 cg	N40E	68SE	
d=?	5 cg	N60E	79SE	
e=?	2 cg	N30E	35NW	
c=?		N50E	86SE	
b=?		N55E	90	
a=?	6 cg	N50E	79SE	

Depth Interval: 240 - 245 Well: NNR - 7

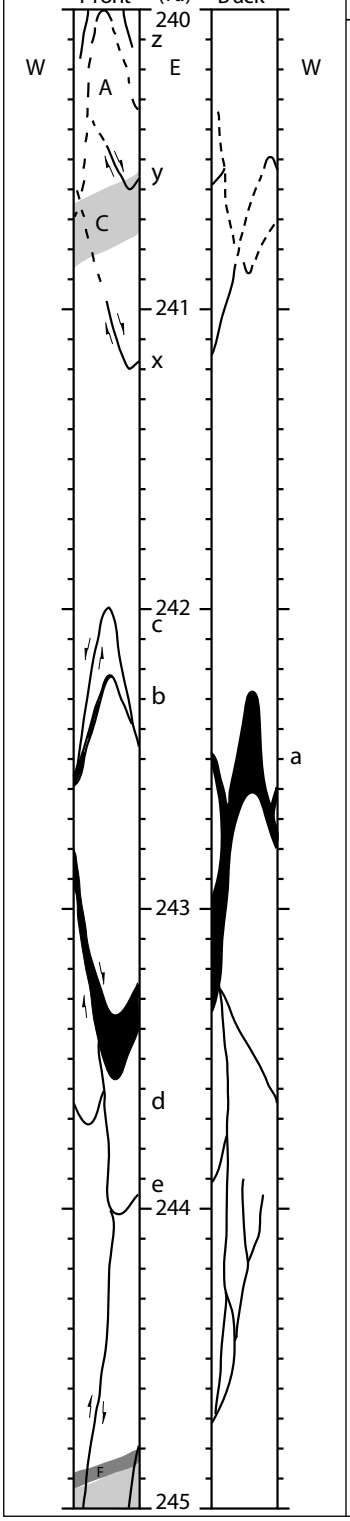

Apparent Disp. (mm)	Fault Thickness (mm)	Fault Strike	Fault Dip	Comments
	6 cg	N50E	74NW	
y=1	1 cg	N20E	56SE	
x=5	2 cg	N15E	67SE	
				Bedding @ 241.7' : N10W 20SW
c=19	7 cg	N80E	81NW	
b=?	7 cg	N80E	79NW	
a=180	3 cg	N70E	78SE	Rake on "a": 45NE Fault "a" correlates w/242.2' in BHTV-log
d=?	4 cg	N60E	57NW	
e=?	3 cg	N70E	63SE	
33 @ 244.8'	6 cg			

Depth Interval: 245 - 250 Well: NNR - 7

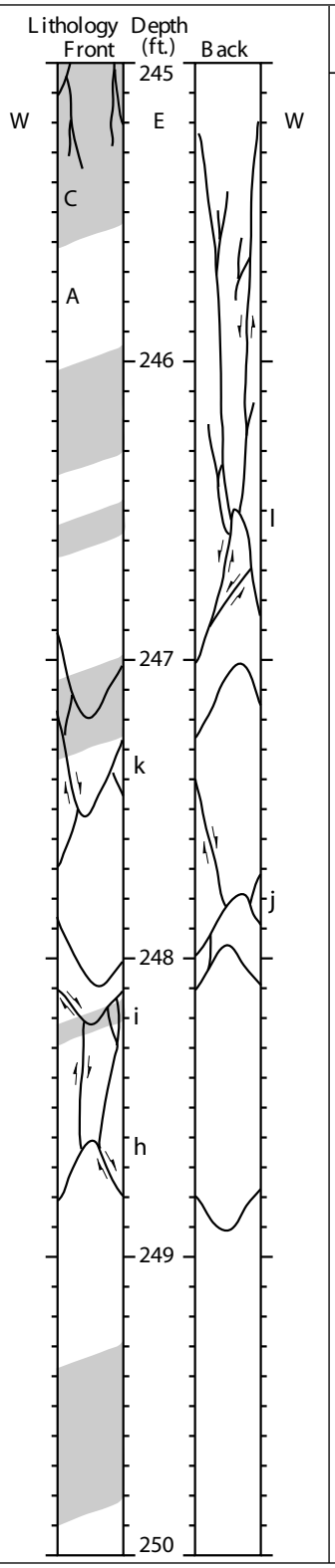

Apparent Disp. (mm)	Fault Thickness (mm)	Fault Strike	Fault Dip	Comments
l=64	6	N50E	75SE	Fault "l" correlates w/247.4' in BHTV-log
k=14	2 cg	N45E	65SE	
j=?	2 mg	N40E	56SE	
i=19	4 mg	N60E	55SE	Fault "i" correlates w/248.4' in BHTV-log
h=6	2 cg	N60E	57NW	
				Bedding @ 249.9' : N60E 21NW

Depth Interval: 250 - 255 Well: NNR - 7

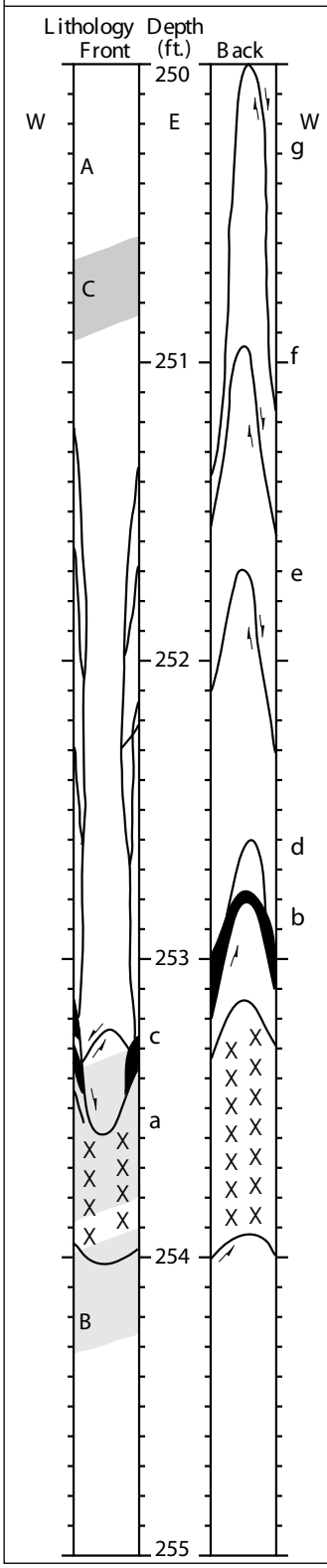

Apparent Disp. (mm)	Fault Thickness (mm)	Fault Strike	Fault Dip	Comments
g=4	2 cg	N70E	83SE	
f=7	2 cg	N80E	75SE	
e=14	2 mg	N60E	81SE	
				Bedding @ 253.8': N1E 23NW [obtained from BHTV-log]
d=?	1 cg	N50E	71SE	
b=?	> 140	N70E	75SE	Run #24 Score card: 253.32' 251.1' - 261.4' Drilled: 10.0'
c=2	1 cg	N65E	67NW	Recovered: 10.3'
a=?	>140	N60E	53SE	Fault "a" correlates w/253.5' in BHTV-log Shear zone is composed of quasi-parallel striking small faults which change to a steeper dip higher in core. High angle faults are younger than lower angle faults due to cross cutting relationship.
				Bedding @ 254.1' : NS 18W
				Bedding @ 254.1': N3E 27NW [obtained from BHTV-log]
				Bedding @ 254.5': N11E 27NW [obtained from BHTV-log]

Depth Interval: 255 - 260 Well: NNR - 7

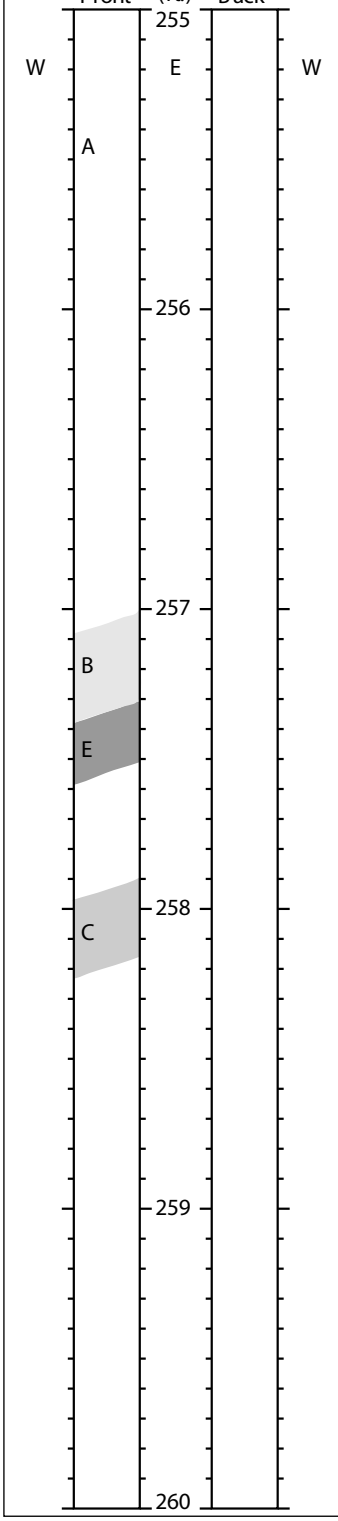

Apparent Disp. (mm)	Fault Thickness (mm)	Fault Strike	Fault Dip	Comments
				Bedding @ 255.9': N10E 26NW [obtained from BHTV-log]
				Bedding @ 257.2': N5E 26NW [obtained from BHTV-log]
				Bedding @ 257.6': N16E 26NW [obtained from BHTV-log]
				Bedding @ 259.7': N13E 26NW [obtained from BHTV-log]
				Bedding @ 259.8' : N30E 21NW

Depth Interval: 260 - 265 Well: NNR - 7

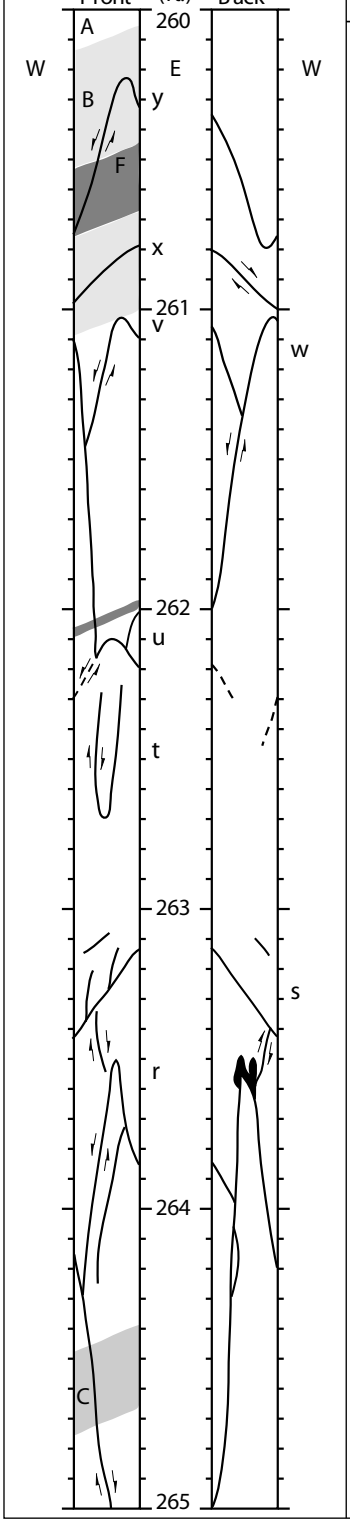

Apparent Disp. (mm)	Fault Thickness (mm)	Fault Strike	Fault Dip	Comments
y=15	3 cg	N40E	71NW	
x=15		NS	65W	
v=2	1 cg	N30E	76NW	Run #25
w=4	1 cg	N40E	84SE	Score card: 181.1' 261.1' - 271.1' Drilled: 10.0' Recovered: 10.0'
				Bedding @ 262.0' : N15W 23NW
u=2	1 cg	N60E	65NW	Bedding @ 262' : NS 26NW [obtained from BHTV-log]
t=2	1 cg	N70E	89SE	
s=?	8 cg	N10E	51NW	Fault "s" correlates w/263.5' in BHTV-log
r=5	2 cg	N60E	74NW	

Depth Interval: 265 - 270 Well: NNR - 7

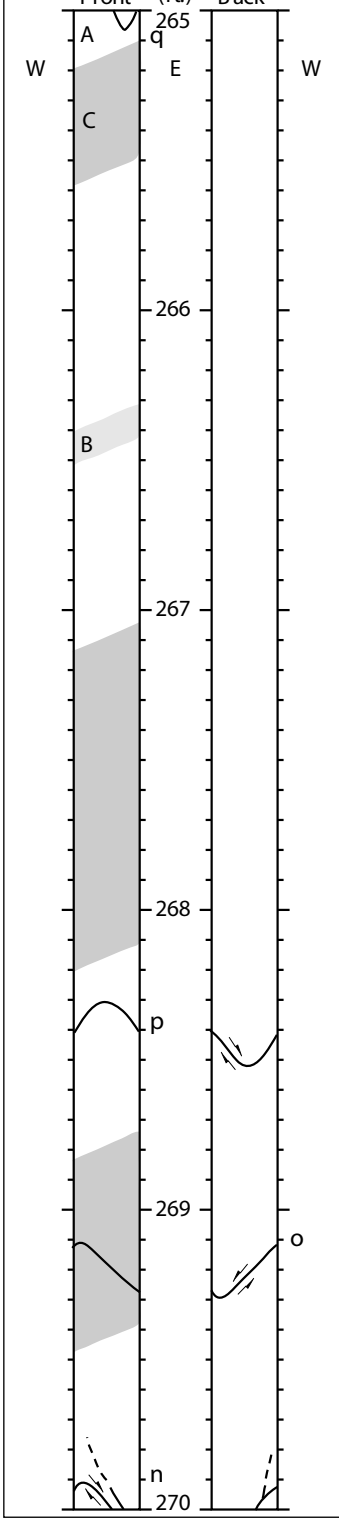

Apparent Disp. (mm)	Fault Thickness (mm)	Fault Strike	Fault Dip	Comments
q=15	3 cg	N50E	84SE	Fault "q" correlates w/265.2' in BHTV-log
				Bedding @ 265.5' : N30E 19NW [obtained from BHTV-log]
				Bedding @ 266.8' : N5E 28NW [obtained from BHTV-log]
p=5	1 mg	N80W	52NE	
o<4	1 fg	N10W	44NE	Fault "o" correlates w/269' in BHTV-log
n=15	2 cg	N20W	51NE	Nice example of mechanical stratigraphy @ 270.05'

Depth Interval: 270 - 275 Well: NNR - 7

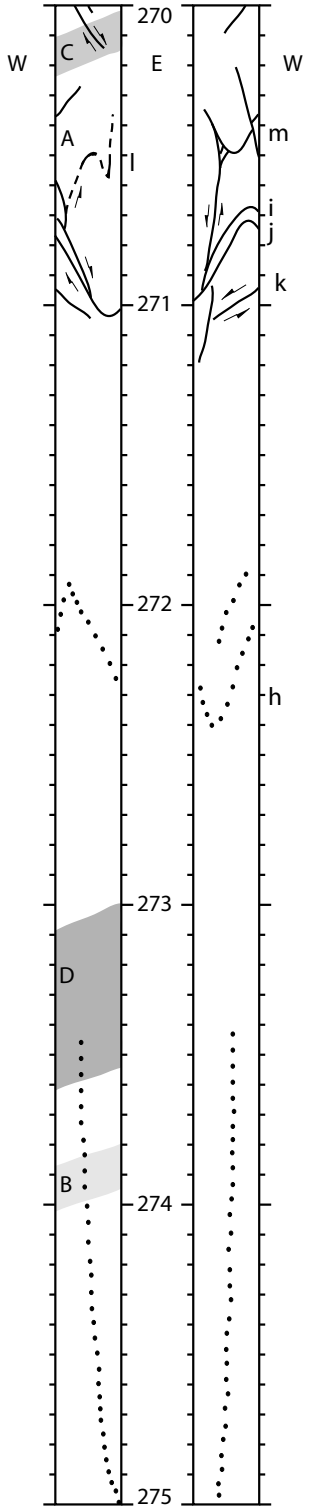

Apparent Disp. (mm)	Fault Thickness (mm)	Fault Strike	Fault Dip	Comments
m=?	0.5 cg	N60E	60NW	
l=5	0.5 cg	N80E	57NW	
i>30	5 cg	N30E	64SE	Faults "i" & "j" correlates w/271.2'
j=?	5 cg	N30E	61SE	in BHTV-log
5 @ 270.7'	1cg			
k=10	2 cg	NS	44E	Run #26 Score card: 271.12' 271.1' - 280.8' Drilled: 10.0' Recovered: 9.7'
				Bedding @ 273.1' : N25E 24NW [obtained from BHTV-log]
h=?		N45W	71NE	Joint "h" correlates w/272.8' in BHTV-log
				Bedding @ 273.2' : N15E 19NW
				Bedding @ 274.1' : N15E 18NW [obtained from BHTV-log]

Depth Interval: 275 - 280 Well: NNR - 7

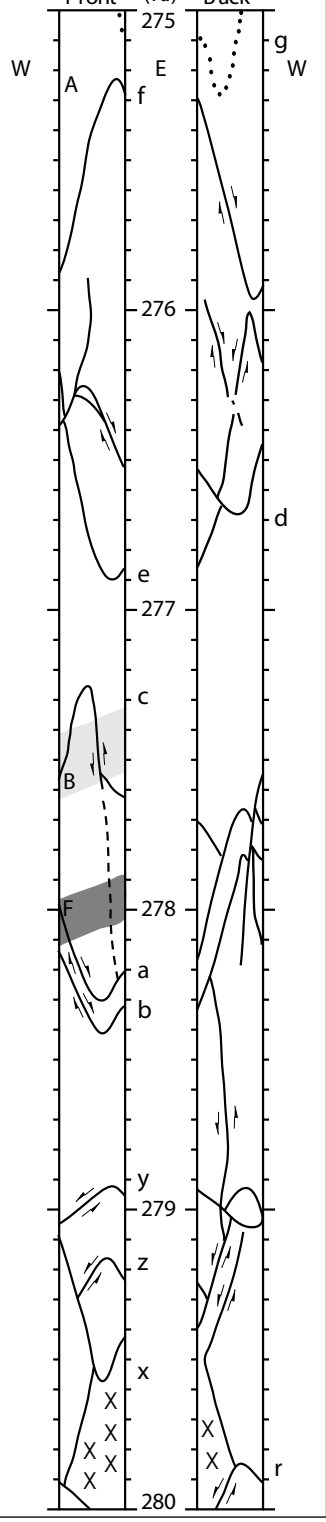

Apparent Disp. (mm)	Fault Thickness (mm)	Fault Strike	Fault Dip	Comments
g=?		N50W	86NE	Joint "g" correlates w/276.1' in BHTV-log
f=9	1 cg	N20E	73NW	
				Bedding @ 275.9' : N10W 2SW
d>20	1 cg	N60E	60NW	appears that "d" is younger than "e" but cross-cutting offset is opposite of "d" displacement.
e=10	2 cg	N20E	74SE	
c=32	2 cg	N70E	71NW	"c" is younger than "a" & "b"
a=34	3 cg	N50E	65SE	
b=16	1 cg	N55E	61SE	
31 @ 278.5'	3 cg			
y=6	1 mg	N10E	42NW	"y" is younger than "x"
z=5	2 mg	N60W	63NE	
				Bedding @ 279.4' : N40E 21NW
x=50	5 cg	N50E	70SE	
r=13	1 mg	N50E	52SE	

Depth Interval: 280 - 285 Well: NNR - 7

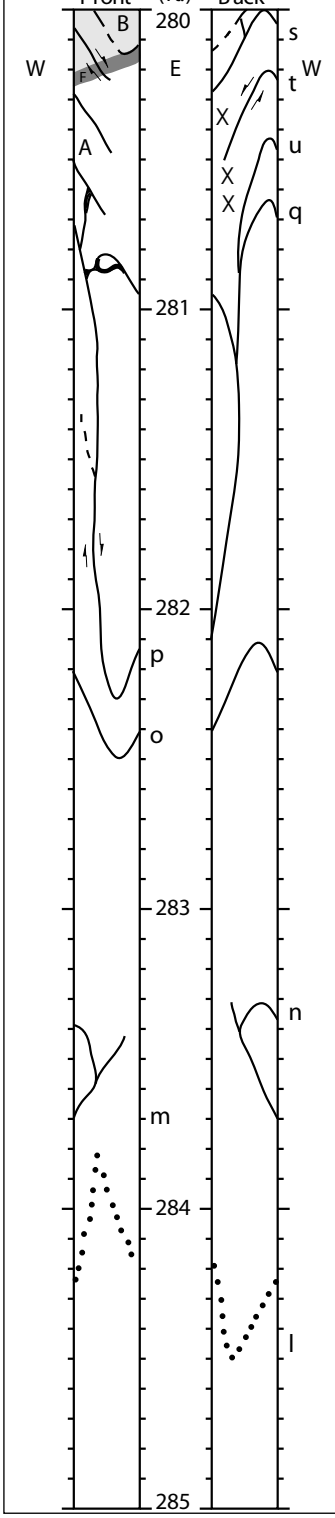

Apparent Disp. (mm)	Fault Thickness (mm)	Fault Strike	Fault Dip	Comments
s=6	1 cg	N40E	56SE	
t=5	1 cg	N30E	55SE	Between 280' and 282' core is 1.7' with no core loss other than one piece which does not affect true length.
u=?	1 cg	N30E	51SE	
q=?	10 cg	N20E	72SE	Fault "q" correlates w/280.5' in BHTV-log
65 @ 281.5'	4 cg			
				Run #27 Score card: 281.9' 281.1' - 291.0' Drilled: 10.0' Recovered: 9.9'
p=?	4 cg	N50E	86SE	
o=?	1 cg	N40E	61SE	Fault "o" correlates w/282.5' in BHTV-log
n=?	2 cg	N30E	54SE	
m=?	1 cg	NS	53W	
l=?		N60W	64NE	Joint "l" correlates w/283.9' in BHTV-log

Depth Interval: 285 - 290 Well: NNR - 7

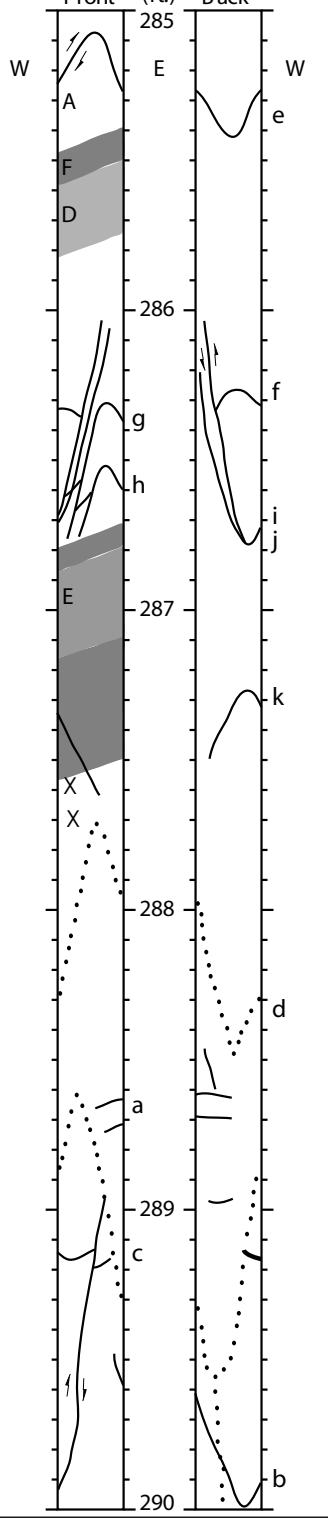

Apparent Disp. (mm)	Fault Thickness (mm)	Fault Strike	Fault Dip	Comments
e=9	2 cg	N70E	54NW	
f=?	2 cg	N60E	36NW	
g=?	2 cg	N50E	70NW	
h=?	2 cg	N40E	68NW	
i+j=11	6 cg	N30E	76NW	
	2 cg	N30E	74NW	
				Bedding @ 287.0' : N30W 18SW
k=?		N30E	54SE	
d=?		N60E	68NW	
a=?		N50W	78NE	Joint "a" correlates w/289.5' in BHTV-log
c=?	3	N40W	14SW	"c" is older than "b"
b=14	4 cg	N40E	64NW	Fault "b" correlates w/290' in BHTV-log

Depth Interval: 290 - 295 Well: NNR - 7

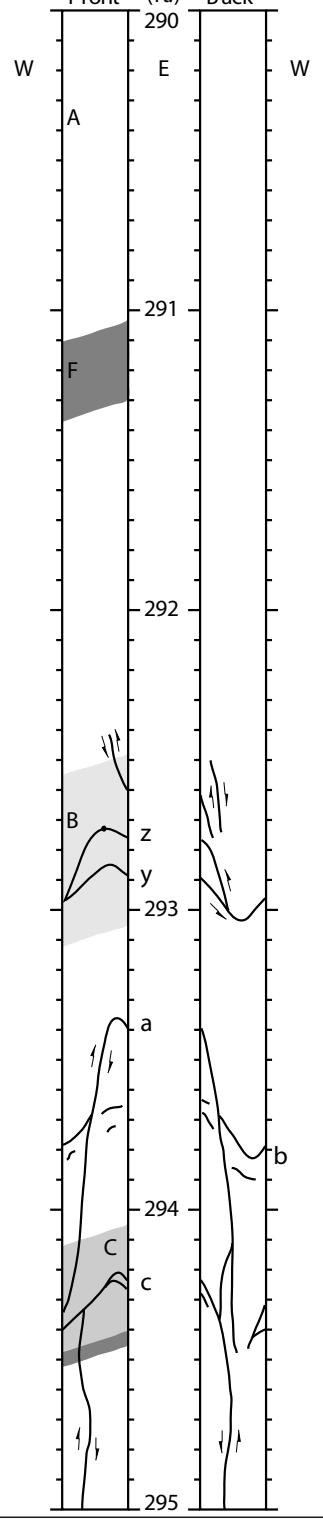

Apparent Disp. (mm)	Fault Thickness (mm)	Fault Strike	Fault Dip	Comments
				Bedding @ 290.5' : N15W 20SW [obtained from BHTV-log]
				Run #28 Score card: 291.06' 291.1' - 301.2' Drilled: 10.0' Recovered: 10.1' Bedding @ 291.4' : N35W 13SW [obtained from BHTV-log] Bedding @ 291.6' : N19W 16SW [obtained from BHTV-log] Bedding @ 291.8' : N30W 18SW
1 @ 292.7'				
z+y=9	z+y=3 fg	N50E	41NW	
		N50E	36NW	
a=12	2 mg	N20E	82NW	
b=?	1	N30E	31NW	
c=?	1	N25E	37NW	
6@ 294.7'	1 mg			

Depth Interval: 295 - 300 Well: NNR - 7

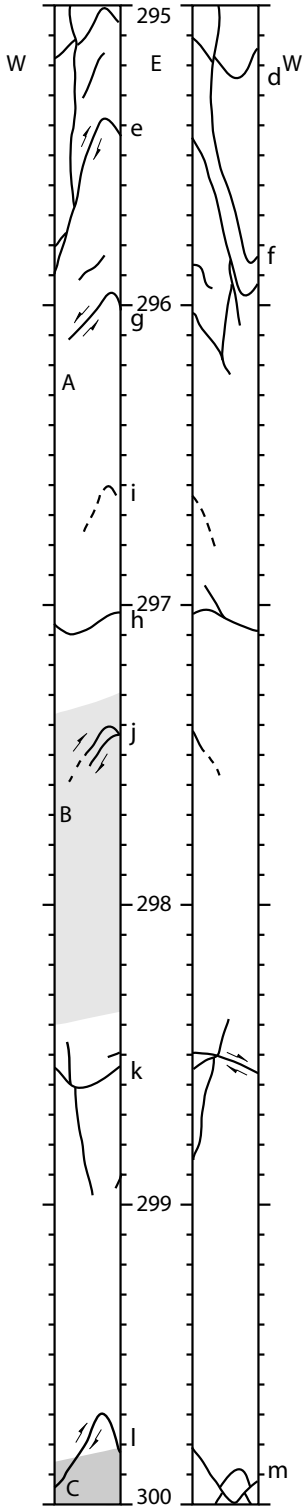

Apparent Disp. (mm)	Fault Thickness (mm)	Fault Strike	Fault Dip	Comments
d=?	1	N40E	40NW	"d" is older than steeper fault
e=23	3 fg	N30E	64NW	
f=?	1	N30E	76NW	
g=11	1 fg	N20E	52NW	
i=?		N30E	62NW	
h=?	1	N40W	19SW	
j=1	1 fg	N20E	40NW	
				Bedding @ 297.7' : N15E 16NW [obtained from BHTV-log]
				Bedding @ 298.2' : N45W 11SW
k=3	1 fg	N60E	17NW	
				Fault "l" correlates w/301.6'
l=7	1 fg	N40E	56NW	in BHTV-log
m=?	1	N60E	65SE	"m" is older than "l"

Depth Interval: 300 - 305 Well: NNR - 7

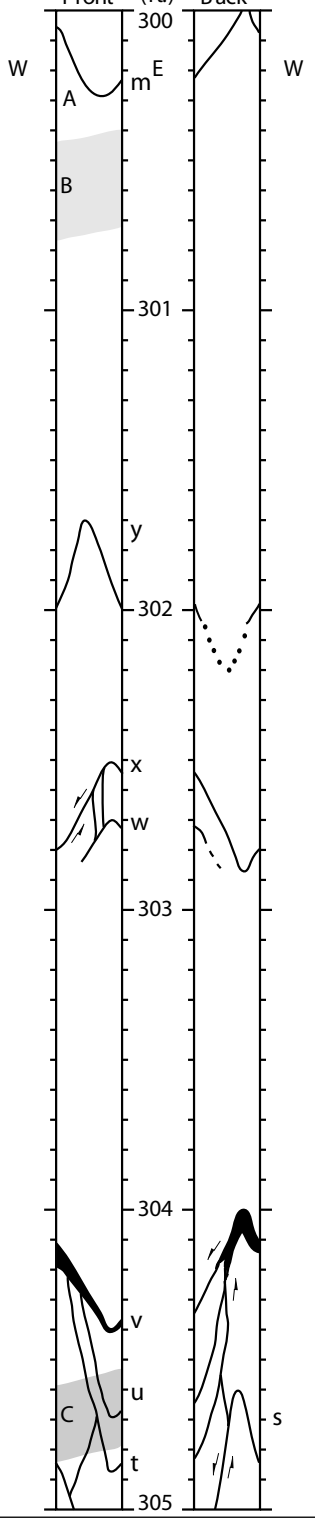

Apparent Disp. (mm)	Fault Thickness (mm)	Fault Strike	Fault Dip	Comments
				details on previous page
				Run # 29 Score card: 301.2' 301.1' - 310.85' Drilled: 9.7' Recovered: 9.75'
y>20	2	N80E	66NW	
x=22	2	N20E	55NW	Bedding @ 302.6' : N10W 14SW
w=?	1	N10E	53NW	
v>10	2 fg/mg	N30E	55SE	Fault "v" correlates w/303.7' in BHTV-log
u=?		N30E	71SE	"v"+"u"+"t" = > 40mm thick
s=23	2 cg	N40E	79SE	
t=?		N30E	72SE	

Depth Interval: 305 - 310 Well: NNR - 7

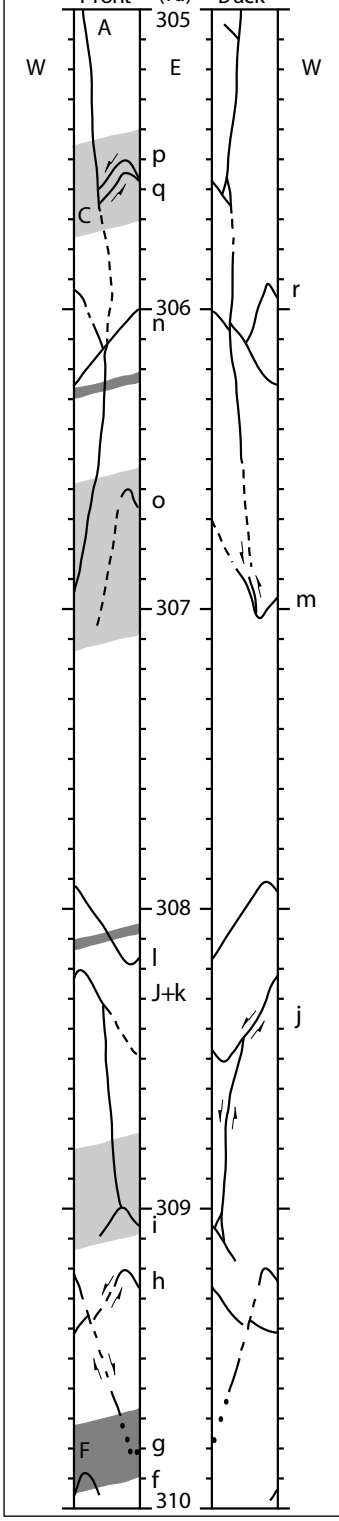

Apparent Disp. (mm)	Fault Thickness (mm)	Fault Strike	Fault Dip	Comments
p+q=9	1 fg	N30E	46NW	
q=?	1	N20E	52NW	
r=?	2	N20E	81SE	
n=?	5	NS	39W	
o=?	1	N20E	73NW	"n" is older than "m"
m=9	2 mg	N40E	83NW	
l=?	1	N10E	55SE	
k=2	1 mg	N10W	82NE	
j=14	2	N10W	56NE	
i=?	0.5	N35E	53NW	
h=14	1 mg	N30E	60NW	"h" is older than "g"
				Bedding @ 309.6' : N10W 19SW [obtained from BHTV-log]
g=2	1 mg	N10E	70SE	
f=2		N20W	67NE	

Depth Interval: 310 - 315 Well: NNR - 7

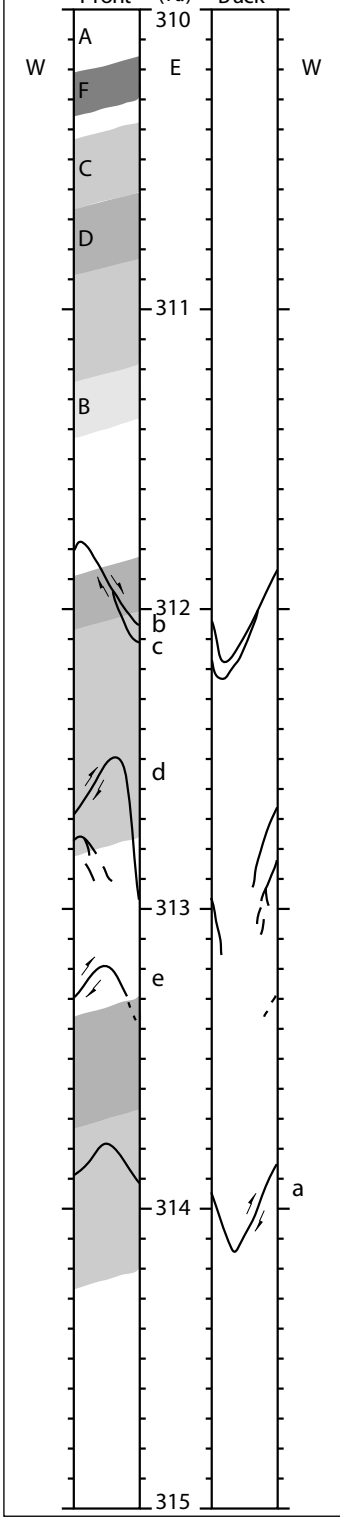

Apparent Disp. (mm)	Fault Thickness (mm)	Fault Strike	Fault Dip	Comments
				Bedding @ 310' : N13W 24SW [obtained from BHTV-log]
				Run # 30 Score card: 310.8' 310.8' - 320.95' Drilled: 10.0' Recovered: 10.15'
				Bedding @ 311.4' : N10W 16SW
b=4	0.5 fg	N15W	62NE	
c=?	0.5	N10W	64NE	
d=1	0.5 fg	N80E	73NW	
e=10		N70E	63NW	Some doubt about fault disp. direction on "e"
a=9	1 mg	N70E	61NW	

Depth Interval: 315 - 320 Well: NNR - 7

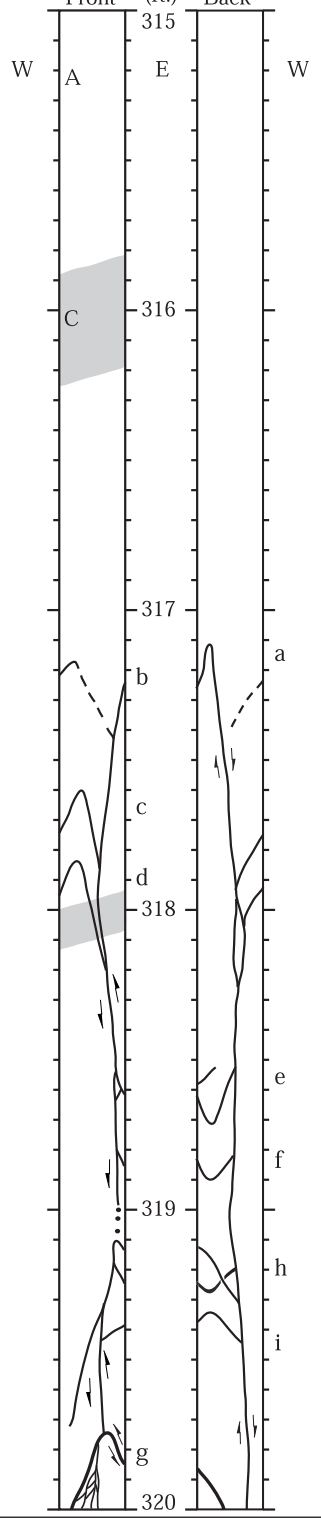

Apparent Disp. (mm)	Fault Thickness (mm)	Fault Strike	Fault Dip	Comments
				Bedding @ 315.0' : N40W 16SW
a=2 b<1	1 mg	N15W N40W	84SW 54NE	
c<1	1	N50W	67NE	
d<1	1	N60W	76NE	
				@ 318.1 fault disp. is 4mm fine-grained sandstone 1mm thick
e=?	0.5 cg	N50W	60NE	
f=?	0.5 cg	N60W	48NE	
				@ 319.0 fault disp. is 11mm coarse-grained sandstone 2mm thick
h=?	0.5 cg	N20W	41NE	
i=?	0.5 cg	N20W	45SW	@ 319.5 fault disp. is 27mm medium-grained sandstone 3mm thick
g=14	2 mg	N40E	60NW	Fault "g" correlates w/319.5' in BHTV-log

Depth Interval: 320 - 325 Well: NNR - 7

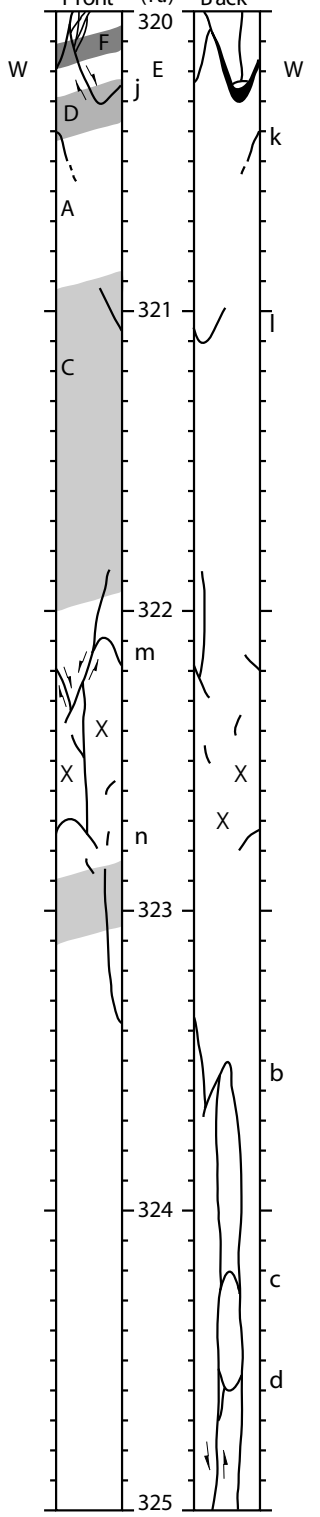

Apparent Disp. (mm)	Fault Thickness (mm)	Fault Strike	Fault Dip	Comments
				Bedding @ 320.1' : N5E 35NW [obtained from BHTV-log]
j=9	1 fg	N50E	57SE	Bedding @ 320.3' : N10E 16NW
k=?	1	NS	38E	
				Run # 31 Score card: 320.7' 320.8' - 331.9' Drilled: 10.1' Recovered: 10.1'
l=?		N50W	65NE	Bedding @ 320.9' : N20E 15NW [obtained from BHTV-log]
m=3	0.5 cg	N40E	60NW	
n=?	0.5 cg	N40W	57NE	
b=?		EW	83S	
c=?	1 cg	N75E	46SE	
d=?	1 cg	N70E	57NW	

Depth Interval: 325 - 330 Well: NNR - 7

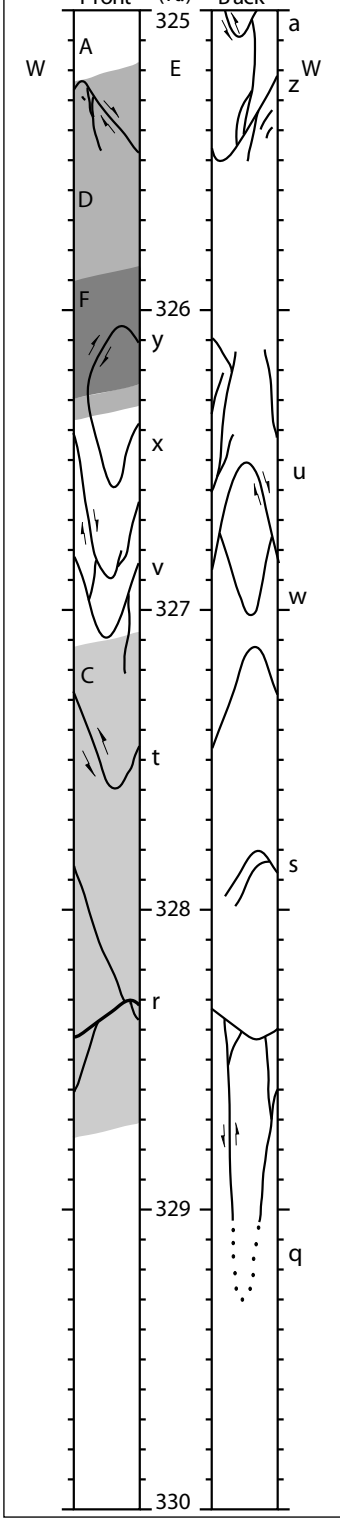

Apparent Disp. (mm)	Fault Thickness (mm)	Fault Strike	Fault Dip	Comments
a=17	2 cg	EW	83N	
z=8	1 fg	N20W	44NE	
				Bedding @ 325.8' : NS 12W
y=5	0.5 clay	N40E	57NW	
x=?		N60E	73SE	
u=7	1 cg	N50E	64SE	Fault "u" correlates w/326.5' in BHTV-log
v=21	3 cg	N60E	71SE	
w=?	1	N60E	64NW	
t=?	9	N60E	65SE	Fault "t" correlates w/327' in BHTV-log
s=?	1	N60E	47SE	
r=?	1	N40E	30NW	Fault "r" correlates w/328.5' in BHTV-log
q=17	7 fg	N70E	85NW	Fault "q" correlates w/329.6' in BHTV-log

Depth Interval: 330 - 335 Well: NNR - 7

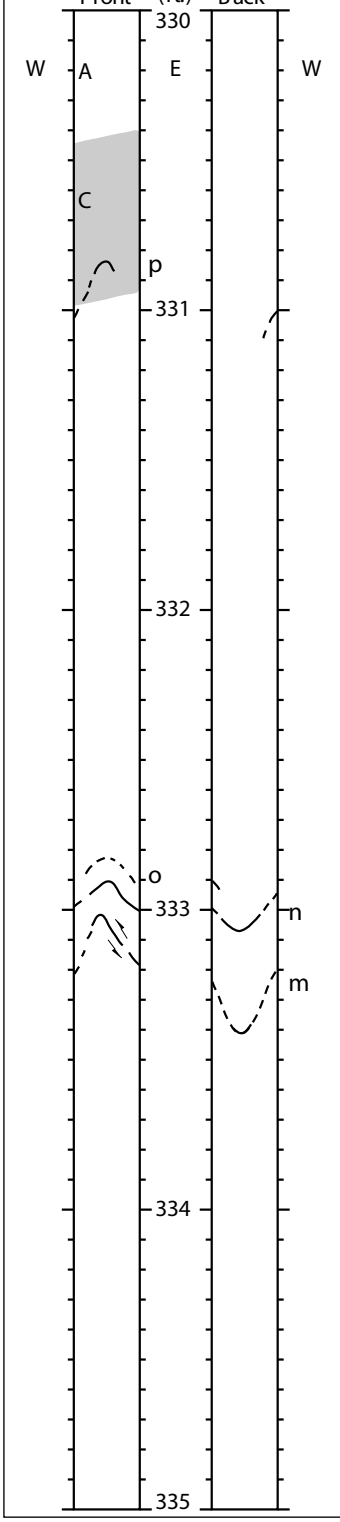

Apparent Disp. (mm)	Fault Thickness (mm)	Fault Strike	Fault Dip	Comments
p=?	1	N70E	56NW	Run # 32 Score card: 330.95' 330.9' - 340.9' Drilled: 10.1' Recovered: 10.0'
o=?	1	N80E	36NW	
n=?	2	N75E	28NW	
m=1	0.5 mg	EW	53N	

Depth Interval: 335 - 340 Well: NNR - 7

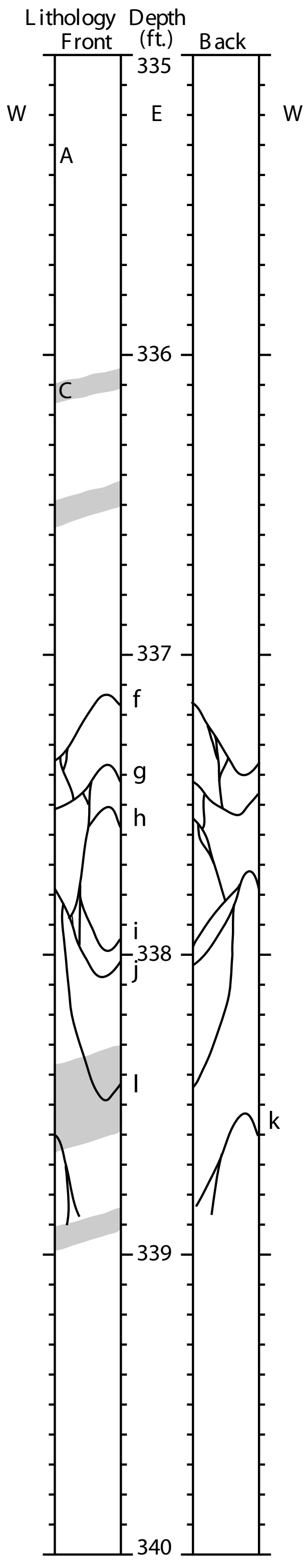

Apparent Disp. (mm)	Fault Thickness (mm)	Fault Strike	Fault Dip	Comments
				Bedding @ 336.4' : N10E 17NW
f=?	5	N40E	51NW	
g=?	3	N30E	61NW	
h=?	3	N35E	56NW	
i=?	2	N25E	47SE	
j=?	3	N30E	52SE	
l=?	2	N40E	65SE	
k=?	3	N50E	64SE	

Depth Interval: 340 - 345 Well: NNR - 7

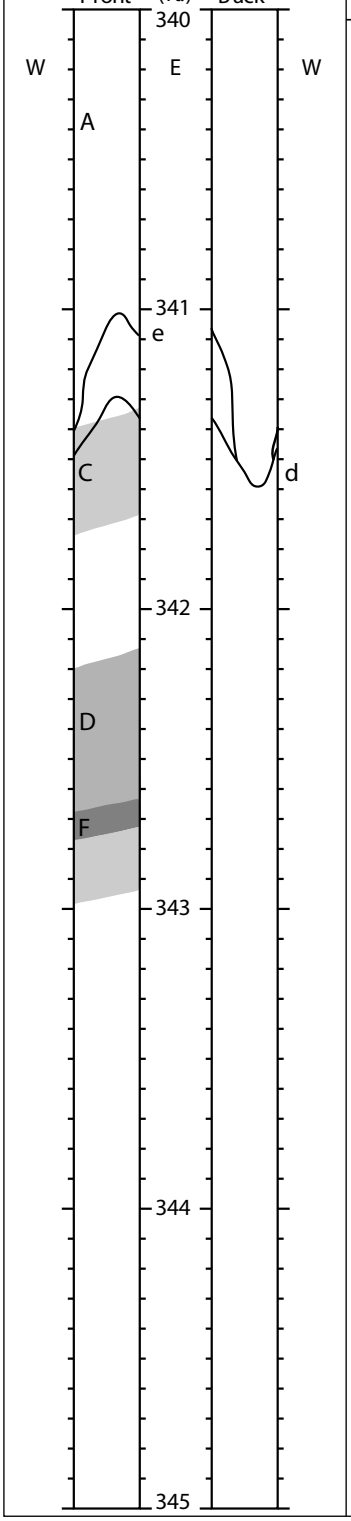

Apparent Disp. (mm)	Fault Thickness (mm)	Fault Strike	Fault Dip	Comments
e=?	1	N45E	64NW	Run # 33 Score card: 341.0' 341.0' - 351.1' Drilled: 10.0' Recovered: 10.5'
d=?	1	N50E	47NW	
				Bedding @ 342.5' : N45W 15SW [obtained from BHTV-log]
				Bedding @ 342.3' : N40W 12SW
				Bedding @ 342.5' : N80W 15SW [obtained from BHTV-log]

Depth Interval: 345 - 350 Well: NNR - 7

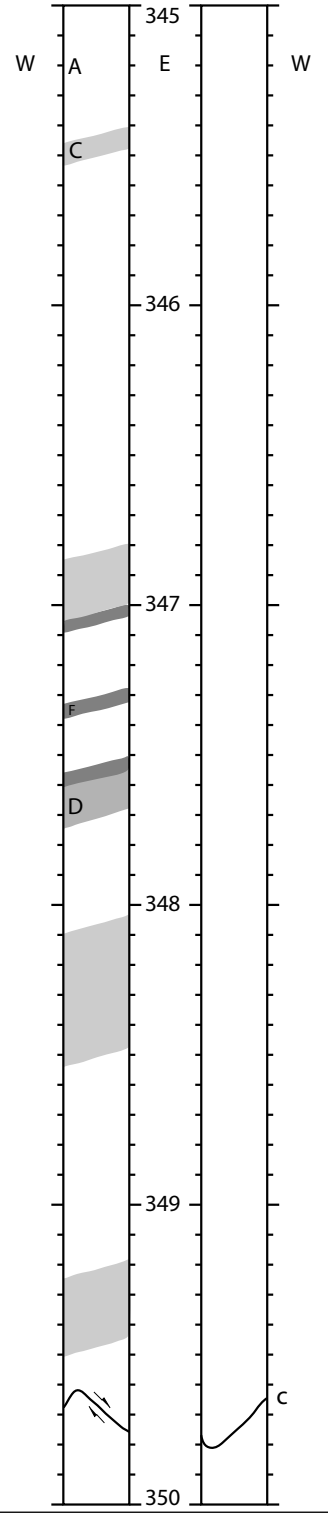

Apparent Disp. (mm)	Fault Thickness (mm)	Fault Strike	Fault Dip	Comments
				Bedding @ 345.3' : N75W 14SW [obtained from BHTV-log]
				Bedding @ 345.5' : N50W 14SW
				Bedding @ 346.9' : N53W 11SW [obtained from BHTV-log]
				Bedding @ 347.2' : N50W 15SW [obtained from BHTV-log]
				Bedding @ 347.7' : N30W 16SW
c=3	2 cg	N30W	32NE	
				Bedding @ 349.9' : N30W 18SW

Depth Interval: 350 - 355 Well: NNR - 7

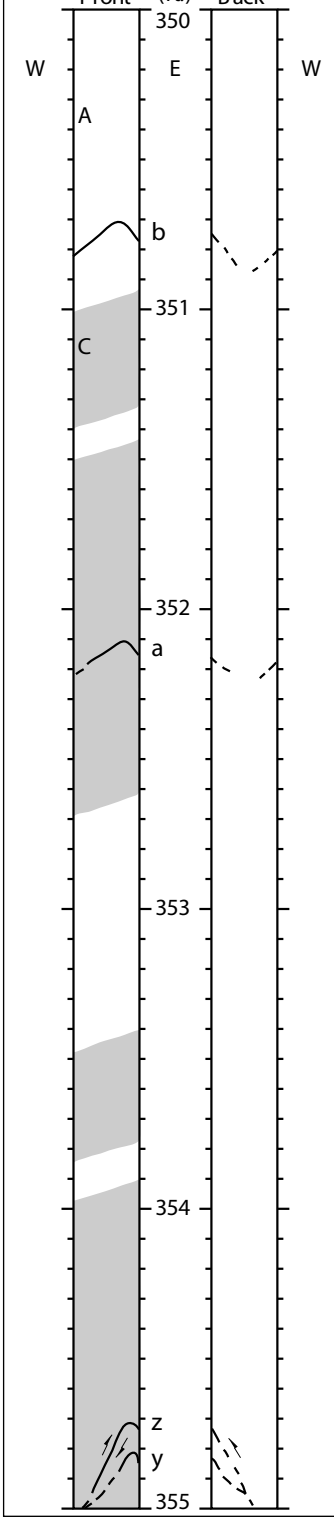

Apparent Disp. (mm)	Fault Thickness (mm)	Fault Strike	Fault Dip	Comments
b=?	1	N50E	37NW	
a=?	0.5	N40E	35NW	
				Bedding @ 352.8' : N60W 13SW [obtained from BHTV-log]
				Bedding @ 353.5' : N25W 15SW [obtained from BHTV-log]
z=3	1 cg	N25E	42NW	
y=?	1	N20E	63NW	

Depth Interval: 355 - 360 Well: NNR - 7

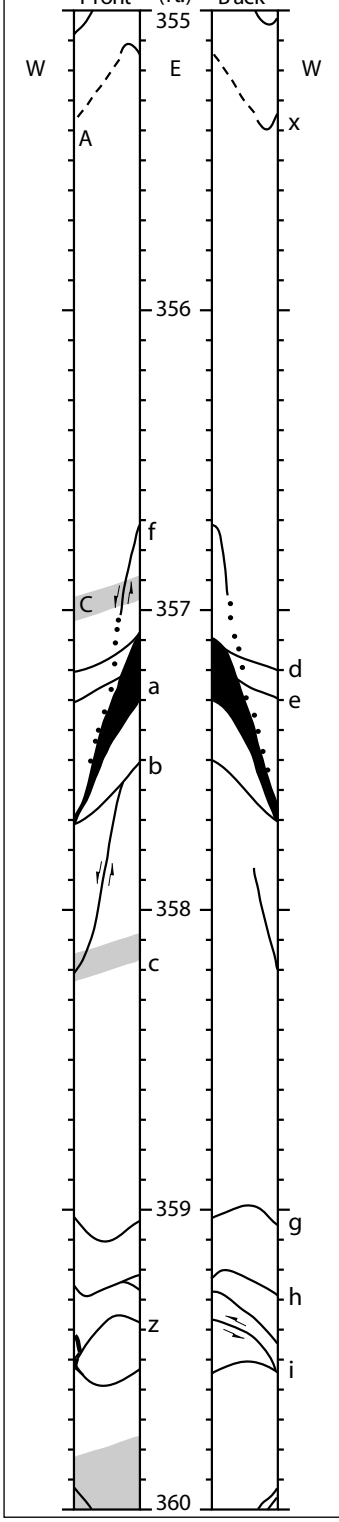

Apparent Disp. (mm)	Fault Thickness (mm)	Fault Strike	Fault Dip	Comments
x=?	1	N25E	59NW	
f=10	2 cg	N10E	60NW	
d=?	3	NS	34W	
e=?	3	N20E	34NW	
a=?	11	NS	71W	Fault "a" correlates w/356.7' in BHTV-log
b=?	4	N10W	34SW	
				Bedding @ 357.9' : N30W 18SW [obtained from BHTV-log]
c=6	3 cg	NS	72W	
g=?	3	N80W	14SW	
h=?	4	N40W	17SW	
z=7	2 mg	N40E	44NW	
i=?	4	N70W	12SW	

Depth Interval: 360 - 365 Well: NNR - 7

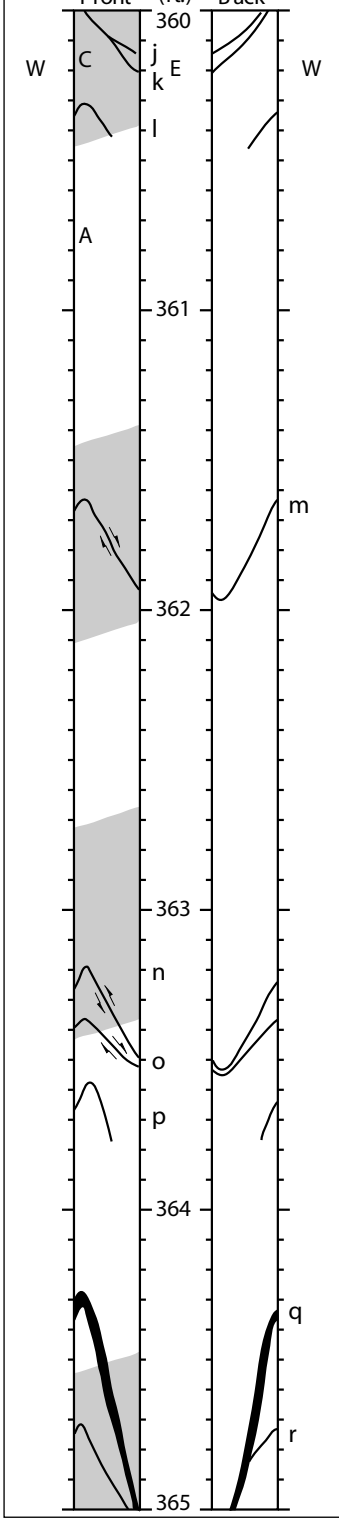

Apparent Disp. (mm)	Fault Thickness (mm)	Fault Strike	Fault Dip	Comments
j=?	3	NS	41E	
k=?	7	NS	42E	Fault "k" correlates w/359.9' in BHTV-log
l=?	1	N30W	38NE	
				Bedding @ 361.2': N82W 11SW [obtained from BHTV-log]
				Run # 35 Score card: 361.0' 361.0' - 371.1' Drilled: 10.0' Recovered: 10.1'
m=5	1 fg	N40W	55NE	Bedding @ 361.9': N57E 11SE [obtained from BHTV-log]
n=3	1 mg	N40W	53NE	
o=10	1 mg	N30W	47NE	
p=?	1	N50W	67NE	
q=?	11	N30W	71NE	
r=?	2	N20W	65NE	

Depth Interval: 365 - 370 Well: NNR - 7

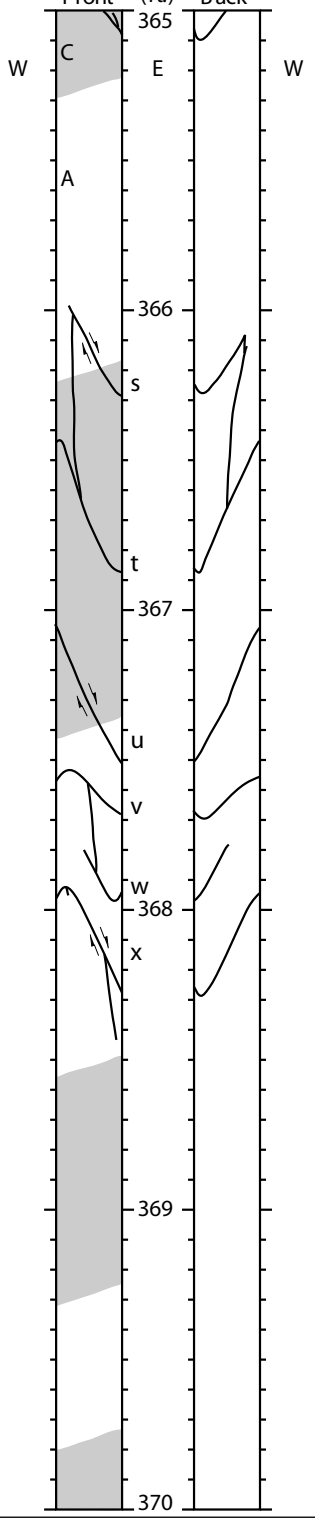

Apparent Disp. (mm)	Fault Thickness (mm)	Fault Strike	Fault Dip	Comments
s=3	1 mg	N20W	48NE	
t=?	1	N10W	56NE	
u>10	1	NS	68E	
v=?	3	N10W	46NE	
w=?	3	N15E	55SE	
x=5	1 cg	N10W	64NE	Bedding @ 368.3': N30W 27SW [obtained from BHTV-log]
				Bedding @ 368.8': N68W 28SW [obtained from BHTV-log]

Depth Interval: 370 - 375 Well: NNR - 7

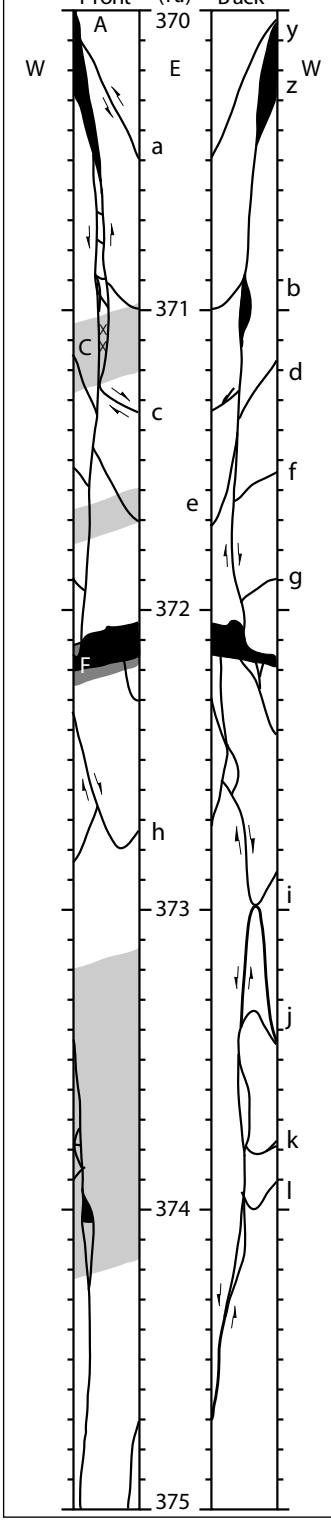

Apparent Disp. (mm)	Fault Thickness (mm)	Fault Strike	Fault Dip	Comments
y+z=40 @ 370.9'	y+z=4 fg	NS	84E	
		NS	83E	
a=10	2 mg	NS	66E	
b=?	1	N10W	30NE	
d=?	1	NS	67E	
c=4	2 fg	N10E	26SE	
f=?	1	N10E	43SE	
e=?	2	N10W	71NE	
g=?	1	N10W	51NE	Bedding @ 371.9': N22W 22SW [obtained from BHTV-log]
23 @ 372.15'				Bedding @ 372.2': N20W 17SW
h=13	2 cg	N50E	71SE	
i=4	1.5 mg	N40E	87SE	
j=?	1	N50E	64SE	
k=?	1	N50E	27NW	
l=?	1	N60E	51NW	
4 @ 374.5'	1 cg			

Depth Interval: 375 - 380 Well: NNR - 7

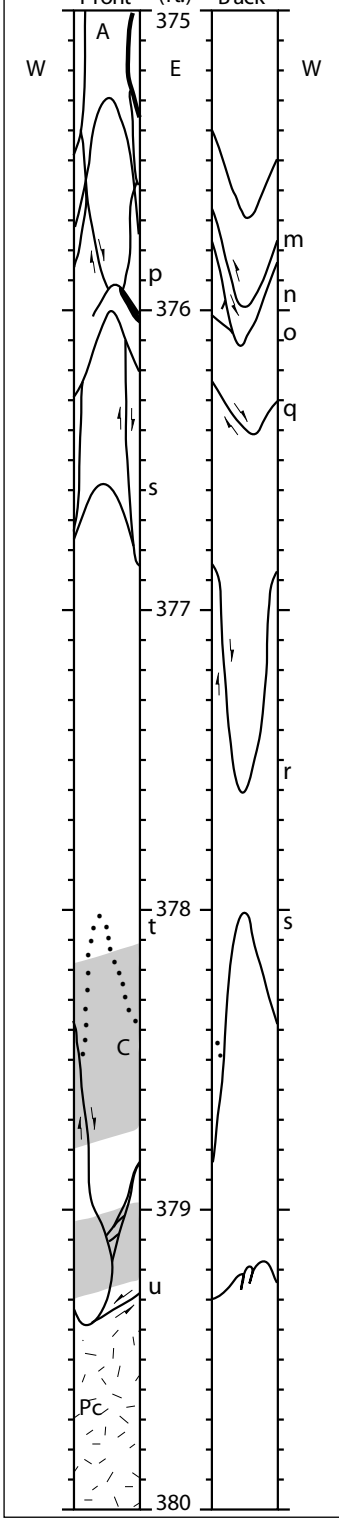

Apparent Disp. (mm)	Fault Thickness (mm)	Fault Strike	Fault Dip	Comments
m=?	1	N70E	62NW	
p=?	2	N60E	41NW	
n=2	1 cg	N75E	66NW	
o=?	1	N80E	71NW	
q=3	3	N70E	71NW	
s=?	1	N70W	68NW	
r=1	2 cg	N80E	76NE	
s=20	2 fg	N80W N80W	79SE 76NE	
u=66	5 cg	N20W	55SW	Fault "u" correlates w/379.6' in BHTV-log

Depth Interval: 170 - 175 Well: NNR - 8

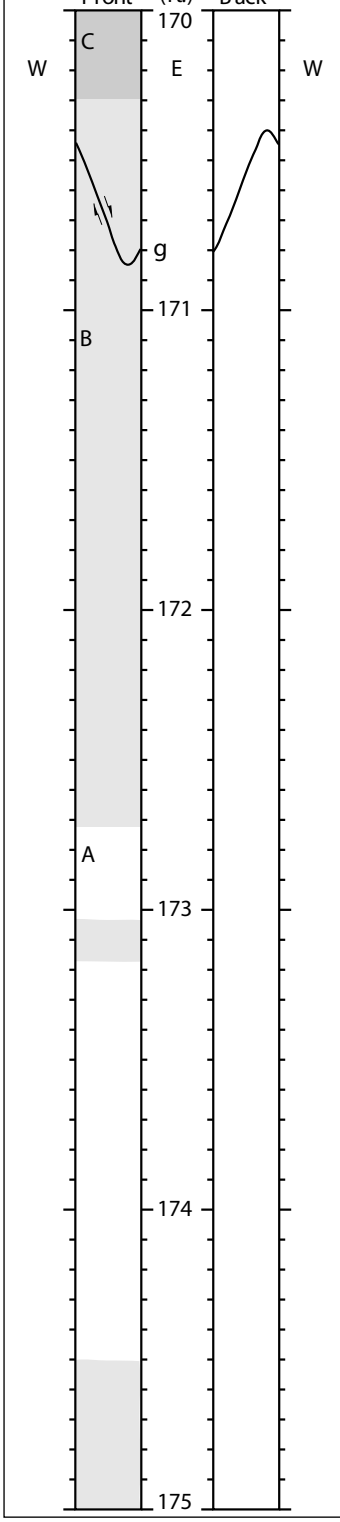

Apparent Disp. (mm)	Fault Thickness (mm)	Fault Strike	Fault Dip	Comments
g=13	0.5 clay	N35E	53SE	Run #18 Score card: 171.0' 170.9' - 181.1' Drilled: 10.0' Recovered: 10.2'
				Bedding @ 172.9' : NS 28W [obtained from BHTV-log]
				Missing core from 173.25' - 174.5'
				Bedding @ 174.2' : N22E 24NW [obtained from BHTV-log]

Depth Interval: 175 - 180 Well: NNR - 8

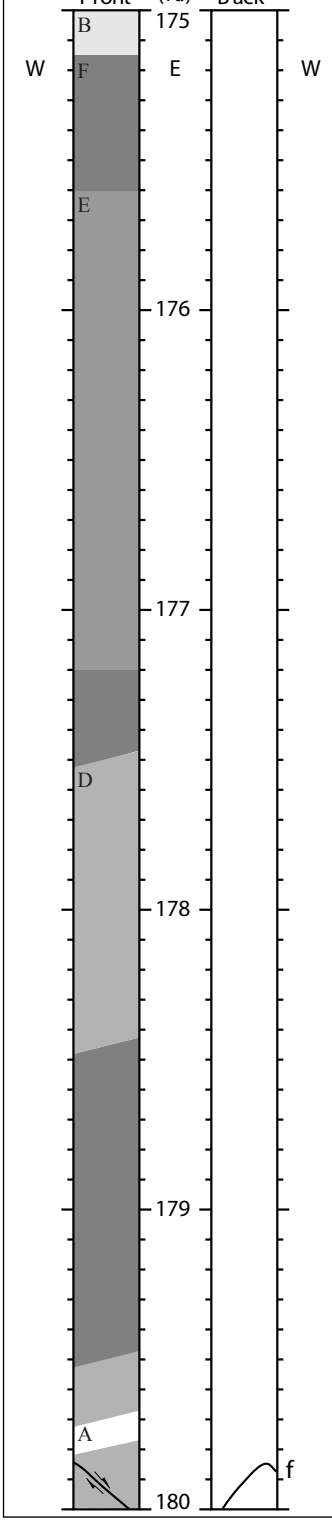

Apparent Disp. (mm)	Fault Thickness (mm)	Fault Strike	Fault Dip	Comments
				Bedding @ 177.25' : N5E 15NW
				Bedding @ 178.7' : N22E 19NW [obtained from BHTV-log]
				Bedding @ 179.65' : N15W 14SW
f=12	0.5 clay	N30E	43SE	

Depth Interval: 180 - 185 Well: NNR - 8

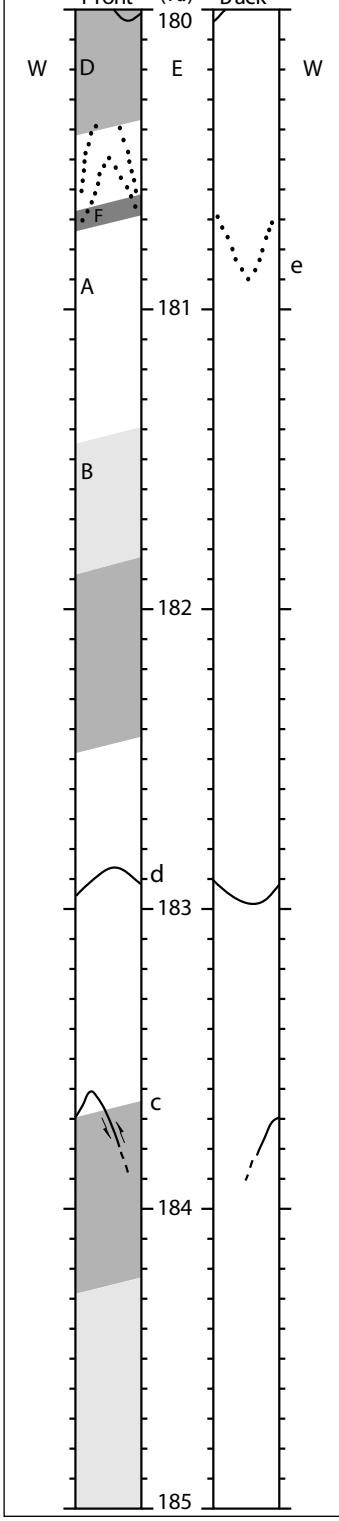

Apparent Disp. (mm)	Fault Thickness (mm)	Fault Strike	Fault Dip	Comments
e=?		N70W	56NE	Joint "e" correlates w/180.7' in BHTV-log
				Run #19 Score card: 181.1' 181.1' - 191.1' Drilled: 10.0' Recovered: 9.9'
				Bedding @ 182.2' : N5W 17SW [obtained from BHTV-log]
d=?	1 fg	N60E	32NW	
c=1	0.5 fg	N30W	57NE	
				Bedding @ 184.05' : N15E 14NW

Depth Interval: 185 - 190 Well: NNR - 8

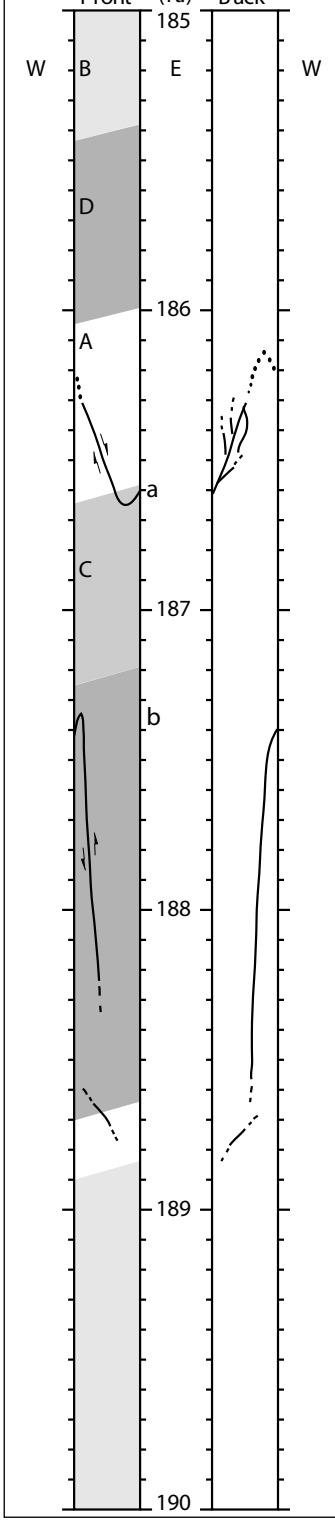

Apparent Disp. (mm)	Fault Thickness (mm)	Fault Strike	Fault Dip	Comments
a=18	2 cg	N25E	58SE	Fault "a" correlates w/185.8' in BHTV-log
				Bedding @ 186.7' : N10E 16NW
b=2	0.5 fg	N10W	87NE	
				Bedding @ 189.2' : N10E 17NW [obtained from BHTV-log]

Depth Interval: 190 - 195 Well: NNR - 8

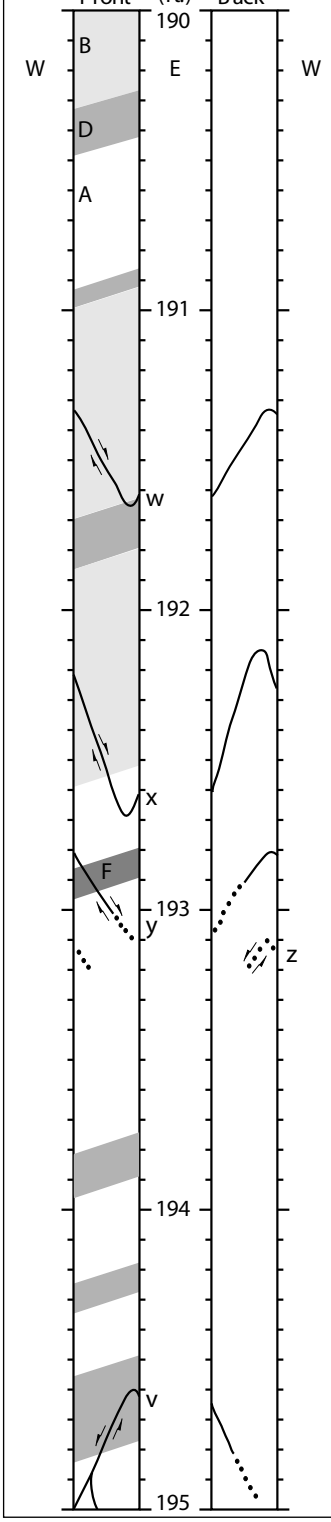

Apparent Disp. (mm)	Fault Thickness (mm)	Fault Strike	Fault Dip	Comments
				Run #20 Score card: 190.1' 191.1' - 201.1' Drilled: 10.0' Recovered: 10.1' Bedding @ 190.45' : N20W 18SW
w=3	0.5 fg	N15W	54NE	
x=5	0.5 mg	N40E	64SE	
y=6	0.5 cg	N10E	51SE	
z=2.5	0.5 cg	N15E	40SE	
v=10	1.5 cg	N20E	66NW	

Depth Interval: 195 - 200 Well: NNR - 8

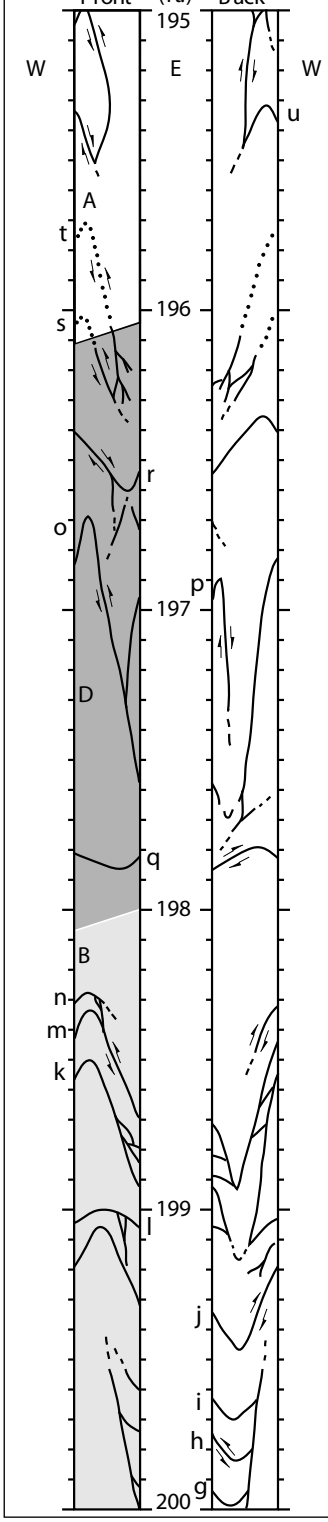

Apparent Disp. (mm)	Fault Thickness (mm)	Fault Strike	Fault Dip	Comments
u=6	0.5 fg	N30E	64SE	
t=4	0.5 fg	N15W	68NE	Faults "t" & "s" are good examples of how sorting & porosity of host Rx effect expression of fault trace
s=2	0.5 fg	N10W	63NE	
r=23	1 clay	N30E	52SE	
o=4	0.5 fg	N35W	81NE	
p=3	0.5 fg	N5E	87NW	
q=4	0.5 fg	N40E	18SE	Bedding @ 197.8' : N15E 24NW [obtained from BHTV-log] Bedding @ 197.9' : NS 17W
n=4	1.5 cg	N30W	54NE	
m=?	1 cg	N40W	66NE	
k=?		N40W	71NE	
l=7	1 cg	N50W	33NE	
j=16		N65W	59NE	
i=?	0.5 fg	N55W	48NE	
h=5	0.5 fg	N60W	43NE	
g=?	0.5 fg	N50W	42NE	

Depth Interval: 200 - 205 Well: NNR - 8

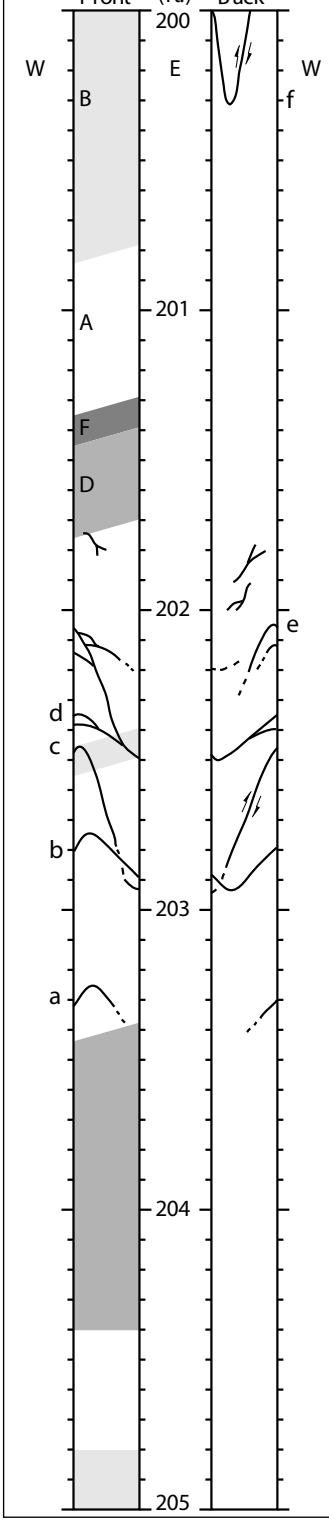

Apparent Disp. (mm)	Fault Thickness (mm)	Fault Strike	Fault Dip	Comments
f=9	1 cg	N40W	73NE	
				Bedding @ 200.9' : N5W 28SW [obtained from BHTV-log]
				Bedding @ 201.0' : N20W 16SW
				Run #21 Score card: 201.25' 201.1' - 211.1' Drilled: 10.0' Recovered: 10.1'
e=?	1 cg	N15E	47NE	
				Bedding @ 202.3' : N10E 34NW [obtained from BHTV-log]
d=?	1 cg	N5W	26NE	
c=1	0.5 fg	N10W	67NE	
b=?	1 cg	N35W	46NE	
a=?	0.5 mg	N30W	43NE	
				Bedding @ 203.6' : N22E 15NW [obtained from BHTV-log]
				Missing core from 204.4' - 204.8'

Depth Interval: 205 - 210 Well: NNR - 8

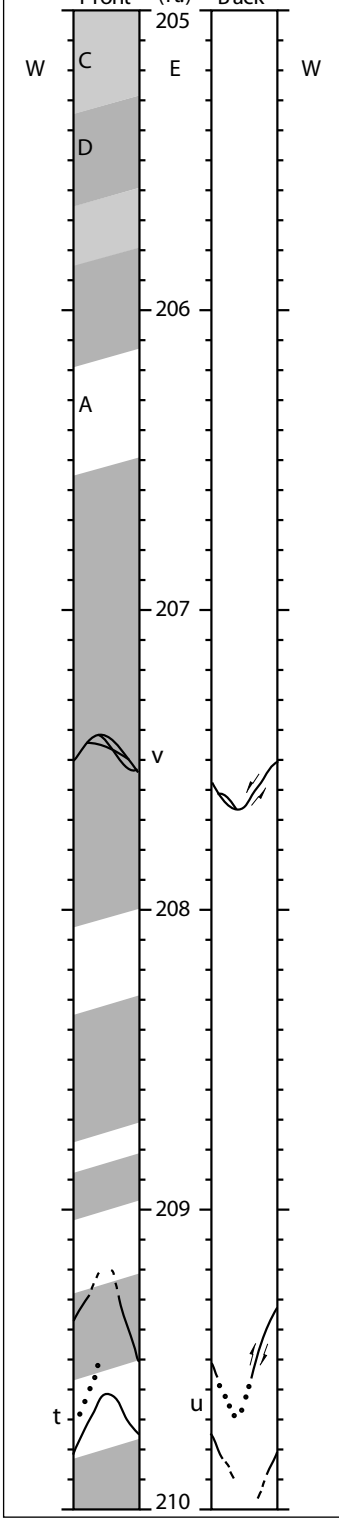

Apparent Disp. (mm)	Fault Thickness (mm)	Fault Strike	Fault Dip	Comments
				Bedding @ 206.5' : N10W 16SW
v=55	1 clay	N55W	49NE	
				Bedding @ 208.6' : N35E 17NW
u=1	0.5 mg	N50W	76NE	
t=?	0.5 mg	N65W	68NE	

Depth Interval: 210 - 215 Well: NNR - 8

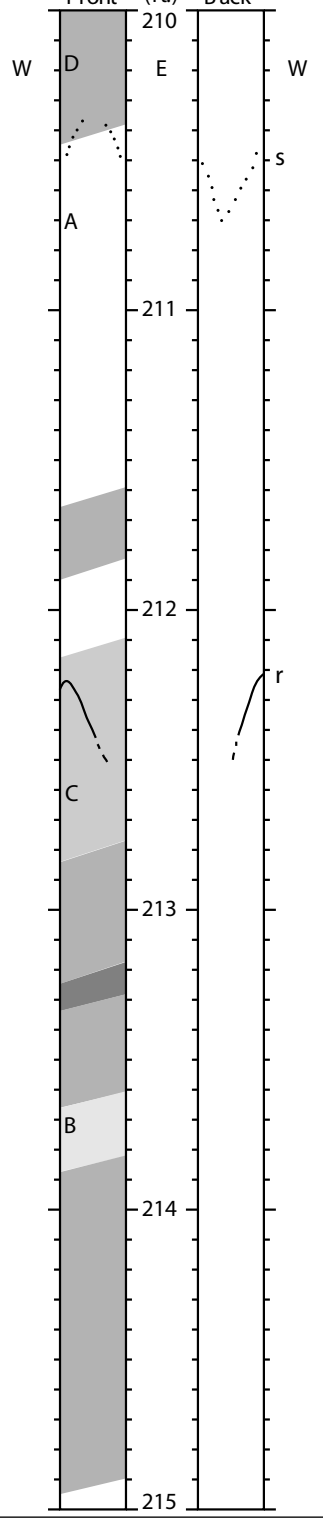

Apparent Disp. (mm)	Fault Thickness (mm)	Fault Strike	Fault Dip	Comments
s=?		N65W	60NE	
				Run # 22 Score card: 211.0' 211.1' - 221.1' Drilled: 10.0' Recovered: 10.0'
r=?	0.5 cg	N15W	57NE	
				Bedding @ 213.3' : NS 13W

Depth Interval: 215 - 220 Well: NNR - 8

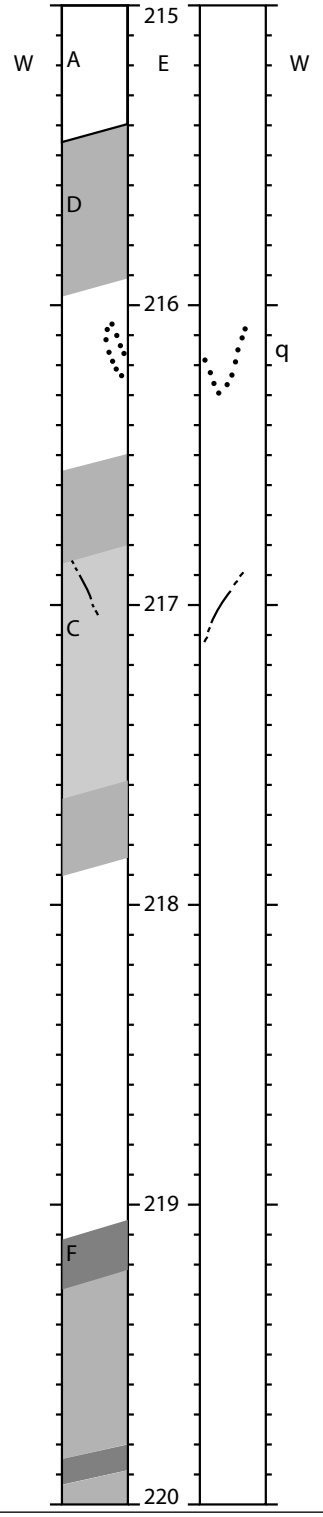

Apparent Disp. (mm)	Fault Thickness (mm)	Fault Strike	Fault Dip	Comments
				Bedding @ 215.6' : N20E 15NW
q=?		N30W	52NE	
				Bedding @ 219.1' : N10W 12SW

Depth Interval: 220 - 225 Well: NNR - 8

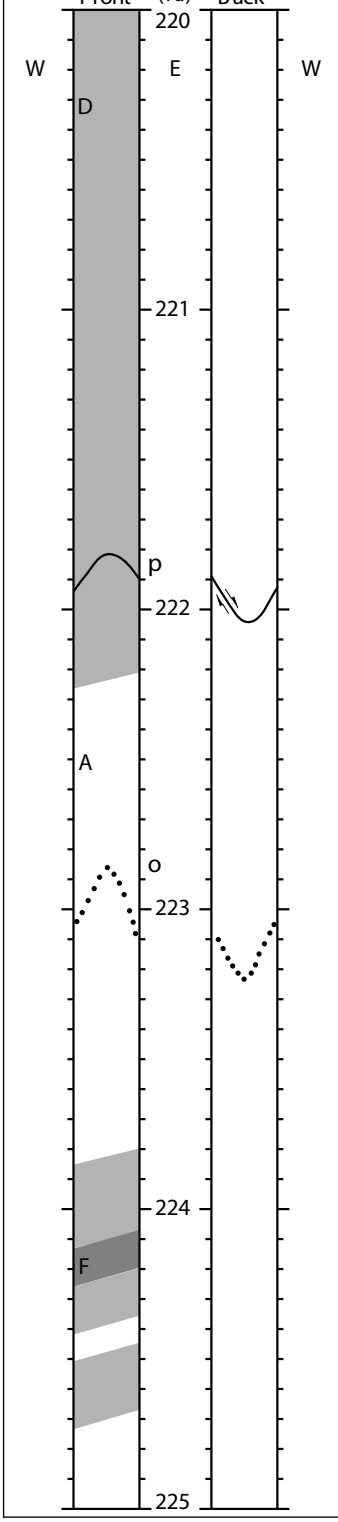

Apparent Disp. (mm)	Fault Thickness (mm)	Fault Strike	Fault Dip	Comments
				Bedding @ 220.05' : N15W 14SW
				Run #23 Score card: 221.1' 221.1' - 231.1' Drilled: 10.0' Recovered: 10.15'
p=5	0.5 fg	N80W	47NE	
o=?		N70W	61NE	
				Bedding @ 224.0' : NS 16W

Depth Interval: 225 - 230 Well: NNR - 8

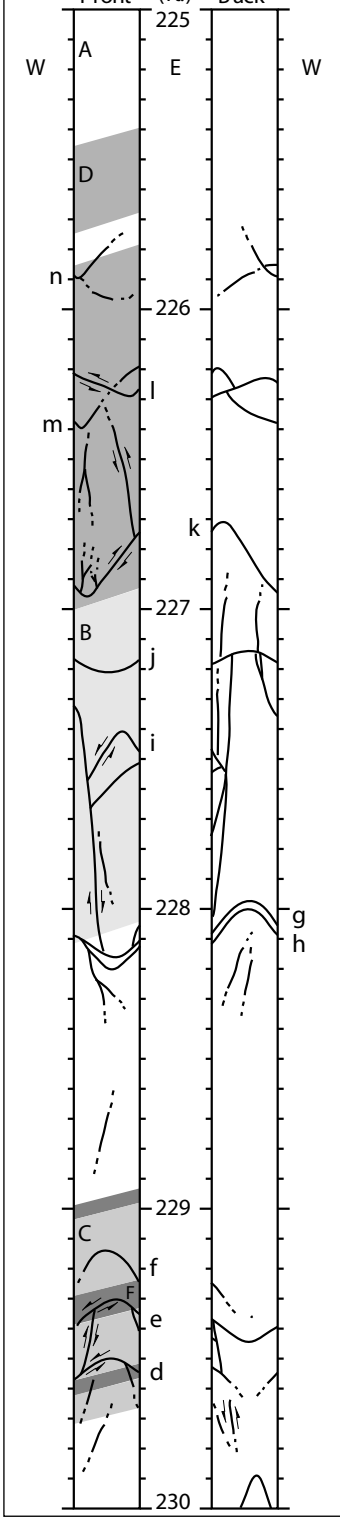

Apparent Disp. (mm)	Fault Thickness (mm)	Fault Strike	Fault Dip	Comments
				Bedding @ 225.3' : N15E 20NW [obtained from BHTV-log]
				Bedding @ 225.7' : N15E 18NW
n=?	1 cg	N5W	47SW	
l=21	1 fg	N15E	11SE	Fault "l" appears to be younger
m=?	0.5 fg	N10W	43SW	than fault "m"
k=4	0.5 fg	N35W	48SW	
j=?		EW	17S	
i=12	1 f g	N50E	41NW	
31 @ 228.0'	1fg			
g=?	1.5 cg	N80E	45SE	Faults "g" & "h" correlates
h=?	3 cg	N85E	42SE	w/227.8' in BHTV-log
f=?	1 mg	N65W	57NE	Bedding @ 229.25' : N10W 16NW
e=7	0.5 fg	N70W	35NE	
d=3	0.5 fg	N60W	42NE	

Depth Interval: 230 - 235 Well: NNR - 8

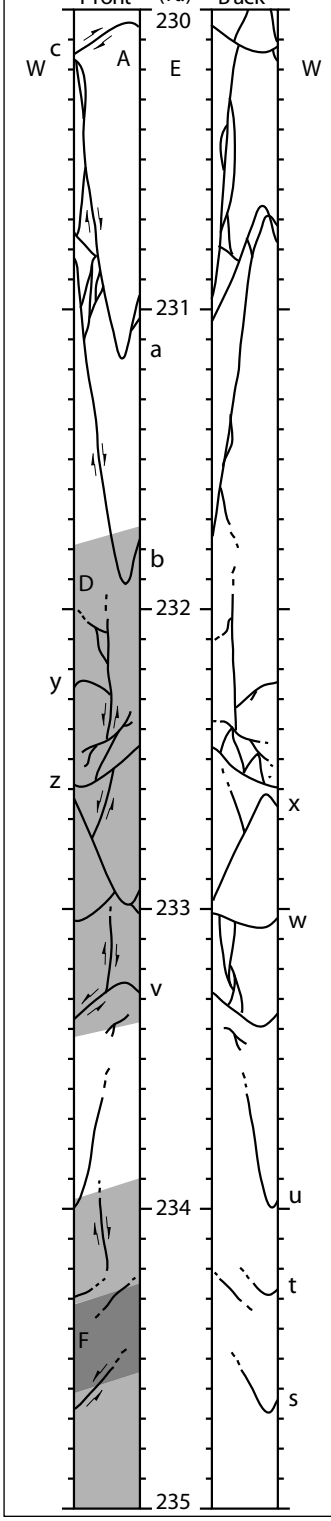

Apparent Disp. (mm)	Fault Thickness (mm)	Fault Strike	Fault Dip	Comments
c=6	1 cg	N5E	26NW	Fault "c" is younger than fault "a"
				Fault "a" correlates w/230.8' in BHTV-log
a=50	2 cg	N45E	83SE	Run # 24 Score card: 231.1' 231.1' - 241.1' Drilled: 10.0' Recovered: 10.1'
b=37	2 cg	N30E	85SE	
				Bedding @ 231.9' : N15W 13NW
y=?	0.5 fg	N5W	21NE	
z=?	0.5 fg	N10W	32SW	
x=?	1 clay	N30E	56SE	
w=?	0.5 fg	N35E	16NW	
v=21	0.5 clay	N40E	24NW	
u=?	1.5 cg	N10E	78NW	
t=?	0.5 fg	N15E	37NW	Bedding @ 234.2' : N15W 18SW
s=4	0.5 fg	N20E	47NW	

Depth Interval: 235 - 240 Well: NNR - 8

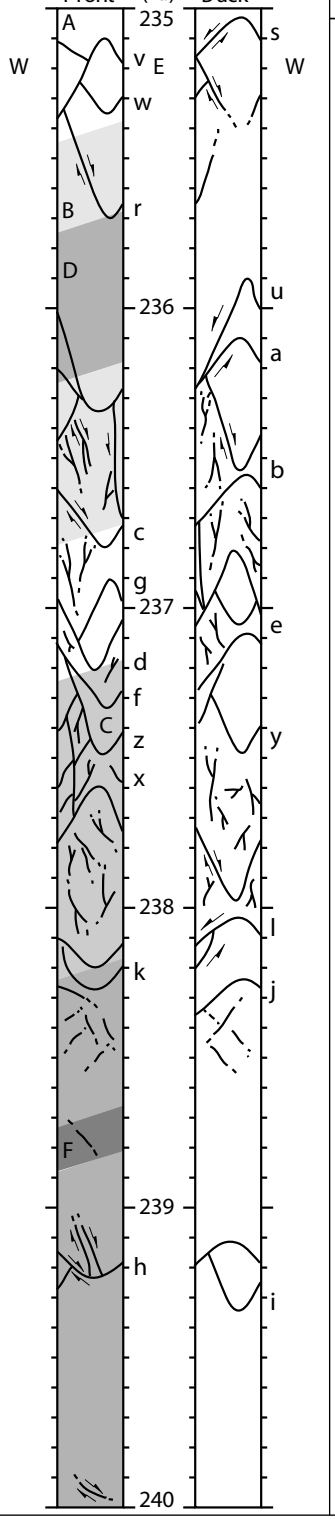

Apparent Disp. (mm)	Fault Thickness (mm)	Fault Strike	Fault Dip	Comments
s=8	1 cg	N45E	67SE	
v=12	1.5 cg	N40E	59NW	Fault "v" correlates w/235' in BHTV-log
w=?	1 cg	N30E	58SE	
r=5	0.5 mg	N35E	71SE	
u=?		N45E	62SE	
a=?	7 mg	N60E	41SE	Fault "a" correlates w/235.9' in BHTV-log
b=18	1.5 mg	N60E	76NW	Nearly verticaly dipping fault is younger than dipping faults.
c=14	2 fg	N50E	52SE	
g=?	1 cg	N40E	72NW	
e=?	2 cg	N55E	61NW	
d=?	2 cg	N70E	57SE	
f=?	2 cg	N35E	45SE	
y=?		N45E	54NW	Between faults "y" & "x" the SE dipping faults are younger than NW dipping faults.
z=?	1.5 mg	N55E	67SE	
x=21	2 fg	N65E	63NW	
l=?	1 clay	N75E	35SE	Fault "l" correlates w/238.9' in BHTV-log
k=?	0.5 fg	N80E	41SE	
j=?	0.5 fg	N55E	36SE	
h=12	3 clay	N80W	34SW	
i=?	1 clay	N45E	56NW	

Depth Interval: 240 - 245 Well: NNR - 8

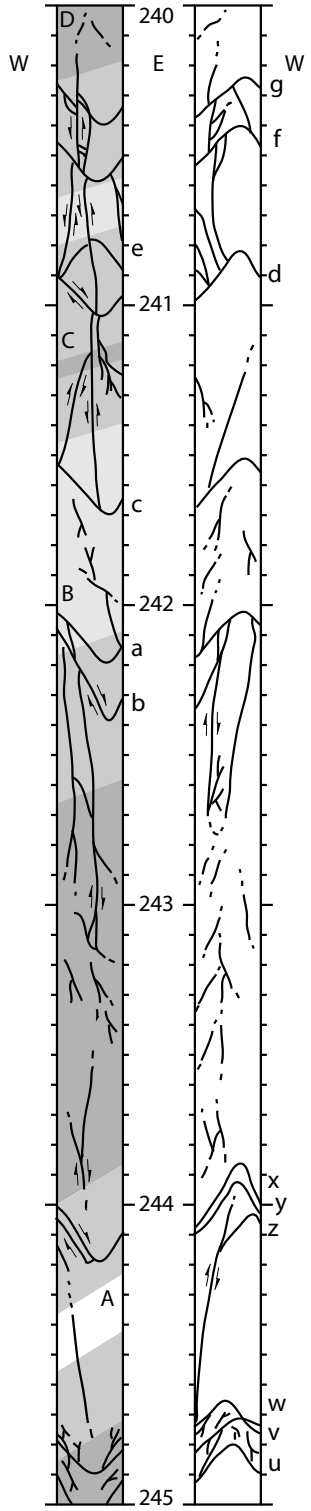

Apparent Disp. (mm)	Fault Thickness (mm)	Fault Strike	Fault Dip	Comments
g=?	1 mg	N45E	37SE	Fault "g" is older than steeper fault
f=?	1 mg	N60E	45SE	
e=?	1 fg	N75E	37NW	Fault "e" is older than steeper fault
d=?	3 fg	N55E	44SE	
c=?	4 cg	N35E	45SE	
				Bedding @ 241.85' : N10W 22SW
a=?	3 fg	N40E	44SE	
b=3	0.5 fg	N35E	54SE	
				Bedding @ 242.7' : N15E 31NW
x=14	1 mg	N60E	56SE	
y=9	0.5 mg	EW	52S	
z=?	0.5 mg	N15E	45SE	
w=?	2 mg	N80E	49SE	
v=?	1 mg	N55E	50SE	Fault "v" correlates w/244.9'
u=?	1 mg	N70E	62SE	in BHTV-log

Depth Interval: 245 - 250 Well: NNR - 8

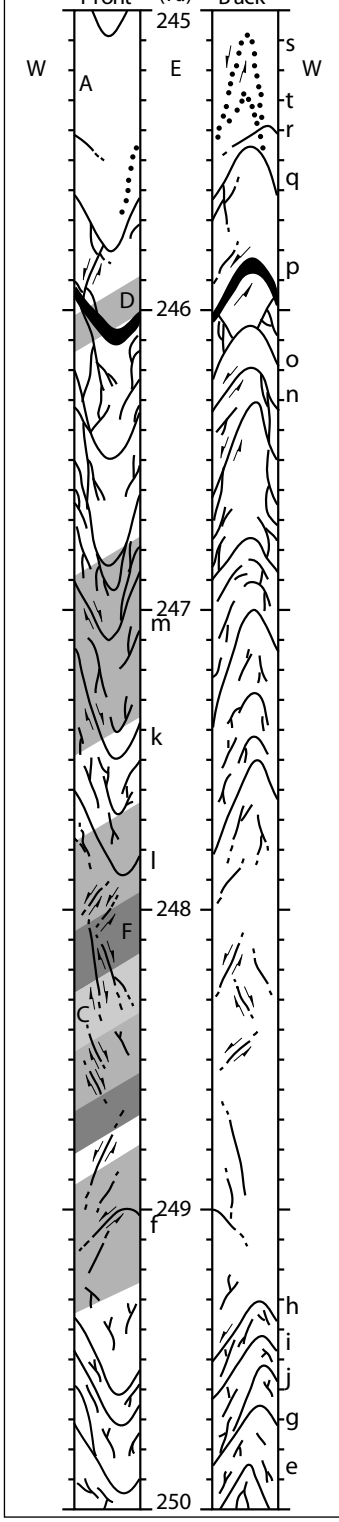

Apparent Disp. (mm)	Fault Thickness (mm)	Fault Strike	Fault Dip	Comments
s=?		EW	74S	
t=?		EW	61S	
r=?	1 cg	N25E	34SE	
q=?		N75E	61SE	NW dipping faults are younger than SE dipping faults near faults "q" & "p"
p=?	17 cg	N60E	46SE	
o=15	2 cg	N80E	54SE	
n=9	1.5 cg	N70E	60SE	
m=63	7 cg	N75E	53SE	
k=57	2 clay	N65E	66SE	
l=?		N60E	68SE	
f=14	<0.5 clay	N40E	38NW	Bedding @ 249.2' : N45W 25SW
h=?	2 cg	N55E	52SE	Bedding @ 249.3' : N45W 24NW [obtained from BHTV-log]
i=?	2 cg	N45E	55SE	
j=?	1 cg	N40E	66SE	
g=?	2 cg	N50E	59SE	
e=?	>5 cg	N70E	74SE	

Depth Interval: 250 - 255 Well: NNR - 8

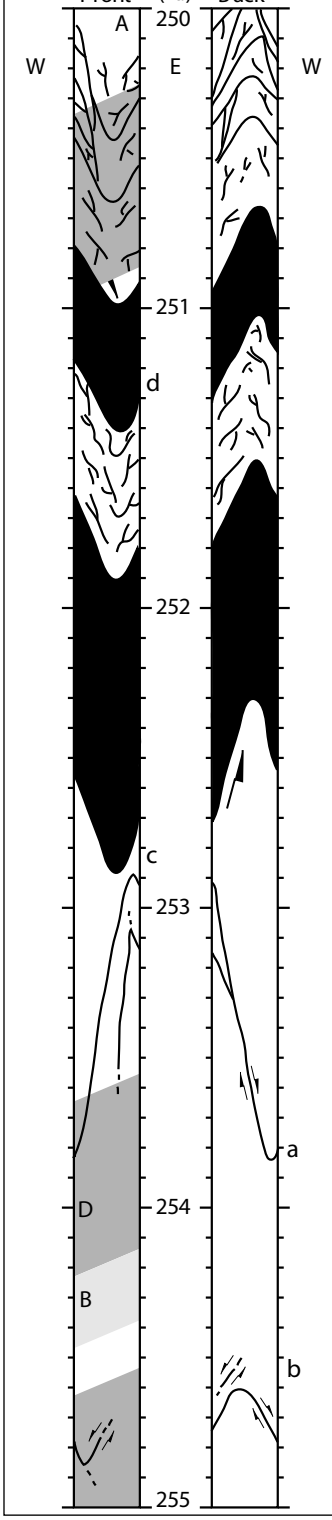

Apparent Disp. (mm)	Fault Thickness (mm)	Fault Strike	Fault Dip	Comments
d=?	43 cg	N50E	60SE	Rake on "d": 52NE Run # 26 Score card: 251.1' 251.1' - 261.1' Drilled: 10.0' Recovered: 10.0'
c=?	>150 cg	N60E	70SE	Fault "c" correlates w/251.6' in BHTV-log
				Bedding @ 253.65' : N25E 23NW
a=12	1.5 cg	N10E	78NW	
b=3	0.5 fg	N65E	62SE	

Depth Interval: 255 - 260 Well: NNR - 8

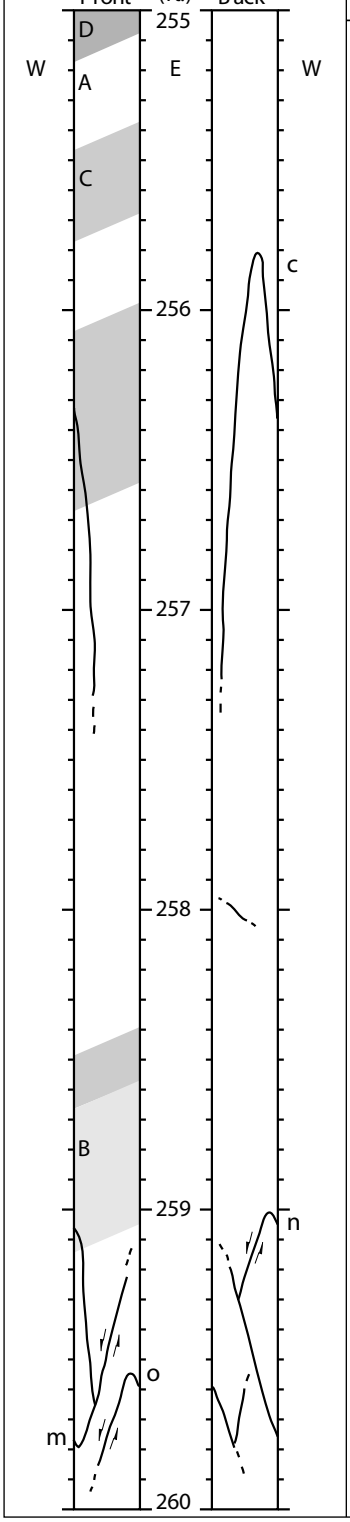

Apparent Disp. (mm)	Fault Thickness (mm)	Fault Strike	Fault Dip	Comments
c=?	0.5 cg	N50E	87SE	
				Bedding @ 257.5' : N3W 28SW [obtained from BHTV-log]
				Bedding @ 258.4' : N3E 16NW [obtained from BHTV-log]
				Bedding @ 258.9' : NS 19W
n=3	1.5 cg	N30E	84SE	
o=2	0.5 cg	N35E	64NW	
m=4	2 cg	N15W	72SW	

Depth Interval: 260 - 265 Well: NNR - 8

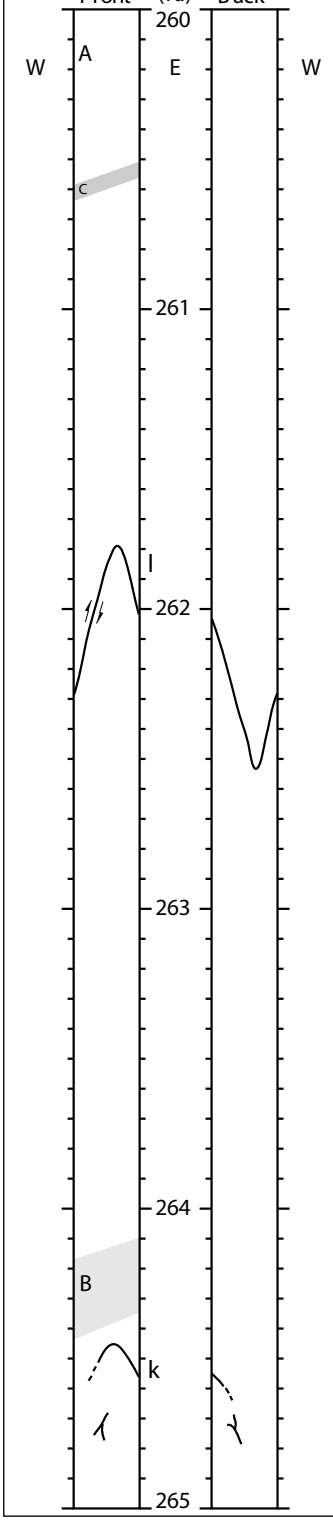

Apparent Disp. (mm)	Fault Thickness (mm)	Fault Strike	Fault Dip	Comments
				Run # 27 Score card: 261.0' 261.1' - 271.1' Drilled: 10.0' Recovered: 9.95'
l=4	1 cg	N60E	72NW	
				Bedding @ 264.4' : N10E 23NW
k=?	1.5 cg	N65E	53NW	

Depth Interval: 265 - 270 Well: NNR - 8

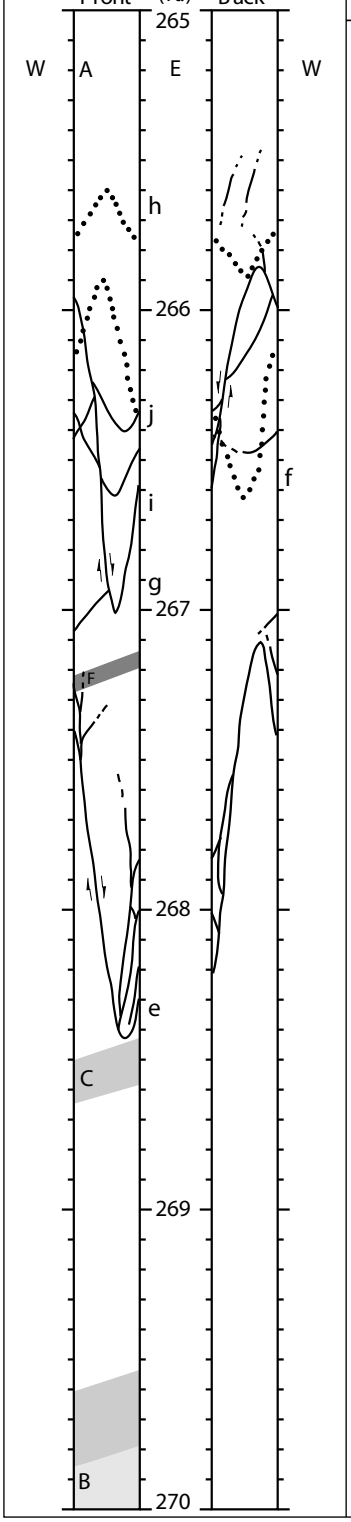

Apparent Disp. (mm)	Fault Thickness (mm)	Fault Strike	Fault Dip	Comments
h=?		N70W	57NE	
39 @ 266.2'	5 cg			
j=?	2 cg	N55E	67SE	
f=?		N60W	73NE	Fault "f" correlates w/265.2' in BHTV-log
i=?	1 cg	N70E	68SE	
g=18	1.5 cg	N60E	84SE	Fault "g" is younger than "i"
				Bedding @ 267.15' : N15E 20NW
e=65	4 cg	N40E	83SE	Fault "e" correlates w/268.3' in BHTV-log

Depth Interval: 270 - 275 Well: NNR - 8

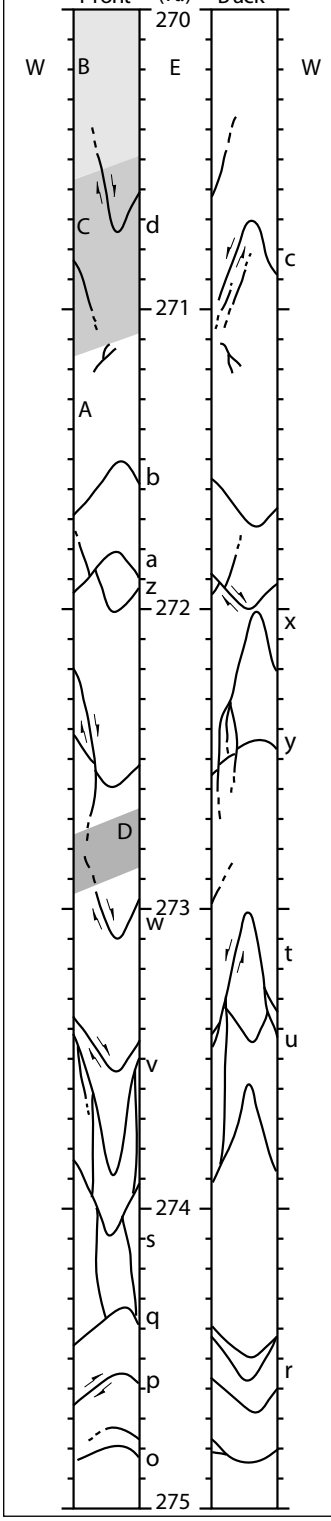

Apparent Disp. (mm)	Fault Thickness (mm)	Fault Strike	Fault Dip	Comments
d=9	0.5 clay	N55E	57SE	
c=18	0.5 clay	N60E	63SE	
				Run # 28 Score card: 271.0' 271.1' - 281.1' Drilled: 10.0' Recovered: 10.0'
b=?	4.5 cg	N45E	49NW	
a=7	1 cg	N65E	38NW	Fault "a" is younger than "z"
z=?	0.5 cg	N60E	64SE	
x=11	1.5 cg	N50E	72SE	Fault "x" is younger than "y"
y=?	1.5 cg	N60E	25SE	
				Bedding @ 272.9' : N40E 22NW
w=11	2.5 cg	N60E	62SE	
t=14	0.5 cg	N70E	77SE	
u=?	0.5 cg	N65E	34NW	
v=1	0.5 cg	N55E	52SE	
s=?	2 cg	N80E	66SE	
q=?	2 cg	N50E	16NW	
r=?	2 cg	N45E	44NW	
p=13	2.5 cg	N45E	30NW	
o=?	1.5 cg	N60E	17NW	

Depth Interval: 275 - 280 Well: NNR - 8

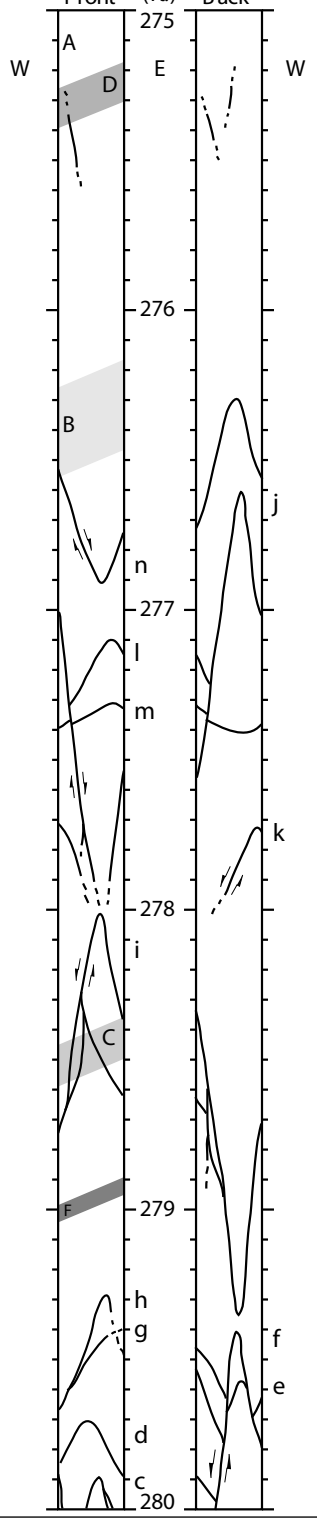

Apparent Disp. (mm)	Fault Thickness (mm)	Fault Strike	Fault Dip	Comments
				Bedding @ 276.2' : N20E 23NW
j=7	1 cg	N45E	83SE	Fault "j" is younger than "m"
n=8	1 cg	N60E	72SE	
l=?	0.5 cg	N30E	59NW	
m=?	0.5 cg	N15E	16NW	
k=5	0.5 cg	N10E	61SE	
i=13	2.5 cg	N50E	81NW	
				Bedding @ 279.0' : N40E 23NW
h=?	1 cg	N65E	69NW	
g=?	1 cg	N10E	51NW	
f=13	1.5 cg	N50E	79SE	
e=?	1 cg	N35E	74SE	
d=?	2 cg	N55W	51NE	
c=?	2 cg	N60E	73NW	

Depth Interval: 280 - 285 Well: NNR - 8

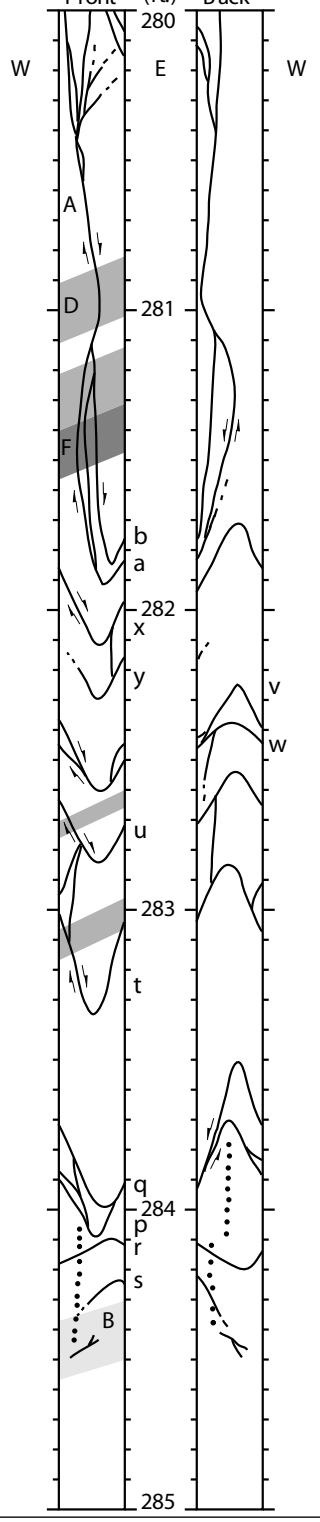

Apparent Disp. (mm)	Fault Thickness (mm)	Fault Strike	Fault Dip	Comments
62@ 280.7'	4.5 cg			Bedding @ 280.9' : N30E 22NW Run # 29 Score card: 281.05' 281.1' - 291.1' Drilled: 10.0' Recovered: 10.1'
				Bedding @ 281.6' : NS 25W
b=26	1.5 cg	N30E	86SE	Fault "b" correlates w/281.7'
a=27		N45E	75SE	in BHTV-log
x=3	1 cg	N60E	59SE	
y=?	0.5 cg	N55E	55SE	
v=26	2.5 cg	N60E	57SE	
w=?	1 cg	EW	43S	
u=14	1 cg	N65E	50SE	
t=8	0.5 mg	N70E	61SE	
q+p=132	7 cg	N50E	61SE	Fault "q" correlates w/283.7'
		N80E	60SE	in BHTV-log
r=?	1 cg	N45E	47NW	
s=?	1 cg	N15E	45NW	
				Bedding @ 284.5' : N35E 17NW

Depth Interval: 285 - 290 Well: NNR - 8

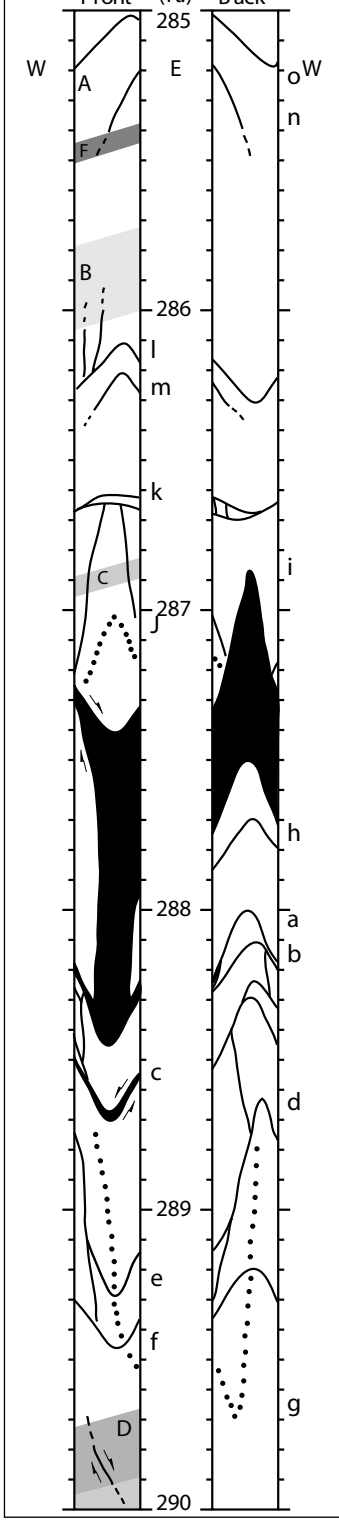

Apparent Disp. (mm)	Fault Thickness (mm)	Fault Strike	Fault Dip	Comments
o=?	1 cg	N10W	47SW	
n=?	1 cg	NS	66W	
				Bedding @ 285.8' : N15E 16NW
l=?	1 cg	N40E	43NW	
m=?	1 cg	N40E	47NW	
k=?	2.5 cg	EW	11N	
i=?	52 cg	N60E	73SE	Fault "i" correlates w/286.3' in BHTV-log
j=?		N60E	68NW	
h=?	2.5 cg	N65E	57SE	
a=?	1.5 cg	N75E	57SE	
b=?	3 mg	N45E	54SE	Fault "b" correlates w/287.7' in BHTV-log
c=58	3 mg	N65E	63SE	
d=?	2 cg	N40E	77SE	
e=?	2 cg	N80E	51SE	
f=?	2 cg	N65E	45SE	Fault "f" correlates w/289.3' in BHTV-log
g=?		N45W	81NE	

Depth Interval: 290 - 295 Well: NNR - 8

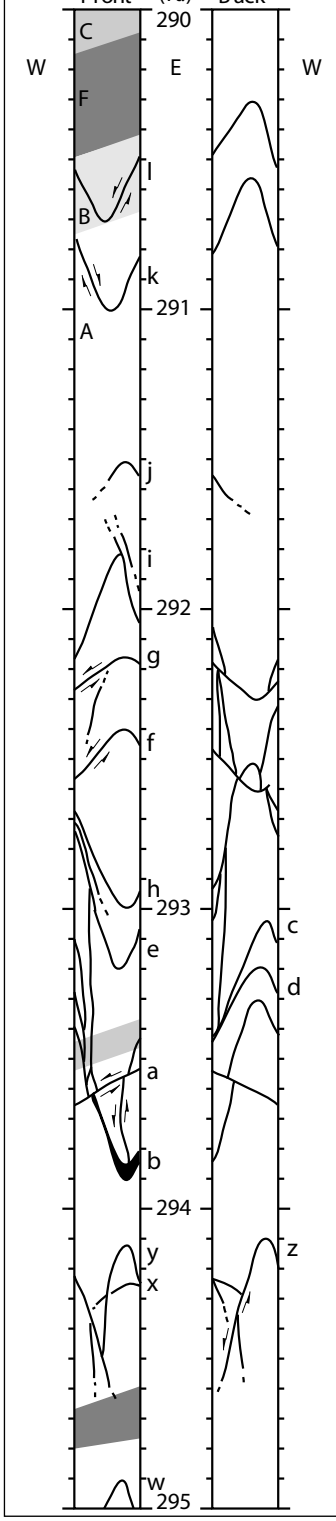

Apparent Disp. (mm)	Fault Thickness (mm)	Fault Strike	Fault Dip	Comments
				Bedding @ 290.0' : N10W 19SW
l=11	0.5 mg	N65W	73SW	
k=18	1.5 cg	N75W	64SW	
				Run # 30 Score card: 291.1' 291.1' - 301.1' Drilled: 10.0' Recovered: 10.05'
j=?	1 cg	N35E	31NW	
i=?	1 cg	N65E	71NW	
g=4	1 cg	N40E	35NW	Fault "g" is younger than "i"
f=14	1.5 cg	N45E	44NW	Fault "f" is younger than "e" & "h"
h=?	3 cg	N40E	68SE	Fault "h" correlates w/292'
c+d=77	2 cg	N20E	66SE	in BHTV-log
e=?	2 cg	N65E	75SE	
	2 cg	N50E	61SE	
a=6	1.5 cg	NS	21W	Fault "a" is younger than "c:", "d", & "b"
b=?	3 cg	N55E	63SE	Fault "b" correlates w/293.7' in BHTV-log
z=7	1 cg	N40E	69SE	
y=?	1 cg	N50E	74NW	
x=?	1 cg	N10W	22SW	
				Bedding @ 294.8' : N20W 9SW
w=?	0.5 cg	N55E	70NW	

Depth Interval: 295 - 300 Well: NNR - 8

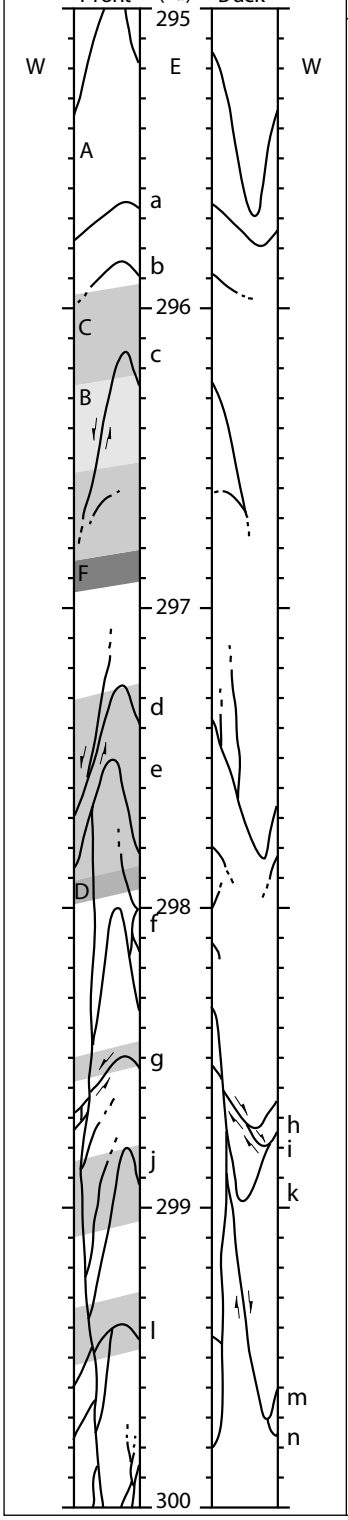

Apparent Disp. (mm)	Fault Thickness (mm)	Fault Strike	Fault Dip	Comments
a=?	2 cg	N45E	27NW	
b=?	0.5 mg	N50E	20NW	
c=5	0.5 mg	N30E	68NW	
				Bedding @ 296.5' : N18W 22SW [obtained from BHTV-log]
				Bedding @ 296.9' : N25W 14SW
d=19	0.5 mg	N45E	64NW	
e=?	0.5 mg	N55E	67NW	
f=?	1 cg	N50E	79NW	
g=2	0.5 cg	N35E	39NW	
h=5	1 cg	N50E	60NW	
i=2	0.5 cg	N30E	52NW	
j=?	0.5 cg	N35E	74NW	
k=?	0.5 cg	N80E	77NW	
l=?	0.5 cg	N65E	55NW	
m+n=8	1 cg	N35E	82NW	
		N5E	6NW	

Depth Interval: 300 - 305 Well: NNR - 8

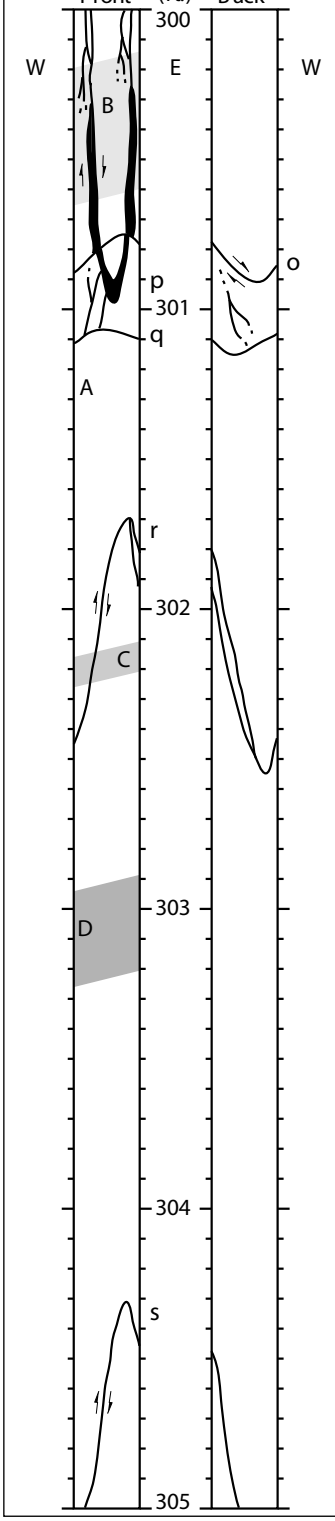

Apparent Disp. (mm)	Fault Thickness (mm)	Fault Strike	Fault Dip	Comments
				Bedding @ 300.8' : N27W 21SW [obtained from BHTV-log]
o=15 p=27	1.5 cg 6 cg	N40E N50E	41NW 87SE	
q=?	1 cg	N65W	14NE	Run # 31 Score card: 301.1' 301.1' - 311.1' Drilled: 10.0' Recovered: 9.9'
r=21	2 cg	N30E	72NW	
				Missing core from 303.25' - 304.1'
s=37	3.5 cg	N45E	75NW	Fault "s" correlates w/303.1' in BHTV-log

Depth Interval: 305 - 310 Well: NNR - 8

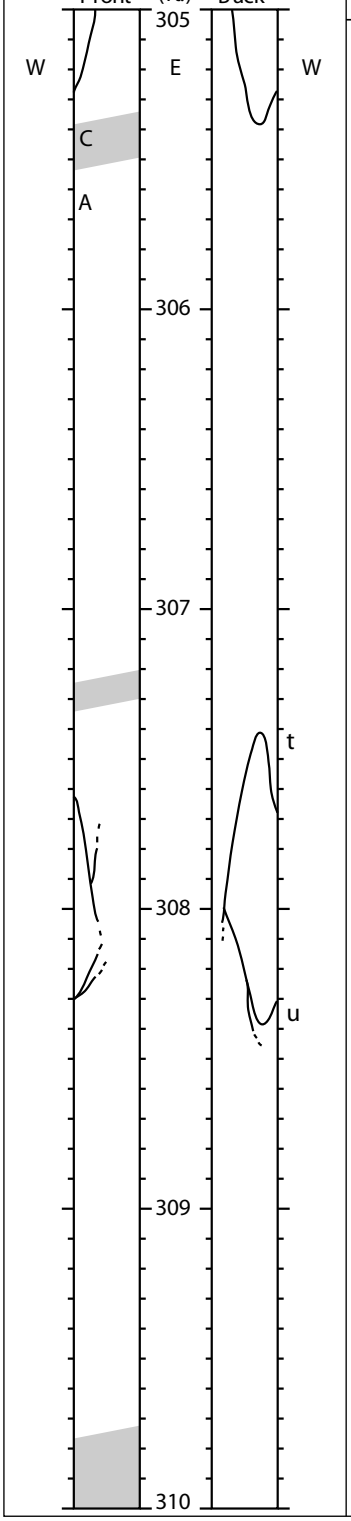

Apparent Disp. (mm)	Fault Thickness (mm)	Fault Strike	Fault Dip	Comments
				Bedding @ 305.5' : N20E 11NW
t=?	4 cg	N45E	76SE	Fault "t" correlates w/306.5' in BHTV-log
u=?	2 cg	N45E	71NW	

Depth Interval: 310 - 315 Well: NNR - 8

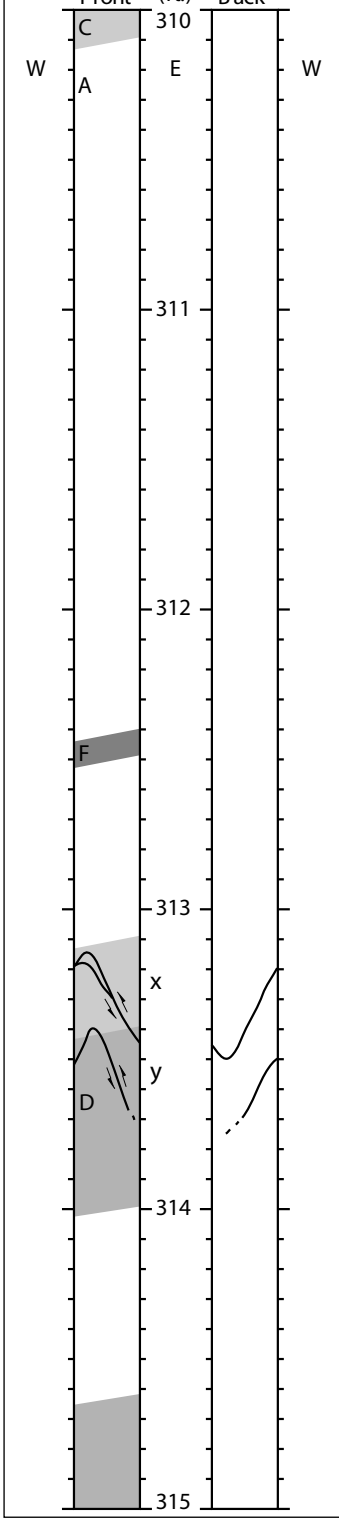

Apparent Disp. (mm)	Fault Thickness (mm)	Fault Strike	Fault Dip	Comments
				Run # 32 Score card: 311.0' 311.1' - 319.7' Drilled: 8.6' Recovered: 8.7' Missing core from 311.0' - 311.85'
x=2	0.5 fg	N25W	57NE	
y=4	0.5 fg	N40W	63NE	
				Bedding @ 313.75' : N25E 9NW

Depth Interval: 315 - 320 Well: NNR - 8

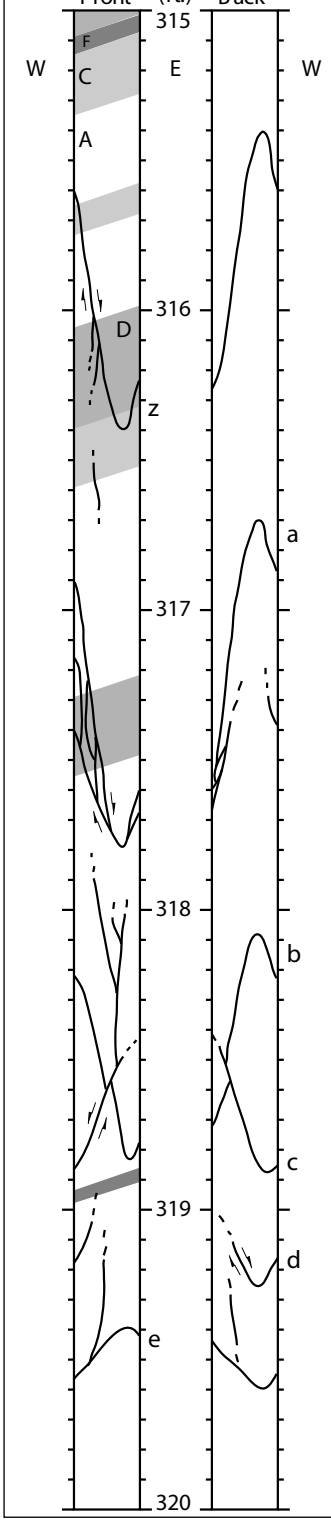

Apparent Disp. (mm)	Fault Thickness (mm)	Fault Strike	Fault Dip	Comments
				Bedding @ 315.1' : N5E 19NW
z=26	1 mg	N45E	83SE	Fault "z" correlates w/315.9' in BHTV-log
a >220		N45E	74SE	Fault "a" correlates w/317.5' in BHTV-log
b=?	3 cg	N50E	79SE	
c=18	1.5 cg	N35E	56NW	Fault "c" is younger than "b"
d=21	2.5 cg	N50E	45NW	
e=?	3 cg	N35E	42NW	
				Run # 33 Score card: 319.7' 319.7' - 321.1' Drilled: 1.4' Recovered: 1.4'

Depth Interval: 320 - 325 Well: NNR - 8

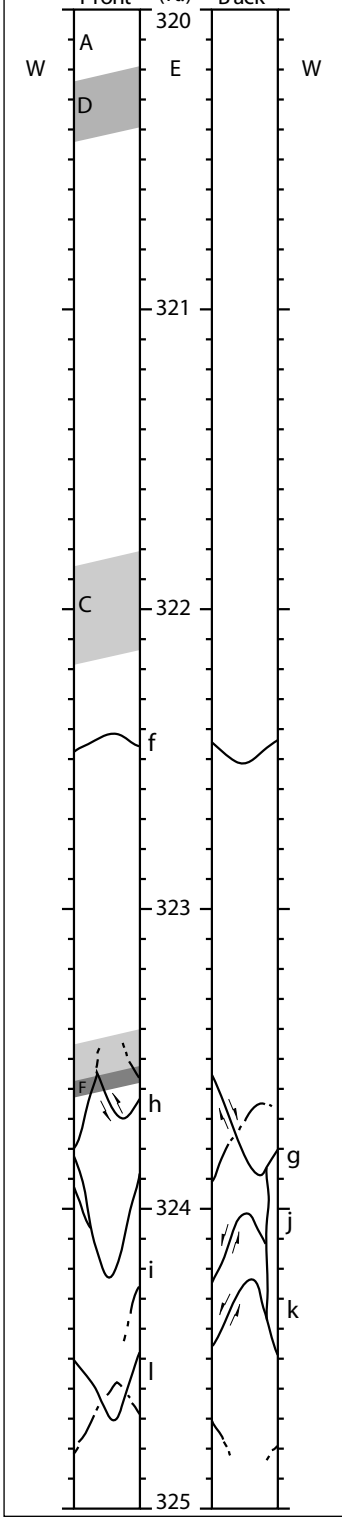

Apparent Disp. (mm)	Fault Thickness (mm)	Fault Strike	Fault Dip	Comments
				Bedding @ 320.3' : N20E 12NW
				Run # 34 Score card: 321.1' 321.1' - 331.1' Drilled: 10.0' Recovered: 10.0'
f=?	2.5 cg	N60E	30NW	
				Bedding @ 323.6' : N10E 11NW
				Bedding @ 323.8' : N12E 29NW [obtained from BHTV-log]
h=6	0.5 mg	N45E	57SE	
g=13	1 mg	N50E	66NW	
j=5	0.5 mg	N75E	61SE	
i=?	0.5 cg	N80E	74SE	
k=6	0.5 cg	N60E	66SE	
l=?	1 cg	N55E	72NW	Fault "l" might be younger than "k" If so, then it is a normal sense of displacement (3 mm)

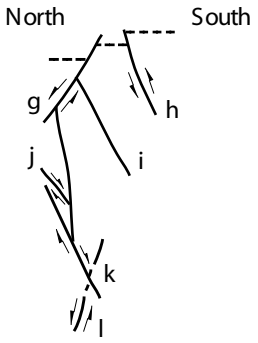

Depth Interval: 325 - 330 Well: NNR - 8

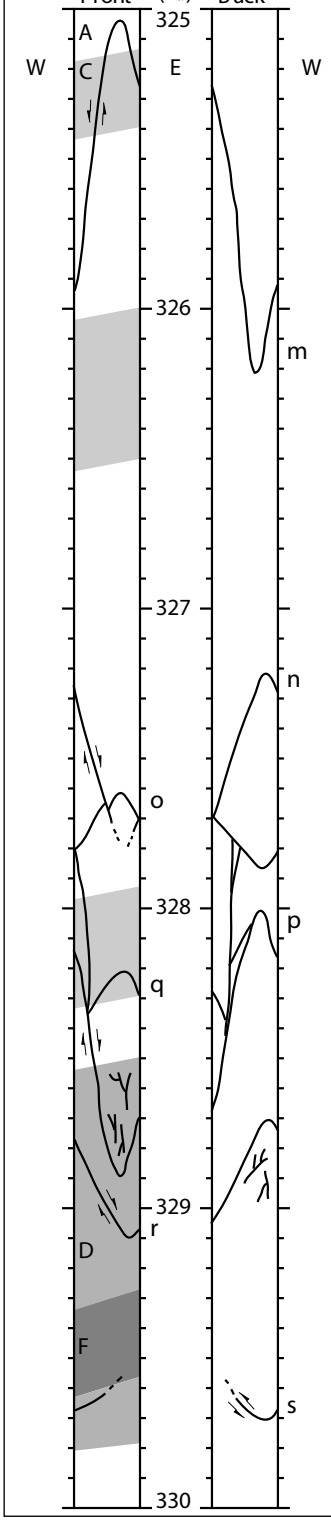

Apparent Disp. (mm)	Fault Thickness (mm)	Fault Strike	Fault Dip	Comments
m=11	1 cg	N45E	79NW	
n=19	1 mg	N15E	67SE	Fault "n" is younger than "o"
o=?	1.5 mg	N35E	44NW	
p=16	2 mg	N40E	78SE	
q=?	1 cg	N35E	67NW	
				Bedding @ 328.7' : N20W 16SW
r=13	0.5 fg	N20E	68SE	
s=23	0.5 clay	N35E	41NW	Bedding @ 329.7' : N20W 5SW

Depth Interval: 330 - 335 Well: NNR - 8

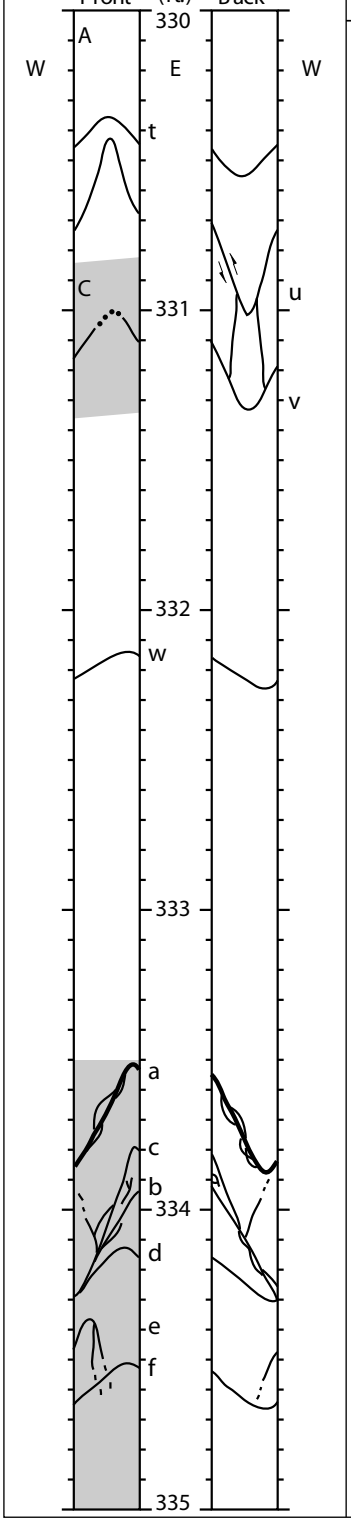

Apparent Disp. (mm)	Fault Thickness (mm)	Fault Strike	Fault Dip	Comments
t=?	0.5 cg	N80W	48NE	
u=7	0.5 cg	N75E	69NW	
				Run # 35 Score card: 331.1'
v=?	0.5 mg	N60E	41NW	331.1' - 341.1' Drilled: 10.0' Recovered: 10.0' Fault "v" correlates w/329.5' in BHTV-log
w=?	1 cg	N20E	31NW	
				Missing core from 332.45' - 333.5'
				Fault "a" correlates w/333' in BHTV-log
a=?	8 mg	N20E	54NW	Fault "a" consists of at least 3 separate faults that range in strike: N10E, N20E, and N30E
c=?	1 mg	N5E	56NW	Each fault is about 1 mm thick
b=?	2 mg	NS	51W	Faults "b", "c", & "d" are three faults amoung many which have a cumulative thickness of 7 mm
d=?	0.5 mg	N40E	33NW	
e=?	0.5 mg	N40W	67NE	
f=?	0.5 mg	N15E	31NW	

Depth Interval: 335 - 340 Well: NNR - 8

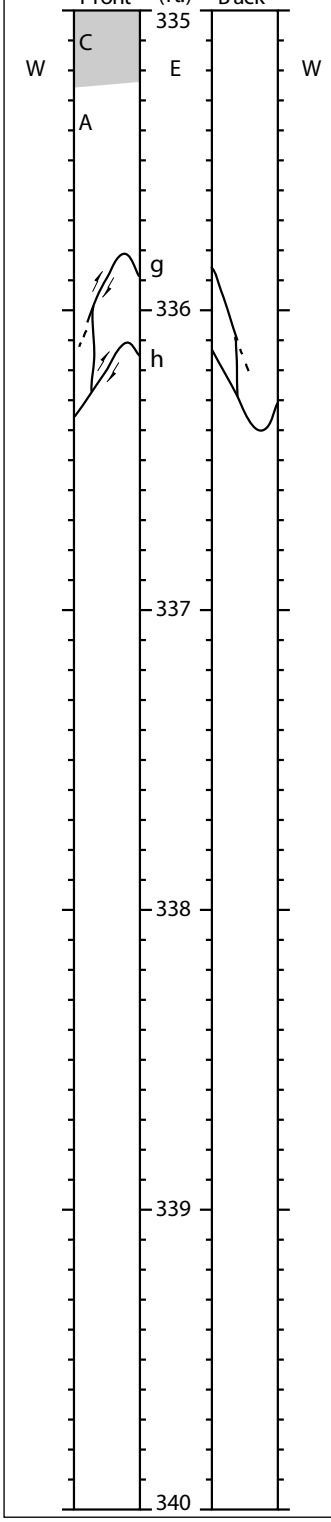

Apparent Disp. (mm)	Fault Thickness (mm)	Fault Strike	Fault Dip	Comments
g=3	1.5 cg	N40E	63NW	
h=2	1.5 cg	N35E	56NW	
				Bedding @ 337.1' : N35W 14SW

Depth Interval: 340 - 345 Well: NNR - 8

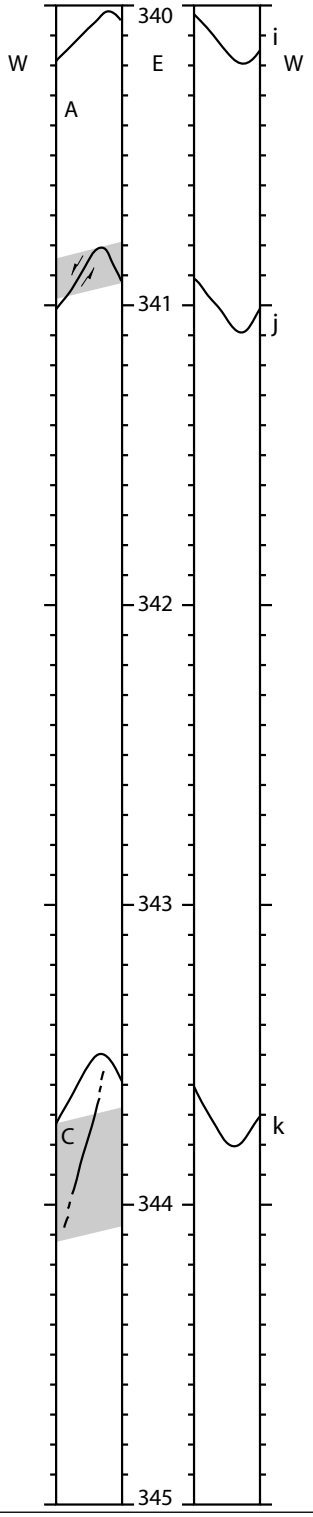

Apparent Disp. (mm)	Fault Thickness (mm)	Fault Strike	Fault Dip	Comments
i=?	1.5 cg	N35E	41NW	
j=25	1 mg	N55E	53NW	Run # 36 Score card: 341.1' 341.1' - 351.1' Drilled: 10.0' Recovered: 10.0'
k=?	1.5 mg	N40E	53NW	Data was rotated 25 degress CCW but figures were not redrawn from 343' - 355'

Depth Interval: 345 - 350 Well: NNR - 8

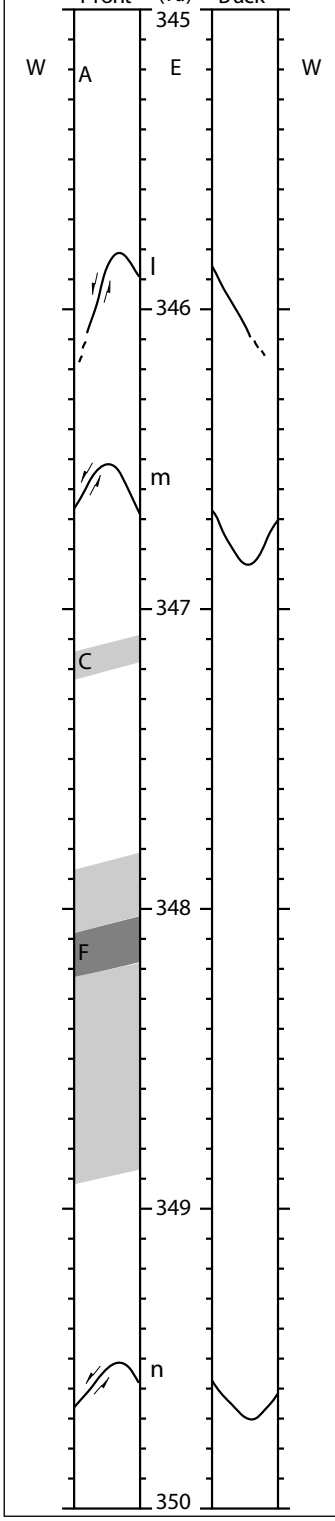

Apparent Disp. (mm)	Fault Thickness (mm)	Fault Strike	Fault Dip	Comments
l=1	0.5 cg	N20E	56NW	
m=14	4 cg	N80E	61NW	
				Bedding @ 348.1' : N45W 12SW
n=1	0.5 cg	N40E	47NW	

Depth Interval: 350 - 355 Well: NNR - 8

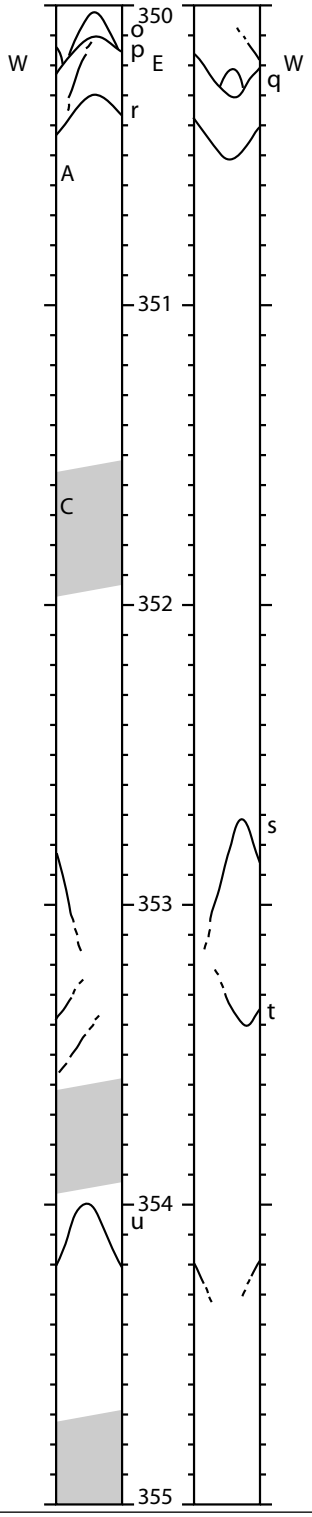

Apparent Disp. (mm)	Fault Thickness (mm)	Fault Strike	Fault Dip	Comments
o=?	1 cg	N60E	48NW	
p=?	1 cg	N45E	40NW	
q=?	1 cg	N45E	64SE	
r=?	1.5 cg	N55E	47NW	
				Run # 37 Score card: 351.1' 351.1' - 361.1' Drilled: 10.0' Recovered: 9.95'
				Bedding @ 351.9' : N30W 10SW
s=?	1 mg	N10E	68SE	Fault "s" correlates w/352' in BHTV-log
t=?	0.5 mg	N10E	55NW	
u=?	1.5 cg	N80E	52NW	

Depth Interval: 355 - 360 Well: NNR - 8

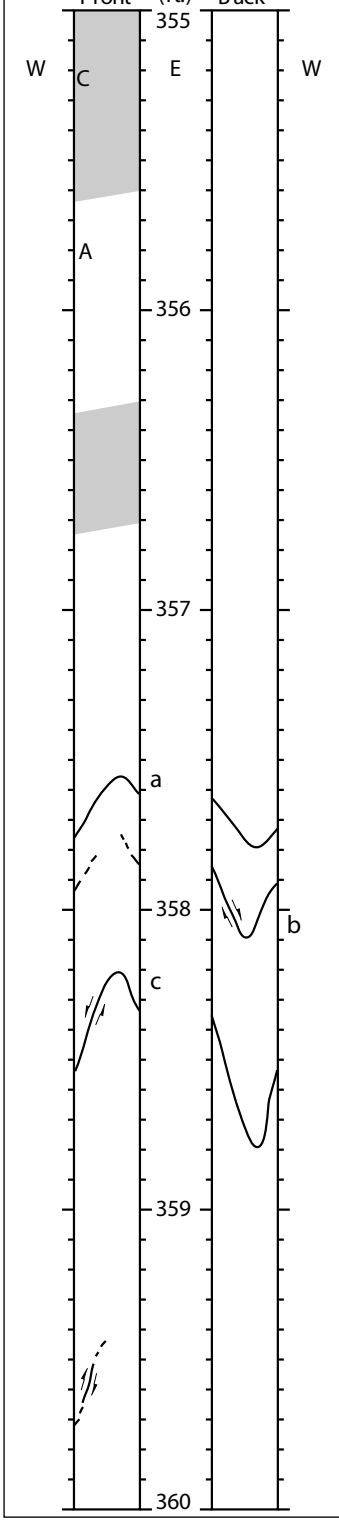

Apparent Disp. (mm)	Fault Thickness (mm)	Fault Strike	Fault Dip	Comments
				Bedding @ 355.8' : N15W 17SW [obtained from BHTV-log]
				Bedding @ 356.3' : N25W 12SW [obtained from BHTV-log]
a=?	2 cg	N45E	54NW	
b=6	1.5 cg	N75E	57NW	
c=31	3 cg	N50E	62NW	
				Bedding @ 358.7' : N20W 20SW
				Bedding @ 358.8' : N30W 19SW [obtained from BHTV-log]
3	2 cg			

Depth Interval: 360 - 365 Well: NNR - 8

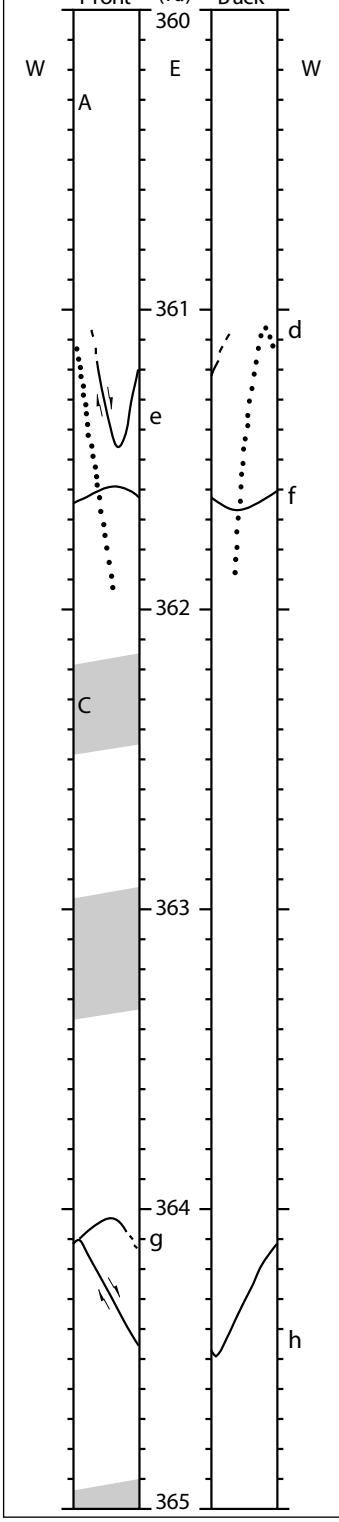

Apparent Disp. (mm)	Fault Thickness (mm)	Fault Strike	Fault Dip	Comments
d=?		N20E	74SE	Run # 38 Score card: 361.03' 361.1' - 371.1' Drilled: 10.0' Recovered: 10.05'
e=9	2 cg	N55E	82SE	
				Bedding @ 361.6' : N35W 9SW
f=?	2 cg	N60E	16NW	[obtained from BHTV-log]
				Bedding @ 362.2' : N35W 9SW
				Bedding @ 362.6' : N25W 20SW [obtained from BHTV-log]
				Bedding @ 362.9' : N30W 23SW [obtained from BHTV-log]
g=?	0.5 cg	N70E	36NW	
				Bedding @ 364.3' : N5W 13SW [obtained from BHTV-log]
h=18	2.5 cg	N5E	59SE	Fault "h" correlates w/364' in BHTV-log
				Bedding @ 364.6' : N20W 13SW [obtained from BHTV-log]

Depth Interval: 365 - 370 Well: NNR - 8

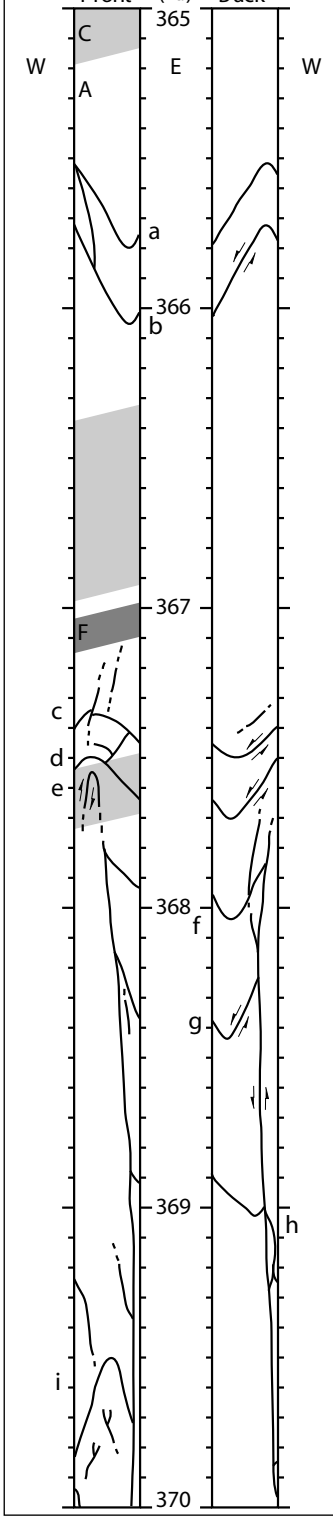

Apparent Disp. (mm)	Fault Thickness (mm)	Fault Strike	Fault Dip	Comments
				Bedding @ 365.15' : N20W 14SW
a=?	1.5 cg	N25E	56SE	
b=7	2 cg	N20E	63SE	
				Bedding @ 366.5' : N30W 11SW [obtained from BHTV-log]
				Bedding @ 367' : N45W 14SW [obtained from BHTV-log]
				Bedding @ 367.2' : NS 22W [obtained from BHTV-log]
c=3	1 cg	N40W	32NE	Steeper faults are younger than fault "c"
d=4	0.5 mg	N30W	44NE	
e=10	1.5 mg	N35W	85NE	
f=?	1 cg	N45W	41NE	
g=5	0.5 mg	N40W	57NE	
h=?	0.5 cg	N50E	40NW	
i=?	1 cg	EW	66N	

Depth Interval: 370 - 375 Well: NNR - 8

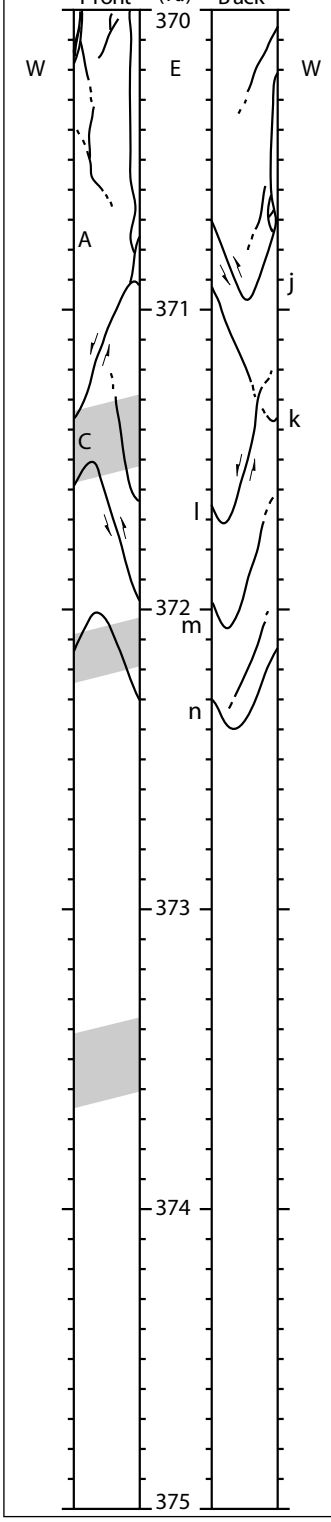

Apparent Disp. (mm)	Fault Thickness (mm)	Fault Strike	Fault Dip	Comments
j=37	2 mg	N80W	68NE	
k=3	0.5 cg	N10E	65NW	Run # 39 Score card: 371.05' 371.1' - 381.1' Drilled: 10.0' Recovered: 10.1'
l=1.5	1 cg	N35W	67NE	
m=1	1 cg	N40W	68NE	
n=?	0.5 mg	N55W	61NE	
				Bedding @ 372.9' : N10W 27SW [obtained from BHTV-log]
				Bedding @ 373.7' : N38W 30SW [obtained from BHTV-log]
				Bedding @ 374.5' : N45W 19SW [obtained from BHTV-log]

Depth Interval: 375 - 380 Well: NNR - 8

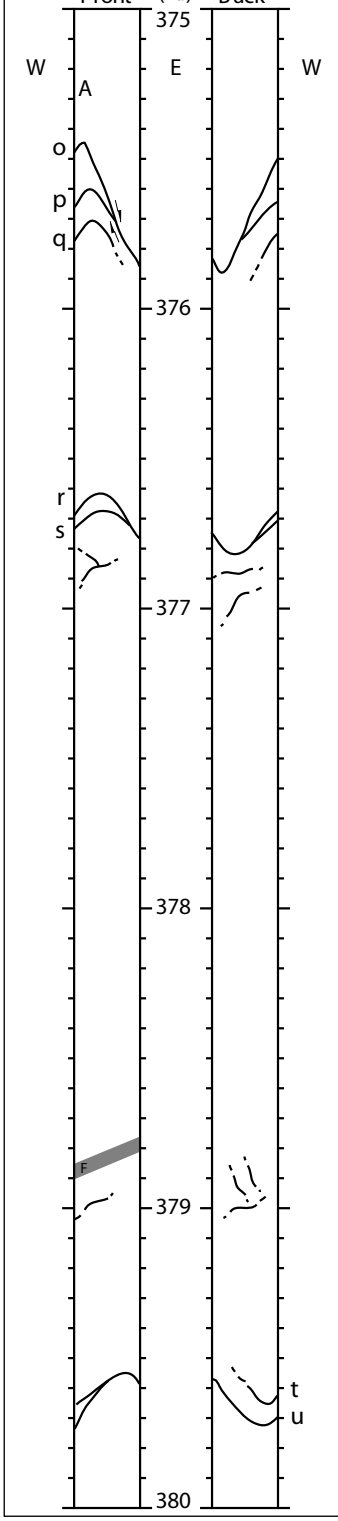

Apparent Disp. (mm)	Fault Thickness (mm)	Fault Strike	Fault Dip	Comments
o=12	2 cg	N15W	65NE	Fault "o" correlates w/375.3' in BHTV-log
p=?	0.5 cg	N30W	68NE	Nice Example of how gouge thickness depends on where measurement is taken.
q=?	1 cg	N40W	61NE	
r=?	1 cg	N50W	47NE	
s=?	1 cg	N50W	42NE	
				Bedding @ 378.8 : N20W 23SE correlates w/378.2' in BHTV-log
				Possible orientation for faults @ 379': N40E, NW dip
t=?	1 cg	N25E	42NW	
u=?	2 cg	N30E	46NW	

Depth Interval: 380 - 385 Well: NNR - 8

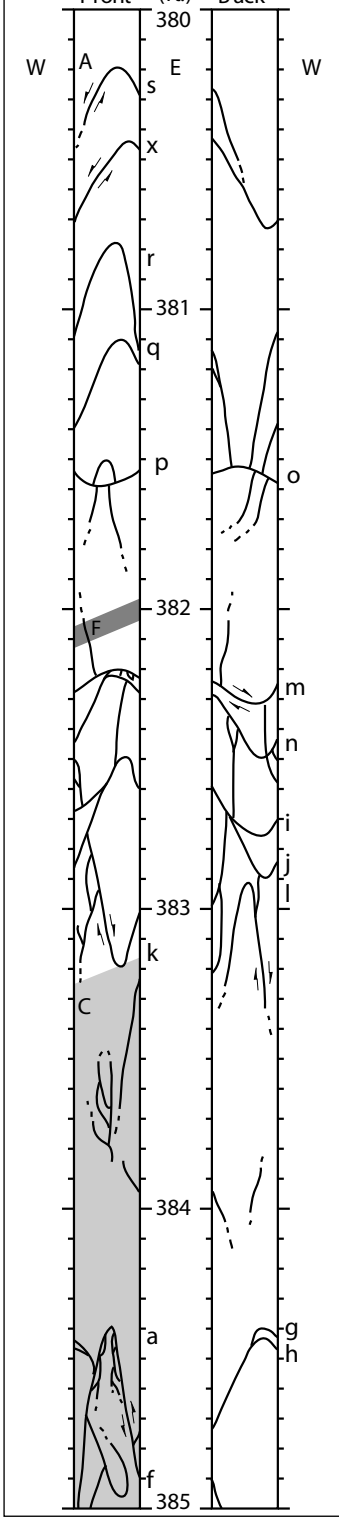

Apparent Disp. (mm)	Fault Thickness (mm)	Fault Strike	Fault Dip	Comments
s=3	1 cg	N60E	55NW	
x=5	1.5 cg	N30E	57NW	
				Rotated "r", "q", "p", & "o" 40° CW but figure not redrawn
r=?	2 cg	N40E	72NW	
				Bedding @ 381.4' : N38W 20SW [obtained from BHTV-log]
q=?	2 cg	N15E	63NW	Run # 40 Score card: 381.2' 381.1' - 391.1' Drilled: 10.0' Recovered: 10.15'
p=?	1.5 cg	N30E	59NW	
o=?	3 cg	NS	17W	Fault "o" is younger than faults "p", "q", & "r". It also has a large strike-slip component
m=24	11 cg	N40E	26NW	Fault "m" is older than steeper fault above it with no orientation data
n=?	2 cg	N35E	53NW	
i=?	1.5 cg	N35E	42NW	
j=?	2 cg	N30E	61NW	
l=4	0.5 mg	N70E	69SE	
k=12	1 cg	N55E	67SE	Fault "k" appears to be older than faults "i" & "j"
a=42	2 mg	N70E	82NW	Fault "a" is the dominant fault
g=?	1 mg	N20E	66SE	Fault "a" correlates w/383.2' in BHTV-log
h=?	1 mg	N15E	61SE	
f=?	0.5 mg	N60E	68SE	

Depth Interval: 385 - 390 Well: NNR - 8

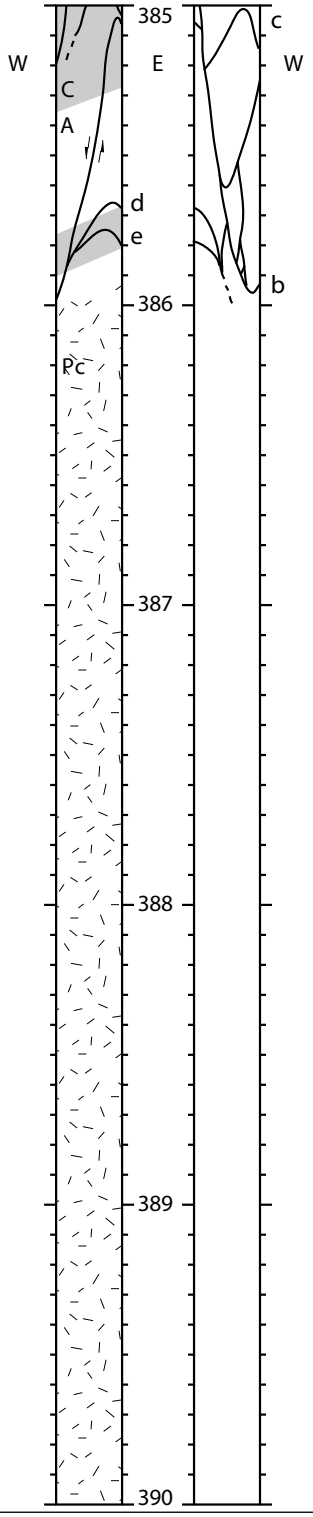

Apparent Disp. (mm)	Fault Thickness (mm)	Fault Strike	Fault Dip	Comments
c=?	0.5 mg	N40E	62SE	
d=?	1 mg	N10E	44NW	
e=?	0.5 mg	N20E	41NW	
b=21	1 mg	N5W	76SW	Fault "b" correlates w/385.3' in BHTV-log

Depth Interval: 170 - 175 Well: NNR - 9

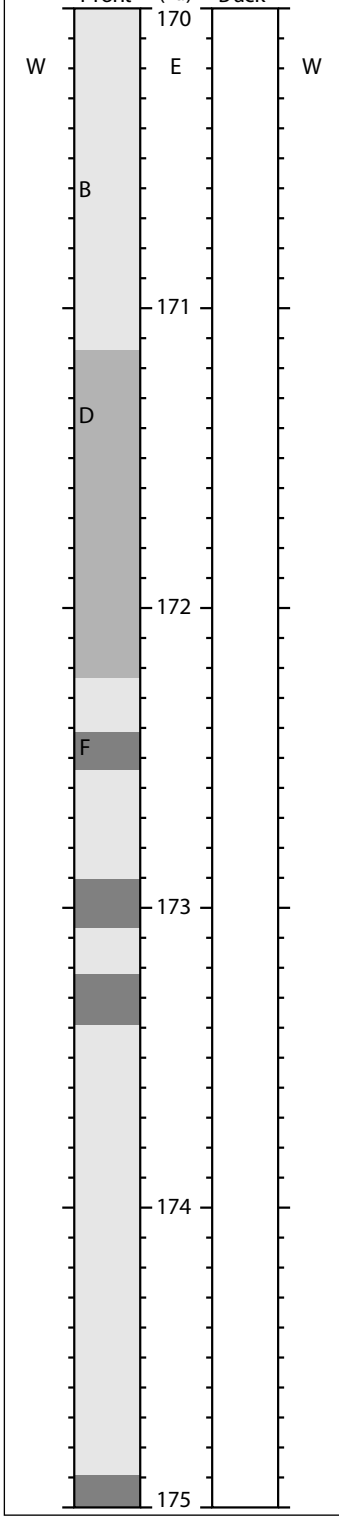

Apparent Disp. (mm)	Fault Thickness (mm)	Fault Strike	Fault Dip	Comments
				Run #17 Score card: 171.3' 171.3' - 181.3' Drilled: 10.0' Recovered: 10.0'

Depth Interval: 175 - 180 Well: NNR - 9

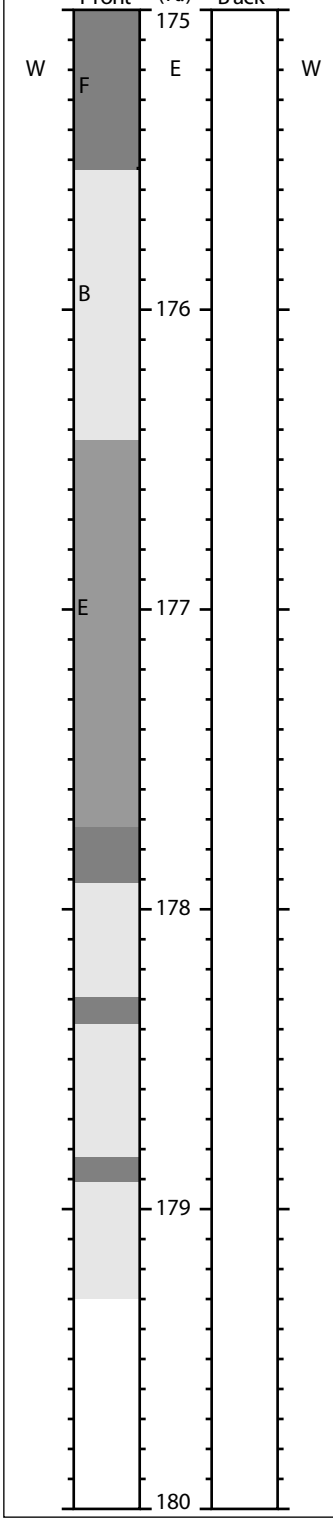

Apparent Disp. (mm)	Fault Thickness (mm)	Fault Strike	Fault Dip	Comments
				Bedding @ 176.4' : N10W 19SW [obtained from BHTV-log] Bedding @ 179.3' : NS 14W [obtained from BHTV-log] Missing core from 179.3' - 180.3'

Depth Interval: 180 - 185 Well: NNR - 9

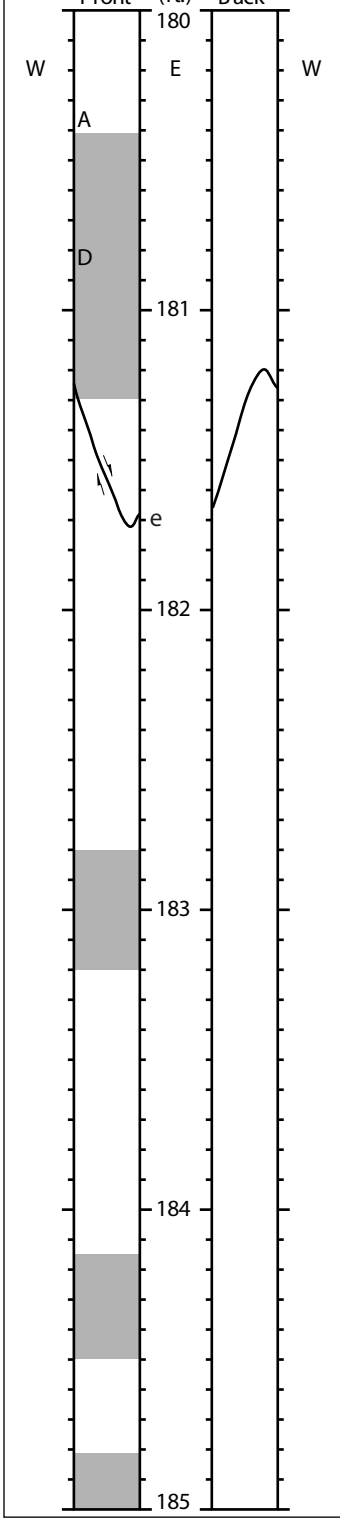

Apparent Disp. (mm)	Fault Thickness (mm)	Fault Strike	Fault Dip	Comments
e=17	1 cg	N30E	67SE	Run #18 Score card: 181.3' 181.3' - 191.55' Drilled: 10.0' Recovered: 10.25'
				Bedding @ 184.4' : NS 13W [obtained from BHTV-log]

Depth Interval: 185 - 190 Well: NNR - 9

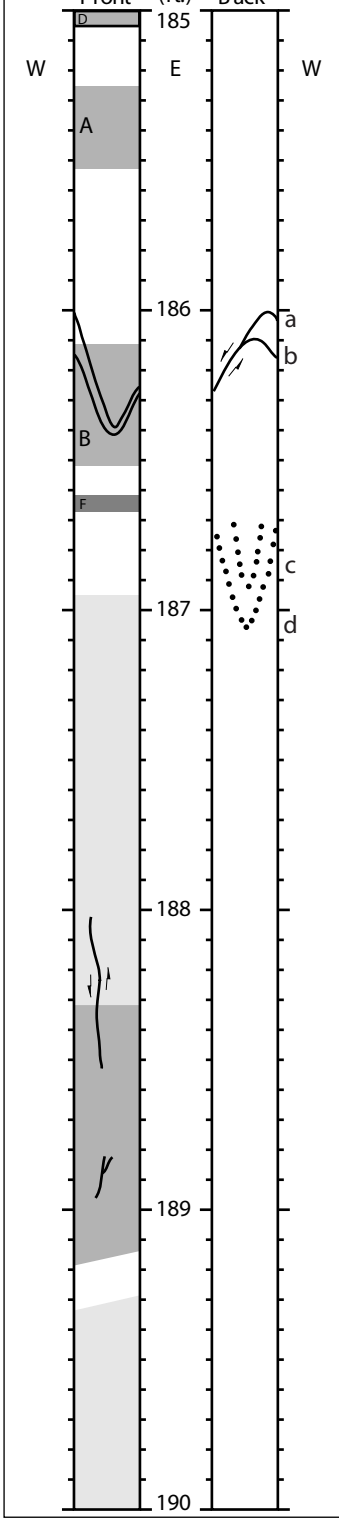

Apparent Disp. (mm)	Fault Thickness (mm)	Fault Strike	Fault Dip	Comments
a=19	1 mg	N20E	62SE	
b=16	1 mg	N60E	45SE	
c=?		N70E	62NW	
d=?		N80E	60NW	
1@ 188.3'	0.5 fg			
				Bedding @ 188.6' : N20E 13NW

Depth Interval: 190 - 195 Well: NNR - 9

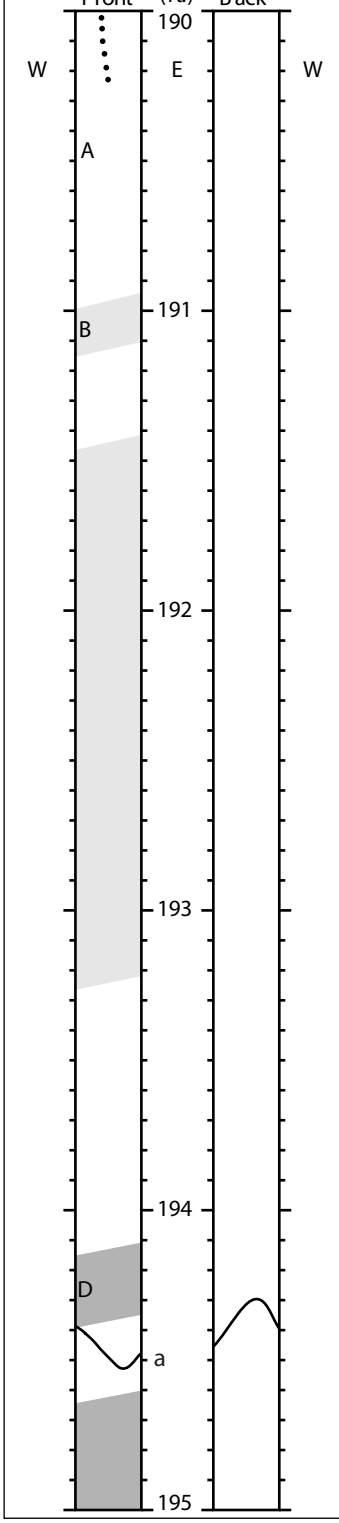

Apparent Disp. (mm)	Fault Thickness (mm)	Fault Strike	Fault Dip	Comments
				Run #19 Score card: 191.5' 191.3.1' - ?? Drilled: ?? Recovered: ??
				Bedding @ 192.8' : N10E 11NW
a=?	1 cg	N50E	47SE	

Depth Interval: 195 - 200 Well: NNR - 9

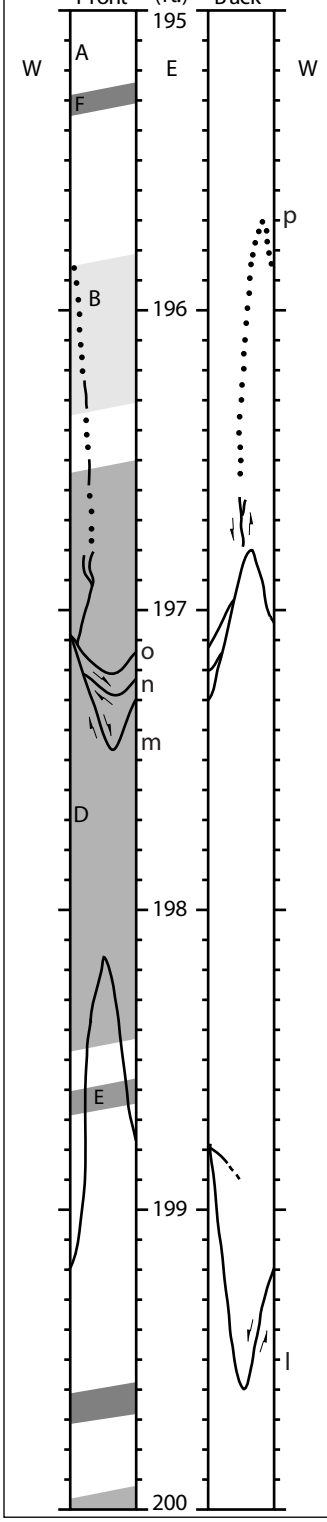

Apparent Disp. (mm)	Fault Thickness (mm)	Fault Strike	Fault Dip	Comments
p=?	?	N20E	85SE	not sure if "p" is a joint or if it is a fault tip
o=?	0.5 fg	N65E	48SE	
n=9	0.5 fg	N55E	56SE	
m=16	0.5 fg	N60E	67SE	
l=7	1 cg	N70E	82NW	

Depth Interval: 200 - 205 Well: NNR - 9

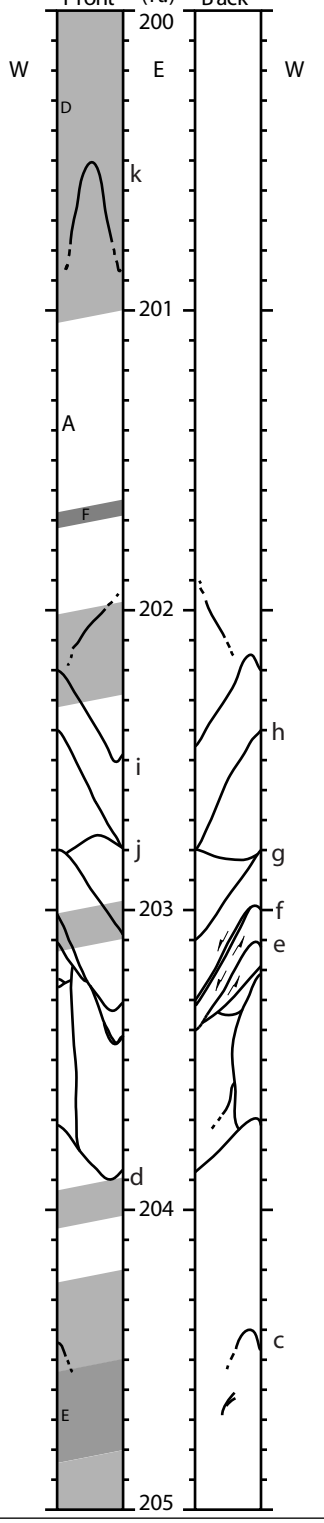

Apparent Disp. (mm)	Fault Thickness (mm)	Fault Strike	Fault Dip	Comments
k=2	1 cg	EW	64N	
				Orientation lost from Run#19 to Run# 20 so bedding dip line is assumed to be N70W from 201' upwards.
				Run #20 Score card: 201.2' 201.3' - 211.3' Drilled: 10.0' Recovered: 10.0'
				Bedding @ 201.8' : N10E 18NW [obtained from BHTV-log]
h=?	1 cg	NS	52E	
i=2	1 cg	N10E	50SE	
j=?	1.5 cg	N60E	29NW	
g=21	2 cg	NS	46E	
f=9	1 cg	N5E	54SE	
e=3	1 cg	N10E	42SE	
d=32	2 clay	N25E	32SE	
				Bedding @ 204.4' : N5E 25NW
c=?	0.5 mg	N20E	55SE	[obtained from BHTV-log]

Depth Interval: 205 - 210 Well: NNR - 9

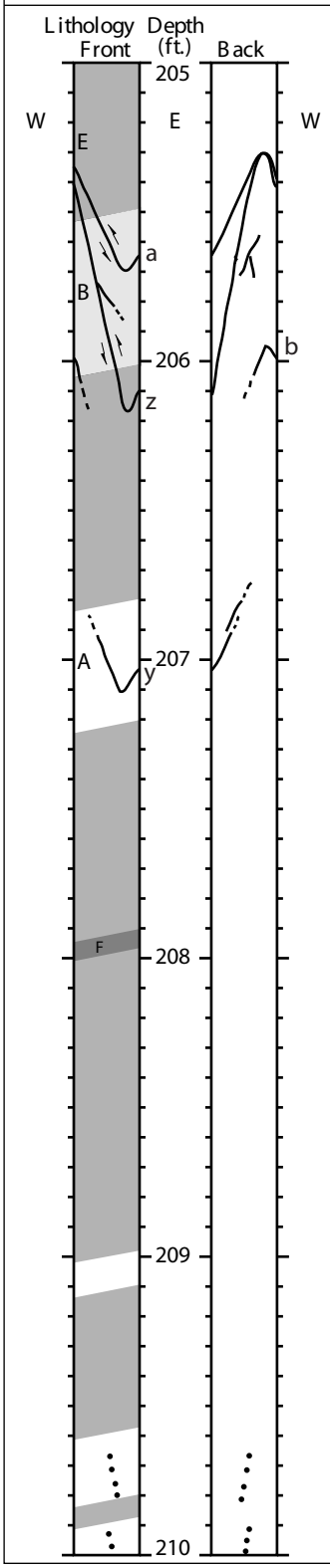

Apparent Disp. (mm)	Fault Thickness (mm)	Fault Strike	Fault Dip	Comments
a=3	0.5 mg	N20E	63SE	
b=?	0.5 mg	N20E	56SE	
z=6	0.5 mg	N20E	81SE	
y=?	0.5 mg	N30E	54SE	
				Bedding @ 208.0' : N20E 14NW
				joints are approximately striking EW

Depth Interval: 210 - 215 Well: NNR - 9

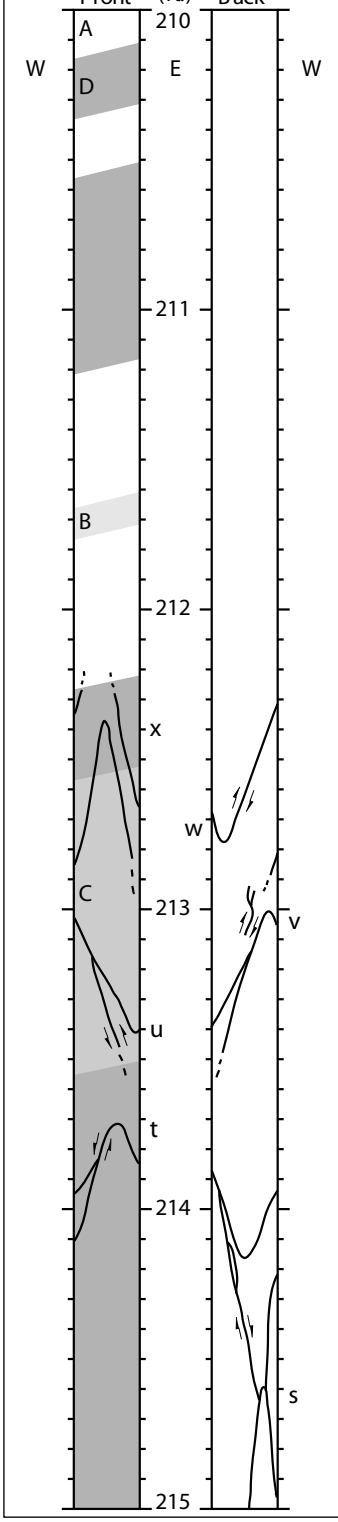

Apparent Disp. (mm)	Fault Thickness (mm)	Fault Strike	Fault Dip	Comments
				Run # 21 Score card: 211.2' 211.3' - 221.3' Drilled: 10.0' Recovered: 10.0' Bedding @ 211.8' : N15E 12NW
x=?	1 mg	N70W	78NE	
w=4	1 mg	N45W	65NE	
v=2	0.5 mg	N30E	76SE	
u=?	0.5 mg	N20E	62SE	
t=30	1 fg	N55E	60NW	
s=25	1 fg	N30E	85SE	

Depth Interval: 215 - 220 Well: NNR - 9

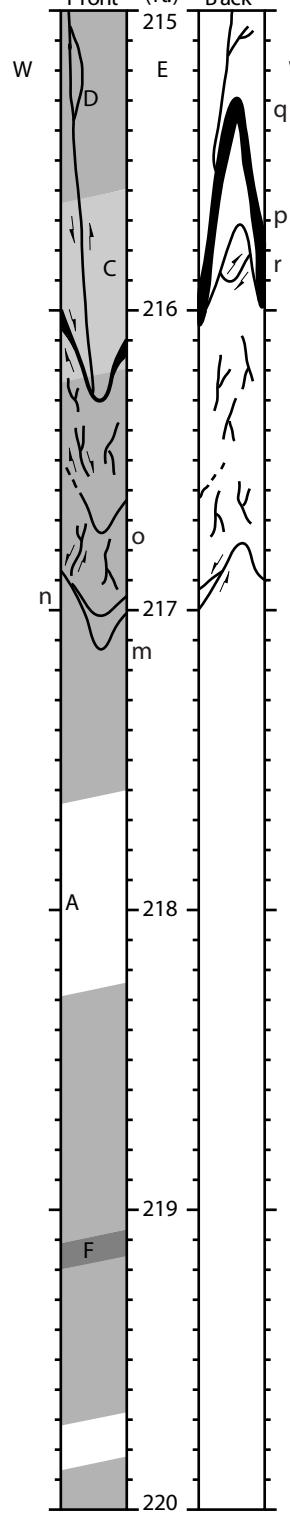

Apparent Disp. (mm)	Fault Thickness (mm)	Fault Strike	Fault Dip	Comments
q=150	13 fg	N80E	82SE	
p=43	2 mg	N70E	70SE	
r=19	1 fg	N70W	67NE	
o=?		N65E	64SE	
n=?	1 fg	N60E	53SE	
m=23	0.5 fg	N55E	65SE	
				Bedding @ 219.1' : N10E 14NW
				Bedding @ 219.6' : N25E 9NW [obtained from BHTV-log]

Depth Interval: 220 - 225 Well: NNR - 9

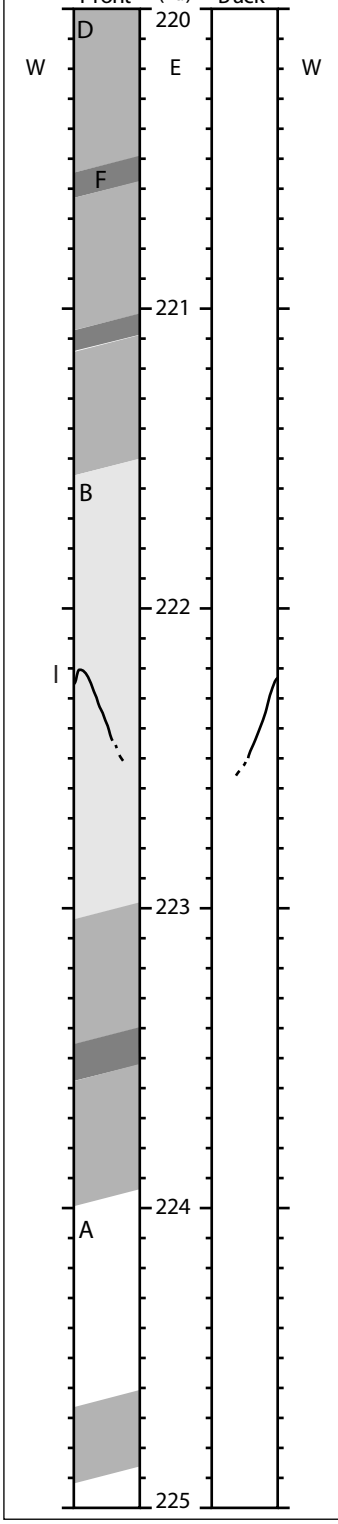

Apparent Disp. (mm)	Fault Thickness (mm)	Fault Strike	Fault Dip	Comments
				Bedding @ 220.9' : NS 13NW [obtained from BHTV-log]
				Lost orientation from Run#21 to Run#22 assumed bedding dip from 221' & up is W.
				Run #22 Score card: 221.3' 121.3' - 131.3' Drilled: 10.0' Recovered: 10.0'
I=?	0.5 cg	N25W	33NE	
				Bedding @ 223.4' : N20E 15NW

Depth Interval: 225 - 230 Well: NNR - 9

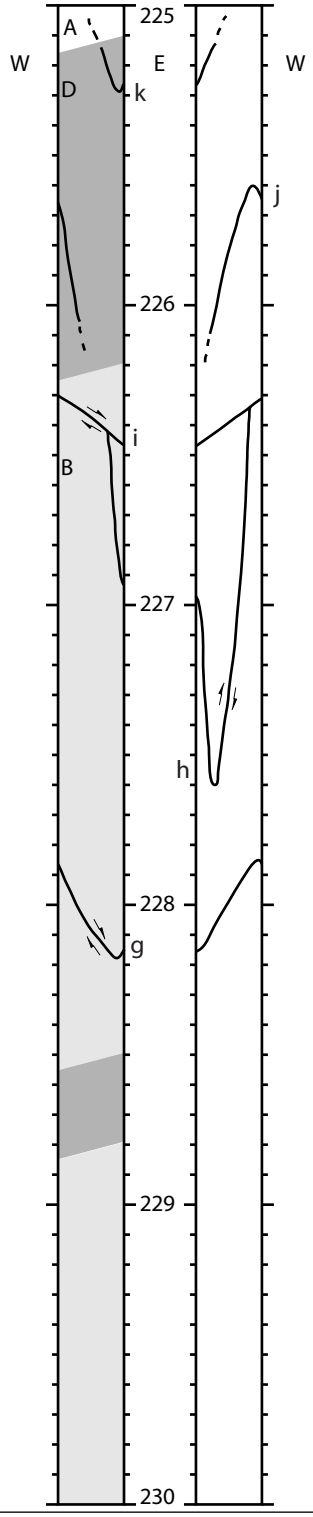

Apparent Disp. (mm)	Fault Thickness (mm)	Fault Strike	Fault Dip	Comments
k=?	0.5 fg	N10E	51SE	
j=?	0.5 fg	N20E	67SE	
i=3	1 cg	NS	26E	
				Bedding @ 227.3' : NS 22W [obtained from BHTV-log]
h=5	1 cg	N40W	82NE	
g=14	1 cg	N10W	52NE	

Depth Interval: 230 - 235 Well: NNR - 9

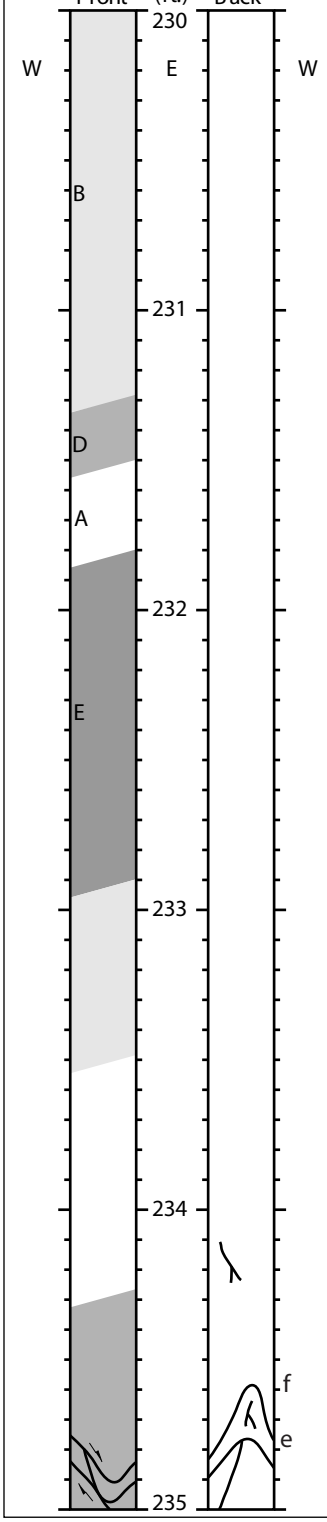

Apparent Disp. (mm)	Fault Thickness (mm)	Fault Strike	Fault Dip	Comments
				Run #23 Score card: 231.3' 231.3' - 241.3' Drilled: 10.0' Recovered: 10.0'
f=30		N50E	57SE	
e=9	1 cg	N60E	42SE	

Depth Interval: 235 - 240 Well: NNR - 9

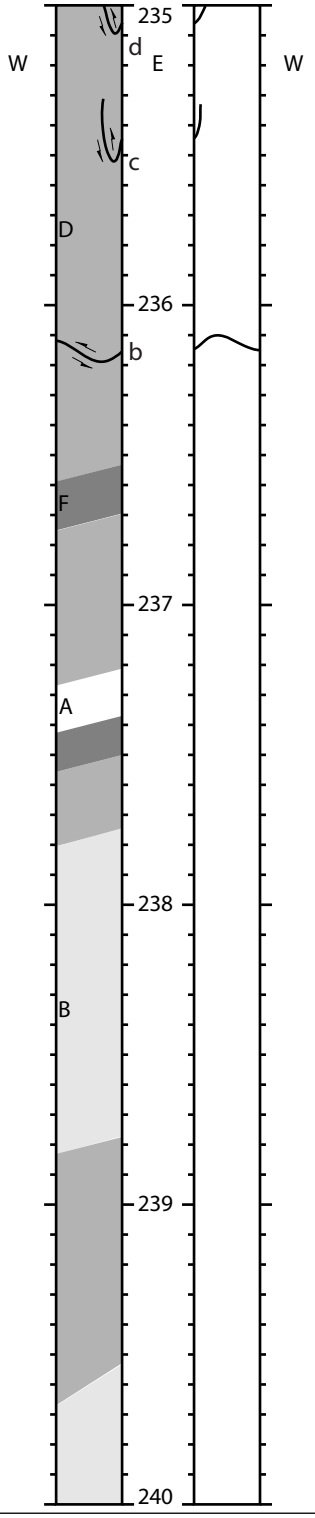

Apparent Disp. (mm)	Fault Thickness (mm)	Fault Strike	Fault Dip	Comments
d=1	0.5 fg	N10E	68SE	
c=1	0.5 fg	N15E	83SE	
b=5	1 fg	N50E	18SE	
				Bedding @ 239.5' : N10E 20NW

Depth Interval: 240 - 245 Well: NNR - 9

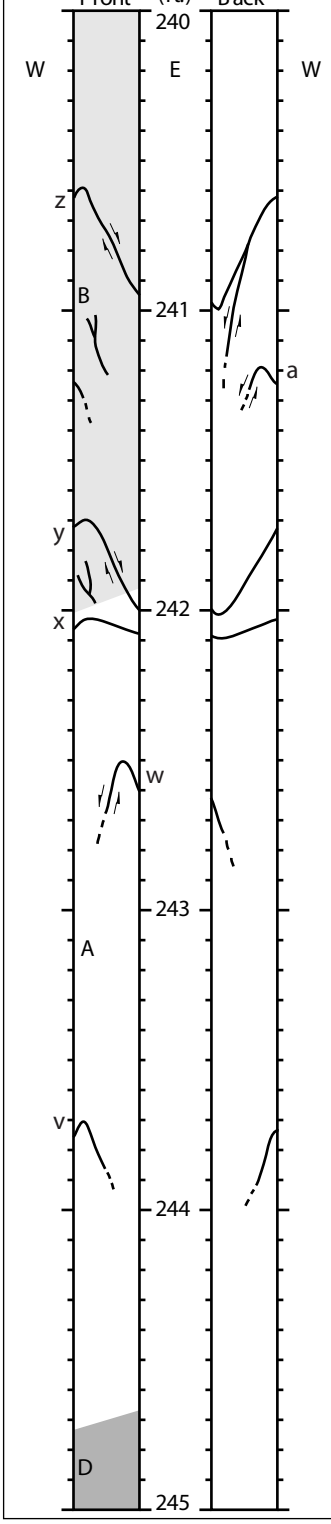

Apparent Disp. (mm)	Fault Thickness (mm)	Fault Strike	Fault Dip	Comments
z=6	0.5 fg	N20W	52NE	
a=3	0.5 fg	N30E	50SE	Run # 27 Score card: 241.3' 241.3' - 251.4' Drilled: 10.0' Recovered: 10.1'
y=3	1 mg	N30W	52NE	
x=?	1 mg	N30W	10NE	
				Bedding @ 242.3 : NS 16W
w=5	1 mg	N45E	67NW	
v=?	1 mg	N20W	56NE	

Depth Interval: 245 - 250 Well: NNR - 9

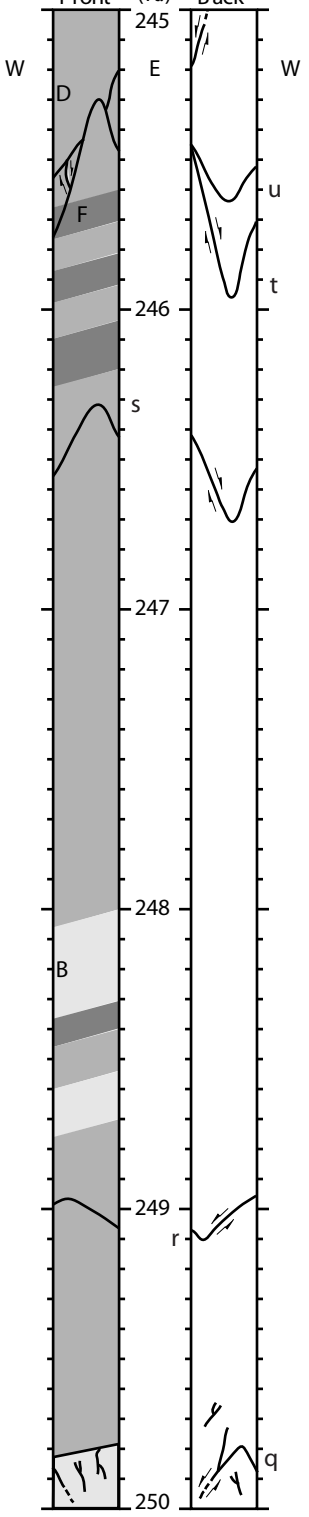

Apparent Disp. (mm)	Fault Thickness (mm)	Fault Strike	Fault Dip	Comments
u=?	1 clay	N60E	47NW	
t=13		N50E	71NW	
s=3	0.5 fg	N60E	60NW	
				Bedding @ 247.2' : N15E 28NW [obtained from BHTV-log]
r=9	0.5 fg	N20W	31NE	Bedding @ 249' : N10E 20NW [obtained from BHTV-log]
				Bedding @ 249.4' : N10E 11NW
q=4	0.5 fg	N35E	41SE	

Depth Interval: 250 - 255 Well: NNR - 9

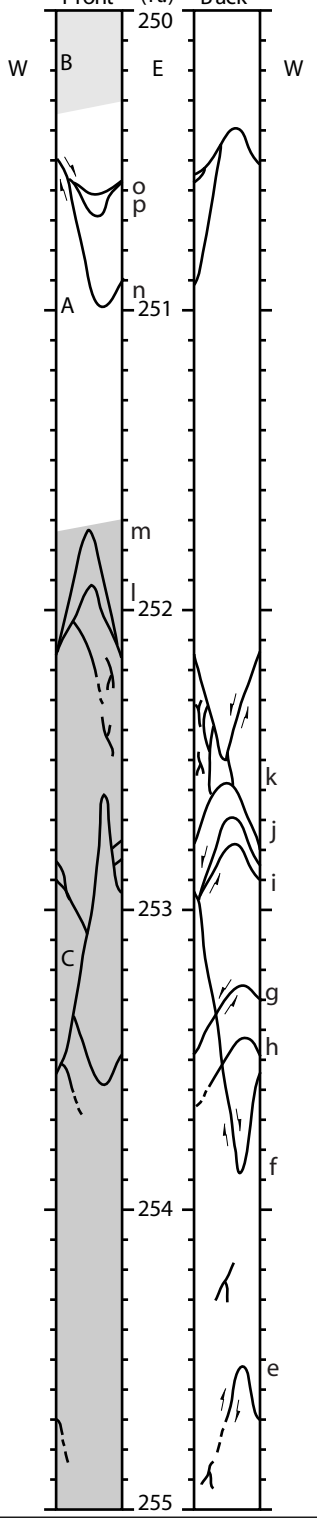

Apparent Disp. (mm)	Fault Thickness (mm)	Fault Strike	Fault Dip	Comments
o=?	1 cg	N55E	39SE	
p=44	3 cg	N60E	46SE	
n=?	1 cg	N40E	67SE	
				Run #25 Score card: 251.3' 251.3' - 261.3' Drilled: 10.0' Recovered: 10.0'
	2 mg	N85E	71NW	
m+l=27				
	1 mg	N70E	63NW	
k=?	1 mg	N70W	55SW	
	1 fg	N80E	68SE	
j+i=14				
	1 fg	N70E	51SE	
g=2	0.5 fg	N50E	42SE	"g" is younger than "f"
h=?	0.5 fg	N50E	42SE	
f=34	3 fg	N45E	81NW	
e=5	0.5 fg	N40E	78SE	

Depth Interval: 255 - 260 Well: NNR - 9

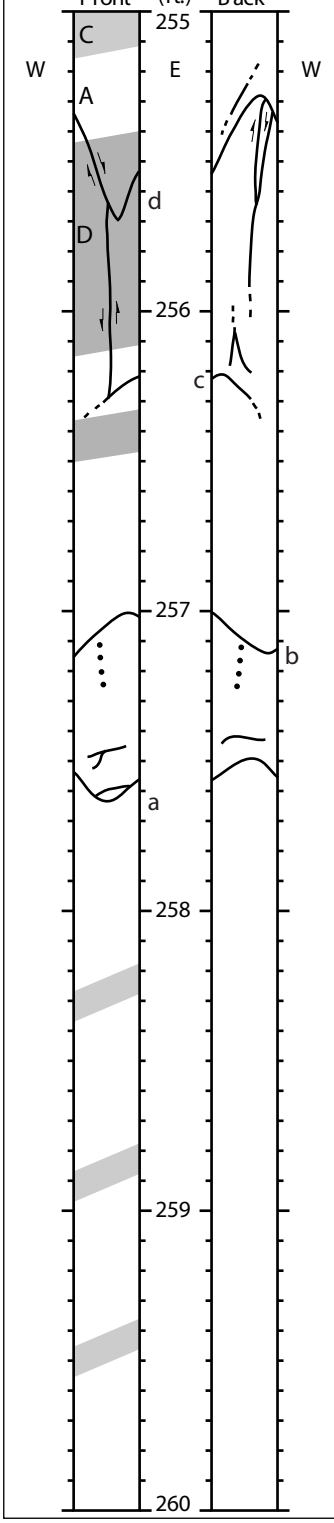

Apparent Disp. (mm)	Fault Thickness (mm)	Fault Strike	Fault Dip	Comments
				Bedding @ 255' : N10E 24NW [obtained from BHTV-log]
d=35	2.5 cg	N50E	64SE	
c=?	1 cg	N10E	28NW	Fault "c" correlates w/256.3' in BHTV-log Bedding @ 256.4' : N20E 22NW
b=?	4cg	N5E	33NW	Fault "b" correlates w/257.1' in BHTV-log Bedding @ 257.4' : N5E 33NW [obtained from BHTV-log]
a=?	2 cg	N70W	26NE	

Depth Interval: 260 - 265 Well: NNR - 9

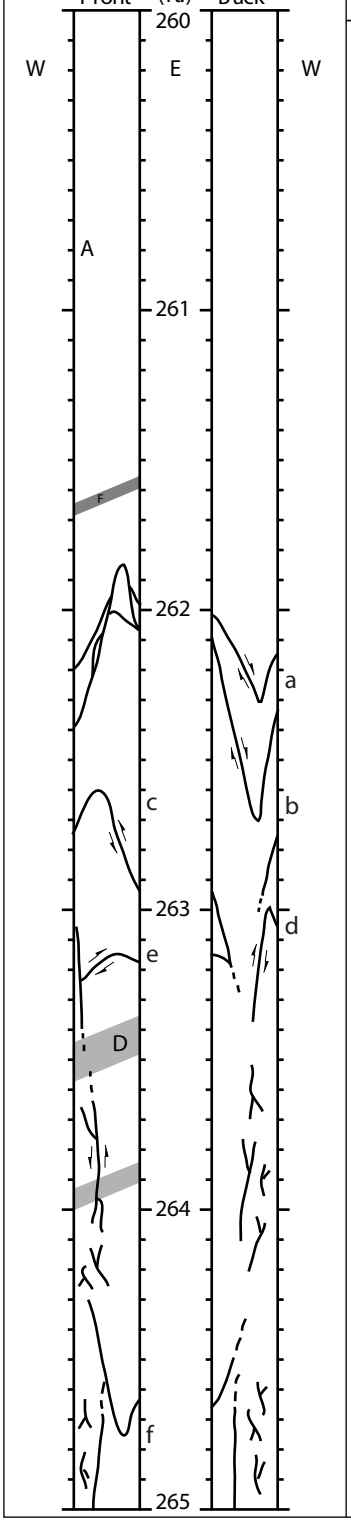

Apparent Disp. (mm)	Fault Thickness (mm)	Fault Strike	Fault Dip	Comments
				Run #26 Score card: 261.3' 261.3' - 271.3' Drilled: 10.0' Recovered: 10.0'
a=3	0.5 mg	N40E	57NW	
c=3	0.5 mg	N50W	73NE	
b=70	1 mg	N55E	76NW	Fault "b" correlates w/261.4' in BHTV-log
d=39	2 mg	N20E	83SE	
e=1	0.5 mg	N80E	37SE	
				Bedding @ 263.3' : N35E 30NW [obtained from BHTV-log]
				@ 263.7' displacement is 18mm and thickness is 0.5mm[mg]
f=?	2 cg	N45E	65SE	Fault "f" correlates w/264.7' in BHTV-log

Depth Interval: 265 - 270 Well: NNR - 9

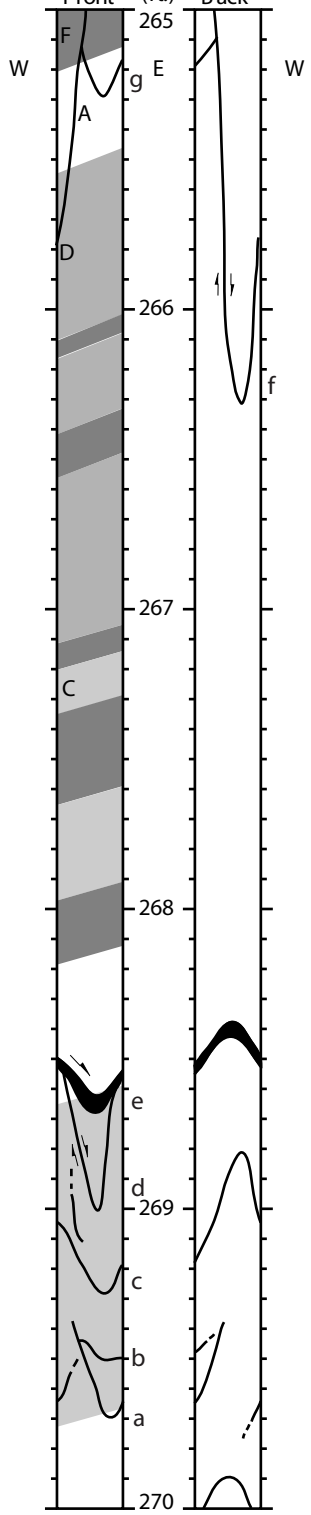

Apparent Disp. (mm)	Fault Thickness (mm)	Fault Strike	Fault Dip	Comments
g=?	1 cg	N50E	58SE	
f=27	2 mg	N50E	83NW	
				Bedding @ 266.5' : N10W 16SW
e=?	24 cg	N75E	57SE	Fault "e" correlates w/268.8' in BHTV-log
d=55	3 cg	N70E	74SE	
c=?	1 clay	N50E	59SE	
b=?	1 mg	N45E	27SE	
a=?	1 mg	N40E	54SE	

Depth Interval: 270 - 275 Well: NNR - 9

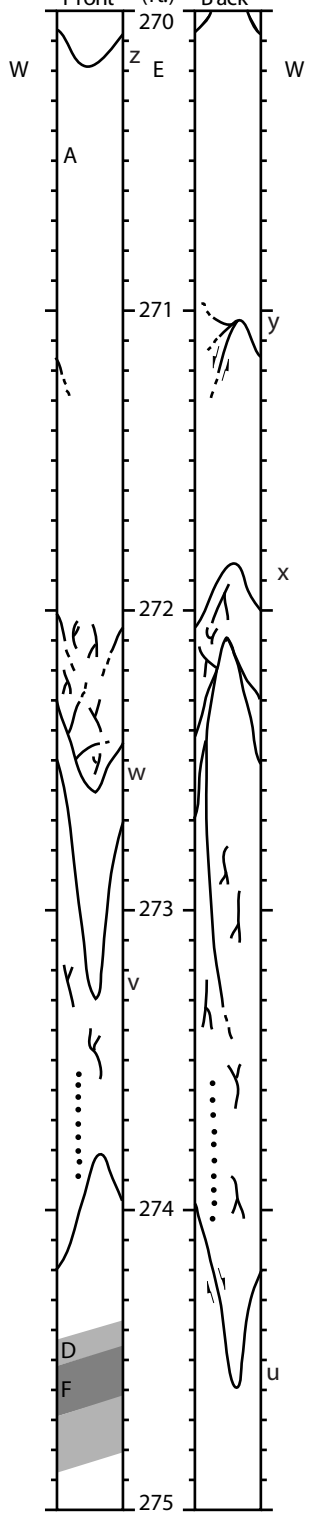

Apparent Disp. (mm)	Fault Thickness (mm)	Fault Strike	Fault Dip	Comments
z=?	4 cg	N80E	49SE	Fault "z" correlates w/270.2' in BHTV-log
y=30	2 mg	N40E	68SE	
				Run #27 Score card: 271.3' 271.3' - 281.5' Drilled: 10.0' Recovered: 10.2'
x=?	4 cg	N70E	50SE	
w=?	2 cg	N75E	62SE	
v=?	3 cg	N75E	80SE	
u=19	0.5 clay	N50E	76NW	Fault "u" correlates w/273.6' in BHTV-log

Depth Interval: 275 - 280 Well: NNR - 9

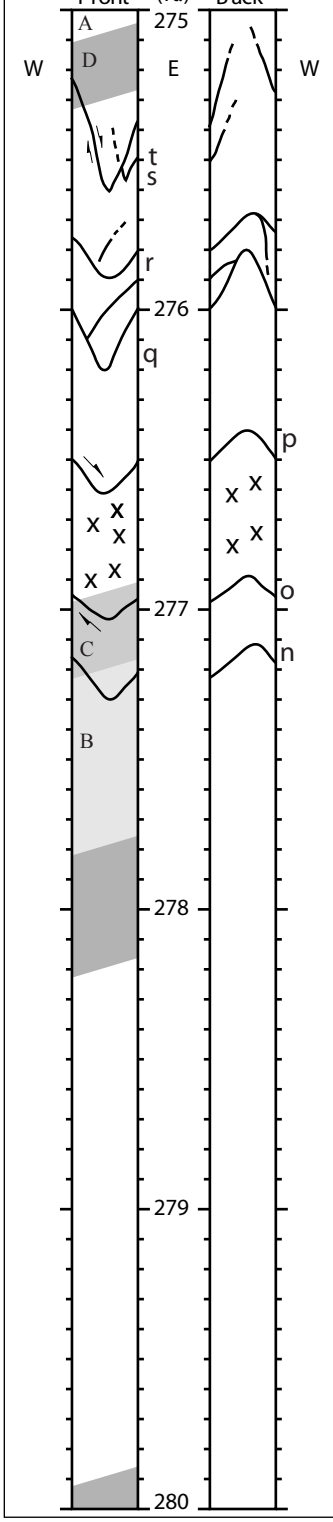

Apparent Disp. (mm)	Fault Thickness (mm)	Fault Strike	Fault Dip	Comments
t=?		N30E	71SE	
s=55	3 mg	N80E	73SE	
r=?	1 cg	N80E	41SE	
q=?	1 cg	EW	56S	
p=?	4 cg	N85E	44SE	Fault "p" correlates w/276.5' in BHTV-log
o=?	4 fg	N80E	41SE	
n=?	6 fg	N70E	53SE	Fault "n" correlates w/277' in BHTV-log

Depth Interval: 280 - 285 Well: NNR - 9

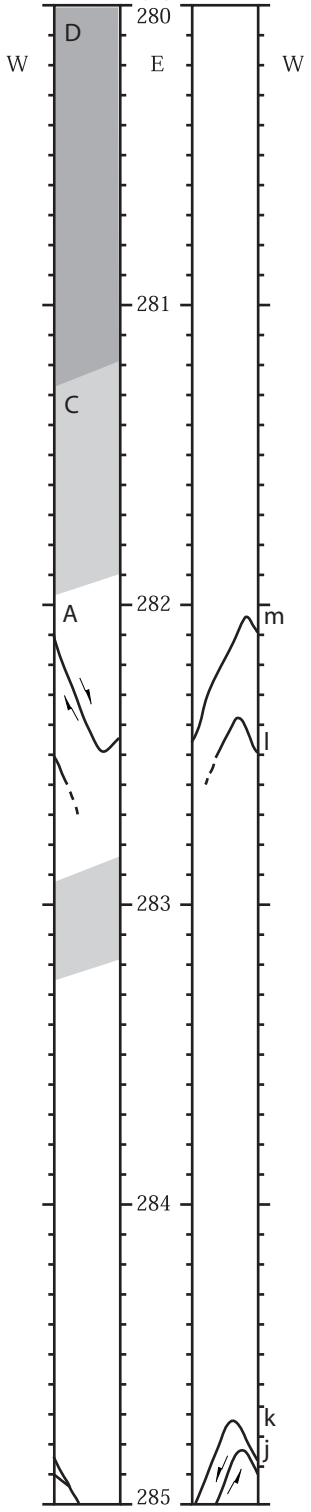

Apparent Disp. (mm)	Fault Thickness (mm)	Fault Strike	Fault Dip	Comments
				Bedding @ 280.3' : N5E 19NW
				Run #28 Score card: 281.5' 281.3' - 291.25' Drilled: 10.0' Recovered: 9.95'
m=14	4 cg	N30E	54SE	
l=?	2 cg	N60E	56SE	
				Bedding @ 284.3' : N15E 18NW [obtained from BHTV-log]
k=?	6 cg	N60E	60SE	Fault "k" correlates w/285.1'
j=3	2 cg	N35E	58SE	in BHTV-log

Depth Interval: 285 - 290 Well: NNR - 9

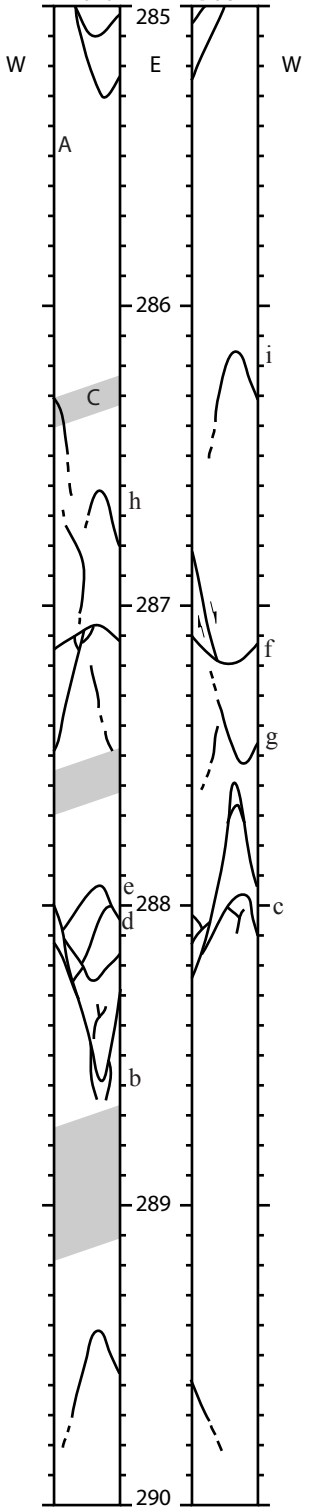

Apparent Disp. (mm)	Fault Thickness (mm)	Fault Strike	Fault Dip	Comments
				Bedding @ 285.8' : N10E 18NW [obtained from BHTV-log]
i=?	1 cg	N50W	78NE	
				Bedding @ 286.4' : N20E 27NW [obtained from BHTV-log]
h=2	1 cg	N35W	80SW	
f=?	2 cg	N35W	73SW	
g=?	7 cg	N40E	29NW	
e=?	1 cg	N50E	36NW	
d=?	1 cg	N20E	64NW	SE dipping set is dominate and younger than fault "d"
c=?	3 cg	N50E	55SE	
b=?	3 cg	N50E	84SE	Fault "b" correlates w/289' in BHTV-log
				Bedding @ 289.2' : N20E 22NW
a=?	1 cg	N55E	56NW	

Depth Interval: 290 - 295 Well: NNR - 9

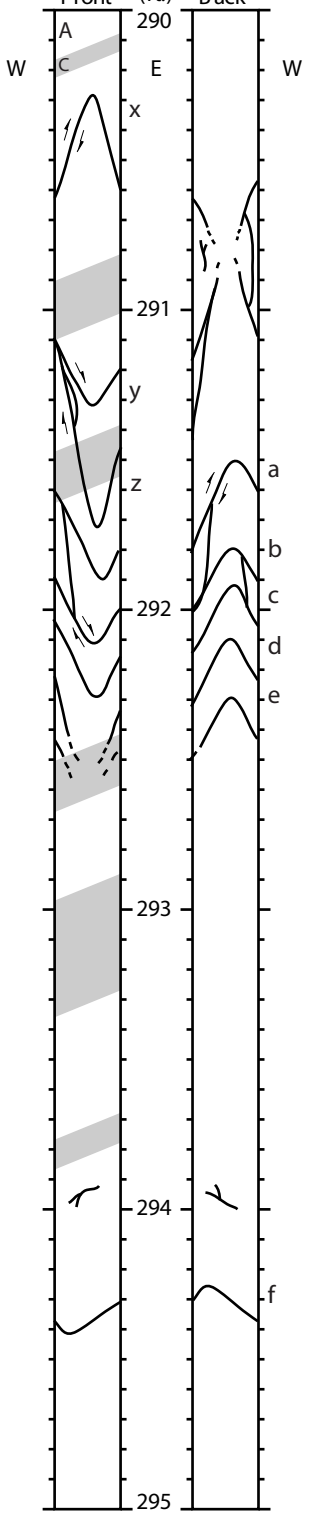

Apparent Disp. (mm)	Fault Thickness (mm)	Fault Strike	Fault Dip	Comments
x=6	1 cg	N60E	65NW	
y=3	1 cg	N50E	66SE	
z=5	1 cg	N60E	79SE	
a=43	3 fg	N45E	50SE	Fault "a" correlates w/292.4' in BHTV-log
b=26	4 cg	N60E	61SE	
c=?	3 cg	N55E	60SE	
d=?	3 cg	N60E	59SE	
e=?	1 cg	N50E	61SE	
				Bedding @ 293.2' : N10E 21NW
f=?	1 cg	N10W	35SW	

Depth Interval: 295 - 300 Well: NNR - 9

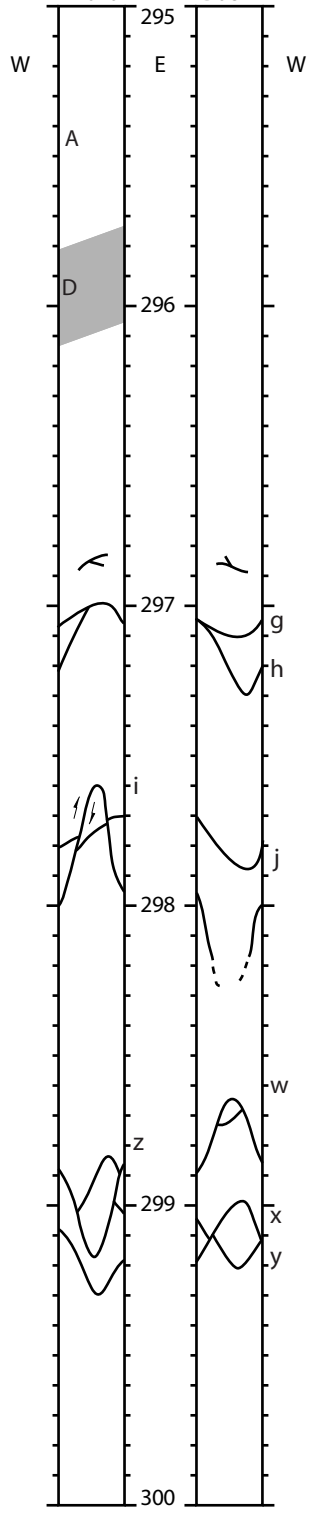

Apparent Disp. (mm)	Fault Thickness (mm)	Fault Strike	Fault Dip	Comments
g=?	2 cg	N40E	18NW	
h=?	2 cg	N40E	54NW	
i=3	1 cg	EW	62N	Fault "i" is younger than "j"
j=?	2 cg	N20E	14NW	
w=?	1 cg	N45E	54NW	
z=?	1 cg	N75E	78SE	Faults "z"& "y" might be the same fault if so than "w"& "x" are younger
x=?	4 cg	N60E	53SE	
y=?	1 cg	N65E	55NW	

Depth Interval: 300 - 305 Well: NNR - 9

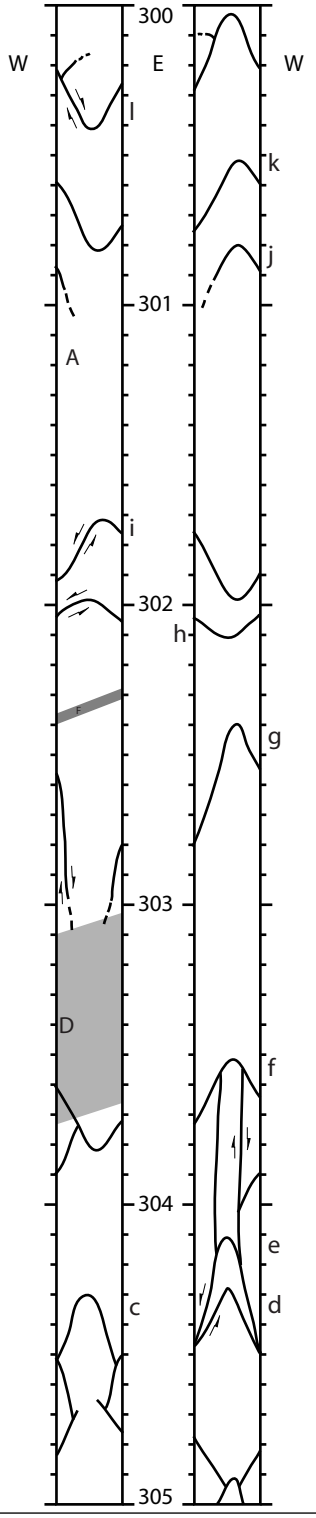

Apparent Disp. (mm)	Fault Thickness (mm)	Fault Strike	Fault Dip	Comments
l=45	3 cg	N70E	58SE	
k=?	0.5 cg	N50E	51SE	
j=?	0.5 cg	N50E	53SE	
				Run #30 Score card: 301.2' 301.3' - 311.3' Drilled: 10.0' Recovered: 10.0'
i=7	1 cg	N40E	41NW	
h=11	1 cg	N80E	34NW	
g=1	1.5 cg	N40E	73SE	
				Bedding @ 303.1' : NS 18W
f=?	13 cg	N50E	47SE	Fault "f" correlates w/303.7' in BHTV-log
e=4	2 cg	N80E	70SE	
d=5	3 cg	N75E	76SE	
c=?	2 cg	EW	59N	

Depth Interval: 305 - 310 Well: NNR - 9

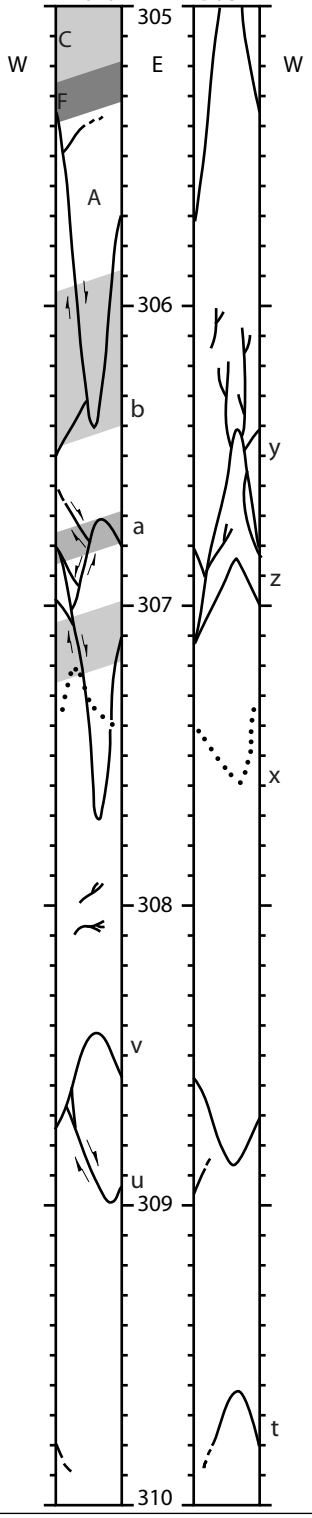

Apparent Disp. (mm)	Fault Thickness (mm)	Fault Strike	Fault Dip	Comments
b=80	6 cg	N60E	84SE	Fault "b" correlates w/306.3' in BHTV-log
y=68	6 cg	N50E	82SE	
a=14	3 cg	N40E	59NW	
z=?	2 cg	N50E	67SE	
x=?		N45W	57NE	Joint "x" correlates w/307.7' in BHTV-log
v=?	2 cg	N65E	58NW	
				Bedding @ 308.8' : N30E 24NW
u=3	1cg	N35E	56SE	
t=?	3 cg	N65E	62SE	

Depth Interval: 310 - 315 Well: NNR - 9

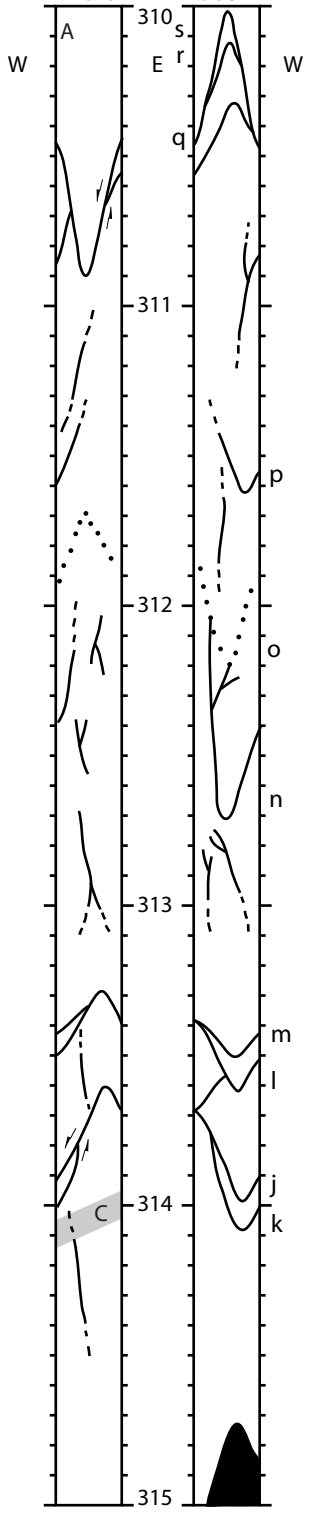

Apparent Disp. (mm)	Fault Thickness (mm)	Fault Strike	Fault Dip	Comments
s=?	3 cg	EW	71S	
r=7	3 cg	N70E	67SE	
q=?	4 cg	N60E	65SE	
p=?	3 cg	N35E	58NW	Run # 31 Score card: 311.3' 311.3' - 321.3' Drilled: 10.0' Recovered: 10.0'
o=?		N70W	66NE	
n=?	2 cg	N85W	74NE	Bedding @ 314.0' : N20E 26NW
m=?	2 cg	N40E	43NW	
l=?	2 cg	N45E	47NW	
j=24	3 cg	N30E	56NW	
k=17	3 cg	N30E	62NW	

Depth Interval: 315 - 320 Well: NNR - 9

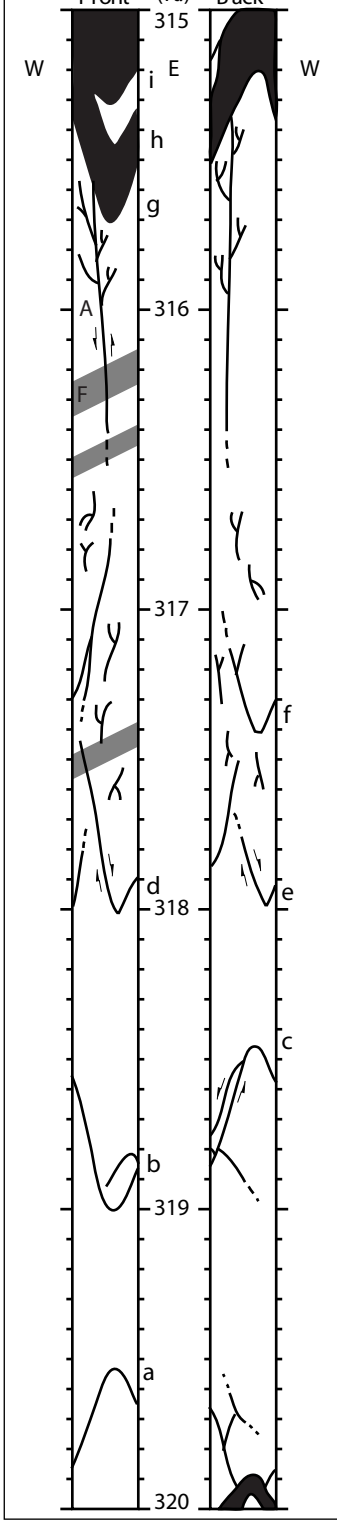

Apparent Disp. (mm)	Fault Thickness (mm)	Fault Strike	Fault Dip	Comments
i=?	48 cg	N65E	71SE	
h=?		N40E	65SE	
g=?	23 cg	N60E	62SE	Fault "g" correlates w/315.7' in BHTV-log
				@ 316.4 displacement is 17mm w/ gouge thickness = 3mm [cg]
f=?		N35E	71NW	
d=2	1 cg	N40E	63SE	
e=8	2 cg	N15W	64SW	
c=4	2 cg	N45E	62SE	
				Fault "b" is older than "c"
b=?	2 cg	N20E	57NW	
				Missing core from 319' - 319.3'
a=?	3 cg	N50E	56NW	

Depth Interval: 320 - 325 Well: NNR - 9

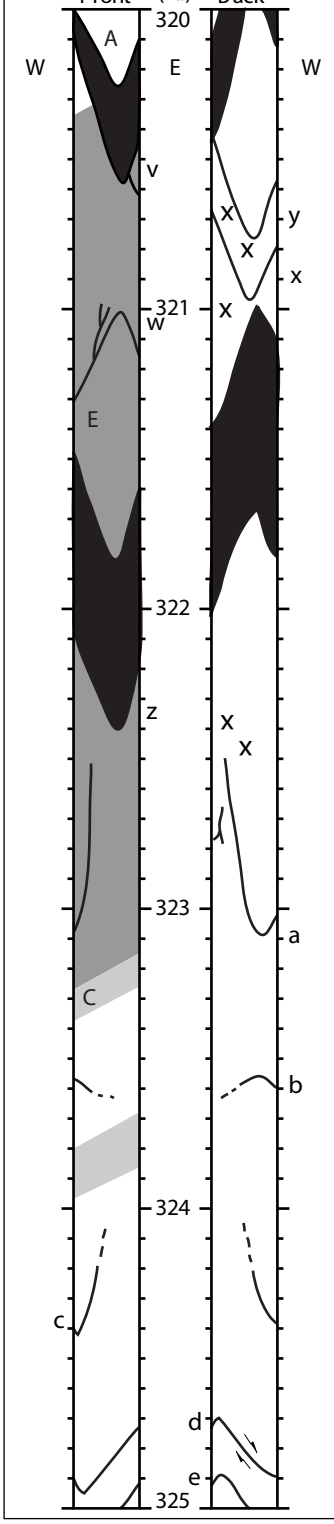

Apparent Disp. (mm)	Fault Thickness (mm)	Fault Strike	Fault Dip	Comments
v=?	50 cg	N40E	72SE	Fault "v" correlates w/319.6' in BHTV-log
y=?	3 mg	N50E	64NW	
x=?	3 mg	N45E	71NW	
w=?	3 mg	N40E	53NW	
z=?	140 mg	N40E	63SE	Fault "z" correlates w/322.3' in BHTV-log
a=?	2 cg	N35E	72NW	
b=?	1 cg	N30E	11SE	
c=?	0.5 mg	N5W	62SW	
d=1	1 mg	N20W	45SW	
e=?	2 cg	N20W	38SW	

Depth Interval: 325 - 330 Well: NNR - 9

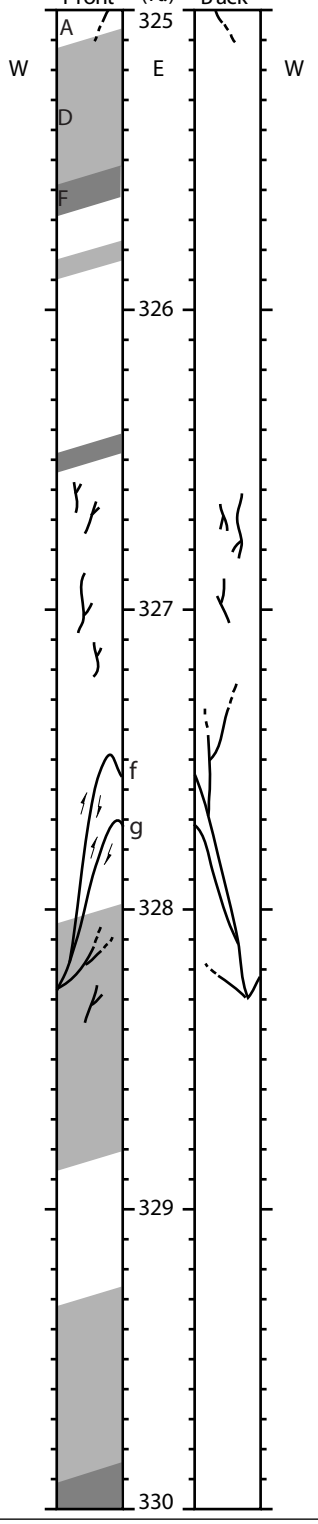

Apparent Disp. (mm)	Fault Thickness (mm)	Fault Strike	Fault Dip	Comments
				Bedding @ 325.1' : N20E 16SW
f=7	1 mg	N30E	67NW	
g=8	1 mg	N15E	65NW	

Depth Interval: 330 - 335 Well: NNR - 9

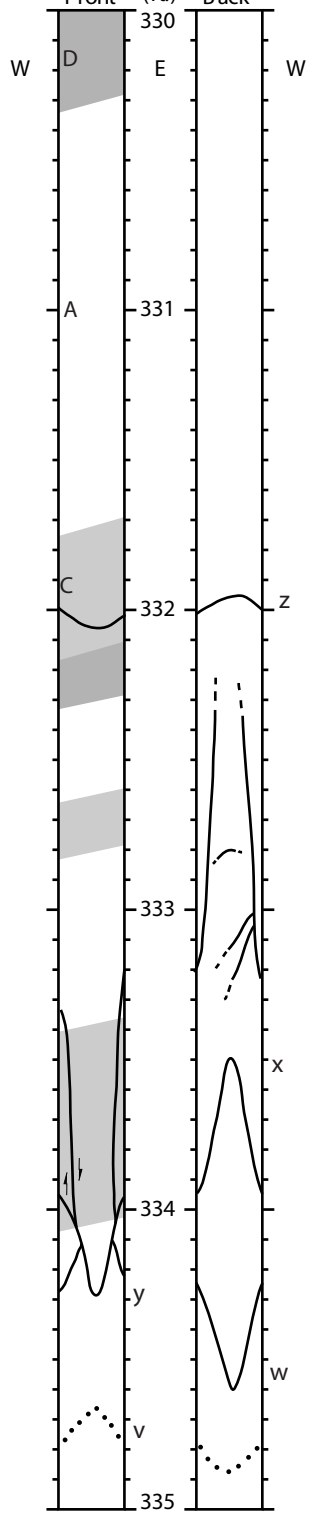

Apparent Disp. (mm)	Fault Thickness (mm)	Fault Strike	Fault Dip	Comments
				Bedding @ 330.3' : N80E 16SE
				Run #23 Score card: 331.3' 331.3' - 341.3' Drilled: 10.0' Recovered: 9.9'
z=?	0.5 cg	N40E	11SE	
				Bedding @ 332.3' : N20E 12SW
x=?	1 cg	N45E	67SE	
y=16	1 cg	N35E	86SE	
w=?	0.5 cg	N30W	57NE	
v=?		N65E	50NW	Joint "v" correlates w/334.8' in BHTV-log

Depth Interval: 335 - 340 Well: NNR - 9

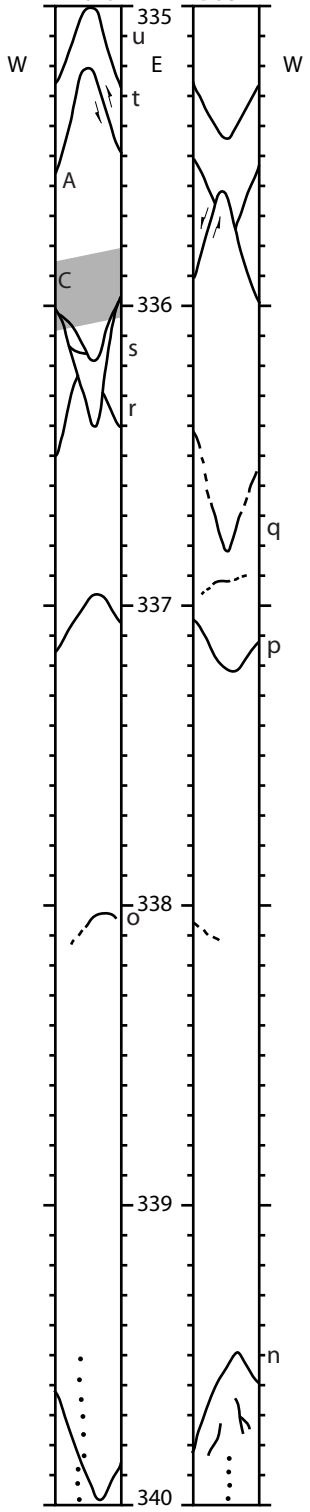

Apparent Disp. (mm)	Fault Thickness (mm)	Fault Strike	Fault Dip	Comments
u=?	1 cg	N50W	55NE	
t=2	1 cg	N50W	54NE	
	2 cg	N35E	52SE	
s+r>30				
	2 cg	N40E	55SE	
q=?	0.5 cg	N50W	62NE	
p=16	1 cg	N55W	57NE	
o=?	1 cg	N30E	17NW	
n=?	1 cg	N30E	64SE	Fault "n" correlates w/340' in BHTV-log

Depth Interval: 340 - 345 Well: NNR - 9

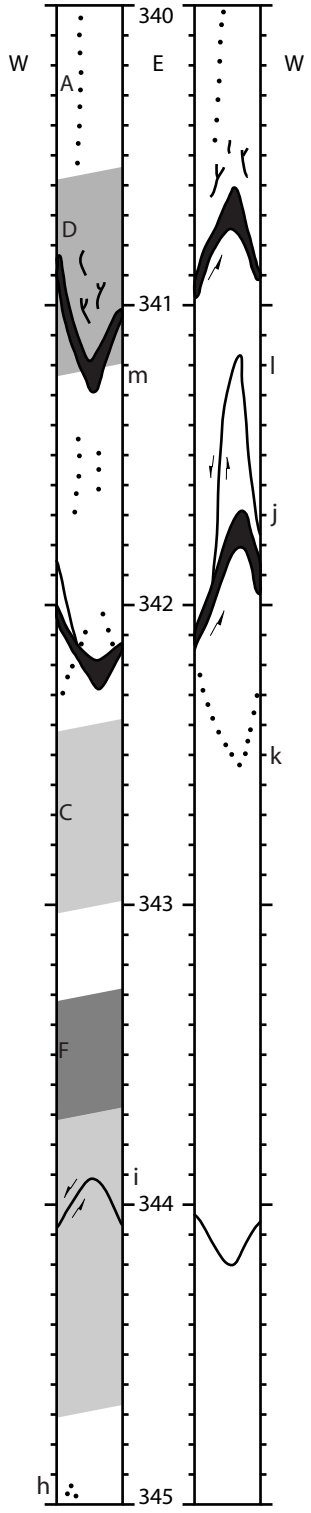

Apparent Disp. (mm)	Fault Thickness (mm)	Fault Strike	Fault Dip	Comments
m=?	28 clay	N60E	66SE	Fault "m" correlates w/341.3'
l=80	5 mg	N40E	84SE	in BHTV-log
j=?	16 mg	N45E	71SE	Fault "j" correlates w/342.3' in BHTV-log
k=?		N65E	60NW	
				Bedding @ 343.5' : N15W 15SW [obtained from BHTV-log]
				Bedding @ 343.7' : N20W 11SW
i=2	0.5 mg	N80W	56NE	
h=?		N50W	77NE	Joint "h" correlates w/344.4' in BHTV-log

Depth Interval: 345 - 350 Well: NNR - 9

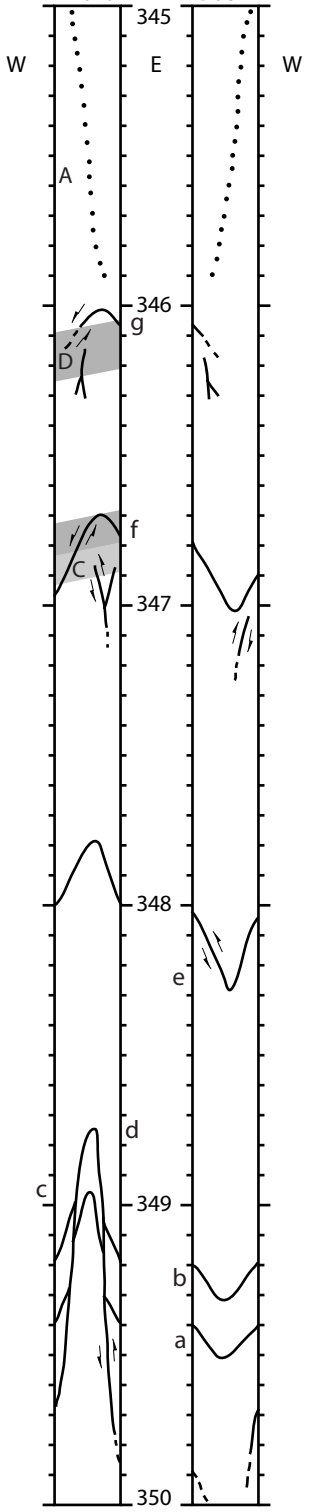

Apparent Disp. (mm)	Fault Thickness (mm)	Fault Strike	Fault Dip	Comments
g=30	4 mg	N40E	42NW	
f=9	1 mg	N40E	63NW	@ 347.0' Fg to Mg Sandstone with 1mm Fault displacement and 0.5mm fault gouge.
e=2	0.5 mg	N75E	64NW	
d=3	1 mg	N60E	81NW	
c=?	1 mg	N65E	66NW	
b=?	1 mg	EW	41N	
a=?	1mg	N80E	56NW	

Depth Interval: 350 - 355 Well: NNR - 9

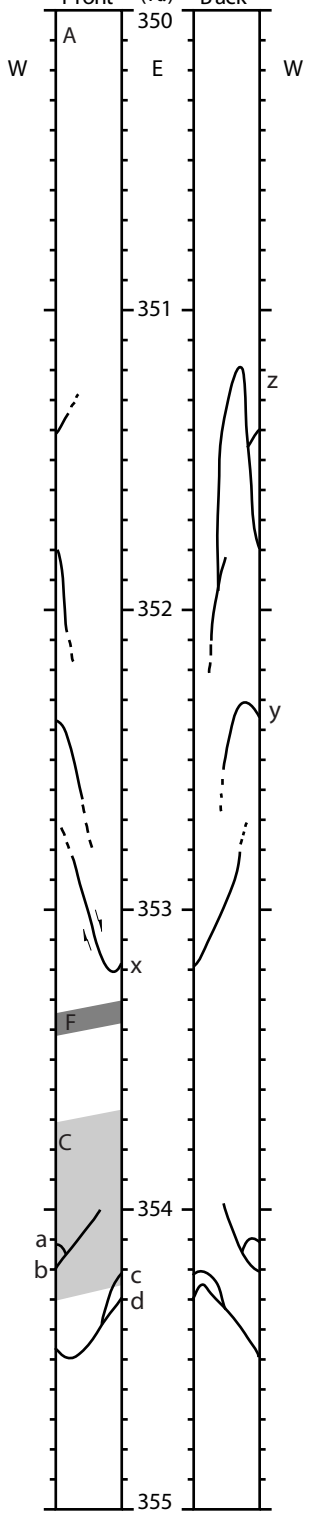

Apparent Disp. (mm)	Fault Thickness (mm)	Fault Strike	Fault Dip	Comments
z=?	0.5 mg	N40E	77SE	
y=?	1 cg	N30E	54SE	
				Bedding @ 352.6' : N18W 18SW [obtained from BHTV-log]
x=2	2 cg	N15E	64SE	
				Bedding @ 353.9' : N30W 15SW
a=?	1 mg	N10W	56NE	
b=?	1 mg	NS	58W	
c=?	c+d=9 cg	N5W	46SW	Fault "c" & "d" correlates w/354.4' in BHTV-log
d=?		N5W	44SW	

Depth Interval: 355 - 360 Well: NNR - 9

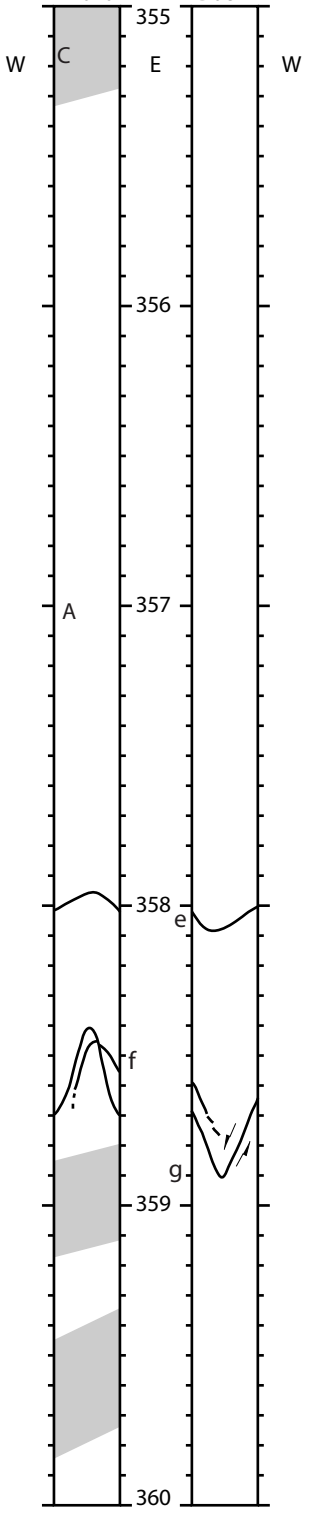

Apparent Disp. (mm)	Fault Thickness (mm)	Fault Strike	Fault Dip	Comments
e=?	1 mg	N60E	24NW	
f=?	1 mg	N65E	56NW	Fault "f" is most likely older than "g"
g=1	1.5 mg	N80E	59NW	
				Bedding @ 359.3' : N40W 26SW

Depth Interval: 360 -365 Well: NNR - 9

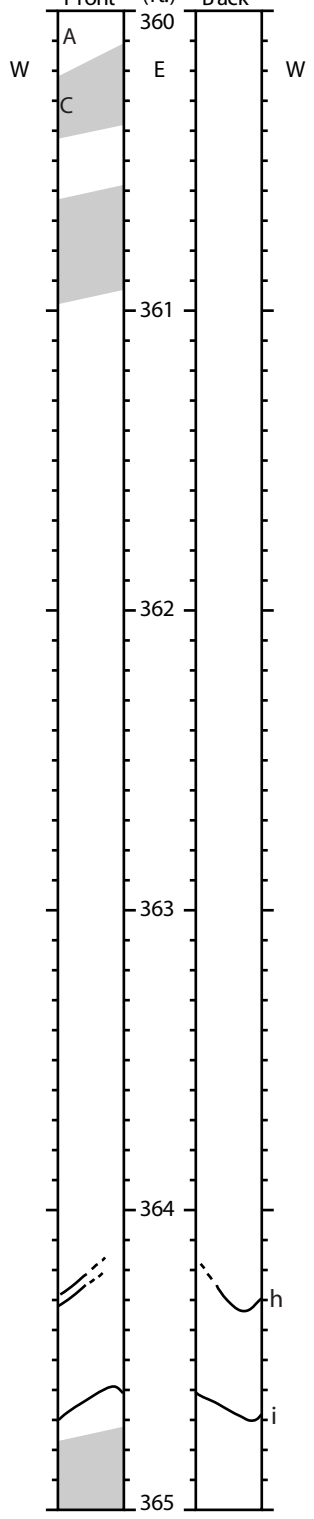

Apparent Disp. (mm)	Fault Thickness (mm)	Fault Strike	Fault Dip	Comments
				Bedding @ 360.3' : N30W 20SW [obtained from BHTV-log]
				Bedding @ 360.4' : N35W 12SW
				Bedding @ 363.9' : N22W 15SW [obtained from BHTV-log]
h=?	1 cg	N25E	17NW	
i=?	1 cg	N5E	18NW	

Depth Interval: 365 - 370 Well: NNR - 9

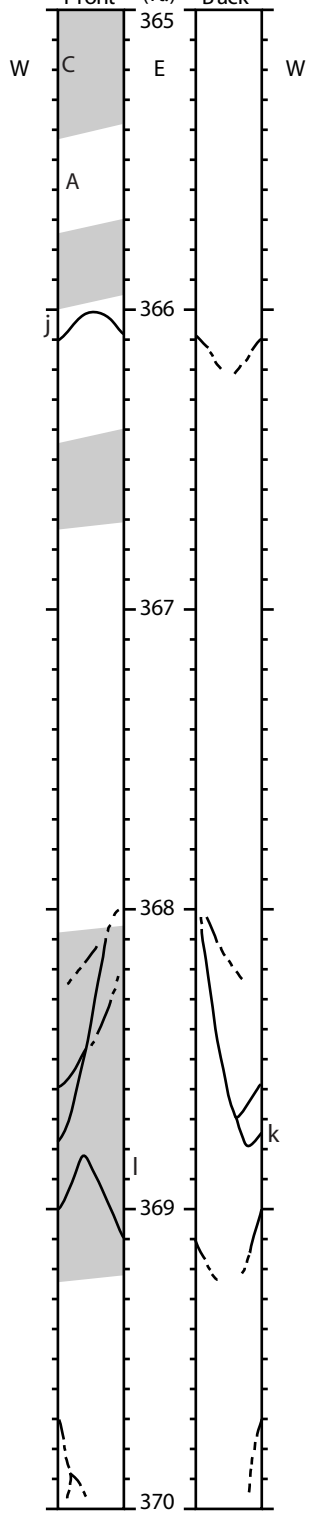

Apparent Disp. (mm)	Fault Thickness (mm)	Fault Strike	Fault Dip	Comments
j=?	4 cg	N80W	27NE	
				Bedding @ 366.6' : N55W 6SW
				Bedding @ 367.6' : N50W 18SW [obtained from BHTV-log]
k=?	0.5 mg	N35E	74NW	
l=?	0.5 mg	N75E	57NW	
				potential NS fault

Depth Interval: 370 - 375 Well: NNR - 9

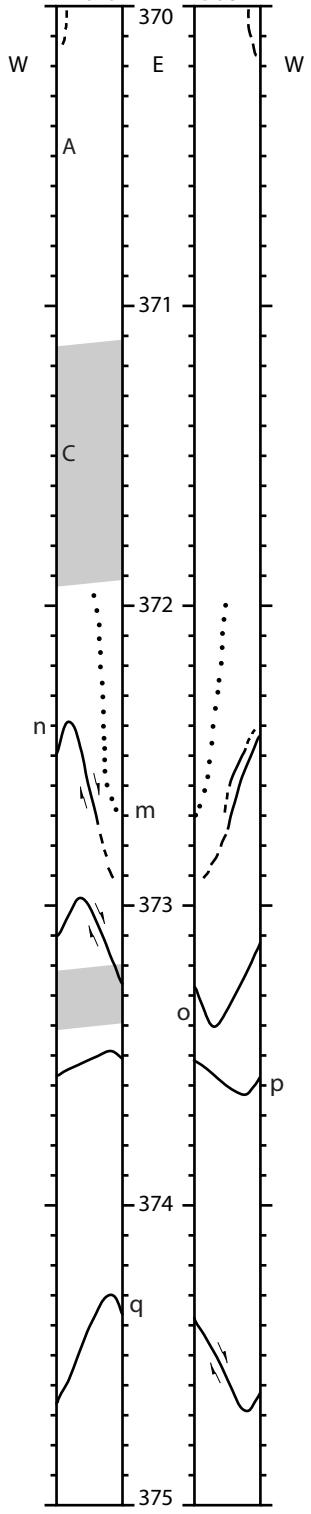

Apparent Disp. (mm)	Fault Thickness (mm)	Fault Strike	Fault Dip	Comments
				Run #37 Score card: 371.3' 371.3' - 381.2' Drilled: 10.0' Recovered: 9.9' orientation from run #37 & below could be off by as much as 30° to the N below run #37 w w above run #37
n=8	1 cg	N50W	49NE	
m=?	?	NS	83E	
o=38	2 mg	N40W	48NE	
p=?	2 cg	N15E	37NW	
				Bedding @ 373.8' : N52W 32SW [obtained from BHTV-log]
q=6	1 cg	N25E	43NW	

Depth Interval: 375 - 380 Well: NNR - 9

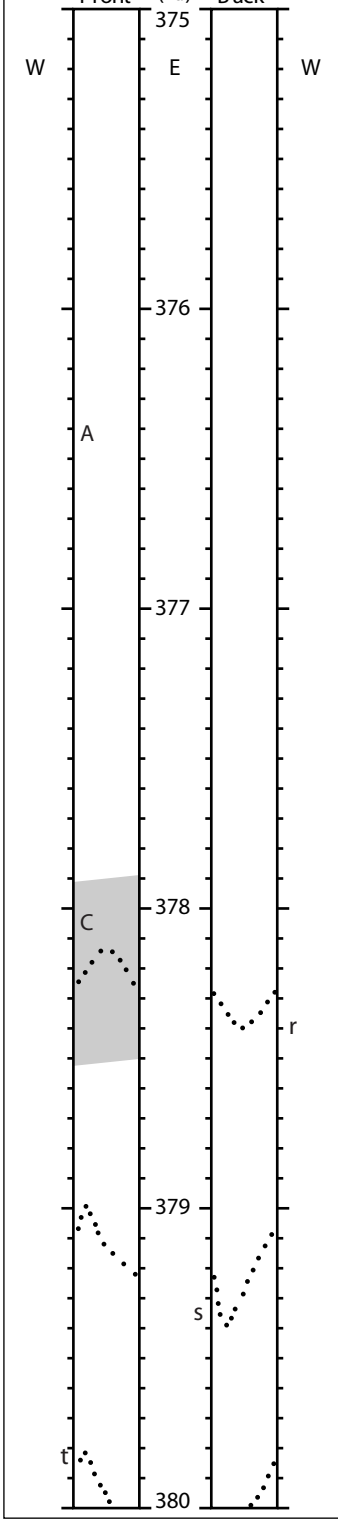

Apparent Disp. (mm)	Fault Thickness (mm)	Fault Strike	Fault Dip	Comments
				Bedding @ 376.9' : N40W 31SW [obtained from BHTV-log]
r=?		N75E	50NW	
s=?		N25W	54NE	Bedding @ 379.6' : N20W 25SW [obtained from BHTV-log]
t=?		N20W	57NE	

Depth Interval: 380 - 385 Well: NNR - 9

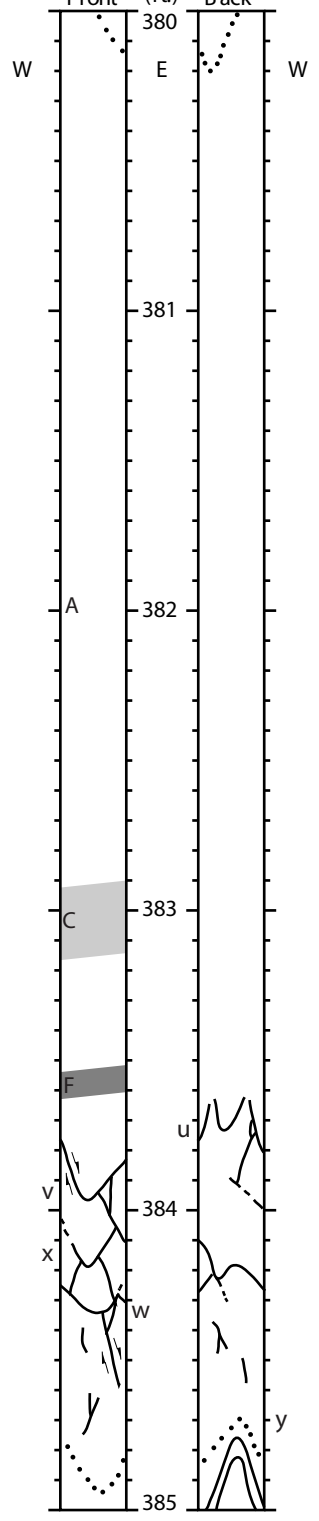

Apparent Disp. (mm)	Fault Thickness (mm)	Fault Strike	Fault Dip	Comments
				Run # 38 Score card: 381.3' 381.3' - 391.3' Drilled: 10.0' Recovered: 10.0'
				Bedding @ 381.9' : N40W 19SW [obtained from BHTV-log]
				Bedding @ 383.3' : N18W 13SW [obtained from BHTV-log]
				Bedding @ 383.5' : N15W 13SW
u=?	3 mg	N65E	52NW	
v=>50	6 cg	N75E	55SE	
x=?	?	N75E	56SE	
w=?	4 cg	N65E	35SE	
y=?	?	N55E	52SE	

Depth Interval: 385 - 390 Well: NNR - 9

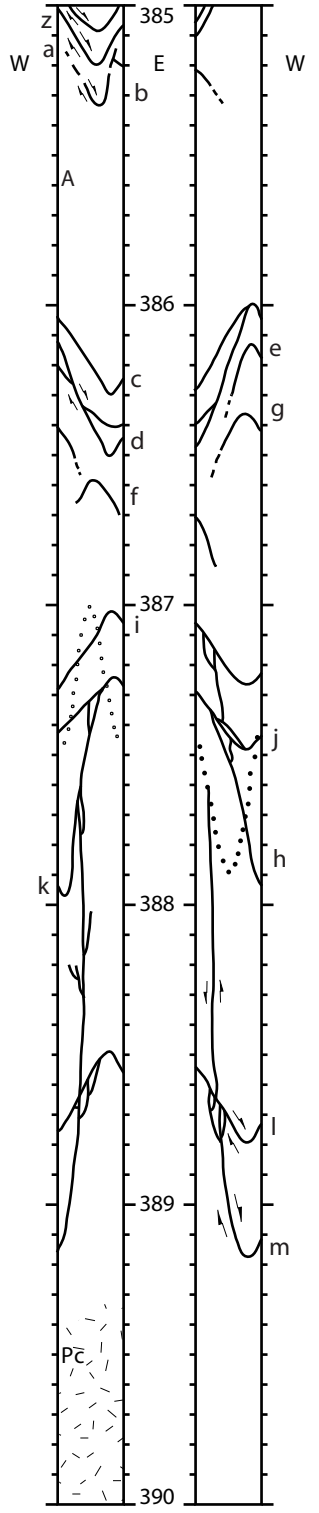

Apparent Disp. (mm)	Fault Thickness (mm)	Fault Strike	Fault Dip	Comments
	4 cg	N50E	58SE	
z+a>50	4 cg	N55E	62SE	
b=3	1 cg	N50E	68SE	
e=?	1 mg	N20W	43NE	
c=?	2 mg	N10W	49NE	
g=?	1 mg	N50W	57NE	
d=10	1.5 mg	N15W	56NE	
f=?	1 mg	N30E	49NW	
i=?	4 cg	N20W	45SW	
j=?	4 cg	N10W	56SW	
h=?		N85E	77NW	
k=?	3 cg	N30W	62SW	
l=5	1.5 cg	N50E	52NW	
m=3	1 cg	N50E	76NW	

Depth Interval: 170 - 175 Well: NNR - 10

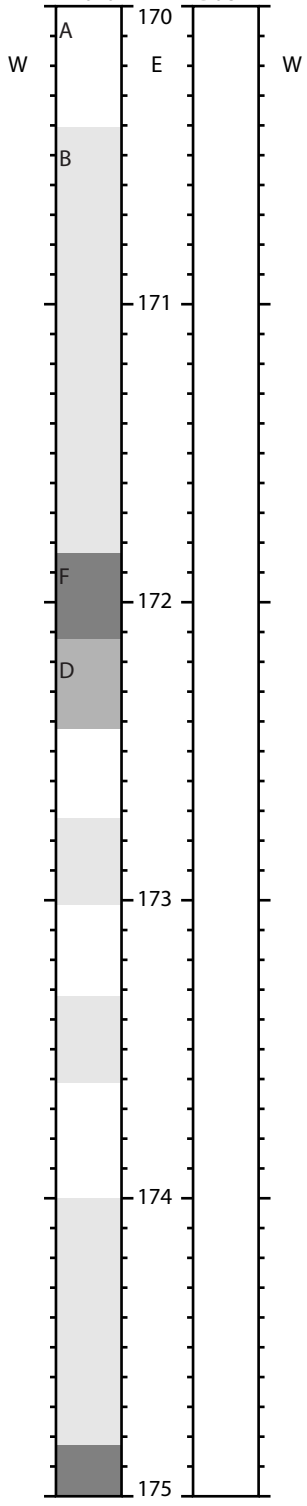

Apparent Disp. (mm)	Fault Thickness (mm)	Fault Strike	Fault Dip	Comments
				Run #17 Score card: 171.32' 171.3' - 181.3' Drilled: 10.0' Recovered: 10.0'

Depth Interval: 175 - 180 Well: NNR - 10

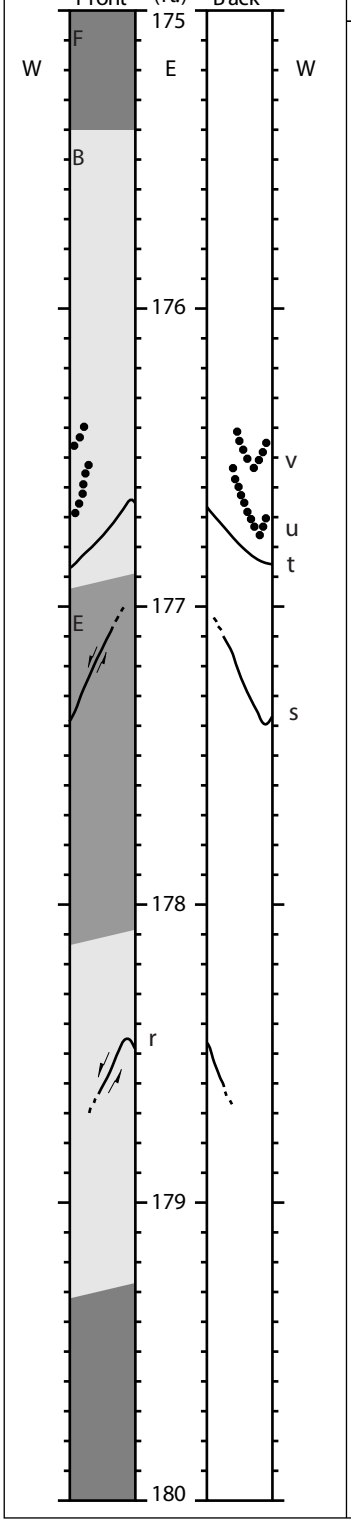

Apparent Disp. (mm)	Fault Thickness (mm)	Fault Strike	Fault Dip	Comments
				Bedding @ 176.0' : N20W 13SW
v=?		N40E	57NW	
u=?		N20E	67NW	
t=?	1 cg	N5W	36SW	
s=7	0.25 clay	N20E	54NW	
r=7	0.5 mg	N15E	67NW	
				Bedding @ 179.4' : N10W 15SW
				Missing core from 179.6' - 179.8'

Depth Interval: 180 - 185 Well: NNR - 10

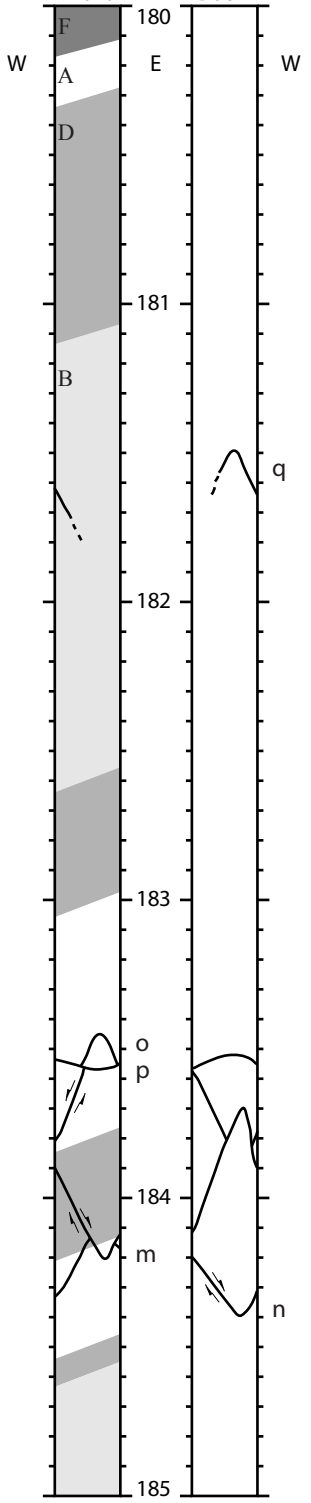

Apparent Disp. (mm)	Fault Thickness (mm)	Fault Strike	Fault Dip	Comments
				Bedding @ 180.5' : N20E 17NW
q=?	1 cg	N50E	66SE	Run #18 Score card: 181.3' 181.3' - 191.3' Drilled: 10.0' Recovered: 10.0'
				Bedding @ 182.3' : N10E 21NW
o=13	1 cg	N45E	69NW	Fault "p" is younger than "o" and has an apparent reverse sense of displacement
p=1	0.5 cg	N75W	13SW	
m=54		N35E	64SE	Rake on "m" is 80NE
n=9	0.5 mg	N40E	62NW	

Depth Interval: 185 - 190 Well: NNR - 10

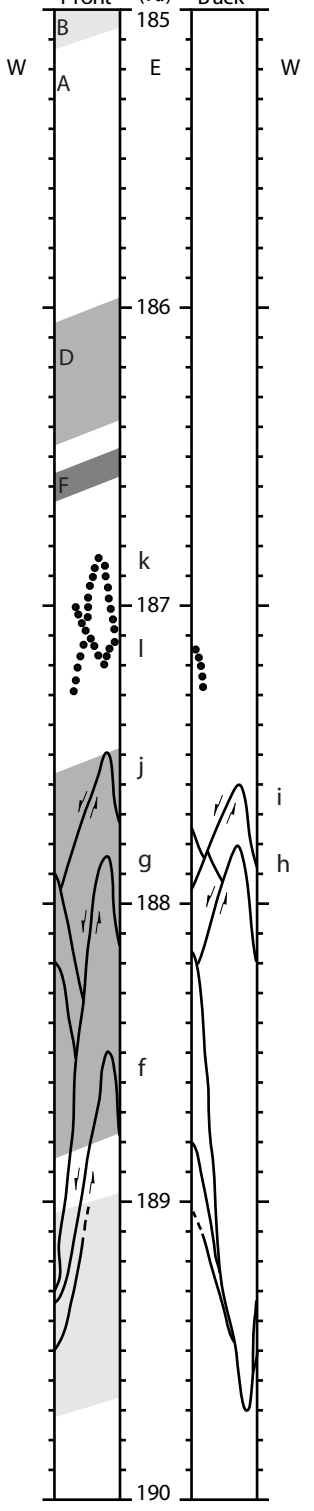

Apparent Disp. (mm)	Fault Thickness (mm)	Fault Strike	Fault Dip	Comments
k=?		N40E	71NW	
l=?		N35E	67SE	
j=8	1 fg	N20E	85NW	
i=6	0.5 fg	N35E	73SE	Fault "i" is younger than "j"
g=2	0.5 fg	N20E	82NW	
h=4	0.5 fg	N40E	68SE	
f=74	4 clay	N25E	78NW	Bedding @ 188.6' : NS 16W

Depth Interval: 190 - 195 Well: NNR - 10

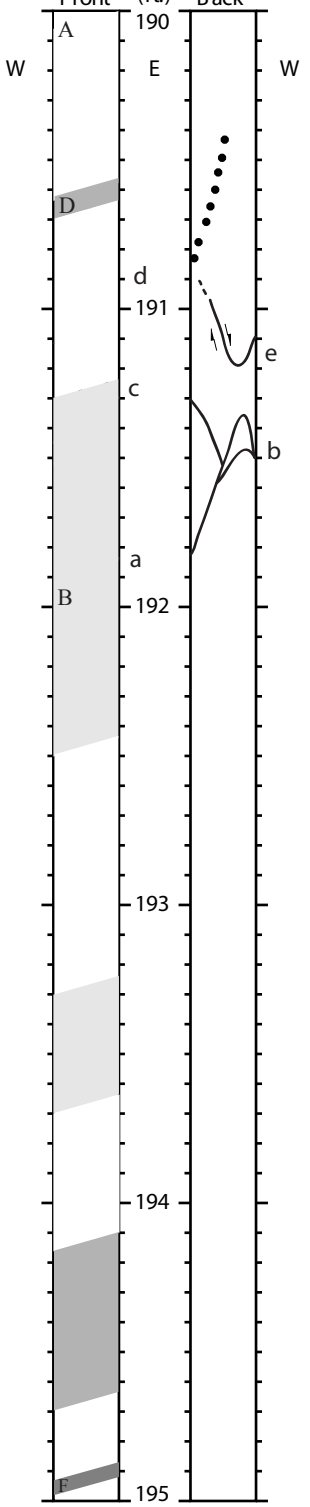

Apparent Disp. (mm)	Fault Thickness (mm)	Fault Strike	Fault Dip	Comments
d=4		N25E	67SE	
e=5	0.5 fg	N40E	61NW	Lost orientation above 191.2', bedding dip line is treated as West
c=8	1 mg	N25E	74NW	
b=?	0.5 mg	N10E	58SE	Run #1920 Score card: 191.3' 191.3' - 201.3' Drilled: 10.0' Recovered: 10.0'
a=57	1.5 clay	N30E	60SE	
				Bedding @ 194.95' : N20E 8NW

Depth Interval: 195 - 200 Well: NNR - 10

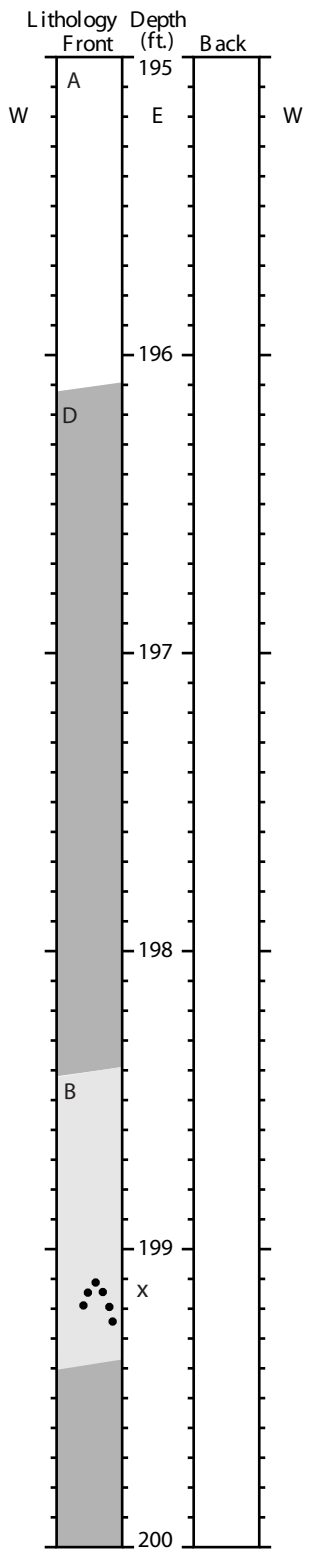

Apparent Disp. (mm)	Fault Thickness (mm)	Fault Strike	Fault Dip	Comments
				Bedding @ 195.3' : N15E 14NW [obtained from BHTV-log]
				Bedding @ 198.0' : NS 9W
x=?		N70W	52NE	

Depth Interval: 200 - 205 Well: NNR - 10

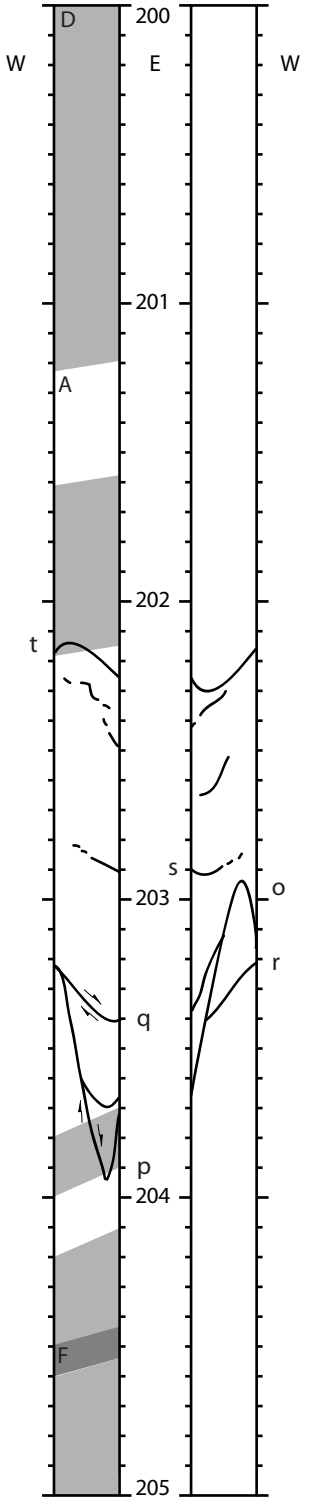

Apparent Disp. (mm)	Fault Thickness (mm)	Fault Strike	Fault Dip	Comments
				Bedding @ 200.5' : N10E 26NW [obtained from BHTV-log]
				Bedding @ 201.1' : N20E 28NW [obtained from BHTV-log] Run # 20 Score card: 201.32' 201.3' - 211.3' Drilled: 10.0' Recovered: 10.0'
				Bedding @ 201.6' : N10E 26NW [obtained from BHTV-log]
t=?	2 cg	N10W	26NE	Bedding @ 202.1' : N15E 24NW
s=?	1 cg	N30W	34NE	
o=17	2 cg	N30E	83SE	
r=?	1 cg	NS	31E	
q=14	2 cg	N10E	63SE	
p=?	1 cg	N20E	44SE	
				Bedding @ 204.6' : NS 14W

Depth Interval: 205 - 210 Well: NNR - 10

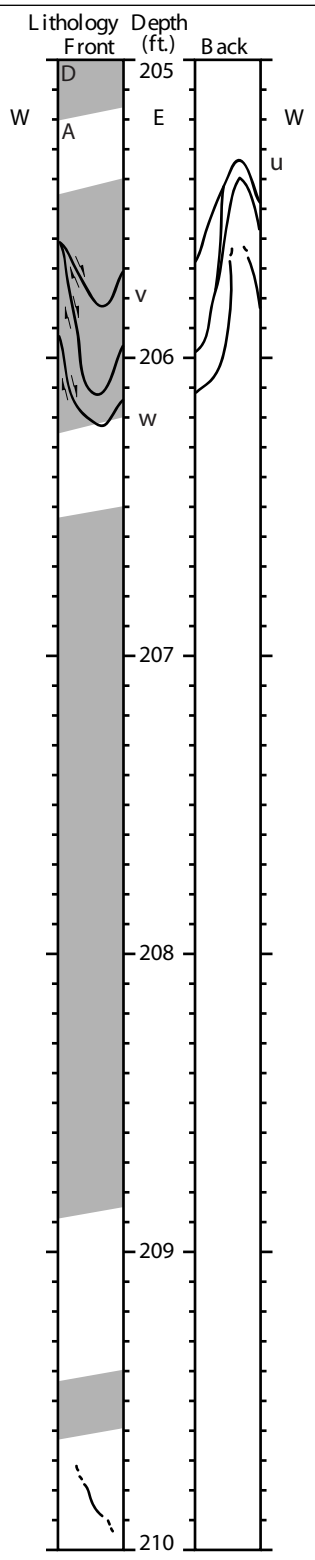

Apparent Disp. (mm)	Fault Thickness (mm)	Fault Strike	Fault Dip	Comments
u>50		N50E	71SE	Rake on "u" is 61NE
v=7	0.5 fg	N65E	73SE	
w=32	0.5 clay	N55E	62SE	
				Bedding @ 206.85' : NS 10W

Depth Interval: 210 - 215 Well: NNR - 10

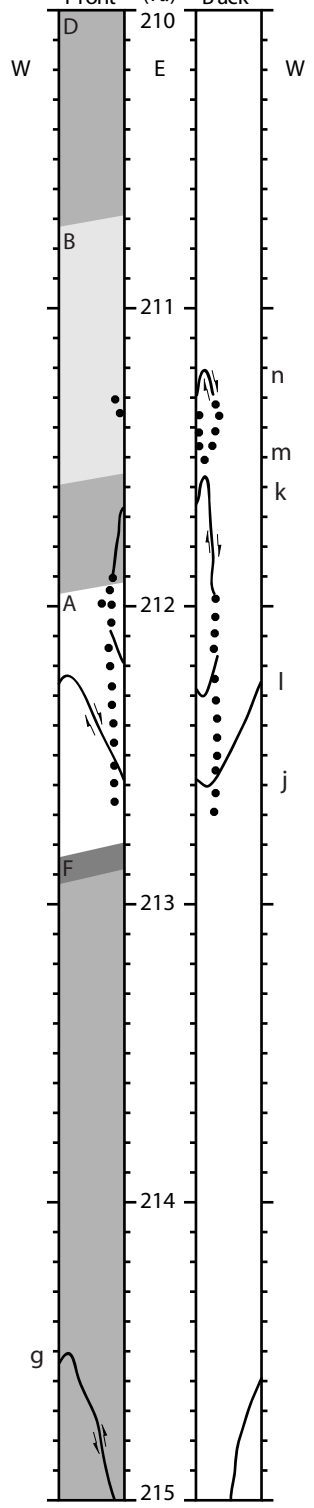

Apparent Disp. (mm)	Fault Thickness (mm)	Fault Strike	Fault Dip	Comments
n=5	1 mg	N30W	84SW	Run # 21 Score card: 211.33' 211.3' - 221.3' Drilled: 10.0' Recovered: 10.0'
m=?		N30W	82NE	
k=6	0.25 clay	N30W	86SW	
l=?	0.5 fg	N30W	75NE	
j=3	0.25 fg	N25W	62NE	
				Bedding @ 212.9' : N15W 13SW
g=7	0.25 clay	N15W	77NE	

Depth Interval: 215 - 220 Well: NNR - 10

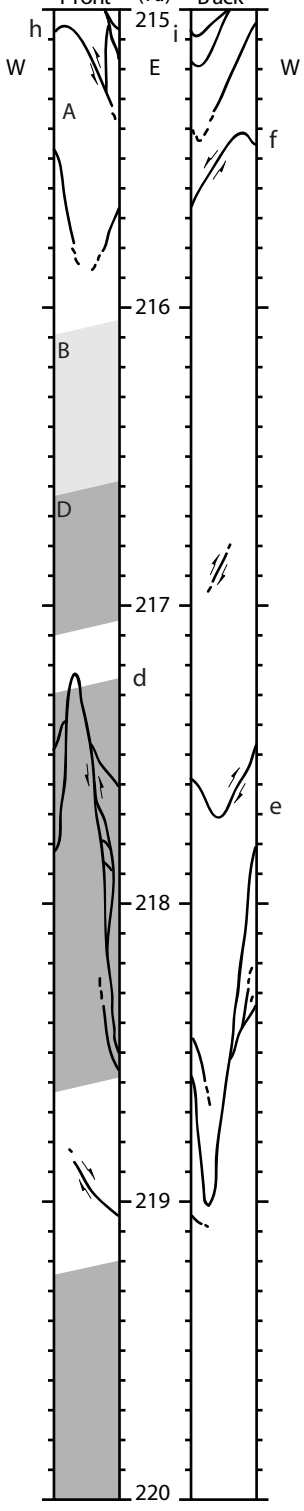

Apparent Disp. (mm)	Fault Thickness (mm)	Fault Strike	Fault Dip	Comments
i=?	0.5 mg	N15W	57NE	
h=7	0.5 fg	N20W	61NE	
f=17	1 fg	N30E	64SE	
d=12	0.5 fg	N40W	87NE	
e=5	0.5 mg	N55W	69NE	
				Bedding @ 218.6' : NS 14W Bedding @ 218.7' : NS 13W [obtained from BHTV-log]
				Bedding @ 219.45' : NS 13W

Depth Interval: 220 - 225 Well: NNR - 10

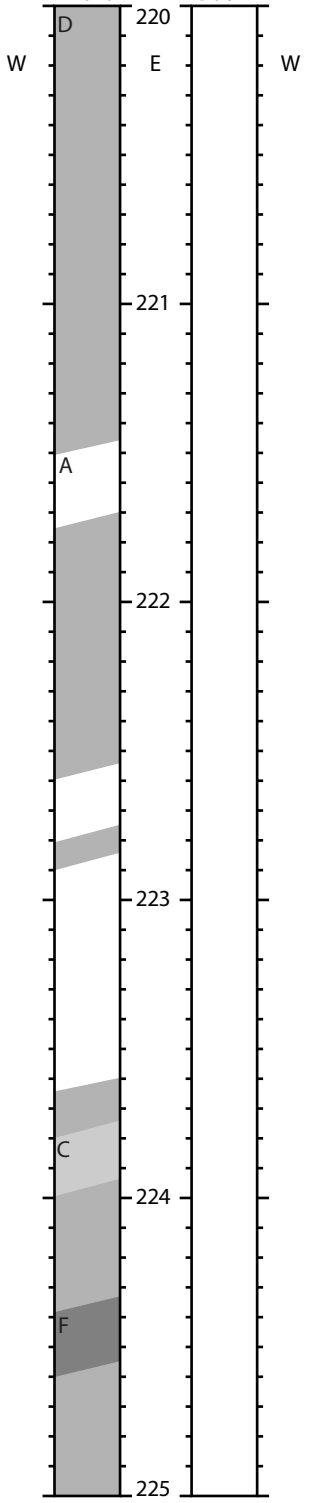

Apparent Disp. (mm)	Fault Thickness (mm)	Fault Strike	Fault Dip	Comments
				Bedding @ 221.45' : N20E 15NW Run # 22 Score card: 221.3' 221.3' - 231.3' Drilled: 10.0' Recovered: 10.05'
				Bedding @ 224.4' : N18E 19NW [obtained from BHTV-log] Bedding @ 224.55' : N15E 13NW

Depth Interval: 225 - 230 Well: NNR - 10

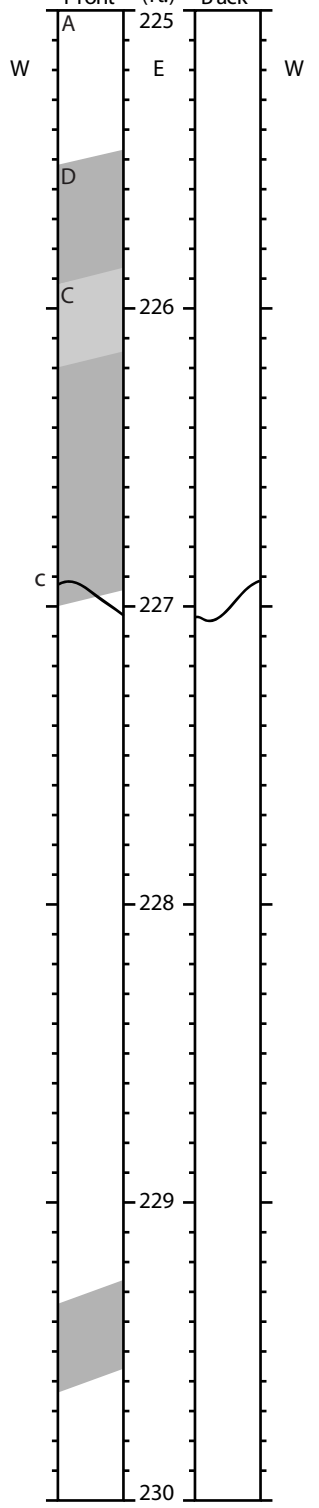

Apparent Disp. (mm)	Fault Thickness (mm)	Fault Strike	Fault Dip	Comments
				Bedding @ 225.4' : N37E 25NW [obtained from BHTV-log]
c>85		N20W	46NE	
				Bedding @ 228.3' : N15E 15NW [obtained from BHTV-log]
				Bedding @ 229.2' : N25E 22NW [obtained from BHTV-log]
				Bedding @ 229.3' : N20E 20NW
				Bedding @ 229.8' : N20E 17NW

Depth Interval: 230 - 235 Well: NNR - 10

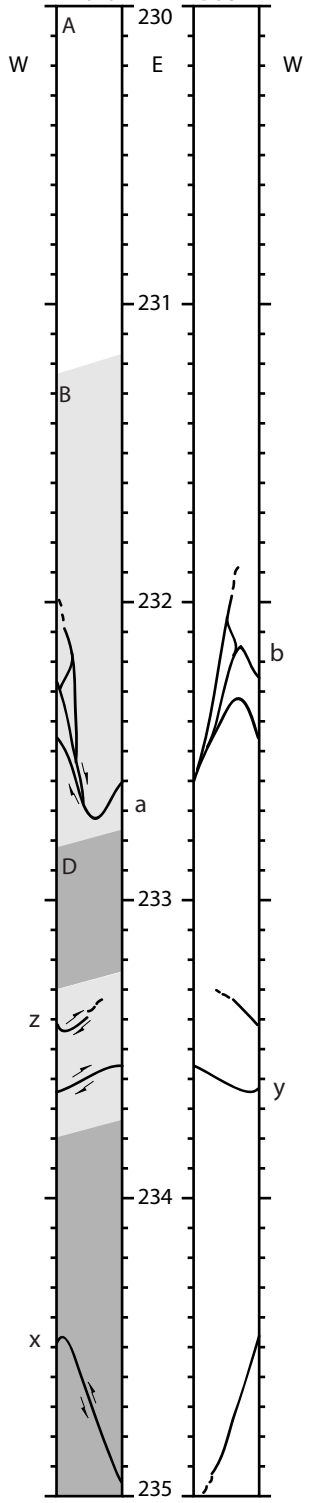

Apparent Disp. (mm)	Fault Thickness (mm)	Fault Strike	Fault Dip	Comments
				Bedding @ 231.45' : N45E 15NW
b=22	2 cg	N55E	68SE	
a=?		N65E	62SE	Fault "a" correlates w/232.7' in BHTV-log Rake on "a" is 54NE
z=4	0.5 mg	N15W	49SW	Bedding @ 233.3' : N15E 15NW
y=25	1 clay	N15E	27NW	
x=1	0.25 fg	N10W	67NE	

Depth Interval: 235 - 240 Well: NNR - 10

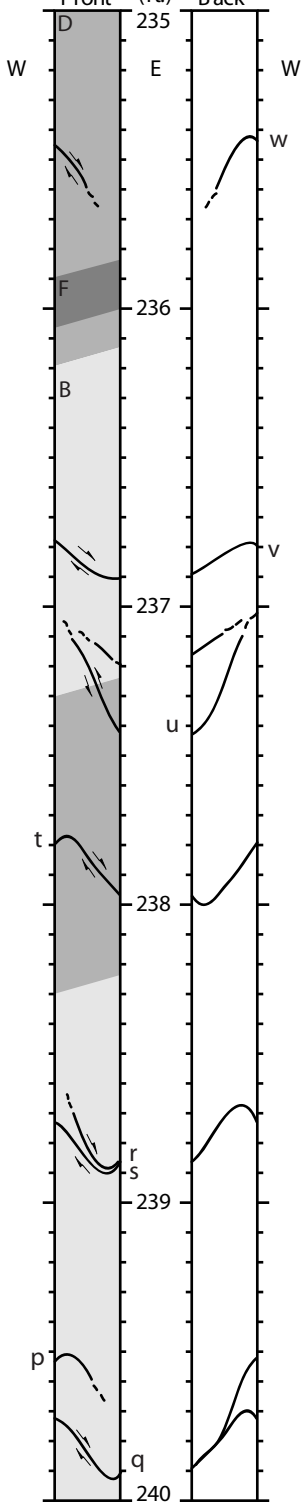

Apparent Disp. (mm)	Fault Thickness (mm)	Fault Strike	Fault Dip	Comments
w=6		N30E	62SE	
				Bedding @ 235.7' : N15E 14NW [obtained from BHTV-log]
				Bedding @ 236' : N22E 14NW [obtained from BHTV-log]
				Bedding @ 236.55' : N30E 16NW
				Bedding @ 236.7' : N30E 31NW [obtained from BHTV-log]
v=23	2 cg	N30E	37SE	
u=6	0.25 fg	NS	68E	
t=6	0.25 fg	N30W	42NE	
r=2	0.5 cg	N40E	66SE	
s=14	1 cg	N45E	47SE	Fault "s" correlates w/238.3' in BHTV-log
p=?	0.5 fg	N20W	55NE	
q=5	0.5fg	N35E	50SE	

Depth Interval: 240 - 245 Well: NNR - 10

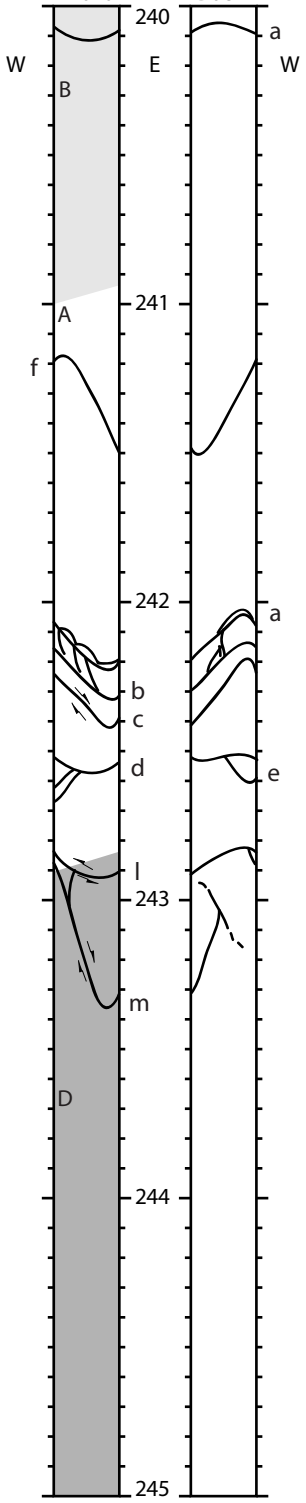

Apparent Disp. (mm)	Fault Thickness (mm)	Fault Strike	Fault Dip	Comments
a=?	0.5 fg	N70E	11SE	Bedding @ 240.3' : N10E 17NW
f=?	1.5 cg	N20W	61NE	
				Run # 24 Score card: 241.35' 241.3' - 251.3' Drilled: 10.0' Recovered: 10.25'
a=?	3 mg	N30E	36SE	Fault "a" correlates w/241.7' in BHTV-log
b=?	1 mg	N25E	44SE	
c=7	1 mg	N30E	54SE	
d=?	1 mg	N70E	11SE	
e=?	0.5 mg	N20E	33NW	
l=2	0.25 fg	N40E	24SE	
m=2	0.25 fg	N30E	63SE	
				Bedding @ 244.5' : N25E 15NW

Depth Interval: 245 - 250 Well: NNR - 10

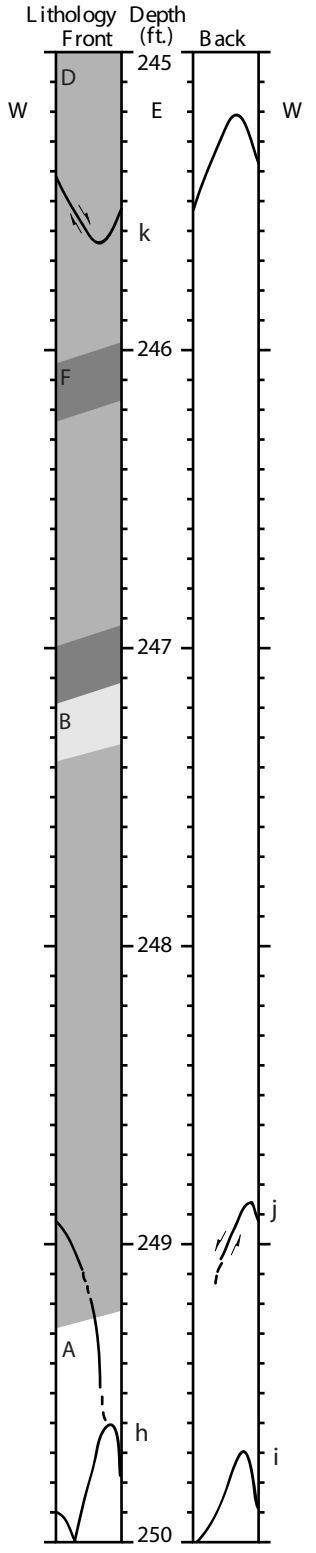

Apparent Disp. (mm)	Fault Thickness (mm)	Fault Strike	Fault Dip	Comments
k=2	0.25 fg	N55E	67SE	
				Bedding @ 246.3' : N20E 18NW
				Bedding @ 248.7' : N15E 15NW
j=?	1 mg	N20E	68SE	
				Bedding @ 249.5' : N15E 24NW
h=8	1 cg	N25E	84NW	
i=5	1 cg	N35E	73SE	

Depth Interval: 250 - 255 Well: NNR - 10

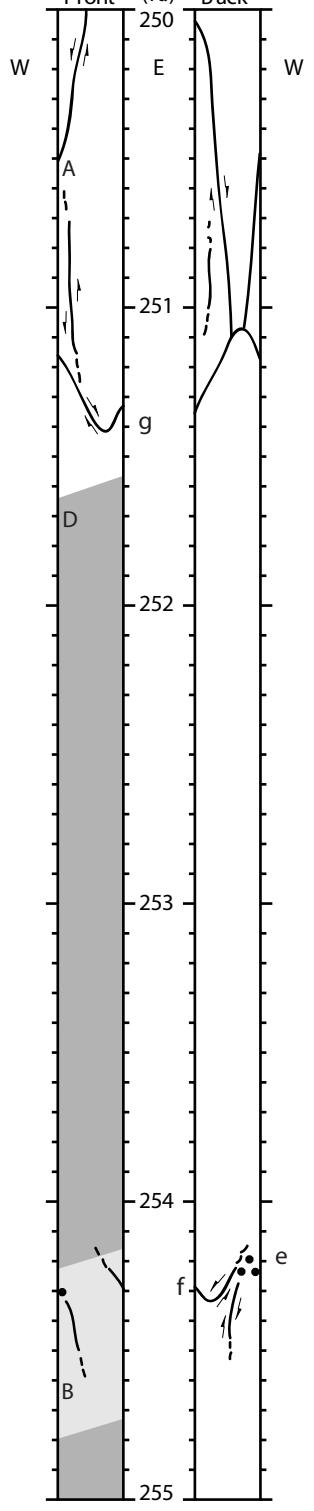

Apparent Disp. (mm)	Fault Thickness (mm)	Fault Strike	Fault Dip	Comments
g=7	1 cg	N40E	57SE	Run # 25 Score card: 251.4' 251.3' - 261.3' Drilled: 10.0' Recovered: 10.1' Bedding @ 251.7' : N30E 22NW [obtained from BHTV-log]
				Bedding @ 252.6' : N30E 19NW
				Bedding @ 254.0' : N20E 17NW
e=4 f=6	0.25 fg 0.5 fg	N15E N40W	83SE 38NE	
				Bedding @ 254.9' : N30E 21NW

Depth Interval: 255 - 260 Well: NNR - 10

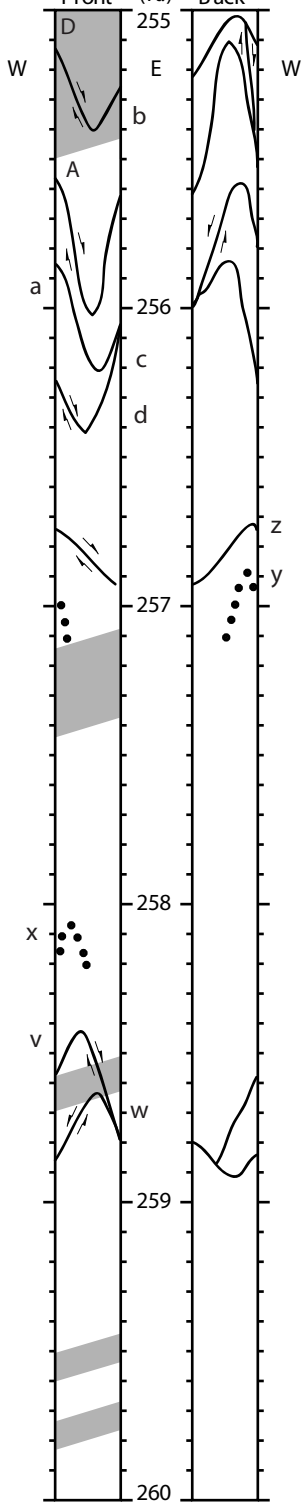

Apparent Disp. (mm)	Fault Thickness (mm)	Fault Strike	Fault Dip	Comments
				North South
b=47	1 clay	N65E	65SE	
a>220	7 cg	N74E	76SE	Fault "a" correlates w/ 255.6' in BHTV-log
c=45	3 cg	N60E	69SE	
d=8	1 cg	N70W	64SW	
z=14	1 cg	N10E	48SE	
y=?		N20E	82SE	
x=?		N40W	76NE	
v=12	1 cg	N50W	55NE	
w=23	2.5 cg	N65E	59NW	
				Bedding @ 259.4' : N5E 36NW [obtained from BHTV-log]
				Bedding @ 259.9' : NS 23W

Depth Interval: 260 - 265 Well: NNR - 10

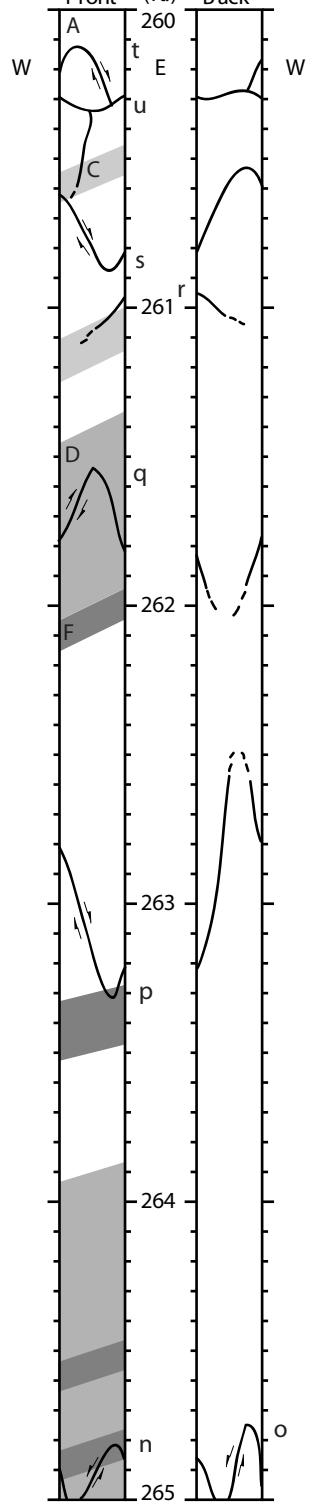

Apparent Disp. (mm)	Fault Thickness (mm)	Fault Strike	Fault Dip	Comments
t=5	1 mg	N55W	54NE	Bedding @ 260' : N3E 22NW [obtained from BHTV-log]
u=?	3 cg	N75W	14SW	Fault "u" appears to be younger than fault "t"
				Bedding @ 260.6' : N10E 22NW [obtained from BHTV-log]
s=2	0.25 fg	N40E	54SE	
r=?	0.5 mg	NS	39W	
				Bedding @ 261.15' : N10E 26NW Bedding @ 261.2' : N30E 25NW [obtained from BHTV-log]
q=2	0.5 mg	N80W	77NE	Run # 26 Score card: 261.43' 261.3' - 271.3' Drilled: 10.0' Recovered: 10.0'
				Bedding @ 262.2' : N20E 14NW
p=3	0.5 cg	N25E	75SE	
				Bedding @ 263.4' : N15E 17NW
o=15	0.25 clay	N35E	83SE	
n=3	0.25 fg	N15E	61NW	

Depth Interval: 265 - 270 Well: NNR - 10

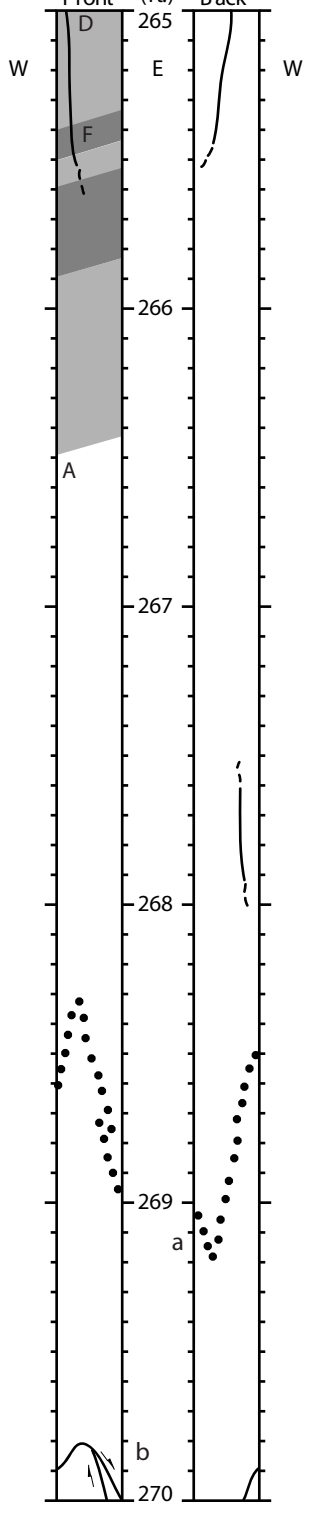

Apparent Disp. (mm)	Fault Thickness (mm)	Fault Strike	Fault Dip	Comments
				Bedding @ 265.9' : N10E 16NW
a=?		N45W	73NE	Joint "a" correlates w/268.3' in BHTV-log
b=3	0.5 cg	N55W	72NE	

Depth Interval: 270 - 275 Well: NNR - 10

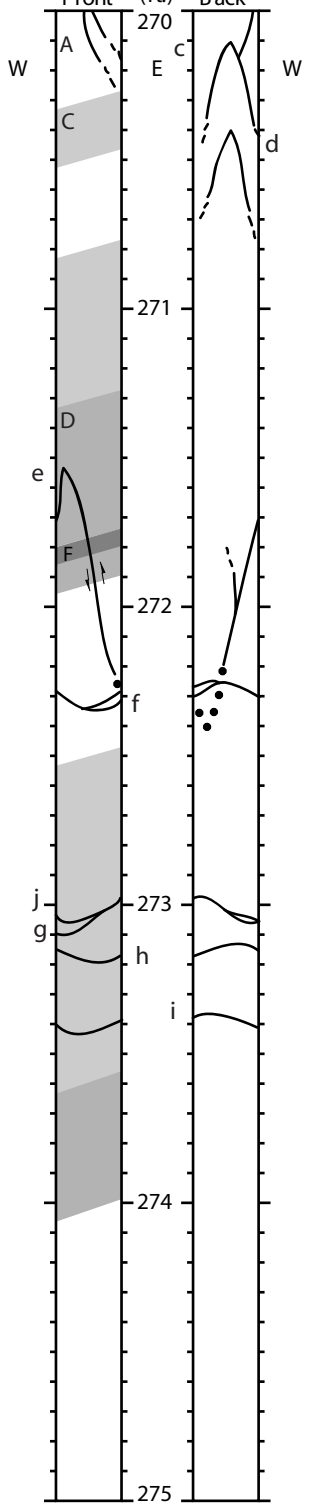

Apparent Disp. (mm)	Fault Thickness (mm)	Fault Strike	Fault Dip	Comments
c=?	0.5 cg	N70W	60SW	
d=?	0.5 cg	N70W	63SW	
				Run # 27 Score card: 271.32' 271.3' - 281.3' Drilled: 10.0' Recovered: 10.0'
e=2	0.5 mg	N20W	78NE	
f=?	1 cg	N85W	25SW	
				Bedding @ 273' : N10E 21NW [obtained from BHTV-log]
j=?	0.25 fg	N5W	16SW	
g=?	0.25 fg	N10E	33NW	
h=?	0.25 fg	N80W	11SW	Faults "j", "g", "h", & "i" are all parallel to bedding and located at a lithological change.
i=?	0.25 fg	N10W	17SW	
				Bedding @ 273.7' : N20E 19NW
				Bedding @ 274.7' : N3E 23NW [obtained from BHTV-log]
				Bedding @ 274.95' : N5E 17NW

Depth Interval: 275 - 280 Well: NNR - 10

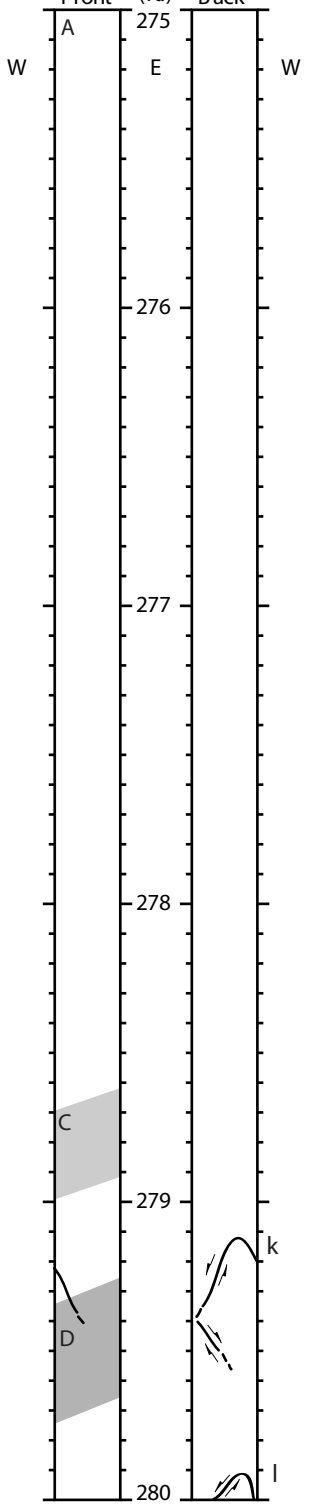

Apparent Disp. (mm)	Fault Thickness (mm)	Fault Strike	Fault Dip	Comments
k=6	0.5 mg	N55E	60SE	Bedding @ 279.4' : N20W 22SW
l>65		N50E	58SE	

Depth Interval: 280 - 285 Well: NNR - 10

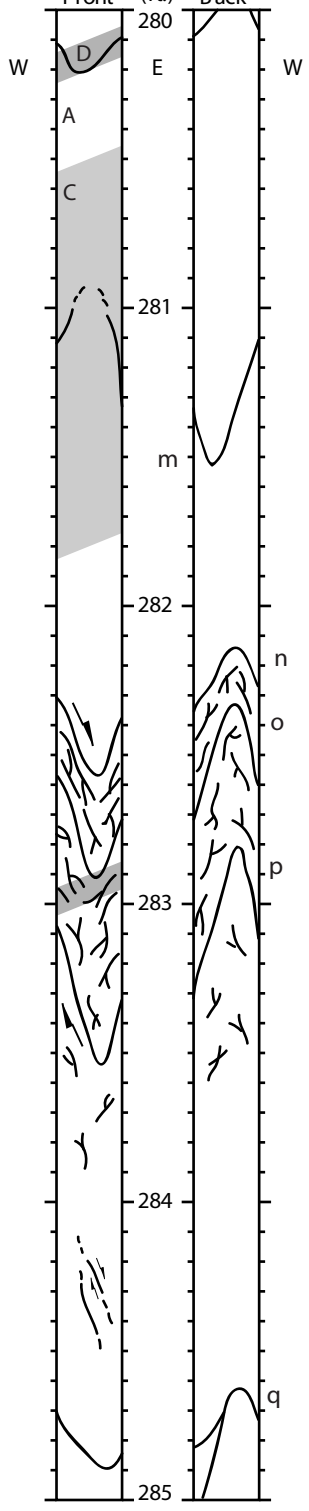

Apparent Disp. (mm)	Fault Thickness (mm)	Fault Strike	Fault Dip	Comments
m=?	1 mg	N45W	73NE	Run # 28 Score card: 281.32' 281.3' - 291.3' Drilled: 10.0' Recovered: 10.15'
n=?	6 fg	N60E	63SE	Fault "n" correlates w/281.2' in BHTV-log
o=?		N65E	67SE	Fault "o" correlates w/282.6' in BHTV-log Rake on "o" is 56NE
p=?		N60E	71SE	Fault "p" correlates w/283.3' in BHTV-log
q>90	5 cg	N55E	51SE	Fault "q" correlates w/284.4' in BHTV-log

Depth Interval: 285 - 290 Well: NNR - 10

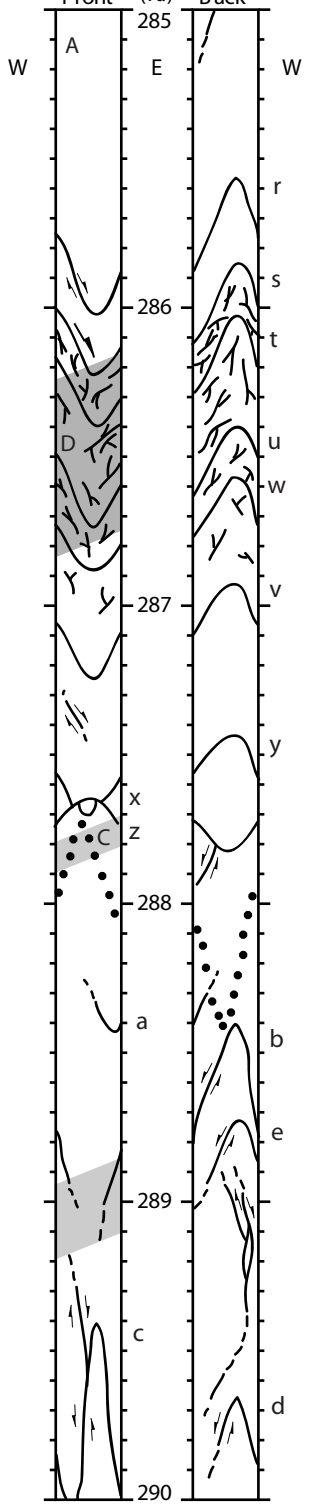

Apparent Disp. (mm)	Fault Thickness (mm)	Fault Strike	Fault Dip	Comments
r=57	2 cg	N65E	62SE	Fault "r" correlates w/284.7' in BHTV-log
s=?	2 cg	N55E	63SE	
t=?		N60E	59SE	
u=?		N65E	58SE	
w=?		N65E	55SE	Fault "w" correlates w/286.5' in BHTV-log
v=?	4 cg	N70E	54SE	
y=?	2 cg	N60E	51SE	Fault "y" appears to be younger than fault "x"
x=?	3 cg	N70E	41NW	
z=?		N60W	75NE	Joint "z" correlates w/287.9' in BHTV-log
a=?	2 cg	N35E	54SE	
b=4	1 cg	N55E	73SE	
e=7	1 cg	N45E	71SE	
c=4	0.5 cg	N50E	83NW	
d=6	0.5 cg	N60E	85SE	

Depth Interval: 290 - 295 Well: NNR - 10

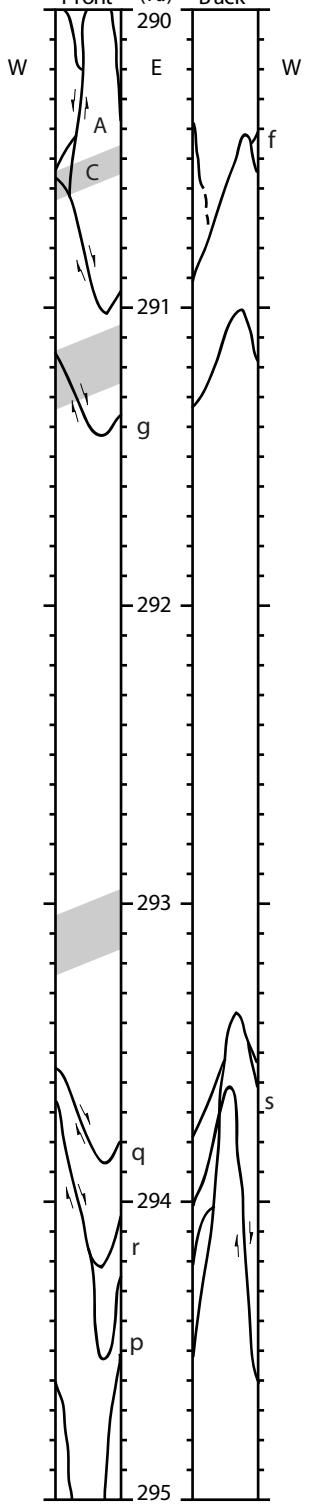

Apparent Disp. (mm)	Fault Thickness (mm)	Fault Strike	Fault Dip	Comments
f=24	1.5 cg	N40E	69SE	Fault "f" correlates w/289.4' in BHTV-log
g>90	8 cg	N45E	60SE	Fault "g" correlates w/290.6' in BHTV-log
				Run # 29 Score card: 291.7' 291.3' - 301.3' Drilled: 10.0' Recovered: 9.9'
s=8	1 cg	N75E	84SE	
q+r=8	1 cg	N40E	61SE	Fault "q" correlates w/293.4' in BHTV-log
	1 cg	N50E	73SE	
p=?	1 cg	N50E	86SE	

Depth Interval: 295 - 300 Well: NNR - 10

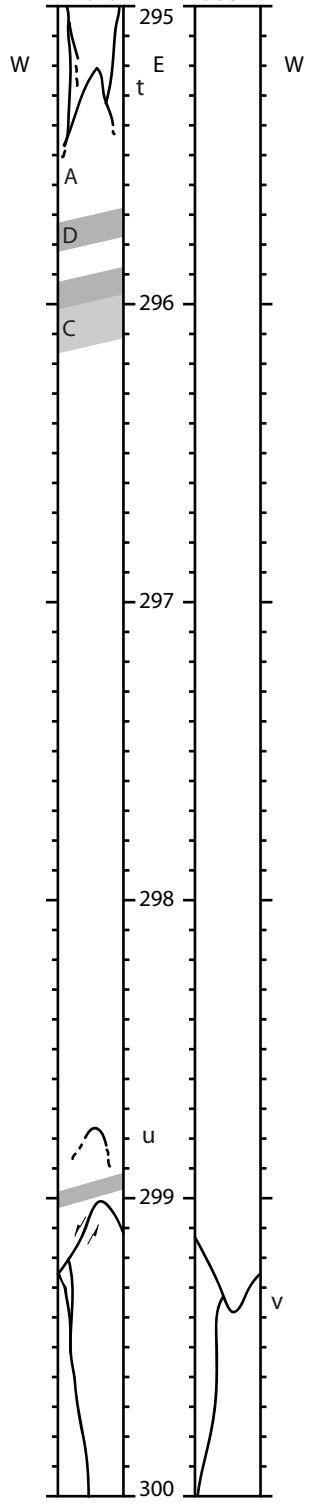

Apparent Disp. (mm)	Fault Thickness (mm)	Fault Strike	Fault Dip	Comments
t=?	1 cg	N80E	72NW	
				Bedding @ 296.0' : N15E 13NW
u=?	0.5 cg	N70E	56NW	
				Bedding @ 299.0' : N10E 16NW
v=8	1 cg	N55E	52NW	
				Bedding @ 299.9' : N15E 27NW

Depth Interval: 300 - 305 Well: NNR - 10

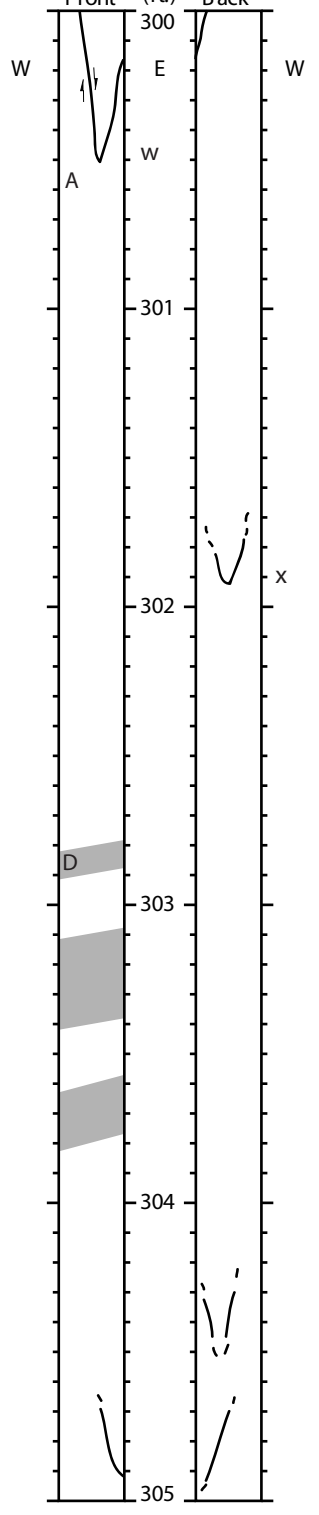

Apparent Disp. (mm)	Fault Thickness (mm)	Fault Strike	Fault Dip	Comments
w=3	1 cg	N60E	85SE	
				Run # 30 Score card: 301.5' 301.3' - 311.3' Drilled: 10.0' Recovered: 9.45'
x=?	1 cg	N80W	69NE	
				Bedding @ 302.5' : N22E 21NW [obtained from BHTV-log]
				Bedding @ 302.8' : N30E 10NW
				Bedding @ 303.8' : N30E 15NW

Depth Interval: 305 - 310 Well: NNR - 10

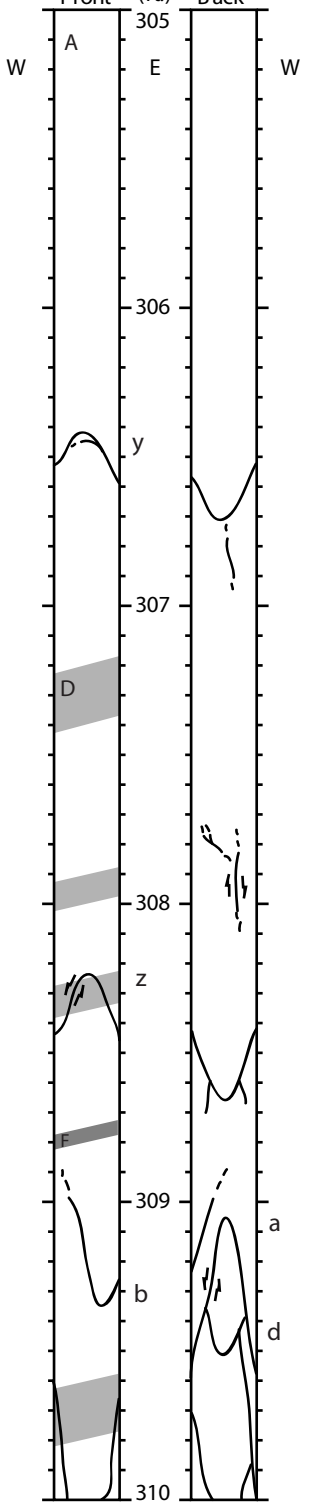

Apparent Disp. (mm)	Fault Thickness (mm)	Fault Strike	Fault Dip	Comments
y=?	1 cg	N60W	57NE	Bedding @ 306.6' : N15E 29NW [obtained from BHTV-log]
				Bedding @ 307.3' : N20E 15NW
				Bedding @ 308.0' : N25E 13NW
z=27	1 clay	N80E	56NW	
a=49	4 cg	N75E	80SE	Fault "a" correlates w/307.95 in BHTV-log
b=?	0.5 cg	N45E	79SE	
d=?	1.5 cg	N75E	62NW	Fault "d" appears to be younger than fault "a"

Depth Interval: 310 - 315 Well: NNR - 10

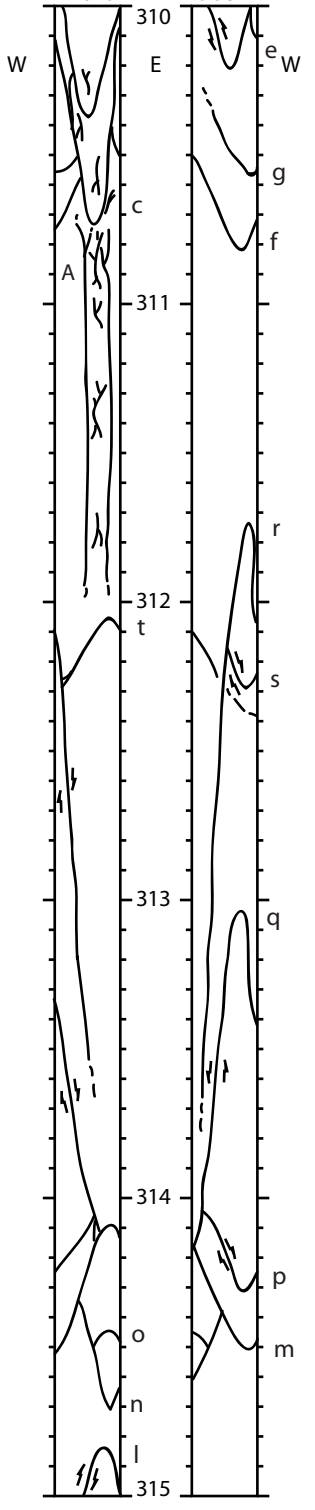

Apparent Disp. (mm)	Fault Thickness (mm)	Fault Strike	Fault Dip	Comments
e=5	1 cg	N70E	86NW	
g=?	1 cg	N35E	74NW	
c=?	4 cg	N70E	83SE	
f=?	2 cg	N50E	59NW	
				Run # 31 Score card: 311.3' 311.3' - 320.7' Drilled: 9.7' Recovered: 10.1'
r=7	1 cg	N30E	84SE	
				Bedding @ 312.0' : N15E 17NW
t=?	1 cg	N35E	62NW	Fault "r" is possible younger than "t" & "s"
s=6	1 cg	N30E	66NW	
q=3	0.5 cg	N40E	81SE	
				Bedding @ 313.3' : N15E 23NW
				Bedding @ 314.0' : N10E 23NW
p=5	1 cg	N45E	68NW	
o=?	1 cg	N40E	57NW	
m=?	1 cg	N35E	64NW	
n=?	1 cg	N40E	77SE	
l=2	0.5 fg	N50E	79NW	

Depth Interval: 315 - 320 Well: NNR - 10

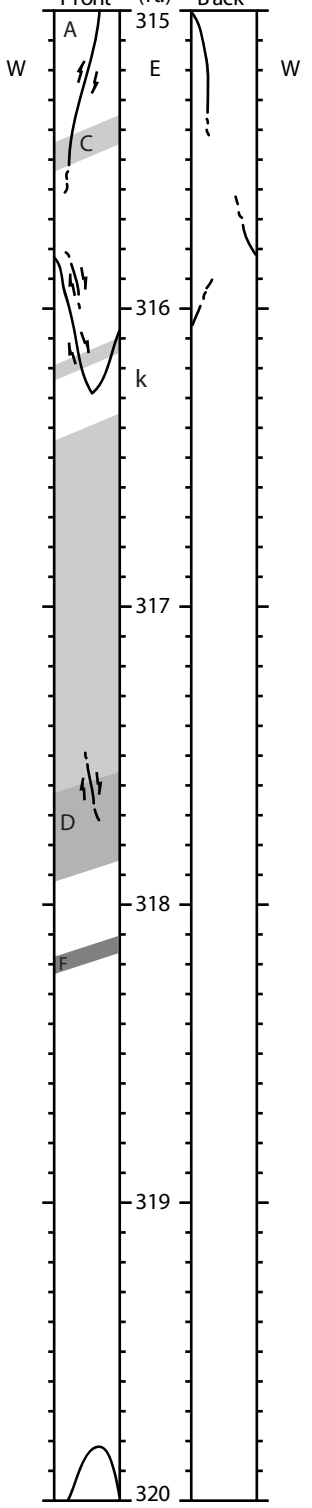

Apparent Disp. (mm)	Fault Thickness (mm)	Fault Strike	Fault Dip	Comments
k=3	0.5 fg	N70E	74SE	
				Bedding @ 317.3' : N7E 26NW [obtained from BHTV-log]
				Bedding @ 317.85' : N20W 18SW
				Bedding @ 319.7' : N20W 29SW Bedding @ 319.8' : NS 29W [obtained from BHTV-log]

Depth Interval: 320 - 325 Well: NNR - 10

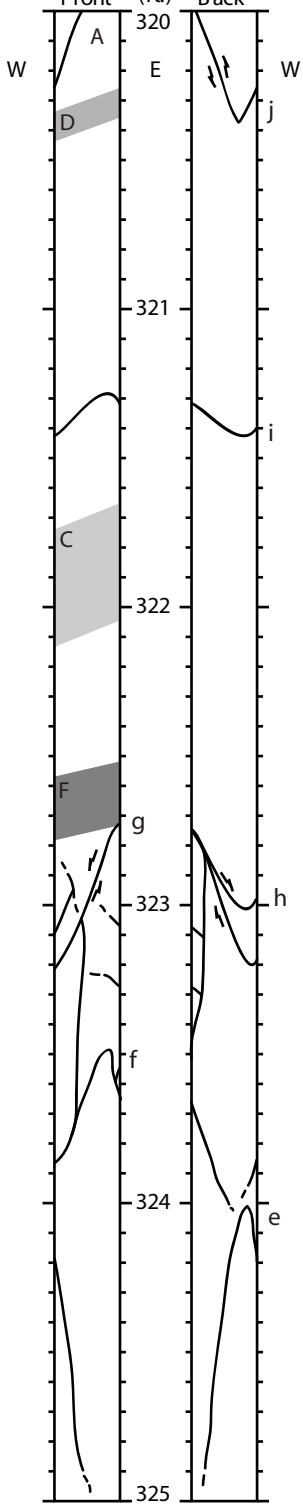

Apparent Disp. (mm)	Fault Thickness (mm)	Fault Strike	Fault Dip	Comments
j=26	1.5 cg	N45E	63NW	Bedding @ 320.4' : N30W 20SW
				Bedding @ 321.0' : N30W 22SW
				Run # 32 Score card: 321.0' 320.7' - 330.8' Drilled: 10.1' Recovered: 9.95'
i=?	1 cg	N35E	36NW	
				Bedding @ 321.8' : N33E 16NW [obtained from BHTV-log]
g=3	1 cg	N10E	60NW	Bedding @ 322.75' : N40W 13SW
h=2	1 cg	N30E	57NW	
f=?	1 cg	N40E	62NW	
e=?	1 cg	N35E	77SE	

Depth Interval: 325 - 330 Well: NNR - 10

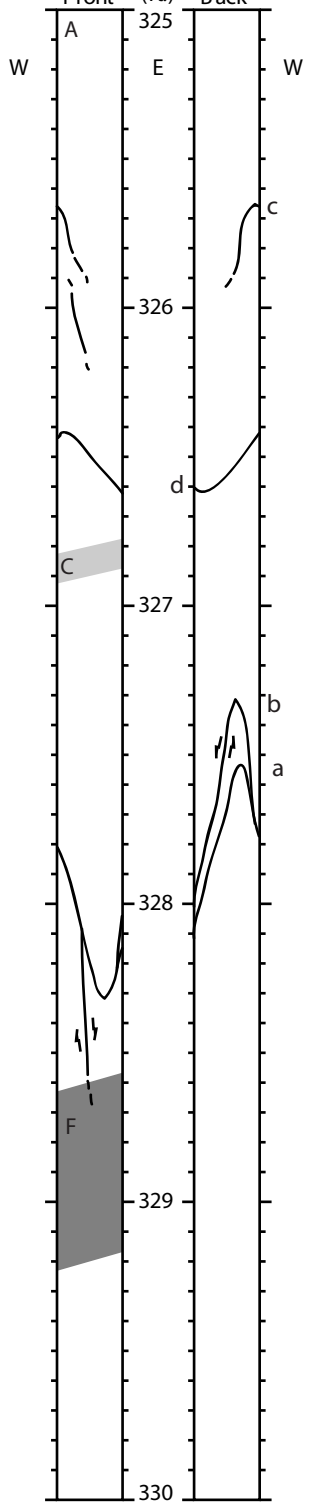

Apparent Disp. (mm)	Fault Thickness (mm)	Fault Strike	Fault Dip	Comments
c=?	1 cg	N10E	71SE	
d=?	1 cg	N25W	46NE	
				Bedding @ 326.9' : N15E 21NW
b=21	1.5 cg	N55E	75SE	Fault "b" correlates w/326.2' in BHTV-log
a=?	3 cg	N55E	71SE	Fault "a" correlates w/326.5' in BHTV-log
				Bedding @ 327.9' : N7W 11SW [obtained from BHTV-log]
				Bedding @ 328.6' : N15E 16SW

Depth Interval: 330 - 335 Well: NNR - 10

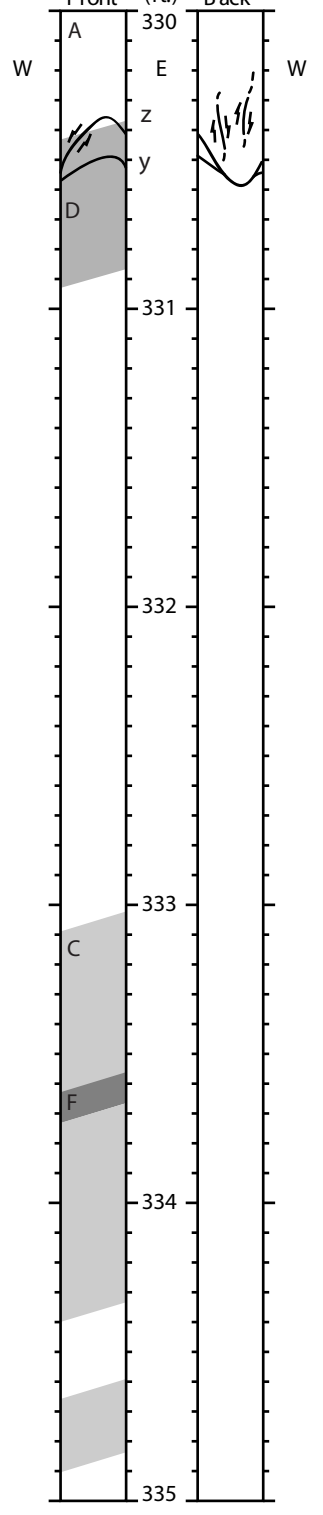

Apparent Disp. (mm)	Fault Thickness (mm)	Fault Strike	Fault Dip	Comments
z=21	0.5 clay	N50E	44NW	
y=?	0.5 fg	N45E	37NW	
				Run # 33 Score card: 330.8' 330.8' - 340.8' Drilled: 10.0' Recovered: 10.1'
				Bedding @ 331.1' : N10W 15SW [obtained from BHTV-log]
				Bedding @ 333.65' : NS 17W

Depth Interval: 335 - 340 Well: NNR - 10

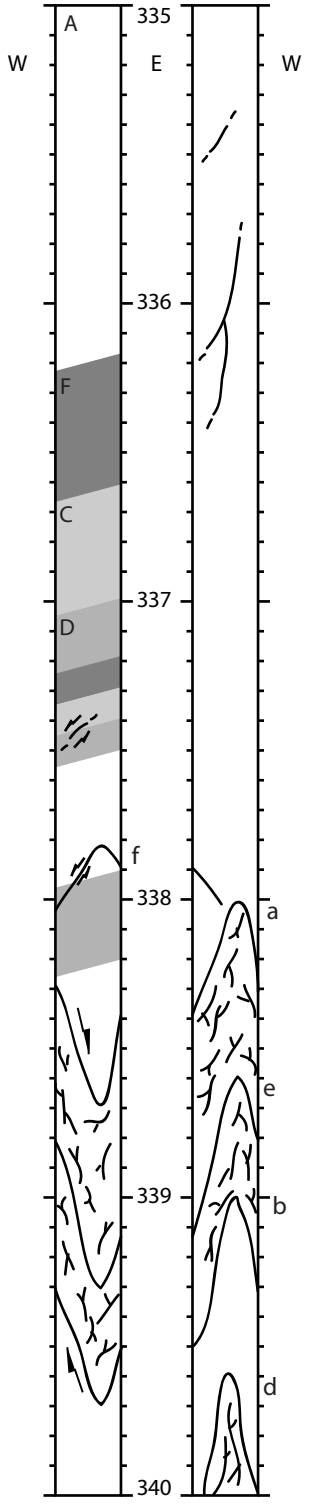

Apparent Disp. (mm)	Fault Thickness (mm)	Fault Strike	Fault Dip	Comments
				Bedding @ 335.6' : NS 20W [obtained from BHTV-log]
				Bedding @ 336.2' : NS 15W
				Bedding @ 336.65' : N5W 13SW
f=9	1 mg	N40E	43NW	
a=?		N50E	74SE	
e=?		N50E	68SE	
b=?		N50E	69SE	Fault "b" correlates w/338' in BHTV-log
d=?	7 cg	N50E	82SE	

Depth Interval: 340 - 345 Well: NNR - 10

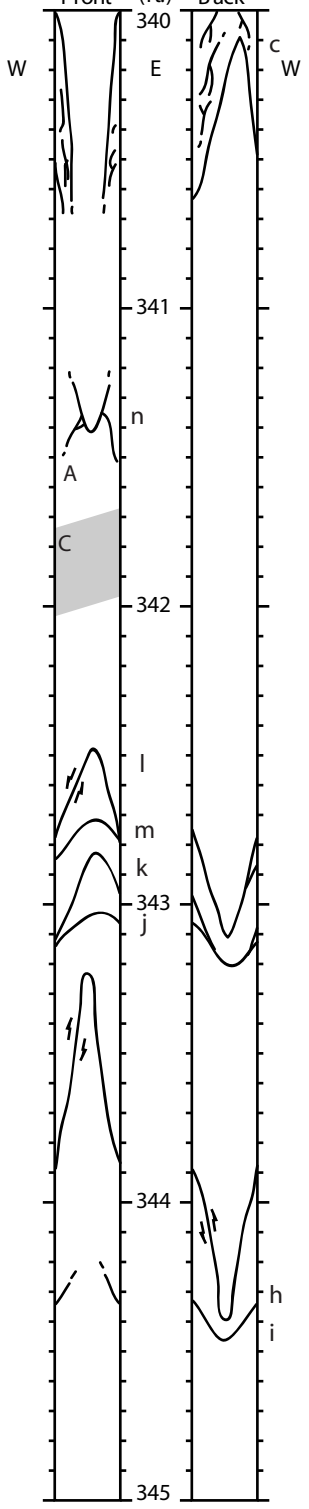

Apparent Disp. (mm)	Fault Thickness (mm)	Fault Strike	Fault Dip	Comments
c=?	4 cg	N55E	79SE	
				Missing core from 340.65' - 341.25
				Data rotated 25 CCW fom 341.25' - 350' but figures are not redrawn
n=?		N45E	76SE	Fault "n" correlates w/340.9' in BHTV-log
				Bedding @ 341.8' : N5E 17NW
l=13	1 cg	N55E	71NW	Fault "l" correlates w/341.6' in BHTV-log
m=?	1 cg	N50E	63NW	
k=?	1 cg	N55E	59NW	
j=?	1 cg	N40E	46NW	
h=32	2.5 cg	N50E	87NW	Fault "h" correlates w/342.1' in BHTV-log
i=?	0.5 cg	N50E	61NW	

Depth Interval: 345 - 350 Well: NNR - 10

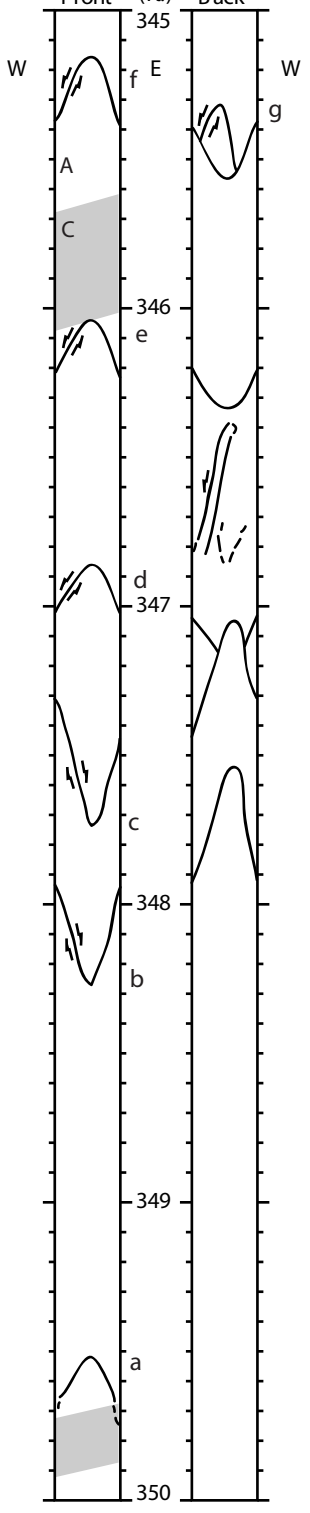

Apparent Disp. (mm)	Fault Thickness (mm)	Fault Strike	Fault Dip	Comments
f=13	1.5 cg	N55W	59NE	
g=4	1 cg	N35W	57SW	
				Bedding @ 345.7' : N5E 16NW
e=5	0.5 cg	N60W	61NE	
d=6	0.5 cg	N55E	66NW	
c=8	1 cg	N40E	69SE	
b=28	2 mg	N45E	74SE	
a=?	0.5 cg	N55E	60NW	
				Bedding @ 349.7' : N10W 13SW

Depth Interval: 350 - 355 Well: NNR - 10

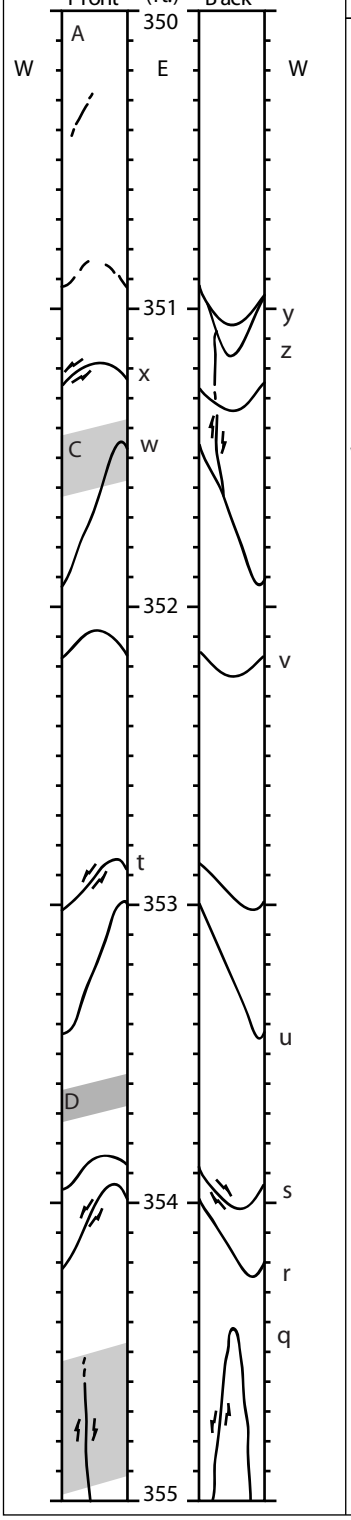

Apparent Disp. (mm)	Fault Thickness (mm)	Fault Strike	Fault Dip	Comments
				Bedding @ 350.1' : NS 25W [obtained from BHTV-log]
				Rotated data 15 CCW from 350.8' - 354.3' but figures were not redrawn
				Bedding @ 350.7' : NS 22W [obtained from BHTV-log]
				Run # 35 Score card: 350.8' 350.8' - 360.8' Drilled: 10.0' Recovered: 10.25'
y=?	0.5 cg	N65E	58NW	
z=?	0.5 cg	N70E	71NW	
x=5	0.5 cg	N55E	40NW	
w=?	0.5 cg	N5W	65NE	Bedding @ 351.4' : N35W 14SW
v=?	1 cg	N65W	33NE	
t=25	3 cg	N15E	51NW	Fault "t" correlates w/352.2' in BHTV-log
u=?	2 cg	N5E	66NW	Fault "u" correlates w/352.8' in BHTV-log
s=23	1.5 cg	N45E	43NW	
r=7	1.5 cg	N25E	52NW	Fault "r" correlates w/352.5' in BHTV-log
q=6	0.5 mg	N65E	82NW	Fault "q" is younger than faults "p" and "o"
				Bedding @ 354.5' : N15E 16NW

Depth Interval: 355 - 360 Well: NNR - 10

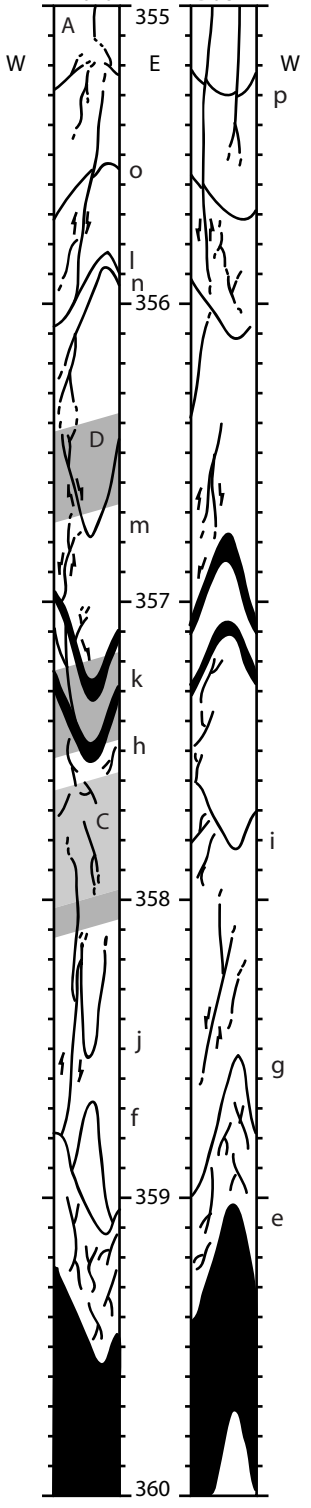

Apparent Disp. (mm)	Fault Thickness (mm)	Fault Strike	Fault Dip	Comments
p=?	2 cg	N70E	37NW	
o=?	2 cg	N30E	35NW	
l=?	2 cg	N40E	51NW	
n=?	2 cg	N45E	78NW	
m=19	1.5 mg	N75E	76SE	
k=?		N60E	68SE	Rake on "k" is 68NE
h=?		N70E	62SE	
i=?	1 mg	N45E	65NW	
				Bedding @ 358.0' : N15E 18NW
j=?		N70E	88SE	
g=?	2 cg	N45E	73SE	
f=?		N70E	86NW	
e=?		N60E	66SE	

Depth Interval: 360 - 365 Well: NNR - 10

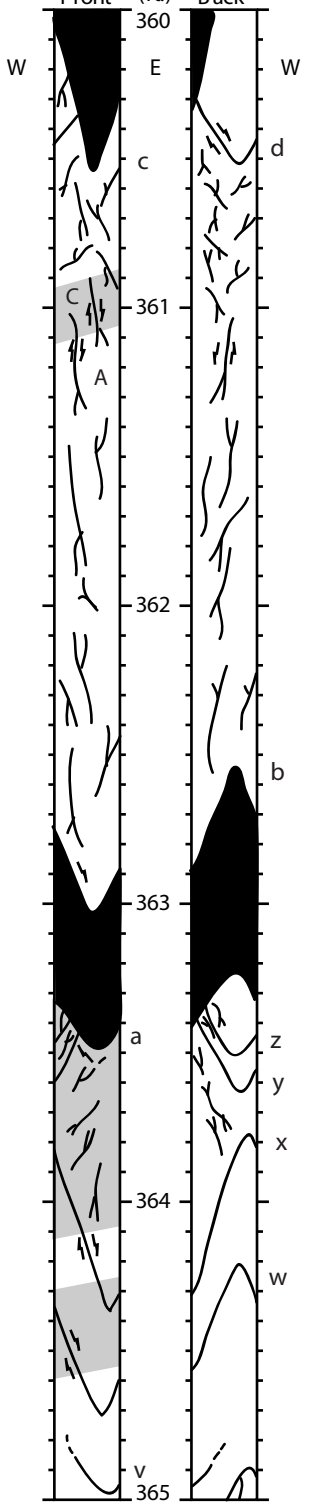

Apparent Disp. (mm)	Fault Thickness (mm)	Fault Strike	Fault Dip	Comments
d=8	1 cg	N50E	46NW	
c=?		N50E	75SE	Fault "c" correlates w/360.1' in BHTV-log Between 360.5' and 361.0' NW dipping faults are predominately younger than SE dipping faults. In instances when NW dipping faults are older than SE dipping faults, the SE dipping faults tend to have a dip greater than 70°.
b=?		N50E	72SE	Fault "b" correlates w/361.6' in BHTV-log
a=?		N50E	56SE	Fault "a" correlates w/362.8' in BHTV-log
z=?	1 mg	N40E	32NW	
y=?	1 mg	N30E	52NW	
x=3	0.5 mg	N25E	67SE	Bedding @ 363.85' : N10W 11SW
w=9	0.5 clay	N50E	61SE	
v=?	1 cg	N35E	54SE	

Depth Interval: 365 - 370 Well: NNR - 10

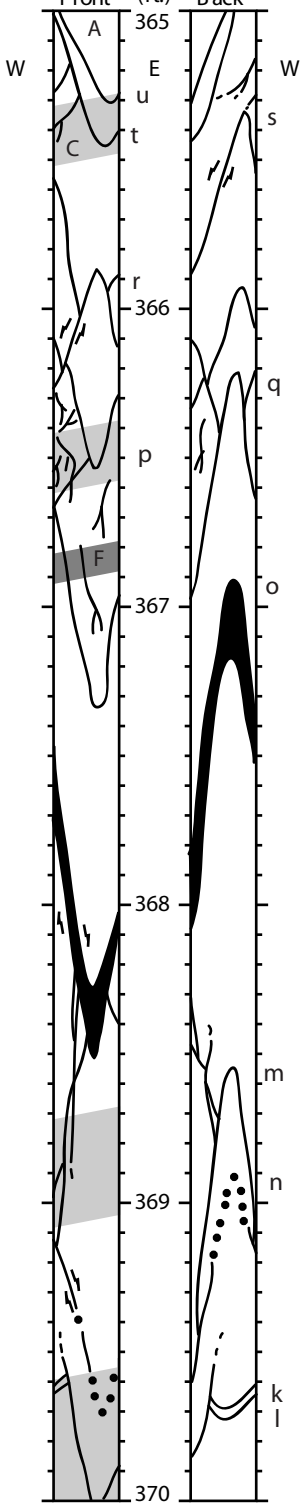

Apparent Disp. (mm)	Fault Thickness (mm)	Fault Strike	Fault Dip	Comments
u=?	1.5 cg	N20E	65SE	
t=?	1 mg	N20E	67SE	
s=12	2 cg	N45E	68SE	
r=14	2 cg	N45E	66NW	Fault "r" is younger than fault "s" & "p", but older than fault "q"
q>180	3 fg	N40E	81SE	
p=?	5 cg	N45E	67SE	
o=?	20 cg	N50E	85SE	
m=?		N45E	81SE	
n=39		N40E	74SE	
k=?	0.5 mg	N70E	39NW	
l=?	0.5 mg	N65E	41NW	

Depth Interval: 370 - 375 Well: NNR - 10

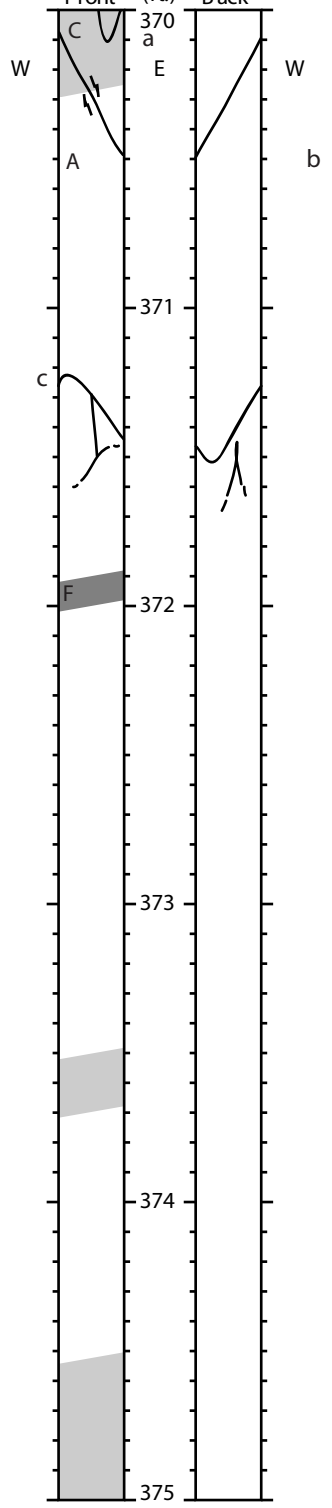

Apparent Disp. (mm)	Fault Thickness (mm)	Fault Strike	Fault Dip	Comments
a>70	4 mg	N45E	71SE	
b=43	2 cg	NS	54E	
				Run # 37 Score card: 370.9' 370.8' - 380.9' Drilled: 10.1' Recovered: 10.05'
c=?	3 cg	N30W	46NE	Bedding @ 371.1' : N15W 6SW [obtained from BHTV-log]
				Bedding @ 372.0' : N15E 10NW
				Bedding @ 372.1' : N10W 15SW [obtained from BHTV-log]
				Bedding @ 372.7' : N7W 15SW [obtained from BHTV-log]
				Bedding @ 373.5' : N20W 9SW
				Bedding @ 373.7' : N45W 15SW [obtained from BHTV-log]
				Bedding @ 374.5' : N25W 10SW

Depth Interval: 375 - 380 Well: NNR - 10

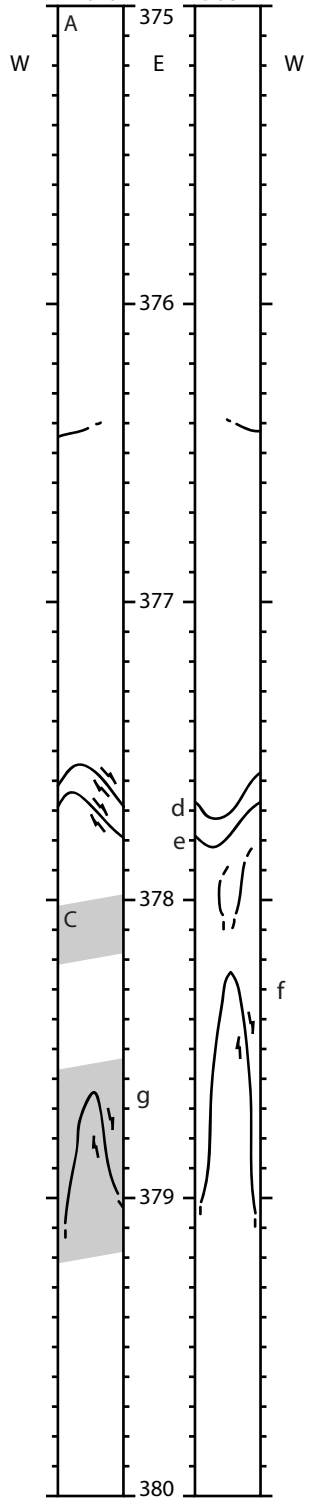

Apparent Disp. (mm)	Fault Thickness (mm)	Fault Strike	Fault Dip	Comments
d=7	1.5 cg	N45W	36NE	
e=28	2 cg	N40W	34NE	
f=5	0.25 mg	EW	81S	Bedding @ 378.4' : N15W 10SW [obtained from BHTV-log]
g=4	0.25 mg	N80E	77NW	Bedding @ 379.2' : N25E 14NW Bedding @ 379.3' : N45W 22SW [obtained from BHTV-log]

Depth Interval: 380 - 385 Well: NNR - 10

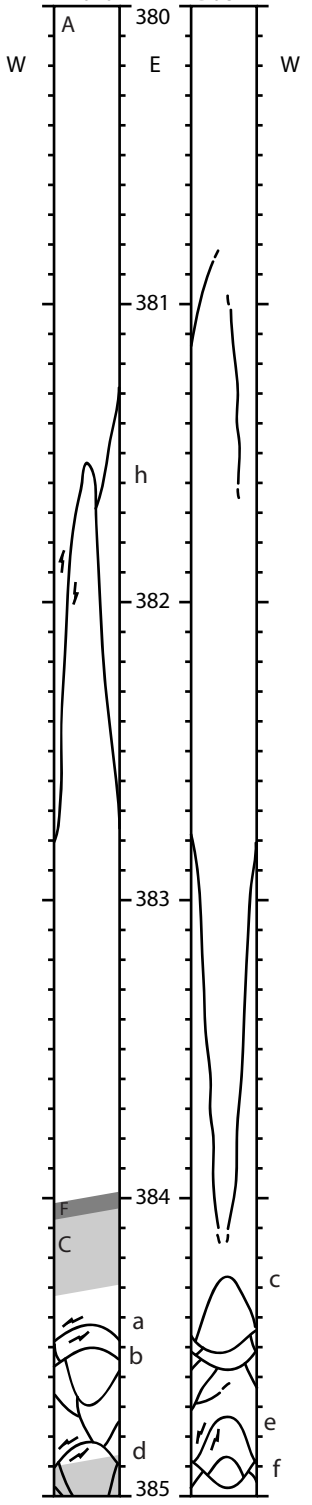

Apparent Disp. (mm)	Fault Thickness (mm)	Fault Strike	Fault Dip	Comments
				Run # 38 Score card: 380.9' 380.9' - 390.9' Drilled: 10.0' Recovered: 10.0'
h=4	1 cg	N80E	88NW	
				Bedding @ 383.4' : N30W 19SW [obtained from BHTV-log]
				Bedding @ 384.1' : N35E 15NW
c=?	3 cg	N75W	56SW	Fault "c" is older than faults "a" and "b"
a=?	2 cg	N80W	34NE	
b=13	2.5 cg	N80W	31NE	
e=11	1 mg	N70W	46SW	Fault "d" is younger than faults "e" and "f"
d=7	1 cg	N70W	39NE	
f=?	2 mg	N75W	37SW	

Depth Interval: 385 - 390 Well: NNR - 10

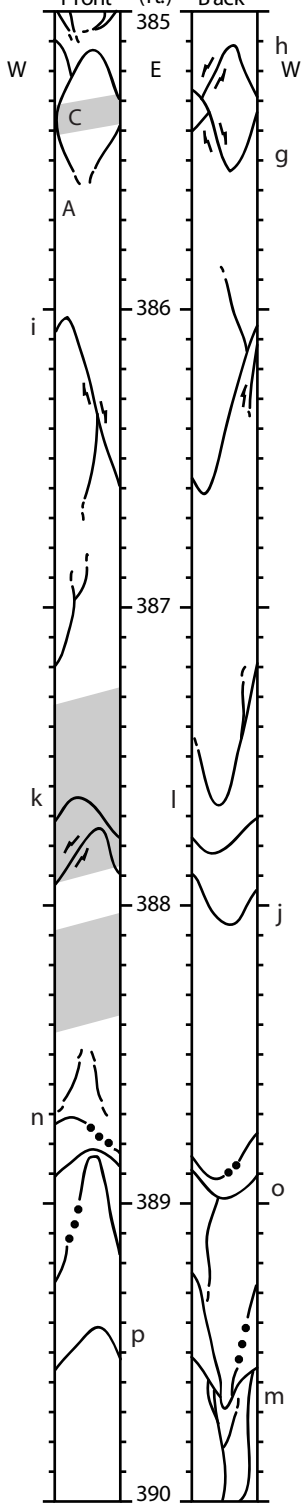

Apparent Disp. (mm)	Fault Thickness (mm)	Fault Strike	Fault Dip	Comments
h=14	1.5 cg	EW	57S	Fault "h" is older than fault "g"
g=18	2 mg	N85E	51NW	
i=10	1.5 cg	N30W	66NE	
l=?	1 cg	N60W	74NE	
k=?	0.5 mg	N55W	56NE	
j=23	1.5 mg	N75E	55NW	
n=?		N45W	47NE	
o=?	1 cg	N60W	40NE	
p=?	1 cg	N75W	46NE	
m=?		N80W	78NE	Rake on "m" is 68SE

Depth Interval: 390 - 395 Well: NNR - 10

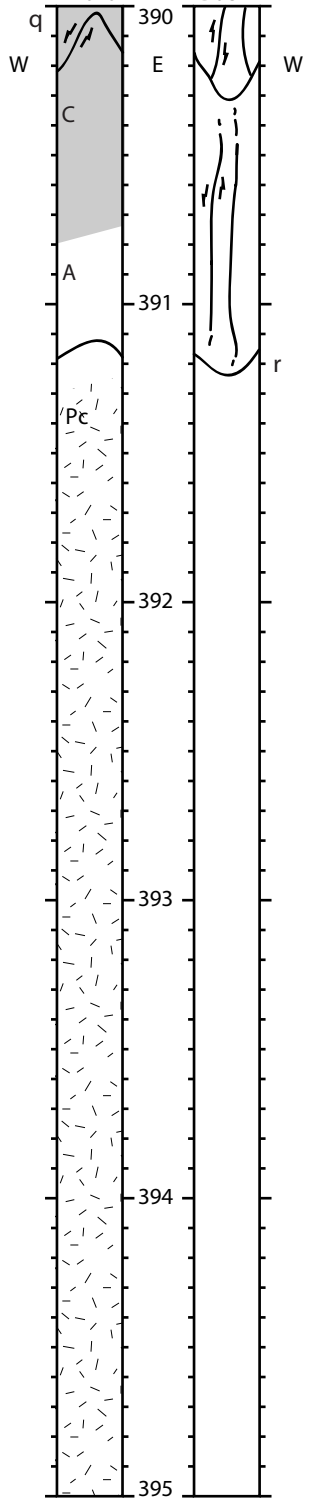

Apparent Disp. (mm)	Fault Thickness (mm)	Fault Strike	Fault Dip	Comments
q=27	1.5 cg	N85E	56NW	
r=?	1.5 cg	EW	27N	Run # 39 Score card: 390.9' 390.5' - 400.9' Drilled: 10.0' Recovered: 10.15'

Depth Interval: 170 - 175 Well: NNR - 4

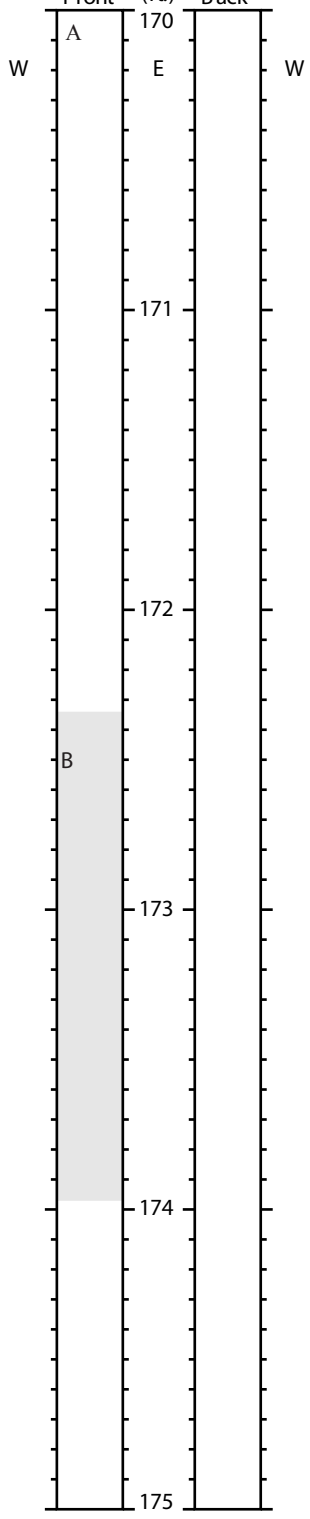

Apparent Disp. (mm)	Fault Thickness (mm)	Fault Strike	Fault Dip	Comments
				Run #19 Score card: 171.7' 171.6' - 181.6' Drilled: 10.0' Recovered: 9.75' Bedding @ 172.1: N10W, 26SW [obtained from BHTV-log] Bedding @ 175: N5E, 21NW [obtained from BHTV-log]

Depth Interval: 175 - 180 Well: NNR - 4

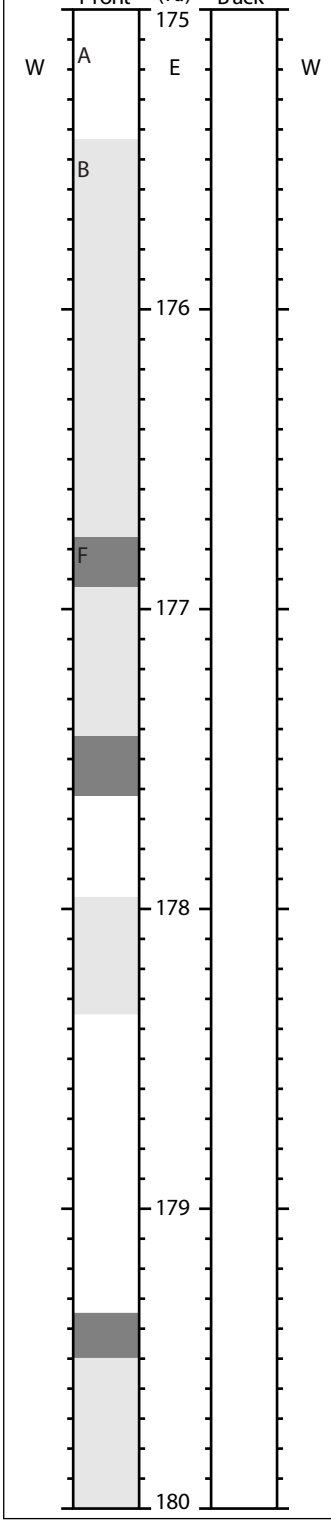

Apparent Disp. (mm)	Fault Thickness (mm)	Fault Strike	Fault Dip	Comments
				Bedding @ 178.4: N7E, 23NW [obtained from BHTV-log]

Depth Interval: 180 - 185 Well: NNR - 4

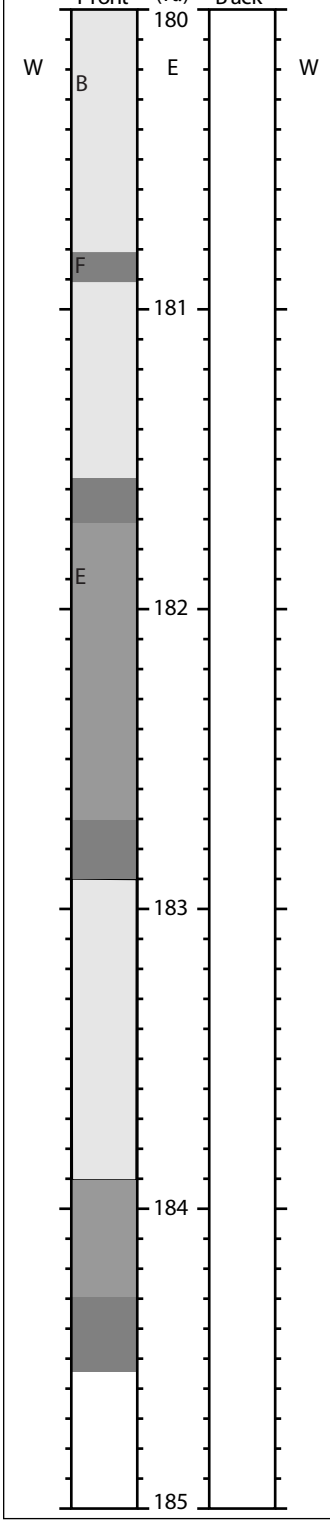

Apparent Disp. (mm)	Fault Thickness (mm)	Fault Strike	Fault Dip	Comments
				Run #20 Score card: 181.6' 181.6' - 191.6' Drilled: 10.0' Recovered: 10.1'
				Bedding @ 184.4: NS, 23W [obtained from BHTV-log]
				Missing core from 184.55' - 185.2'

Depth Interval: 185 - 190 Well: NNR - 4

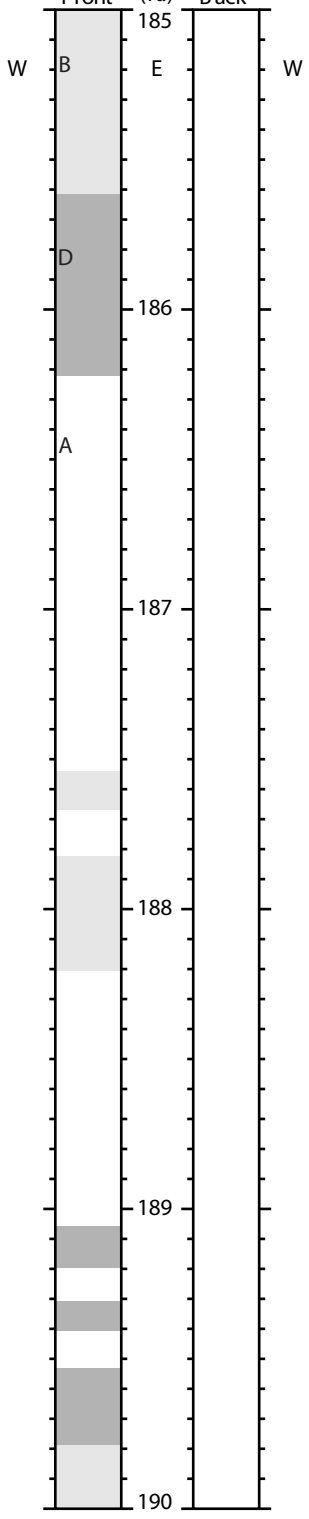

Apparent Disp. (mm)	Fault Thickness (mm)	Fault Strike	Fault Dip	Comments

Depth Interval: 190 - 195 Well: NNR - 4

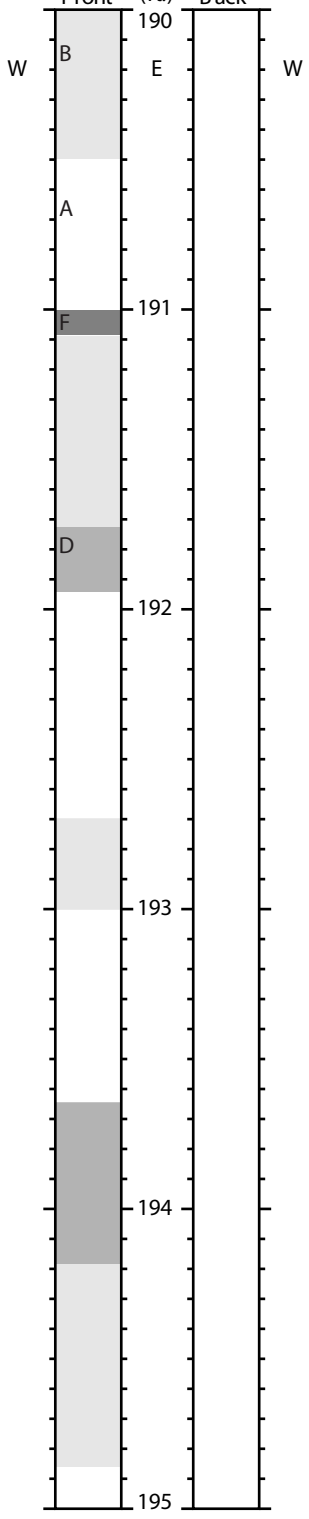

Apparent Disp. (mm)	Fault Thickness (mm)	Fault Strike	Fault Dip	Comments
				Run #21 Score card: 191.7' 191.6' - 201.6' Drilled: 10.0' Recovered: 10.1'
				Missing core from 193.0' - 193.65'

Depth Interval: 195 - 200 Well: NNR - 4

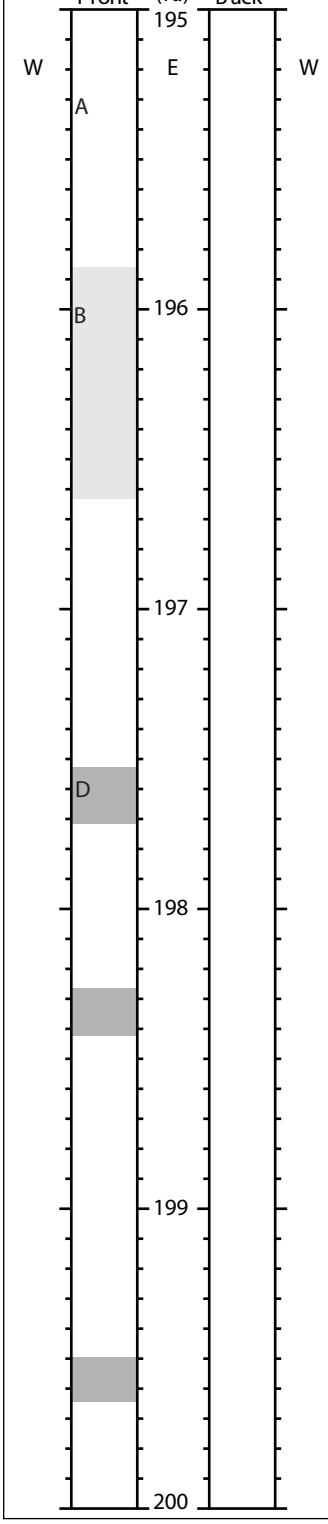

Apparent Disp. (mm)	Fault Thickness (mm)	Fault Strike	Fault Dip	Comments

Depth Interval: 200 - 205 Well: NNR - 4

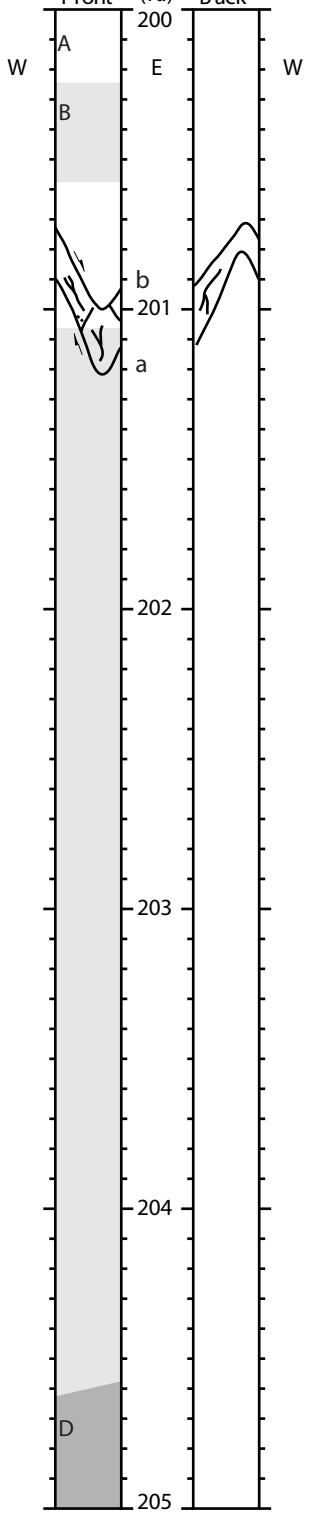

Apparent Disp. (mm)	Fault Thickness (mm)	Fault Strike	Fault Dip	Comments
b=?		N30E	57SE	
a=?	20	N50E	76SE	Fault "a" correlates with 201' in BHTV-log
				Run #22 Score card: 201.6' 201.6' - 211.6' Drilled: 10.0' Recovered: 10.0'
				Bedding @ 202.0' : N15E 13NW
				Bedding @ 202.9' : N15E 27NW [obtained from BHTV-log]

Depth Interval: 205 - 210 Well: NNR - 4

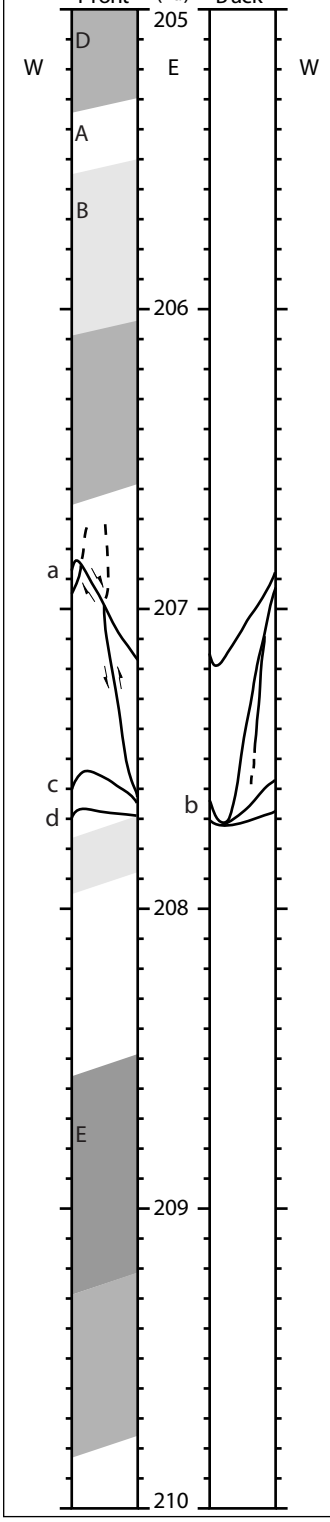

Apparent Disp. (mm)	Fault Thickness (mm)	Fault Strike	Fault Dip	Comments
				Bedding @ 205.9' : NS 24W [obtained from BHTV-log]
				Bedding @ 206.4' : N22E 35NW [obtained from BHTV-log]
				Bedding @ 206.7' : N30E 18NW
a=9	1 cg	N10W	47NE	
c=?	1 cg	N30W	43NE	
b=6	1 cg	N40W	83NE	
d=?	1 cg	N30W	31NE	
				Bedding @ 208.6' : N30E 24NW [obtained from BHTV-log]

Depth Interval: 210 - 215 Well: NNR - 4

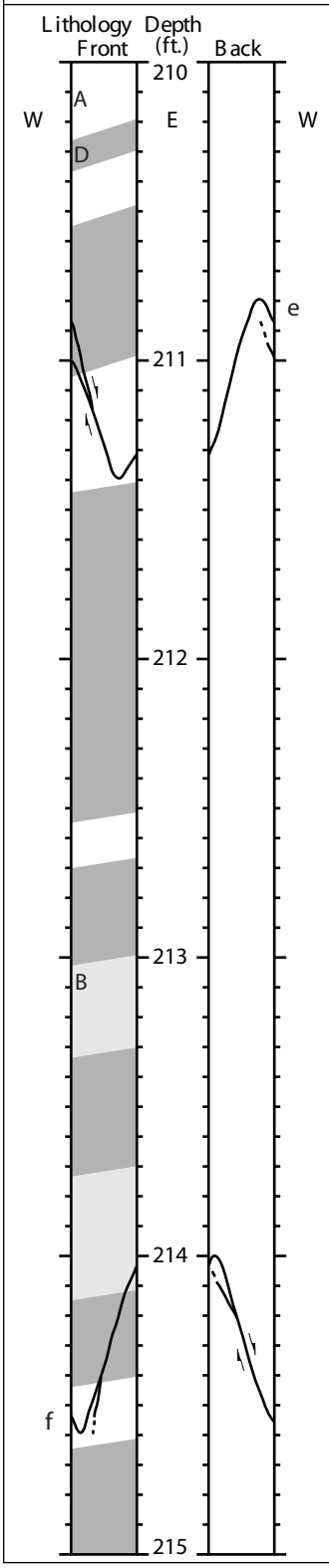

Apparent Disp. (mm)	Fault Thickness (mm)	Fault Strike	Fault Dip	Comments
e=12	0.5 clay	N40E	66SE	
				Bedding @ 211.3' : N25E 9NW
				Run #23 Score card: 211.6' 211.6' - 221.6' Drilled: 10.0' Recovered: 10.1'
f=24	0.5 clay	N5W	63SW	

Depth Interval: 215 - 220 Well: NNR - 4

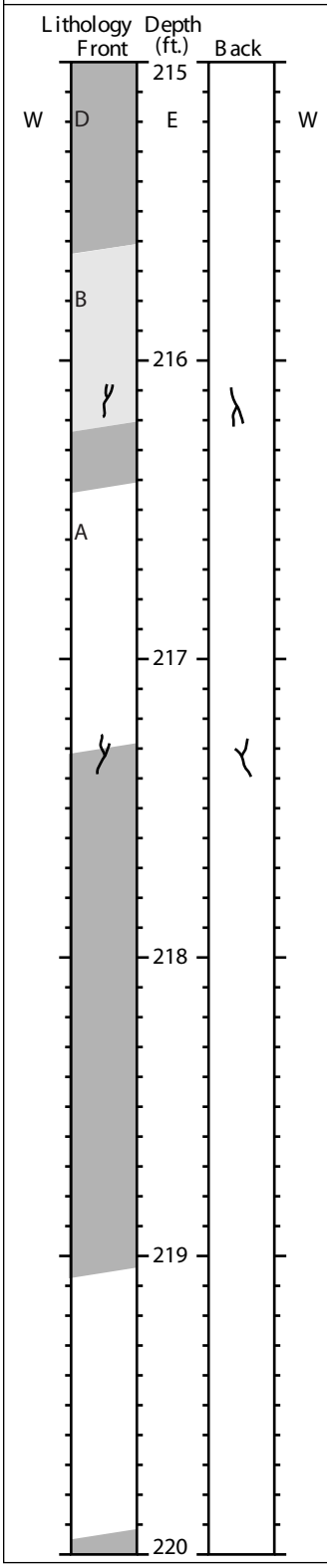

Apparent Disp. (mm)	Fault Thickness (mm)	Fault Strike	Fault Dip	Comments
				Bedding @ 217.4' : N20W 9SW
				Missing core from 219.05' - 219.5'

Depth Interval: 220 - 225 Well: NNR - 4

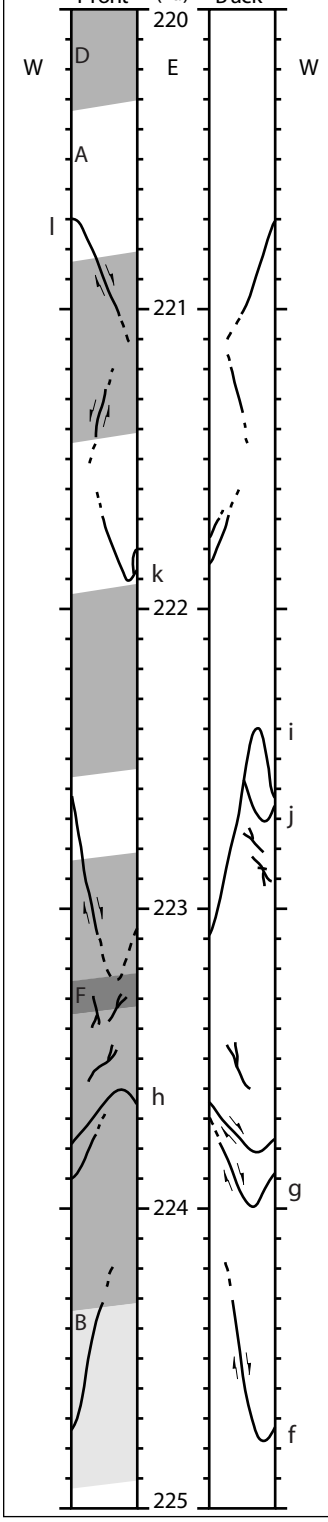

Apparent Disp. (mm)	Fault Thickness (mm)	Fault Strike	Fault Dip	Comments
l=11	0.5 fg	N5E	64SE	
k=?	0.5 fg	N20E	63SE	Run #24 Score card: 221.72' 221.6' - 229.9' Drilled: 8.25' Recovered: 8.25'
i=68		N45E	83SE	Bedding @ 222.4' : N15E 7NW
j=?	1 cg	N30E	57NW	
h=6	0.5 mg	N40E	42NW	
g=3	0.5 mg	N50E	53NW	
f=3	0.5 cg	N40E	65NW	

Depth Interval: 225 - 230 Well: NNR - 4

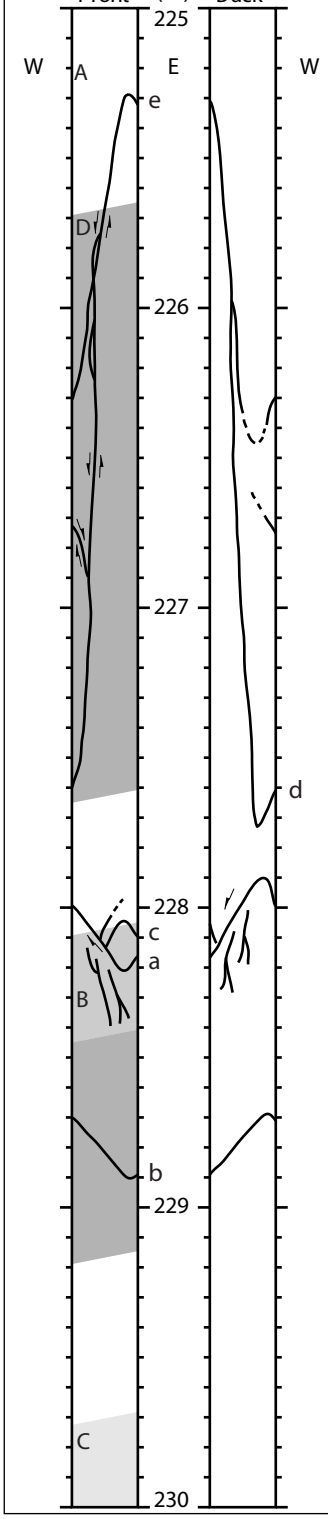

Apparent Disp. (mm)	Fault Thickness (mm)	Fault Strike	Fault Dip	Comments
				Bedding @ 225.0' : N30E 11NW
e=28		N30E	81NW	Rake = 65NE on fault "e" fault "e" correlates with 225' in BHTV-log
d=25	1 fg	N50E	84NW	Rake = 55 NE on fault "d"
c=?	1.5 cg	N40E	71NW	
a=610	27.5 cg	N30E	54SE	Fault "a" correlates with 227.7' in BHTV-log
b=?		N10E	44SE	
				Bedding @ 229.5': NS, 22W

Depth Interval: 230 - 235 Well: NNR - 4

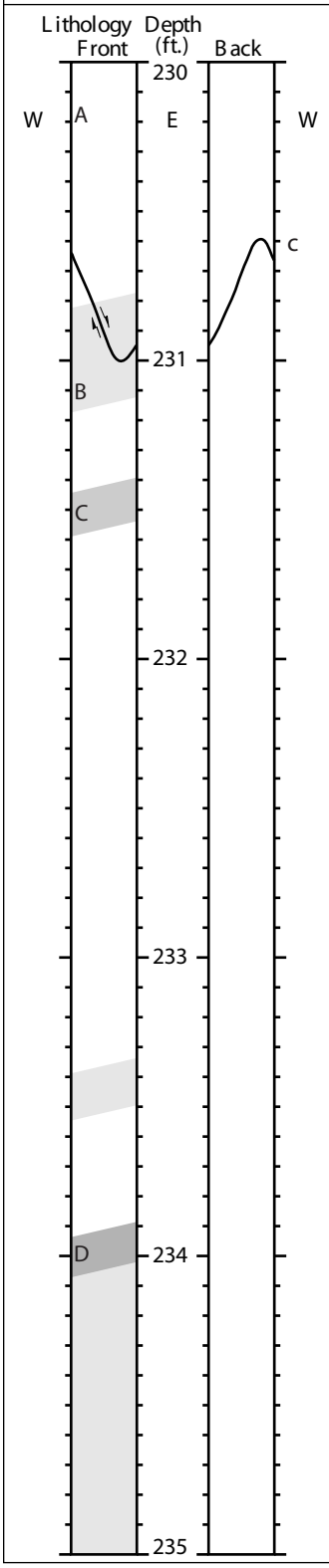

Apparent Disp. (mm)	Fault Thickness (mm)	Fault Strike	Fault Dip	Comments
c=13	1.5 cg	N40E	61SE	fault "c" correlates with 230.6' in BHTV-log
				Bedding @ 231.1' : N20E 13NW
				Missing core from 232.4' - 233.25'
				Bedding @ 234.7' : N30E 29NW [obtained from BHTV-log]

Depth Interval: 235 - 240 Well: NNR - 4

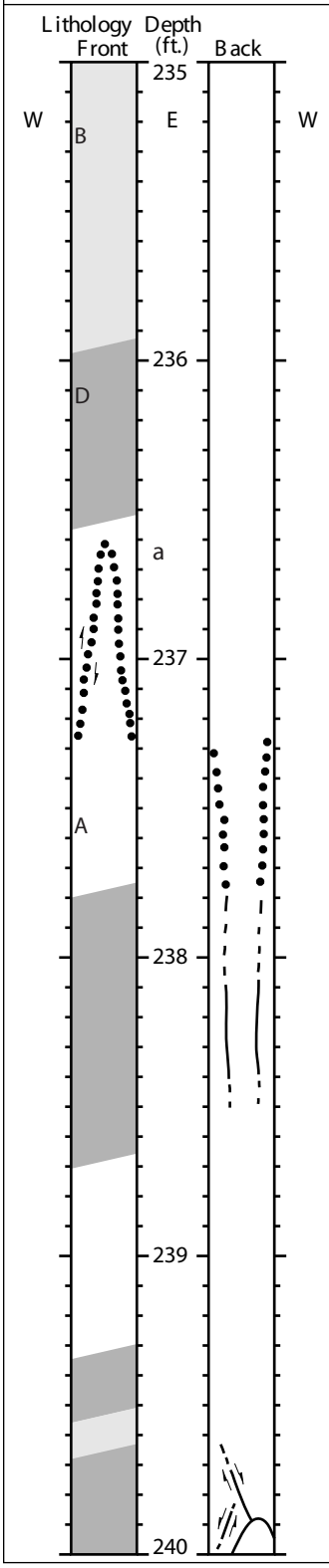

Apparent Disp. (mm)	Fault Thickness (mm)	Fault Strike	Fault Dip	Comments
				Bedding @ 235.2' : N37E 25NW [obtained from BHTV-log]
				Bedding @ 236.3' : N10E 18NW [obtained from BHTV-log]
a=2	0.5 fg	N75W	84NE	
				Bedding @ 238.6' : N30E 21NW

Depth Interval: 240 - 245 Well: NNR - 4

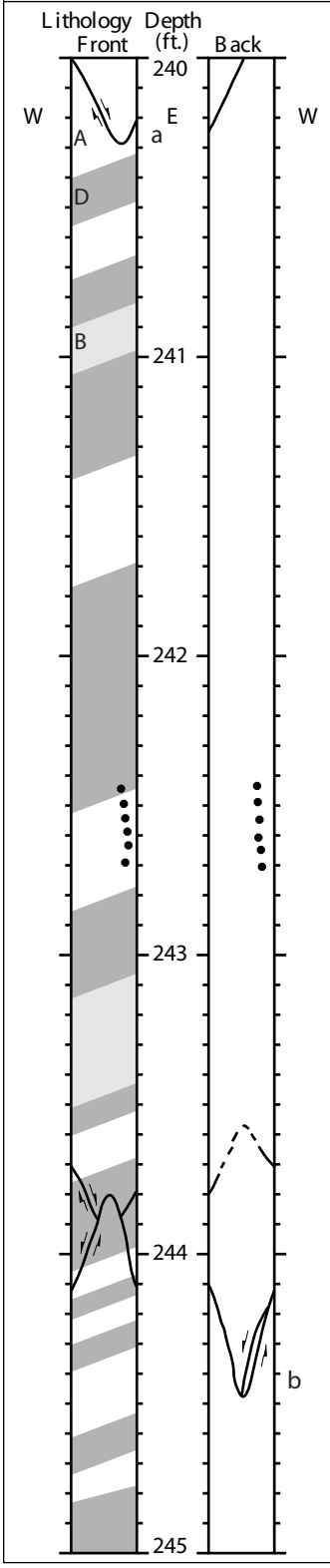

Apparent Disp. (mm)	Fault Thickness (mm)	Fault Strike	Fault Dip	Comments
a=50		N40E	65SE	fault "a" correlates with 239.6' in BHTV-log
b=33	1 fg	N70E	64NW	
				Bedding @ 244.8' : N15E 14NW

Depth Interval: 245 - 250 Well: NNR - 4

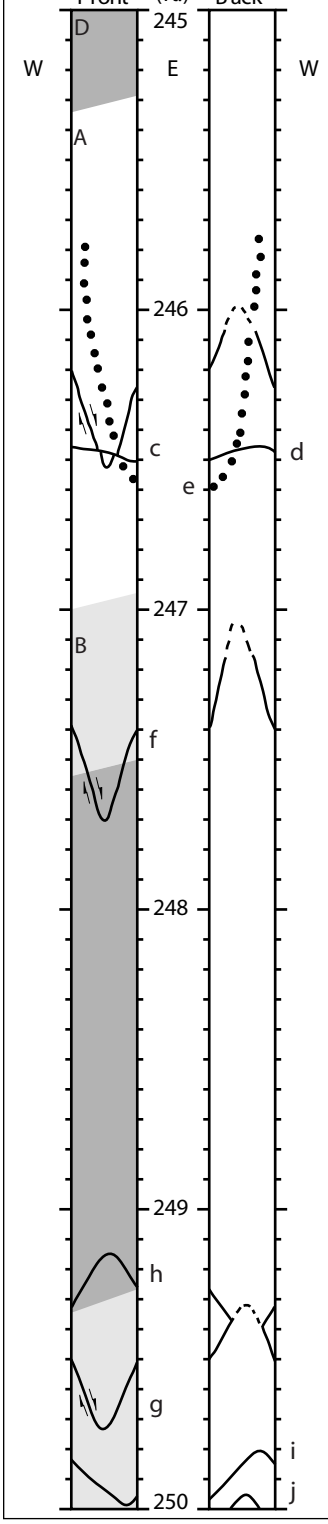

Apparent Disp. (mm)	Fault Thickness (mm)	Fault Strike	Fault Dip	Comments
c=23	1.5 mg	N70E	64SE	"c" is older than "d"
d=4	1 mg	N10E	12SE	Fault "d" might have more of a strike-slip component than dip-slip
e=?		N10W	77NE	
f=6	0.5 fg	N80W	63SW	
				Bedding @ 247.9' : N20E 21NW
h=?	0.5 clay	N60E	61NW	
g=21	1 clay	N70E	67SE	fault "g" correlates with 249.1' in BHTV-log
i=?	0.5 clay	N30E	33SE	
j=?	0.5 clay	N80E	60SE	

Depth Interval: 250 - 255 Well: NNR - 4

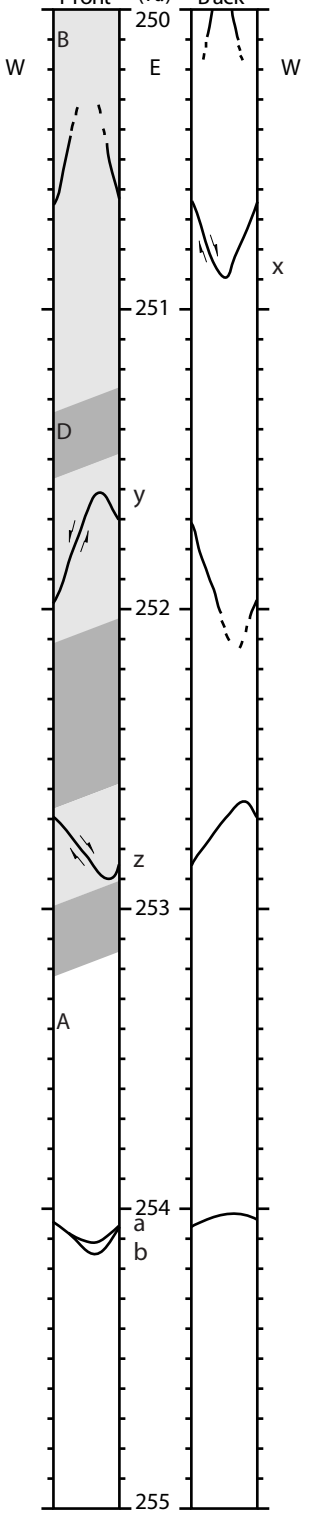

Apparent Disp. (mm)	Fault Thickness (mm)	Fault Strike	Fault Dip	Comments
				Run #27 Score card: 250.2' 250.0' - 259.0' Drilled: 9.1' Recovered: 9.15'
x=6	1 cg	N70E	76NW	Bedding @ 251.1' : N5W 28NW [obtained from BHTV-log]
y=9	1 cg	N60E	71NW	
z=16	1 mg	N50E	47SE	
				Bedding @ 253.0' : N30E 21NW Bedding @ 253.5' : N7W 29SW [obtained from BHTV-log]
a=? b=?	1 mg 1 mg	N70E N75E	21SE 26SE	Bedding @ 254.0' : N15W 35SW Bedding @ 254.2' : NS 41W [obtained from BHTV-log]
				Bedding @ 254.2' : N5W 39SW [obtained from BHTV-log]

Depth Interval: 255 - 260 Well: NNR - 4

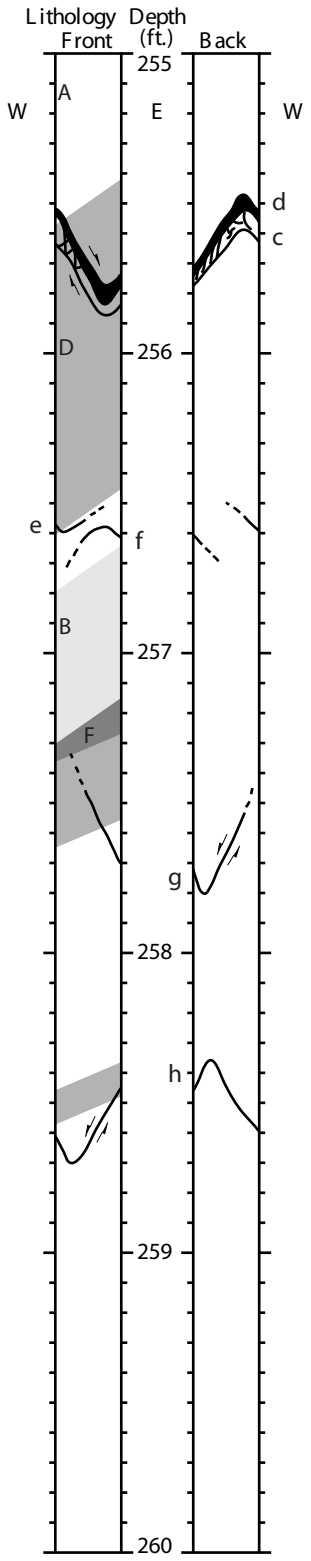

Apparent Disp. (mm)	Fault Thickness (mm)	Fault Strike	Fault Dip	Comments
				Multiple smaller faults associated with the general orientation and displacement of fault "d". Some anithetic dipping faults are also found between faults "c" and "d".
d=?	10	N45E	57SE	
c=4	0.5 fg	N40E	53SE	fault "d" correlates with 255.6' in BHTV-log
				Bedding @ 256.3' : N22E 27NW [obtained from BHTV-log]
e=?	1 mg	N10W	23SW	
f=?	1 mg	N50E	34NW	
				Bedding @ 257.3' : N40E 23NW
				Bedding @ 257.6' : N25E 23NW [obtained from BHTV-log]
g=3	0.5 fg	N40W	57NE	
h=16	1.5 cg	N50W	50SW	
				Run #28 Score card: 259.2' 259.0' - 261.6' Drilled: 2.8' Recovered: 2.85'
				Bedding @ 259.9' : N20E 21NW [obtained from BHTV-log]

Depth Interval: 260 - 265 Well: NNR - 4

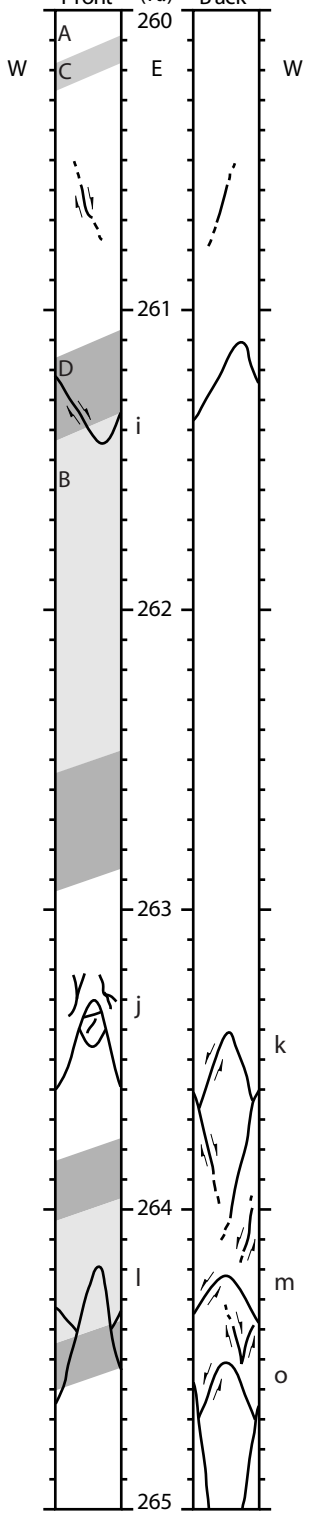

Apparent Disp. (mm)	Fault Thickness (mm)	Fault Strike	Fault Dip	Comments
3	1 cg			Bedding @ 260.8' : NS 23W [obtained from BHTV-log]
i=6	0.5 fg	N60E	42SE	Bedding @ 261.7' : N45E 19NW
				Run #29 Score card: 261.6' 261.6' - 271.6' Drilled: 10.0' Recovered: 10.0'
				Bedding @ 261.9' : N7E 19NW [obtained from BHTV-log]
				Bedding @ 262.2' : N30E 21NW [obtained from BHTV-log]
j=11	1 mg	N80W	77NE	Bedding @ 263.1' : N22E 23NW [obtained from BHTV-log]
k=4	0.5 mg	N60W	62SW	
l=?		N60E	82NW	"l" is most likely a normal fault
m=3	1 cg	EW	57S	fault "l" correlates with 265.8' in BHTV-log
o=5	1 cg	EW	59S	

Depth Interval: 265 - 270 Well: NNR - 4

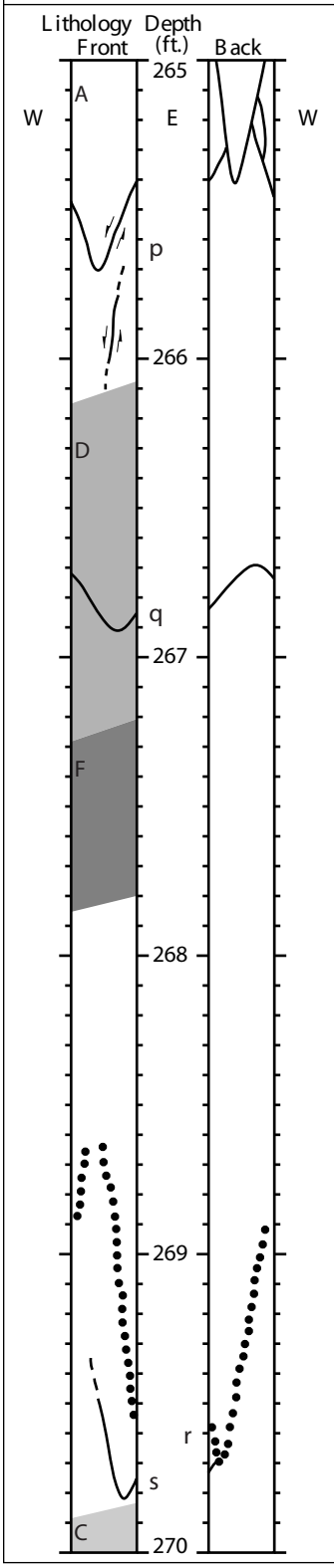

Apparent Disp. (mm)	Fault Thickness (mm)	Fault Strike	Fault Dip	Comments
p=10	1 cg	N60E	57SE	
q=?		N50E	42SE	
				Bedding @ 267.8' : N35E 14NW
r=?		N30W	83NE	joint "r" correlates with 270.1' in BHTV-log
s=?	2 cg	N40E	67SE	

Depth Interval: 270 - 275 Well: NNR - 4

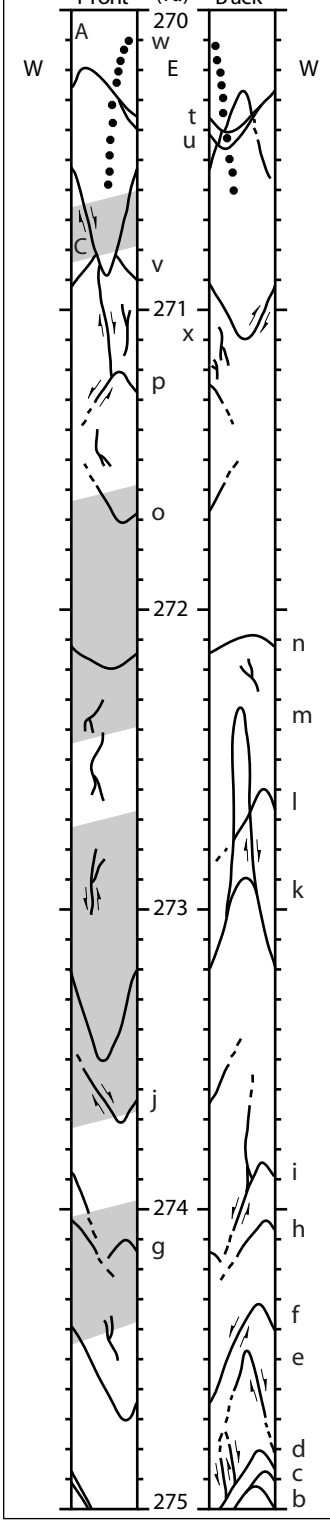

Apparent Disp. (mm)	Fault Thickness (mm)	Fault Strike	Fault Dip	Comments
w=?		N10E	84NW	
t=2	1 cg	N30W	50NE	"t" and "u" are younger than "v"
u=2	1cg	N30W	56NE	
v=23	2 cg	N70E	70SE	
x=3	0.5 fg	EW	68N	
p=7	1 cg	N40E	47NW	
o=?	1 cg	N30E	52SE	Run #30 Score card: 271.5' 271.6' - 281.6' Drilled: 10.0' Recovered: 10.05'
n=?	0.5 fg	N60E	22SE	
m=18	2 cg	N75E	87SE	
l=?	1 cg	N25E	59SE	"l" is younger than "m" Bedding @ 272.9' : N15E 19NW [obtained from BHTV-log]
k=?		N70E	73SE	Rake = 46NE, fault "k"
j=9	1 cg	N40E	53SE	
i=11	1.5 cg	N45E	51SE	
h=?		N35E	52SE	Rake = 67NE, fault "h"
g=?		N40E	68NW	
f=7	0.5 fg	N40E	54SE	Bedding @ 274.3' : N30E 20NW
e=6	1 cg	EW	68S	
d=?	1 cg	N35E	52SE	Bedding @ 274.5' : N30E 27NW
c=?	1 cg	N25E	56SE	[obtained from BHTV-log]
b=?	1 cg	N60E	49SE	

Depth Interval: 275 - 280 Well: NNR - 4

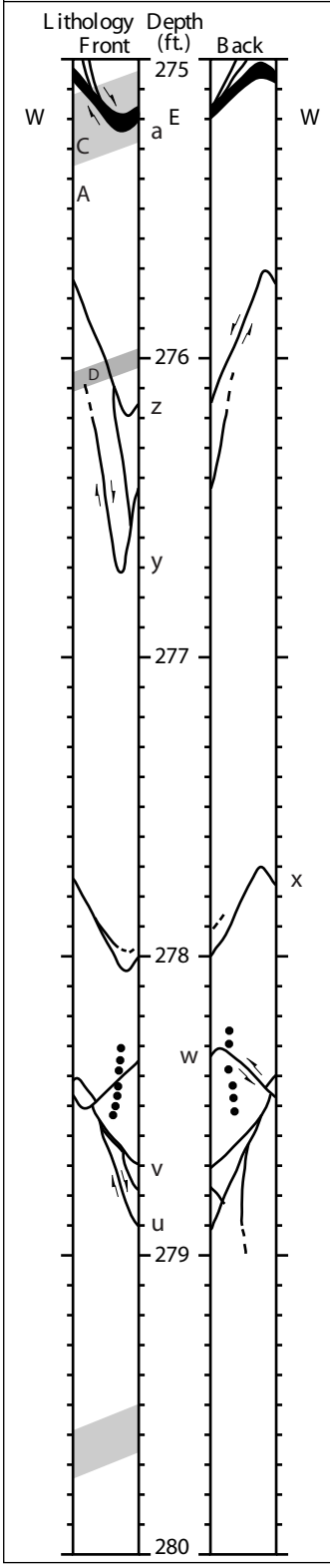

Apparent Disp. (mm)	Fault Thickness (mm)	Fault Strike	Fault Dip	Comments
a>10	13 cg for a+b+c+d	N45E	43SE	Rake = 54 NE, fault "a" fault "a" correlates with 274.9' in BHTV-log
z=4	2.5 cg	N35E	61SE	Bedding @ 276.1' : N30E 33NW [obtained from BHTV-log]
y=4	2 cg	N50E	71SE	fault "y" correlates with 276.9 in BHTV-log
				Bedding @ 277.6' : N30E 35NW [obtained from BHTV-log]
x=?	3 cg	N40E	61SE	
w=9	1.5 cg	N30E	42NW	"w" is younger than "v" and "u"
v=?	1 cg	NS	47SE	
u=3	1 cg	N10W	55NE	
				Bedding @ 279.4' : N25E 30NW [obtained from BHTV-log]
				Bedding @ 279.5' : N30E 22NW

Depth Interval: 280 - 285 Well: NNR - 4

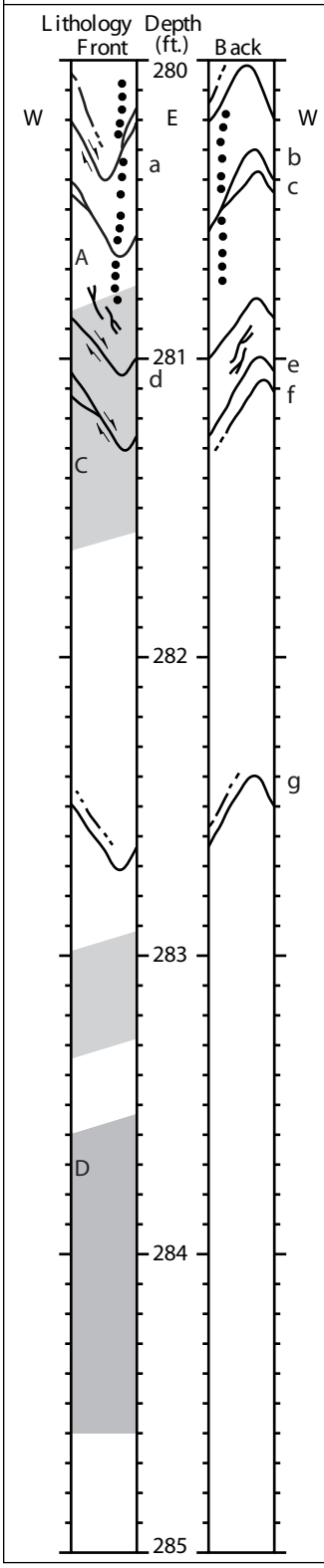

Apparent Disp. (mm)	Fault Thickness (mm)	Fault Strike	Fault Dip	Comments
a=3	1 cg	EW	51S	
b=?	6 cg	N60E	55SE	fault "b" correlates with 280.3' in BHTV-log
c=?	4 cg	N40E	42SE	
d=9	0.5 fg	N50E	37SE	
e=3	1 cg	N35E	53SE	
f=2	1 cg	N30E	58SE	
				Bedding @ 281.4' : N50E 17NW
				Run #31 Score card: 281.7' 281.6' - 291.6' Drilled: 10.0' Recovered: 9.8'
				Bedding @ 282.2' : N22E 30NW [obtained from BHTV-log]
g=?	1.5 cg	N50E	57SE	
				Bedding @ 283.7' : N30E 22NW [obtained from BHTV-log]
				Missing core from 284.6' - 285.35'

Depth Interval: 285 - 290 Well: NNR - 4

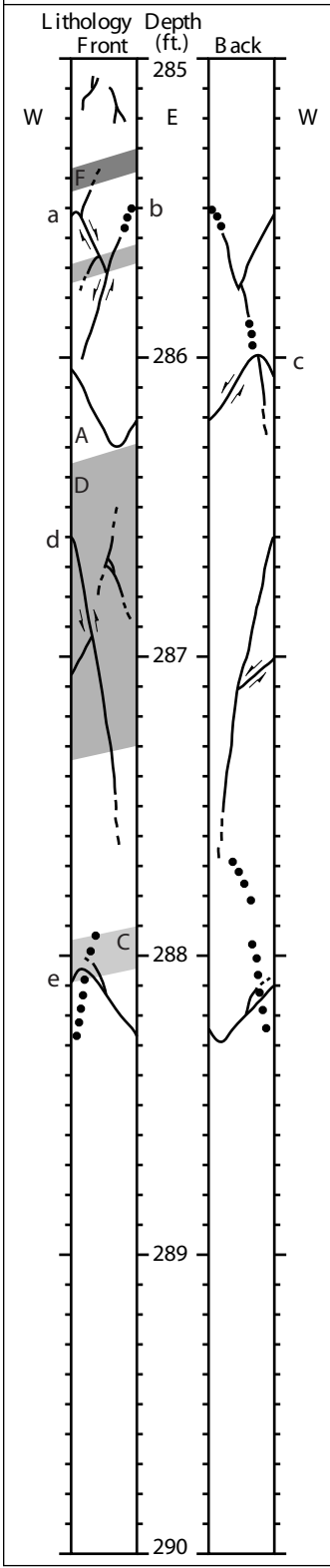

Apparent Disp. (mm)	Fault Thickness (mm)	Fault Strike	Fault Dip	Comments
				Bedding @ 285.4' : N20E 20NW [obtained from BHTV-log]
a=3 b=19	0.5 fg 1 fg	N5W N10W	62NE 69SW	
c=13	3 cg	N50E	57SE	Bedding @ 286.2' : N15E 20NW [obtained from BHTV-log]
d=17	1 mg	NS	85E	
				Bedding @ 287.0' : N30E 12NW
				Bedding @ 287.3' : N25E 26NW [obtained from BHTV-log]
e=?	2 cg	N25W	43NE	Bedding @ 288.1' : N52E 22NW [obtained from BHTV-log]
				Missing core from 288.8' - 289.35'
				Bedding @ 289.5' : N22E 21NW [obtained from BHTV-log]

Depth Interval: 290 - 295 Well: NNR - 4

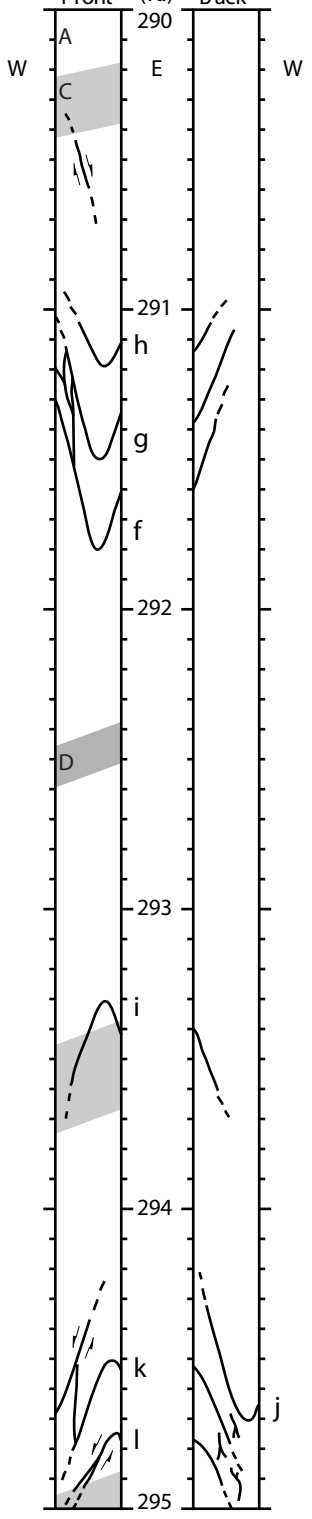

Apparent Disp. (mm)	Fault Thickness (mm)	Fault Strike	Fault Dip	Comments
				fault "h" correlates with 291.2' in
h=?	13 cg	N50E	56SE	BHTV-log
				fault "g" correlates with 291.9 in
g=?	12 cg	N65E	69SE	BHTV-log
				Run #32
				Score card: 291.6'
f=?	2 cg	N60E	72SE	291.6' - 301.6'
				Drilled: 10.0'
				Recovered: 9.95'
				Bedding @ 292.4' : N35E 20NW
i=?	0.5 mg	N35E	65NW	
				Bedding @ 293.8' : N52E 23NW
				[obtained from BHTV-log]
k=?	1 cg	N10E	62NW	
j=9	1 cg	N25E	67NW	
l=8	1 mg	N5E	60NW	

Depth Interval: 295 - 300 Well: NNR - 4

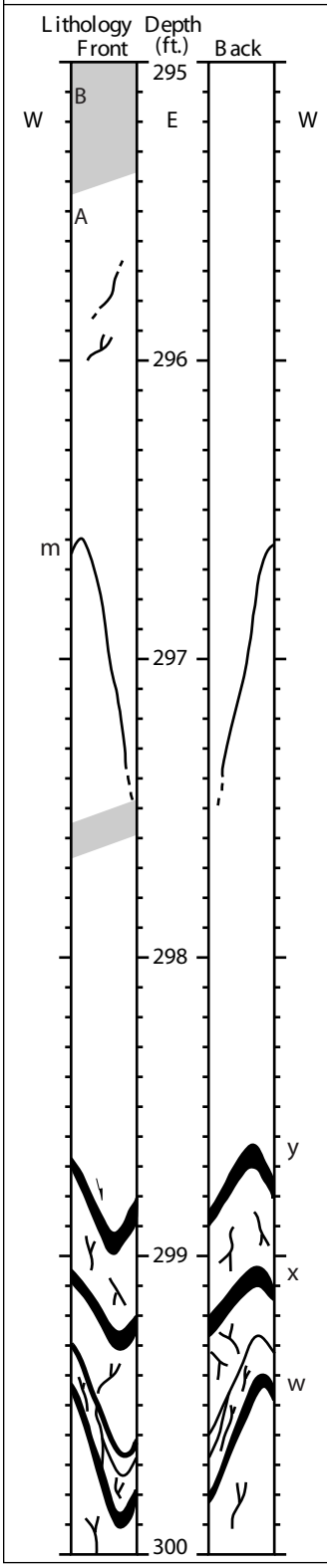

Apparent Disp. (mm)	Fault Thickness (mm)	Fault Strike	Fault Dip	Comments
				Bedding @ 295.8' : N45E 18NW [obtained from BHTV-log]
m=?	2 cg	N30W	78NE	
y=?	15 cg	N65E	60SE	fault "y" correlates with 298.6 in BHTV-log
x=?	10 cg	N45E	60SE	
w=?	5 cg	N35E	70SE	

Depth Interval: 300 - 305 Well: NNR - 4

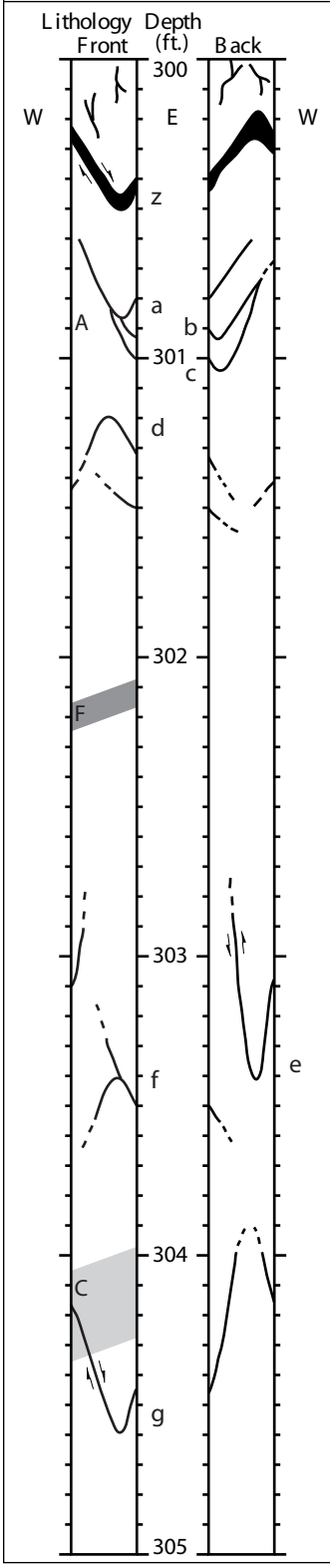

Apparent Disp. (mm)	Fault Thickness (mm)	Fault Strike	Fault Dip	Comments
z=?	15 clay	N50E	65SE	fault "z" correlates with 300.7' in BHTV-log
a=?	2 cg	N45E	52SE	
b=?	2 cg	N30W	39NE	
c=?	2 cg	N35W	46NE	
d=?	2 cg	N60E	63NW	
				Run # 33 Score card: 301.62' 301.6' - 311.6' Drilled: 10.0' Recovered: 9.9'
				Bedding @ 302.1' : N20W 20SW
				Bedding @ 303.7' : N10E 19NW [obtained from BHTV-log]
e=3	2 cg	N55E	83NW	
f=?	2 cg	N60W	54NE	
g=6	0.5 fg	N40E	74SE	

Depth Interval: 305 - 310 Well: NNR - 4

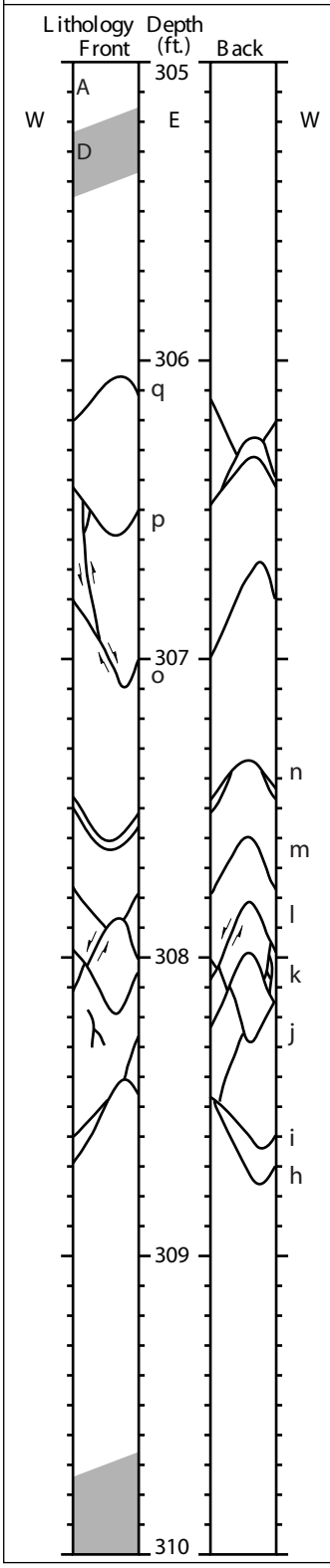

Apparent Disp. (mm)	Fault Thickness (mm)	Fault Strike	Fault Dip	Comments
				Bedding @ 305.4' : N20E 21NW Bedding @ 304.45' : N30E 15NW [obtained from BHTV-log]
q=?	1 cg	N40E	57NW	
p=?	4 cg	N45E	45SE	fault "p" correlates with 306.5' in BHTV-log
o=7	1 cg	N40E	63SE	fault "o" correlates with 307.1' in BHTV-log
n=?	2 cg	N65E	37SE	
m=?	1 cg	N70E	54SE	
l=11	1 cg	N70E	64SE	SE set is younger than NW set, but if interpretation is correct then SE set has a larger strike slip component
k=?	1 cg	N80E	66SE	
j=?	4 cg	N60E	68NW	
i=?	2 cg	N35E	42NW	fault "i" correlates with 308.2 in BHTV-log
h=?	2 cg	N40E	55NW	

Depth Interval: 310 - 315 Well: NNR - 4

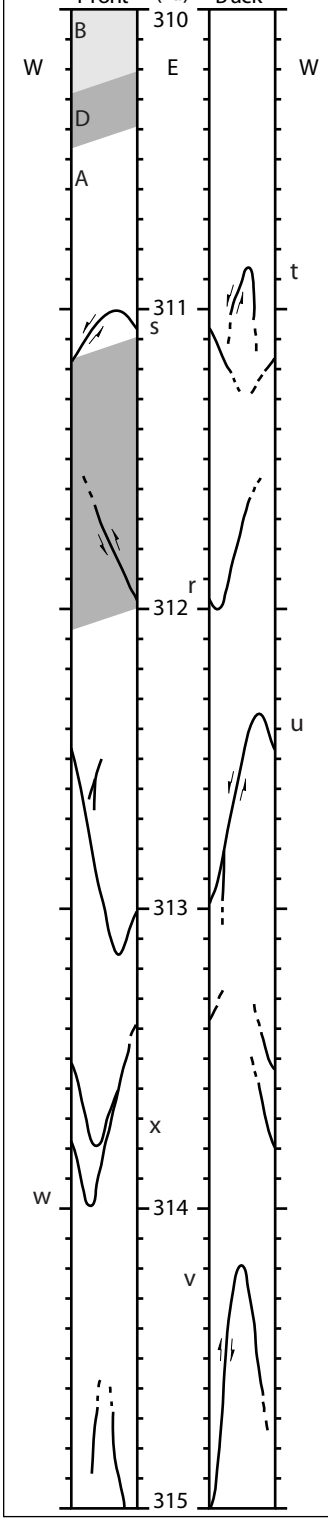

Apparent Disp. (mm)	Fault Thickness (mm)	Fault Strike	Fault Dip	Comments
				Bedding @ 310.7' : N30E 19NW
t=1	1 cg	N65E	82SE	
s=1	1 cg	N45E	57NW	Bedding @ 311.4' : N15E 23NW [obtained from BHTV-log]
				Run # 34 Score card: 311.4' 311.6' - 321.6' Drilled: 10.0' Recovered: 10.1'
r=3	0.5 fg	N20W	59NE	
u=9	2 cg	N40E	73SE	
x=?	2 cg	N65W	82SW	
w=?	2 cg	N40W	78SW	
v=13	2 cg	N80E	79SE	

Depth Interval: 315 - 320 Well: NNR - 4

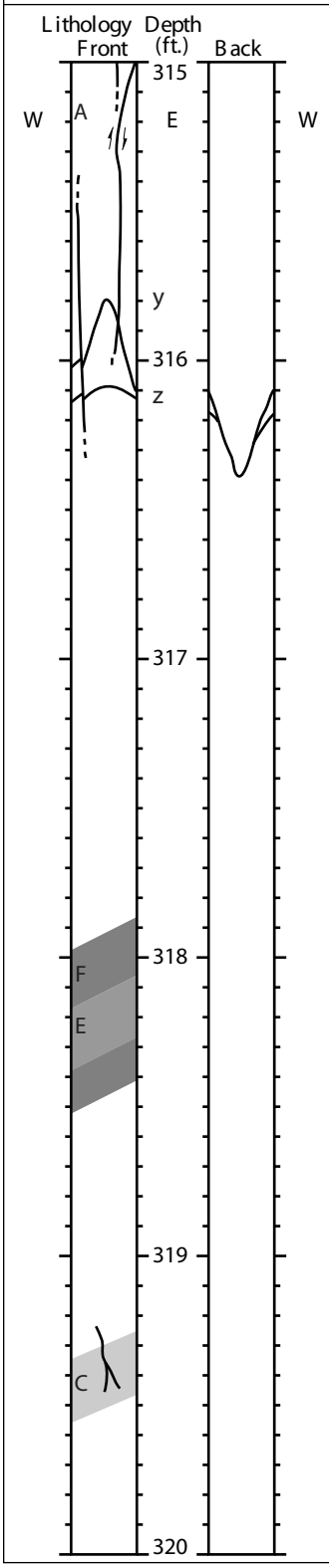

Apparent Disp. (mm)	Fault Thickness (mm)	Fault Strike	Fault Dip	Comments
				Bedding @ 315.9' : N25E 36NW [obtained from BHTV-log]
y=?	2 cg	N80E	66NW	Steep fault appears to be younger than y and z
z=?	2 cg	N70E	46NW	
				Bedding @ 316.4' : N25E 27NW
				Bedding @ 317.9' : NS 21W [obtained from BHTV-log]
				Bedding @ 319.5' : N25W 23SW
				Bedding @ 319.5' : N25W 24SW [obtained from BHTV-log]

Depth Interval: 320 - 325 Well: NNR - 4

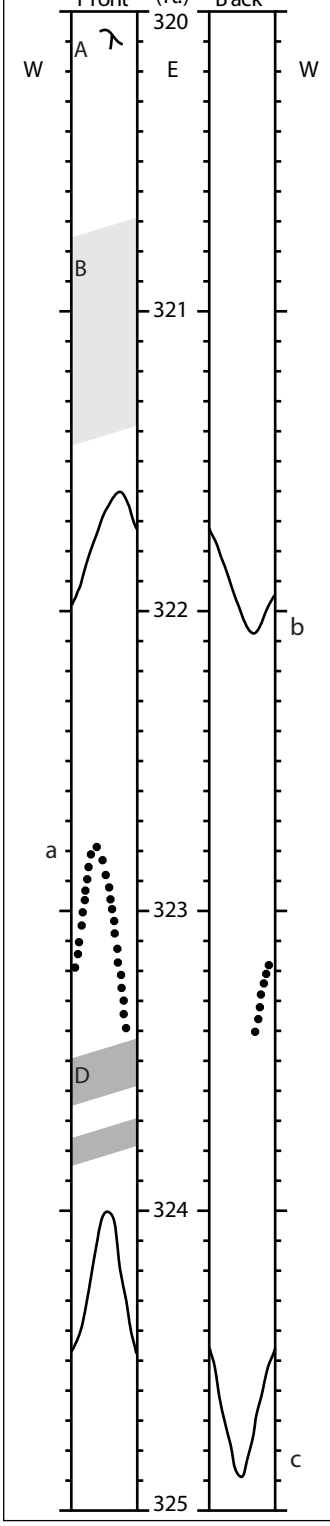

Apparent Disp. (mm)	Fault Thickness (mm)	Fault Strike	Fault Dip	Comments
				Bedding @ 321.3' : N20E 17NW
				Run # 35 Score card:321.55' 321.6' - 331.6' Drilled: 10.0' Recovered: ?
b=?	3 cg	N55E	58NW	fault "b" correlates with 321.5 in BHTV-log
a=?		N60W	74NE	joint "a" correlates with 322.5 in BHTV-log
				Bedding @ 323.8' : N22E 26NW [obtained from BHTV-log]
c=?	0.5 mg	N75W	74NE	

Depth Interval: 325 - 330 Well: NNR - 4

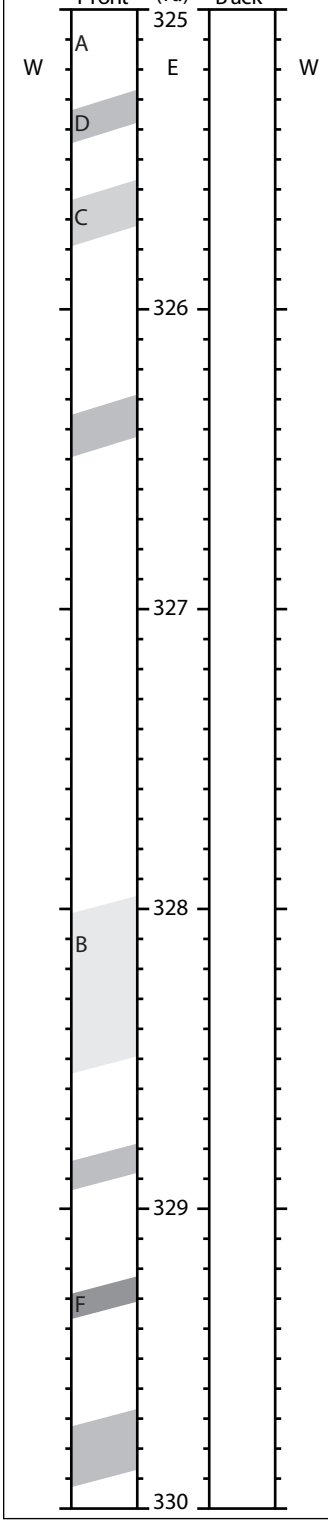

Apparent Disp. (mm)	Fault Thickness (mm)	Fault Strike	Fault Dip	Comments
				Missing core from 326.8' - 327.7'
				Bedding @ 327.8' : N20E 13NW [obtained from BHTV-log]
				Bedding @ 328.5' : N15E 15NW

Depth Interval: 330 - 335 Well: NNR - 4

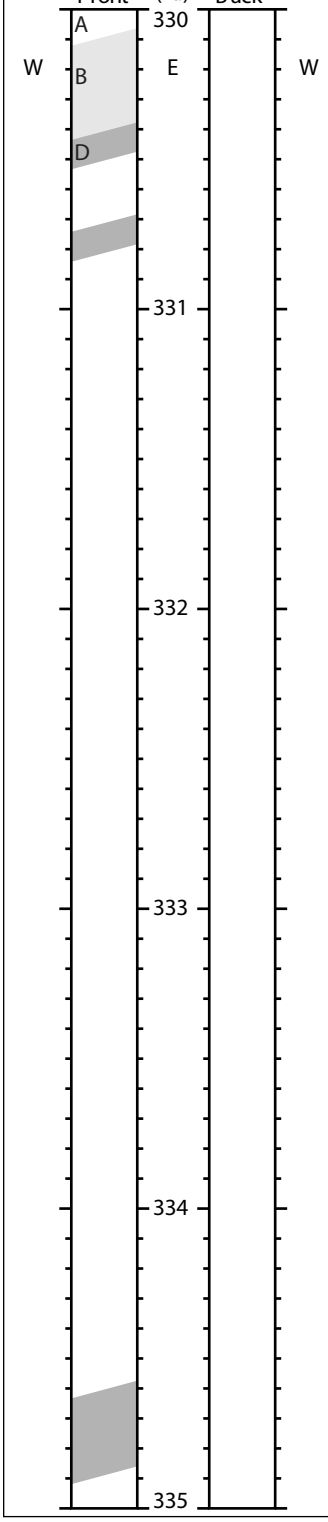

Apparent Disp. (mm)	Fault Thickness (mm)	Fault Strike	Fault Dip	Comments
				Run # 36 Score card: 331.6' 331.6' - 341.6' Drilled: 10.0' Recovered: 10.1'
				Bedding @ 333.6' : N7E 16NW [obtained from BHTV-log]

Depth Interval: 335 - 340 Well: NNR - 4

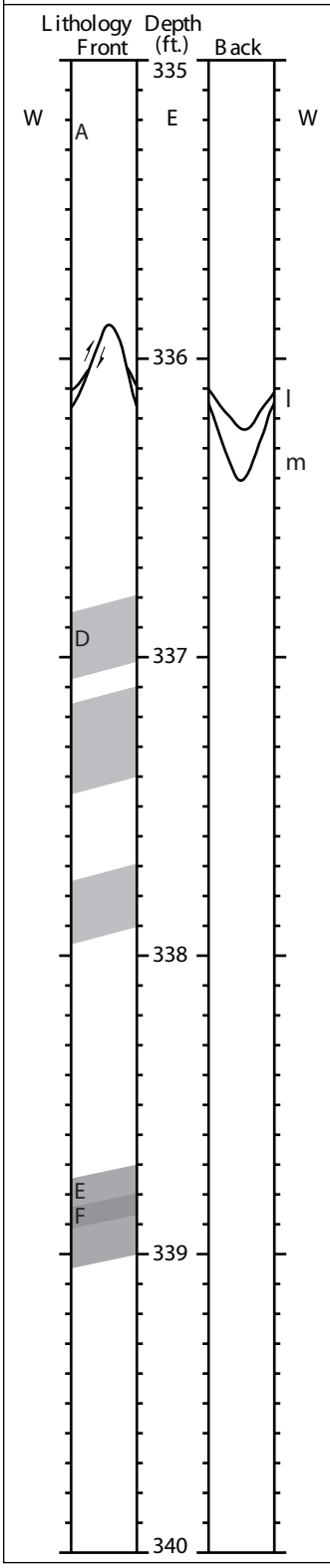

Apparent Disp. (mm)	Fault Thickness (mm)	Fault Strike	Fault Dip	Comments
l=4	1 cg	N70E	50NW	fault "l" and "m" correlate with 335.6 in BHTV-log
m=3	1 cg	EW	56N	
				Bedding @ 338.4' : N25W 12SW

Depth Interval: 340 - 345 Well: NNR - 4

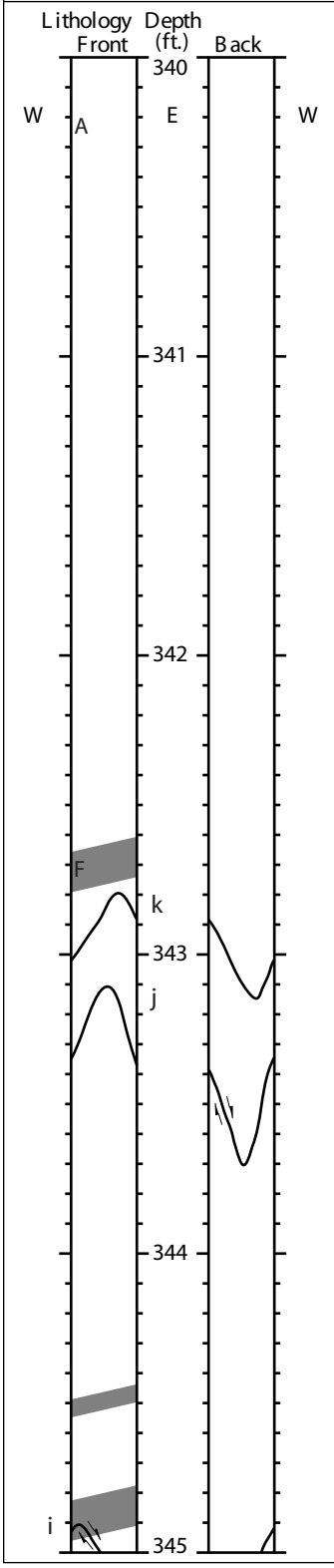

Apparent Disp. (mm)	Fault Thickness (mm)	Fault Strike	Fault Dip	Comments
				Bedding @ 340.2' : N18E 21NW [obtained from BHTV-log]
				Run # 37 Score card: 341.7' 341.6' - 351.6' Drilled: 10.0' Recovered: 10.1'
				Bedding @ 342.2' : NS 27W [obtained from BHTV-log]
				Bedding @ 342.7' : N20E 13NW
k=?	1 cg	N45E	54NW	
j=3	1 cg	N70E	61NW	
				Bedding @ 344.5' : N3E 17NW [obtained from BHTV-log]
i=7	0.5 clay	N10W	49NE	

Depth Interval: 345 - 350 Well: NNR - 4

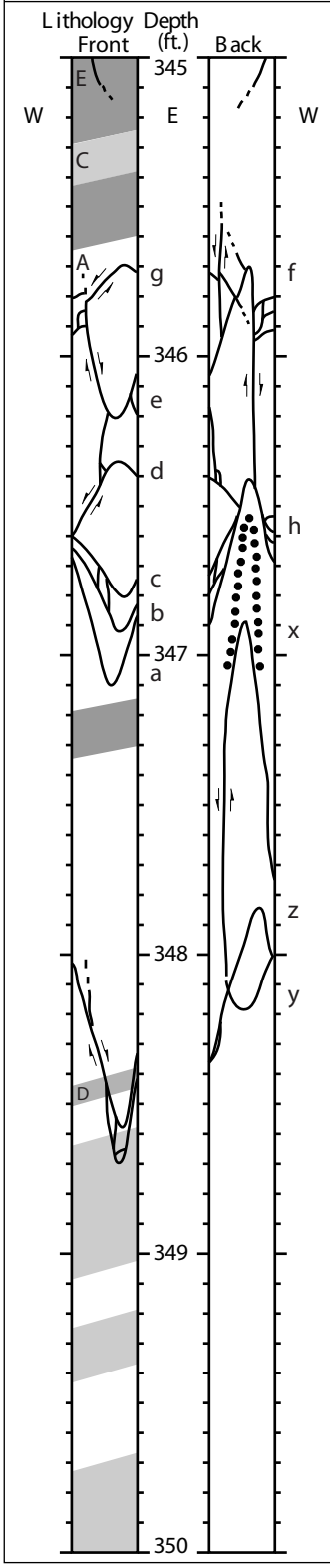

Apparent Disp. (mm)	Fault Thickness (mm)	Fault Strike	Fault Dip	Comments
				Bedding @ 345.8' : N30W 11SW
g=5	1 cg	N35E	43NW	"g" is older then steeper SE dipping fault, but younger than "f"
f=6	1 cg	N70E	82SE	
e=14	2 cg	N50E	59SE	fault "e" correlates with 346.6' in BHTV-log
d=17	2 cg	N50E	52NW	
h=?		N35E	81SE	"h" is a joint
c=?	1.5 fg	N30E	53SE	Very photogenic fault system
b=?	2 fg	N45E	61SE	
x=7	1 cg	N80E	86SE	
a=?	4 fg	N60E	76SE	fault "a" correlates with 347.3' in BHTV-log
z=11	1 cg	N45E	71SE	
y=?	0.5 cg	N85E	53NW	
				Bedding @ 348.4' : N10E 16NW
				Bedding @ 349.8' : N7E 23NW [obtained from BHTV-log]

Depth Interval: 350 - 355 Well: NNR - 4

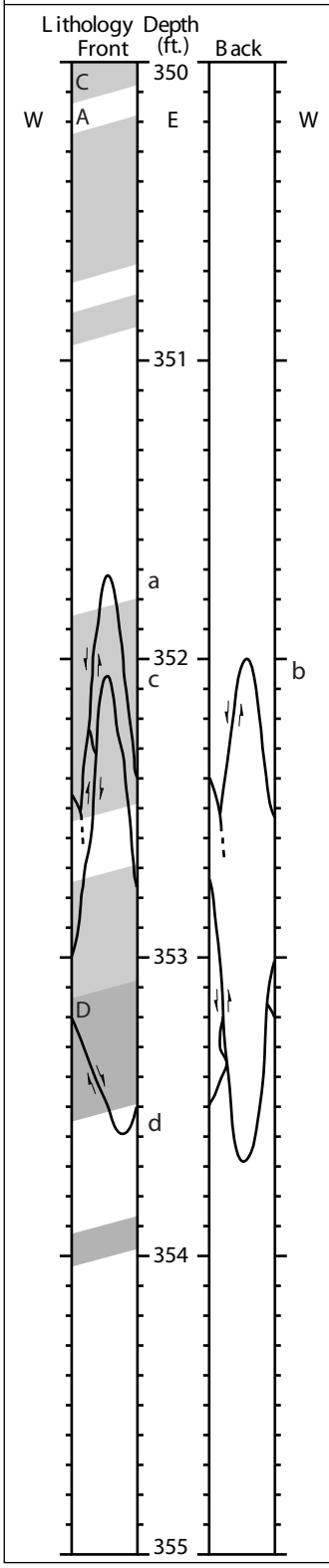

Apparent Disp. (mm)	Fault Thickness (mm)	Fault Strike	Fault Dip	Comments
				Bedding @ 351.0' : N30E 15NW
a=4	0.5 fg	N75E	79NW	Run # 38 Score card: 351.43' 351.6' - 361.6' Drilled: 10.0' Recovered: 10.0'
b=2	0.5 fg	N65E	75SE	Bedding @ 351.7' : N8E 25NW [obtained from BHTV-log]
c=3	0.5 fg	N80E	84NW	
				Bedding @ 352.7' : N3E 25NW [obtained from BHTV-log]
d=4	0.5 cg	N40E	57SE	
				Bedding @ 354.5' : N10W 18SW [obtained from BHTV-log]

Depth Interval: 355 - 360 Well: NNR - 4

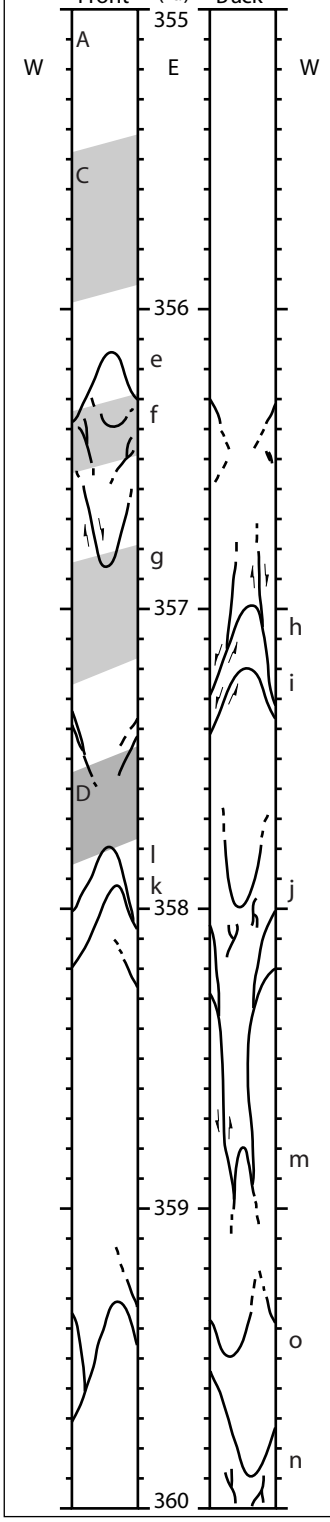

Apparent Disp. (mm)	Fault Thickness (mm)	Fault Strike	Fault Dip	Comments
e=?	0.5 mg	N75E	61NW	
f=?	1 mg	N70E	67SE	
g=2	2 cg	N80E	63SE	Bedding @ 356.95' : N35E 22NW
h>60	4 cg	N65E	62SE	fault "h" correlates with 356.6' in BHTV-log
i>80	4 cg	N70E	67SE	
l=?	1 cg	N80E	73NW	
k=?	1 cg	N55E	64NW	
j=?	1 cg	N80W	71NE	
m=?	1 cg	N85W	84SW	
o=?	0.5 cg	N40W	62NE	
n=?	2 cg	N60E	66NW	

Depth Interval: 360 - 365 Well: NNR - 4

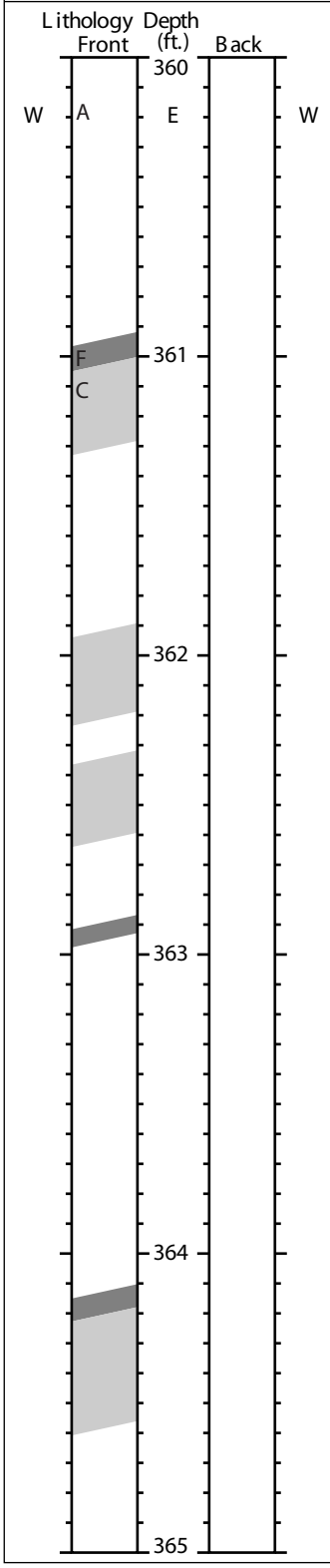

Apparent Disp. (mm)	Fault Thickness (mm)	Fault Strike	Fault Dip	Comments
				Bedding @ 360.1' : N3W 27SW [obtained from BHTV-log]
				Bedding @ 361.0' : N5E 12NW
				Run # 39 Score card: 361.64' 361.6' - 371.6' Drilled: 10.0' Recovered: 10.15'
				Bedding @ 364.1' : N10E 17NW [obtained from BHTV-log]

Depth Interval: 365 - 370 Well: NNR - 4

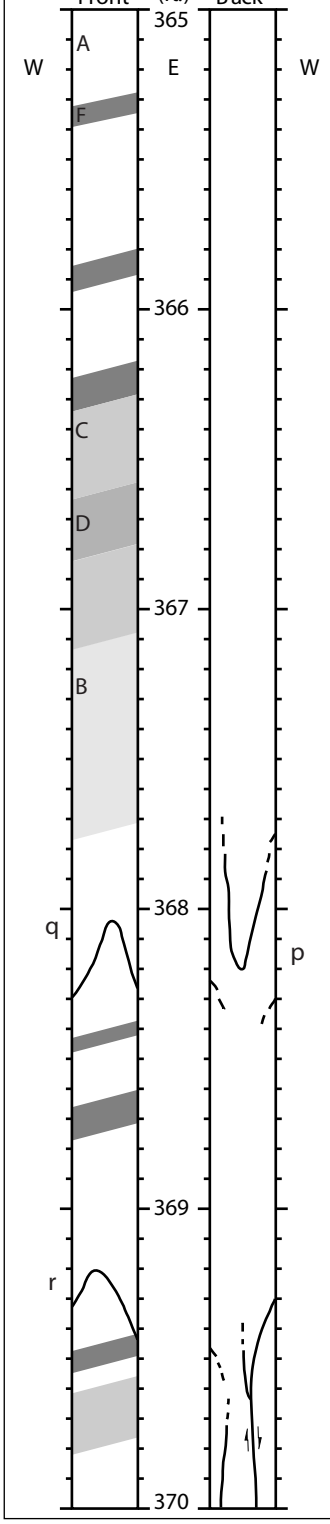

Apparent Disp. (mm)	Fault Thickness (mm)	Fault Strike	Fault Dip	Comments
				Bedding @ 365.9' : N15E 15NW
				Bedding @ 366.5' : N3E 15SW [obtained from BHTV-log]
q=?	1 cg	N70W	57NE	
p=?	2 cg	N75W	84NE	Bedding @ 368.3' : NS 15SW [obtained from BHTV-log]
r=?	1 cg	N60W	58NE	

Depth Interval: 370 - 375 Well: NNR - 4

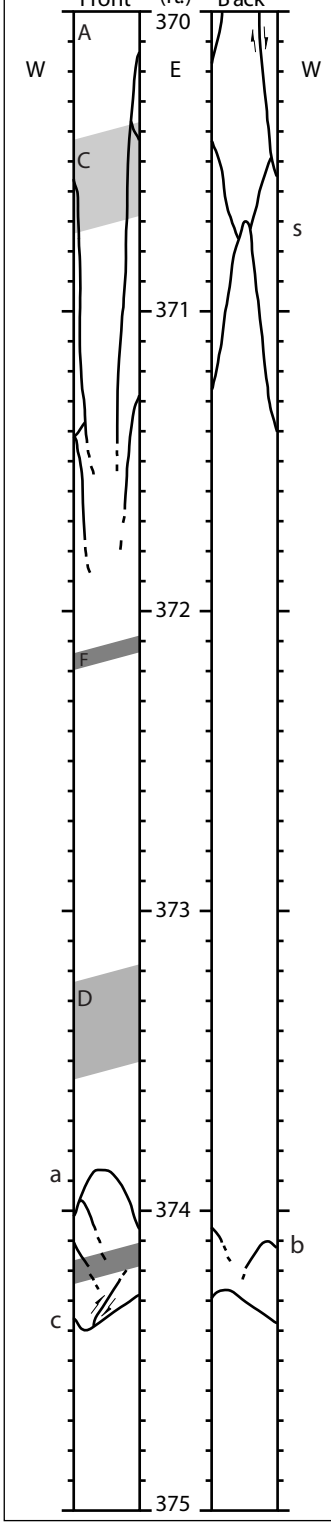

Apparent Disp. (mm)	Fault Thickness (mm)	Fault Strike	Fault Dip	Comments
s=?	1 cg	N80E	86SE	
				Run # 40 Score card: 371.71' 371.6' - 381.1' Drilled: 9.5' Recovered: 9.55'
				Bedding @ 373.5' : N30E 15NW
a=?	2 cg	N65W	46NE	Bedding @ 374.2' : N5W 15SW [obtained from BHTV-log]
b=?	3 cg	N5E	60SE	Missing core from 374.2' - 375.6'
c=?	2 cg	N20E	50NW	Fault "c" orientation was taken from previous strip map

Depth Interval: 375 - 380 Well: NNR - 4

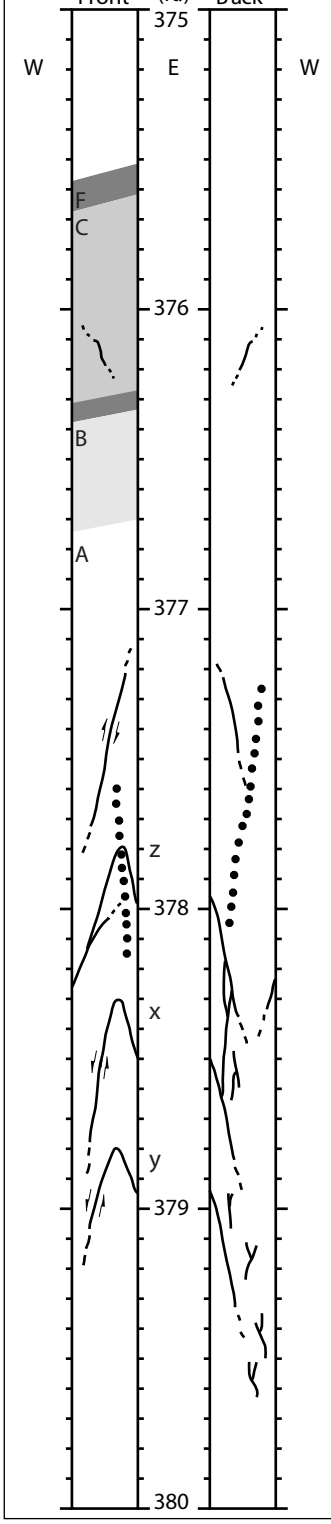

Apparent Disp. (mm)	Fault Thickness (mm)	Fault Strike	Fault Dip	Comments
				Bedding @ 376' : N10E 18NW [obtained from BHTV-log]
				Bedding @ 376.3' : N15W 11SW
				Bedding @ 376.4' : N15W 17SW [obtained from BHTV-log]
z=?	3 cg	N55E	75NW	
x=50	3.5 cg	N55E	73NW	
y=35	2 cg	N60E	67NW	

Depth Interval: 380 - 385 Well: NNR - 4

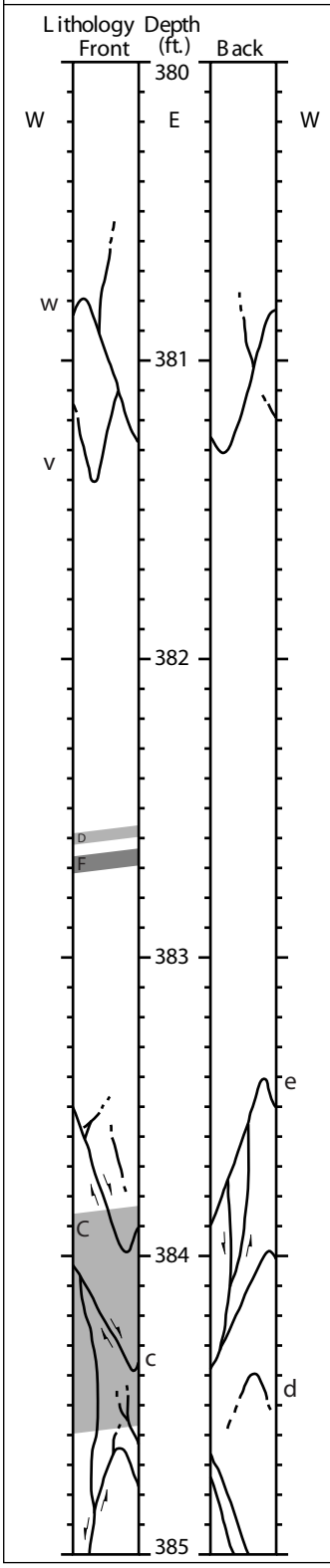

Apparent Disp. (mm)	Fault Thickness (mm)	Fault Strike	Fault Dip	Comments
w =?	3 cg	N25W	59NE	
				Missing core from 381.1' - 382.1'
				Run # 41 Score card: 381.1'
v=?	2 cg	N60W	80SW	381.1' - 391.1' Drilled: 10.0' Recovered: 9.9'
				Bedding @ 382.7' : N45W 7SW
e=19	2 cg	N20E	64SE	
c=21	1 fg	N5E	61SE	
d=?	0.5 fg	N60E	56SE	

Depth Interval: 385 - 390 Well: NNR - 4

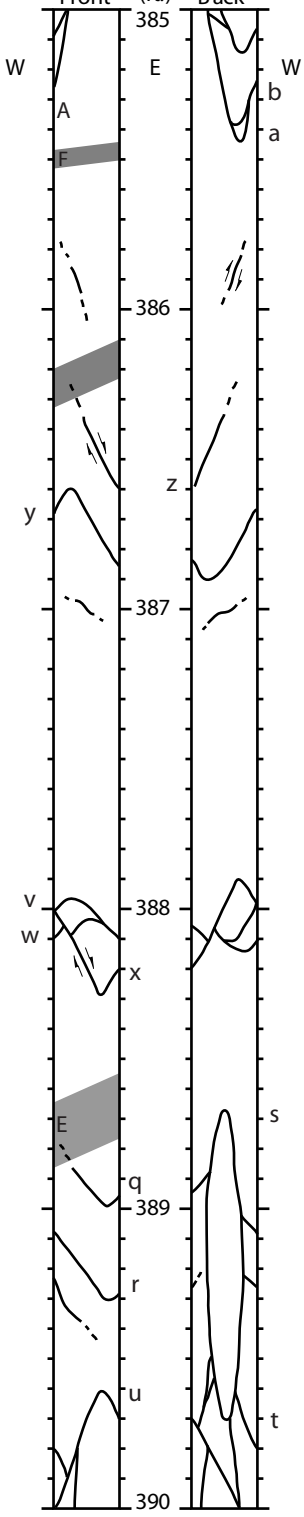

Apparent Disp. (mm)	Fault Thickness (mm)	Fault Strike	Fault Dip	Comments
b+a=44	1.5 mg	N50E	68NW	
	1.5 mg	N55E	71NW	fault "a" correlates with 385.4' in BHTV-log
				Bedding @ 386.2' : N30W 24SW
				Bedding @ 386.25' : N25W 30SW [obtained from BHTV-log]
z=11	1 mg	NS	59E	
y=?	1.5 cg	N35W	45NE	
v=?	4 cg	N35E	47NW	"x" is younger than "w" and "v"
w=?	9 cg	N50E	44NW	
x=24	4 cg	N40E	58SE	fault "x" correlates with 386.2' in BHTV-log
s=?	2 cg	N65E	87SE	
q=?	1 cg	N20E	47SE	
r=?	1 cg	N10E	52SE	
u=?	3 cg	N45E	59NW	fault "u" correlates with 389.6' in BHTV-log
t=?	2 cg	N75E	87NW	

Depth Interval: 390 - 395 Well: NNR - 4

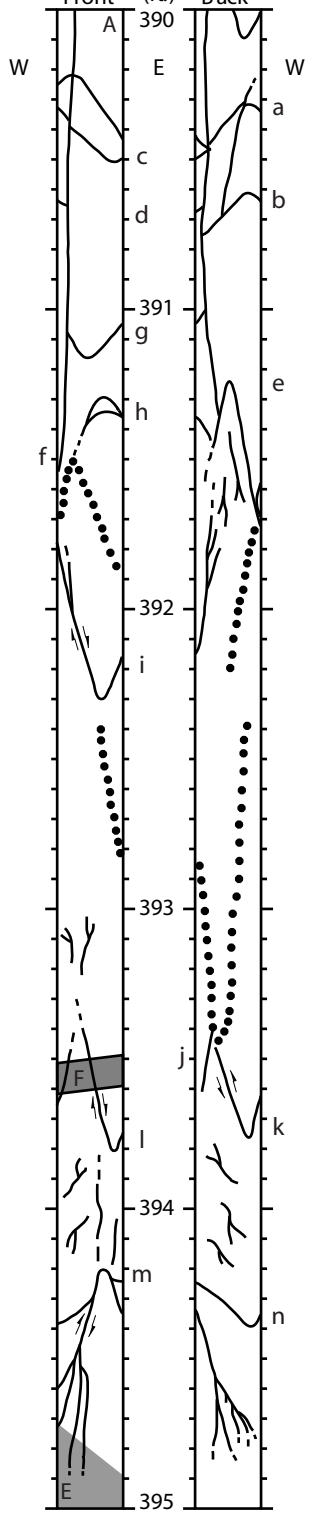

Apparent Disp. (mm)	Fault Thickness (mm)	Fault Strike	Fault Dip	Comments
a=?	2 cg	N25E	40SE	Bedding @ 390.3' : N35W 7SW
c=?	1 cg	N20E	31SE	
d=?	2 cg	N30E	37SE	
b=?	2 cg	N35E	49SE	
g=?	1 cg	N65E	51SE	
e=?	2 cg	EW	73S	
h=?	2 cg	N50E	54NW	
f=?		N45W	71NE	joint "f" correlates with 391' in BHTV-log
i>80	8 cg	N45E	73SE	fault "i" correlates with 392.8' in BHTV-log
j=?		N70W	84NE	
k=14	2 cg	N30E	73NW	
l=19	2 cg	N35E	77SE	
m=19	1.5 cg	N50E	75NW	fault "m" correlates with 394.5' in BHTV-log
n=?	3 cg	N10E	34NW	
				Bedding @ 394.7' : N38E 52SE [obtained from BHTV-log]
				Bedding @ 395.0' : N45E 39SE
				Nice example of bedding rotation

Depth Interval: 395 - 400 Well: NNR - 4

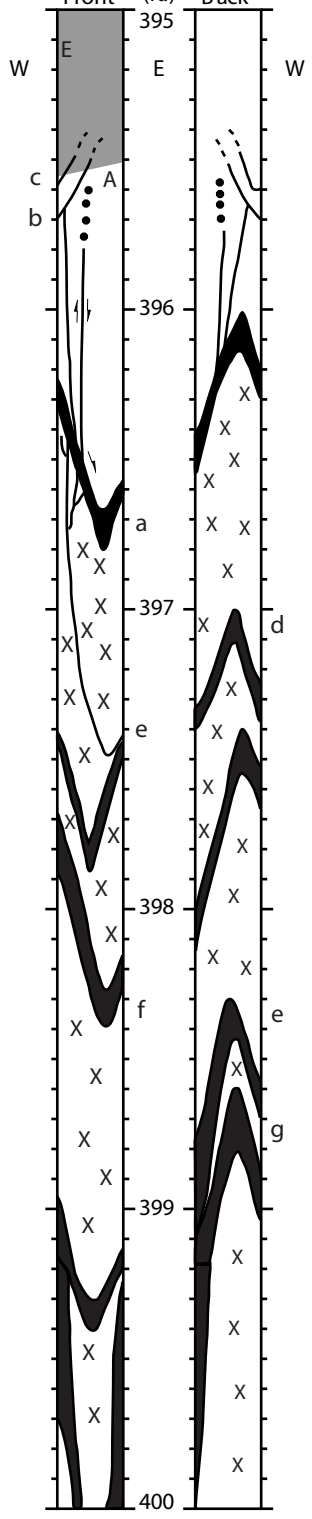

Apparent Disp. (mm)	Fault Thickness (mm)	Fault Strike	Fault Dip	Comments
c=?	1 cg	N5W	54SW	Bedding @ 395.55' : N80W 11SW
b=?	1 cg	NS	49W	
a=?	24 cg	N55E	77SE	fault "a" correlates with 395.7' in BHTV-log
d=?	10 cg	N80E	81SE	
e=?	4 cg	N40E	84SE	
f=?	10 cg	N50E	74SE	
e=?	10 cg	N70E	71SE	
g=?	10 cg	N65E	82SE	

Depth Interval: 400 - 405 Well: NNR - 4

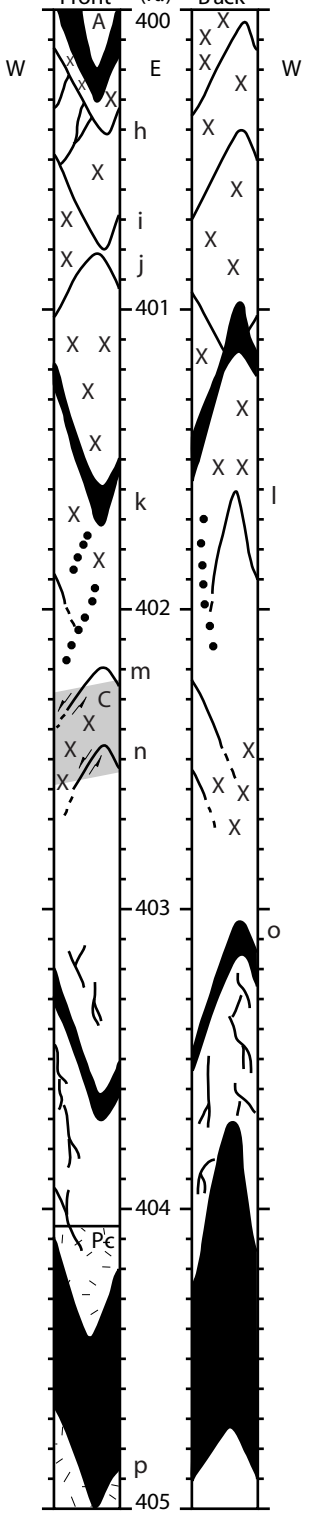

Apparent Disp. (mm)	Fault Thickness (mm)	Fault Strike	Fault Dip	Comments
				Rake = 62 NE for fault "h"
h>50		N35E	60SE	Run # 43 Score card: 400.4' 401.1' - 411.1' Drilled: 10.0' Recovered: 10.1'
i>50		N30E	64SE	
j=?	5 cg	N40E	60NW	
k=?	10 cg	N55E	69SE	
l>30		N55E	83SE	
m=24	2 fg	N40E	48NW	
n=18	2 fg	N35E	55NW	
o=?	40 cg	N45E	75SE	
				Bedding @ 403.5' : N23W 22NE [obtained from BHTV-log]
p=?	52 cg	N73E	77SE	Rake = 62 NE for fault "p"

APPENDIX B

In order to facilitate quantitative analysis of data recorded from the core and illustrated in strip maps, data were tabulated in a Microsoft Excel spread sheet. The data recorded within the spread sheet is outlined below and presented in the following pages.

Column 1…… Borehole in which structural element resides
Column 2…… Midpoint depth of structural element (ft)
Column 3…… Type of structural feature:
- f = fault
- j = joint
- f/j = faulted joint
- b= bedding

Column 4…… Minimum depth of fault, joint or faulted joint in borehole (ft)
Column 5…… Maximum depth of fault, joint or faulted joint in borehole (ft)
Columns 6 – 8….. Strike of structural feature (quadrant format)
Columns 9 – 10… Dip of structural feature
Column 11…….... Gouge thickness of small fault (mm)
Column 12…….... Sorting of protolith:
- 1 = Lower Middle Hickory
- 2 = Lower Hickory

Column 13…….... Grain Size of protolith:
- 1 = Very coarse grained (2 to 0.5 mm)
- 2 = Medium Grained (0.5 to 0.25 mm)
- 3 = Fine Grained (0.25 to 0.0625 mm)
- 4 = Mudstone (< 0.0625 mm)

Column 14…….... Displacement magnitude (mm)
Column 15…….... Estimated displacement (mm)
Column 16…….... Displacement direction
- n = normal
- r = reverse

Column 17…….... Slip striae (trend and plunge)
Column 18…….... Notes
- Cross-cutting relationships
- BHTV-log correlation points
- Bedding attitudes determined from BHTV-logs

GKR-5	24.15	j	24.20	24.20										
GKR-5	28.40	j	28.20	28.60										
GKR-5	49.20	f	49.10	49.30	N	70	E	36	NW	0.50		1.50		n
GKR-5	49.60	b						12	W					
GKR-5	50.40	f	50.35	50.45	N	0	S	46	E	0.50		2.50		n
GKR-5	50.70	f	50.60	50.80	N	30	W	51	NE	0.50		2.50		r
GKR-5	50.83	f	50.65	51.00	N	0	S	56	E	0.50		2.50		r
GKR-5	50.85	f	50.80	50.90	N	20	W	53	NE	0.50		2.50		r
GKR-5	51.60	f	51.30	51.90	N	0	S	63	E	0.50		13.00		r
GKR-5	52.00	f	51.95	52.05	N	70	W	44	NE	0.50			0.50	
GKR-5	52.13	f	52.05	52.20	N	10	E	32	SE	0.50		1.00		n
GKR-5	52.30	b						12	W					
GKR-5	56.30	f	56.10	56.50	N	70	E	47	NW	1.00		2.50		r
GKR-5	58.78	f	58.60	58.95	N	80	E	52	NW	1.00			10.63	
GKR-5	59.00	b						17	W					
GKR-5	60.48	j	60.25	60.70	N	40	W	65	NE					
GKR-5	61.25	f	61.20	61.30	N	70	E	20	SE	1.00			8.17	
GKR-5	61.55	f	61.50	61.60	N	20	W	51	SW	1.00			9.77	
GKR-5	61.63	f	61.60	61.65	N	70	W	9	SW	2.50			43.65	
GKR-5	61.80	f	61.70	61.90	N	30	W	40	SW	1.00			4.18	
GKR-5	64.10	b						11	W					
GKR-5	64.63	f	64.40	64.85	N	70	W	62	NE	0.50		5.00		n
GKR-5	64.70	f	64.50	64.90				71	NE	0.50			5.82	r
GKR-5	74.25	f	74.20	74.30	N	10	E	15	SE	0.50		5.00		n
GKR-5	74.85	j	74.75	74.95	N	10	W	54	NE					
GKR-5	75.00	j	74.85	75.15	N	10	E	76	SE					
GKR-5	75.40	b						21	W					
GKR-5	79.98	j	79.80	80.15	N	10	W	56	NE					
GKR-5	80.80	j	80.70	80.90	N	20	E	60	NW					
GKR-5	81.55	j	81.50	81.60	N	50	E	27	SE					
GKR-5	83.20	j	83.10	83.30	N	0	S	37	E					
GKR-5	83.80	b						20	W					
GKR-5	84.93	f	84.80	85.05	N	50	E	41	NW	1.00		5.00		n
GKR-5	85.80	j	85.50	86.10	N	20	W	72	NE					

GKR-5	85.90	f	85.80	86.00	N	60	E	58	NW	2.50			16.77		
GKR-5	86.40	b						20	W						
GKR-5	90.25	f	90.10	90.40	N	40	E	46	SE	2.50		5.00		n	
GKR-5	90.33	f						52	SE					n	
GKR-5	90.53	f	90.45	90.60	N	10	W	27	NE	1.00		13.00		n	
GKR-5	90.58	f	90.50	90.65	N	0	S	27	E	1.00		25.40		n	
GKR-5	90.75	f	90.70	90.80	N	40	W	28	NE	2.50		7.50		n	
GKR-5	90.83	f	90.75	90.90	N	20	E	36	SE						
GKR-5	91.00	f	90.80	91.20	N	40	E	62	SE	2.50		1.00		n	
GKR-5	91.50	b						22	W						
GKR-5	91.68	f	91.60	91.75	N	10	E	33	SE						
GKR-5	92.80	f	92.25	93.35	N	50	E	67	SE	0.50	1	2.50		r	
GKR-5	92.80	f	92.40	93.20	N	60	E	56	NW	0.50	1	2.50			
GKR-5	93.00	f	92.05	93.95	N	50	E	61	NW	0.50	1	5.00		n	
GKR-5	94.90	f	94.80	95.00	N	10	W	54	NE	0.50	1	10.00		n	
GKR-5	95.03	f	95.05	95.05	N	20	E	82	SE	0.50	1	30.50		r	
GKR-5	95.08	f	95.35	96.70	N	20	E	57	NW	2.50	1	15.00		n	348, 39
GKR-5	95.80	f	95.50	96.10	N	40	E	70	NW	1.00	1	7.50		n	
GKR-5	95.85	f	95.60	96.10	N	40	E	72	NW	1.00	1	10.00		n	
GKR-5	96.00	f	95.35	96.80	N	20	E	53	NW	2.50	1	28.00		n	357, 28
GKR-5	97.30	b						8	W						
GKR-5	97.90	f	97.50	98.30	N	70	E	71	NW	0.50	1	2.50		n	
GKR-5	98.00	f	97.70	98.30	N	80	E	67	NW	0.50	1	2.50		n	
GKR-5	98.25	f	98.15	98.35	N	80	E	55	NW	0.50	1		8.66		
GKR-5	99.00	f								2.00	1		9.86		
GKR-5	100.20	f								1.00	1		8.44		
GKR-5	101.68	f	101.60	101.75				31	NW		1				
GKR-5	102.50	b						20	W						
GKR-5	103.28	f	103.15	103.40	N	50	E	48	SE	2.50	1	25.40		n	
GKR-5	105.80	b						8	W						
GKR-5	111.05	b						24	W						
GKR-5	111.63	f	111.45	111.80	N	40	E	46	SE	1.00	1	28.00		n	
GKR-5	115.40	b						14	W						
GKR-5	116.85	f	116.70	117.00	N	20	E	61	SE	2.50	1	15.00		n	

GKR-5	119.83	f	119.75	119.90	N	50	W	25	SW	0.50	1	7.50		n	289, 9
GKR-5	120.30	f	119.90	120.70	N	50	E	76	SE	0.50	1	13.00		n	
GKR-5	120.93	f	120.80	121.05	N	60	W	47	SW	0.50	1	5.00		n	
GKR-5	121.45	f	121.30	121.60	N	80	E	50	NW	0.50	1	20.00		n	
GKR-5	122.40	b						14	W						
GKR-5	123.40	j	122.90	123.90	N	10	W	74	NE						
GKR-5	123.73	f	123.45	124.00	N	70	E	63	NW	1.00	1	7.50		n	
GKR-5	124.50	f	124.30	124.70	N	40	E	63	SE	2.50	1	2.50		n	
GKR-5	124.90	j	124.80	125.00	N	0	S	75	E						
GKR-5	125.65	f	125.40	125.90	N	70	E	67	SE	1.00	1	20.00		n	
GKR-5	125.90	f	125.70	126.10	N	40	E	66	SE	1.00	1	13.00		n	
GKR-5	126.20	f	126.00	126.40	N	10	E	63	SE	cum 5	1	cum 61		n	
GKR-5	126.23	f	126.05	126.40	N	20	E	59	SE	cum 5	1	cum 61		n	
GKR-5	126.58	f	126.45	126.70	N	10	W	51	NE	0.50	1	5.00		n	
GKR-5	126.60	f	126.45	126.75	N	10	W	45	NE	0.50	1	5.00		n	
GKR-5	126.73	f	126.50	126.95	N	50	E	68	SE	1.00	1	35.50		n	93, 59
GKR-5	127.15	f	127.00	127.30	N	40	W	45	NE	2.50	1	5.00		n	
GKR-5	127.20	f						57	NE		1				
GKR-5	127.23	f	127.15	127.30	N	30	W	34	NE	2.50	1	2.00		n	
GKR-5	127.35	f	127.15	127.55	N	30	W	58	NE	2.50	1	5.00		n	
GKR-5	127.70	b						14	W						
GKR-5	128.10	f	128.00	128.20	N	0	S	70	E		1	2.00		n	
GKR-5	128.20	f	128.00	128.40	N	0	S	68	E		1	2.00		n	
GKR-5	128.60	f	128.50	128.70	N	20	W	40	NE	2.50	1		35.48		
GKR-5	129.20	f								1.00	1		18.27		
GKR-5	129.80	f	129.60	130.00	N	30	E	57	SE	1.00	1	2.50		n	
GKR-5	129.85	f	129.65	130.05	N	30	E	72	SE	1.00	1		9.24		
GKR-5	130.80	b						18	W						
GKR-5	131.60	f	131.40	131.80	N	0	S	72	E	0.50	1	cum 13		r	
GKR-5	131.80	f	131.60	132.00	N	10	W	63	NE	0.50	1	cum 13		r	
GKR-5	132.08	j	132.00	132.15	N	50	W	44	NE						
GKR-5	132.20	f	132.00	132.40	N	30	E	64	SE	2.50	1		14.40		
GKR-5	132.60	f	132.15	133.05	N	20	E	80	SE	2.50	1		9.11		
GKR-5	133.00	f								4.00	1	43.00		r	

GKR-5	133.35	f	133.10	133.60	N	20	E	59	SE	2.50	1		19.52	
GKR-5	133.35	f	133.20	133.50	N	20	E	51	SE	1.00	1		2.37	
GKR-5	133.80	f	133.45	134.15	N	10	E	83	SE	0.50	1	5.00		r
GKR-5	135.05	f	134.85	135.25	N	40	E	54	SE	2.50	1		33.63	
GKR-5	135.08	f	134.90	135.25	N	20	E	50	SE	2.50	1		26.78	
GKR-5	135.10	f	135.00	135.20	N	20	E	50	SE	2.50	1	25.50		n
GKR-5	135.35	f	135.25	135.45	N	0	S	49	E	1.00	1	10.00		n
GKR-5	135.55	f	135.30	135.80	N	50	E	70	SE	1.00	1	76.00		n
GKR-5	135.63	f	135.35	135.90	N	50	E	77	SE	1.00	1	10.00		n
GKR-5	136.63	f	136.05	137.20	N	40	E	68	SE	51.00	1		964.89	
GKR-5	137.30	b						20	W					
GKR-5	137.65	f	137.50	137.80	N	80	E	42	NW	0.50	1		1.03	
GKR-5	139.60	f	139.50	139.70	N	70	W	48	NE	1.00	1		6.86	
GKR-5	139.63	f	139.50	139.75	E	90	W	51	N	1.00	1		9.38	
GKR-5	139.65	f	139.50	139.80	N	80	W	53	SW	1.00	1		8.06	
GKR-5	140.60	f									1	3.00		
GKR-5	141.60	f	141.50	141.70	N	70	E	40	NW	2.50	1		25.28	
GKR-5	141.70	f	141.60	141.80	N	40	E	43	NW	2.50	1	1.00		r
GKR-5	142.30	b						20	W					
GKR-5	143.00	f	142.90	143.10	N	50	E	50	SE	2.50	1		30.04	
GKR-5	143.10	f						80	SE		1			
GKR-5	143.50	f	143.15	143.85	N	50	E	61	SE	2.50	1		18.18	
GKR-5	144.40	f	144.25	144.55	E	90	W	67	N	0.50	1	10.00		n
GKR-5	144.70	f	144.60	144.80	N	80	W	37	NE	1.00	1	7.50		
GKR-5	144.78	f	144.70	144.85	N	80	W	34	NE	0.50	1	5.00		n
GKR-5	145.50	j	145.30	145.70	N	20	E	76	SE					
GKR-5	146.50	b						18	W					
GKR-5	150.03	f	149.90	150.15	N	20	E	47	SE	0.50	1	5.00		n
GKR-5	150.20	j												
GKR-5	153.10	f								0.50	1		13.51	
GKR-5	153.90	f								0.50	1		9.09	
GKR-5	154.80	b						14	W					
GKR-5	155.70	f	155.25	156.15	N	40	E	78	SE	1.00	1		8.55	
GKR-5	155.80	f								1.00	1	2.50		n

GKR-5	155.90	f	155.85	155.95	N	30	E	47	SE	0.50	1	2.50		n	
GKR-5	156.63	f	156.50	156.75	N	10	E	56	SE		1	>50		n	55, 45
GKR-5	156.90	f	156.60	157.20	N	60	E	60	NW	2.50	1	94.00		r	
GKR-5	157.35	f	157.30	157.40	N	80	E	61	NW	0.50	1	1.00		n	
GKR-5	157.53	f	157.35	157.70	N	80	E	61	NW	0.50	1	1.00		n	
GKR-5	157.60	f	157.50	157.70	N	80	E	59	NW	0.50	1	1.00		n	
GKR-5	157.98	f	157.75	158.20	N	80	E	60	NW	1.00	1	cum 2.5		n	
GKR-5	158.03	f	157.85	158.20	N	80	E	61	NW	1.00	1	cum 2.5		n	
GKR-5	158.10	f	157.95	158.25	N	80	E	60	NW	1.00	1		9.52		
GKR-5	159.20	b						10	W						
GKR-5	159.30	f	159.20	159.40	N	10	E	72	NW	0.50	1	2.50		n	
GKR-5	161.80	f	161.30	162.30	N	45	W	82	NE	0.50	1	2.50		r	
GKR-5	163.20	b						10	W						
GKR-5	163.20	f						86	NE		1	6.00		r	
GKR-5	163.70	f	163.40	164.00	N	5	W	85	NE	0.50	1	2.00		r	
GKR-5	164.10	f	163.95	164.25	N	0	S	63	E	0.50	1	1.00		n	
GKR-5	164.20	f						79	NE		1			r	
GKR-5	164.28	f	164.15	164.40	N	5	E	52	SE	2.00	1	2.50		n	
GKR-5	164.45	f						82	NE		1			r	
GKR-5	164.85	f	164.70	165.00	N	0	S	60	E	0.50	1	2.50		n	
GKR-5	165.30	b						13	W						
GKR-5	165.30	f								0.50	1	0.50		r	
GKR-5	165.95	f	165.80	166.10	N	30	E	62	NW	0.50	1	2.50		n	
GKR-5	166.80	f	166.50	167.10	N	30	E	65	NW	cum 35.5	1	cum 30.5		n	
GKR-5	166.80	f	166.60	167.00	N	30	E	64	NW	cum 35.5	1	cum 30.5		n	
GKR-5	166.90	f	166.70	167.10	N	50	E	70	SE	0.50	1	2.50		r	
GKR-5	169.70	f	169.50	170.00	N	10	E	76	SE	1.00	1	cum 10		n	
GKR-5	169.75	f	169.50	170.00	N	50	E	62	SE	1.00	1	cum 10		n	
GKR-5	171.20	b						16	W						
GKR-5	175.90	b						15	W						
GKR-5	178.40	b						17	W						
GKR-5	179.10	f	179.00	179.20	N	85	E	63	NW	0.50	1		5.82		
GKR-5	179.25	f	179.10	179.40	N	80	W	75	NE	0.50	1	2.00		r	
GKR-5	179.55	f	179.45	179.65	N	60	W	60	NE	0.50	1		1.26		

GKR-5	181.35	j	181.00	181.70	N	10	W	15	NE						
GKR-5	181.70	f						76	SE		1				
GKR-5	181.75	f	181.60	181.90	N	40	E	32	SE	0.50	1	10.00		n	
GKR-5	182.05	f						78	SE		1	4.00		r	
GKR-5	182.38	f	182.25	182.50	N	60	E	36	SE		1	>50			115, 30
GKR-5	183.75	f	183.50	184.00	N	30	W	52	NE	0.50	1	0.50		r	
GKR-5	184.10	f	184.05	184.15	N	30	W	61	NE	0.50	1		1.17		
GKR-5	184.60	b						17	W						
GKR-5	185.05	f	185.00	185.10	N	30	E	26	SE	0.50	1	5.00		n	
GKR-5	185.25	f						61	SE		1			r	
GKR-5	185.48	f	185.40	185.55	N	32	E	29	SE	0.50	1	4.00		n	
GKR-5	186.38	f	186.10	186.65	N	0	S	70	E	1.00	1	18.00		r	
GKR-5	187.10	b						17	W						
GKR-5	187.85	f	187.70	188.00	E	90	W	65	N	0.50	1		7.65		
GKR-5	188.20	f	188.00	188.40	N	80	E	71	NW	0.50	1	1.00		n	
GKR-5	188.58	f	188.50	188.65	N	10	W	40	NE	2.50	1	7.50		n	
GKR-5	188.81	f	188.51	189.10	N	10	W	74	NE	2.50	1	cum 23		r	
GKR-5	188.88	f	188.65	189.10	N	20	W	21	NE	1.00	1	cum 23		r	
GKR-5	188.98	f	188.80	189.15	N	0	S	64	E	2.50	1	7.50		r	
GKR-5	189.83	f	189.65	190.00	N	15	E	65	SE	0.50	1		3.73	r	
GKR-5	189.85	f	189.65	190.05	N	15	E	68	SE	1.00	1	2.50		r	
GKR-5	190.05	f	189.90	190.20	N	0	S	46	E	0.50	1		0.71	r	
GKR-5	190.10	f	190.00	190.20	N	5	E	56	SE	0.50	1	cum 5		n	
GKR-5	190.15	f	190.00	190.30	N	5	W	59	NE	0.50	1	cum 5		n	
GKR-5	190.33	f	190.20	190.45	N	20	E	42	SE	0.50	1	5.00		n	
GKR-5	192.50	b						16	W						
GKR-5	195.80	f	195.70	195.90	N	0	S	56	E	0.50	1		3.56		
GKR-5	195.95	j	195.70	196.20	N	10	W	67	NE						
GKR-5	196.05	j	195.90	196.20	N	10	E	55	SE						
GKR-5	196.80	b						23	W						
GKR-5	199.10	b						17	W						
GKR-5	199.85	f	199.65	200.05	N	20	E	54	SE	0.50	2	1.00		n	
GKR-5	201.30	f	201.20	201.40	N	30	E	40	SE		2	>30		n	77, 27
GKR-5	201.33	f	201.25	201.40	N	10	E	35	SE	0.50	2	7.50		n	

GKR-5	201.80	f	201.70	201.90	N	0	S	40	E	1.00	2		0.95	n
GKR-5	202.00	f	201.90	202.10	N	20	W	40	NE	0.50	2	4.00		n
GKR-5	203.40	f	203.20	203.60	N	20	W	75	NE	0.50	2		10.65	
GKR-5	203.50	b						17	W					
GKR-5	206.25	f	206.10	206.40	N	20	E	59	SE	2.00	2		2.53	
GKR-5	207.40	f								2.50	2		36.00	
GKR-5	208.10	b						20	W					
GKR-5	208.50	f								1.00	2	10.00		n
GKR-5	210.10	f	209.70	210.50	N	40	E	76	NW	0.50	2		19.21	
GKR-5	214.80	b						18	W					
GKR-5	216.30	b						16	W					
GKR-5	218.75	f	218.40	219.10	N	10	E	80	SE	2.00	2	7.50		n
GKR-5	223.60	b						17	W					
GKR-5	223.80	f	223.65	223.95	N	0	S	51	E	2.00	2	13.00		n
GKR-5	223.83	f	223.70	223.95	N	10	E	50	SE	2.00	2		18.41	n
GKR-5	224.35	f	224.10	224.60	N	10	W	61	SW	2.00	2		7.63	
GKR-5	224.40	f	224.00	224.80	N	20	E	63	SE	2.00	2		1.80	
GKR-5	224.85	f	224.70	225.00	N	10	E	53	SE	2.00	2		18.25	
GKR-5	224.90	f	224.80	225.00	N	0	S	52	E	2.00	2		5.08	
GKR-5	225.18	f	224.95	225.40	N	0	S	56	E	2.00	2		16.55	
GKR-5	226.30	b						16	W					
GKR-5	226.50	f	226.20	226.80	N	50	E	45	SE	0.50	2		10.08	
GKR-5	229.70	f	229.50	229.90	N	50	E	45	SE	1.00	2	2.50		n
GKR-5	230.10	f	229.90	230.30	N	0	S	64	E	1.00	2	2.50		n
GKR-5	230.70	b						14	W					
GKR-5	233.90	f								1.00	2		6.11	
GKR-5	235.10	f	234.90	235.30	N	15	W	60	NE	1.00	2	1.00		r
GKR-5	235.70	f	235.40	236.00	N	0	S	67	E	1.00	2	2.50		r
GKR-5	235.90	f	235.80	236.00	N	10	W	50	SW	1.00	2		1.97	
GKR-5	238.90	f	238.80	239.00	N	70	E	52	NW	0.50	2		6.50	
GKR-5	239.40	b						19	W					
GKR-5	239.55	f	239.50	239.60	N	50	W	14	NE	0.50	2		5.32	
GKR-5	239.95	f	239.90	240.00	E	90	W	40	N	0.50	2		1.85	
GKR-5	240.60	f	240.00	241.20	E	90	W	75	S	19.00	2		225.82	240, 60

GKR-5	240.95	f	240.70	241.20	N	0	S	64	W	1.00	2		16.53	
GKR-5	241.30	f	241.10	241.50	N	50	E	47	NW	3.00	2		46.25	
GKR-5	241.85	f	241.55	242.15	N	10	E	80	NW	3.00	2		25.32	
GKR-5	241.90	f	241.60	242.20	N	40	E	78	NW	1.00	2		23.20	
GKR-5	242.07	f	241.70	242.44	N	40	E	63	SE	1.00	2	2.50		n
GKR-5	242.08	f	241.70	242.46	N	40	E	87	SE	1.00	2	5.00		n
GKR-5	242.58	f	242.35	242.80	N	0	S	61	E	1.00	2		12.57	
GKR-5	242.58	f	242.35	242.80	N	31	E	58	SE	1.00	2		4.72	
GKR-5	242.80	f	242.50	243.10	N	30	E	73	SE	1.00	2		10.13	
GKR-5	243.30	f	243.20	243.40						2.50	2		25.33	
GKR-5	243.50	f	243.30	243.70						2.50	2		22.28	
GKR-5	243.80	f	243.50	244.10						2.50	2		30.56	
GKR-5	244.63	f	244.50	244.75	N	40	E	74	SE	1.00	2		4.69	
GKR-5	245.50	f	244.80	246.20	N	50	E	75	NW	1.00	2		9.77	
GKR-5	245.53	f	244.85	246.20	N	50	E	75	NW	1.00	2		9.67	
GKR-5	245.60	f	245.00	246.20	N	60	E	75	NW	1.00	2		2.29	
GKR-5	245.65	f								2.00	2	38.00		n
GKR-5	245.70	f	245.20	246.20	N	30	E	75	NW	1.00	2		8.29	
GKR-5	245.93	f	245.60	246.25	N	80	E	70	NW	2.50	2	7.50		n
GKR-5	247.40	f	246.05	248.75	N	60	E	79	NW	2.50	2	26.00		n
GKR-5	248.78	f	248.70	248.85	N	10	E	25	NW	1.00	2		5.73	
GKR-5	249.90	b						14	W					
GKR-5	251.90	f								1.00	2	1.00		r
GKR-5	252.55	f	252.35	252.75	N	60	E	55	SE	1.00	2	1.00		n
GKR-5	253.30	b						14	W					
GKR-5	255.05	f	254.00	256.10	N	0	S	85	E	2.00	2	13.00		r
GKR-5	255.45	f	254.80	256.10	N	30	E	70	SE	1.00	2	10.00		r
GKR-5	255.80	f	255.50	256.10	N	10	W	65	NE	2.50	2	11.00		r
GKR-5	258.45	f	258.35	258.55	N	0	S	63	E		2			
GKR-5	258.63	f	258.35	258.90	E	90	W	63	N		2			
GKR-5	258.95	f	258.70	259.20	N	70	E	61	NW	4.00	2	35.00		n
GKR-5	259.30	f	259.05	259.55	N	20	E	67	NW	2.50	2		43.70	
GKR-5	260.40	f	259.60	261.20	N	30	E	80	NW	3.00	2	56.00		n
GKR-5	261.50	b						19	W					

GKR-5	264.50	f	264.40	264.60	N	80	W	36	NE	0.50	2		5.82	
GKR-5	265.00	f	264.40	265.60	N	20	E	75	SE	1.00	2		0.95	
GKR-5	267.40	f	267.15	267.65	N	30	E	66	SE	1.00	2		9.77	
GKR-5	267.75	f	267.70	267.80	N	10	E	11	SE	5.00	2		62.27	
GKR-5	267.90	f	267.70	268.10	N	50	E	57	NW	2.00	2		17.92	
GKR-5	268.23	f	268.05	268.40	N	50	W	41	NE	2.00	2		9.20	
GKR-5	268.28	f	268.15	268.40	N	30	W	41	NE	2.50	2		21.84	
GKR-5	268.85	f	268.50	269.20	N	40	W	85	NE	2.50	2		30.61	
GKR-5	271.08	j	270.90	271.25	N	10	W	54	NE					
GKR-5	272.50	b						22	W					
GKR-5	272.80	f	272.70	272.90	N	40	W	51	NE	2.50	2		13.71	
GKR-5	272.85	f	272.65	273.05	N	20	W	53	NE	2.50	2		21.39	
GKR-5	272.88	f	272.70	273.05	N	20	E	55	NW	1.00	2		11.85	
GKR-5	273.50	f	273.40	273.60	N	40	W	37	NE	2.00	2		16.54	
GKR-5	273.60	f	273.40	273.80	N	50	W	54	NE	1.00	2	5.00		n
GKR-5	273.90	f	273.40	274.40	N	80	W	71	NE	1.00	2	4.00		r
GKR-5	274.85	f	274.80	274.90	N	70	E	64	SE	2.00	2	16.00		n
GKR-5	275.30	f	274.90	275.70	N	60	E	80	SE	3.00	2	25.00		n
GKR-5	275.85	j	275.40	276.30	N	30	E	83	SE					
GKR-5	275.90	f	275.80	276.00	N	60	E	46	SE	1.00	2		0.98	
GKR-5	276.18	f	276.05	276.30	N	50	E	47	SE	4.00	2		14.31	
GKR-5	276.20	f	276.00	276.40	N	50	E	45	SE	0.50	2		5.82	
GKR-5	279.60	f	279.30	279.90	N	20	E	51	NW		2	25.00		n
GKR-5	279.70	f	279.60	279.80	N	0	S	43	E	0.50	2		5.82	
GKR-5	280.55	f	280.40	280.70	N	10	W	37	SW	2.00	2		19.32	
GKR-5	280.63	j	280.30	280.95	N	50	W	76	NE					
GKR-5	281.15	f	281.00	281.30	N	30	W	47	NE	1.00	2		12.23	
GKR-5	282.30	b						25	W					
GKR-5	283.40	f	283.30	283.50	N	30	W	28	SW	2.50	2		19.31	
GKR-5	283.45	f	283.30	283.60	N	30	W	47	SW	2.50	2		11.37	
GKR-5	283.50	f	283.40	283.60	N	70	E	20	SE	1.00	2		4.21	
GKR-5	283.75	f	283.30	284.20	N	40	E	85	SE	2.00	2	7.50		
GKR-5	284.20	f	283.80	284.60	N	10	E	76	SE	2.00	2		28.77	
GKR-5	284.30	f	283.90	284.70	N	20	E	72	SE	1.00	2		7.39	

GKR-5	284.30	f	284.25	284.35	N	60	E	45	SE	1.00	2		6.38		
GKR-5	284.30	f	284.25	284.35	N	70	E	38	NW	1.00	2		18.81		
GKR-5	284.60	f	284.55	284.65	N	20	E	52	SE	2.50	2		27.02		
GKR-5	284.65	f	284.50	284.80	N	40	E	45	NW	5.00	2		69.70		
GKR-5	284.65	f	284.60	284.70	N	10	W	46	NE	2.00	2		5.05		
GKR-5	284.65	f	284.60	284.70	N	30	W	47	NE	2.00	2		14.60		
GKR-5	284.80	f	284.75	284.85	N	10	E	27	NW	2.00	2		5.72		
GKR-5	284.90	f	284.80	285.00	N	20	E	51	NW	1.00	2		37.66		
GKR-5	285.00	f	284.65	285.35	N	20	E	74	SE	2.50	2	10.00			
GKR-5	285.80	b						25	W						
GKR-5	286.10	f	285.90	286.30	N	20	E	54	NW	5.00	2		85.93		
GKR-5	286.20	f	286.10	286.30	N	10	E	31	NW	5.00	2		40.85		
GKR-5	286.45	f	286.20	286.70	N	50	E	67	SE	5.00	2		75.36		
GKR-5	286.90	f	286.80	287.00	N	80	E	42	NW	0.50	2		0.85		
GKR-5	287.13	f	287.00	287.25	N	20	E	23	SE	23.00	2		257.94		89, 22
GKR-5	287.83	f	287.65	288.00	N	60	E	43	SE	7.50	2		94.41		
GKR-5	288.40	f	288.20	288.60	N	65	E	51	SE		2	>50			100, 36
GKR-5	288.50	f	288.20	288.80	N	20	W	33	NE	0.50	2		6.60		
GKR-5	288.83	f	288.60	289.05	N	50	E	65	SE	0.50	2	12.00		n	
GKR-5	289.40	f	289.20	289.60	N	60	E	64	SE	2.00	2	18.00		n	
GKR-5	289.90	f	289.70	290.10	N	80	E	62	SE	0.50	2		22.97	n	
GKR-5	290.00	f	289.80	290.20	N	80	E	65	SE	0.50	2	2.50		n	
GKR-5	290.10	f	289.85	290.35	N	80	E	62	SE	0.50	2	7.00		n	
GKR-5	290.75	f	290.60	290.90	N	10	E	52	NW	2.00	2		22.92		
GKR-5	290.75	f	290.70	290.80	N	30	E	40	SE	2.00	2		3.42		
GKR-5	290.78	f	290.60	290.95	N	0	S	55	W	2.50	2		28.24		
GKR-5	290.85	f	290.40	291.30	N	20	W	81	NE	2.50	2		27.72		
GKR-5	290.98	f	290.90	291.05	N	50	W	33	SW	1.00	2		13.05		
GKR-5	291.50	f	291.30	291.70	N	10	W	52	NE	2.50	2		28.60		
GKR-5	292.80	b						21	W						
GKR-5	293.38	f	293.25	293.50	N	30	W	50	NE	1.00	2		17.66		
GKR-5	293.40	f	293.25	293.55	N	30	E	47	SE	1.00	2		9.02		
GKR-5	293.40	f	293.30	293.50	N	80	E	33	NW	1.00	2		10.99		
GKR-5	293.70	f	293.60	293.80	N	10	W	42	NE	1.00	2		1.05		

GKR-5	294.23	f	293.85	294.60	N	30	E	67	NW		2	>50		4, 47
GKR-5	294.40	f	290.10	298.70	N	10	E	62	SE	7.50	2		60.95	
GKR-5	294.65	j	294.60	294.70	N	20	E	70	SE					
GKR-5	294.85	f	294.40	295.30	N	40	E	72	NW	25.00	2		329.78	
GKR-5	294.90	j	294.60	295.20	N	20	E	54	SE					
GKR-5	296.90	f	296.00	297.80	N	30	E	66	NW		2	>100		
GKR-5	298.15	f	297.60	298.70	N	40	E	59	NW	76.00	2		1858.45	
GKR-5	299.15	f	299.10	299.20	N	30	E	24	NW		2			
GKR-5	299.40	f	299.30	299.50	N	30	E	35	SE	2.50	2		27.43	
GKR-5	299.65	f	299.60	299.70	N	20	E	49	NW		2			
GKR-5	299.68	f	299.60	299.75	N	50	E	45	SE	0.50	2		6.45	
GKR-5	299.98	f	299.90	300.05	N	0	S	28	E	1.00	2		7.70	
GKR-5	300.33	f	300.25	300.40	N	70	E	21	SE	5.00	2		74.26	
GKR-5	300.40	b						47	W					
GKR-5	300.40	f						53	SE		2			
GKR-5	300.55	f	300.50	300.60	N	30	E	14	SE	5.00	2		35.32	
GKR-5	300.60	f						57	SE		2			
GKR-5	300.70	f	300.60	300.80	N	20	E	46	SE	0.50	2		5.82	
GKR-5	301.00	f	300.95	301.05	N	30	E	40	SE	0.50	2		0.87	
GKR-5	301.05	f	301.00	301.10	N	20	E	40	SE	0.50	2		19.36	
GKR-5	301.15	f	301.00	301.30	N	20	E	47	SE	0.50	2		3.45	
GKR-5	301.15	f	301.10	301.20	N	20	E	55	SE	0.50	2		3.32	
GKR-5	301.38	f	301.30	301.45	N	40	E	27	SE	0.50	2	cum 10		n
GKR-5	301.40	b						21	W					
GKR-5	301.40	f	301.35	301.45	N	20	E	71	SE	0.50	2	cum 10		r
GKR-5	301.48	f	301.35	301.60	N	40	E	39	SE	0.50	2	12.00		n
GKR-5	301.60	f	301.50	301.70	N	20	E	51	SE	1.00	2		22.40	
GKR-5	301.95	f	301.70	302.20	N	20	E	65	SE	1.00	2		6.22	
GKR-5	302.35	f	302.30	302.40	N	70	W	33	SW	2.00	2		8.79	
GKR-5	303.40	b						23	W					
GKR-5	303.80	f	303.50	304.10	N	80	E	73	SE	1.00	2		9.52	
GKR-5	304.13	j	303.85	304.40	E	90	W	65	N					
GKR-5	304.50	f	304.40	304.60	N	80	E	66	NW	2.50	2		37.27	
GKR-5	306.28	f	305.50	307.05	N	60	W	86	NE	2.00	2	5.00		

GKR-5	306.50	f	306.30	306.70	N	50	W	55	NE	2.00	2	2.50		r
GKR-5	307.70	f	307.60	307.80	N	80	W	43	NE	2.00	2		10.12	
GKR-5	307.80	b						19	W					
GKR-5	309.98	f	309.95	310.00	N	70	W	16	SW	2.00	2		9.85	
GKR-5	310.05	f	310.00	310.10	N	70	W	16	SW	2.00	2		6.53	
GKR-5	310.60	j	309.80	311.40	N	30	W	84	NE					
GKR-5	311.75	f	311.50	312.00	E	90	W	66	N	1.00	2		26.79	
GKR-5	313.50	b						14	W					
GKR-5	314.85	f	314.80	314.90	N	20	E	17	NW	1.00	2		1.87	
GKR-5	317.30	b						20	W					
GKR-5	318.65	f	318.55	318.75	N	70	W	55	NE	0.50	2		7.53	
GKR-5	319.00	f	318.85	319.15	N	50	W	50	NE	0.50	2	5.00		n
GKR-5	319.50	f	319.30	319.70	N	60	W	55	NE	1.00	2	1.00		r
GKR-5	319.58	f	319.45	319.70	N	60	W	37	NE	1.00	2	4.00		n
GKR-5	320.30	f	319.70	320.90	N	60	E	80	SE	2.00	2	2.50		n
GKR-5	320.68	f	320.20	321.15	N	70	E	76	SE	2.50	2	2.50		n
GKR-5	322.20	f	322.00	322.40	N	50	E	60	SE	5.00	2		55.59	n
GKR-5	322.30	f	322.00	322.60	N	20	E	56	SE	2.50	2	10.00		n
GKR-5	322.53	f	322.20	322.85	N	50	E	74	SE	5.00	2		40.27	n
GKR-5	322.75	f	322.60	322.90	N	70	W	68	SW	1.00	2	2.50		n
GKR-5	323.10	f	322.40	323.80	N	20	E	86	SE	1.50	2	5.00		n
GKR-5	323.30	b						12	W					
GKR-5	323.40	f	323.35	323.45	N	40	E	37	NW	1.00	2		7.37	
GKR-5	324.25	f	324.05	324.45	N	40	W	46	NE	1.00	2		9.77	
GKR-5	324.50	f	324.35	324.65	N	60	W	39	NE	1.00	2		1.07	
GKR-5	324.65	f	324.50	324.80	N	60	W	35	NE	1.00	2		10.45	
GKR-5	325.60	f	325.50	325.70	N	30	W	61	NE	0.50	2		5.81	
GKR-5	326.55	f	326.40	326.70	N	10	W	46	NE	0.50	2		5.82	
GKR-5	326.65	f	326.50	326.80	N	20	W	53	NE	0.50	2		2.90	
GKR-5	327.88	f	327.70	328.05	N	0	S	52	E	0.50	2	6.00		n
GKR-5	327.93	f	327.80	328.05	N	10	W	50	NE	1.00	2	7.50		n
GKR-5	328.18	f	328.00	328.35	N	40	W	58	NE	1.00	2		10.07	
GKR-5	328.25	f	328.20	328.30	N	20	W	19	NE	1.00	2		10.82	
GKR-5	328.50	b						30	W					

GKR-5	329.18	f	329.00	329.35	N	20	W	58	NE	2.00	2		19.17	
GKR-5	329.90	f	329.40	330.40	N	50	E	82	SE	0.50	2		6.00	
GKR-5	333.90	b						29	W					
GKR-5	334.60	f	334.50	334.70	N	10	W	42	NE	2.50	2	5.00		n
GKR-5	335.03	f	334.60	335.45	N	10	W	73	NE	0.50	2		12.55	
GKR-5	337.60	f	337.50	337.70	N	70	W	45	NE	2.50	2	10.00		n
GKR-5	338.05	f	338.00	338.10	N	80	E	22	NW	1.50	2		19.21	
GKR-5	339.05	f	338.90	339.20	N	70	E	69	SE	0.50	2		6.56	
GKR-5	339.45	f	339.20	339.70	N	40	W	61	NE	3.00	2		17.97	
GKR-5	339.85	f	339.70	340.00	N	20	W	51	NE	3.00	2	10.00		n
GKR-5	348.28	f	348.20	348.35	N	70	W	22	NE	7.50	2		69.12	
GKR-5	348.48	f	348.35	348.60	N	60	E	45	SE	6.00	2		67.13	
GKR-5	348.65	f	348.50	348.80	E	90	W	66	N	1.00	2		11.83	
GKR-5	349.30	f	349.10	349.50	N	70	W	55	NE	0.50	2		4.88	
GKR-5	349.30	f	349.20	349.40	N	70	W	37	NE	0.50	2		1.53	
GKR-5	349.65	f	349.40	349.90	N	70	W	74	NE		2			
GKR-5	350.00	b						11	W					
GKR-5	350.28	f	350.05	350.50	N	0	S	60	E	4.00	2	7.50		r
GKR-5	350.60	f	350.40	350.80	N	0	S	80	E	2.50	2		12.38	
GKR-5	350.90	f	350.80	351.00	N	20	W	73	NE	2.50	2	7.50		r
GKR-5	351.60	f	351.35	351.85	N	80	E	67	SE	2.00	2	8.00		n
GKR-5	351.65	f	351.50	351.80	N	10	W	47	NE	cum 3	2			
GKR-5	351.75	f	351.70	351.80	N	70	W	37	NE	cum 3	2			
GKR-5	352.03	f	351.95	352.10	N	80	W	40	NE	2.50	2	28.00		n
GKR-5	352.25	f	352.20	352.30	E	90	W	47	N	0.50	2		6.66	
GKR-5	352.31	f						85	NE		2			
GKR-5	352.50	f	352.45	352.55	N	80	W	32	NE	0.50	2		5.73	
GKR-5	352.55	f	352.50	352.60	N	80	W	29	NE	1.00	2		6.89	
GKR-5	352.60	f	352.60	352.60	E	90	W	41	N	0.50	2	5.00		n
GKR-5	352.70	f						82	NE		2			
GKR-5	352.85	f	352.80	352.90	N	70	W	43	NE	0.50	2		6.08	
GKR-5	352.90	f	351.95	353.85	N	80	W	88	NE	2.00	2	13.00		n
GKR-5	353.40	j	353.20	353.60	N	0	S	62	E					
GKR-5	354.10	f	354.00	354.20	N	50	W	46	NE	1.50	2		19.36	

GKR-5	354.80	b						10	W					
GKR-5	356.85	f	356.50	357.20	N	10	W	76	NE	1.00	2		9.77	
GKR-5	357.20	f	357.00	357.40	N	80	E	60	NW	3.00	2	23.00		n
GKR-5	357.45	f	357.30	357.60	N	50	E	45	SE	1.50	2		16.51	
GKR-5	357.65	f	357.60	357.70	N	50	E	18	SE	1.50	2		6.39	
GKR-5	357.73	f	357.60	357.85	N	50	E	47	SE	2.50	2		14.58	
GKR-5	358.90	f	358.80	359.00	N	60	E	35	SE	0.50	2		6.40	
GKR-5	359.45	f	358.85	360.05	N	80	E	71	SE	2.50	2	15.00		n
GKR-5	359.50	b						12	W					
GKR-5	359.60	f	359.00	360.20	N	70	E	72	NW	2.50	2	12.50		n
GKR-5	360.30	f	360.20	360.40	N	30	E	53	SE	0.50	2		1.33	
GKR-5	360.65	f	360.55	360.75	N	40	E	68	NW	2.00	2		28.12	
GKR-5	360.65	f	360.60	360.70	N	20	E	52	SE	2.50	2		31.05	
GKR-5	361.75	f	361.70	361.80	N	50	E	65	NW	3.00	2	7.50		n
GKR-5	364.60	f	364.30	364.90	N	60	E	55	SE	56.00	2		1121.41	
GKR-5	365.10	f	364.80	365.40	N	20	E	82	NW	2.50	2	17.50		n
GKR-5	366.18	f	366.05	366.30	N	10	E	32	SE	1.50	2		9.77	
GKR-5	366.33	f	366.05	366.60	N	20	E	56	SE	1.50	2		22.46	
GKR-5	366.43	f	366.05	366.80	N	40	E	63	SE	1.50	2		9.81	
GKR-5	367.83	f	367.60	368.05	N	40	E	65	NW	10.50	2		105.88	
GKR-5	368.50	f	368.20	368.80	N	50	E	63	SE	33.00	2		493.25	
GKR-5	369.05	f	369.00	369.10	E	90	W	11	S	0.50	2		6.76	
GKR-5	369.55	f	369.50	369.60	N	10	E	22	NW	1.00	2		8.38	
GKR-5	370.00	f	369.90	370.10	N	70	E	51	NW	0.50	2	7.50		n
GKR-5	371.00	f	370.70	371.30	N	30	E	60	NW	5.00	2		60.63	
GKR-5	371.40	f	371.30	371.50	N	20	E	51	NW		2			
GKR-5	372.15	f	371.80	372.50	N	50	E	66	SE	0.50	2	63.00		n
GKR-5	372.50	f	372.40	372.60	N	50	E	43	SE	0.50	2	2.50		n
GKR-5	372.83	f	372.55	373.10	N	50	E	65	SE	1.00	2	cum 12.5		n
GKR-5	373.80	f	372.50	373.10	N	50	E	68	SE	1.00	2	cum 12.5		n
GKR-5	375.90	f						64		1.00	2		6.10	
GKR-5	376.10	f						62		1.00	2		2.37	
GKR-5	376.15	f						51			2	>50		
GKR-5	376.80	f						57		64.00	2		1394.93	

NNR-10	176.00	b			N	20	W	13	SW								
NNR-10	176.53	j	176.50	176.55	N	40	E	57	NW								
NNR-10	176.63	j	176.50	176.75	N	20	E	67	NW								
NNR-10	176.75	f	176.65	176.85	N	5	W	36	SW	1.00	1	1		6.58			
NNR-10	177.40	f	177.05	177.40	N	20	E	54	NW	0.25	1	4	7.00		n		
NNR-10	178.65	f	178.45	178.65	N	15	E	67	NW	0.50	1	2	7.00		n		
NNR-10	179.40	b			N	10	W	15	SW								
NNR-10	180.50	b			N	20	E	17	NW								
NNR-10	181.65	f	181.50	181.70	N	50	E	66	SE	1.00	1	1		8.37			
NNR-10	182.30	b			N	10	E	21	NW								
NNR-10	183.55	f	183.50	183.60	N	75	W	13	SW	0.50	1	1	1.00		r		younger than 183.65
NNR-10	183.65	f	183.45	183.85	N	45	E	69	NW	1.00	1	1	13.00		n		
NNR-10	183.95	f	183.70	184.20	N	35	E	64	SE		1		54.00		n	103, 62	
NNR-10	184.25	f	184.10	184.40	N	40	E	62	NW	0.50	1	2	9.00		n		probably younger than 183.95
NNR-10	187.08	j	186.85	187.30	N	40	E	71	NW								
NNR-10	187.10	j	187.00	187.20	N	35	E	67	SE								
NNR-10	187.73	f	187.50	187.95	N	20	E	85	NW	1.00	1	3	8.00		n		
NNR-10	187.80	f	187.60	188.00	N	35	E	73	SE	0.50	1	3	6.00		n		younger than 187.725
NNR-10	188.15	f	187.80	188.50	N	40	E	68	SE	0.50	1	3	4.00		n		
NNR-10	188.53	f	187.85	189.20	N	20	E	82	NW	0.50	1	3	2.00		n		
NNR-10	188.60	b			N	0	S	16	W								
NNR-10	188.60	f	188.50	189.70	N	25	E	78	NW	4.00	1	4	74.00		n		
NNR-10	190.63	f/j	190.35	190.90	N	25	E	67	SE		1		4.00		n		
NNR-10	191.10	f	191.00	191.20	N	40	E	61	NW	0.50	1	3	5.00		n		
NNR-10	191.33	f	191.25	191.50	N	25	E	74	NW	1.00	1	2	8.00		n		
NNR-10	191.60	f	191.35	191.85	N	30	E	60	SE	1.50	1	4	57.00		n		probably younger than 191.325
NNR-10	194.95	b			N	20	E	8	NW								
NNR-10	195.50	b			N	15	E	14	NW								Obtained from BHTV-log
NNR-10	198.00	b			N	0	S	9	W								
NNR-10	199.15	j	199.10	199.20	N	70	W	52	NE								
NNR-10	200.50	b			N	10	E	26	NW								Obtained from BHTV-log
NNR-10	201.10	b			N	20	E	28	NW								Obtained from BHTV-log
NNR-10	201.60	b			N	10	E	26	NW								Obtained from BHTV-log
NNR-10	202.10	b			N	15	E	24	NW								

NNR-10	202.18	f	202.10	202.25	N	10	W	26	NE	2.00	1	1		20.74			
NNR-10	202.88	f	202.85	202.90	N	30	W	34	NE	1.00	1	1		9.25			
NNR-10	203.28	f	203.15	203.40	N	10	E	63	SE	2.00	1	1	14.00		n		
NNR-10	203.30	f	203.20	203.40	N	0	S	31	E	1.00	1	1		10.36			
NNR-10	203.43	f	202.90	203.95	N	30	E	83	SE	2.00	1	1	17.00		n		
NNR-10	203.68	f	203.65	203.70	N	20	E	44	SE	1.00	1	1		8.86			
NNR-10	204.60	b			N	0	S	14	W								
NNR-10	205.58	f	205.35	205.80	N	65	E	73	SE	0.50	1	3	7.00		n		
NNR-10	205.75	f	205.40	206.10	N	50	E	71	SE				>50		n	80, 56	
NNR-10	205.98	f	205.75	206.20	N	55	E	62	SE	0.50	1	4	32.00		n		
NNR-10	206.85	b			N	0	S	10	W								
NNR-10	211.25	f	211.20	211.30	N	30	W	84	SW	1.00	1	2	5.00		n		
NNR-10	211.43	j	211.35	211.50	N	30	W	82	NE								
NNR-10	212.08	f	212.05	212.00	N	30	W	75	NE	0.50	1	3		9.99			
NNR-10	212.13	f/j	211.55	212.70	N	30	W	86	SW	0.25	1	4	6.00		n		
NNR-10	212.38	f	212.20	212.55	N	25	W	62	NE	0.25	1	3	3.00		n		
NNR-10	212.90	b			N	15	W	13	SW								
NNR-10	214.60	f	214.00	215.20	N	15	W	77	NE	0.25	1	4	7.00		r		
NNR-10	215.05	f	215.00	215.10	N	15	W	57	NE	0.50	1	2		2.42			
NNR-10	215.20	f	215.05	215.35	N	20	W	61	NE	0.50	1	3	7.00		r		
NNR-10	215.60	f	215.40	215.80	N	30	E	64	SE	1.00	1	3	17.00		n		
NNR-10	217.55	f	217.40	217.70	N	55	W	69	NE	0.50	1	2	5.00		r		
NNR-10	218.10	f	217.20	219.00	N	40	W	87	NE	0.50	1	3	12.00		r		
NNR-10	218.60	b			N	30	W	14	SW								
NNR-10	218.70	b			N	0	S	13	W								Obtained from BHTV-log
NNR-10	219.45	b			N	0	S	13	W								
NNR-10	221.45	b			N	20	E	15	NW								
NNR-10	224.40	b			N	18	E	19	NW								Obtained from BHTV-log
NNR-10	224.55	b			N	15	E	13	NW								
NNR-10	225.40	b			N	37	E	25	NW								Obtained from BHTV-log
NNR-10	226.93	f	226.85	227.00	N	20	W	46	NE				>85				
NNR-10	228.30	b			N	15	E	15	NW								Obtained from BHTV-log
NNR-10	229.20	b			N	25	E	22	NW								Obtained from BHTV-log
NNR-10	229.30	b			N	20	E	20	NW								

NNR-10	229.80	b			N	20	E	17	NW								
NNR-10	231.45	b			N	45	E	15	NW								
NNR-10	232.30	f	232.10	232.50	N	55	E	68	SE	2.00	1	1	22.00		n		
NNR-10	232.48	f	232.25	232.70	N	65	E	62	SE			1			n	97, 45	BHTV-Log correlation
NNR-10	233.30	b			N	15	E	15	NW								
NNR-10	233.38	f	233.35	233.40	N	15	W	49	SW	0.50	1	2	4.00		r		
NNR-10	233.55	f	233.50	233.60	N	15	E	27	NW	1.00	1	4	25.00		r		
NNR-10	234.65	f	234.40	234.90	N	10	W	67	NE	0.25	1	3	1.00		r		
NNR-10	235.50	f	235.40	235.60	N	30	E	62	SE		1		6.00		n		
NNR-10	235.70	b			N	15	E	14	NW								Obtained from BHTV-log
NNR-10	236.00	b			N	22	E	14	NW								Obtained from BHTV-log
NNR-10	236.55	b			N	30	E	16	NW								
NNR-10	236.70	b			N	30	E	31	NW								Obtained from BHTV-log
NNR-10	236.80	f	236.75	236.85	N	30	E	37	SE	2.00	1	1	23.00		n		
NNR-10	237.23	f	237.10	237.35	N	0	S	68	E	0.25	1	3	6.00		r		
NNR-10	237.85	f	237.70	238.00	N	30	W	42	NE	0.25	1	3	6.00		n		
NNR-10	238.78	f	238.65	238.90	N	45	E	47	SE	1.00	1	1	14.00		n		BHTV-Log correlation
NNR-10	238.83	f	238.70	238.95	N	40	E	66	SE	0.50	1	1	2.00		n		
NNR-10	239.65	f	239.50	239.80	N	20	W	55	NE	0.50	1	3		12.41			
NNR-10	239.83	f	239.70	239.95	N	35	E	50	SE	0.50	1	3	5.00		n		
NNR-10	240.08	f	240.05	240.10	N	70	E	11	SE	0.50	1	3		4.43			
NNR-10	240.30	b			N	10	E	17	NW								
NNR-10	241.30	f	241.10	241.50	N	20	W	61	NE	1.50	1	1		10.07			
NNR-10	242.10	f	242.00	242.20	N	30	E	36	SE	3.00	1	2		31.09			BHTV-log correlation
NNR-10	242.20	f	242.10	242.30	N	25	E	44	SE	1.00	1	2		10.63			
NNR-10	242.28	f	242.15	242.40	N	30	E	54	SE	1.00	1	2	7.00		n		
NNR-10	242.53	f	242.50	242.55	N	70	E	11	SE	1.00	1	2		3.77			
NNR-10	242.55	f	242.50	242.60	N	20	E	33	NW	0.50	1	2		8.23			
NNR-10	242.85	f	242.80	242.90	N	40	E	24	SE	0.25	1	3	2.00		r		
NNR-10	243.10	f	242.85	243.35	N	30	E	63	SE	0.25	1	3	2.00		n		
NNR-10	244.50	b			N	25	E	15	NW								
NNR-10	245.43	f	245.20	245.65	N	55	E	67	SE	0.25	1	3	2.00		n		
NNR-10	246.30	b			N	20	E	18	NW								
NNR-10	248.95	f	248.85	249.05	N	20	E	68	SE	1.00	1	2	5.00				

NNR-10	249.50	b			N	15	E	24	NW							Obtained from BHTV-log
NNR-10	249.85	f	249.70	250.00	N	35	E	73	SE	1.00	1	1		7.81		
NNR-10	250.33	f	249.60	251.05	N	25	E	84	NW	1.00	1	1	8.00		n	
NNR-10	251.23	f	251.05	251.40	N	40	E	57	SE	1.00	1	1	7.00		n	
NNR-10	251.70	b			N	30	E	22	NW							Obtained from BHTV-log
NNR-10	252.60	b			N	30	E	19	NW							
NNR-10	254.00	b			N	20	E	17	NW							
NNR-10	254.28	f/j	254.20	254.35	N	15	E	83	SE	0.25	1	3	4.00		r	
NNR-10	254.40	f	254.30	254.50	N	40	W	38	NE	0.50	1	3	6.00		n	
NNR-10	254.90	b			N	30	E	21	NW							
NNR-10	255.20	f	255.00	255.40	N	65	E	65	SE	1.00	1	4	47.00		n	
NNR-10	255.55	f	255.10	256.00	N	75	E	76	SE	7.00	1	1	>220	71.73	n	BHTV-Log correlation
NNR-10	256.10	f	255.80	256.40	N	70	W	64	SW	1.00	1	1	8.00		n	
NNR-10	256.20	f	255.55	256.20	N	60	E	69	SE	3.00	1	1	45.00		n	
NNR-10	256.80	f	256.70	256.90	N	10	E	48	SE	1.00	1	1	14.00		n	
NNR-10	256.98	j	256.85	257.10	N	20	E	82	SE							
NNR-10	258.13	j	258.05	258.20	N	40	W	76	NE							
NNR-10	258.65	f	258.40	258.90	N	50	W	55	NE	1.00	1	1	12.00		n	
NNR-10	258.75	f	258.60	258.90	N	65	E	59	NW	2.50	1	1	23.00		n	
NNR-10	259.40	b			N	5	E	36	NW							Obtained from BHTV-log
NNR-10	259.90	b			N	0	S	23	W							
NNR-10	260.00	b			N	3	E	22	NW							Obtained from BHTV-log
NNR-10	260.20	f	260.10	260.30	N	55	W	54	NE	1.00	1	2	5.00		n	
NNR-10	260.28	f	260.25	260.30	N	75	W	14	SW	3.00	1	1		35.50		probably younger than 260.2
NNR-10	260.60	b			N	10	E	22	NW							Obtained from BHTV-log
NNR-10	260.68	f	260.50	260.85	N	40	E	54	SE	0.25	1	3	2.00		n	
NNR-10	261.00	f	260.95	261.05	N	0	S	39	W	0.50	1	2		4.54		
NNR-10	261.15	b			N	10	E	26	NW							
NNR-10	261.20	b			N	30	E	25	NW							Obtained from BHTV-log
NNR-10	261.70	f	261.50	261.90	N	80	W	77	NE	0.50	1	2	2.00		r	
NNR-10	262.20	b			N	20	E	14	NW							
NNR-10	262.93	f	262.55	263.30	N	25	E	75	SE	0.50	2	1	3.00		n	
NNR-10	263.40	b			N	15	E	17	NW							
NNR-10	264.80	f	264.80	265.00	N	15	E	61	NW	0.25	2	3	3.00		n	

NNR-10	265.10	f	264.70	265.50	N	35	E	83	SE	0.25	2	4	15.00		n	
NNR-10	265.40	b			N	10	E	16	NW							
NNR-10	268.53	j	268.30	269.20	N	45	W	73	NE							BHTV-Log correlation
NNR-10	269.98	f	269.80	270.15	N	55	W	72	NE	0.50	2	1	3.00		n	
NNR-10	270.25	f	270.10	270.40	N	70	W	60	SW	0.50	2	1		5.80		
NNR-10	270.55	f	270.40	270.70	N	70	W	63	SW	0.50	2	1		4.17		
NNR-10	271.95	f/j	271.50	272.40	N	20	W	78	NE	0.50	2	2	2.00		r	
NNR-10	272.25	f	272.20	272.30	N	85	W	25	SW	1.00	2	1		11.73		
NNR-10	273.00	b			N	10	E	21	NW							Obtained from BHTV-log
NNR-10	273.00	f	272.95	273.05	N	5	W	16	SW	0.25	2	3		2.10		
NNR-10	273.03	f	273.00	273.05	N	10	E	33	NW	0.25	2	3		0.71		
NNR-10	273.13	f	273.10	273.15	N	80	W	11	SW	0.25	2	3		1.68		
NNR-10	273.38	f	273.35	273.40	N	10	W	17	SW	0.25	2	3		4.17		
NNR-10	273.70	b			N	20	E	19	NW							
NNR-10	274.70	b			N	3	E	23	NW							Obtained from BHTV-log
NNR-10	274.95	b			N	5	E	17	NW							
NNR-10	279.23	f	279.10	279.35	N	55	E	60	SE	0.50	2	2	6.00		n	
NNR-10	279.40	b			N	20	W	22	SW							
NNR-10	280.05	f	279.90	280.20	N	50	E	58	SE		2	1	>65		n	
NNR-10	281.25	f	281.00	281.50	N	45	W	73	NE	1.00	2	2		16.16		
NNR-10	282.33	f	282.10	282.55	N	60	E	63	SE	6.00	2	3		66.52	n	BHTV-Log correlation
NNR-10	282.60	f	282.30	282.90	N	65	E	67	SE		2	3			n	95, 50 BHTV-Log correlation
NNR-10	283.15	f	282.80	283.50	N	60	E	71	SE		2	3			n	BHTV-Log correlation
NNR-10	284.75	f	284.60	284.90	N	55	E	51	SE	5.00	2	1	>90	123.40		BHTV-Log correlation
NNR-10	285.78	f	285.55	286.00	N	65	E	62	SE	2.00	2	1	57.00		n	BHTV-Log correlation
NNR-10	286.03	f	285.85	286.20	N	55	E	63	SE	2.00	2	1		15.57	n	
NNR-10	286.20	f	286.00	286.40	N	60	E	59	SE		2	1			n	
NNR-10	286.53	f	286.35	286.70	N	65	E	58	SE		2	1			n	
NNR-10	286.70	f	286.55	286.85	N	65	E	55	SE		2	1			n	BHTV-Log correlation
NNR-10	287.05	f	286.90	287.20	N	70	E	54	SE	4.00	2	1		34.37	n	
NNR-10	287.55	f	287.40	287.70	N	60	E	51	SE	2.00	2	1		4.08		older than 287.7
NNR-10	287.70	f	287.60	287.80	N	70	E	41	NW	3.00	2	1	14.00		n	
NNR-10	288.10	j	287.70	288.50	N	60	W	75	NE							BHTV-Log correlation
NNR-10	288.35	f	288.30	288.40	N	35	E	54	SE	2.00	2	1		9.66		

NNR-10	288.70	f	288.40	289.00	N	55	E	73	SE	1.00	2	1	4.00		n	
NNR-10	288.83	f	288.70	288.95	N	45	E	71	SE	1.00	2	1	7.00		n	
NNR-10	289.93	f	289.65	290.20	N	60	E	85	SE	0.50	2	1	6.00		n	
NNR-10	290.00	f	289.40	290.60	N	50	E	83	NW	0.50	2	1	4.00		n	
NNR-10	290.70	f	290.40	291.00	N	40	E	69	SE	1.50	2	1	24.00		n	BHTV-Log correlation
NNR-10	291.20	f	291.00	291.40	N	45	E	60	SE	8.00	2	1	>90	89.04	n	BHTV-Log correlation
NNR-10	293.60	f	293.35	293.85	N	40	E	61	SE	1.00	2	1	4.00		n	BHTV-Log correlation
NNR-10	294.15	f	293.50	294.80	N	50	E	73	SE	1.00	2	1	4.00		n	
NNR-10	294.25	f	294.00	294.50	N	50	E	86	SE	1.00	2	1		11.28		
NNR-10	294.45	f	293.60	295.30	N	75	E	84	SE	1.00	2	1	8.00		n	
NNR-10	295.35	f	295.20	295.50	N	80	E	72	SE	1.00	2	1		13.35		
NNR-10	296.00	b			N	15	E	13	NW							
NNR-10	298.80	f	298.75	298.85	N	70	E	56	NW	0.50	2	1		2.76		
NNR-10	299.00	b			N	10	E	16	NW							
NNR-10	299.20	f	299.00	299.40	N	55	E	52	NW	1.00	2	1	8.00		n	
NNR-10	299.85	f	299.20	300.50	N	60	E	85	SE	1.00	2	1	3.00		n	
NNR-10	299.90	b			N	15	E	27	NW							Obtained from BHTV-log
NNR-10	301.83	f	301.75	301.90	N	80	W	69	NE	1.00	2	1		6.09		
NNR-10	302.50	b			N	22	E	21	NW							Obtained from BHTV-log
NNR-10	302.80	b			N	30	E	10	NW							
NNR-10	303.80	b			N	30	E	15	NW							
NNR-10	306.55	f	306.40	306.70	N	60	W	57	NE	1.00	2	1		8.31		
NNR-10	306.60	b			N	15	E	29	NW							Obtained from BHTV-log
NNR-10	307.30	b			N	20	E	15	NW							
NNR-10	308.00	b			N	25	E	13	NW							
NNR-10	308.43	f	308.20	308.65	N	80	E	65	NW	1.00	2	4	27.00		n	
NNR-10	309.15	f	308.95	309.35	N	45	E	79	SE	0.50	2	1		0.67		
NNR-10	309.43	f	309.35	309.50	N	75	E	62	NW	1.50	2	1		2.59		
NNR-10	309.70	f	309.05	310.35	N	75	E	80	SE	4.00	2	1	24.50		n	BHTV-Log correlation
NNR-10	310.00	f	309.70	310.20	N	70	E	86	NW	1.00	2	1	5.00		r	
NNR-10	310.15	f	309.60	310.70	N	70	E	83	SE	4.00	2	1	24.50		n	
NNR-10	310.45	f	310.35	310.55	N	35	E	74	NW	1.00	2	1		5.05		
NNR-10	310.65	f	310.50	310.80	N	50	E	59	NW	2.00	2	1		32.88		
NNR-10	312.00	b			N	15	E	17	NW							

NNR-10	312.10	f	312.00	312.20	N	35	E	62	NW	1.00	2	1		4.49		
NNR-10	312.20	f	312.15	312.25	N	30	E	66	NW	1.00	2	1	6.00		n	
NNR-10	312.68	f	311.70	313.65	N	30	E	84	SE	1.00	2	1	7.00		n	probably younger than faults 312.1 and 312.2
NNR-10	313.30	b			N	15	E	23	NW							Obtained from BHTV-log
NNR-10	313.55	f	313.00	314.10	N	40	E	81	SE	0.50	2	1	3.00		n	
NNR-10	314.00	b			N	10	E	23	NW							
NNR-10	314.15	f	314.00	314.30	N	45	E	68	NW	1.00	2	1	5.00		n	
NNR-10	314.25	f	314.00	314.50	N	35	E	64	NW	1.00	2	1		5.88		
NNR-10	314.45	f	314.40	315.50	N	40	E	57	NW	1.00	2	1		0.57		
NNR-10	314.53	f	314.35	314.70	N	40	E	77	SE	1.00	2	1		2.63		
NNR-10	315.15	f	314.80	315.50	N	50	E	79	NW	0.50	2	3	2.00		r	
NNR-10	315.23	f	315.80	316.25	N	70	E	74	SE	0.50	2	3	3.00		n	
NNR-10	317.30	b			N	7	E	26	NW							Obtained from BHTV-log
NNR-10	317.85	b			N	20	W	18	SW							
NNR-10	319.70	b			N	20	W	29	SW							
NNR-10	319.80	b			N	0	S	29	W							Obtained from BHTV-log
NNR-10	320.08	f	319.80	320.35	N	45	E	63	NW	1.50	2	1	26.00		r	
NNR-10	320.40	b			N	30	W	20	SW							
NNR-10	321.00	b			N	30	W	22	SW							
NNR-10	321.33	f	321.25	321.40	N	35	E	36	NW	1.00	2	1		11.07		
NNR-10	321.80	b			N	33	E	16	NW							Obtained from BHTV-log
NNR-10	322.75	b			N	40	W	13	SW							
NNR-10	322.95	f	322.70	323.20	N	10	E	60	NW	1.00	2	1	3.00		n	
NNR-10	323.00	f	322.80	323.20	N	30	E	57	NW	1.00	2	1	2.00		n	
NNR-10	323.70	f	323.40	324.00	N	40	E	62	NW	1.00	2	1		7.20		
NNR-10	324.45	f	324.00	324.90	N	35	E	77	SE	1.00	2	1		7.02		
NNR-10	325.74	f	325.65	325.85	N	10	E	71	SE	1.00	2	1		9.92		
NNR-10	326.50	f	326.40	326.60	N	25	W	46	NE	1.00	2	1		8.92		
NNR-10	326.90	b			N	15	E	21	NW							
NNR-10	327.70	f	327.30	328.10	N	55	E	75	SE	1.50	2	1	21.00		n	BHTV-Log correlation
NNR-10	327.90	b			N	7	W	11	SW							Obtained from BHTV-log
NNR-10	327.90	f	327.50	328.30	N	55	E	71	SE	3.00	2	1		15.25		BHTV-Log correlation
NNR-10	328.60	b			N	15	W	16	SW							
NNR-10	330.48	f	330.35	330.60	N	50	E	44	NW	0.50	2	4	21.00		n	

NNR-10	330.53	f	330.50	330.55	N	45	E	37	NW	0.50	2	3		14.78		
NNR-10	333.10	b			N	10	W	15	SW							Obtained from BHTV-log
NNR-10	333.65	b			N	0	S	17	W							
NNR-10	335.60	b			N	0	S	20	W							Obtained from BHTV-log
NNR-10	336.20	b			N	0	S	15	W							
NNR-10	336.65	b			N	5	W	13	SW							
NNR-10	337.90	f	337.80	338.00	N	40	E	43	NW	1.00	2	2	9.00		n	
NNR-10	338.35	f	338.00	338.70	N	50	E	74	SE		2	1			n	
NNR-10	338.95	f	338.60	339.30	N	50	E	69	SE		2	1			n	BHTV-Log correlation
NNR-10	339.35	f	339.00	339.70	N	50	E	68	SE		2	1			n	
NNR-10	340.13	f	339.60	340.65	N	50	E	82	SE	7.00	2	1		62.13		
NNR-10	340.38	f	340.10	340.65	N	55	E	79	SE	4.00	2	1		26.46		
NNR-10	341.30	f	341.20	341.40	N	45	E	76	SE		2					BHTV-Log correlation
NNR-10	341.80	b			N	5	E	17	NW							
NNR-10	342.75	f	342.40	343.10	N	55	E	71	NW	1.00	2	1	13.00		n	BHTV-Log correlation
NNR-10	342.80	f	342.70	342.90	N	50	E	63	NW	1.00	2	1		9.40		
NNR-10	342.95	f	342.80	343.10	N	55	E	59	NW	1.00	2	1		9.38		
NNR-10	343.10	f	343.00	343.20	N	40	E	46	NW	1.00	2	1		10.79		
NNR-10	343.80	f	343.20	344.40	N	50	E	87	NW	2.50	2	1	32.00		r	BHTV-Log correlation
NNR-10	344.33	f	344.20	344.45	N	50	E	61	NW	0.60	2	1		3.68		
NNR-10	345.35	f	345.15	345.55	N	55	W	59	NE	1.50	2	1	13.00		n	
NNR-10	345.40	f	345.30	345.50	N	35	W	57	SW	1.00	2	1	4.00		n	
NNR-10	345.70	b			N	5	E	16	NW							
NNR-10	346.13	f	346.00	346.25	N	60	W	61	NE	0.50	2	1	5.00		n	
NNR-10	346.95	f	346.80	347.10	N	55	E	66	NW	0.50	2	1	6.00		n	
NNR-10	347.35	f	347.00	347.70	N	40	E	69	SE	1.00	2	1	8.00		n	
NNR-10	347.88	f	347.50	348.25	N	45	E	74	SE	2.00	2	2	28.00		n	
NNR-10	349.60	f	349.50	349.70	N	55	E	60	NW	0.50	2	1		0.63		
NNR-10	349.70	b			N	10	W	13	SW							
NNR-10	350.10	b			N	0	S	25	W							Obtained from BHTV-log
NNR-10	350.40	b			N	0	S	22	W							Obtained from BHTV-log
NNR-10	350.95	f	350.90	351.00	N	65	E	58	NW	0.50	2	1		3.59		
NNR-10	351.08	f	351.00	351.15	N	70	E	71	NW	0.50	2	1		1.87		
NNR-10	351.23	f	351.15	351.30	N	55	E	40	NW	0.50	2	1	5.00		n	

NNR-10	351.40	b			N	35	W	14	SW								
NNR-10	351.65	f	351.40	351.90	N	5	W	65	NE	0.50	2	1		0.50			
NNR-10	352.13	f	352.05	352.20	N	65	W	33	NE	1.00	2	1		3.40			
NNR-10	352.90	f	352.80	353.00	N	15	E	51	NW	3.00	2	1	25.00		n		BHTV-Log correlation
NNR-10	353.20	f	352.95	353.45	N	5	E	66	NW	2.00	2	1		33.74			BHTV-Log correlation
NNR-10	353.90	f	353.80	354.00	N	45	E	43	NW	1.50	2	1	23.00		n		BHTV-Log correlation
NNR-10	354.08	f	353.90	354.25	N	25	E	52	NW	1.50	2	1	7.00		n		
NNR-10	354.50	b			N	15	E	16	NW								
NNR-10	355.15	f	354.40	355.90	N	65	E	82	NW	0.50	2	2	6.00		n		younger than faults 355.25 and 355.6
NNR-10	355.25	f	355.20	355.30	N	70	E	37	NW	2.00	2	1		5.63			
NNR-10	355.60	f	355.50	355.70	N	30	E	35	NW	2.00	2	1		7.92			
NNR-10	355.95	f	355.80	356.10	N	40	E	51	NW	2.00	2	1		12.46			
NNR-10	356.08	f	355.85	356.30	N	45	E	78	NW	2.00	2	1		14.75			
NNR-10	356.40	f	356.05	356.75	N	75	E	76	SE	1.50	2	2	19.00		n		
NNR-10	357.03	f	356.75	357.30	N	60	E	68	SE		2	3			n	102, 60	
NNR-10	357.28	f	357.05	357.50	N	70	E	62	SE		2	3			n		
NNR-10	357.70	f	357.60	357.80	N	45	E	65	NW	1.00	2	2		8.83			
NNR-10	358.00	b			N	15	E	18	NW								
NNR-10	358.50	f	358.15	358.50	N	70	E	88	SE	2.00	2	1		22.52			
NNR-10	358.80	f	358.50	359.10	N	45	E	73	SE	2.00	2	1		12.77			
NNR-10	358.85	f	358.65	359.05	N	70	E	86	NW	1.00	2	1		3.18			
NNR-10	359.28	f	359.00	359.55	N	60	E	66	SE		2	1			n		
NNR-10	360.10	f	359.70	360.50	N	50	E	75	SE		2	1			n		BHTV-Log correlation
NNR-10	360.40	f	360.30	360.50	N	50	E	46	NW	1.00	2	1	8.00		n		
NNR-10	362.75	f	362.50	363.00	N	50	E	72	SE		2	2			n		BHTV-Log correlation
NNR-10	363.33	f	363.20	363.45	N	50	E	56	SE		2	2			n		BHTV-Log correlation
NNR-10	363.43	f	363.35	363.50	N	40	E	32	NW	1.00	2	2		12.60			
NNR-10	363.48	f	363.35	363.60	N	30	E	52	NW	1.00	2	2		5.65			
NNR-10	363.85	b			N	10	W	11	SW								
NNR-10	364.05	f	363.75	364.35	N	25	E	67	SE	0.50	2	2	3.00		n		
NNR-10	364.45	f	364.20	364.70	N	50	E	61	SE	0.50	2	4	9.00		n		
NNR-10	364.93	f	364.85	365.00	N	35	E	54	SE	1.00	2	1		11.01			
NNR-10	365.10	f	364.90	365.30	N	20	E	65	SE	1.50	2	1		8.49			
NNR-10	365.20	f	364.95	365.45	N	20	E	67	SE	1.00	2	2		6.93			

NNR-10	365.68	f	365.35	366.00	N	45	E	68	SE	2.00	2	1	12.00		n	
NNR-10	366.10	f	365.85	366.35	N	45	E	66	NW	2.00	2	1	14.00		n	younger than 366.2 and 365.68
NNR-10	366.20	f	365.90	366.50	N	45	E	67	SE	5.00	2	1		44.73		
NNR-10	366.75	f	366.20	367.30	N	40	E	81	SE	3.00	2	3	>180	207.35		older than 366.1
NNR-10	367.70	f	366.90	368.50	N	50	E	85	SE	20.00	2	1		209.50	n	
NNR-10	368.98	f	368.50	369.45	N	45	E	81	SE	8.00	2	1		77.09		
NNR-10	369.30	f/j	368.90	369.70	N	40	E	74	SE		2		39.00		n	
NNR-10	369.63	f	369.55	369.70	N	70	E	39	NW	0.50	2	2		4.47		
NNR-10	369.68	f	369.60	369.75	N	65	E	41	NW	0.50	2	2		4.58		
NNR-10	369.80	f	369.50	370.10	N	45	E	71	SE	4.00	2	2	>70	93.50	n	
NNR-10	370.30	f	370.10	370.50	N	0	S	54	E	2.00	2	1	43.00			
NNR-10	371.10	b			N	15	W	6	SW							Obtained from BHTV-log
NNR-10	371.35	f	371.20	371.50	N	30	W	46	NE	3.00	2	1		25.59		
NNR-10	372.00	b			N	15	E	10	NW							
NNR-10	372.10	b			N	10	W	15	SW							Obtained from BHTV-log
NNR-10	372.70	b			N	7	W	15	SW							Obtained from BHTV-log
NNR-10	373.50	b			N	20	W	9	SW							
NNR-10	373.70	b			N	45	W	15	SW							Obtained from BHTV-log
NNR-10	374.50	b			N	25	W	10	SW							
NNR-10	377.60	f	377.50	377.70	N	45	W	36	NE	1.50	2	1	7.00		n	
NNR-10	377.70	f	377.60	377.80	N	40	W	34	NE	2.00	2	1	28.00		n	
NNR-10	378.40	b			N	15	W	10	SW							Obtained from BHTV-log
NNR-10	378.58	f	378.20	378.95	E	90	W	81	S	0.25	2	2	5.00		n	
NNR-10	378.80	f	378.60	379.00	N	80	E	77	NW	0.25	2	2	4.00		n	
NNR-10	379.20	b			N	25	E	14	NW							
NNR-10	379.30	b			N	45	W	22	SW							Obtained from BHTV-log
NNR-10	382.78	f	381.50	384.05	N	80	E	88	NW	1.00	2	1	4.00		n	
NNR-10	383.40	b			N	30	W	19	SW							Obtained from BHTV-log
NNR-10	384.10	b			N	35	E	15	NW							
NNR-10	384.45	f	384.40	384.50	N	80	W	34	NE	2.00	2	1	15.00		n	
NNR-10	384.48	f	384.25	384.70	N	75	W	56	SW	3.00	2	1		35.60		older than 384.45 and 384.55
NNR-10	384.55	f	384.50	384.60	N	80	W	31	NE	2.50	2	1	13.00		n	
NNR-10	384.85	f	384.75	385.05	N	70	W	46	SW	1.00	2	2	11.00		n	
NNR-10	384.90	f	384.80	385.00	N	70	W	39	NE	1.00	2	1	7.00		n	younger than 384.85 and 384.975

NNR-10	384.98	f	384.90	385.05	N	75	W	37	SW	2.00	2	2		19.12			
NNR-10	385.30	f	385.10	385.50	N	85	E	51	NW	2.00	2	2	18.00		n		
NNR-10	385.33	f	385.10	385.55	E	90	W	57	S	1.50	2	1	14.00		n		older than 385.3
NNR-10	386.30	f	386.00	386.60	N	30	W	66	NE	1.50	2	1	10.00		n		
NNR-10	387.28	f	386.90	387.65	N	60	W	74	NE	1.00	2	1		7.12			
NNR-10	387.70	f	387.60	387.80	N	55	W	56	NE	0.50	2	2		1.70			
NNR-10	387.88	f	387.70	388.05	N	75	E	55	NW	1.50	2	2	23.00		n		
NNR-10	388.80	f	388.70	388.90	N	45	W	47	NE		2						
NNR-10	388.88	f/j	388.80	388.95	N	60	W	40	NE	1.00	2	1		7.20			
NNR-10	389.25	f/j	388.80	389.70	N	80	W	78	NE		2		>50			307, 65	
NNR-10	389.55	f	389.40	389.70	N	75	W	46	NE	1.00	2	1		9.72			
NNR-10	390.15	f	390.00	390.30	N	85	E	56	NW	1.50	2	1	27.00		n		
NNR-10	391.15	f	391.10	391.20	E	90	W	27	N	1.50	2	1		7.13			
NNR-3	174.30	b			N	15	W	27	SW								Obtained from BHTV-log
NNR-3	174.80	b			N	0	S	27	W								Obtained from BHTV-log
NNR-3	175.60	b			N	3	E	25	NW								Obtained from BHTV-log
NNR-3	180.70	b			N	0	S	19	W								Obtained from BHTV-log
NNR-3	181.20	b			N	15	E	21	NW								Obtained from BHTV-log
NNR-3	181.50	b			N	7	E	23	NW								Obtained from BHTV-log
NNR-3	182.10	b			N	10	W	21	SW								Obtained from BHTV-log
NNR-3	182.30	b			N	5	E	22	NW								
NNR-3	184.10	b			N	10	E	18	NW								
NNR-3	185.00	b			N	15	E	15	NW								
NNR-3	187.23	f	187.15	187.30	N	70	E	41	SE		1		>25				BHTV-log correlation
NNR-3	188.03	f	187.95	188.10	N	50	W	33	NE	1.00	1	1		8.01			
NNR-3	188.23	f	188.05	188.40	N	60	W	66	NE	1.00	1	1		9.69			
NNR-3	189.35	f	189.30	189.40	N	80	W	21	SW	1.00	1	1		10.31			
NNR-3	189.65	f	189.60	189.70	N	75	E	18	SE	1.00	1	2		0.50			
NNR-3	190.80	b			N	15	W	19	SW								Obtained from BHTV-log
NNR-3	191.15	b			N	5	E	12	NW								
NNR-3	191.20	b			N	5	E	29	NW								Obtained from BHTV-log
NNR-3	192.45	f	192.20	192.70	N	30	E	71	NW	4.00		2	>110	144.77	n		BHTV-log correlation
NNR-3	192.63	f	192.50	192.75	N	50	E	57	NW								BHTV-log correlation
NNR-3	193.15	f	193.00	193.30	N	50	E	57	SE	1.00	1	3	23.00		n		

NNR-3	194.30	b			N	20	E	14	SW							
NNR-3	194.45	f	194.40	194.50	N	45	E	67	NW	1.50	1	1	13.00		n	BHTV-log correlation
NNR-3	194.90	f	194.70	195.10	N	40	E	61	NW	2.00	1	3	54.00		n	
NNR-3	195.38	f	195.35	193.40	N	70	E	15	SE	1.00	1	2	4.00		r	younger than fault 195.5
NNR-3	195.50	f	195.30	195.70	N	65	E	57	NW	2.00	1	2		6.04		
NNR-3	196.63	f	196.30	196.95	N	50	E	72	NW	1.00	1	3	42.00		n	
NNR-3	197.15	f	196.90	197.40	N	45	E	73	NW	1.00	1	2	9.00		n	
NNR-3	198.08	f	198.00	198.15	N	70	E	32	SE	0.50	1	1	3.00		r	younger than fault 198.475
NNR-3	198.40	b			N	83	W	29	SW							Obtained from BHTV-log
NNR-3	198.48	f	197.95	199.00	N	50	E	82	NW	1.50	1	2	9.00		r	
NNR-3	198.53	f	198.20	198.85	N	65	E	83	NW	1.00	1	2	7.00		r	
NNR-3	198.98	f	198.85	199.10	N	55	E	62	NW	1.00	1	2		19.13		
NNR-3	199.50	f	199.30	199.70	N	35	E	63	SE	1.50	1	2	17.00		n	
NNR-3	199.53	f	199.45	199.60	N	30	E	56	NW	1.50	1	2		15.19		
NNR-3	199.60	b			N	42	E	33	SE							Obtained from BHTV-log
NNR-3	199.78	f	199.65	199.90	N	50	E	55	NW	1.50	1	2	16.00		n	
NNR-3	200.20	b			N	45	W	20	SW							Obtained from BHTV-log
NNR-3	200.30	f	200.20	200.40	N	70	E	39	SE	2.00	1	1		12.79		younger than fault 200.725
NNR-3	200.35	j	200.10	200.80	N	35	W	77	NE							
NNR-3	200.73	f	200.40	201.10	N	70	E	74	NW	1.50	1	1		27.74		
NNR-3	200.78	f	200.60	200.95	N	45	E	76	SE	1.50	1	1		17.84		
NNR-3	201.15	f	201.00	201.30	N	55	E	58	SE		1					BHTV-log correlation
NNR-3	202.93	f	202.80	203.05	N	60	E	56	SE		`	4		2185.59	132, 56	BHTV-log correlation
NNR-3	203.35	f	203.10	203.60	N	50	E	62	SE	3.00	1	1		22.79	69, 32	BHTV-log correlation
NNR-3	203.60	f	203.25	203.95	N	35	E	67	SE	2.00	1	1	21.00		n	
NNR-3	204.08	f	204.00	204.15	N	55	E	36	SE	1.00	1	1		9.19		
NNR-3	204.30	b			N	20	W	20	SW							
NNR-3	204.50	f	204.10	204.90	N	60	E	73	SE	0.50	1	2		8.36		
NNR-3	204.80	f	204.70	204.90	N	80	W	61	SW	0.50	1	2		7.35		
NNR-3	204.90	f	204.80	205.00	N	80	W	53	SW	0.50	1	2		4.78		
NNR-3	205.10	f	205.00	205.20	N	60	E	73	SE	0.50	1	2		6.49		
NNR-3	205.50	f	205.20	205.80	N	45	E	75	SE	0.50	1	3	3.00		n	
NNR-3	205.85	f	205.60	206.10	N	40	E	80	SE	0.50	1	3	3.00		r	
NNR-3	206.05	f	205.60	206.50	N	25	E	78	SE	0.50	1	3	4.00		r	

NNR-3	206.90	b			N	20	W	18	SW						
NNR-3	208.60	b			N	10	E	16	NW						
NNR-3	210.28	f/j	210.10	210.45	N	10	E	51	NW	1.50	1	1	10.00		n
NNR-3	210.58	f	210.40	210.75	N	30	E	55	NW	1.50	1	1		9.43	
NNR-3	211.13	f	210.80	211.45	N	35	E	76	SE	2.00	1	3	33.00		n
NNR-3	211.45	b			N	10	E	17	NW						
NNR-3	211.80	f	211.75	211.85	N	10	E	21	SE	0.50	1	3	4.00		r
NNR-3	212.10	b			N	30	E	22	NW						
NNR-3	212.15	b			N	30	E	28	NW						Obtained from BHTV-log
NNR-3	212.40	b			N	33	E	28	NW						Obtained from BHTV-log
NNR-3	212.90	b			N	20	E	14	NW						
NNR-3	213.20	f	212.95	213.45	N	35	E	66	NW	0.50	1	1	2.00		n
NNR-3	213.45	f	213.20	213.70	N	40	E	68	NW	0.50	1	1	2.00		n
NNR-3	213.70	b			N	0	S	22	W						Obtained from BHTV-log
NNR-3	213.90	b			N	15	E	24	NW						
NNR-3	214.23	f	214.05	214.40	N	35	E	69	NW	1.50	1	1	13.00		n
NNR-3	214.40	b			N	0	S	29	W						
NNR-3	215.20	f	215.00	215.40	N	50	E	60	NW	2.00	1	1	22.00		n
NNR-3	215.25	j	214.90	215.60	N	45	W	76	NE						BHTV-log correlation
NNR-3	216.80	f	216.65	216.95	N	65	E	54	NW	1.00	1	2		7.28	
NNR-3	216.90	f	216.70	217.10	N	60	E	52	NW	1.00	1	2		10.63	
NNR-3	217.15	f	216.30	218.00	N	80	E	86	SE	0.50	1	2	7.00		n younnger than faults 216.8 and 216.9
NNR-3	217.60	b			N	7	E	34	NW						Obtained from BHTV-log
NNR-3	217.80	b			N	22	E	25	NW						Obtained from BHTV-log
NNR-3	217.93	f	217.70	218.15	N	55	E	67	NW	2.50	1	2	36.00		n
NNR-3	218.15	f	218.00	218.30	N	60	E	71	SE	0.50	1	4	10.00		n
NNR-3	218.58	f	218.90	218.25	N	50	E	83	NW	0.50	1	4	8.00		n
NNR-3	218.90	b			N	30	E	26	NW						
NNR-3	218.95	b			N	20	E	34	NW						Obtained from BHTV-log
NNR-3	219.20	b			N	15	E	38	NW						Obtained from BHTV-log
NNR-3	220.00	b			N	7	E	17	NW						Obtained from BHTV-log
NNR-3	220.40	b			N	25	E	20	NW						
NNR-3	221.00	b			N	30	E	21	NW						
NNR-3	221.05	b			N	30	E	21	NW						Obtained from BHTV-log

NNR-3	222.28	j	222.10	222.45	N	15	W	66	NE								BHTV-log correlation
NNR-3	222.63	f	222.10	223.15	N	50	E	78	NW	1.00	2	2	9.00		n		BHTV-log correlation
NNR-3	223.00	b			N	30	E	16	NW								
NNR-3	223.30	f	223.00	223.60	N	45	E	86	NW	1.00	2	2	8.00		n		
NNR-3	224.13	f	223.75	224.50	N	40	E	74	NW	1.50	2	2	20.00		n		BHTV-log correlation
NNR-3	225.50	b			N	22	E	17	NW								Obtained from BHTV-log
NNR-3	228.30	b			N	22	E	24	NW								Obtained from BHTV-log
NNR-3	228.70	b			N	20	E	34	NW								Obtained from BHTV-log
NNR-3	229.70	b			N	15	E	29	NW								Obtained from BHTV-log
NNR-3	230.30	f	230.10	230.50	N	60	E	51	SE	43.00	2	3		460.68			BHTV-log correlation
NNR-3	230.83	f	230.60	231.05	N	65	E	64	SE	5.00	2	1		54.27			BHTV-log correlation
NNR-3	231.90	b			N	10	E	30	NW								
NNR-3	232.00	b			N	7	E	31	NW								Obtained from BHTV-log
NNR-3	232.90	f	232.80	233.00	N	45	E	31	NW	1.00	2	2	11.00		n		younger than fault 233.05
NNR-3	233.05	f	232.70	233.40	N	75	E	70	SE	1.50	2	2	31.00		n		
NNR-3	233.80	b			N	35	E	34	NW								
NNR-3	233.93	f	233.85	234.00	N	65	E	33	NW	1.00	2	2		16.04			
NNR-3	234.30	f	234.10	234.50	N	80	E	57	SE	3.00	2	3	62.00		n		BHTV-log correlation
NNR-3	234.38	f	234.25	234.50	N	70	E	51	SE	1.00	2	2		14.69			
NNR-3	235.30	b			N	35	E	25	NW								Obtained from BHTV-log
NNR-3	235.50	b			N	30	E	30	NW								
NNR-3	236.25	f	236.15	236.35	N	85	W	37	SW	3.00	2	2	47.00		n		BHTV-log correlation
NNR-3	236.55	f	236.40	236.70	N	85	E	66	SE	1.50	2	2	21.00		n		
NNR-3	236.73	f	236.65	236.80	E	90	W	54	S	0.50	2	2		8.19			
NNR-3	236.98	f	236.85	237.10	N	80	E	50	SE	0.50	2	2	7.00		n		BHTV-log correlation
NNR-3	237.90	f	237.70	238.10	N	75	E	64	SE	1.00	2	1		11.06			BHTV-log correlation
NNR-3	238.80	f	238.60	239.00	N	60	E	60	NW	1.00	2	1		6.41			
NNR-3	239.10	f	239.00	239.20	N	50	E	61	NW	1.50	2	1		14.42			
NNR-3	240.28	f	240.05	240.50	N	70	W	64	SW	0.50	2	1		2.94			
NNR-3	242.50	b			N	18	E	31	NW								Obtained from BHTV-log
NNR-3	244.80	b			N	20	E	28	NW								
NNR-3	245.00	f	244.90	245.10	N	65	E	55	SE		2		>50			104, 42	
NNR-3	245.28	f	245.15	245.40	N	75	E	49	SE	1.50	2	4	40.00		n		BHTV-log correlation
NNR-3	245.55	f	245.45	245.65	N	80	E	45	SE	4.00	2	1		14.13			

NNR-3	245.98	f	245.90	246.05	N	60	E	36	SE	1.00	2	1		6.86		
NNR-3	246.18	f	246.10	246.25	N	50	E	33	SE	1.00	2	1		15.83		
NNR-3	246.55	f	246.50	246.60	N	60	E	44	SE	1.00	2	1	8.00		n	
NNR-3	247.00	f	246.80	247.20	N	35	E	53	SE	2.00	2	1		36.69		
NNR-3	247.30	f	247.20	247.40	N	40	E	31	SE	21.00	2	1		220.32		NW dipping faults are younger
NNR-3	247.60	f	247.40	247.80	N	65	W	58	SW	1.50	2	1	12.00		n	
NNR-3	247.70	f	247.60	247.80	N	60	E	44	SE	3.00	2	1		27.85		
NNR-3	248.30	f	248.20	248.40	N	70	E	42	SE	2.00	2	1	18.00		n	
NNR-3	248.60	f	248.50	248.70	N	35	E	38	NW	1.50	2	1	9.00		r	younger than 248.75
NNR-3	248.75	f	248.60	248.90	N	65	E	51	SE	1.50	2	1	13.00		r	
NNR-3	249.03	f	248.90	249.15	N	45	E	57	NW	0.50	2	1	3.00		n	
NNR-3	249.38	f	249.25	249.50	N	65	E	51	SE	1.50	2	1	9.00		n	
NNR-3	249.77	f	249.65	249.90	N	60	E	54	SE	2.00	2	1		17.80		
NNR-3	249.90	b			N	25	E	34	NW							Obtained from BHTV-log
NNR-3	249.90	f	249.80	250.00	N	20	E	36	SE	3.00	2	1	26.00		n	
NNR-3	250.20	b			N	25	E	34	NW							
NNR-3	250.28	f	250.10	250.45	N	75	E	45	SE	1.00	2	1	16.00		n	
NNR-3	251.00	f	250.45	251.55	N	65	E	81	SE	2.00	2	1	21.00		n	
NNR-3	251.68	f	251.60	251.75	N	10	E	32	SE		2					
NNR-3	252.05	f	252.00	252.10	N	10	E	33	NW	0.50	2	1		2.82		
NNR-3	252.28	f	252.10	252.45	N	0	S	57	E	0.50	2	1		2.10		
NNR-3	252.35	f	252.25	252.45	N	0	S	40	E	1.00	2	1		9.12		
NNR-3	252.70	f	252.60	252.80	N	10	E	40	SE	1.00	2	1		10.70		
NNR-3	253.05	f	253.00	253.10	N	20	W	39	NE	1.00	2	1		8.34		
NNR-3	253.10	f	253.00	253.20	N	20	W	25	NE	1.00	2	1		7.55		
NNR-3	253.88	f	253.65	254.10	N	65	E	62	SE	1.00	2	1		3.17		
NNR-3	254.50	f	254.20	254.80	N	40	E	73	SE	0.50	2	4	26.00		n	
NNR-3	254.88	f	254.20	255.55	N	45	E	82	SE	1.50	2	1	18.00		n	BHTV-log correlation
NNR-3	256.20	f	256.10	256.30	N	25	E	79	SE	2.00	2	1		32.68		
NNR-3	256.50	f	256.30	256.70	N	25	E	67	SE	3.00	2	1		12.05		
NNR-3	256.98	f	256.70	257.25	N	20	E	73	NW	1.50	2	1		11.28		
NNR-3	257.50	b			N	10	W	30	SW							
NNR-3	257.60	f	257.55	257.65	N	40	E	31	NW	2.00	2	1		15.57		BHTV-log correlation
NNR-3	257.63	f	257.55	257.70	N	45	E	34	NW	2.00	2	1		5.97		

NNR-3	259.40	b			N	0	S	19	W						
NNR-3	259.45	b			N	22	E	29	NW						Obtained from BHTV-log
NNR-3	259.90	b			N	0	S	31	NW						Obtained from BHTV-log
NNR-3	260.85	f	260.60	261.10	N	55	E	76	NW	0.50	2	1	3.00		r	
NNR-3	261.20	b			N	30	E	25	NW							
NNR-3	261.63	f	261.25	262.00	N	20	E	66	SE	2.00	2	1		22.59		
NNR-3	261.85	f	261.65	262.05	N	30	E	56	SE	5.00	2	4	106.00		n	BHTV-log correlation
NNR-3	262.18	f/j	262.00	262.35	N	55	E	57	NW	1.00	2	1		7.00		
NNR-3	262.43	f	262.35	262.50	N	35	E	39	NW	0.50	2	3	7.00		n	
NNR-3	262.80	b			N	0	S	24	W							
NNR-3	263.10	f	263.00	263.20	N	60	E	54	NW	1.00	2	1		12.13		
NNR-3	263.18	f	262.90	263.45	N	70	E	67	SE	1.00	2	1	11.00		n	
NNR-3	263.50	b			N	25	E	27	NW							
NNR-3	264.40	b			N	5	E	27	NW							Obtained from BHTV-log
NNR-3	265.78	f	265.15	266.40	N	30	E	80	SE	2.00	2	1	23.00		r	
NNR-3	266.70	b			N	25	E	23	NW							
NNR-3	266.95	f	266.60	267.30	N	55	E	72	NW	3.00	2	1	72.00		n	
NNR-3	267.10	b			N	20	E	48	NW							Obtained from BHTV-log
NNR-3	267.40	f	267.20	267.60	N	60	E	69	SE	1.00	2	1		6.34		
NNR-3	267.43	f	267.20	267.65	N	40	E	60	SE	1.00	2	1		7.76		
NNR-3	267.70	f	267.55	267.85	N	25	E	67	NW	1.00	2	1	8.00		n	
NNR-3	268.55	f	268.40	268.70	N	30	E	62	SE	1.00	2	1		13.32		
NNR-3	269.15	f	268.80	269.50	N	50	E	72	SE	55.00	2	1		588.15	n	BHTV-log correlation
NNR-3	269.75	f	269.60	269.90	N	25	E	55	NW	15.00	2	1		169.81		
NNR-3	270.10	b			N	20	E	15	NW							
NNR-3	270.35	f	270.00	270.70	N	20	E	67	SE	0.50	2	3	2.00		n	
NNR-3	270.50	b			N	10	E	18	NW							Obtained from BHTV-log
NNR-3	270.60	f	270.30	270.90	N	15	E	71	SE				32.00		n	
NNR-3	270.80	b			N	0	S	26	NW							Obtained from BHTV-log
NNR-3	271.10	b			N	10	W	28	SW							
NNR-3	271.70	b			N	15	E	23	NW							
NNR-3	272.10	f	271.90	272.30	N	15	E	64	SE	1.00	2	1	8.00		n	
NNR-3	272.30	b			N	0	S	33	W							Obtained from BHTV-log
NNR-3	272.80	b			N	0	S	25	W							

NNR-3	273.15	f	272.95	273.35	N	20	E	68	SE	0.50	2	1	4.00		n	
NNR-3	273.60	b			N	10	E	36	NW							Obtained from BHTV-log
NNR-3	274.60	b			N	15	E	22	NW							Obtained from BHTV-log
NNR-3	274.78	f	274.55	275.00	N	5	W	69	NE	0.50	2	1	5.00		n	
NNR-3	276.50	b			N	10	E	28	NW							Obtained from BHTV-log
NNR-3	276.80	b			N	10	E	24	NW							
NNR-3	277.00	b			N	15	E	23	NW							Obtained from BHTV-log
NNR-3	277.30	b			N	10	E	27	NW							
NNR-3	277.70	b			N	20	E	24	NW							
NNR-3	278.55	f	278.35	278.75	N	40	E	59	NW	1.00	2	1	6.00		n	younger than 278.85
NNR-3	278.85	f	278.50	278.85	N	40	E	57	SE	1.00	2	1		4.20		
NNR-3	279.40	f	279.10	279.70	N	40	E	63	SE	3.00	2	1		9.80		
NNR-3	279.55	f	279.40	279.70	N	25	E	47	SE		2		>50			BHTV-log correlation
NNR-3	279.90	f	279.60	280.20	N	25	E	67	SE	1.00	2	1		6.85		
NNR-3	280.40	b			N	5	E	21	NW							
NNR-3	281.35	f	281.20	281.50	N	50	E	71	NW	0.50	2	1	4.00		r	
NNR-3	281.98	f	281.85	282.10	N	15	W	61	NE	0.50	2	1		1.40		probably younger than 281.975
NNR-3	281.98	f	281.85	282.10	N	30	E	37	NW	1.00	2	1		3.16		
NNR-3	282.33	f	282.20	282.45	N	30	W	64	NE	0.50	2	1		2.46		
NNR-3	282.38	f	282.25	282.50	N	45	E	47	NW	0.50	2	1	4.00		n	younger than 282.325
NNR-3	282.73	f	282.50	282.95	N	20	W	68	NE	0.50	2	1		2.76		
NNR-3	283.00	f	282.90	283.10	N	25	W	63	NE	0.50	2	1		2.81		
NNR-3	283.20	b			N	10	E	18	NW							
NNR-3	283.70	b			N	25	E	20	NW							Obtained from BHTV-log
NNR-3	284.10	b			N	20	E	16	NW							
NNR-3	285.00	b			N	37	E	17	NW							Obtained from BHTV-log
NNR-3	285.60	b			N	35	E	17	NW							Obtained from BHTV-log
NNR-3	285.90	b			N	35	E	17	NW							
NNR-3	286.15	f	286.00	286.30	N	5	E	64	NW	0.50	2	1		2.64		
NNR-3	286.98	f	286.55	287.40	N	25	E	74	SE	1.00	2	1	3.00			
NNR-3	287.35	f	287.20	287.50	N	30	E	60	SE	1.00	2	1	3.00			
NNR-3	287.60	b			N	10	E	23	NW							
NNR-3	287.95	f	287.65	288.25	N	15	E	67	SE	1.50	2	1	23.00		n	
NNR-3	288.38	f	288.15	288.60	N	30	E	65	SE	4.00	2	1	>105	116.03	n	BHTV-log correlation

NNR-3	288.55	f	288.30	288.80	N	20	E	62	SE	2.00	2	1		17.57		
NNR-3	289.00	f	288.60	289.40	N	25	E	79	SE	2.00	2	1	28.00		n	
NNR-3	291.50	b			N	15	E	19	NW							Obtained from BHTV-log
NNR-3	291.70	b			N	20	E	17	NW							
NNR-3	292.20	b			N	5	E	15	NW							
NNR-3	292.48	f	292.30	292.65	N	35	W	48	NE	1.00	2	1		3.77		
NNR-3	292.53	f	292.35	292.70	N	40	E	60	SE	1.00	2	1		8.13		
NNR-3	292.75	f	292.60	292.90	N	45	E	61	NW	1.00	2	1		7.98		younger than 292.525
NNR-3	293.08	f	292.60	293.55	N	45	E	81	SE	1.50	2	1	17.00		n	
NNR-3	293.10	f	293.00	293.20	N	35	E	56	SE	1.00	2	1	13.00		n	
NNR-3	293.55	f	293.30	293.80	N	40	E	67	NW	1.00	2	1	7.00		n	
NNR-3	294.88	f	294.80	294.95	N	0	S	23	E	1.00	2	1		8.27		
NNR-3	295.70	b			N	10	E	20	NW							Obtained from BHTV-log
NNR-3	295.90	b			N	20	E	19	NW							
NNR-3	296.05	f	295.60	296.50	N	25	E	77	NW	1.00	2	3	6.00		n	
NNR-3	296.25	f	295.80	296.70	N	50	E	81	NW	1.00	2	3	5.00		r	
NNR-3	296.65	f	296.55	296.75	N	50	E	66	SE	2.00	2	3		23.15		
NNR-3	296.75	f	296.55	296.95	N	20	E	64	NW		2		>5		n	
NNR-3	297.00	f	296.85	297.15	N	35	E	71	SE	3.00	2	1	21.00		n	BHTV-log correlation
NNR-3	297.35	f	297.20	297.50	N	35	E	67	NW	1.00	2	2	7.00		n	
NNR-3	297.55	f	297.10	298.00	N	40	E	79	SE	1.50	2	2	52.00		n	
NNR-3	298.45	j	298.30	298.60	N	40	W	54	NE							
NNR-3	298.75	j	298.55	298.95	N	50	W	62	NE							BHTV-log correlation
NNR-3	299.53	f	299.35	299.70	N	5	E	60	NW	3.00	2	1		14.24		
NNR-3	300.05	f	300.00	300.10	N	50	E	62	SE	1.00	2	4	17.00		n	
NNR-3	300.20	f	300.10	300.30	N	5	E	44	NW		2		>40			BHTV-log correlation, younger than 300.05
NNR-3	302.35	f	301.90	302.80	N	65	E	74	SE	3.00	2	4	66.00		n	BHTV-log correlation
NNR-3	303.43	f	303.30	303.55	N	50	E	52	NW	2.50	2	1		19.99		BHTV-log correlation
NNR-3	303.70	f	303.60	303.80	N	30	E	43	NW	5.00	2	1		49.24		
NNR-3	303.80	f	303.75	303.85	N	75	E	46	SE	2.50	2	1	23.00		n	
NNR-3	304.10	f	304.00	304.20	N	20	E	39	NW	2.00	2	3	9.00		r	younger than 304.225
NNR-3	304.23	f	304.05	304.40	N	50	E	66	SE	2.00	2	4	50.00		n	
NNR-3	304.38	f	304.25	304.50	N	50	E	54	SE	1.50	2	3	6.00		n	
NNR-3	304.45	f	304.35	304.55	N	55	E	51	SE	1.00	2	3		8.30		

NNR-3	304.55	f	304.40	304.70	N	50	E	58	NW		2					
NNR-3	304.93	f	304.90	304.95	N	40	E	42	SE	1.00	2	1		8.66		
NNR-3	305.18	f	304.75	305.60	N	30	E	82	NW	2.00	2	1	26.00		n	BHTV-log correlation
NNR-3	305.43	f	305.05	305.80	N	55	E	74	NW	1.00	2	1		6.64		
NNR-3	305.65	f	305.25	306.05	N	45	E	72	NW	1.00	2	1		2.46		
NNR-3	305.85	b			N	15	E	16	NW							
NNR-3	306.88	f	306.20	307.55	N	40	E	86	SE	0.50	2	3	18.00		n	
NNR-3	307.20	f	306.50	307.90	N	50	E	74	SE	6.00	2	1		55.95		BHTV-log correlation
NNR-3	307.90	f	307.30	308.50	N	45	E	77	SE	1.00	2	1	12.00		n	
NNR-3	308.50	b			N	60	E	13	NW							
NNR-3	312.68	f	312.35	313.00	N	50	E	71	SE	3.00	2	1	36.00		n	BHTV-log correlation
NNR-3	312.85	f	312.50	313.20	N	40	E	67	SE	3.00	2	1	36.00		n	
NNR-3	313.95	f	313.05	314.85	N	75	E	86	NW	5.50	2	1	73.00		r	BHTV-log correlation
NNR-3	315.90	f	315.70	316.10	N	45	E	74	NW	2.50	2	1	46.00		n	
NNR-3	316.80	f	316.60	317.00	N	65	E	77	SE	0.50	2	4	23.00		n	
NNR-3	317.10	b			N	35	E	22	NW							
NNR-3	318.30	b			N	20	E	16	NW							
NNR-3	319.13	f/j	318.05	320.20	N	80	E	86	NW	0.50	2	1	6.00		r	
NNR-3	319.30	b			N	25	E	10	NW							
NNR-4	172.10	b			N	10	W	26	SW							Obtained from BHTV-log
NNR-4	175.00	b			N	5	E	21	NW							Obtained from BHTV-log
NNR-4	178.40	b			N	7	E	23	NW							Obtained from BHTV-log
NNR-4	184.40	b			N	0	S	23	W							Obtained from BHTV-log
NNR-4	200.85	f	200.70	201.00	N	30	E	57	SE		1	2				
NNR-4	201.00	f	200.80	201.20	N	50	E	76	SE	20.00	1	2		215.01	n	BHTV-log correlation
NNR-4	202.00	b			N	15	E	13	NW							
NNR-4	202.90	b			N	7	E	27	NW							Obtained from BHTV-log
NNR-4	205.90	b			N	0	S	24	W							Obtained from BHTV-log
NNR-4	206.40	b			N	22	E	35	NW							Obtained from BHTV-log
NNR-4	206.70	b			N	30	E	18	NW							
NNR-4	207.03	f	206.85	207.20	N	10	W	47	NE	1.00	1	1	9.00		n	
NNR-4	207.30	f	206.90	207.70	N	40	W	83	NE	1.00	1	1	6.00		r	
NNR-4	207.63	f	207.55	207.70	N	30	W	43	NE	1.00	1	1		9.76		
NNR-4	207.70	f	207.65	207.75	N	30	W	31	NE	1.00	1	1		8.68		

NNR-4	208.60	b			N	30	E	24	NW								Obtained from BHTV-log
NNR-4	211.10	f	210.80	211.40	N	40	E	66	SE	0.50	1	4	12.00		n		
NNR-4	211.30	b			N	25	E	9	NW								
NNR-4	214.28	f	214.00	214.55	N	5	W	63	SW	0.50	1	4	24.00		n		
NNR-4	217.40	b			N	20	W	9	SW								
NNR-4	220.85	f	220.70	221.00	N	5	E	64	SE	0.50	1	3	11.00		n		
NNR-4	221.80	f	221.70	221.90	N	20	E	63	SE	0.50	1	3		6.80			
NNR-4	222.40	b			N	15	W	7	SW								
NNR-4	222.65	f	222.60	222.70	N	30	E	57	NW	1.00	1	1		7.80			
NNR-4	222.85	f	222.60	223.10	N	45	E	83	SE		1		68.00		n		
NNR-4	223.70	f	223.60	223.80	N	40	E	42	NW	0.50	1	2	6.00		n		
NNR-4	223.90	f	223.80	224.00	N	50	E	53	NW	0.50	1	2	3.00		n		
NNR-4	224.55	f	224.30	224.80	N	40	E	65	NW	0.50	1	1	3.00		n		
NNR-4	225.00	b			N	30	E	11	NW								
NNR-4	225.80	f	225.30	226.30	N	30	E	81	NW		1		28.00		n	12, 63	BHTV-log correlation
NNR-4	226.83	f	225.90	227.75	N	50	E	84	NW	1.00	1	3	25.00		n	42, 54	
NNR-4	228.05	f	227.90	228.20	N	30	E	54	SE		1	1			n		BHTV-log correlation
NNR-4	228.10	f	228.05	228.15	N	40	E	71	NW	1.50	1	1		12.93			
NNR-4	228.80	f	228.70	228.90	N	10	E	44	SE		1		>25				
NNR-4	229.50	b			N	0	S	22	W								Obtained from BHTV-log
NNR-4	230.80	f	230.60	231.00	N	40	E	61	SE	1.50	1	1	13.00		n		BHTV-log correlation
NNR-4	231.10	b			N	20	E	13	NW								
NNR-4	234.70	b			N	30	E	29	NW								Obtained from BHTV-log
NNR-4	235.20	b			N	37	E	25	NW								Obtained from BHTV-log
NNR-4	236.30	b			N	10	E	18	NW								Obtained from BHTV-log
NNR-4	237.50	f/j	236.60	238.40	N	75	W	84	NE	0.50	1	3	2.00		r		
NNR-4	238.60	b			N	30	E	21	NW								
NNR-4	240.10	f	239.90	240.30	N	40	E	65	SE		1		50.00		n		BHTV-log correlation
NNR-4	244.15	f	243.80	244.50	N	70	E	64	NW	1.00	1	3	33.00		n		
NNR-4	244.80	b			N	15	E	14	NW								
NNR-4	246.20	j	245.80	246.60	N	10	W	77	NE								
NNR-4	246.30	f	246.10	246.50	N	70	E	64	SE	1.50	1	2	23.00		n		
NNR-4	246.48	f	246.45	246.50	N	10	E	12	SE	1.00	1	2	4.00				younger than 246.3
NNR-4	247.43	f	247.15	247.70	N	80	W	63	SW	0.50	1	3	6.00		n		

NNR-4	247.90	b			N	20	E	21	NW							
NNR-4	249.25	f	249.10	249.40	N	60	E	61	NW	0.50	1	4		33.65		
NNR-4	249.58	f	249.40	249.75	N	70	E	67	SE	1.00	1	4	21.00			BHTV-log correlation
NNR-4	249.90	f	249.80	250.00	N	30	E	33	SE	0.50	1			8.63		
NNR-4	250.03	f	249.95	250.10	N	80	E	60	SE	0.50	1	4		4.37		
NNR-4	250.65	f	250.40	250.90	N	70	E	76	NW	1.00	1	1	6.00		n	
NNR-4	251.10	b			N	5	W	28	SW							Obtained from BHTV-log
NNR-4	251.80	f	251.60	252.00	N	60	E	71	NW	1.00	1	1	9.00		n	
NNR-4	252.78	f	252.65	252.90	N	50	E	47	SE	1.00	1	2	16.00		n	
NNR-4	253.00	b			N	30	E	21	NW							
NNR-4	253.50	b			N	7	W	29	SW							Obtained from BHTV-log
NNR-4	254.00	b			N	15	W	35	SW							
NNR-4	254.05	f	254.00	254.10	N	70	E	21	SE	1.00	1	2		10.63		
NNR-4	254.08	f	254.00	254.15	N	75	E	26	SE	1.00	1	2		1.51		
NNR-4	254.20	b			N	0	S	41	W							Obtained from BHTV-log
NNR-4	254.80	b			N	5	W	39	SW							Obtained from BHTV-log
NNR-4	255.65	f	255.45	255.85	N	45	E	57	SE	10.00	1	3		106.53	n	BHTV-log correlation
NNR-4	255.73	f	255.60	255.85	N	40	E	53	SE	0.50	1	3	4.00		n	
NNR-4	256.30	b			N	22	E	27	NW							Obtained from BHTV-log
NNR-4	256.55	f	256.50	256.60	N	10	W	23	SW	1.00	1	2		10.63		
NNR-4	256.65	f	256.60	256.70	N	50	E	34	NW	1.00	1	2		10.63		
NNR-4	257.30	b			N	40	E	23	NW							
NNR-4	257.60	b			N	25	E	23	NW							Obtained from BHTV-log
NNR-4	257.65	f	257.50	257.80	N	40	W	57	NE	0.50	1	3	3.00		n	
NNR-4	258.53	f	258.35	258.70	N	50	W	50	SW	1.50	1	1	16.00		n	
NNR-4	259.90	b			N	20	E	21	NW							Obtained from BHTV-log
NNR-4	260.80	b			N	0	S	23	W							Obtained from BHTV-log
NNR-4	261.28	f	261.10	261.45	N	60	E	42	SE	0.50	1	3	6.00		n	
NNR-4	261.70	b			N	45	E	19	NW							
NNR-4	261.90	b			N	7	E	19	NW							Obtained from BHTV-log
NNR-4	262.20	b			N	30	E	21	NW							Obtained from BHTV-log
NNR-4	263.10	b			N	22	E	23	NW							Obtained from BHTV-log
NNR-4	263.50	f	263.40	263.60	N	60	W	62	SW	0.50	1	2	4.00		n	
NNR-4	263.68	f	263.30	264.05	N	80	W	77	NE	1.00	1	2	11.00		n	

NNR-4	264.30	f	264.20	264.40	E	90	W	57	SE	1.00	1	1	3.00		n		
NNR-4	264.60	f	264.50	264.70	E	90	W	59	S	1.00	1	1	5.00		n		
NNR-4	264.80	f	264.20	265.40	N	60	E	82	NW		1		>25				BHTV-log correlation
NNR-4	265.50	f	265.30	265.70	N	60	E	57	SE	1.00	2	1	10.00		n		
NNR-4	266.80	f	266.70	266.90	N	50	E	42	SE		2						
NNR-4	267.80	b			N	35	E	14	NW								
NNR-4	269.15	j	268.60	269.70	N	30	W	83	NE								BHTV-log correlation
NNR-4	269.68	f	269.50	269.85	N	40	E	67	SE	2.00	2	1		3.43			
NNR-4	270.30	f	270.20	270.40	N	30	W	50	NE	1.00	2	1		7.29			
NNR-4	270.33	f	270.20	270.45	N	30	W	56	NE	1.00	2	1		13.81			
NNR-4	270.40	j	270.10	270.70	N	10	E	84	NW								
NNR-4	270.73	f	270.25	270.90	N	70	E	70	SE	2.00	2	1	23.00		n		older than 270.3 and 270.325
NNR-4	270.95	f	270.80	271.10	E	90	W	68	N	0.50	2	3	3.00		r		
NNR-4	271.25	f	271.20	271.30	N	40	E	47	NW	1.00	2	1	7.00		n		
NNR-4	271.63	f	271.55	271.70	N	30	E	52	SE	1.00	2	1		8.55			
NNR-4	272.20	f	272.10	272.30	N	60	E	22	SE	0.50	2	3		8.04			
NNR-4	272.65	f	272.30	273.00	N	75	E	87	SE	2.00	2	1	18.00		n		
NNR-4	272.70	f	272.60	272.80	N	25	E	59	SE	1.00	2	1		6.28			younger than 272.65
NNR-4	272.90	b			N	15	E	19	NW								Obtained from BHTV-log
NNR-4	273.20	f	272.90	273.50	N	70	E	73	SE		2		>50			87, 44	
NNR-4	273.60	f	273.50	273.70	N	40	E	53	SE	1.00	2	1	9.00		n		
NNR-4	273.95	f	273.85	274.05	N	45	E	51	SE	1.50	2	1	11.00		n		
NNR-4	274.13	f	274.05	274.20	N	35	E	52	SE		2		>50			90, 47	
NNR-4	274.13	f	274.10	274.15	N	40	E	68	NW		2						
NNR-4	274.30	b			N	30	E	20	NW								
NNR-4	274.50	b			N	30	E	27	NW								Obtained from BHTV-log
NNR-4	274.58	f	274.45	274.70	E	90	W	68	S	1.00	2	1	6.00		n		
NNR-4	275.00	f	274.80	275.20	N	35	E	52	SE	1.00	2	1		4.47			
NNR-4	275.03	f	274.85	275.20	N	25	E	56	SE	1.00	2	1		8.63			
NNR-4	275.08	f	274.95	275.20	N	60	E	49	SE	1.00	2	1		8.25			
NNR-4	275.13	f	275.00	275.25	N	45	E	43	SE	13.00	2	1	>10	136.58	n	88, 33	BHTV-log correlation
NNR-4	275.95	f	275.70	276.20	N	35	E	61	SE	2.50	2	1	4.00		n		
NNR-4	276.10	b			N	30	E	33	NW								Obtained from BHTV-log
NNR-4	276.45	f	276.20	276.70	N	50	E	71	SE	2.00	2	1	4.00		n		BHTV-log correlation

NNR-4	277.60	b			N	30	E	35	NW							Obtained from BHTV-log
NNR-4	277.88	f	277.70	278.05	N	40	E	61	SE	3.00	2	1		20.75		
NNR-4	278.40	f	278.30	278.50	N	30	E	42	NW	1.50	2	1	9.00		r	younger than 278.55 and 278.65
NNR-4	278.55	f	278.40	278.70	N	0	S	47	E	1.00	2	1		7.20		
NNR-4	278.65	f	278.40	278.90	N	10	W	55	NE	1.00	2	1	3.00			
NNR-4	279.40	b			N	25	E	30	NW							Obtained from BHTV-log
NNR-4	279.50	b			N	30	E	22	NW							
NNR-4	280.20	f	280.00	280.40	E	90	W	51	S	1.00	2	1	3.00		n	
NNR-4	280.48	f	280.30	280.65	N	60	E	55	SE	6.00	2	1		47.58		BHTV-log correlation
NNR-4	280.53	f	280.40	280.65	N	40	E	42	SE	4.00	2	1		62.86		
NNR-4	280.93	f	280.80	281.05	N	50	E	37	SE	0.50	2	3	9.00		n	
NNR-4	281.15	f	281.00	281.30	N	35	E	53	SE	1.00	2	1	3.00		n	
NNR-4	281.20	f	281.10	281.30	N	30	E	58	SE	1.00	2	1	2.00		n	
NNR-4	281.40	b			N	50	E	17	NW							
NNR-4	282.20	b			N	22	E	30	NW							Obtained from BHTV-log
NNR-4	282.55	f	282.40	282.70	N	50	E	57	SE	1.50	2	1		11.28		
NNR-4	283.70	b			N	30	E	22	NW							Obtained from BHTV-log
NNR-4	285.40	b			N	20	E	20	NW							Obtained from BHTV-log
NNR-4	285.63	f	285.50	285.75	N	5	W	62	NE	0.50	2	3	3.00		n	
NNR-4	285.75	f/j	285.50	286.00	N	10	W	69	SW	1.00	2	3	19.00		r	
NNR-4	286.15	f	286.00	286.30	N	50	E	57	SE	3.00	2	1	13.00		n	
NNR-4	286.20	b			N	15	E	20	NW							Obtained from BHTV-log
NNR-4	287.00	b			N	30	E	12	NW							
NNR-4	287.05	f	286.60	287.50	N	0	S	85	E	1.00	2	2	17.00		r	
NNR-4	287.30	b			N	25	E	26	NW							Obtained from BHTV-log
NNR-4	288.10	b			N	52	E	22	NW							Obtained from BHTV-log
NNR-4	288.18	f	288.05	288.30	N	25	W	43	NE	2.00	2	1		25.01		
NNR-4	289.50	b			N	22	E	21	NW							Obtained from BHTV-log
NNR-4	291.10	f	291.00	291.20	N	50	E	56	SE	13.00	2	1		112.71		BHTV-log correlation
NNR-4	291.30	f	291.10	291.50	N	65	E	69	SE	12.00	2	1		122.96		BHTV-log correlation
NNR-4	291.55	f	291.30	291.80	N	60	E	72	SE	2.00	2	1		9.19		
NNR-4	292.40	b			N	35	E	20	NW							
NNR-4	293.45	f	293.30	293.60	N	35	E	65	NW	0.50	2	2		5.10		
NNR-4	293.80	b			N	52	E	23	NW							Obtained from BHTV-log

NNR-4	294.50	f	294.30	294.70	N	25	E	67	NW	1.00	2	1	9.00		n	
NNR-4	294.65	f	294.50	294.80	N	10	E	62	NW	1.00	2	1		7.13		
NNR-4	294.88	f	294.75	295.00	N	5	E	60	NW	1.00	2	2	8.00		n	
NNR-4	295.80	b			N	45	E	18	NW							Obtained from BHTV-log
NNR-4	297.00	f	296.60	297.40	N	30	W	78	NE	2.00	2	1		6.09		
NNR-4	298.83	f	298.65	299.00	N	65	E	60	SE	15.00	2	1		148.98	n	BHTV-log correlation
NNR-4	299.15	f	299.00	299.30	N	45	E	60	SE	10.00	2	1		108.99	n	
NNR-4	299.68	f	299.40	299.95	N	35	E	70	SE	5.00	2	1		27.70	n	
NNR-4	300.33	f	300.15	300.50	N	50	E	65	SE	15.00	2	4		170.48	n	BHTV-log correlation
NNR-4	300.73	f	300.60	300.85	N	45	E	52	SE	2.00	2	1		22.31		
NNR-4	300.83	f	300.70	300.95	N	30	W	39	NE	2.00	2	1		5.32		
NNR-4	300.88	f	300.70	301.05	N	35	W	46	NE	2.00	2	1		15.57		
NNR-4	301.28	f	301.20	301.35	N	60	E	63	NW	2.00	2	1		10.85		
NNR-4	302.10	b			N	20	W	20	SW							
NNR-4	302.70	b			N	10	E	19	NW							Obtained from BHTV-log
NNR-4	303.15	f	302.90	303.40	N	55	E	83	NW	2.00	2	1	3.00		r	
NNR-4	303.48	f	303.40	303.55	N	60	W	54	NE	2.00	2	1		0.62		
NNR-4	304.30	f	304.00	304.60	N	40	E	74	SE	0.50	2	3	6.00			
NNR-4	305.40	b			N	20	E	21	NW							
NNR-4	305.45	b			N	30	E	15	NW							Obtained from BHTV-log
NNR-4	306.18	f	306.05	306.30	N	40	E	57	NW	1.00	2	1		10.62		
NNR-4	306.45	f	306.30	306.60	N	45	E	45	SE	4.00	2	1		32.74		BHTV-log correlation
NNR-4	306.90	f	306.70	307.10	N	40	E	63	SE	1.00	2	1	7.00		n	BHTV-log correlation
NNR-4	307.48	f	307.35	307.60	N	65	E	37	SE	2.00	2	1		13.13		
NNR-4	307.75	f	307.60	307.90	N	70	E	54	SE	1.00	2	1		10.39		
NNR-4	308.00	f	307.80	308.20	N	70	E	64	SE	1.00	2	1		9.93	n	younger than 308.225, also large strike-slip component
NNR-4	308.20	f	308.00	308.40	N	80	E	66	SE	1.00	2	1		10.25		younger than 308.225, also large strike-slip component
NNR-4	308.23	f	308.10	308.30	N	60	E	68	NW	4.00	2	1		31.02		
NNR-4	308.53	f	308.40	308.65	N	35	E	42	NW	2.00	2	1		15.57		BHTV-log correlation
NNR-4	308.58	f	308.40	308.75	N	40	E	55	NW	2.00	2	1		34.02		
NNR-4	310.70	b			N	30	E	19	NW							
NNR-4	310.93	f	310.85	311.00	N	65	E	82	SE	1.00	2	1	1.00		n	
NNR-4	311.10	f	311.00	311.20	N	45	E	57	NW	1.00	2	1	1.00		n	
NNR-4	311.40	b			N	15	E	23	NW							Obtained from BHTV-log

NNR-4	311.80	f	311.60	312.00	N	20	W	59	NE	0.50	2	3	3.00		r	
NNR-4	312.75	f	312.35	313.15	N	40	E	73	SE	2.00	2	1	9.00		n	
NNR-4	313.53	f	313.45	313.80	N	65	W	82	SW	2.00	2	1		12.91		
NNR-4	313.80	f	313.60	314.00	N	40	W	78	SW	2.00	2	1		32.98		
NNR-4	315.10	f	314.20	316.00	N	80	E	79	SE	2.00	2	1	13.00		r	younger than 316.1 and 316.15
NNR-4	315.90	b			N	25	E	36	NW							Obtained from BHTV-log
NNR-4	316.10	f	315.80	316.40	N	80	E	66	NW	2.00	2	1		3.67		
NNR-4	316.15	f	316.10	316.20	N	70	E	46	NW	2.00	2	1		20.28		
NNR-4	316.40	b			N	25	E	27	NW							
NNR-4	317.90	b			N	0	S	21	W							Obtained from BHTV-log
NNR-4	319.50	b			N	25	W	23	SW							
NNR-4	319.55	b			N	25	W	24	SW							Obtained from BHTV-log
NNR-4	321.30	b			N	20	E	17	NW							
NNR-4	321.85	f	321.60	322.10	N	55	E	58	NW	3.00	2	1		36.08		BHTV-log correlation
NNR-4	323.10	j	322.80	323.40	N	60	W	74	NE							BHTV-log correlation
NNR-4	323.80	b			N	22	E	26	NW							Obtained from BHTV-log
NNR-4	324.45	f	324.00	324.90	N	75	W	74	NE	0.50	2	2		4.02		
NNR-4	327.80	b			N	20	E	13	NW							Obtained from BHTV-log
NNR-4	328.50	b			N	15	E	15	NW							
NNR-4	333.60	b			N	7	E	16	NW							Obtained from BHTV-log
NNR-4	336.08	f	335.90	336.25	N	70	E	50	NW	1.00	2	1	4.00		r	BHTV-log correlation
NNR-4	336.15	f	335.90	336.40	E	90	W	56	N	1.00	2	1	3.00		r	BHTV-log correlation
NNR-4	338.40	b			N	25	W	12	SW							
NNR-4	340.20	b			N	18	E	21	NW							Obtained from BHTV-log
NNR-4	342.20	b			N	0	S	27	W							Obtained from BHTV-log
NNR-4	342.70	b			N	20	E	13	NW							
NNR-4	342.98	f	342.80	343.15	N	45	E	54	NW	1.00	2	1		7.45		
NNR-4	343.40	f	343.10	343.70	N	70	E	61	NW	1.00	2	1	3.00		n	
NNR-4	344.50	b			N	3	E	17	NW							Obtained from BHTV-log
NNR-4	345.00	f	344.90	345.10	N	10	W	49	NE	0.50	2	4	7.00		n	
NNR-4	345.75	f	345.70	345.80	N	35	E	43	NW	1.00	2	1	5.00		n	younger than 346.05
NNR-4	345.80	b			N	30	W	11	SW							
NNR-4	346.00	f	345.80	346.20	N	50	E	59	SE	2.00	2	1	14.00		n	BHTV-log correlation
NNR-4	346.05	f	345.70	346.40	N	70	E	82	SE	1.00	2	1	6.00		n	

NNR-4	346.48	f	346.35	346.60	N	50	E	52	NW	2.00	2	1	17.00		n	
NNR-4	346.60	f	346.40	346.80	N	30	E	53	SE	1.50	2	3		11.33		
NNR-4	346.65	f	346.40	346.90	N	45	E	61	SE	2.00	2	3		17.26		
NNR-4	346.75	f	346.40	347.10	N	60	E	76	SE	4.00	2	3		23.67		BHTV-log correlation
NNR-4	346.78	j	346.50	347.05	N	35	E	81	SE							
NNR-4	347.50	f	346.90	348.10	N	80	E	86	SE	1.00	2	1	7.00		n	
NNR-4	347.80	b			N	3	E	21	NW							Obtained from BHTV-log
NNR-4	348.10	f	348.00	348.20	N	85	E	53	NW	0.50	2	1		1.54		
NNR-4	348.23	f	347.85	348.60	N	45	E	71	SE	1.00	2	1	11.00		n	
NNR-4	348.40	b			N	10	E	16	NW							
NNR-4	349.80	b			N	7	E	23	NW							Obtained from BHTV-log
NNR-4	351.00	b			N	30	E	15	NW							
NNR-4	351.70	b			N	8	E	25	NW							Obtained from BHTV-log
NNR-4	352.10	f	351.70	352.50	N	75	E	79	NW	0.50	2	3	4.00		n	
NNR-4	352.25	f	352.00	352.50	N	65	E	75	SE	0.50	2	3	2.00		n	
NNR-4	352.70	b			N	3	E	25	NW							Obtained from BHTV-log
NNR-4	352.88	f	352.05	353.70	N	80	E	84	NW	0.50	2	3	3.00		r	
NNR-4	353.38	f	353.15	353.60	N	40	E	57	SE	0.50	2	1	4.00		n	
NNR-4	354.50	b			N	10	W	18	SW							Obtained from BHTV-log
NNR-4	356.28	f	356.15	356.40	N	75	E	61	NW	0.50	2	2		0.64		
NNR-4	356.35	f	356.30	356.40	N	70	E	67	SE	1.00	2	2		15.84		
NNR-4	356.73	f	356.60	356.85	N	80	E	63	SE	2.00	2	1	2.50		n	
NNR-4	356.95	b			N	35	E	22	NW							
NNR-4	357.20	f	357.00	357.40	N	65	E	62	SE	4.00	2	1	>60	74.68	n	BHTV-log correlation
NNR-4	357.38	f	357.20	357.55	N	70	E	67	SE	4.00	2	1	>80	91.35	n	
NNR-4	357.60	f	357.20	358.00	N	80	W	71	NE	1.00	2	1		6.76		
NNR-4	358.00	f	357.80	358.20	N	80	E	73	NW	1.00	2	1		4.24		
NNR-4	358.10	f	357.90	358.30	N	55	E	64	NW	1.00	2	1		6.32		
NNR-4	358.90	f	358.80	359.00	N	85	W	84	SW	1.00	2	1		5.44		
NNR-4	359.35	f	359.20	359.50	N	40	W	62	NE	0.50	2	1		3.04		
NNR-4	359.60	f	359.30	359.90	N	60	E	66	NW	2.00	2	1		5.25		
NNR-4	360.10	b			N	3	W	27	SW							Obtained from BHTV-log
NNR-4	361.00	b			N	5	E	12	NW							
NNR-4	364.10	b			N	10	E	17	NW							Obtained from BHTV-log

NNR-4	365.90	b			N	15	E	15	NW							
NNR-4	366.50	b			N	3	W	15	SW							Obtained from BHTV-log
NNR-4	368.03	f	367.85	368.20	N	70	W	57	NE	1.00	2	1		0.73		
NNR-4	368.18	f	368.05	368.30	N	75	W	84	NE	2.00	2	1		6.16		
NNR-4	368.30	b			N	0	S	15	SW							Obtained from BHTV-log
NNR-4	369.33	f	369.20	369.45	N	60	W	58	NE	1.00	2	1		6.78		
NNR-4	371.23	f	370.70	371.75	N	80	E	86	SE	1.00	2	1		8.22		
NNR-4	373.50	b			N	30	E	15	NW							
NNR-4	373.98	f	373.85	374.10	N	65	W	46	NE	2.00	2	1		17.15		
NNR-4	374.15	f	374.10	374.20	N	5	E	60	SE	3.00	2	1		26.59		
NNR-4	374.20	b			N	5	W	15	SW							Obtained from BHTV-log
NNR-4	374.33	f	374.25	374.40	N	20	E	50	NW	2.00	2	1		25.67		
NNR-4	376.00	b			N	10	E	18	NW							Obtained from BHTV-log
NNR-4	376.30	b			N	15	W	11	SW							
NNR-4	376.40	b			N	15	W	17	SW							Obtained from BHTV-log
NNR-4	378.10	f	377.80	378.40	N	55	E	75	NW	3.00	2	1		41.57		
NNR-4	378.55	f	378.30	378.80	N	55	E	73	NW	3.50	2	1	50.00		n	
NNR-4	379.05	f	378.80	379.30	N	60	E	67	NW	2.00	2	1	35.00		n	
NNR-4	381.05	f	380.80	381.30	N	25	W	59	NE	3.00	2	1		15.47		
NNR-4	381.25	f	381.10	381.40	N	60	W	80	SW	2.00	2	1		12.66		
NNR-4	382.70	b			N	45	W	7	SW							
NNR-4	383.70	f	383.40	384.00	N	20	E	64	SE	2.00	2	1	19.00		n	
NNR-4	384.20	f	384.00	384.40	N	5	E	61	SE	1.00	2	3	21.00		n	
NNR-4	384.45	f	384.40	384.50	N	60	E	56	SE	0.50	2	3		9.84		
NNR-4	384.83	f	384.50	385.15	N	50	E	68	NW	1.50	2	2	22.00		n	
NNR-4	385.03	f	384.65	385.40	N	55	E	71	NW	1.50	2	2	22.00		n	BHTV-log correlation
NNR-4	386.20	b			N	30	W	24	SW							
NNR-4	386.25	b			N	25	W	30	SW							Obtained from BHTV-log
NNR-4	386.48	f	386.35	386.60	N	0	S	59	E	1.00	2	2	11.00		n	
NNR-4	386.75	f	386.60	386.90	N	35	W	45	NE	1.50	2	1		13.02		
NNR-4	388.08	f	388.00	388.15	N	50	E	44	NW	9.00	2	1		90.50		
NNR-4	388.10	f	387.90	388.30	N	40	E	58	SE	4.00	2	1	24.00		n	BHTV-log correlation, younger than 388.075 and 388.15
NNR-4	388.15	f	387.95	388.15	N	35	E	47	NW	4.00	2	1		24.09		
NNR-4	388.90	f	388.70	389.10	N	65	E	87	SE	2.00	2	1		26.38		

NNR-4	388.93	f	388.85	389.00	N	30	E	47	SE	1.00	2	1		9.58			
NNR-4	389.15	f	389.00	389.30	N	10	E	52	SE	1.00	2	1		12.64			
NNR-4	389.45	f	389.10	389.70	N	75	E	87	NW	2.00	2	1		18.99			BHTV-log correlation
NNR-4	389.85	f	389.60	390.10	N	45	E	59	NW	3.00	2	1		14.00			
NNR-4	390.30	b			N	35	W	7	SW								
NNR-4	390.38	f	390.30	390.45	N	25	E	40	SE	2.00	2	1		17.40			
NNR-4	390.45	f	390.40	390.50	N	20	E	31	SE	1.00	2	1		12.79			
NNR-4	390.65	f	390.60	390.70	N	30	E	37	SE	2.00	2	1		1.28			
NNR-4	390.68	f	390.60	390.75	N	35	E	49	SE	2.00	2	1		9.46			
NNR-4	391.08	f	391.00	391.15	N	65	E	51	SE	1.00	2	1		7.68			
NNR-4	391.38	f	391.30	391.45	N	50	E	54	NW	2.00	2	1		15.39			
NNR-4	391.43	f	391.25	391.60	E	90	W	73	SE	2.00	2	1		6.07			
NNR-4	391.85	j	391.50	392.20	N	45	W	71	NE								BHTV-log correlation
NNR-4	392.00	f	391.70	392.30	N	45	E	73	SE	8.00	2	1	>80		n		BHTV-log correlation
NNR-4	392.90	j	392.40	393.40	N	70	W	84	NE								
NNR-4	393.60	f	393.40	393.80	N	35	E	77	SE	2.00	2	1	19.00		n		
NNR-4	393.60	f	393.45	393.75	N	30	E	73	NW	2.00	2	1	14.00		r		
NNR-4	394.30	f	394.20	394.40	N	10	E	34	NW	3.00	2	1		25.59			
NNR-4	394.40	f	394.20	394.80	N	50	E	75	NW	1.50	2	1	19.00		r		BHTV-log correlation
NNR-4	394.70	b			N	38	E	52	SE								Obtained from BHTV-log
NNR-4	395.00	b			N	45	E	39	SE								
NNR-4	395.55	f	395.50	395.60	N	5	W	54	SW	1.00	2	1		6.86			
NNR-4	395.60	f	395.50	395.70	N	0	S	49	W	1.00	2	1		13.19			
NNR-4	396.40	f	396.00	396.80	N	55	E	77	SE	24.00	2	1		237.62	n		BHTV-log correlations
NNR-4	397.00	f	396.50	397.50	N	40	E	84	SE	4.00	2	1		31.96			
NNR-4	397.43	f	397.00	397.85	N	80	E	81	SE	10.00	2	1		89.09			
NNR-4	397.90	f	397.40	398.40	N	50	E	74	SE	10.00	2	1		101.14			
NNR-4	398.85	f	398.30	399.40	N	70	E	71	SE	10.00	2	1		106.84			
NNR-4	399.45	f	398.60	400.30	N	65	E	82	SE	10.00	2	1		135.75			
NNR-4	400.20	f	400.00	400.40	N	35	E	60	SE		2		>50			78, 50	
NNR-4	400.60	f	400.40	400.80	N	30	E	64	SE		2		>50				
NNR-4	400.95	f	400.80	401.10	N	40	E	60	NW	5.00	2	1		56.32			
NNR-4	401.35	f	401.00	401.70	N	55	E	69	SE	10.00	2	1		104.60			
NNR-4	401.80	f	401.60	402.00	N	55	E	83	SE		2		>30				

NNR-4	402.30	f	402.20	402.40	N	40	E	48	NW	2.00	2	3	24.00		n		
NNR-4	402.53	f	402.45	402.60	N	35	E	55	NW	2.00	2	3	18.00		n		
NNR-4	403.35	f	403.00	403.70	N	45	E	75	SE	40.00	2	1		425.87	n		
NNR-4	403.50	b			N	23	W	22	NE								Obtained from BHTV-log
NNR-4	404.53	f	403.70	405.00	N	73	E	77	SE	52.00	2	1		558.39	n	96, 60	
NNR-7	171.60	b			N	7	W	9	SW								Obtained from BHTV-log
NNR-7	175.00	b			N	0	S	14	W								
NNR-7	175.70	b			N	2	E	18	NW								Obtained from BHTV-log
NNR-7	175.90	b			N	2	W	14	SW								Obtained from BHTV-log
NNR-7	178.00	b			N	0	S	12	W								
NNR-7	178.40	f	178.30	178.50	N	40	E	53	NW		1						
NNR-7	179.83	f	179.70	179.95	N	70	E	57	NW	1.00	1	3	4.00		n		
NNR-7	180.43	f	180.05	180.80	N	45	E	66	NW	1.00	1	2	16.00		n		
NNR-7	180.50	f	180.40	180.60	N	0	S	50	E	1.50	1	2	2.00		r		
NNR-7	182.50	b			N	18	E	14	NW								Obtained from BHTV-log
NNR-7	182.90	b			N	20	E	16	NW								
NNR-7	183.50	f	183.30	183.70	N	30	E	56	SE	1.00	1	3	3.00		n		
NNR-7	183.55	f	183.40	183.70	N	35	E	52	SE	2.00	1	3	7.00		n		
NNR-7	184.10	b			N	5	E	12	NW								Obtained from BHTV-log
NNR-7	186.40	f	186.20	186.60	N	80	E	60	NW	1.00	1	2	2.00		n		
NNR-7	186.48	f	186.30	186.65	N	30	E	61	NW	1.00	1	2	1.00		n		
NNR-7	187.55	f	187.10	188.00	N	80	E	69	SE	0.50	1	3	3.00		n		
NNR-7	188.10	f	187.80	188.40	N	50	E	65	SE	1.00	1	3	27.00		n		
NNR-7	188.50	b			N	10	E	14	NW								
NNR-7	191.13	f	191.05	191.20	N	70	E	30	NW	0.50	1	3		3.04			
NNR-7	192.70	b			N	22	W	14	SW								Obtained from BHTV-log
NNR-7	193.40	f	193.30	193.50	N	50	E	49	NW	1.00	1	2	6.00		n		
NNR-7	193.50	f	193.40	193.60	N	85	E	61	NW	1.00	1	2		26.35			
NNR-7	193.60	b			N	5	W	16	SW								
NNR-7	195.00	b			N	5	E	19	NW								Obtained from BHTV-log
NNR-7	195.65	f	195.30	196.00	N	55	E	78	SE	1.00	1	2	2.50		n		
NNR-7	195.70	f	195.40	196.00	N	55	E	75	SE	1.00	1	2	2.50		n		
NNR-7	196.10	f	195.90	196.30	N	50	E	58	SE		1	3			n		
NNR-7	196.50	f	196.00	197.00	N	50	E	80	SE		1	3			n	64, 54	BHTV-Log correlation

NNR-7	196.85	f	196.70	197.00	N	60	E	61	NW	1.00	1	2		14.13			
NNR-7	197.10	f	197.00	197.20	N	60	E	64	SE	1.00	1	2		19.41			
NNR-7	197.70	b			N	35	W	16	SW								
NNR-7	197.93	f	197.85	198.00	N	35	E	32	NW	1.00	1	2	5.00		r		
NNR-7	198.05	f	198.00	198.10	N	30	E	30	NW	1.00	1	2		10.63			
NNR-7	198.65	f	198.20	199.10	N	40	E	72	SE		1	1			n		
NNR-7	202.13	f	202.05	202.20	N	60	E	41	SE		1	3			n		
NNR-7	203.00	f	202.80	203.20	N	60	E	60	SE		1	3			n	95, 44	
NNR-7	203.28	f	203.05	203.50	N	50	E	56	SE	1.00	1	3	9.00		n		
NNR-7	203.65	f	203.40	203.90	N	70	E	63	SE	7.00	1	3	47.00		n		
NNR-7	204.05	f	203.90	204.20	N	40	E	51	SE	0.50	1	4	7.00		n		younger than fault 204.3
NNR-7	204.30	f	203.90	204.70	N	40	E	74	NW		1		6.00		n		
NNR-7	205.13	f	205.00	205.25	N	50	E	37	SE	1.00	1	1		9.47	n		
NNR-7	205.20	f	205.00	205.40	N	50	E	45	SE	21.00	1	1		223.19	n		
NNR-7	205.35	f	205.00	205.70	N	50	E	67	SE	0.50	2	3	1.00		n		
NNR-7	205.95	f	205.80	206.05	N	60	E	55	NW	0.50	2	3	11.00		n		
NNR-7	206.08	f	205.95	206.20	N	60	E	58	SE	2.00	2	3	32.00		n		
NNR-7	206.35	f	206.20	206.50	N	70	E	51	SE	2.00	2	1	28.00		n		
NNR-7	206.60	b			N	30	E	23	NW								
NNR-7	206.85	f	206.70	207.00	N	50	E	41	SE	1.00	2	3	19.00		n		
NNR-7	207.05	f	206.90	207.20	N	60	E	56	SE	0.50	2	3	7.00		n		
NNR-7	207.25	f	207.10	207.40	N	55	E	54	SE	0.50	2	3	3.00		n		
NNR-7	207.60	f	207.30	207.90	N	50	E	70	SE	2.00	2	3	16.00		n		
NNR-7	207.80	f	207.70	207.90	N	60	E	53	SE	0.50	2	3	3.00		n		
NNR-7	208.28	f	207.95	208.60	N	80	W	62	NE	0.50	2	3	26.00		n		
NNR-7	208.40	f	208.30	208.50	N	45	E	65	SE	0.50	2	3	3.00		n		
NNR-7	208.65	f	208.50	208.80	N	40	E	63	SE	0.50	2	3	3.00		r		
NNR-7	208.80	b			N	30	W	33	SW								
NNR-7	208.90	f	208.80	209.00	N	50	E	37	SE	0.50	2	3	2.00		n		
NNR-7	209.10	f	209.00	209.20	N	40	E	44	SE	2.00	2	2	3.00		n		
NNR-7	209.30	f	209.25	209.35	N	20	E	24	SE	1.00	2	2		9.50			
NNR-7	210.05	f	209.90	210.20	N	25	E	51	SE	2.50	2	1	33.50		n		
NNR-7	210.10	f	209.90	210.30	N	40	E	67	SE	2.50	2	1	33.50		n		
NNR-7	210.23	f	210.05	210.40	N	70	E	52	SE	7.00	2	1		53.78	n		

NNR-7	210.35	f	210.30	210.40	N	55	E	31	SE	3.00	2	1		9.60	n	
NNR-7	211.40	f	211.20	211.60	N	20	E	54	SE	1.00	2	2	3.00		n	
NNR-7	211.80	f	211.70	211.90	N	60	E	43	SE	1.00	2	2		16.44		
NNR-7	212.00	f	211.95	212.05	N	55	E	41	SE	1.00	2	2		15.34		
NNR-7	212.40	b			N	50	W	29	SW							
NNR-7	213.00	f	212.80	213.20	N	20	E	61	SE	1.00	2	3		7.52	n	
NNR-7	213.15	f	213.00	213.30	N	30	E	46	SE	1.00	2	3	3.00		n	
NNR-7	213.25	f	213.10	213.40	N	30	E	68	SE	1.00	2	3	7.00		r	
NNR-7	213.40	f	213.20	213.60	N	50	E	61	SE	4.00	2	3		59.26	n	
NNR-7	213.75	f	213.40	214.10	N	10	W	71	NE	2.00	2	2	8.00		r	
NNR-7	215.10	f	215.00	215.20	N	50	E	43	NW	1.50	2	2		5.74		
NNR-7	215.40	f	215.30	215.50	N	30	E	32	SE	2.00	2	2		18.82		
NNR-7	215.48	f	215.35	215.60	N	20	E	31	SE	2.00	2	2		28.72		
NNR-7	215.50	f	215.20	215.80	N	70	E	72	SE	1.50	2	2	7.00		n	younger than faults 215.4 and 215.475
NNR-7	215.90	f	215.80	216.00	N	10	E	42	SE	1.00	2	2		2.29		
NNR-7	216.15	f	216.00	216.30	N	70	E	60	SE	1.00	2	3	12.00		n	
NNR-7	216.25	f	216.10	216.40	N	70	E	62	SE	0.50	2	3	4.00		n	
NNR-7	216.40	f	216.20	216.60	N	75	E	66	SE	0.50	2	4	12.00		n	
NNR-7	216.90	b			N	0	S	25	W							
NNR-7	217.05	f	216.90	217.20	N	0	S	42	E	0.25	2	4	3.00		n	
NNR-7	217.95	f	217.60	218.30	N	0	S	61	E	1.00	2	3	10.00		r	
NNR-7	218.60	f	218.20	219.00	N	10	E	80	NW	1.00	2	1	5.00		n	
NNR-7	218.75	f	218.60	218.90	N	10	E	41	SE	0.50	2	2	3.00		n	
NNR-7	219.48	f	219.20	219.75	N	20	E	65	NW	1.00	2	2	4.00		n	
NNR-7	219.60	f	219.50	219.70	N	20	E	41	SE	1.00	2	2		15.26		older than 219.475
NNR-7	222.60	b			N	15	E	24	NW							
NNR-7	227.90	f	227.50	228.30	N	30	E	77	NW	1.00	2	1	1.50		n	
NNR-7	227.98	f	227.90	227.95				14	S	1.00	2	1		3.03		
NNR-7	228.30	b			N	0	S	21	W							
NNR-7	229.05	f	228.90	229.20	N	20	E	51	SE	0.50	2	3		2.14		
NNR-7	229.40	f	229.00	229.80	N	40	E	73	SE	1.00	2	3	19.00		n	
NNR-7	229.45	f	229.00	229.90	N	40	E	69	SE	0.50	2	3		8.48		
NNR-7	230.78	f	230.50	231.05	N	40	E	63	SE	3.00	2	1	9.00		n	
NNR-7	231.00	f	230.70	231.30	N	45	E	64	SE	2.00	2	1		12.20		

NNR-7	231.10	f	230.70	231.50	N	50	E	76	SE	4.00	2	1	24.00		n		
NNR-7	231.60	b			N	30	E	26	NW								
NNR-7	231.80	b			N	7	E	22	NW								Obtained from BHTV-log
NNR-7	232.08	f	231.95	232.20	N	70	E	75	NW	1.00	2	4	21.00		n		
NNR-7	232.15	f	232.00	232.30	N	60	E	57	SE	1.00	2	1		10.66			
NNR-7	232.55	f	232.40	232.70	N	70	E	51	SE	4.00	2	1	14.00		n		
NNR-7	233.08	f	232.80	233.35	N	30	E	74	SE	4.00	2	1	39.00		n		
NNR-7	233.60	f	233.50	233.70	N	30	E	43	NW		2		1.00		r		
NNR-7	233.68	f	233.50	233.85	N	30	E	46	SE	4.00	2		22.00		n		
NNR-7	234.20	f	234.00	235.00	N	50	E	77	SE	3.00	2	1		7.11	n		younger than 234.7
NNR-7	234.70	f	234.50	234.90	N	70	E	74	NW	5.00	2	1	21.00		r		
NNR-7	235.80	f	235.60	236.00	N	50	W	43	NE		2				n		
NNR-7	235.90	f	235.70	236.10	N	50	E	64	NW		2				n		
NNR-7	236.35	f	236.00	236.70	N	60	E	70	SE		2	1			n	79, 42	BHTV-Log correlation
NNR-7	236.95	f	236.50	237.40	N	60	E	72	SE		2	1			n	95, 60	BHTV-Log correlation
NNR-7	237.70	f	237.50	237.90	N	40	E	79	SE	3.50	2	1		31.00			
NNR-7	237.73	f	237.60	237.85	N	40	E	66	SE	2.00	2	1	9.00		n		
NNR-7	237.90	f	237.80	238.00	N	40	E	68	SE	3.00	2	1		44.55			
NNR-7	238.18	f	238.05	238.30	N	60	E	79	SE	5.00	2	1		27.76			
NNR-7	238.33	f	238.25	238.40	N	30	E	35	NW	2.00	2	1		22.03			
NNR-7	238.60	f	238.30	238.90	N	50	E	86	SE		2						
NNR-7	239.30	f	238.90	239.70	N	55	E	90			2						
NNR-7	239.80	f	239.60	240.00	N	50	E	79	SE	6.00	2	1		67.39			
NNR-7	240.45	f	240.00	240.90	N	50	E	74	NW	6.00	2	1		100.14			
NNR-7	240.50	f	240.40	240.60	N	20	E	56	SE	1.00	2	1	1.00		n		
NNR-7	240.85	f	240.50	241.20	N	15	E	67	SE	2.00	2	1	5.00		n		
NNR-7	241.70	b			N	10	W	20	SW								
NNR-7	242.20	f	242.00	242.40	N	80	E	81	NW	7.00	2	1	19.00		n		
NNR-7	242.35	f	242.20	242.50	N	80	E	79	NW	7.00	2	1		62.02			
NNR-7	242.90	f	242.30	243.50	N	70	E	78	SE	3.00	2	1	180.00		n	81, 43	BHTV-Log correlation
NNR-7	243.50	f	243.30	243.70	N	60	E	57	NW	4.00	2	1		17.69			
NNR-7	243.85	f	243.70	244.00	N	70	E	63	SE	3.00	2	1		42.59			
NNR-7	244.80	f								6.00	2	1	33.00		r		
NNR-7	246.85	f	246.50	247.20	N	50	E	75	SE	6.00	2		64.00		n		BHTV-Log correlation

NNR-7	247.25	f	247.00	247.50	N	45	E	65	SE	2.00	2	1	14.00		n	
NNR-7	247.95	f	247.80	248.10	N	40	E	56	SE	2.00	2	2		7.41		
NNR-7	248.08	f	247.95	248.20	N	60	E	55	SE	4.00	2	2	19.00		n	BHTV-Log correlation
NNR-7	248.75	f	248.60	248.90	N	60	E	57	NW	2.00	2	1	6.00		n	
NNR-7	249.90	b			N	60	E	21	NW							
NNR-7	251.00	f	250.00	252.00	N	70	E	83	SE	2.00	2	1	4.00		n	
NNR-7	251.50	f	251.00	252.00	N	80	E	75	SE	2.00	2	1	7.00		n	
NNR-7	252.20	f	251.70	252.70	N	60	E	81	SE	2.00	2	2	14.00		n	
NNR-7	252.75	f	252.60	252.90	N	50	E	71	SE	1.00	2	1		8.66		
NNR-7	253.20	f	252.80	253.60	N	70	E	75	SE		2		>140		n	
NNR-7	253.25	f	253.20	253.30	N	65	E	67	NW	1.00	2	1	2.00		n	
NNR-7	253.80	b			N	1	E	23	NW							Obtained from BHTV-log
NNR-7	253.95	f	253.90	254.00	N	60	E	53	SE		2		>140		n	BHTV-Log correlation
NNR-7	254.10	b			N	0	S	18	W							
NNR-7	254.10	b			N	3	E	27	NW							Obtained from BHTV-log
NNR-7	254.50	b			N	12	E	27	NW							Obtained from BHTV-log
NNR-7	255.90	b			N	10	E	26	NW							Obtained from BHTV-log
NNR-7	257.20	b			N	5	E	26	NW							Obtained from BHTV-log
NNR-7	257.60	b			N	16	E	26	NW							Obtained from BHTV-log
NNR-7	259.70	b			N	13	E	26	NW							Obtained from BHTV-log
NNR-7	259.80	b			N	30	E	21	NW							
NNR-7	260.50	f	260.20	260.80	N	40	E	71	NW	3.00	2	1	15.00		n	
NNR-7	260.90	f	260.80	261.00	N	0	S	65	W		2		15.00		n	
NNR-7	261.20	f	261.00	261.40	N	30	E	76	NW	1.00	2	1	2.00		n	
NNR-7	261.55	f	261.00	262.10	N	40	E	84	SE	1.00	2	1	4.00		n	
NNR-7	262.00	b			N	0	S	26	W							Obtained from BHTV-log
NNR-7	262.00	b			N	15	W	23	NW							
NNR-7	262.30	f	262.20	262.40	N	60	E	65	NW	1.00	2	1	2.00		n	
NNR-7	262.50	f	262.30	262.70	N	70	E	89	SE	1.00	2	1	2.00		n	
NNR-7	263.28	f	263.13	263.43	N	10	E	51	NW	8.00	2	1		87.24		BHTV-Log correlation
NNR-7	263.85	f	263.50	264.20	N	60	E	74	NW	2.00	2	1	5.00		n	
NNR-7	264.30	f	263.50	265.10	N	50	E	84	SE	3.00	2	1	15.00		n	BHTV-Log correlation
NNR-7	265.50	b			N	30	E	19	NW							Obtained from BHTV-log
NNR-7	266.80	b			N	5	E	28	NW							Obtained from BHTV-log

NNR-7	268.40	f	268.30	268.50	N	80	W	52	NE	1.00	2	2	5.00		n	
NNR-7	269.20	f	269.10	269.30	N	10	W	44	NE	1.00	2	3	4.00		n	BHTV-Log correlation
NNR-7	270.03	f	269.90	270.15	N	20	W	51	NE	2.00	2	1	15.00		n	
NNR-7	270.40	f	270.30	270.50	N	60	E	57	NW	0.50	2	1		5.24		
NNR-7	270.60	f	270.50	270.70	N	80	E	60	NW	0.50	2	1	5.00		n	
NNR-7	270.70	f								1.00	2	1	5.00		n	
NNR-7	270.78	f	270.65	270.90	N	30	E	64	SE	5.00	2	1	>30	39.56	n	BHTV-Log correlation
NNR-7	270.88	f	270.70	271.05	N	30	E	61	SE	5.00	2	1		47.47		BHTV-Log correlation
NNR-7	271.00	f	270.95	271.05	N	0	S	44	E	2.00	2	1	10.00		n	
NNR-7	272.15	j	271.90	272.40	N	45	W	71	NE							BHTV-Log correlation
NNR-7	273.10	b			N	25	E	24	NW							Obtained from BHTV-log
NNR-7	273.20	b			N	15	E	19	NW							
NNR-7	274.10	b			N	15	E	18	NW							Obtained from BHTV-log
NNR-7	274.35	j	273.40	275.30	N	50	W	86	NE							BHTV-Log correlation
NNR-7	275.60	f	275.20	276.00	N	20	E	73	NW	1.00	2	1	9.00		n	
NNR-7	275.90	b			N	10	W	2	SW							
NNR-7	276.45	f	276.20	276.70	N	60	E	60	NW	1.00	2	1	>20	24.58	r	
NNR-7	276.48	f	276.00	276.95	N	20	E	74	SE	2.00	2	1	10.00		n	
NNR-7	277.70	f	277.20	278.20	N	70	E	71	NW	2.00	2	1	32.00		r	younger than faults 277.975 and 278.1
NNR-7	277.98	f	277.65	278.30	N	50	E	65	SE	3.00	2	1	34.00		n	
NNR-7	278.10	f	277.80	278.40	N	55	E	61	SE	1.00	2	1	16.00		n	
NNR-7	278.50	f								3.00	2	1	31.00		r	
NNR-7	279.00	f	278.90	279.10	N	10	E	42	NW	1.00	2	2	6.00		n	younger than fault 279.3
NNR-7	279.23	f	279.15	279.30	N	60	W	63	NE	2.00	2	2	5.00		n	
NNR-7	279.30	f	278.90	279.70	N	50	E	70	SE	5.00	2	1	50.00		n	
NNR-7	279.40	b			N	40	E	21	NW							
NNR-7	280.00	f	279.85	280.15	N	50	E	52	SE	1.00	2	2	13.00		n	
NNR-7	280.15	f	280.00	280.30	N	40	E	56	SE	1.00	2	1	6.00		n	
NNR-7	280.35	f	280.20	280.50	N	30	E	55	SE	1.00	2	1	5.00		n	
NNR-7	280.60	f	280.40	280.80	N	30	E	51	SE	1.00	2	1		4.99		
NNR-7	280.90	f	280.60	281.20	N	20	E	72	SE	10.00	2	1		114.01		BHTV-Log correlation
NNR-7	281.50	f								4.00	2	1	65.00		n	
NNR-7	281.70	f	281.10	282.30	N	50	E	86	SE	4.00	2	1		32.77		BHTV-Log correlation
NNR-7	282.30	f	282.10	282.50	N	40	E	61	SE	1.00	2	1		5.30		

NNR-7	283.35	f	283.30	283.40	N	30	E	54	SE	2.00	2	1		23.56		
NNR-7	283.50	f	283.30	283.70	N	0	S	53	W	3.00	2	1		25.59		
NNR-7	284.15	j	283.80	284.50	N	60	W	64	NE							BHTV-Log correlation
NNR-7	285.25	f	285.10	285.40	N	70	E	54	NW	2.00	2	1	9.00		r	
NNR-7	286.40	f	286.00	286.80	N	30	E	74	NW	2.00	2	1	11.00		r	
NNR-7	286.43	f	286.05	286.80	N	30	E	76	NW	6.00	2	1		59.83		
NNR-7	286.53	f	286.30	286.75	N	50	E	70	NW	2.00	2	1		16.82		
NNR-7	286.65	f	286.50	286.80	N	40	E	68	NW	2.00	2	1		8.52		
NNR-7	287.00	b			N	30	W	18	SW							
NNR-7	287.43	f	287.25	287.60	N	30	E	54	SE		2					
NNR-7	288.10	j	287.70	288.50	N	60	E	68	NW							
NNR-7	289.05	j	288.60	289.50	N	50	W	78	NE							BHTV-Log correlation
NNR-7	289.13	f	289.10	289.15	N	40	W	14	SW	3.00	2			14.89		older than fault 289.475
NNR-7	289.48	f	288.95	290.00	N	40	E	64	NW	4.00	2	1	14.00		r	BHTV-Log correlation
NNR-7	290.50	b			N	15	W	20	SW							Obtained from BHTV-log
NNR-7	291.40	b			N	35	W	13	SW							Obtained from BHTV-log
NNR-7	291.60	b			N	19	W	16	SW							Obtained from BHTV-log
NNR-7	291.80	b			N	30	W	18	SW							
NNR-7	292.83	f	292.70	292.95	N	50	E	41	NW	1.50	2	3	4.50		r	
NNR-7	292.90	f	292.80	293.00	N	50	E	36	NW	1.50	2	3	4.50		r	
NNR-7	293.70	f	293.60	293.80	N	30	E	31	NW	1.00	2			24.21		
NNR-7	293.88	f	293.30	294.45	N	20	E	82	NW	2.00	2	2	12.00		r	
NNR-7	294.30	f	294.20	294.40	N	25	E	37	NW	1.00	2			24.77		
NNR-7	294.80	f								1.00	2	2	6.00			
NNR-7	295.10	f	295.00	295.20	N	40	E	40	NW	1.00	2			9.33		older than fault 295.425
NNR-7	295.43	f	295.00	295.85	N	30	E	76	NW	1.00	2			7.38		
NNR-7	295.68	f	295.40	295.95	N	30	E	64	NW	3.00	2	3	23.00		r	
NNR-7	296.08	f	295.95	296.20	N	20	E	52	NW	1.00	2	3	11.00		n	
NNR-7	296.70	f	296.60	296.80	N	30	E	62	NW		2					
NNR-7	297.05	f	297.00	297.10	N	40	W	19	SW	1.00	2			26.28		
NNR-7	297.50	f	297.40	297.60	N	20	E	40	NW	1.00	2	3	1.00		r	
NNR-7	297.70	b			N	15	E	16	NW							Obtained from BHTV-log
NNR-7	298.20	b			N	45	W	11	SW							
NNR-7	298.55	f	298.50	298.60	N	60	E	17	NW	1.00	2	3	3.00		n	

NNR-7	299.85	f	299.70	300.00	N	40	E	56	NW	1.00	2	3	7.00		r	BHTV-Log correlation
NNR-7	300.10	f	299.90	300.30	N	60	E	65	SE	1.00	2			9.77		older than fault 299.85
NNR-7	301.95	f/j	301.70	302.20	N	80	E	66	NW	2.00	2			22.88		
NNR-7	302.60	b			N	10	W	14	SW							
NNR-7	302.70	f	302.50	302.90	N	20	E	55	NW	2.00	2		22.00		n	
NNR-7	302.80	f	302.70	302.90	N	10	E	53	NW	1.00	2			17.55		
NNR-7	304.20	f	304.00	304.40	N	30	E	55	SE	2.00	2	1	>10	28.46	n	BHTV-Log correlation
NNR-7	304.50	f	304.30	304.70	N	30	E	71	SE		2	1			n	
NNR-7	304.55	f	304.20	304.90	N	30	E	72	SE		2	1			n	
NNR-7	305.15	f	304.60	305.70	N	40	E	79	SE	2.00	2	1	23.00		n	
NNR-7	305.55	f	305.50	305.60	N	30	E	46	NW	1.00	2	3	4.50		n	
NNR-7	305.65	f	305.60	305.70	N	20	E	52	NW	1.00	2	3	4.50		n	
NNR-7	306.00	f	305.90	306.10	N	20	E	81	SE	2.00	2			5.45		
NNR-7	306.13	f	306.00	306.25	N	0	S	39	W	5.00	2			33.83		older than fault 306.375
NNR-7	306.38	f	305.75	307.00	N	40	E	83	NW	2.00	2	2	9.00		r	
NNR-7	306.85	f	306.60	307.10	N	20	E	73	NW	1.00	2			11.82		
NNR-7	308.05	f	307.90	308.20	N	10	E	55	SE	1.00	2			0.99		
NNR-7	308.35	f	308.20	308.50	N	10	W	56	NE	2.00	2	2	14.00		n	
NNR-7	308.73	f	308.45	309.00	N	10	W	82	NE	1.00	2	2	2.00		n	
NNR-7	309.10	f	309.00	309.20	N	35	E	53	NW	0.50	2			4.33		
NNR-7	309.30	f	309.20	309.40	N	30	E	60	NW	1.00	2	2	14.00		n	older than fault 309.5
NNR-7	309.50	f/j	309.20	309.80	N	10	E	70	SE	1.00	2	2	2.00		n	
NNR-7	309.60	b			N	10	W	19	SW							Obtained from BHTV-log
NNR-7	309.90	f	309.85	309.95	N	20	W	67	NE		2					
NNR-7	310.00	b			N	13	W	24	SW							Obtained from BHTV-log
NNR-7	311.40	b			N	10	W	16	SW							
NNR-7	312.03	f	311.80	312.25	N	10	W	64	NE	0.50	2			1.22		
NNR-7	312.05	f	311.90	312.20	N	15	W	62	NE	0.50	2	3	4.00		n	
NNR-7	312.80	f	312.50	313.10	N	80	E	73	NW	0.50	2	3	1.00		r	
NNR-7	313.30	f	313.20	313.40	N	70	E	63	NW		2		10.00		r	
NNR-7	313.98	f	313.80	314.15	N	70	E	61	NW	1.00	2	2	9.00		r	
NNR-7	315.00	b			N	40	W	16	SW							
NNR-7	317.28	f	317.15	317.40	N	40	W	54	NE		2					
NNR-7	317.50	f	317.10	317.90	N	15	W	84	SW	1.00	2	2	2.00		n	

NNR-7	317.78	f	317.60	317.90	N	50	W	67	NE	1.00	2		3.39			
NNR-7	318.05	f	317.80	318.30	N	60	W	76	NE	1.00	2		4.01			
NNR-7	318.10	f								1.00	2	3	4.00		r	
NNR-7	318.60	f	318.50	318.70	N	50	W	60	NE		2	1	0.50			
NNR-7	318.85	f	318.80	318.90	N	60	W	48	NE		2	1	0.50			
NNR-7	319.00	f								2.00	2	1	11.00		r	
NNR-7	319.25	f	319.20	319.30	N	20	W	41	NE	0.50	2	1		2.76		
NNR-7	319.40	f	319.35	319.45	N	20	W	45	SW	0.50	2	1		2.76		
NNR-7	319.50	f								3.00	2	2	27.00			
NNR-7	320.03	f	319.75	320.30	N	40	E	60	NW	2.00	2	2	14.00		r	BHTV-Log correlation
NNR-7	320.10	b			N	5	E	35	NW							Obtained from BHTV-log
NNR-7	320.20	f	320.10	320.30	N	50	E	57	SE	1.00	2	3	9.00		n	
NNR-7	320.30	b			N	10	E	16	NW							
NNR-7	320.50	f	320.40	320.60	N	0	S	38	E	1.00	2			11.39		
NNR-7	320.90	b			N	20	E	15	NW							Obtained from BHTV-log
NNR-7	321.00	f	320.90	321.10	N	50	W	65	NE		2					
NNR-7	322.25	f	322.10	322.40	N	40	E	60	NW	0.50	2	1	3.00		n	
NNR-7	322.75	f	322.70	322.80	N	40	W	57	NE	0.50	2	1		0.50		
NNR-7	323.60	f	323.50	323.70	E	90	W	83	S		2					
NNR-7	324.25	f	324.20	324.30	N	75	E	46	SE	1.00	2	1		8.49		
NNR-7	324.55	f	324.50	324.60	N	70	E	57	NW	1.00	2	1		12.09		
NNR-7	324.80	f	324.50	325.10	E	90	W	83	N	2.00	2	1	17.00		r	
NNR-7	325.35	f	325.20	325.50	N	20	W	44	NE	1.00	2	3	8.00		n	
NNR-7	325.80	b			N	0	S	12	W							
NNR-7	326.13	f	326.05	326.20	N	40	E	57	NW	0.50	2	4	5.00		r	
NNR-7	326.43	f	326.25	326.60	N	60	E	73	SE		2					
NNR-7	326.50	f	326.10	326.90	N	60	E	71	SE	3.00	2	1	21.00		n	
NNR-7	326.80	f	326.50	327.10	N	50	E	64	SE	1.00	2	1	7.00		n	BHTV-Log correlation
NNR-7	326.88	f	326.75	327.00	N	60	E	64	NW	1.00	2			9.77		
NNR-7	327.35	f	327.10	327.60	N	60	E	65	SE	9.00	2	3		92.85	n	BHTV-Log correlation
NNR-7	328.05	f	327.80	328.30	N	60	E	47	SE	1.00	2			9.02		
NNR-7	328.35	f	328.30	328.40	N	40	E	30	NW	1.00	2			15.14		BHTV-Log correlation
NNR-7	328.85	f/j	328.40	329.30	N	70	E	85	NW	7.00	2	3	17.00		r	BHTV-Log correlation
NNR-7	330.95	f	330.80	331.10	N	70	E	56	NW	1.00	2			14.32		

NNR-7	332.85	f	332.80	332.90	N	80	E	36	NW	1.00	2			30.77		
NNR-7	333.00	f	332.90	333.10	N	75	E	28	NW	2.00	2			34.00		
NNR-7	333.20	f	333.00	333.40	E	90	W	53	NW	0.50	2	2	1.00		r	
NNR-7	336.40	b			N	10	E	17	NW							
NNR-7	337.30	f	337.20	337.40	N	40	E	51	NW	5.00	2			24.63		
NNR-7	337.45	f	337.40	337.50	N	30	E	61	NW	3.00	2			40.49		
NNR-7	337.55	f	337.50	337.60	N	35	E	56	NW	3.00	2			43.37		
NNR-7	337.90	f	337.80	338.00	N	25	E	47	SE	2.00	2			28.41		
NNR-7	337.93	f	337.75	338.10	N	30	E	52	SE	3.00	2			52.58		
NNR-7	338.20	f	337.90	338.50	N	40	E	65	SE	2.00	2			7.20		
NNR-7	338.70	f	338.50	338.90	N	50	E	64	SE	3.00	2			5.18		
NNR-7	341.20	f	341.00	341.40	N	45	E	64	NW	1.00	2			8.11		
NNR-7	341.45	f	341.30	341.60	N	50	E	47	NW	1.00	2			6.97		
NNR-7	342.20	b			N	45	W	15	SW							Obtained from BHTV-log
NNR-7	342.30	b			N	40	W	12	SW							
NNR-7	342.50	b			N	80	W	15	SW							Obtained from BHTV-log
NNR-7	345.30	b			N	75	W	14	SW							Obtained from BHTV-log
NNR-7	345.50	b			N	50	W	12	SW							
NNR-7	346.90	b			N	53	W	11	SW							Obtained from BHTV-log
NNR-7	347.20	b			N	50	W	15	SW							Obtained from BHTV-log
NNR-7	347.70	b			N	30	W	16	SW							
NNR-7	349.70	f	349.60	349.80	N	30	W	32	NE	2.00	2	1	3.00		n	
NNR-7	349.90	b			N	30	W	18	SW							
NNR-7	350.80	f	350.70	350.90	N	50	E	37	NW	1.00	2			7.24		
NNR-7	352.15	f	352.10	352.20	N	40	E	35	NW	0.50	2			8.84		
NNR-7	352.80	b			N	60	W	13	SW							Obtained from BHTV-log
NNR-7	353.50	b			N	25	W	15	SW							Obtained from BHTV-log
NNR-7	354.85	f	354.70	355.00	N	25	E	42	NW	1.00	2	1	3.00		r	
NNR-7	354.93	f	354.80	355.05	N	20	E	63	NW	1.00	2			1.19		
NNR-7	355.25	f	355.10	355.40	N	25	E	59	NW	1.00	2			5.19		
NNR-7	356.90	f/j	356.70	357.10	N	10	E	60	NW	2.00	2	1	10.00		n	
NNR-7	357.15	f	357.10	357.20	N	0	S	34	W	3.00	2			43.53		
NNR-7	357.25	f	357.20	357.30	N	20	E	34	NW	3.00	2			19.59		
NNR-7	357.40	f	357.10	357.70	N	0	S	71	W	11.00	2			127.71		BHTV-Log correlation

NNR-7	357.60	f	357.50	357.70	N	10	W	34	SW	4.00	2			12.57		
NNR-7	357.90	b			N	30	W	18	SW							Obtained from BHTV-log
NNR-7	357.90	f	357.60	358.20	N	0	S	72	W	3.00	2	1	6.00			
NNR-7	359.05	f	359.00	359.10	N	80	W	14	SW	3.00	2			12.30		
NNR-7	359.25	f	359.20	359.30	N	40	W	17	SW	4.00	2			26.64		
NNR-7	359.40	f	359.30	359.50	N	40	E	44	NW	2.00	2	2	7.00		r	
NNR-7	359.55	f	359.50	359.60	N	70	W	12	SW	4.00	2			56.64		
NNR-7	360.05	f	359.95	360.15	N	0	S	41	E	3.00	2			31.11		
NNR-7	360.08	f	359.95	360.20	N	0	S	42	E	7.00	2			85.04		BHTV-Log correlation
NNR-7	360.38	f	360.30	360.45	N	30	w	38	NE	1.00	2			11.01		
NNR-7	361.20	b			N	82	W	11	SW							Obtained from BHTV-log
NNR-7	361.78	f	361.60	361.95	N	40	W	55	NE	1.00	2	3	5.00		n	
NNR-7	361.90	b			N	57	E	11	SE							Obtained from BHTV-log
NNR-7	363.35	f	363.20	363.50	N	40	W	53	NE	1.00	2	2	3.00		r	
NNR-7	363.48	f	363.40	363.55	N	30	W	47	NE	1.00	2	2	10.00		n	
NNR-7	363.70	f	363.60	363.80	N	50	W	67	NE	1.00	2			9.77		
NNR-7	364.68	f	364.25	365.10	N	30	W	71	NE	11.00	2		>10	152.83		
NNR-7	364.90	f	364.70	365.10	N	20	W	65	NE	2.00	2			21.73		
NNR-7	366.15	f	366.00	366.30	N	20	W	48	NE	1.00	2	2	3.00		n	
NNR-7	366.63	f	366.40	366.85	N	10	W	56	NE	1.00	2			1.70		
NNR-7	367.28	f	367.05	367.50	N	0	S	68	E	1.00	2		>10	13.86	n	
NNR-7	367.60	f	367.50	367.70	N	10	W	46	NE	3.00	2			10.46		
NNR-7	367.88	f	367.80	367.95	N	15	E	55	SE	3.00	2			45.06		
NNR-7	368.10	f	367.90	368.30	N	10	W	64	NE	1.00	2	1	5.00		n	
NNR-7	368.30	b			N	30	W	27	SW							Obtained from BHTV-log
NNR-7	368.80	b			N	68	W	28	SW							Obtained from BHTV-log
NNR-7	370.10	f	370.00	371.20	N	0	S	84	E	4.00	2	3	20.00		r	
NNR-7	370.30	f	370.10	370.50	N	0	S	66	E	2.00	2	2	10.00		r	
NNR-7	370.63	f	370.00	371.25	N	0	S	83	E	4.00	2	3	20.00		r	
NNR-7	370.95	f	370.90	371.00	N	10	W	30	NE	1.00	2			17.81		
NNR-7	371.25	f	371.15	371.35	N	0	S	67	E	1.00	2			0.99		
NNR-7	371.30	f	371.25	371.35	N	10	E	26	SE	2.00	2	3	4.00		n	
NNR-7	371.55	f	371.40	371.70	N	10	W	71	NE	2.00	2			27.53		
NNR-7	371.58	f	371.50	371.65	N	10	E	43	SE	1.00	2			0.85		

NNR-7	371.90	b			N	22	W	22	SW							Obtained from BHTV-log
NNR-7	371.93	f	371.90	371.95	N	10	W	51	NE	1.00	2		5.42			
NNR-7	372.15	f									2		23.00			
NNR-7	372.20	b			N	20	W	17	SW							
NNR-7	372.40	f	372.00	372.80	N	50	E	71	SE	2.00	2	1	13.00		n	
NNR-7	373.20	f	373.00	373.40	N	40	E	87	SE	1.50	2	2	4.00		n	
NNR-7	373.45	f	373.30	373.60	N	50	E	64	SE	1.00	2			2.46		
NNR-7	373.70	f	373.60	373.80	N	50	E	27	NW	1.00	2			29.90		
NNR-7	373.90	f	373.80	374.00	N	60	E	51	NW	1.00	2			12.74		
NNR-7	374.50	f							SE	1.00	2	1	4.00		n	
NNR-7	375.45	f	375.20	375.70	N	70	E	62	NW	1.00	2			10.80		
NNR-7	375.75	f	375.50	376.00	N	75	E	66	NW	1.00	2	1	2.00		r	
NNR-7	375.80	f	375.50	376.10	N	80	E	71	NW	1.00	2			11.78		
NNR-7	375.95	f	375.90	376.00	N	60	E	41	NW	2.00	2			13.85		
NNR-7	376.20	f	376.00	376.40	N	60	E	71	NW	3.00	2		3.00		n	
NNR-7	376.70	f	376.60	376.80	N	70	E	68	NW	1.00	2			21.01		
NNR-7	376.85	f	376.10	377.60	N	70	W	76	NE	2.00	2	1	1.00		n	
NNR-7	378.20	j	378.00	378.40	N	80	W	76	NE							
NNR-7	378.45	f	378.00	378.90	N	80	E	79	SE	2.00	2	3	20.00		n	
NNR-7	379.30	f	379.20	379.40	N	20	W	55	SW	5.00	2	1	66.00		n	BHTV-Log correlation
NNR-7	380.60	b			N	10	W	32	SW							Obtained from BHTV-log
NNR-8	170.63	f	170.40	170.85	N	35	E	53	SE	0.50	1	4	13.00		n	
NNR-8	172.90	b			N	0	S	28	W							obtained from BHTV-log
NNR-8	174.20	b			N	22	E	24	NW							obtained from BHTV-log
NNR-8	177.25	b			N	5	E	15	NW							
NNR-8	178.70	b			N	22	E	19	NW							obtained from BHTV-log
NNR-8	179.65	b			N	15	W	14	SW							
NNR-8	179.95	f	179.85	180.05	N	30	E	43	SE	0.50	1	4	12.00		n	
NNR-8	180.70	j	180.50	180.90	N	70	W	56	NE							BHTV-log correlation
NNR-8	182.20	b			N	5	W	17	SW							obtained from BHTV-log
NNR-8	182.93	f	182.85	183.00	N	60	E	32	NW	1.00	1	3		5.70		
NNR-8	183.75	f	183.60	183.90	N	30	W	57	NE	0.50	1	3	1.00		r	
NNR-8	184.05	b			N	15	E	14	NW							
NNR-8	186.70	b			N	10	E	16	NW							

NNR-8	186.93	f/j	186.10	186.65	N	25	E	58	SE	2.00	1	4	18.00		n	BHTV-log correlation
NNR-8	187.95	f	187.30	188.60	N	10	W	87	NE	0.50	1	3	2.00		r	
NNR-8	189.20	b			N	10	E	17	NW							obtained from BHTV-log
NNR-8	190.45	b			N	20	W	18	SW							
NNR-8	191.50	f	191.35	191.65	N	15	W	54	NE	0.50	1	3	3.00		n	
NNR-8	192.90	f	192.10	192.70	N	40	E	64	SE	0.50	1	2	5.00		n	
NNR-8	192.95	f/j	192.80	193.10	N	10	E	51	SE	0.50	1	1	6.00		n	
NNR-8	193.15	f/j	193.10	193.20	N	15	E	40	SE	0.50	1	1	2.50		n	
NNR-8	194.80	f/j	194.60	195.00	N	20	E	66	NW	1.50	1	1	10.00		n	
NNR-8	195.43	f	195.30	195.55	N	30	E	64	SE	0.50	1	3	6.00		n	
NNR-8	195.95	f/j	195.70	196.20	N	15	W	68	NE	0.50	1	3	4.00		r	
NNR-8	196.18	f/j	196.00	196.35	N	10	W	63	NE	0.50	1	3	2.00		r	
NNR-8	196.48	f	196.35	196.60	N	30	E	52	SE	1.00	1	4	23.00		n	
NNR-8	197.15	f	196.90	197.40	N	5	E	87	NW	0.50	1	3	3.00		n	
NNR-8	197.20	f	196.70	197.70	N	35	W	81	NE	0.50	1	3	4.00		r	
NNR-8	197.80	b			N	15	E	24	NW							obtained from BHTV-log
NNR-8	197.83	f	197.80	197.85	N	40	E	18	SE	0.50	1	3	4.00		r	
NNR-8	197.90	b			N	0	S	17	W							
NNR-8	198.40	f	198.30	198.50	N	30	W	54	NE	1.50	1	1	4.00		r	
NNR-8	198.65	f	198.35	198.95	N	40	W	66	NE	1.00	1	1	7.00		r	
NNR-8	198.83	f	198.50	199.15	N	40	W	71	NE		1					
NNR-8	199.05	f	199.00	199.10	N	50	W	33	NE	1.00	1	1		11.52		
NNR-8	199.28	f	199.05	199.50	N	65	W	59	NE		1		16.00		r	
NNR-8	199.63	f	199.55	199.70	N	55	W	48	NE	0.50	1	3		5.60		
NNR-8	199.78	f	199.70	199.85	N	60	W	43	NE	0.50	1	3	5.00		r	
NNR-8	199.90	f	199.50	200.30	N	40	W	73	NE	1.00	1	3	9.00		r	
NNR-8	199.95	f	199.90	200.00	N	50	W	42	NE	0.50	1	3		6.86		
NNR-8	200.90	b			N	5	W	28	SW							obtained from BHTV-log
NNR-8	201.00	b			N	20	W	16	SW							
NNR-8	202.23	f	202.05	202.40	N	15	E	47	SE	1.00	1	1		7.93		
NNR-8	202.30	b			N	10	E	34	NW							obtained from BHTV-log
NNR-8	202.43	f	202.35	202.50	N	5	W	26	NE	1.00	1	1		9.57		
NNR-8	202.70	f	202.45	202.95	N	10	W	67	NE	0.50	1	3	1.00		r	
NNR-8	202.85	f	202.75	202.95	N	35	W	46	NE	1.00	1	1		10.90		

NNR-8	203.33	f	203.25	203.40	N	30	W	43	NE	0.50	1	2		7.15		
NNR-8	203.60	b			N	22	E	15	NW							obtained from BHTV-log
NNR-8	206.50	b			N	10	W	16	SW							
NNR-8	207.53	f	207.40	207.65	N	55	W	49	NE	1.00	1	4	55.00		n	
NNR-8	208.60	b			N	35	E	17	NW							
NNR-8	209.48	f/j	209.25	209.70	N	50	W	76	NE	0.50	1	2	1.00		r	
NNR-8	209.78	f	209.65	209.90	N	65	W	68	NE	0.50	1	2		3.48		
NNR-8	210.53	j	210.35	210.70	N	65	W	60	NE							
NNR-8	212.35	f	212.25	212.45	N	15	W	57	NE	0.50	1	1		4.80		
NNR-8	213.30	b			N	0	S	13	W							
NNR-8	215.60	b			N	20	E	15	NW							
NNR-8	216.18	j	216.05	216.30	N	30	W	52	NE							
NNR-8	219.10	b			N	10	W	12	SW							
NNR-8	220.05	b			N	15	W	14	SW							
NNR-8	221.93	f	221.80	222.05	N	80	W	47	NE	0.50	1	3	5.00		n	
NNR-8	223.05	j	222.85	223.25	N	70	W	61	NE							
NNR-8	224.00	b			N	0	S	16	W							
NNR-8	225.30	b			N	15	E	20	NW							obtained from BHTV-log
NNR-8	225.70	b			N	15	E	18	NW							
NNR-8	225.93	f	225.85	226.00	N	5	W	47	SW	1.00	1	1		8.74		
NNR-8	226.28	f	226.25	226.30	N	15	E	11	SE	1.00	1	3	21.00		r	younger than fault 226.3
NNR-8	226.30	f	226.20	226.40	N	10	W	43	SW	0.50	1	3		6.21		
NNR-8	226.83	f	226.70	226.95	N	35	W	48	SW	0.50	1	3	4.00		r	
NNR-8	227.18	f	227.15	227.20	E	90	W	17	S		1					
NNR-8	227.48	f	227.40	227.55	N	50	E	41	NW	1.00	1	3	12.00		n	
NNR-8	228.05	f	227.95	228.15	N	80	E	45	SE	1.50	1	1		30.31	n	BHTV-log correlation
NNR-8	228.10	f	228.00	228.20	N	85	E	42	SE	3.00	1	1		33.04	n	BHTV-log correlation
NNR-8	229.20	f	229.10	229.30	N	65	W	57	NE	1.00	1	2		14.53		
NNR-8	229.25	b			N	10	W	16	NW							
NNR-8	229.38	f	229.30	229.45	N	70	W	35	NE	0.50	1	3	7.00		n	
NNR-8	229.55	f	229.50	229.60	N	60	W	42	NE	0.50	1	3	3.00		n	
NNR-8	230.10	f	230.00	230.20	N	5	E	26	NW	1.00	1	1	6.00			younger than 230.525
NNR-8	230.53	f	229.90	231.15	N	45	E	83	SE	2.00	1	1	50.00		n	BHTV-log correlation
NNR-8	231.28	f	230.65	231.90	N	30	E	85	SE	2.00	1	1	37.00		n	

NNR-8	231.90	b			N	15	W	13	SW							
NNR-8	232.28	f	232.25	232.30	N	5	W	21	NE	0.50	1	3		6.46		
NNR-8	232.53	f	232.45	232.60	N	10	W	32	SW	0.50	1	3		6.68		
NNR-8	232.83	f	232.65	233.00	N	30	E	56	SE	1.00	1	4		48.50		
NNR-8	233.33	f	232.95	233.50	N	35	E	16	NW	0.50	1	3		2.88		
NNR-8	233.33	f	233.25	233.40	N	40	E	24	NW	0.50	1	4	21.00		n	
NNR-8	233.80	f	233.60	234.00	N	10	E	78	NW	1.50	1	1		7.70		
NNR-8	234.15	b			N	4	W	16	SW							obtained from BHTV-log
NNR-8	234.20	b			N	15	W	18	SW							
NNR-8	234.28	f	234.25	234.30	N	15	E	37	NW	0.50	1	3		6.93		
NNR-8	234.60	f	234.50	234.70	N	20	E	47	NW	0.50	1	3	4.00		n	
NNR-8	235.13	f	235.05	235.20	N	45	E	67	SE	1.00	1	1	8.00		n	
NNR-8	235.23	f	235.10	235.35	N	40	E	59	NW	1.50	1	1	12.00		n	BHTV-log correlation
NNR-8	235.30	f	235.25	235.35	N	40	E	58	SE	1.00	1	1		10.48		
NNR-8	235.53	f	235.35	235.70	N	35	E	71	SE	0.50	1	2	5.00		n	
NNR-8	236.13	f	235.90	236.35	N	45	E	62	SE		1					
NNR-8	236.23	f	236.10	236.35	N	60	E	41	SE	7.00	1	2		74.37	n	BHTV-log correlation
NNR-8	236.40	f	236.25	236.55	N	60	E	76	NW	1.50	1	2	18.00		n	
NNR-8	236.68	f	236.55	236.80	N	50	E	52	SE	2.00	1	3	14.00		n	
NNR-8	236.98	f	236.90	237.10	N	40	E	72	NW	1.00	1	1		9.56		
NNR-8	237.00	f	236.95	237.05	N	55	E	61	NW	2.00	1	1		16.56		
NNR-8	237.03	f	236.80	237.20	N	70	E	57	SE	2.00	1	1		26.49		
NNR-8	237.23	f	237.10	237.35	N	35	E	45	SE	2.00	1	1		17.40		
NNR-8	237.30	f	237.10	237.50	N	55	E	67	SE	1.50	1	2		15.82		between 237.3 and 237.8 SE dipping faults are younger
NNR-8	237.40	f	237.30	237.50	N	45	E	54	NW		1					
NNR-8	237.80	f	237.60	238.00	N	65	E	63	NW	2.00	1	3	21.00		n	
NNR-8	238.10	f	238.00	238.20	N	75	E	35	SE	1.00	1	3		10.10	n	BHTV-log correlation
NNR-8	238.13	f	238.00	238.25	N	80	E	41	SE	0.50	1	3		4.68		
NNR-8	238.30	f	238.25	238.35	N	55	E	36	SE	0.50	1	3		5.13		
NNR-8	239.18	f	239.10	239.25	N	80	W	34	SW	3.00	1	4	21.00		n	
NNR-8	239.25	f	239.15	239.35	N	45	E	56	NW	1.00	1	4		15.16		
NNR-8	240.33	f	240.25	240.40	N	45	E	37	SE	1.00	1	2		10.63		older than steeper dipping fault
NNR-8	240.50	f	240.40	240.60	N	60	E	45	SE	1.00	1	2		33.24		
NNR-8	240.85	f	240.80	240.90	N	75	E	37	NW	1.00	1	3		8.44		older than steeper dipping fault

NNR-8	240.93	f	240.80	241.05	N	55	E	44	SE	3.00	1	3		31.30			
NNR-8	241.85	b			N	10	W	22	SW								
NNR-8	242.10	f	242.00	242.20	N	40	E	44	SE	3.00	1	3		5.49			
NNR-8	242.20	f	242.00	242.40	N	35	E	54	SE	0.50	1	3	3.00		n		
NNR-8	242.60	f	242.50	242.70	N	35	E	45	SE	4.00	1	1		32.84			
NNR-8	242.70	b			N	15	E	31	NW								
NNR-8	244.03	f	243.85	244.20	N	60	E	56	SE	1.00	1	2	14.00		n		
NNR-8	244.08	f	243.95	244.20	E	90	W	52	S	0.50	1	2	9.00		n		
NNR-8	244.10	f	244.05	244.15	N	15	E	45	SE	0.50	1	2		6.54			
NNR-8	244.78	f	244.65	244.90	N	80	E	49	SE	2.00	1	2		27.52			
NNR-8	244.80	f	244.70	244.90	N	55	E	50	SE	1.00	1	2		8.79			BHTV-log correlation
NNR-8	245.05	f	244.80	245.10	N	70	E	62	SE	1.00	1	2		14.67			
NNR-8	245.30	j	245.10	245.50	E	90	W	74	S								
NNR-8	245.43	f	245.40	245.45	N	25	E	34	SE	1.00	1	1		8.04			
NNR-8	245.50	j	245.30	245.70	E	90	W	61	S								
NNR-8	245.63	f	245.45	245.80	N	75	E	61	SE		1						NW dipping faults are younger 245.95 and 245.625
NNR-8	245.95	f	245.80	246.10	N	60	E	46	SE	17.00	1	1		179.91	n		
NNR-8	246.35	f	246.20	246.50	N	80	E	54	SE	2.00	1	1	15.00		n		
NNR-8	246.53	f	246.30	246.75	N	70	E	60	SE	1.50	1	1	9.00		n		
NNR-8	246.93	f	246.75	247.10	N	75	E	53	SE	7.00	1	1	63.00		n		
NNR-8	247.25	f	247.00	247.50	N	65	E	66	SE	2.00	1	4	57.00		n		
NNR-8	247.70	f	247.50	247.90	N	60	E	68	SE		1						
NNR-8	249.05	f	249.00	249.10	N	40	E	38	NW	0.50	1	4	14.00		n		
NNR-8	249.20	b			N	45	W	25	SW								
NNR-8	249.30	b			N	45	W	24	SW								obtained from BHTV-log
NNR-8	249.45	f	249.30	249.60	N	55	E	52	SE	2.00	1	1		13.33			
NNR-8	249.55	f	249.40	249.70	N	45	E	55	SE	2.00	1	1		15.33			
NNR-8	249.65	f	249.50	249.80	N	40	E	66	SE	1.00	1	1		7.84			
NNR-8	249.80	f	249.65	249.95	N	50	E	59	SE	2.00	1	1		5.78			
NNR-8	250.13	f	249.85	250.40	N	70	E	74	SE	5.00	1	1		50.09			
NNR-8	251.05	f	250.70	251.40	N	50	E	60	SE	43.00	1	1		461.19	n	82, 43	
NNR-8	252.20	f	251.50	252.90	N	60	E	70	SE	>150	1	1			n		BHTV-log correlation
NNR-8	253.38	f	252.90	253.85	N	10	E	78	NW	1.50	2	1	12.00				
NNR-8	253.65	b			N	25	E	23	NW								

NNR-8	254.75	f	254.60	254.90	N	65	E	62	SE	0.50	2	3	3.00		n	
NNR-8	256.55	f	255.80	257.30	N	60	E	87	SE	0.50	2	1		6.40		
NNR-8	257.50	b			N	3	W	28	SW							obtained from BHTV-log
NNR-8	258.40	b			N	3	E	16	NW							obtained from BHTV-log
NNR-8	258.90	b			N	0	S	19	W							
NNR-8	259.15	f	259.00	259.30	N	30	E	84	SE	1.50	2	1	3.00		n	
NNR-8	259.50	f	259.20	259.80	N	35	E	64	NW	0.50	2	1	2.00		n	
NNR-8	259.73	f	259.55	259.90	N	15	W	72	SW	2.00	2	1	4.00		n	
NNR-8	262.18	f	261.80	262.55	N	60	E	72	NW	1.00	2	1	4.00		r	
NNR-8	264.40	b			N	10	E	23	NW							
NNR-8	264.53	f	264.45	264.60	N	65	E	53	NW	1.00	2	1		5.98		
NNR-8	265.75	j	265.60	265.90	N	70	W	57	NE							
NNR-8	266.25	j	265.90	266.60	N	60	W	73	NE							BHTV-log correlation
NNR-8	266.28	f	265.95	266.60	N	70	E	68	SE	1.00	2	1		2.90		
NNR-8	266.30	f	266.20	266.40	N	55	E	67	SE	2.00	2	1		17.76		
NNR-8	266.43	f	265.85	267.00	N	60	E	84	SE	1.50	2	1	18.00		n	younger than 266.275
NNR-8	267.15	b			N	15	E	20	NW							
NNR-8	267.78	f	267.10	268.45	N	40	E	83	SE	4.00	2	1	65.00		n	BHTV-log correlation
NNR-8	270.63	f	270.50	270.75	N	55	E	57	SE	0.50	2	4	9.00		n	
NNR-8	270.85	f	270.70	271.00	N	60	E	63	SE	0.50	2	4	18.00		n	
NNR-8	271.63	f	271.50	271.75	N	45	E	49	NW	4.50	2	1		68.44		
NNR-8	271.85	f	271.75	272.00	N	60	E	64	SE	0.50	2	1		2.76		
NNR-8	272.00	f	271.80	272.00	N	65	E	38	NW	1.00	2	1	7.00		n	yonger than 271.85
NNR-8	272.35	f	272.00	272.70	N	60	E	72	SE	1.50	2	1	11.00		n	younger than 272.525
NNR-8	272.40	f	273.35	273.45	N	65	E	34	NW	0.50	2	1		2.76		
NNR-8	272.53	f	272.45	272.60	N	60	E	25	SE	1.50	2	1		6.28		
NNR-8	272.90	b			N	40	E	22	NW							
NNR-8	273.00	f	272.90	273.10	N	60	E	62	SE	2.50	2	1	11.00		n	
NNR-8	273.45	f	273.35	273.55	N	55	E	52	SE	0.50	2	1	1.00		n	
NNR-8	273.48	f	273.00	273.90	N	70	E	77	SE	0.50	2	1	14.00		n	
NNR-8	273.85	f	273.60	274.10	N	80	E	66	SE	2.00	2	1		14.30		
NNR-8	274.40	f	274.30	274.50	N	50	E	16	NW	2.00	2	1		16.24		
NNR-8	274.45	f	274.30	274.60	N	45	E	44	NW	2.00	2	1		21.39		
NNR-8	274.63	f	274.55	274.70	N	45	E	30	NW	2.50	2	1	13.00		r	

NNR-8	274.85	f	274.80	274.90	N	60	E	17	NW	1.50	2	1		9.33		
NNR-8	276.20	b			N	20	E	23	NW							
NNR-8	276.60	f	276.30	276.90	N	60	E	72	SE	1.00	2	1	8.00		n	
NNR-8	277.20	f	277.10	277.30	N	30	E	59	NW	0.50	2	1		2.97		
NNR-8	277.25	f	276.60	277.90	N	45	E	83	SE	1.00	2	1	7.00		n	younger than 277.35
NNR-8	277.35	f	277.30	277.40	N	15	E	16	NW	0.50	2	1		5.14		
NNR-8	277.85	f	277.75	277.95	N	10	E	61	SE	0.50	2	1	5.00		n	
NNR-8	278.68	f	278.00	279.35	N	50	E	81	NW	2.50	2	1	13.00		n	
NNR-8	279.00	b			N	40	E	23	NW							
NNR-8	279.45	f	279.30	279.60	N	65	E	69	NW	1.00	2	1		7.55		
NNR-8	279.50	f	279.40	279.60	N	10	E	51	NW	1.00	2	1		9.86		
NNR-8	279.53	f	279.50	279.55	N	35	E	74	SE	1.00	2	1		9.57		
NNR-8	279.83	f	279.70	279.95	N	55	W	51	NE	2.00	2	1		37.05		
NNR-8	280.15	f	279.90	280.40	N	60	E	73	NW	2.00	2	1		1.53		
NNR-8	280.20	f	279.40	281.00	N	50	E	79	SE	1.50	2	1	13.00		n	
NNR-8	280.90	b			N	30	E	22	NW							
NNR-8	281.48	f	281.10	281.85	N	30	E	86	SE	1.50	2	1	26.00		n	BHTV-log correlation
NNR-8	281.50	f	281.10	281.90	N	45	E	75	SE	27.00	2			367.99	n	
NNR-8	281.60	b			N	0	S	25	W							
NNR-8	281.90	f	281.70	282.10	N	60	E	59	SE	1.00	2	1	3.00		n	
NNR-8	282.23	f	282.15	282.30	N	55	E	55	SE	0.50	2	1		3.99		
NNR-8	282.43	f	282.25	282.60	N	60	E	57	SE	2.50	2	1	26.00		n	
NNR-8	282.50	f	282.40	282.60	E	90	W	43	S	1.00	2	1		14.31		
NNR-8	282.70	f	282.55	282.85	N	65	E	50	SE	1.00	2	1	14.00		n	
NNR-8	283.10	f	282.85	283.35	N	70	E	61	SE	0.50	2	2	8.00		n	
NNR-8	283.75	f	283.50	284.00	N	50	E	61	SE	3.50	2	1	66.00		n	BHTV-log correlation
NNR-8	283.90	f	283.70	284.10	N	80	E	60	SE	3.50	2	1	66.00		n	
NNR-8	284.15	f	284.10	284.20	N	45	E	47	NW	1.00	2	1		7.17		
NNR-8	284.30	f	284.25	284.35	N	15	E	45	NW	1.00	2	1		6.68		
NNR-8	284.50	b			N	35	E	17	NW							
NNR-8	285.10	f	285.00	285.20	N	10	W	47	SW	1.00	2	1		6.79		
NNR-8	285.30	f	285.20	285.40	N	0	S	66	W	1.00	2	1		3.84		
NNR-8	285.80	b			N	15	E	16	NW							
NNR-8	286.20	f	286.10	286.30	N	40	E	43	NW	1.00	2	1		5.87		

NNR-8	286.25	f	286.20	286.30	N	40	E	47	NW	1.00	2	1		8.35		
NNR-8	286.65	f	286.60	286.70	E	90	W	11	N	2.50	2	1		30.03		
NNR-8	287.13	j	287.00	287.25	N	60	E	68	NW							
NNR-8	287.23	f	286.85	287.60	N	60	E	73	SE	52.00	2	1		600.15	n	BHTV-log correlation
NNR-8	287.80	f	287.70	287.90	N	65	E	57	SE	2.50	2	1		15.58		
NNR-8	288.23	f	288.00	288.45	N	75	E	57	SE	1.50	2	1		11.28		
NNR-8	288.33	f	288.20	288.45	N	45	E	54	SE	3.00	2	2		26.43		BHTV-log correlation
NNR-8	288.50	f	288.30	288.70	N	65	E	63	SE	3.00	2	2	58.00		n	
NNR-8	289.00	f	288.60	289.40	N	50	E	77	SE	2.00	2	1		4.14		
NNR-8	289.13	f	289.00	289.25	N	80	E	51	SE	2.00	2	1		7.10		
NNR-8	289.25	j	288.80	289.70	N	45	W	81	NE							
NNR-8	289.33	f	289.20	289.45	N	65	E	45	SE	2.00	2	1		27.65		BHTV-log correlation
NNR-8	290.00	b			N	10	W	19	SW							
NNR-8	290.50	f	290.30	290.70	N	65	W	73	SW	0.50	2	2	11.00		n	
NNR-8	290.78	f	290.55	291.00	N	75	W	64	SW	1.50	2	1	18.00		n	
NNR-8	291.55	f	291.50	291.60	N	35	E	31	NW	1.00	2	1		2.99		
NNR-8	292.15	f	291.80	292.50	N	65	E	71	NW	1.00	2	1		4.11		
NNR-8	292.23	f	292.15	292.30	N	40	E	35	NW	1.00	2	1	4.00		n	younger than 292.15
NNR-8	292.50	f	292.40	292.60	N	45	E	44	NW	1.50	2	1	14.00		n	younger than 292.75 and 292.85
NNR-8	292.75	f	292.50	293.00	N	40	E	68	SE	3.00	2	1		17.09		BHTV-log correlation
NNR-8	292.85	f	292.50	293.20	N	65	E	75	SE	2.00	2	1		25.15		
NNR-8	293.45	f	293.05	293.85	N	20	E	66	SE	2.00	2	1	38.50		n	
NNR-8	293.53	f	293.20	293.85	N	50	E	61	SE	2.00	2	1	38.50		n	
NNR-8	293.55	f	293.55	293.65	N	0	S	21	W	1.50	2	1	6.00		n	younger than 293.45, 293.525 and 293.6
NNR-8	293.60	f	293.30	293.90	N	55	E	63	SE	3.00	2	1		36.28		BHTV-log correlation
NNR-8	294.28	f	294.25	294.30	N	10	W	22	SW	1.00	2	1		5.64		
NNR-8	294.30	f	294.10	294.50	N	50	E	74	NW	1.00	2	1		10.74		
NNR-8	294.35	f	294.10	294.60	N	40	E	69	SE	1.00	2	1	7.00		n	
NNR-8	294.80	b			N	20	W	9	SW							
NNR-8	295.30	f	294.90	295.70	N	55	E	70	NW	0.50	2	1		0.50		
NNR-8	295.73	f	295.65	295.80	N	45	E	27	NW	2.00	2	1		19.24		
NNR-8	295.90	f	295.85	295.95	N	50	E	20	NW	0.50	2	2		4.58		
NNR-8	296.43	f	296.15	296.70	N	30	E	68	NW	0.50	2	2	5.00		n	
NNR-8	296.50	b			N	18	W	22	SW							obtained from BHTV-log

NNR-8	296.90	b			N	25	W	14	SW							
NNR-8	297.55	f	297.25	297.85	N	45	E	64	NW	0.50	2	2	19.00		n	
NNR-8	297.70	f	297.50	297.90	N	55	E	67	NW	0.50	2	2		4.58		
NNR-8	298.45	f	298.00	298.90	N	50	E	79	NW	1.00	2	1		3.22		
NNR-8	298.55	f	298.50	298.60	N	35	E	39	NW	0.50	2	1	2.00			
NNR-8	298.70	f	298.60	298.75	N	50	E	60	NW	1.00	2	1	5.00		n	
NNR-8	298.73	f	298.60	298.80	N	30	E	52	NW	0.50	2	1	2.00		n	
NNR-8	298.88	f	298.75	299.00	N	80	E	77	NW	0.50	2	1		2.76		
NNR-8	299.10	f	298.80	299.40	N	35	E	74	NW	0.50	2	1		2.50		
NNR-8	299.33	f	298.90	299.75	N	35	E	82	NW	1.00	2	1	4.00		n	
NNR-8	299.35	f	298.90	299.80	N	5	E	76	NW	1.00	2	1	4.00		n	
NNR-8	299.45	f	299.40	299.50	N	65	E	55	NW	0.50	2	1		2.76		
NNR-8	299.98	f	299.00	300.95	N	50	E	87	SE	6.00	2	1	27.00		n	
NNR-8	300.80	b			N	27	W	21	SW							obtained from BHTV-log
NNR-8	300.83	f	300.75	300.90	N	40	E	41	NW	1.50	2	1	15.00		n	
NNR-8	301.10	f	301.05	301.15	N	65	W	14	NE	1.00	2	1		3.38		
NNR-8	302.13	f	301.70	302.55	N	30	E	72	NW	2.00	2	1	21.00		r	
NNR-8	304.85	f	304.30	305.40	N	45	E	75	NW	3.50	2	1	37.00		r	BHTV-log correlation
NNR-8	305.50	b			N	20	E	11	NW							
NNR-8	307.73	f	307.40	308.05	N	45	E	76	SE	4.00	2	1		51.69		BHTV-log correlation
NNR-8	308.20	f	308.00	308.40	N	45	E	71	NW	2.00	2	1		0.49		
NNR-8	313.33	f	313.15	313.50	N	25	W	57	NE	0.50	2	3	2.00		r	
NNR-8	313.53	f	313.40	313.65	N	40	W	63	NE	0.50	2	3	4.00		r	
NNR-8	313.75	b			N	25	E	9	NW							
NNR-8	315.10	b			N	5	E	19	NW							
NNR-8	315.90	f	315.40	316.40	N	45	E	83	SE	1.00	2	2	26.00		n	BHTV-log correlation
NNR-8	317.25	f	316.70	317.80	N	45	E	74	SE		2		220.00		n	BHTV-log correlation
NNR-8	318.48	f	318.10	318.85	N	50	E	79	SE	3.00	2	1		31.37		
NNR-8	318.70	f	318.50	318.90	N	35	E	56	NW	1.50	2	1	18.00		n	younger than 318.475
NNR-8	319.15	f	319.05	319.25	N	50	E	45	NW	2.50	2	1	21.00		n	
NNR-8	319.50	f	319.40	319.60	N	35	E	42	NW	3.00	2	1		31.83		
NNR-8	320.30	b			N	20	E	12	NW							
NNR-8	322.45	f	322.40	322.50	N	60	E	30	NW	2.50	2	1		27.63		
NNR-8	323.60	b			N	10	E	11	NW							

NNR-8	323.63	f	323.55	323.70	N	45	E	57	SE	0.50	2	2	6.00		r	
NNR-8	323.73	f	323.55	323.90	N	50	E	66	NW	1.00	2	2	13.00		n	
NNR-8	323.80	b			N	12	E	29	NW							obtained from BHTV-log
NNR-8	323.95	f	323.65	324.25	N	80	E	74	SE	0.50	2	1		2.87		
NNR-8	324.20	f	324.05	324.35	N	75	E	61	SE	0.50	2	2	5.00		n	
NNR-8	324.48	f	324.25	324.70	N	60	E	66	SE	0.50	2	1	6.00		n	
NNR-8	324.65	f	324.55	324.75	N	55	E	72	NW	1.00	2	1		5.97		
NNR-8	325.63	f	325.05	326.20	N	45	E	79	NW	1.00	2	1	11.00		n	
NNR-8	327.45	f	327.20	327.70	N	15	E	67	SE	1.00	2	2	19.00		n	younger than 327.725
NNR-8	327.73	f	327.60	327.85	N	35	E	44	NW	1.50	2	2		17.53		
NNR-8	328.28	f	328.20	328.35	N	35	E	67	NW	1.00	2	1		4.52		
NNR-8	328.45	f	328.00	328.90	N	40	E	78	SE	2.00	2	2	16.00		n	
NNR-8	328.70	b			N	20	W	16	SW							
NNR-8	328.90	f	328.70	329.10	N	20	E	68	SE	0.50	2	3	13.00		n	
NNR-8	329.65	f	329.60	329.70	N	35	E	41	NW	0.50	2	4	23.00		r	
NNR-8	329.70	b			N	20	W	5	SW							
NNR-8	330.45	f	330.35	330.55	N	80	W	48	NE	0.50	2	1		2.76		
NNR-8	330.70	f	330.40	331.00	N	75	E	69	NW	0.50	2	1		2.19	r	
NNR-8	331.15	f/j	331.00	331.30	N	60	E	41	NW	0.50	2	2		4.58		BHTV-log correlation
NNR-8	332.20	f	332.15	332.25	N	20	E	31	NW	1.00	2	1		14.10		
NNR-8	333.70	f	333.50	333.90	N	20	E	54	NW	8.00	2	2		82.32		BHTV-log correlation
NNR-8	334.05	f	333.80	334.30	N	0	S	51	NW	2.00	2	2		7.49		
NNR-8	334.13	f	333.95	334.30	N	5	E	56	NW	1.00	2	2		17.63		
NNR-8	334.23	f	334.15	334.30	N	40	E	33	NW	0.50	2	2		4.58		
NNR-8	334.43	f	334.35	334.50	N	40	W	67	NE	0.50	2	2		5.19		
NNR-8	334.58	f	334.50	334.65	N	15	E	31	NW	0.50	2	2		17.29		
NNR-8	335.95	f	335.80	336.10	N	40	E	63	NW	1.50	2	1	3.00		r	
NNR-8	336.25	f	336.10	336.40	N	35	E	56	NW	1.50	2	1	2.00		r	
NNR-8	337.10	b			N	35	W	14	SW							
NNR-8	340.10	f	340.00	340.20	N	35	E	41	NW	1.50	2	1		19.04		
NNR-8	340.95	f	340.80	341.10	N	55	E	53	NW	1.00	2	2	25.00		n	
NNR-8	343.65	f	343.50	343.80	N	40	E	53	NW	1.50	2	2		10.13		
NNR-8	345.95	f	345.80	346.10	N	20	E	56	NW	0.50	2	1	1.00		n	
NNR-8	346.68	f	346.50	346.85	N	80	E	61	NW	4.00	2	1	14.00		n	

NNR-8	348.10	b			N	45	W	12	SW						
NNR-8	349.60	f	349.50	349.70	N	40	E	47	NW	0.50	2	1	1.00	n	
NNR-8	350.15	f	350.00	350.30	N	60	E	48	NW	1.00	2	1	9.00		
NNR-8	350.20	f	350.10	350.30	N	45	E	40	NW	1.00	2	1	8.27		
NNR-8	350.23	f	350.20	350.25	N	45	E	64	SE	1.00	2	1	8.64		
NNR-8	350.40	f	350.30	350.50	N	55	E	47	NW	1.50	2	1	15.64		
NNR-8	351.90	b			N	30	W	10	SW						
NNR-8	352.88	f	352.70	353.05	N	10	E	68	SE	1.00	2	2	8.29		BHTV-log correlation
NNR-8	353.35	f	353.30	353.40	N	10	E	55	NW	0.50	2	2	5.06		
NNR-8	354.13	f	354.00	354.25	N	80	E	52	NW	1.50	2	1	25.94		
NNR-8	355.80	b			N	15	W	17	SW						obtained from BHTV-log
NNR-8	356.30	b			N	25	W	12	SW						
NNR-8	357.68	f	357.55	357.80	N	45	E	54	NW	2.00	2	1	16.88		
NNR-8	357.98	f	357.85	358.10	N	75	E	57	NW	1.50	2	1	6.00	n	
NNR-8	358.50	f	358.20	358.80	N	50	E	62	NW	3.00	2	1	31.00	n	
NNR-8	358.70	b			N	20	W	20	SW						
NNR-8	358.80	b			N	30	W	20	SW						obtained from BHTV-log
NNR-8	361.33	f	361.20	361.45	N	55	E	82	SE	2.00	2	1	9.00	n	
NNR-8	361.45	j	361.00	361.90	N	20	E	74	SE						
NNR-8	361.60	b			N	35	W	9	SW						obtained from BHTV-log
NNR-8	361.63	f	361.60	361.65	N	60	E	16	NW	2.00	2	1	34.24		
NNR-8	362.20	b			N	35	W	9	SW						
NNR-8	362.60	b			N	25	W	20	SW						obtained from BHTV-log
NNR-8	362.90	b			N	30	W	23	SW						obtained from BHTV-log
NNR-8	364.05	f	364.00	364.10	N	70	E	36	NW	0.50	2	1	0.50		
NNR-8	364.30	b			N	5	W	13	SW						obtained from BHTV-log
NNR-8	364.35	f	364.10	364.50	N	5	E	59	SE	2.50	2	1	18.00	n	BHTV-log correlation
NNR-8	364.60	b			N	20	W	13	SW						obtained from BHTV-log
NNR-8	365.15	b			N	20	W	14	SW						
NNR-8	365.65	f	365.50	365.80	N	25	E	56	SE	1.50	2	1	18.62		
NNR-8	365.88	f	365.70	366.05	N	20	E	63	SE	2.00	2	1	7.00	n	
NNR-8	366.50	b			N	30	W	11	SW						obtained from BHTV-log
NNR-8	367.00	b			N	45	W	14	SW						
NNR-8	367.20	b			N	0	S	22	SW						obtained from BHTV-log

NNR-8	367.43	f	367.35	367.50	N	40	W	32	NE	1.00	2	1	3.00		n	stepper faults are younger
NNR-8	367.60	f	367.50	367.70	N	30	W	44	NE	0.50	2	2	4.00		n	
NNR-8	367.60	f	367.55	367.65	N	35	W	85	NE	1.50	2	2	10.00		r	
NNR-8	367.93	f	367.80	368.05	N	45	W	41	NE	1.00	2	1		11.73		
NNR-8	368.30	f	368.15	368.45	N	40	W	57	NE	0.50	2	2	5.00		n	
NNR-8	368.95	f	368.85	369.05	N	50	E	40	NW	0.50	2	1		0.50		
NNR-8	369.68	f	369.50	369.85	E	90	W	66	NW	1.00	2	1		2.29		
NNR-8	370.83	f	370.70	370.95	N	80	W	68	NE	2.00	2	2	37.00		r	
NNR-8	371.13	f	370.90	371.35	N	10	E	65	NW	0.50	2	1	3.00		n	
NNR-8	371.48	f	371.25	371.70	N	35	W	67	NE	1.00	2	1	1.50		n	
NNR-8	371.78	f	371.50	372.05	N	40	W	68	NE	1.00	2	1	1.00		r	
NNR-8	372.20	f	372.00	372.40	N	55	W	61	NE	0.50	2	2		4.58		
NNR-8	372.90	b			N	10	W	27	SW							obtained from BHTV-log
NNR-8	373.70	b			N	38	W	30	SW							obtained from BHTV-log
NNR-8	374.50	b			N	45	W	19	SW							
NNR-8	375.68	f	375.45	375.90	N	15	W	65	NE	2.00	2	1	12.00		n	BHTV-log correlation
NNR-8	375.75	f	375.60	375.90	N	30	W	68	NE	0.50	2	1		1.51		
NNR-8	375.78	f	375.70	375.85	N	40	W	61	NE	1.00	2	1		9.33		
NNR-8	376.70	f	376.60	376.80	N	50	W	47	NE	1.00	2	1		8.51		
NNR-8	376.73	f	376.65	376.80	N	50	W	42	NE	1.00	2	1		7.65		
NNR-8	378.80	b			N	20	W	23	SE							BHTV-log correlation
NNR-8	379.60	f	379.55	379.65	N	25	E	42	NW	1.00	2	1		3.76		
NNR-8	379.63	f	379.55	379.70	N	30	E	46	NW	2.00	2	1		17.72		
NNR-8	380.35	f	380.20	380.50	N	60	E	55	NW	1.00	2	1	3.00		n	
NNR-8	380.60	f	380.45	380.75	N	30	E	57	NW	1.50	2	1	5.00		n	
NNR-8	381.18	f	380.80	381.55	N	40	E	72	NW	2.00	2	1		26.29		
NNR-8	381.33	f	381.10	381.55	N	15	E	63	NW	2.00	2	1		20.27		
NNR-8	381.40	b			N	38	W	20	SW							obtained from BHTV-log
NNR-8	381.53	f	381.50	381.55	N	30	E	59	NW	1.50	2	1		11.28		
NNR-8	381.55	f	381.50	381.60	N	80	W	17	SW	3.00	2	1		3.05		younger than 381.175, 381.315 and 381.525
NNR-8	382.25	f	382.20	382.30	N	40	E	26	NW	11.00	2	1	24.00		n	
NNR-8	382.38	f	382.25	382.50	N	35	E	53	NW	2.00	2	1		26.10		
NNR-8	382.63	f	382.50	382.75	N	35	E	42	NW	1.50	2	1		20.86		
NNR-8	382.70	f	382.50	382.90	N	30	E	61	NW	2.00	2	1		12.73		

NNR-8	382.95	f	382.70	383.20	N	55	E	67	SE	1.00	2	1	12.00		n	older than 382.625 and 382.7
NNR-8	383.10	f	382.90	383.30	N	70	E	69	SE	0.50	2	2	4.00		n	
NNR-8	384.60	f	384.40	384.80	N	20	E	66	SE	1.00	2	2		6.40		
NNR-8	384.63	f	384.45	384.80	N	15	E	61	SE	1.00	2	2		15.01		
NNR-8	384.83	f	384.70	384.95	N	60	E	68	SE	0.50	2	2		4.58		
NNR-8	385.00	f	384.40	385.60	N	70	E	82	NW	2.00	2	2	42.00		r	BHTV-log correlation
NNR-8	385.10	f	385.00	385.20	N	40	E	62	SE	0.50	2	2		15.03		
NNR-8	385.50	f	385.05	385.95	N	5	W	76	SW	1.00	2	2	21.00		n	BHTV-log correlation
NNR-8	385.78	f	385.65	385.90	N	10	E	44	NW	1.00	2	2		2.79		
NNR-8	385.83	f	385.75	385.90	N	20	E	41	NW	0.50	2	2		2.23		
NNR-9	176.40	b			N	10	W	19	SW							Obtained from BHTV-log
NNR-9	179.30	b			N	0	S	14	W							Obtained from BHTV-log
NNR-9	181.45	f	181.20	181.70	N	30	E	67	SE	1.00	1	1	17.00		n	
NNR-9	184.80	b			N	0	S	13	W							Obtained from BHTV-log
NNR-9	186.18	f	186.00	186.35	N	20	E	62	SE	1.00	1	2	19.00		n	
NNR-9	186.25	f	186.10	186.40	N	60	E	45	SE	1.00	1	2	16.00		n	
NNR-9	186.85	j	186.70	187.00	N	70	E	62	NW							
NNR-9	186.88	j	186.70	187.05	N	80	E	60	NW							
NNR-9	188.60	b			N	20	E	13	NW							
NNR-9	190.10	j														
NNR-9	192.80	b			N	10	E	11	NW							
NNR-9	194.43	f	194.30	194.55	N	50	E	47	SE	1.00	1	1		8.99		
NNR-9	196.25	j	195.70	196.80	N	20	E	85	SE							
NNR-9	197.10	f	197.00	197.20	N	65	E	48	SE	0.50	1	3		4.65		
NNR-9	197.13	f	196.80	197.45	N	60	E	67	SE	0.50	1	3	16.00		n	
NNR-9	197.20	f	197.15	197.25	N	55	E	56	SE	0.50	1	3	9.00		n	
NNR-9	198.88	f	198.15	199.60	N	70	E	82	NW	1.00	1	1	7.00		n	
NNR-9	200.68	f	200.50	200.85	E	90	W	64	N	1.00	1	1	2.00		n	
NNR-9	201.80	b			N	10	E	18	NW							Obtained from BHTV-log
NNR-9	202.33	f	202.15	202.50	N	10	E	50	SE	1.00	1	1		7.12		
NNR-9	202.60	f	202.40	202.80	N	0	S	52	E	1.00	1	1		8.67		
NNR-9	202.80	f	202.75	202.85	N	60	E	29	NW	1.00	1	1		8.78		
NNR-9	202.95	f	202.80	203.10	N	0	S	46	E	2.00	1	1	21.00		n	
NNR-9	203.18	f	203.00	203.35	N	5	E	54	SE	1.00	1	1	9.00		n	

NNR-9	203.28	f	203.10	203.45	N	10	E	42	SE	1.00	1	1	3.00		n	
NNR-9	203.80	f	203.70	203.90	N	25	E	32	SE	2.00	1	4	32.00		n	
NNR-9	204.40	b			N	5	E	25	NW							Obtained from BHTV-log
NNR-9	204.45	f	204.40	204.50	N	20	E	55	SE	0.50	1	2		5.31		
NNR-9	205.50	f	205.30	205.70	N	20	E	63	SE	0.50	1	2	3.00		r	
NNR-9	205.73	f	205.30	206.15	N	20	E	81	SE	0.50	1	2	6.00		r	
NNR-9	206.00	f	205.95	206.05	N	20	E	56	SE	0.50	1	2		2.71		
NNR-9	206.95	f	206.80	207.10	N	30	E	54	SE	0.50	1	2		6.49		
NNR-9	208.00	b			N	20	E	14	NW							
NNR-9	209.80	j			E	90	W									
NNR-9	211.80	b			N	15	E	12	NW							
NNR-9	212.53	f	212.40	212.85	N	70	W	78	NE	1.00	1	2		10.63		
NNR-9	212.63	f	212.25	212.80	N	45	W	65	NE	1.00	1	2	4.00		r	
NNR-9	213.20	f	213.00	213.40	N	20	E	62	SE	0.50	1	2		8.08		
NNR-9	213.25	f	213.00	213.50	N	30	E	76	SE	0.50	1	2	2.00		r	
NNR-9	213.90	f	213.70	214.10	N	55	E	60	NW	1.00	1	3	30.00		n	
NNR-9	215.40	f	214.60	216.20	N	30	E	85	SE	1.00	1	3	25.00		r	
NNR-9	215.80	f	215.30	216.30	N	80	E	82	SE	13.00	1	3	>150	138.99	n	
NNR-9	215.85	f	215.80	215.90	N	70	W	67	NE	1.00	1	3	19.00		r	
NNR-9	216.00	f	215.70	216.30	N	70	E	70	SE	2.00	1	2	43.00		n	
NNR-9	216.68	f	216.60	216.75	N	65	E	64	SE		1					
NNR-9	216.95	f	216.90	217.00	N	60	E	53	SE	1.00	1	3		6.41		
NNR-9	216.96	f	216.75	217.15	N	55	E	65	SE	0.50	1	3	23.00		n	
NNR-9	219.10	b			N	10	E	14	NW							
NNR-9	219.60	b			N	25	E	9	NW							Obtained from BHTV-log
NNR-9	220.90	b			N	0	S	13	NW							Obtained from BHTV-log
NNR-9	222.35	f	222.20	222.50	N	25	W	33	NE	0.50	1	1		10.31		
NNR-9	223.40	b			N	20	E	15	NW							
NNR-9	225.23	f	225.15	225.30	N	10	E	51	SE	0.50	1	3		1.60		
NNR-9	225.85	f	225.60	226.10	N	20	E	67	SE	0.50	1	3		5.20		
NNR-9	226.38	f	226.30	226.45	N	0	S	26	E	1.00	1	1	3.00		n	
NNR-9	227.00	f	226.40	227.60	N	40	W	82	NE	1.00	1	1	5.00		r	
NNR-9	227.30	b			N	0	S	22	W							Obtained from BHTV-log
NNR-9	228.03	f	227.85	228.20	N	10	W	52	NE	1.00	1	1	14.00		n	

NNR-9	234.73	f	234.55	234.90	N	50	E	57	SE		1		30.00		n	
NNR-9	234.85	f	234.75	234.95	N	60	E	42	SE	1.00	1	1	9.00		n	
NNR-9	234.95	f	234.80	235.10	N	10	E	68	SE	0.50	1	3	1.00		r	
NNR-9	235.40	f	235.30	235.50	N	15	E	83	SE	0.50	1	3	1.00		r	
NNR-9	236.15	f	236.10	236.20	N	50	E	18	SE	1.00	1	3	5.00		r	
NNR-9	239.50	b			N	10	E	20	NW							
NNR-9	240.80	f	240.60	241.00	N	20	W	52	NE	0.50	1	3	6.00		n	
NNR-9	241.25	f	241.20	241.30	N	30	E	50	SE	0.50	1	3	3.00		n	
NNR-9	241.85	f	241.70	242.00	N	30	W	52	NE	1.00	1	2	3.00		n	
NNR-9	242.05	f	242.00	242.10	N	30	W	10	NE	1.00	1	2		10.63		
NNR-9	242.30	b			N	0	S	16	W							
NNR-9	242.63	f	242.50	242.75	N	45	E	67	NW	1.00	1	2	5.00		n	
NNR-9	243.80	f	243.70	243.90	N	20	W	56	NE	1.00	1	2		10.63		
NNR-9	245.53	f	245.40	245.65	N	60	E	47	NW	1.00	1	4		16.80		
NNR-9	245.63	f	245.30	245.95	N	50	E	71	NW		1		13.00		n	
NNR-9	246.50	f	246.30	246.70	N	60	E	60	NW	0.50	1	3	3.00		n	
NNR-9	247.20	b			N	15	E	28	NW							Obtained from BHTV-log
NNR-9	249.00	b			N	10	E	20	NW							Obtained from BHTV-log
NNR-9	249.03	f	248.95	249.10	N	20	W	31	NE	0.50	1	3	9.00		n	
NNR-9	249.40	b			N	10	E	11	NW							
NNR-9	249.85	f	249.80	249.90	N	35	E	41	SE	0.50	1	3	4.00		n	
NNR-9	250.50	f	250.40	250.60	N	60	E	46	SE	3.00	1	1	44.00		n	
NNR-9	250.55	f	250.40	250.70	N	55	E	39	SE	1.00	1	1		9.66		
NNR-9	250.73	f	250.45	251.00	N	40	E	67	SE	1.00	1	1		8.24		
NNR-9	252.10	f	251.70	252.50	N	85	E	71	NW	2.00	1	2	13.50		n	
NNR-9	252.20	f	251.90	252.50	N	70	E	63	NW	1.00	1	2	13.50		n	
NNR-9	252.70	f	252.60	252.80	N	70	W	55	SW	1.00	1	2		16.34		
NNR-9	252.85	f	252.70	253.00	N	80	E	68	SE	1.00	1	3	7.00		n	
NNR-9	252.95	f	252.80	253.10	N	70	E	51	SE	1.00	1	3	7.00		n	
NNR-9	253.23	f	252.60	253.85	N	45	E	81	NW	3.00	1	3	34.00		n	
NNR-9	253.43	f	253.25	253.60	N	50	E	42	SE	0.50	1	3	2.00		n	younger than fault 253.225
NNR-9	253.58	f	253.55	253.60	N	50	E	42	SE	0.50	1	3		2.79		
NNR-9	254.60	f	254.50	254.70	N	40	E	78	SE	0.50	1	3	5.00		r	
NNR-9	255.00	b			N	10	E	24	NW							Obtained from BHTV-log

NNR-9	255.50	f	255.30	255.70	N	50	E	64	SE	2.50	1	1	35.00		n	
NNR-9	256.25	f	256.20	256.30	N	10	E	28	NW	1.00	1	1		10.05		
NNR-9	256.40	b			N	20	E	22	NW							BHTV-Log correlation
NNR-9	257.08	f	257.00	257.15	N	5	E	33	NW	4.00	1	1		57.50		BHTV-Log correlation
NNR-9	257.40	b			N	5	E	24	NW							Obtained from BHTV-log
NNR-9	257.58	f	257.50	257.65	N	70	W	26	NE	2.00	1	1		24.70		
NNR-9	262.13	f	261.95	262.30	N	40	E	57	NW	0.50	1	2	3.00		n	
NNR-9	262.28	f	261.85	262.70	N	55	E	76	NW	1.00	1	2	70.00		n	BHTV-Log correlation
NNR-9	262.83	f	262.50	263.15	N	50	W	73	NE	0.50	1	2	3.00		r	
NNR-9	263.20	f	263.00	263.40	N	20	E	83	SE	2.00	1	2	39.00		r	
NNR-9	263.25	f	263.15	263.25	N	80	E	37	SE	0.50	1	2	1.00		r	
NNR-9	263.30	b			N	35	E	30	NW							Obtained from BHTV-log
NNR-9	263.70	f								0.50	1	2	18.00		r	
NNR-9	264.55	f	264.30	264.80	N	45	E	65	SE	2.00	1	1		17.17		BHTV-Log correlation
NNR-9	265.20	f	265.10	265.30	N	50	E	58	SE	1.00	1	1		7.98		
NNR-9	265.50	f	264.70	266.30	N	50	E	83	NW	2.00	2	2	27.00			
NNR-9	266.50	b			N	10	W	16	SW							
NNR-9	268.53	f	268.35	268.70	N	75	E	57	SE	24.00	2	1		248.38	n	BHTV-Log correlation
NNR-9	268.80	f	268.60	269.00	N	70	E	74	SE	3.00	2	1	55.00		n	
NNR-9	269.05	f	268.80	269.30	N	50	E	59	SE	1.00	2	4		17.46		
NNR-9	269.45	f	269.40	269.50	N	45	E	27	SE	1.00	2	2		3.27		
NNR-9	269.55	f	269.40	269.70	N	40	E	54	SE	1.00	2	2		8.17		
NNR-9	270.00	f	269.80	270.20	N	80	E	49	SE	4.00	2	1		38.46		BHTV-Log correlation
NNR-9	271.15	f	271.00	271.30	N	40	E	68	SE	2.00	2	2	30.00		n	
NNR-9	272.00	f	271.80	272.20	N	70	E	50	SE	4.00	2	1		16.96		
NNR-9	272.35	f	272.10	272.60	N	75	E	62	SE	2.00	2	1		2.67		
NNR-9	272.70	f	272.10	273.30	N	75	E	80	SE	3.00	2	1		35.16		
NNR-9	274.20	f	273.80	274.60	N	50	E	76	NW	0.50	2	4	19.00		n	BHTV-Log correlation
NNR-9	275.35	f	275.10	275.60	N	80	E	73	SE	3.00	2	2	55.00		n	
NNR-9	275.48	f	275.40	275.55	N	30	E	71	SE		2					
NNR-9	275.80	f	275.70	275.90	N	80	E	41	SE	1.00	2	1		15.24		
NNR-9	276.00	f	275.80	276.20	E	90	W	56	S	1.00	2	1		9.43		
NNR-9	276.50	f	276.40	276.60	N	85	E	44	SE	4.00	2	1		17.37	n	BHTV-Log correlation
NNR-9	276.95	f	276.90	277.00	N	80	E	41	SE	4.00	2	3		24.69	n	

NNR-9	277.20	f	277.10	277.30	N	70	E	53	SE	6.00	2	3		71.01		BHTV-Log correlation
NNR-9	280.30	b			N	5	E	19	NW							
NNR-9	282.28	f	282.05	282.50	N	30	E	54	SE	4.00	2	1	14.00			
NNR-9	282.50	f	282.40	282.60	N	60	E	56	SE	2.00	2	1		29.13		
NNR-9	284.30	b			N	15	E	18	NW							Obtained from BHTV-log
NNR-9	284.90	f	284.70	285.10	N	60	E	60	SE	6.00	2	1		68.45		BHTV-Log correlation
NNR-9	285.05	f	284.80	285.30	N	35	E	58	SE	2.00	2	1	3.00			
NNR-9	285.80	b			N	10	E	18	NW							Obtained from BHTV-log
NNR-9	286.33	f	286.15	286.50	N	50	W	78	NE	1.00	2	1		8.08		
NNR-9	286.40	b			N	20	E	27	NW							Obtained from BHTV-log
NNR-9	286.88	f	286.60	287.15	N	35	W	80	SW	1.00	2	1	2.00		n	
NNR-9	287.13	f	287.05	287.20	N	40	E	29	NW	7.00	2	1		83.91		
NNR-9	287.33	f	287.10	287.55	N	35	W	73	SW	2.00	2	1		14.52		
NNR-9	288.00	f	287.90	288.10	N	50	E	36	NW	1.00	2	1		8.88		
NNR-9	288.10	f	288.00	288.20	N	20	E	64	NW	1.00	2	1		7.52		
NNR-9	288.13	f	288.00	288.25	N	50	E	55	SE	3.00	2	1		53.42		younger than 288.1
NNR-9	288.20	f	287.60	288.60	N	50	E	84	SE	3.00	2	1		72.68		BHTV-Log correlation
NNR-9	289.20	b			N	20	E	22	NW							
NNR-9	289.55	f	289.40	289.70	N	55	E	65	NW	1.00	2	1		5.33		
NNR-9	290.50	f	290.30	290.70	N	60	E	65	NW	1.00	2	1	6.00		r	
NNR-9	291.10	f	290.90	291.30	N	50	E	66	SE	1.00	2	1	3.00		n	
NNR-9	291.33	f	290.90	291.75	N	60	E	79	SE	1.00	2	1	5.00		n	
NNR-9	291.70	f	291.50	291.90	N	45	E	50	SE	3.00	2	3	43.00		r	BHTV-Log correlation
NNR-9	291.95	f	291.80	292.10	N	60	E	61	SE	4.00	2	1	26.00		n	
NNR-9	292.10	f	291.90	292.30	N	55	E	60	SE	3.00	2	1		41.40		
NNR-9	292.25	f	292.10	292.40	N	60	E	59	SE	3.00	2	1		9.23		
NNR-9	292.40	f	292.30	292.50	N	50	E	61	SE	1.00	2	1		4.76		
NNR-9	293.20	b			N	10	E	21	NW							
NNR-9	294.30	f	294.20	294.40	N	10	W	35	SW	1.00	2	1		5.85		
NNR-9	297.05	f	297.00	297.10	N	40	E	18	NW	2.00	2	1		5.38		
NNR-9	297.15	f	297.00	297.30	N	40	E	54	NW	2.00	2	1		18.15		
NNR-9	297.75	f	297.70	297.80	N	20	E	14	NW	2.00	2	1		30.60		
NNR-9	297.90	f	297.60	298.20	E	90	W	62	N	1.00	2	1	3.00		r	younger than 297.75
NNR-9	298.90	f	298.65	299.15	N	75	E	78	SE	1.00	2	1		5.43		

NNR-9	298.93	f	298.85	299.00	N	45	E	54	NW	1.00	2	1		11.59		
NNR-9	299.15	f	299.00	299.30	N	60	E	53	SE	4.00	2	1		70.94		
NNR-9	299.15	f	299.10	299.20	N	65	E	55	NW	1.00	2	1		8.35		
NNR-9	300.30	f	300.00	300.60	N	70	E	58	SE	3.00	2	1	45.00		n	
NNR-9	300.65	f	300.50	300.80	N	50	E	51	SE	0.50	2	1		2.76		
NNR-9	300.85	f	300.80	300.90	N	50	E	53	SE	0.50	2	1		4.00		
NNR-9	301.85	f	301.70	302.00	N	40	E	41	NW	1.00	2	1	7.00		n	
NNR-9	302.03	f	301.95	302.10	N	80	E	34	NW	1.00	2	1	11.00		n	
NNR-9	302.70	f	302.40	303.00	N	40	E	73	SE	1.50	2	1	1.00		n	
NNR-9	303.10	b			N	0	E	18	W							
NNR-9	303.68	f	303.50	303.85	N	50	E	47	SE	13.00	2	1		135.14	n	BHTV-Log correlation
NNR-9	304.40	f	304.10	304.70	N	80	E	70	SE	2.00	2	1	4.00		n	
NNR-9	304.40	f	304.30	304.50	E	90	W	59	N	2.00	2	1		13.19		
NNR-9	304.50	f	304.30	304.70	N	75	E	76	SE	3.00	2	1	5.00		n	
NNR-9	305.65	f	304.90	306.40	N	60	E	84	SE	6.00	2	1	80.00		n	BHTV-Log correlation
NNR-9	306.85	f	306.70	307.00	N	40	E	59	NW	3.00	2	1	14.00		n	
NNR-9	307.05	f	306.40	307.70	N	50	E	82	SE	6.00	2	1	68.00		n	
NNR-9	307.28	f	306.85	307.70	N	50	E	67	SE	2.00	2	1		21.63		
NNR-9	307.40	j	307.20	307.60	N	45	E	57	NE							BHTV-Log correlation
NNR-9	308.63	f	308.40	308.85	N	65	E	58	NW	2.00	2	1		15.22		
NNR-9	308.80	b			N	30	E	24	NW							
NNR-9	308.85	f	308.70	309.00	N	35	E	56	SE	1.00	2	1	3.00		n	
NNR-9	309.70	f	309.60	309.80	N	65	E	62	SE	3.00	2	1		18.20		
NNR-9	310.45	f	310.00	310.90	E	90	W	71	S	3.00	2	1		8.50		
NNR-9	310.50	f	310.10	310.90	N	70	E	67	SE	3.00	2	1	7.00		n	
NNR-9	310.60	f	310.30	310.90	N	60	E	65	SE	4.00	2	1		50.22		
NNR-9	311.50	f	311.40	311.60	N	35	E	58	NW	3.00	2	1		50.50		
NNR-9	311.95	j	311.70	312.20	N	70	E	66	NE							
NNR-9	312.38	f	312.05	312.70	N	85	E	74	NE	2.00	2	1		16.88		
NNR-9	313.38	f	313.25	313.50	N	40	E	43	NW	2.00	2	1		31.98		
NNR-9	313.45	f	313.25	313.65	N	45	E	47	NW	2.00	2	1		31.98		
NNR-9	313.80	f	313.60	314.00	N	30	E	56	NW	3.00	2	1	24.00		n	
NNR-9	313.85	f	313.60	314.10	N	30	E	26	NW	3.00	2	1	17.00		n	
NNR-9	314.00	b			N	20	E	26	NW							

NNR-9	315.00	f	314.70	315.30	N	65	E	71	SE	48.00	2	1		512.42	n	
NNR-9	315.08	f	314.70	315.45	N	40	E	65	SE		2	1			n	
NNR-9	315.20	f	314.70	315.70	N	60	E	62	SE	23.00	2	1		241.96	n	BHTV-Log correlation
NNR-9	316.40	f								3.00	2	1	17.00		r	
NNR-9	317.10	f	316.80	317.40	N	35	E	71	NW		2					
NNR-9	317.75	f	317.50	318.00	N	40	E	63	SE	1.00	2	1	2.00		n	
NNR-9	317.85	f	317.70	318.00	N	15	W	64	SW	2.00	2	1	8.00		n	
NNR-9	318.70	f	318.40	319.00	N	45	E	62	SE	2.00	2	1	4.00		n	
NNR-9	318.85	f	318.80	318.90	N	20	E	57	NW	2.00	2	1		32.15		older than 318.7
NNR-9	319.70	f	319.50	319.90	N	50	E	56	NW	3.00	2	1		12.60		
NNR-9	320.23	f	319.85	320.60	N	40	E	72	SE	50.00	2	2		536.70	n	BHTV-Log correlation
NNR-9	320.65	f	320.50	320.80	N	50	E	64	NW	3.00	2	2		46.29		
NNR-9	320.85	f	320.70	321.00	N	45	E	71	NW	3.00	2	2		30.20		
NNR-9	321.20	f	321.00	321.40	N	40	E	53	NW	3.00	2	2		16.65		
NNR-9	321.70	f	321.00	322.40	N	40	E	63	SE	140.00	2	2		1510.36	n	BHTV-Log correlation
NNR-9	322.80	f	322.50	323.10	N	35	E	72	NW	2.00	2	1		17.11		
NNR-9	323.58	f	323.55	323.60	N	30	E	11	SE	1.00	2	1		5.26		
NNR-9	324.33	f	324.20	324.45	N	5	W	62	SW	0.50	2	2		2.11		
NNR-9	324.83	f	324.70	324.95	N	20	W	45	SW	1.00	2	2	1.00		n	
NNR-9	324.95	f	324.85	325.05	N	20	W	38	SW	2.00	2	1		30.10		
NNR-9	325.10	b			N	20	E	16	SW							
NNR-9	327.88	f	327.45	328.30	N	30	E	67	NW	1.00	2	2	7.00		r	
NNR-9	328.00	f	327.70	328.30	N	15	E	56	NW	1.00	2	2	8.00		r	
NNR-9	330.30	b			N	80	E	16	SE							
NNR-9	332.30	b			N	20	E	12	SW							
NNR-9	332.50	f	332.95	332.05	N	40	E	11	SE	0.50	2	1		5.58		
NNR-9	333.90	f	333.50	334.30	N	35	E	86	SE	1.00	2	1	16.00			
NNR-9	334.25	f	334.10	334.60	N	30	W	57	NE	0.50	2	1		2.52		
NNR-9	334.78	j	334.65	334.90	N	65	E	50	NW							BHTV-Log correlation
NNR-9	335.20	f	335.00	335.40	N	50	W	55	NE	1.00	2	1		4.30		
NNR-9	335.45	f	335.20	335.70	N	50	W	54	NE	1.00	2	1	2.00		r	
NNR-9	335.90	f	335.60	336.20	N	35	E	52	SE	2.00	2	1	15.00		n	
NNR-9	336.00	f	335.60	336.40	N	40	E	55	SE	2.00	2	1	15.00		n	
NNR-9	336.53	f	336.25	336.80	N	50	W	62	NE	0.50	2	1		0.55		

NNR-9	337.08	f	336.95	337.20	N	55	W	57	NE	1.00	2	1		5.84		
NNR-9	338.05	f	338.00	338.10	N	30	E	17	NW	1.00	2	1		8.30		
NNR-9	339.75	f	339.50	340.00	N	30	E	64	SE	1.00	2	1		13.44		BHTV-Log correlation
NNR-9	340.95	f	340.60	341.30	N	60	E	66	SE	28.00	2	4		311.13	n	BHTV-Log correlation
NNR-9	341.53	f	341.15	341.90	N	40	E	84	SE	5.00	2	2	80.00		n	
NNR-9	342.00	f	341.70	342.30	N	45	E	71	SE	16.00	2	2		168.87	n	BHTV-Log correlation
NNR-9	342.28	j	342.00	342.55	N	65	E	60	NW							
NNR-9	343.50	b			N	15	W	15	SW							Obtained from BHTV-log
NNR-9	343.70	b			N	20	W	11	SW							
NNR-9	344.05	f	343.90	344.20	N	80	W	56	NE	0.50	2	2	2.00		n	
NNR-9	345.40	j	344.90	345.90	N	50	W	77	NE							BHTV-Log correlation
NNR-9	346.05	f	346.00	346.10	N	40	E	42	NW	4.00	2	2	30.00		n	
NNR-9	346.85	f	346.70	347.00	N	40	E	63	NW	1.00	2	2	9.00		n	
NNR-9	348.05	f	347.80	348.30	N	75	E	64	NW	0.50	2	2	2.00		r	
NNR-9	349.15	f	349.00	349.30	E	90	W	41	N	1.00	2	2		5.06		
NNR-9	349.28	f	348.75	349.80	N	60	E	81	NW	1.00	2	2	3.00		r	
NNR-9	349.40	f	349.30	349.50	N	80	E	56	NW	1.00	2	2		9.29		
NNR-9	349.55	f	349.95	349.15	N	65	E	66	NW	1.00	2	2		12.47		
NNR-9	352.45	f	352.30	352.60	N	30	E	54	SE	1.00	2	1		11.19		
NNR-9	352.55	f	351.20	352.10	N	40	E	77	SE	0.50	2	2		4.39		
NNR-9	352.60	b			N	18	W	18	SW							Obtained from BHTV-log
NNR-9	353.00	f	352.80	353.20	N	15	E	64	SE	2.00	2	1	2.00		n	
NNR-9	353.90	b			N	30	W	15	SW							
NNR-9	354.10	f	354.00	354.20	N	0	S	58	W	1.00	2	2		12.73		
NNR-9	354.15	f	354.10	354.20	N	10	W	56	NE	1.00	2	2		11.87		
NNR-9	354.35	f	354.20	354.50	N	5	W	46	SW	4.50	2	1		40.45		BHTV-Log correlation
NNR-9	354.43	f	354.35	354.50	N	5	W	44	SW	4.50	2	1		26.61		BHTV-Log correlation
NNR-9	358.00	f	357.95	358.05	N	60	E	24	NW	1.00	2	2		17.52		
NNR-9	358.65	f	358.40	358.90	N	80	E	59	NW	1.50	2	2	1.00		n	
NNR-9	358.68	f	358.45	358.90	N	65	E	56	NW	1.00	2	2		6.74		older than 358.65
NNR-9	359.30	b			N	40	W	26	SW							
NNR-9	360.30	b			N	30	W	20	SW							Obtained from BHTV-log
NNR-9	360.40	b			N	35	W	12	SW							
NNR-9	363.90	b			N	22	W	15	SW							Obtained from BHTV-log

NNR-9	364.28	f	364.20	364.35	N	25	E	17	NW	1.00	2	1		12.53		
NNR-9	364.65	f	364.60	364.70	N	5	E	18	NW	1.00	2	1		12.29		
NNR-9	366.05	f	366.00	366.10	N	80	W	27	NE	4.00	2	1		71.05		
NNR-9	366.60	b			N	55	W	6	SW							
NNR-9	367.60	b			N	50	W	18	SW							Obtained from BHTV-log
NNR-9	368.45	f	368.10	368.80	N	35	E	74	NW	0.50	2	2		4.58		
NNR-9	368.98	f	368.80	369.15	N	75	E	57	NW	0.50	2	2		6.02		
NNR-9	372.33	j	371.95	372.70	N	0	S	83	E							
NNR-9	372.53	f	372.35	372.70	N	50	W	49	NE	1.00	2	1	8.00		n	
NNR-9	373.18	f	372.95	373.40	N	40	W	48	NE	2.00	2	2	38.00		n	
NNR-9	373.55	f	373.50	373.60	N	15	E	37	NW	2.00	2	1		11.76		
NNR-9	373.80	b			N	52	W	32	SW							Obtained from BHTV-log
NNR-9	374.50	f	374.30	374.70	N	25	E	43	NW	1.00	2	1	6.00		n	
NNR-9	376.90	b			N	40	W	31	SW							Obtained from BHTV-log
NNR-9	378.25	j	378.10	378.40	N	75	E	50	NW							
NNR-9	379.20	j	379.00	379.40	N	25	W	54	NE							
NNR-9	379.60	b			N	70	W	25	SW							Obtained from BHTV-log
NNR-9	380.00	j	379.80	380.20	N	20	W	57	NE							
NNR-9	381.90	b			N	40	W	19	SW							Obtained from BHTV-log
NNR-9	383.30	b			N	18	W	13	SW							Obtained from BHTV-log
NNR-9	383.50	b			N	15	W	13	SW							
NNR-9	383.65	f	383.60	383.70	N	65	E	52	NW	3.00	2	2		25.31		
NNR-9	383.80	f	383.65	383.95	N	75	E	55	SE	6.00	2	1	50.00		n	
NNR-9	384.13	f	384.05	384.20	N	75	E	56	SE		2					
NNR-9	384.28	f	384.20	384.35	N	65	E	35	SE	4.00	2	1		52.48		older than NW faults
NNR-9	384.85	j	384.70	385.00	N	55	E	52	SE							
NNR-9	384.90	f	384.70	385.10	N	50	E	58	SE	4.00	2	1	25.00		n	
NNR-9	385.00	f	384.80	385.20	N	55	E	62	SE	4.00	2	1	25.00		n	
NNR-9	385.30	f	385.25	385.35	N	50	E	68	SE	1.00	2	1	3.00		n	
NNR-9	386.15	f	386.00	386.30	N	10	W	49	NE	2.00	2	2		14.55		
NNR-9	386.23	f	386.15	386.30	N	20	W	43	NE	1.00	2	2		12.29		
NNR-9	386.25	f	386.00	386.50	N	15	W	56	NE	1.50	2	2	10.00		n	
NNR-9	386.43	f	386.35	386.50	N	50	W	57	NE	1.00	2	2		7.82		
NNR-9	386.73	f	386.60	386.85	N	30	E	49	NW	1.00	2	2		9.62		

NNR-9	387.15	f	387.00	387.30	N	20	W	45	SW	4.00	2	1		38.37	
NNR-9	387.38	f	387.25	387.50	N	10	W	56	SW	4.00	2	1		31.02	
NNR-9	387.45	j	387.00	387.90	N	85	E	77	NW						
NNR-9	387.63	f	387.30	387.95	N	30	W	62	SW	3.00	2	1		26.96	
NNR-9	388.65	f	388.50	388.80	N	20	E	52	NW	1.50	2	1	5.00		n
NNR-9	388.95	f	388.70	389.20	N	30	E	76	NW	1.00	2	1	3.00		n

VITA

Name: Mitchell C. Graff

Address: BP America Inc.
501 Westlake Park Blvd.
P.O. Box 3092 (77253-3092)
Houston Tx, 77079

E-mail: Mitchell.Graff@bp.com

Education: B.S. in Geology, December 2000
The University of Texas of the Permian Basin